NEXT-GENERATION CANCER THERAPIES BASED ON A (R)EVOLUTION OF THE BIOMARKER LANDSCAPE

EDITED BY: Claudia Cerella, Katia Aquilano, Marc Diederich and Anne Lorant

PUBLISHED IN: Frontiers in Pharmacology and Frontiers in Oncology

frontiers Research Topics

frontiers

Frontiers eBook Copyright Statement

The copyright in the text of individual articles in this eBook is the property of their respective authors or their respective institutions or funders. The copyright in graphics and images within each article may be subject to copyright of other parties. In both cases this is subject to a license granted to Frontiers.

The compilation of articles constituting this eBook is the property of Frontiers.

Each article within this eBook, and the eBook itself, are published under the most recent version of the Creative Commons CC-BY licence. The version current at the date of publication of this eBook is CC-BY 4.0. If the CC-BY licence is updated, the licence granted by Frontiers is automatically updated to the new version.

When exercising any right under the CC-BY licence, Frontiers must be attributed as the original publisher of the article or eBook, as applicable.

Authors have the responsibility of ensuring that any graphics or other materials which are the property of others may be included in the CC-BY licence, but this should be checked before relying on the CC-BY licence to reproduce those materials. Any copyright notices relating to those materials must be complied with.

Copyright and source acknowledgement notices may not be removed and must be displayed in any copy, derivative work or partial copy which includes the elements in question.

All copyright, and all rights therein, are protected by national and international copyright laws. The above represents a summary only. For further information please read Frontiers' Conditions for Website Use and Copyright Statement, and the applicable CC-BY licence.

ISSN 1664-8714
ISBN 978-2-88974-787-0
DOI 10.3389/978-2-88974-787-0

About Frontiers

Frontiers is more than just an open-access publisher of scholarly articles: it is a pioneering approach to the world of academia, radically improving the way scholarly research is managed. The grand vision of Frontiers is a world where all people have an equal opportunity to seek, share and generate knowledge. Frontiers provides immediate and permanent online open access to all its publications, but this alone is not enough to realize our grand goals.

Frontiers Journal Series

The Frontiers Journal Series is a multi-tier and interdisciplinary set of open-access, online journals, promising a paradigm shift from the current review, selection and dissemination processes in academic publishing. All Frontiers journals are driven by researchers for researchers; therefore, they constitute a service to the scholarly community. At the same time, the Frontiers Journal Series operates on a revolutionary invention, the tiered publishing system, initially addressing specific communities of scholars, and gradually climbing up to broader public understanding, thus serving the interests of the lay society, too.

Dedication to Quality

Each Frontiers article is a landmark of the highest quality, thanks to genuinely collaborative interactions between authors and review editors, who include some of the world's best academicians. Research must be certified by peers before entering a stream of knowledge that may eventually reach the public - and shape society; therefore, Frontiers only applies the most rigorous and unbiased reviews.
Frontiers revolutionizes research publishing by freely delivering the most outstanding research, evaluated with no bias from both the academic and social point of view. By applying the most advanced information technologies, Frontiers is catapulting scholarly publishing into a new generation.

What are Frontiers Research Topics?

Frontiers Research Topics are very popular trademarks of the Frontiers Journals Series: they are collections of at least ten articles, all centered on a particular subject. With their unique mix of varied contributions from Original Research to Review Articles, Frontiers Research Topics unify the most influential researchers, the latest key findings and historical advances in a hot research area! Find out more on how to host your own Frontiers Research Topic or contribute to one as an author by contacting the Frontiers Editorial Office: frontiersin.org/about/contact

NEXT-GENERATION CANCER THERAPIES BASED ON A (R)EVOLUTION OF THE BIOMARKER LANDSCAPE

Topic Editors:
Claudia Cerella, Fondation de Recherche Cancer et Sang, Luxembourg
Katia Aquilano, University of Rome Tor Vergata, Italy
Marc Diederich, Seoul National University, South Korea
Anne Lorant, Laboratoire de Biologie Moléculaire et Cellulaire du Cancer (LBMCC), Luxembourg

Citation: Cerella, C., Aquilano, K., Diederich, M., Lorant, A., eds. (2022). Next-Generation Cancer Therapies Based on a (R)evolution of the Biomarker Landscape. Lausanne: Frontiers Media SA. doi: 10.3389/978-2-88974-787-0

Table of Contents

frontiers in Pharmacology

EDITORIAL
published: 07 March 2022
doi: 10.3389/fphar.2022.861424

Editorial: Next-Generation Cancer Therapies Based on a (R)evolution of the Biomarker Landscape

Claudia Cerella[1]*, *Anne Lorant*[1], *Katia Aquilano*[2] and *Marc Diederich*[3]

[1]Laboratoire de Biologie Moléculaire du Cancer, Hôpital Kirchberg, Luxembourg, Luxembourg, [2]Laboratory of Biochemistry, Department of Biology, University of Rome Tor Vergata, Rome, Italy, [3]Department of Pharmacy, College of Pharmacy, Seoul National University, Seoul, South Korea

Keywords: cancer biomarkers, precision oncology, targeted agents, immunotherapy, therapy response prediction

Editorial on the Research Topic

Next-Generation Cancer Therapies Based on a (R)evolution of the Biomarker Landscape

Targeted and immunomodulatory agents have driven the field of cancer therapy toward precision oncology. Therapeutic protocols can now be tailored to each patient after identifying molecular alterations and vulnerabilities to provide the most case-effective therapeutic option. Even though personalized therapies have offered clinical benefits to responsive patients, they also reveal limitations (Gambardella et al., 2020; Malone et al., 2020). The multi-arm precision clinical trial NCI-MATCH (National Cancer Institute-Molecular Analysis for Therapy Choice) applied DNA sequencing to assign the most appropriate targeted therapies to individual cancer patients. As a result, 18% of the 38% of patients with an actionable mutation could benefit from such a personalized treatment; moreover, a significant proportion of them did not respond to these therapies (Flaherty et al., 2020; Commentary, 2021). Similarly, immunotherapies hold potential in cancer therapy; however, the benefit of these approaches is counterbalanced by early disease progression and frequent adverse events (AEs) in real-world experience (McKean et al., 2020). The robustness of biomarkers predicting patient response or AEs must be improved. To reach this goal, several ongoing clinical trials have been launched to validate innovative precision immuno-oncology markers with the intent to improve patient stratification and drug response prediction (NCT03833440; NCT03493581; NCT04589845; NCT03917537). Robust indicators are required to: 1) monitor and predict the cellular fates of intratumor subclones presenting heterogeneous genetic profiles and therapeutic vulnerabilities; 2) identify stem cells; 3) track cell communication within the tumor microenvironment (TME); 4) characterize determinants of metabolic plasticity and 5) cancer immune evasion. Furthermore, therapies need to be adapted. This approach requires the integration of multi-parametric models, including *in vitro*/*ex vivo* drug screening platforms, *in vivo* patient-derived models, computational methods, and retrospective/prospective cancer patient studies (Letai et al., 2021).

This special issue discusses the evolving concept of biomarkers in cancer therapy, considering the rapid evolution of the treatment landscape. The volume includes 14 contributions encompassing reviews, metadata studies, and original articles. Globally, they provide a comprehensive overview of the current classification of biomarkers, suggest innovative approaches, or rediscuss/implement the validity of biomarker-driven treatments. Discussions involve conventional and personalized therapies.

THE EVOLVING CONCEPT OF THE CANCER BIOMARKERS

Diversified and innovative investigational technologies in pharmacological and medical sciences require a continuous update of biomarker classification. Worldwide medical agencies are developing guidelines for biomarker qualifications (e.g., the FDA-NHI Biomarker Working Group,

OPEN ACCESS

Edited and reviewed by:
Olivier Feron,
Université catholique de Louvain, Belgium

***Correspondence:**
Claudia Cerella
claudia.cerella@lbmcc.lu

Specialty section:
This article was submitted to Pharmacology of Anti-Cancer Drugs, a section of the journal Frontiers in Pharmacology

Received: *24 January 2022*
Accepted: *17 February 2022*
Published: *07 March 2022*

Citation:
Cerella C, Lorant A, Aquilano K and Diederich M (2022) Editorial: Next-Generation Cancer Therapies Based on a (R)evolution of the Biomarker Landscape. Front. Pharmacol. 13:861424. doi: 10.3389/fphar.2022.861424

https://www.fda.gov/about-fda/center-drug-evaluation-and-research-cder/fda-biomarkers-working-group; the EMA Concept Paper EMA/CHMP/800914/2016, https://www.ema.europa.eu/en/predictive-biomarker-based-assay-development-context-drug-development-lifecycle). The field of cancer biomarkers mirrors this dynamic scenario. Louie et al. provide a comprehensive overview of the evolving field of cancer biomarkers. After defining the different categories, the authors discuss their clinical application and utility by examples. The article integrates the contribution of different technologies to facilitate the discovery of cancer biomarkers, ranging from omics assays (genomics, transcriptomics, proteomics, and metabolomics) to the most recent approaches (machine learning, analysis of tissues, biological fluids, and liquid biopsies).

BIOMARKERS FOR PERSONALIZED IMMUNO-ONCOLOGY

Cancer immunotherapy drives recent therapy breakthroughs. The cellular and molecular complexity of the immune system mirrors multiple subverted processes that innovative compounds can efficiently target to harness the immune response (Waldman et al., 2020). Despite this exciting premise, most patients do not respond to immunotherapies while developing severe AEs. Although some alterations are associated with immunotherapy response, the underwhelming therapeutic outcomes indicate the limited predictive power of most of these putative response biomarkers (McKean et al., 2020). Tian et al. describe the lack of prediction of T cell exhaustion as a significant limitation of the currently used indicators of response to immune checkpoints inhibitors (ICIs), like the microsatellite instability/stability (MSI/MSS) status or the tumor mutational burden (TMB). Consequently, they developed the TMEPRE computational method, which integrates two scores respectively measuring the level of T cell infiltration in the TME (TME1. TCellInfiltration) and their ability to respond to ICIs (TME2. CellResponse). Their approach, specific for colorectal cancer (CRC), matches the expected percentages of responders among MSI or MSS CRC, providing mechanistic insights about their resistance. Abdolahi et al. investigate the antitumor potential of *ex vivo*-expanded, IL-2 activated NK cells combined with an anti-PD1 antibody (Nivolumab) using a xenograft model of gastric cancer. The authors show that anti-PD1 treatment improves the efficacy of adaptive NK cell therapy by using an integrated analysis including morphometric, immunohistochemical, and flow cytometric analyses. A maximal response was achieved when anti-PD1-pretreated NK cells were injected. Interested readers will find a comprehensive and up-to-date overview of clinically approved and investigational ICIs in the review article of Lee et al. Each ICI description comprises the molecular structure, the mechanism of action, cell expression pattern, targeting agents, and ongoing clinical trials, further summarized in accompanying tables.

MAXIMIZING THE CLINICAL BENEFITS IN CANCER THERAPY

Improving responder prediction and progressively adapting therapies remain urgent needs. Nikanen et al. use an *ex vivo* drug screening platform as a functional diagnostic method for therapy decision-making. They report a case study of a patient affected by a metastatic parotid squamous cell carcinoma, a rare and aggressive type of cancer generally diagnosed at an advanced stage. They combined a phenotypic-based assay with a reverse-phase protein array (RPPA) drug screening using 318 anti-cancer agents. They applied this setup on tumor cells isolated in two stages to adapt the treatment to the disease progression. They further improved the control of the disease by the off-label use of drugs providing the most efficient *ex vivo* results. AEs cause therapy discontinuation. Tawk et al. reflect on current strategies to minimize morbidities by optimizing treatment intensity. Human papillomavirus (HPV)-driven head and neck squamous cell carcinoma (HNSCC) is the topic of this overview. The authors suggest that a deeper molecular characterization of the HNSCC TME may identify new biomarkers to be validated in next-generation de-escalation trials.

IMPLEMENTING THE PROGNOSTIC/PREDICTIVE POTENTIAL OF CANCER BIOMARKER

Protocol conditions are critical when establishing the potential of biomarkers. Ungureanu et al. performed a meta-analysis of the clinicopathological relevance of claudin (CLDN) 18.2 expression in gastric cancer. The authors did not establish significant correlations between CLDN 18.2 and clinical features (including TNM stages, Laurent classification, human epidermal growth factor receptor 2 (HER), grading, and overall survival (OS)) when using two different cutoff values to classify CLDN 18.2 positivity. However, higher CLDN 18.2 expression could be observed in specific T/N stages when the cutoff for CLDN 18.2 positivity was set higher. The authors predict that a re-evaluation of classification criteria (e.g., more specific assays for staining and quantification and the cutoff threshold for CLDN 18.2 positivity) might improve the CLDN 18.2 prognostic value. Hsiao et al. aim at validating c-Myc expression levels as a new marker of resistance to the "7 + 3" induction regimen of *de novo* acute myeloid leukemia (AML) patients. They used the complete remission (CR) rates of a cohort of 75 patients from one prospective and one retrospective study as a readout. They discovered that patients unable to reach a CR display higher c-Myc gene expression levels. Of note, responder prediction is facilitated by combining c-Myc positivity to high-risk cytogenetics. This study establishes the gene (but not the protein) expression level combined with the cut-off of expression positivity as critical determinants for consistent results.

CLINICOPATHOLOGICAL SIGNIFICANCE OF SPECIFIC ALTERATION PATTERNS

Tian et al. review the dual role of the integrated stress response (ISR) on cell survival/death and autophagy. The authors discuss strategies to manipulate the ISR to sensitize tumor cells to specific agents (protease and tyrosine kinase inhibitors, ISR activators, and ICIs). Raufi et al. discuss the role of autophagy in pancreatic ductal carcinoma (PDAC). In this aggressive type of cancer, autophagy is upregulated and contributes to carcinogenesis and therapy resistance.

Functional studies document the dependency of PDAC on this process to sustain metabolism and modulate immunity. Mechanistically, a hypoxic TME promotes autophagy and the unfolded protein response (UPR) as adaptive responses to ISR. The authors suggest MEK inhibitors and ICIs targeting the ISR as promising candidates for combinatorial therapies. This article provides extensive tables summarizing autophagy inhibitors and overviewing clinical trials with autophagy modulators in PDAC. The lack of biomarker-driven treatments in selected cancer types is a major challenge. Liguori et al. discuss the therapeutic potential of the ISR as a pharmacological target. The authors investigate the effect of preclinical drug candidates against small cell lung cancer (SCLC) without actionable biomarkers. Chang et al. review chromosomal rearrangements in pediatric solid tumors outside the central nervous system (CNS). Promising therapeutic regimens and ongoing clinical trials are reported for each type of cancer.

The aberrant regulation of lipid metabolism causes carcinogenesis and therapy resistance (Bacci et al., 2021). Tomacha et al. characterize the metabolic profile of 155 cholangiocarcinoma (CCA) patients, identifying an inverse correlation between fatty acid synthase (FASN) expression and OS. FASN knockdown inhibits CCA cell proliferation and survival, while metabolomics suggests the purine metabolism as the most relevant pathway affected by FASN knockdown. Approaches targeting FASN might thus represent a potential strategy for this aggressive type of cancer.

BEYOND GENE AND PROTEIN BIOMARKERS

Gene or protein expression networks commonly constitute prognostic signatures. Li et al. analyze the potential of long coding RNAs (lncRNAs) in the prognosis of papillary thyroid cancer (PTC). Using four different databases, the authors identify 5 promising hub lncRNAs and develop two prognostic risk models for PTC OS and disease-free survival (DFS) based on lncRNA-miRNA-mRNA competing endogenous RNA (ceRNA) network. The resulting connectivity Map predicts candidate compounds for PTC treatment.

Overall, this special issue provides new ideas of cancer biomarkers and offers a discussion forum to design and improve clinical trials and validate novel biomarkers predictive of therapy response and optimization. We thank all authors for their valuable contributions.

AUTHOR CONTRIBUTIONS

All authors listed have made a substantial, direct, and intellectual contribution to the work and approved it for publication.

FUNDING

CC, AL, and MD: "Recherche Cancer et Sang" Foundation, "Recherches Scientifiques Luxembourg", "Een Häerz fir kriibskrank Kanner", Action Lions "Vaincre le Cancer" (Luxembourg), and Télévie Luxembourg. M.D.: National Research Foundation (NRF) (Grant number 019R1A2C-1009231), Brain Korea (BK21) FOUR and the Creative-Pioneering Researchers Program at Seoul National University (funding number: 370C-20160062). KA: Italian Association for Cancer Research (AIRC) IG 2019—ID. 23562.

REFERENCES

Bacci, M., Lorito, N., Smiriglia, A., and Morandi, A. (2021). Fat and Furious: Lipid Metabolism in Antitumoral Therapy Response and Resistance. *Trends Cancer* 7, 198–213. doi:10.1016/j.trecan.2020.10.004

Commentary and Dolgin, E. (2021). NCI-MATCH Sets "Benchmark of Actionability. *Cancer Discov.* 11, 6–7. doi:10.1158/2159-8290.CD-NB2020-100

Flaherty, K. T., Gray, R. J., Chen, A. P., Li, S., Mcshane, L. M., Patton, D., et al. (2020). Molecular Landscape and Actionable Alterations in a Genomically Guided Cancer Clinical Trial: National Cancer Institute Molecular Analysis for Therapy Choice (NCI-MATCH). *J. Clin. Oncol.* 38, 3883–3894. doi:10.1200/JCO.19.03010

Gambardella, V., Tarazona, N., Cejalvo, J. M., Lombardi, P., Huerta, M., Rosello, S., et al. (2020). Personalized Medicine: Recent Progress in Cancer Therapy. *Cancers (Basel)* 12 (4), 1009. doi:10.3390/cancers12041009

Letai, A., Bhola, P., and Welm, A. L. (2021). Functional Precision Oncology: Testing Tumors with Drugs to Identify Vulnerabilities and Novel Combinations. *Cancer Cell* 40 (1), 26–35. doi:10.1016/j.ccell.2021.12.004

Malone, E. R., Oliva, M., Sabatini, P. J. B., Stockley, T. L., and Siu, L. L. (2020). Molecular Profiling for Precision Cancer Therapies. *Genome Med.* 12, 8. doi:10.1186/s13073-019-0703-1

McKean, W. B., Moser, J. C., Rimm, D., and Hu-Lieskovan, S. (2020). Biomarkers in Precision Cancer Immunotherapy: Promise and Challenges. *Am. Soc. Clin. Oncol. Educ. Book* 40, e275–e291. doi:10.1200/EDBK_280571

Waldman, A. D., Fritz, J. M., and Lenardo, M. J. (2020). A Guide to Cancer Immunotherapy: from T Cell Basic Science to Clinical Practice. *Nat. Rev. Immunol.* 20, 651–668. doi:10.1038/s41577-020-0306-5

Conflict of Interest: The authors declare that the research was conducted in the absence of any commercial or financial relationships that could be construed as a potential conflict of interest.

Publisher's Note: All claims expressed in this article are solely those of the authors and do not necessarily represent those of their affiliated organizations, or those of the publisher, the editors and the reviewers. Any product that may be evaluated in this article, or claim that may be made by its manufacturer, is not guaranteed or endorsed by the publisher.

Copyright © 2022 Cerella, Lorant, Aquilano and Diederich. This is an open-access article distributed under the terms of the Creative Commons Attribution License (CC BY). The use, distribution or reproduction in other forums is permitted, provided the original author(s) and the copyright owner(s) are credited and that the original publication in this journal is cited, in accordance with accepted academic practice. No use, distribution or reproduction is permitted which does not comply with these terms.

frontiers in Oncology

SYSTEMATIC REVIEW
published: 04 March 2021
doi: 10.3389/fonc.2021.643872

Clinicopathologic Relevance of Claudin 18.2 Expression in Gastric Cancer: A Meta-Analysis

Bogdan Silviu Ungureanu[1], Cristian-Virgil Lungulescu[2], Daniel Pirici[3], Adina Turcu-Stiolica[4], Dan Ionut Gheonea[1], Victor Mihai Sacerdotianu[1], Ilona Mihaela Liliac[3], Emil Moraru[5], Felix Bende[6] and Adrian Saftoiu[1]*

[1] Gastroenterology Department, University of Medicine and Pharmacy of Craiova, Craiova, Romania, [2] Oncology Department, University of Medicine and Pharmacy of Craiova, Craiova, Romania, [3] Histology Department, University of Medicine and Pharmacy of Craiova, Craiova, Romania, [4] Pharmacoeconomics Department, University of Medicine and Pharmacy of Craiova, Craiova, Romania, [5] Surgical Department, University of Medicine and Pharmacy of Craiova, Craiova, Romania, [6] Gastroenterology Department, University of Medicine and Pharmacy "Victor Babes", Timisoara, Romania

An increasing number of tumor markers have been discovered to have potential efficacy as diagnostic and prognostic tools in gastric cancer. We aimed to assess putative correlations between claudin 18.2 expression and pathological or prognosis features in patients with gastric cancer. MEDLINE, Web of Science, EBSCO, and ClinicalTrials.gov were used to search for relevant studies from their inception to 30 October 2020. Finally, a total of six articles were included in this meta-analysis. Review Manager 5 software was applied to examine the heterogeneity among the studies and to calculate the odds ratio with 95% CI by selecting corresponding models, in evaluating the strength of the relationship. Publication bias test was also conducted. No bias and no significant correlations were found between CLDN 18.2 and TNM stages, Lauren classification, HER2, grading, or overall survival. This meta-analysis expounded that the relationship with CLDN 18.2 and pathological features depends on the percentage of staining of tumor cells for which CLDN 18.2 is considered positive. Our pooled outcomes suggest that targeted therapy for CLDN 18.2 could be effective if certain criteria were established.

Keywords: claudin 18.2, gastric cancer, TNM stages, HER2, Lauren classification

OPEN ACCESS

Edited by:
Claudia Cerella, Fondation de Recherche Cancer et Sang, Luxembourg

Reviewed by:
Matteo Fassan, University of Padua, Italy
Hye Seung Lee, Seoul National University, South Korea

****Correspondence:***
Adina Turcu-Stiolica
adina.turcu@gmail.com

Specialty section:
This article was submitted to Pharmacology of Anti-Cancer Drugs, a section of the journal Frontiers in Oncology

Received: *19 December 2020*
Accepted: *08 February 2021*
Published: *04 March 2021*

Citation:
Ungureanu BS, Lungulescu C-V, Pirici D, Turcu-Stiolica A, Gheonea DI, Sacerdotianu VM, Liliac IM, Moraru E, Bende F and Saftoiu A (2021) Clinicopathologic Relevance of Claudin 18.2 Expression in Gastric Cancer: A Meta-Analysis. Front. Oncol. 11:643872. doi: 10.3389/fonc.2021.643872

INTRODUCTION

Gastric cancer (GC) is one of the most commonly diagnosed malignancies worldwide and the second cause of cancer-related death. Despite the variability of GC incidence and mortality, an estimated 1,033,701 new stomach cancers and 782,685 deaths occurred in 2018[1]. Frequently, patients are diagnosed at an advanced stage, especially in countries where GC screening is not routinely performed, aggravating its poor prognosis.

Targeted agents approved for GC like trastuzumab (anti-HER2) or ramucirumab (anti-VEGF receptor) have shortcomings such as modest survival benefits and second resistance development. New suitable biomarkers that can serve as targets have to be found for highly effective targeted therapies for GC (1).

Claudins are a family of at minimum 27 proteins with roles in maintaining the intercellular tight junction adhesion, which create a paracellular barrier. The impossibility of these molecules

[1]GLOBOCAN, https://gco.iarc.fr/today/data/factsheets/populations/900-world-fact-sheets.pdf (accessed November 20, 2020).

to accomplish their function is linked with tumor development and progression (2, 3). Different claudins expression may have prognostic value in colon cancer [claudin (CLDN)-1] (4), pancreatic cancer (CLDN-18), and hepatocellular carcinoma and thyroid cancer (CLDN-10) (5, 6). CLDN 18 has two isoforms (CLDN 18.1 and CLDN 18.2), which are present in differentiated epithelial cells of gastric mucosa. CLDN 18 splice variant 2 is the dominant isoform that occurs in normal gastric tissue, gastric adenocarcinomas, and their metastases. Furthermore, CLDN 18.2 is aberrantly expressed in pancreatic, esophageal, ovarian, and lung adenocarcinomas (7). CLDN 18.2 is an attractive surface biomarker as it is located on the outer cell membrane, therefore easy accessible for targeted therapies (8).

IMAB362 (known as zolbetuximab or claudiximab), a novel chimeric immunoglobulin G1 antibody, is the first type of ideal monoclonal antibodies (IMAB) used for the treatment of GC. After IMAB362 binds to CLDN 18.2, immune effectors activate antibody-dependent cellular cytotoxicity and complement-dependent cytotoxicity. This change induces apoptosis and promotes the inhibition of cell proliferation, with beneficial effects for patients (9).

Our objective was to assess all available studies that involve CLDN 18.2 expression in GC and its relation to clinicopathological or prognosis features in patients with GC, in order to offer more insights on its potential as a target in future clinical trials.

MATERIALS AND METHODS

Literature Search

We used the PICOS (populations, interventions, comparators, outcomes, and study designs) model and PRISMA guidelines to design our search strategy (10).

To identify studies, we searched the following databases: MEDLINE, Web of Science, EBSCO, and ClinicalTrials.gov (inception to 30 October 2020) to see if they evaluated the expression of CLDN 18.2 in order to find correlations with clinicopathological patient characteristics with GC. We studied reference lists as well as published systematic review articles. The search terms included ("claudin 18.2" AND "gastric cancer") OR ("claudin18.2" AND "gastric cancer").

Inclusion and Exclusion Criteria

Studies evaluating the expression of CLDN 18.2 in adults with GC were included in our meta-analysis. The inclusion criteria for selection were: (1) clear definition of scoring for CLDN 18.2 staining; (2) assessment of clinicopathological patient characteristics; (3) histologically confirmed adenocarcinoma of the stomach. Exclusion criteria were: (1) tumor types other than adenocarcinoma; (2) patients who had undergone a perioperative or neoadjuvant chemo- or radiotherapy; (3) studies as case reports, systematic reviews, abstracts.

Data Extraction and Quality Assessment

Two review authors (BSU and VMS) independently extracted all data using a standardized data extraction table. Any disagreements regarding eligible articles were resolved after consulting a third review author (AT-S). The risk of bias was assessed through a funnel plot.

Statistical Analysis

We conducted a standard meta-analysis using the Review Manager 5 software (RevMan 5. Version 5.4.1, the Cochrane Collaboration, 2020). We used both the random-effects model and the fixed-effects model based on the assessment of heterogeneity, when the inverse-variance approach was implemented. We used the I^2 statistic, which gave us the proportion of the observed variance that reflects real differences in effect size, for quantifying heterogeneity of the results in individual studies, which combined the Chi^2 statistic and the number of studies contributing to each summary estimate in the forest plot (11).

We used odds ratio (OR) as the effect measure for dichotomous outcomes, that is the number of participants achieving TNM clinical stage, HER2, Lauren classification, and grading. Analysis and comparisons for all outcomes were performed where data were available. We considered *P*-values <0.05 and 95% confidence intervals (CI) that did not include 1 to be statistically significant.

Time-to-event data for overall-survival (OS) were analyzed using hazard ratio (HR), which was estimated using the calculation methods described by Tierney et al. (12). If these parameters were not available in the studies, we used WebPlot Digitizer version 4.3 (Austin, Texas, USA) to extract the specific survival rates from the Kaplan-Meier curves.

To assure our results were robust, the presence of any publication bias was analyzed with a funnel plot, based on the visual inspection of the symmetry.

RESULTS

Figure 1 shows the overall study selection process. We identified a total of six eligible studies, including 2,440 patients. A total of 86 studies were excluded, and the main reasons for exclusion included lack of information about the correlation of CLDN 18.2 expression and clinicopathological patient features and duplicate studies or abstracts.

Baseline Characteristics of All Included Studies

The characteristics of the included studies are provided in **Table 1**. The study sample size ranged from 263 to 485 participants. The six studies revealed a prevalence of 34.2% from the total of 2,055 patients.

Correlation Between CLDN 18.2, Pathological Characteristics, and Prognosis of GC Patients

We conducted the following analysis using the standard meta-analysis to find correlations between CLDN 18.2 and pathological features and prognosis of GC patients. Two subgroups of studies were analyzed according to the definition of CLDN 18.2's positivity and the outcomes were assessed where data

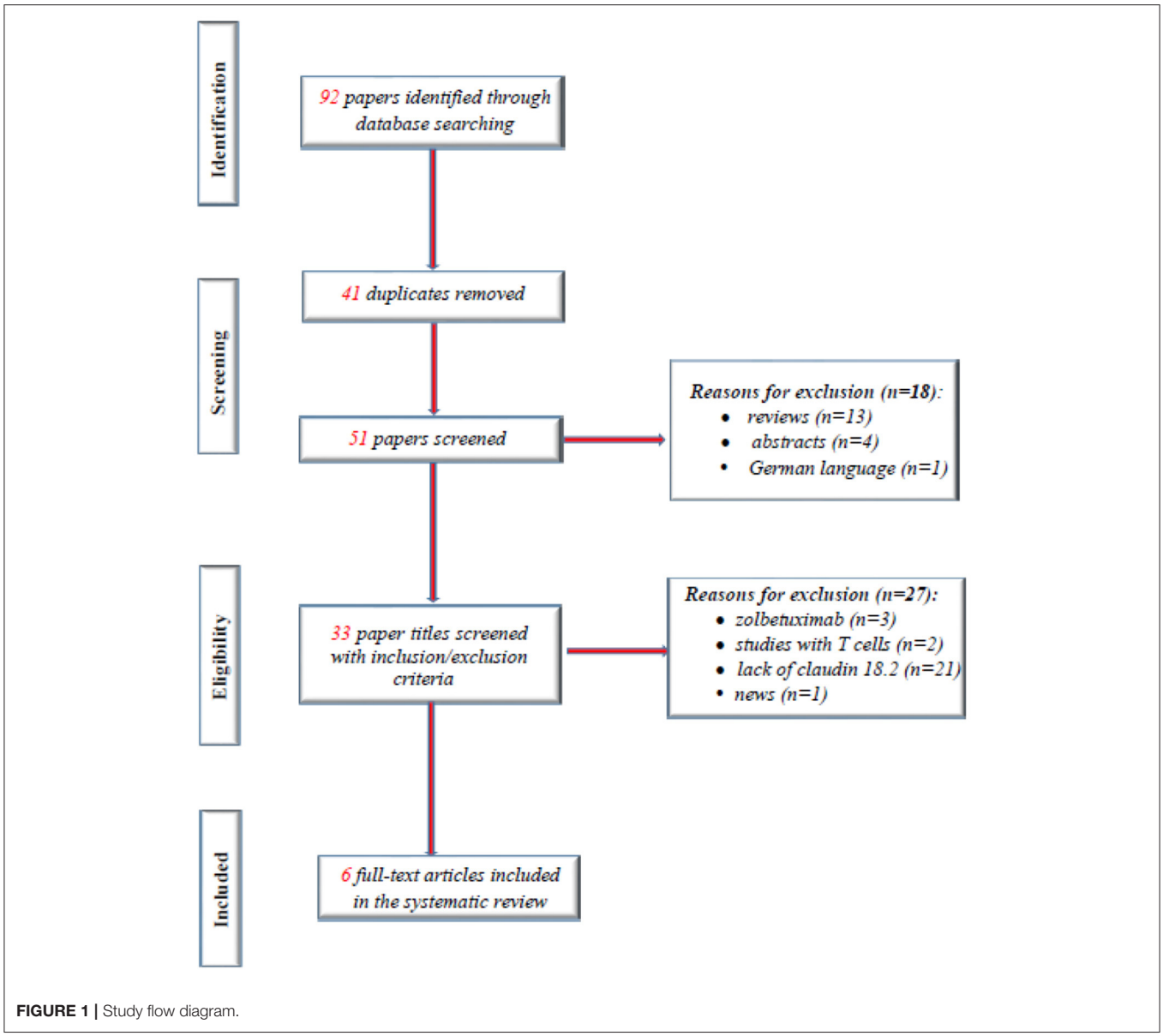

FIGURE 1 | Study flow diagram.

were available. The two subgroups were: A (positivity was defined as CLDN 18.2 staining intensity was present in any percentage of tumor cells) and B (positivity was defined as CLDN 18.2 staining intensity was present in more than 40% of tumor cells).

By T Clinical Stage

The results are illustrated in the forest plots in **Figure 2**. If the samples were defined as CLDN 18.2-positive showing specific staining with any fraction of tumor cells, there was no evidence ($p = 0.12$) to indicate correlation between CLDN 18.2 expression and T1 + T2 vs. T3 + T4 clinical stage, with an OR of 0.83 (95% CI 0.66–1.05). The fixed-effect model was used with an I^2 of 11% ($p = 0.34$) indicating no heterogeneity.

If the samples were defined as CLDN 18.2-positive showing specific staining with more than 40% of tumor cells, there was no evidence ($p = 0.28$) to indicate correlation between CLDN 18.2 expression and T1 + T2 vs. T3 + T4 clinical stage, with an OR of 1.26 (95% CI 0.83–1.91). The fixed-effect model was used with an I^2 of 0% ($p = 0.42$) indicating no heterogeneity.

The effect estimates and confidence intervals for both individual studies and meta-analysis showed the importance of how CLDN 18.2 was defined as positive. We observed, for example in Baek et al. (14), that the results of OR was 0.68 (95% CI 0.43–1.07) for a positive CLDN 18.2 expression in any percentage staining and 1.54 (95% CI 0.80–2.96) for more than 40% staining. The overall effect was also different in the two subgroups of studies: for subgroup A, but without statistical significance, CLDN 18.2 exhibited more positive expression in patients with T1 + T2 stage than in those with T3 + T4 stage GC; while for subgroup B, but also without statistical significance, CLDN 18.2 exhibited more positive expression in

TABLE 1 | Baseline characteristics of the six included studies.

References	Country	No. of patients (No. of positive by predefined criteria, %)	Definition of positive CLDN 18.2	Immunohistochemical analysis
(13)	Germany	381 (65, 17%)	IRS > 8	Anti-CLDN 18.2 clone EPR19202 (Abcam, Cambridge, UK, rabbit Mab, dilution: 1:500) and clone 43-14A (Roche Ventana Medical Systems, mouse Mab, dilution: 1:1); FFPE tissue immunostained on a Leica Bond-Max Autostainer (Leica Biosystems, Wetzlar, Germany), with heat-induced epitope retrieval and the Leica Bond HRP Polymer Detection Kit
(14)	Korea	367 (108, 29.4%[a] or 46, 12.5%[b])	H-score	Anti-CLDN 18.2 (Abcam, dilution 1:75); FFPE tissue immunostained on a Leica Bond-Max Autostainer, with the Leica Red Refine HRP Polymer Detection Kit
(15)	Germany	481 (203, 42.3%)	H-score	Anti-CLDN 18.2 clone EPR19202 (Abcam, rabbit Mab, dilution: 1:200); FFPE tissue immunostained on a Leica Bond-Max Autostainer, with heat-induced epitope retrieval (ER-2 buffer, Leica, 20 min) and the Leica Refine HRP Polymer Detection Kit
(16)	Korea	82 (12, 14.6%)	Staining was visible in >5% of tumor cells	Anti-CLDN 18.2 rabbit Pab (Thermo Fisher Scientific, Carlsbad, CA, USA, dilution 1:150 with incubation for 15 min at room temperature); FFPE tissue immunostained on a Leica Bond-Max Autostainer, with heat-induced epitope retrieval (pH 6 at 97°C for 20 min) and the Leica Bond Polymer Refine Detection Kit (DS9800)
(17)	Germany	483 (89, 18.4%)	Staining was visible in >5% of tumor cells	Anti-CLDN 18.2 clone EPR19202 (Abcam, cat. no. ab222512, rabbit Mab, dilution: 1:200, incubation for 20 min at 37°C); FFPE tissue immunostained on a Leica Bond-Max Autostainer, with autoclave heat-induced epitope retrieval (Tris-EDTA pH 9 buffer at 121°C for 5 min) and the Leica Bond Polymer Refine Detection Kit for 5 min at 37°C (DS9800)
(18)	Japan	263 (227, 86.6%[c] or 135, 51.5%[d])	At least 1+ (weak membrane or cytoplasmic reactivity) intensity in any fraction of tumor cells	Anti-CLDN 18.2 clone 43-14A recognizing the C-terminus of claudin 18 (Ganymed Pharmaceuticals AG, Mainz, DE, mouse Mab, incubation for 30 min at room temperature); FFPE tissue manually immunostained after heat-induced epitope retrieval (10 mM Tris, 1 mM EDTA pH 9 buffer at 95–99°C for 15 min) and a goat anti-mouse horseradish peroxidase conjugated Fab polymer detection system (Nichirei Biosciences, Inc., Tokyo, Japan) for 30 min at room temperature.

CLDN, claudin; FFPE, formalin fixed paraffin embedded tissue; IRS, immunoreactivity score; H-score, histoscore; Mab, monoclonal antibody; Pab, polyclonal antibody.
[a]Positivity was defined as a percentage of staining >10%; [b]positivity was defined as a percentage of staining ≥ 51%; [c]positivity was defined as at least 1+intensity in any percentage; [d]positivity was defined as a percentage of staining ≥ 40%.

patients with T3 + T4 stage than in those with T1 + T2 stage GC.

By N Clinical Stage

As demonstrated in **Figure 3**, no statistically significant correlation was found between positivity of CLDN 18.2 and N clinical stage (N+ vs. N0), neither for subgroup A [$p = 0.71$, with an OR of 1.17 (95% CI 0.51–2.68)] nor for subgroup B [$p = 0.20$, with an OR of 1.29 (95% CI 0.87–1.90)]. We used a random-effect model for the A subgroup with an I^2 of 93% ($p < 0.00001$) and a fixed-effect model for the B subgroup with an I^2 of 65% ($p = 0.09$). The high heterogeneity of the A subgroup ($Chi^2 = 54.88$) was not observed in subgroup B ($Chi^2 = 2.83$).

By M Clinical Stage

The lack of statistical significance at $p < 0.05$ ($p = 0.89$) proved no correlation between CLDN 18.2 expression and the M clinical stage. The fixed-effect model was used for no heterogeneity of the two studies included in this meta-analysis ($I^2 = 57\%$, $p = 0.13$). The overall effect OR was close to 1 as shown in **Figure 4**: 1.03 (95% 0.71–1.49).

By HER2

There were no significant differences between CLDN 18.2 positive and CLDN 18.2 negative GC patients with respect to HER2 statuses, as showed in **Figure 5** ($p = 0.80$).

A random-effect model was used for moderate heterogeneity of the five studies included in this meta-analysis ($I^2 = 76\%$, $p = 0.002$). The overall effect OR was 1.12 (95% 0.47–2.63).

By Lauren Classification

If the samples were defined as CLDN 18.2-positive showing specific staining with any fraction of tumor cells (>5 or >10%), there was no evidence ($p = 0.74$) to indicate correlation between CLDN 18.2 expression and diffuse vs. other Lauren classifications, with an OR of 0.91 (95% CI 0.54–1.56), as shown in **Figure 6**. A random-effect model was used with an I^2 of 73% ($p = 0.005$) indicating moderate heterogeneity.

If the samples were defined as CLDN 18.2-positive showing specific staining with more than 40% of tumor cells, there was no evidence ($p = 0.76$) to indicate correlation between CLDN 18.2 expression and diffuse vs. other Lauren classifications, with an OR of 1.24 (95% CI 0.31–4.95). A random-effect model was used with an I^2 of 88% ($p = 0.004$) indicating high heterogeneity.

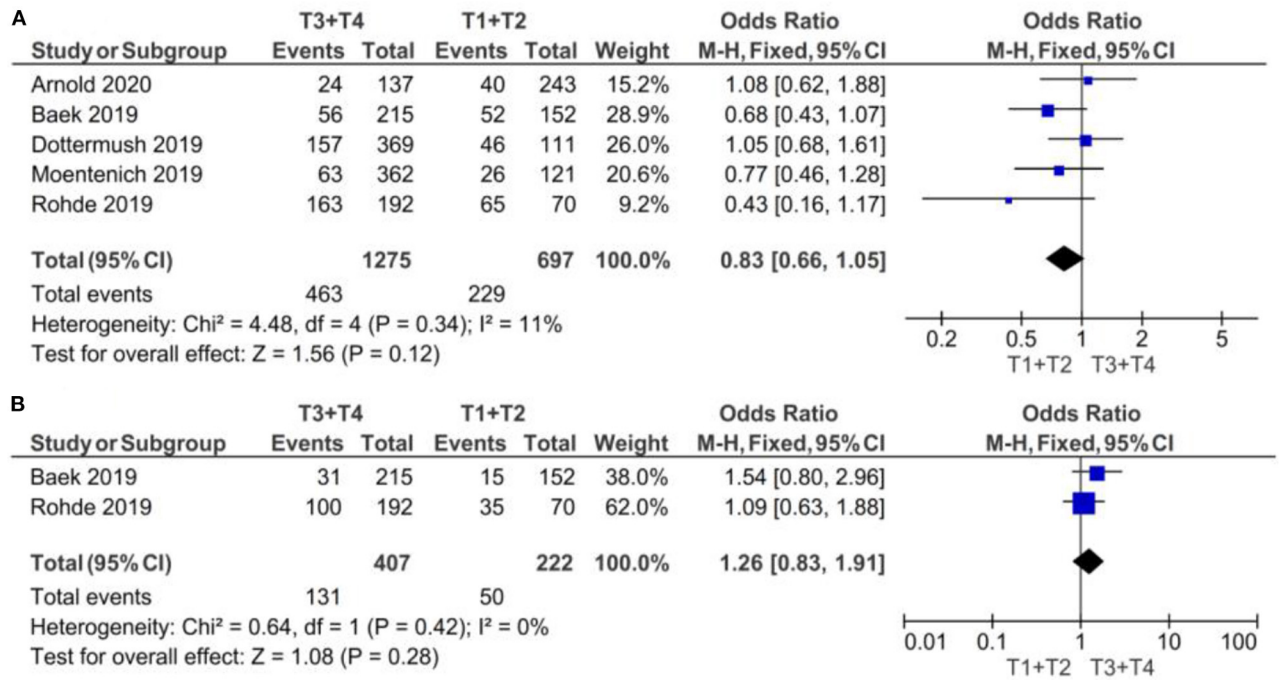

FIGURE 2 | Forest plot on the association between CLDN 18.2 and invasive grade (T3 + T4 vs. T1 + T2). **(A)** The proportion of staining scored in any percentage of tumor cells; **(B)** the proportion of staining scored as ≥40% of tumor cells.

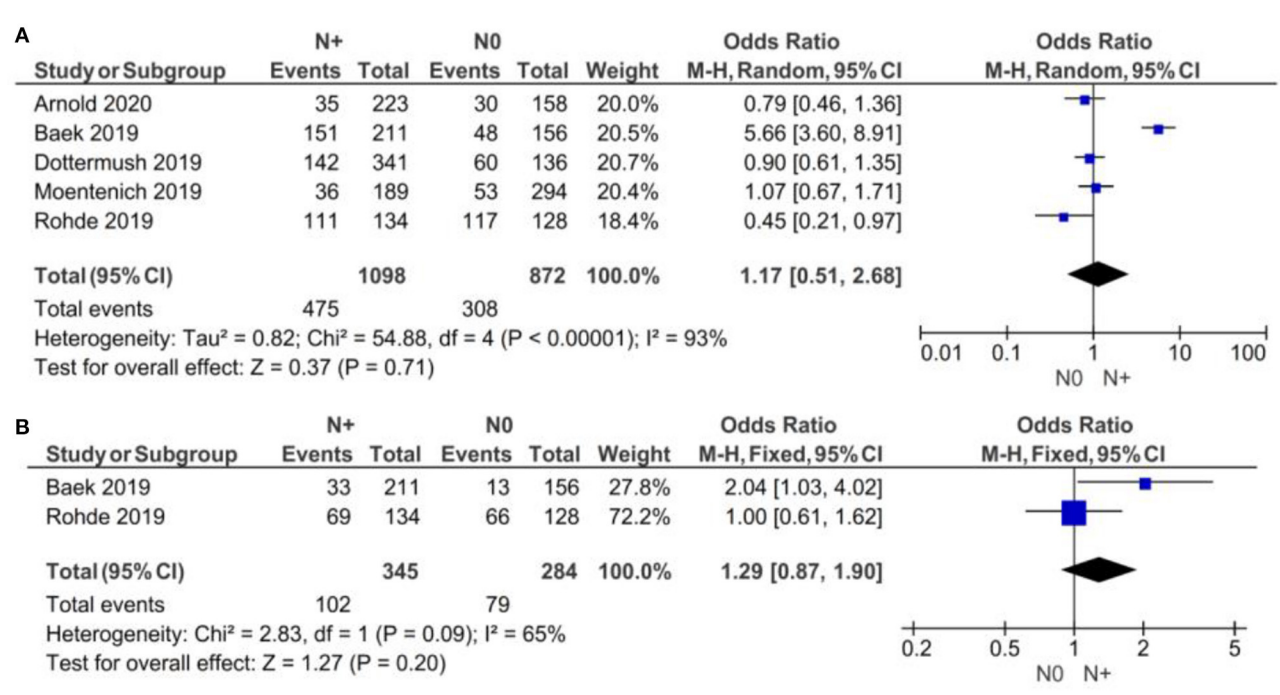

FIGURE 3 | Forest plot on the association between CLDN 18.2 and invasive grade (N+ vs. N0). **(A)** The proportion of staining scored in any percentage of tumor cells; **(B)** the proportion of staining scored as ≥40% of tumor cells.

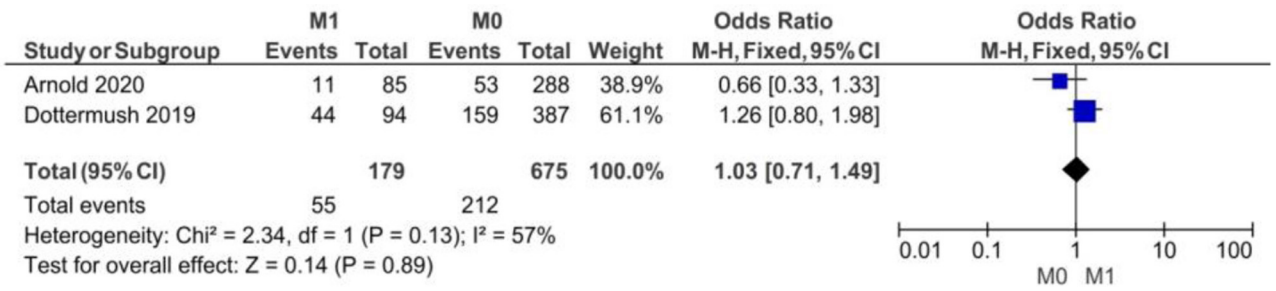

FIGURE 4 | Forest plot on the association between CLDN 18.2 and invasive grade (M1 vs. M0) at the proportion of staining scored in any percentage of tumor cells.

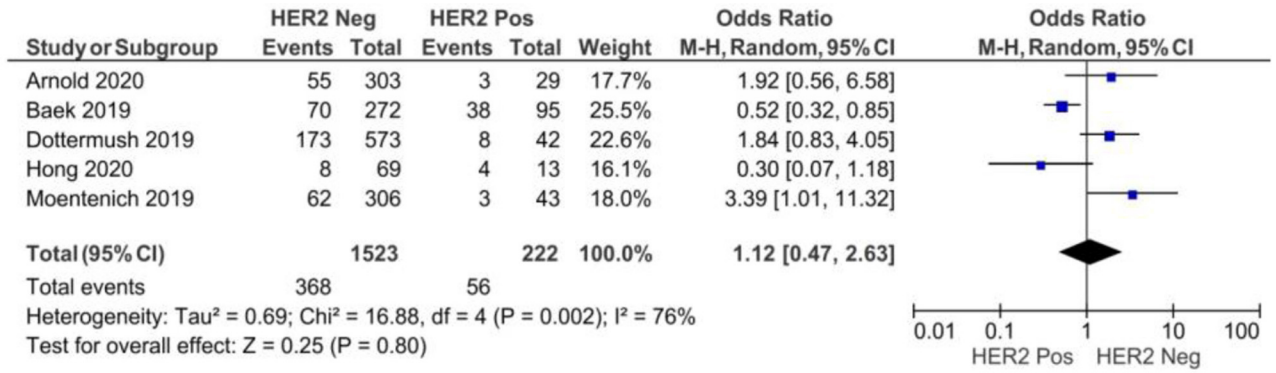

FIGURE 5 | Forest plot on the association between CLDN 18.2 and HER2 at the proportion of staining scored in any percentage of tumor cells.

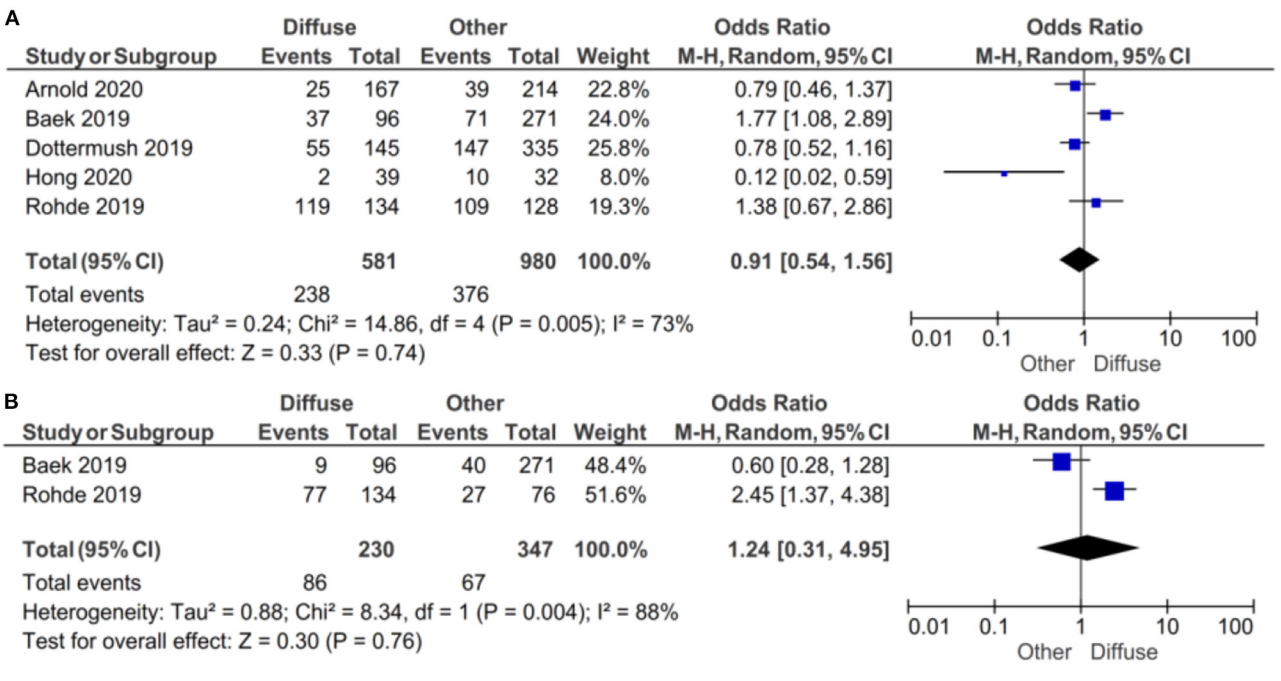

FIGURE 6 | Forest plot on the association between CLDN 18.2 and Lauren classification (diffuse vs. other). **(A)** The proportion of staining scored in any percentage of tumor cells; **(B)** the proportion of staining scored as ≥40% of tumor cells.

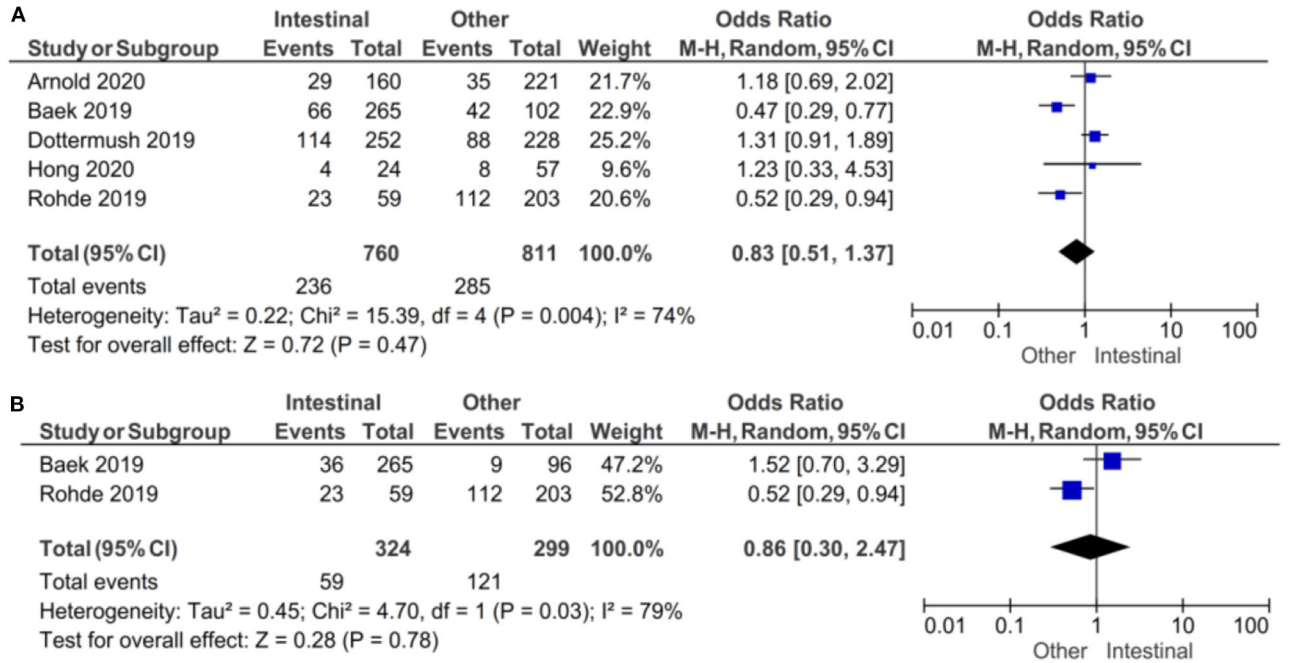

FIGURE 7 | Forest plot on the association between CLDN 18.2 and Lauren classification (intestinal vs. other). **(A)** The proportion of staining scored in any percentage of tumor cells; **(B)** the proportion of staining scored as ≥40% of tumor cells.

The effect estimates and confidence intervals for both individual studies and the meta-analysis showed the importance of CLDN 18.2 being defined as positive. We observed, for example in Baek et al. (14), that the result of OR was 1.77 (95% CI 1.08–2.89) for a positive CLDN 18.2 expression in any percentage staining and 0.60 (95% CI 0.28–1.28) for more than 40% staining. The overall effect was also different in the two subgroups of studies.

In the subgroup of studies where positive CLDN 18.2 was defined as more than 5% staining of tumor cells, there was no evidence ($p = 0.47$) to indicate correlation between CLDN 18.2 expression and intestinal vs. other Lauren classifications, with an OR of 0.83 (95% CI 0.51–2.47). A random-effect model was used with an I^2 of 74% ($p = 0.004$) indicating moderate heterogeneity, as shown in **Figure 7**.

In the subgroup of studies where positive CLDN 18.2 was defined as more than 40% staining of tumor cells, there was no evidence ($p = 0.78$) to indicate correlation between CLDN 18.2 expression and intestinal vs. other Lauren classifications, with an OR of 0.86 (95% CI 0.30–2.47). A random-effect model was used with an I^2 of 79% ($p = 0.03$) indicating moderate heterogeneity.

The effect estimates and confidence intervals for both individual studies and meta-analysis showed the importance of how CLDN 18.2 was defined as positive. We observed, for example in Baek et al. (14), that the results of OR was 0.47 (95% CI 0.29–0.77) for a positive CLDN 18.2 expression of more than 5% staining and 1.52 (95% CI 0.70–3.29) for more than 40% staining. The overall effect was almost the same in the two subgroups of studies.

By Grading

There were no significant differences between CLDN 18.2-positive and CLDN 18.2-negative GC patients with respect to grading, as **Figure 8** shows ($p = 0.69$).

As for the grading, we found that CLDN 18.2 expression was almost the same in GC tumors with G1/G2 when compared with G3/G4 (OR = 0.94; 95% CI 0.69–1.28). The fixed-effect model was used for no heterogeneity between the three studies included in this meta-analysis ($I^2 = 62\%$, $p = 0.07$).

By Overall Survival (OS)

Three studies were included in the meta-analysis of assessing the hazard ratio (HR) for overall survival (OS) for patients who were CLDN 18.2-positive vs. CLDN 18.2-negative. The fixed-effect model was used (no heterogeneity $I^2 = 0\%$ and $p = 0.99$). No significant difference in OS was found between CLDN 18.2-positive and CLDN 18.2-negative: HR = 1.01 (95%CI 0.69–1.48), $p = 0.95$, as **Figure 9** shows.

Publication Bias

Moderately sized and large studies were included in our meta-analysis, as it can be seen in the funnel plots in **Figure 10**, where no smaller studies appeared toward the bottom of the graph. There was no evidence of any bias because of the observed symmetry: the effect size on the x axis showed that the studies were distributed symmetrically about the mean effect size.

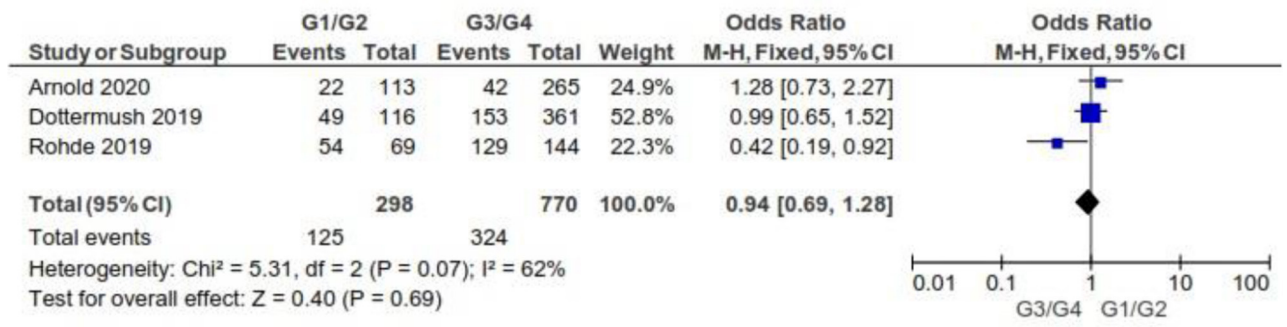

FIGURE 8 | Forest plot on the association between CLDN 18.2 and grading at the proportion of staining scored in any percentage of tumor cells.

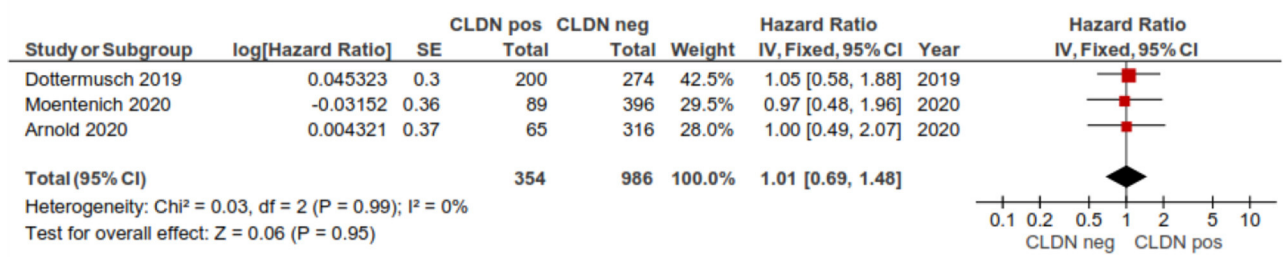

FIGURE 9 | Hazard ratio for OS for patients with positive CLDN vs. negative CLDN.

DISCUSSION

In this meta-analysis, we observed the relationship between CLDN 18.2 expression and GC pathologic features. This tight junction protein CLDN 18.2 is currently considered as a potential target for GC adenocarcinoma and could enlarge the panel of therapeutic options (19). Our results point out that there is no significant connection between CLDN 18.2 and TNM stage, histologic and invasive grade as well as with the Lauren classification.

The claudins are a family of surface proteins which lay the ground for tight cell junctions. Different isoforms are associated with different types of tissue, of which CLDN 18 relates more to GC. CLDN 18.2 is considered a gastric-specific isoform with higher expression in cancer cells than in normal tissue. Generally, it is located within the upper foveolar epithelial cells and is not present within the stem cells areas. However, when carcinogenesis occurs, the tight junctions are disrupted and CLDN 18.2 epitopes are expressed by tumor cells. Thus, this process has proposed the development of a monoclonal antibody against CLDN 18.2 such as zolbetuximab (IMAB362, claudiximab). This new targeted therapy is validated in preclinical studies, and several phase I and II trials are underway with positive results published so far. The FAST study (NCT01630083) (20) showed that combined with first-line chemotherapy, it might improve overall survival (OS) and progression-free survival rate. Zolbetuximab is an IgG1 monoclonal antibody that generates a cascade of processes leading to apoptosis and cell proliferation inhibition. However, it seems to be related so far to higher outcomes only if CLDN 18.2 is expressed in at least 70% of tumor cells (21).

Our meta-analysis reveals that there is no significant correlation between CLDN 18.2 tissue expression and clinicopathologic features. None of the available studies showed any correlation with the TNM stage, however, in T3 + T4 we emphasized a more abundant expression than for T1 + T2, if the positivity of CLDN 18.2 was defined through a higher percentage of stained tumor cells. This was similar for the N stage showing that along with an increased positivity, no correlation was observed (the pooled results showed that CLDN 18.2 was more correlated with the N+ status, in the case of a higher proportion of staining tumor cells).

While our results did not show any positive correlation with Lauren classification, Coati et al. observed that higher prevalence of CLDN 18 had a diffuse type. They also found that higher expression was found in the corpus than the antrum (22).

Regarding the HER2+ status, CLDN 18.2 staining did not correlate with it, even though one study suggested higher expression rates for HER2+ (2+, 3+) statuses (14). On the other hand, two phase III clinical trials (NCT03504397 and NCT03653507) on HER2-negative cases are looking for promising results and might promote CLDN 18.2-directed therapy as a solution for HER2 GC negative patients (23, 24).

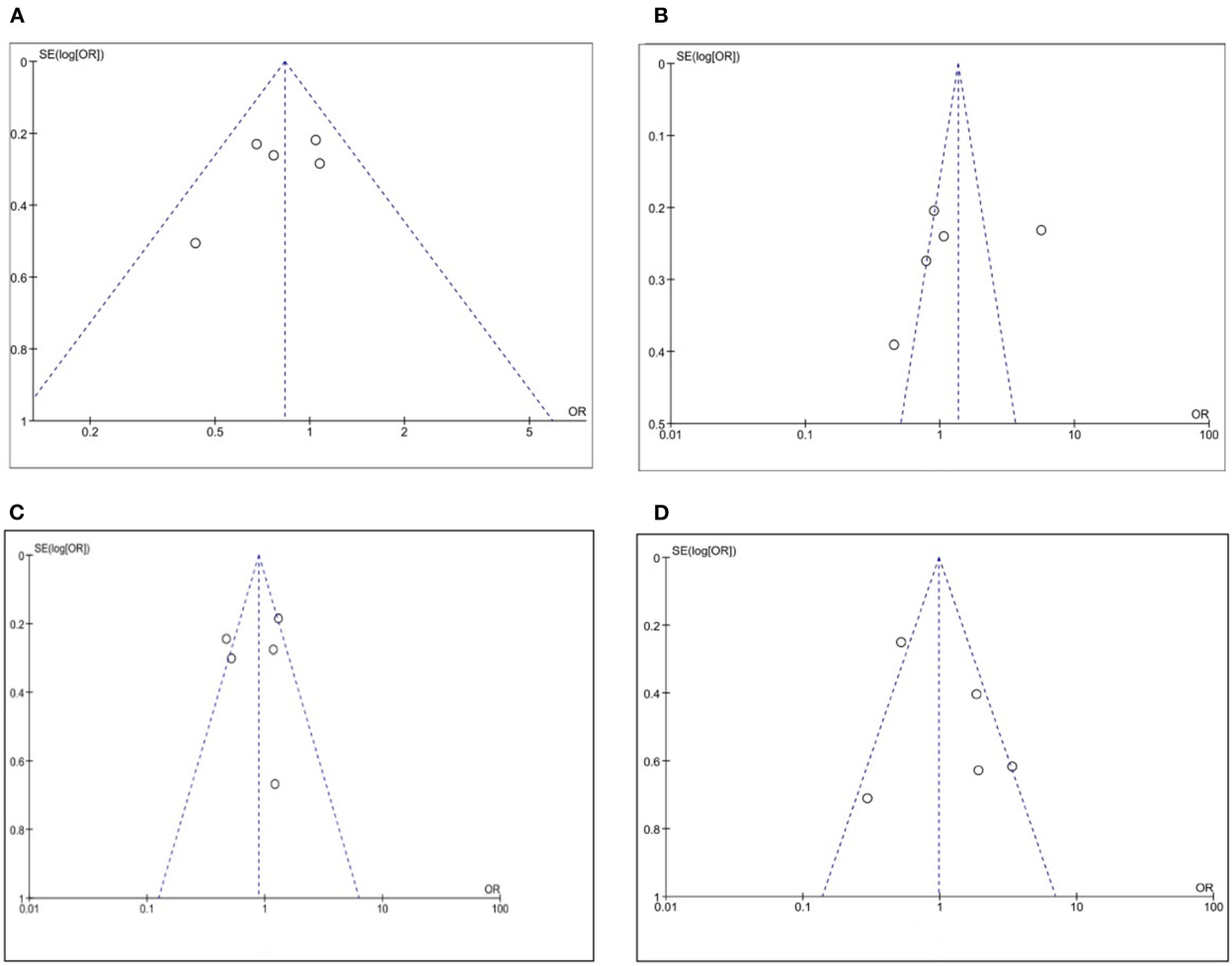

FIGURE 10 | Funnel plot on the association between CLDN 18.2 and pathological characteristics at the proportion of staining scored in any percentage of tumor cells: **(A)** T stage; **(B)** N stage; **(C)** Lauren classification; **(D)** HER2.

Due to the heterogeneity of studies some questions should be raised. First, there is a need for uniformity when differentiating CLDN 18.2 from other variants, currently the only IVD (*in vitro* diagnostics) approved test is the CLAUDETECT 18.2 Kit (developed by Ganymed Pharmaceuticals AG, acquired by Astellas, partnership with Ventana for automated immunohistochemical staining assay on platform). The CLAUDETECT 18.2 Kit was introduced for *in vitro* diagnosis of expression level assessment. This immunohistochemical assay which recognizes the C terminus of claudin 18 is not specific for the isoform 18.2. However, the Anti-CLDN EPR19202 kit (Abcam, Cambridge, UK) is specific for a synthetic peptide within human claudin 18.2 amino acids 1-100, thus it can only detect this isoform. CLDN 18.2 histopathological staining status is important because it will validate patients for future therapy.

However, the cut-off seems to be the key point. Our meta-analysis focused on any percentage of positive staining and > 40% positive cells and showed no correlation with any of the clinicopathologic features, which strongly suggests that standard criteria are yet to be established. Some studies used IRS score or H-score for the definition of positive CLDN 18.2. Perhaps more studies focusing on a higher level of positive staining might obtain better results in relation to TNM stage, grading, as well as OS. This is confirmed by some trial studies which suggest that higher intensity (>75%) will result in better efficacy (longer OS) (20). On the same line of uniformizing the results, it should be mentioned that automated computer-aided image-analysis offers a more objective and reproducible way of quantifying any immunohistochemical staining, for example using parameters like signal area and integrated optical density. Moreover, the advent of multispectral microscopy has opened the avenue for true quantitative staining analysis at the tissue level, a multispectral filter allowing the camera to quantify only the spectral signature of the chromophore has been utilized to visualize the antibody without any interference from the tissue and any counterstaining (25).

Ethnicity represents a main factor in GC response to therapy. The percentage of positive patients varied in both European and Asian countries. While two studies from Germany showed rather similar results with 17 and 18%, Dottermuch et al. (15) had 42% of the patients positive for CLDN 18.2. Results are rather similar in Asia with two Korean studies displaying 15 and 29% positive results and a study from Japan with 87% positive cells. This might emphasize that race involvement in positive staining should be further pursued.

This is the first meta-analysis on CLDN 18.2 and its expression on GC patients. Even though it may represent a new addition for current therapies, our results show a low prevalence with 34.2% in 2,055 patients. The data so far suggest that targeted therapy for CLDN 18.2 could be effective if certain criteria will be established. Clinical trials might help providing more data about the expression of CLD18.2 in assessing claudiximab productivity.

Our results suggest that a new cut-off value for CLDN 18.2 positivity should be taken into account, and that computer generated analysis might be an option for further studies, as it may provide more accurate results. This was actually discussed by clinical trials which achieved better efficacy if higher expression levels were taken into account. Perhaps selecting only patients with high intensity levels and correlated with clinicopathologic data could provide more candidates to establish the therapy candidates.

Our study has some limitations due to the small number of included studies, but it pooled the outcomes for a large number of patients with international findings, recruiting both Caucasians and Asians.

CONCLUSION

Even though our results did not show any correlation between CLDN 18.2 staining and the patient's clinicopathologic features, we believe that more specific assays for staining and quantification, as well as a cut-off value for CLDN 18.2 level, might help solve this issue. Hopefully the available trials will shed more light on this new targeted therapy much needed for GC treatment.

DATA AVAILABILITY STATEMENT

The original contributions presented in the study are included in the article/supplementary material, further inquiries can be directed to the corresponding author.

AUTHOR CONTRIBUTIONS

BSU and DIG: conceptualization. BSU and AT-S: methodology. AT-S: software. C-VL, DP, IML, EM, and FB: formal analysis. BSU and VMS: data curation. BSU and AT-S: writing—original draft preparation. DP, DIG, and AS: writing-review and editing. All authors contributed to the article and approved the submitted version.

FUNDING

This work was supported by a grant from the Ministry of Research and Innovation, CNCS-UEFISCDI, project number PN-III-P4-ID-PCCF2016-0158 (THERRES), within PN III.

REFERENCES

1. Hsu A, Chudasama R, Almhanna K, Raufi A. Targeted therapies for gastroesophageal cancers. *Ann. Transl. Med.* (2020) 8:1104. doi: 10.21037/atm-20-3265
2. Chen Z, Li Y, Tan B, Zhao Q, Fan L, Li F, et al. Progress and current status of molecule-targeted therapy and drug resistance in gastric cancer. *Drugs Today*. (2020) 56:469–82. doi: 10.1358/dot.2020.56.7.3112071
3. Kyuno D, Yamaguchi H, Ito T, Kono T, Kimura Y, Imamura M, et al. Targeting tight junctions during epithelial to mesenchymal transition in human pancreatic cancer. *World J. Gastroenterol.* (2014) 20:10813–24. doi: 10.3748/wjg.v20.i31.10813
4. Ouban A. Claudin-1 role in colon cancer: an update and a review. *Histol. Histopathol.* (2018) 33:1013–9. doi: 10.14670/HH-11-980
5. Huang GW, Ding X, Chen SL, Zeng L. Expression of claudin 10 protein in hepatocellular carcinoma: impact on survival. *J. Cancer Res. Clin. Oncol.* (2011) 137:1213–8. doi: 10.1007/s00432-011-0987-z
6. Zhou Y, Xiang J, Bhandari A, Guan Y, Xia E, Zhou X, et al. CLDN10 is associated with papillary thyroid cancer progression. *J. Cancer*. (2018) 9:4712–7. doi: 10.7150/jca.28636
7. Li WT, Jeng YM, Yang CY. Claudin-18 as a marker for identifying the stomach and pancreatobiliary tract as the primary sites of metastatic adenocarcinoma. *Am. J. Surg. Pathol.* (2020) 44:1643–8. doi: 10.1097/PAS.0000000000001583
8. Bednarz-Misa I, Fortuna P, Diakowska D, Jamrozik N, Krystek-Korpacka M. Distinct local and systemic molecular signatures in the esophageal and gastric cancers: possible therapy targets and biomarkers for gastric cancer. *Int. J. Mol. Sci.* (2020) 21:4509. doi: 10.3390/ijms21124509
9. Zhang J, Dong R, Shen L. Evaluation and reflection on claudin 18.2 targeting therapy in advanced gastric cancer. *Chin. J. Cancer Res.* (2020) 32:263–70. doi: 10.21147/j.issn.1000-9604.2020.02.13
10. Moher D, Liberati A, Tetzlaff J, Altman DG, The PRISMA Group. Preferred reporting items for systematic reviews and meta-analyses: the PRISMA statement. *PLoS Med.* (2009) 6:e1000097. doi: 10.1371/journal.pmed.1000097
11. Higgins JP, Thompson SG, Deeks JJ, Altman DG. Measuring inconsistency in meta-analyses. *BMJ.* (2003) 327:557–60. doi: 10.1136/bmj.327.7414.557
12. Tierney JF, Stewart LA, Ghersi D, Burdett S, Sydes MR. Practical methods for incorporating summary time-to-event data into meta-analysis. *Trials.* (2007) 8:16. doi: 10.1186/1745-6215-8-16
13. Arnold A, Daum S, von Winterfeld M, Berg E, Hummel M, Rau B, et al. Prognostic impact of Claudin 18.2 in gastric and esophageal adenocarcinomas. *Clin. Transl. Oncol.* (2020) 22:2357–63. doi: 10.1007/s12094-020-02380-0
14. Baek JH, Park DJ, Kim GY, Cheon J, Kang BW, Cha HJ, et al. Clinical implications of Claudin18.2 expression in patients with gastric cancer. *Antican Res.* (2019) 39:6973–9. doi: 10.21873/anticanres.13919
15. Dottermush M, Kruger S, Behrens H-M, Halske C, Rocken C. Expression of the potential therapeutic target claudin-18.2 is frequently decreased in gastric cancer: results from a large Caucasian cohort study. *Virchows Arch.* (2019) 475:563–71. doi: 10.1007/s00428-019-02624-7
16. Hong JY, An JY, Lee J, Park SH, Park JO, Park YS, et al. Claudin 18.2 expression in various tumor types and its role as a potential target in advanced gastric cancer. *Transl. Cancer Res.* (2020) 9:3367–74. doi: 10.21037/tcr-19-1876
17. Moentenich V, Gebauer F, Comut E, Tuchscherer A, Bruns C, Schroeder W, et al. Claudin 18.2 expression in esophageal adenocarcinoma and its potential impact on future treatment strategies. *Oncol. Lett.* (2020) 19:3665–70. doi: 10.3892/ol.2020.11520

18. Rohde C, Yamaguchi R, Mukhina S, Sahin U, Itoh K, Tureci, O. Comparison of claudin 18.2 expression in primary tumors and lymph node metastases in Japanese patients with gastric adenocarcinoma. *Jpn. J. Clin. Oncol*. (2019) 9:870–6. doi: 10.1093/jjco/hyz068
19. Sahin U, Koslowski M, Dhaene K, Usener D, Brandenburg G, Seitz G, et al. Claudin-18 splice variant 2 is a pan-cancer target suitable for therapeutic antibody development. *Clin. Cancer Res*. (2008) 14:7624–34. doi: 10.1158/1078-0432.CCR-08-1547
20. Al-Batran S, Schuler M, Zvirbule Z, Manikhas G, Lordick F, Rusyn A, et al. FAST: an international, multicenter, randomized, phase II trial of epirubicin, oxaliplatin, and capecitabine (EOX) with or without IMAB362, a first-in-class anti-CLDN18.2 antibody, as first-line therapy in patients with advanced CLDN18.2+ gastric and gastroesophageal junction (GEJ) adenocarcinoma. *J. Clin. Oncol*. (2016) 34(18 Suppl.):LBA4001. doi: 10.1200/JCO.2016.34.15_suppl.LBA4001
21. Sahin U, Tureci Ö, Manikhas GM, Lordick F, Rusyn A, Vynnychenko I, et al. Zolbetuximab combined with EOX as first-line therapy in advanced CLDN18.2+ gastric (G) and gastroesophageal junction (GEJ) adenocarcinoma: updated results from the FAST trial. *J. Clin. Oncol*. (2019) 37:16. doi: 10.1200/JCO.2019.37.4_suppl.16
22. Coati I, Lotz G, Fanelli GN, Brignola S, Lanza C, Cappellesso R, et al. Claudin-18 expression in oesophagogastric adenocarcinomas: a tissue microarray study of 523 molecularly profiled cases. *Br. J. Cancer*. (2019) 121:257–63. doi: 10.1038/s41416-019-0508-4
23. Yamaguchi K, Shitara K, Al-Batran SE, Bang YJ, Catenacci D, Enzinger P, et al. SPOTLIGHT: comparison of zolbetuximab or placebo + mFOLFOX6 as first-line treatment in patients with claudin18.2+/HER2– locally advanced unresectable or metastatic gastric or gastroesophageal junction adenocarcinoma (GEJ): a randomized phase III study. *Ann. Oncol*. (2019) 30:966–7. doi: 10.1093/annonc/mdz422.074
24. Türeci O, Sahin U, Schulze-Bergkamen H, Zvirbule Z, Lordick F, Koeberle D, et al. A multicentre, phase IIa study of zolbetuximab as a single agent in patients with recurrent or refractory advanced adenocarcinoma of the stomach or lower oesophagus: the MONO study. *Ann. Oncol*. (2019) 30:1487–95. doi: 10.1093/annonc/mdz199
25. Ciurea RN, Rogoveanu I, Pirici D, Tartea G-C, Streba CT, Florescu C, et al. B2 adrenergic receptors and morphological changes of the enteric nervous system in colorectal adenocarcinoma. *World J. Gastroenterol*. (2017) 23:1250–61. doi: 10.3748/wjg.v23.i7.1250

Conflict of Interest: The authors declare that the research was conducted in the absence of any commercial or financial relationships that could be construed as a potential conflict of interest.

Copyright © 2021 Ungureanu, Lungulescu, Pirici, Turcu-Stiolica, Gheonea, Sacerdotianu, Liliac, Moraru, Bende and Saftoiu. This is an open-access article distributed under the terms of the Creative Commons Attribution License (CC BY). The use, distribution or reproduction in other forums is permitted, provided the original author(s) and the copyright owner(s) are credited and that the original publication in this journal is cited, in accordance with accepted academic practice. No use, distribution or reproduction is permitted which does not comply with these terms.

frontiers in Pharmacology

ORIGINAL RESEARCH
published: 08 April 2021
doi: 10.3389/fphar.2021.649267

Chemoresponse of de novo Acute Myeloid Leukemia to "7+3" Induction can Be Predicted by c-Myc-facilitated Cytogenetics

*Tzu-Hung Hsiao[1†], Ren Ching Wang[2,3†], Tsai-Jung Lu[1], Chien-Hung Shih[1], Yu-Chen Su[4], Jia-Rong Tsai[4], Pei-Pei Jhan[1], Cai-Sian Lia[1], Han-Ni Chuang[1], Kuang-Hsi Chang[5,6,7] and Chieh-Lin Teng[4,8,9]**

[1]Department of Medical Research, Taichung Veterans General Hospital, Taichung, Taiwan, [2]Department of Pathology, Taichung Veterans General Hospital, Taichung, Taiwan, [3]Department of Nursing, College of Nursing, Hungkuang University, Taichung, Taiwan, [4]Division of Hematology/Medical Oncology, Department of Medicine, Taichung Veterans General Hospital, Taichung, Taiwan, [5]Department of Medical Research, Tungs' Taichung Metroharbor Hospital, Taichung, Taiwan, [6]Graduate Institute of Biomedical Sciences, China Medical University, Taichung, Taiwan, [7]General Education Center, Jen-The Junior College of Medicine, Nursing and Management, Miaoli, Taiwan, [8]Department of Life Science, Tunghai University, Taichung, Taiwan, [9]School of Medicine, Chung Shan Medical University, Taichung, Taiwan

OPEN ACCESS

Edited by:
Claudia Cerella, Fondation de Recherche Cancer et Sang, Luxembourg

Reviewed by:
Seongseok Yun, Moffitt Cancer Center, United States
Wei Cui, University of Kansas Medical Center, United States

***Correspondence:**
Chieh-Lin Teng
drteng@vghtc.gov.tw

[†]*These authors have contributed equally to this work*

Specialty section:
This article was submitted to Pharmacology of Anti-Cancer Drugs, a section of the journal Frontiers in Pharmacology

Received: *04 January 2021*
Accepted: *01 March 2021*
Published: *08 April 2021*

Citation:
Hsiao T-H, Wang RC, Lu T-J, Shih C-H, Su Y-C, Tsai J-R, Jhan P-P, Lia C-S, Chuang H-N, Chang K-H and Teng C-L (2021) Chemoresponse of de novo Acute Myeloid Leukemia to "7+3" Induction can Be Predicted by c-Myc-facilitated Cytogenetics. Front. Pharmacol. 12:649267. doi: 10.3389/fphar.2021.649267

Background: Identifying patients with *de novo* acute myeloid leukemia (AML) who will probably respond to the "7 + 3" induction regimen remains an unsolved clinical challenge. This study aimed to identify whether c-Myc could facilitate cytogenetics to predict a "7 + 3" induction chemoresponse in *de novo* AML.

Methods: We stratified 75 untreated patients (24 and 51 from prospective and retrospective cohorts, respectively) with *de novo* AML who completed "7 + 3" induction into groups with and without complete remission (CR). We then compared Myc-associated molecular signatures between the groups in the prospective cohort after gene set enrichment analysis. The expression of c-Myc protein was assessed by immunohistochemical staining. We defined high c-Myc-immunopositivity as > 40% of bone marrow myeloblasts being c-Myc (+).

Results: Significantly more Myc gene expression was found in patients who did not achieve CR by "7 + 3" induction than those who did (2439.92 ± 1868.94 vs. 951.60 ± 780.68; $p = 0.047$). Expression of the Myc gene and c-Myc protein were positively correlated ($r = 0.495$; $p = 0.014$). Although the non-CR group did not express more c-Myc protein than the CR group (37.81 ± 25.13% vs. 29.04 ± 19.75%; $p = 0.151$), c-Myc-immunopositivity could be a surrogate to predict the "7 + 3" induction chemoresponse (specificity: 81.63%). More importantly, c-Myc-immunopositivity facilitated cytogenetics to predict a "7 + 3" induction chemoresponse by increasing specificity from 91.30 to 95.92%.

Conclusion: The "7 + 3" induction remains the standard of care for *de novo* AML patients, especially for those without a high c-Myc-immunopositivity and high-risk cytogenetics. However, different regimens might be considered for patients with high c-Myc-immunopositivity or high-risk cytogenetics.

Keywords: induction chemotherapy, "7+3", myc (c-Myc), acute myeloid leukemia, chemoresponse

INTRODUCTION

With an incidence of 1.3 per 100,000 people, acute myeloid leukemia (AML) is the most common type of leukemia in adults (De Kouchkovsky and Abdul-Hay, 2016). Characterized by clonal expansion of immature myeloid blasts due to abnormal proliferation and differentiation of hematopoietic stem cells, ≥ 20% of nucleated cells from either peripheral blood or bone marrow being myeloblasts meet the World Health Organization AML diagnostic criteria (Vardiman et al., 2009). The current AML treatment flow includes the achievement of complete remission (CR) via induction chemotherapy followed by consolidation chemotherapy. Allogeneic hematopoietic stem cell transplantation (allo-HSCT) further improves the overall survival (OS) of patients with high-risk cytogenetics or genetic mutations, mainly when they are in CR (Burnett et al., 2011). Nevertheless, CR is the most crucial step toward curative intention in AML treatment.

Currently, the cytarabine 100 mg/m^2 for 7 days; idarubicin 12 mg/m^2 for 3 days ("7 + 3") regimen is the standard of care among various types of induction regimens against AML. With relatively tolerable toxicities, this induction therapy can achieve a 70% CR rate in untreated *de novo* AML (Burnett et al., 2011). However, the outcomes for patients who do not achieve CR with "7 + 3" induction chemotherapy are exceptionally dismal. Several studies have focused on the possible mechanisms of induction failure in AML. From the perspective of cell functions, cell quiescence, DNA damage repair, and leukemic stem cell-related leukemogenesis might be associated with chemoresistance in AML (Abdullah and Chow, 2013; Vidal et al., 2014; Walter et al., 2015; Ng et al., 2016). In terms of clinical features, more advanced age, leukocytosis, and high-risk cytogenetics could be risk factors of "7 + 3" induction failure (Ho and Becker, 2013). However, the precise identification of patients with *de novo* AML who will probably respond to the "7 + 3" induction regimen remains an unresolved clinical challenge.

The Myc family consists of the nuclear transcription factors c-Myc, n-Myc, and i-Myc. Among the various Myc proteins, c-Myc plays a crucial role in most oncogenic processes, orchestrating proliferation, apoptosis, differentiation, and metabolism (Chen et al., 2018). Moreover, c-Myc is associated with chemoresistance in various cancers (Lee et al., 2017; Elbadawy et al., 2019). We previously revealed that Myc signature gene expression was higher in patients with *de novo* AML who failed to achieve CR by "7 + 3" induction than patients did (Chiu et al., 2019). Consequently, Myc could be a biomarker, facilitating chemoresistance prediction in *de novo* AML patients undergoing "7 + 3" induction therapy. However, studies of this clinical application remain limited. Therefore, we aimed to determine the value of Myc as part of a timely and practical approach to predict a chemoresponse to "7 + 3" induction.

The present study aimed to validate the role of Myc in chemoresistance to the "7 + 3" regimen in *de novo* AML. We also correlated expression of the Myc gene to that of c-Myc protein in 24 prospective patients with *de novo* AML who completed "7 + 3" or "7 + 3"-like induction chemotherapy. We then investigated whether c-Myc protein could facilitate cytogenetics to precisely predict a chemoresponse to "7 + 3" induction in a timely manner among patients with AML.

MATERIALS AND METHODS

Patients

Between 2017 and 2020, we prospectively screened consecutive patients with untreated *de novo* non-promyelocytic AML (age ≤75 years; Eastern Cooperative Oncology Group Performance Status ≤2) who had completed the first cycle of cytarabine (100 mg/m^2) for 7 days and idarubicin (12 mg/m^2 for 3 days; "7 + 3") or "7 + 3"-like induction chemotherapy. No other chemotherapeutic or novel agents were added to the "7 + 3" induction regimen regardless of the genetic mutation status of the patients. A total of 31 patients met these criteria. Seven patients were excluded from the study because no qualified RNA was extracted from the bone marrow leukemic cells for RNA sequencing at initial diagnosis. Finally, 24 patients were assigned to a prospective cohort (n = 24) and stratified into groups with (n = 15) and without (n = 9) CR according to their responses to the first cycle of "7 + 3" induction therapy.

To expand the number of study participants, we used data from a retrospective cohort comprising 52 patients with *de novo* AML who had completed "7 + 3" induction therapy (Chiu et al., 2019). One patient was excluded because of a disqualified bone marrow specimen that was ineligible for c-Myc immunohistochemical (IHC) staining. Finally, 51 patients were assigned to a retrospective cohort (n = 51). A combined cohort (n = 75) comprising prospective (n = 24) and retrospective (n = 51) patients was established for c-Myc-associated analyses. To avoid pathogenic background heterogeneity, this study did not include patients with therapy-related AML or AML with myelodysplasia-related changes. This study was approved by the Institutional Review Board of Taichung Veterans General Hospital and was in accordance with the Declaration of Helsinki (2013). All patients in the prospective cohort provided written informed consent to participate in the study before enrollment. The Institutional Review Board waived the need for informed consent for the retrospective cohort.

RNA Sequencing

We prepared mononuclear cells from bone marrow aspirate specimens of the prospective cohort using BD Vacutainer® CPT™ Mononuclear Cell Preparation Tube (Becton Dickinson and Co., Franklin Lakes, NJ, United States) as described by the manufacturer. Total RNA was extracted from mononuclear cells using TRIzol (Thermo Fisher Scientific Inc., Waltham, MA, United States) then purified using RNeasy Mini Kits and dnase I (Qiagen, Valencia, CA, United States). After enrichment using oligo (dT)-labelled magnetic beads, mRNA was fragmented, converted into cDNA, which was ligated to adaptors, and amplified. Quality-checked library products were 75-bp paired-end sequenced using a NextSeq 500 sequencer (Illumina Inc., San Diego, CA, United States). The original RNA-sequencing data from the prospective cohort has been deposited in the GEO repository (https://www.ncbi.nlm.nih.gov/geo/query/acc.cgi?acc=GSE164894).

After removing low-quality raw sequencing reads containing adaptor sequences or reads with high content of unknown bases, clean reads were aligned to the Ensembl GRCh38 human reference genome using HISAT2 (Kim et al., 2019). We used featureCounts software to count the mapped reads against Ensembl annotated genes (ENSG IDs) (Liao et al., 2014). Gene-level read counts were then normalized using DESeq2 and differential expression between AML patients with and without CR was assessed (Love et al., 2014).

Myc Gene Set Enrichment Analysis and Myc Gene Quantitation

We identified Myc-associated molecular signatures curated in the Molecular Signatures Database (MSigDB) collections (Liberzon et al., 2011) using gene set enrichment analysis (GSEA) software. For each Myc-associated signature gene panel, GSEA reported leading-edge component genes, accounting for enrichment. We further compared Myc gene expression between the groups with and without CR in the prospective cohort using DESeq2 normalization.

Immunohistochemical Staining for c-Myc Expression

Formalin-fixed paraffin-embedded tissue sections from bone marrow biopsies were stained for c-MYC (clone EP121, BioSB) on a Ventana BenchMark XT slide preparation system (Ventana Medical Systems, Tucson, AZ, United States). We decalcified bone marrow specimens with acid before October 2017. Thereafter, bone marrow biopsy samples were routinely decalcified with EDTA. An experienced hematological pathologist who was blinded to the genetic test results scored portions of c-Myc (+) myeloblasts from 0 to 100% to quantify c-Myc protein expression. We defined high c-Myc-immunopositivity when >40% of myeloblasts in the bone marrow were c-Myc (+) by testing the sensitivity and specificity according to different cutoffs from the combined cohort (**Supplemental Table S1**). We also examined c-Myc-immunopositivity in 20 normal bone marrow biopsy specimens to avoid interference by c-Myc overexpression in normal hematopoietic cells. All 20 bone marrow specimens contained <5% c-Myc (+) hematopoietic cells.

Statistical Analysis

Continuous and categorical variables between the CR and non-CR groups were compared using Student t-tests and the Chi-squared tests, respectively. Numerical data are presented as means ± standard deviation. We applied logistic proportional regression to identify factors for high c-Myc-immunopositivity quantified according to odds ratios (OR) and 95% confidence intervals (CI). Values were considered statistically significant at $p < 0.05$.

RESULTS

Patient Characteristics

Table 1 shows a demographic comparison between the groups with and without CR from the prospective cohort (n = 24). Sex ($p = 0.669$), age ($p = 0.614$), leukocyte count at diagnosis ($p = 0.335$), and cytogenetic risk ($p = 0.057$) did not significant differ between the groups. Proportions of FLT3 ITD ($p = 0.615$) and NPM1 ($p = 0.615$) gene mutations were also comparable between the groups. We also compared demographic data between the prospective and retrospective cohorts. These two cohorts had comparable demographic characteristics. This result revealed the absence of significant clinical heterogeneity between the prospective and retrospective cohorts (**Supplemental Table S2**).

Patients with AML Without CR Under "7 + 3" Induction Therapy had More Myc Gene Expression

To validate our previous findings that Myc overexpression is associated with "7 + 3" induction chemoresistance in AML (Chiu et al., 2019), we compared Myc molecular signature gene expression between the groups with and without CR in the prospective cohort. Using three different Myc molecular signatures from MSigDB selected based on our best knowledge (Schlosser et al., 2005; Sansom et al., 2007), significantly more Myc molecular signature gene expression was found in the group that did not achieve CR than the group that did (**Figure 1A,B,C**).

After confirming that patients with untreated *de novo* AML who did not achieve CR with the "7 + 3″ induction therapy expressed more of the Myc signature gene, we further investigated whether Myc gene expression differ between groups in the prospective cohort. The results showed that mean (±SD) amounts of Myc gene expression in the groups without and with CR were 2439.92 ± 1868.94 vs. 951.60 ± 780.68, $p = 0.047$; **Figure 2**).

C-Myc Protein Expression Comparison Between the CR and non-CR Groups

We aimed to develop a more timely and feasible approach to predict a chemoresponse of *de novo* AML to "7 + 3" based on our findings that patients with AML who did not achieve CR had more Myc gene expression. We assessed bone marrow myeloblasts for c-Myc protein by immunohistochemical (IHC) staining. The average ratio of c-Myc (+) cells in bone marrow myeloblasts in the combined cohort was 32.08% (<1% to >90%; **Figure 3A,B**). Furthermore, Myc gene and c-Myc protein expression significantly correlated in the prospective cohort ($r = 0.495$; $p = 0.014$; **Figure 3C**). However, this correlation did not translate into a meaningful difference in c-Myc protein expression between the groups with and without CR, although the ratio of c-Myc (+) myeloblasts was higher the group without than with CR (37.81 ± 25.13% vs. 29.04 ± 19.75%, $p = 0.151$; **Figure 3D**).

Factors Associated With c-Myc Protein Expression

To identify potential factors that might interfere with the c-Myc expression in *de novo* AML, we compared the demographic and

TABLE 1 | Characteristics of patients in the prospective cohort.

Variable	All patients (n = 24)	Non-CR group (n = 9)	CR group (n = 15)	p
Sex (n, %)				0.669[a]
Male	17 (70.83)	7 (77.78)	10 (66.67)	
Female	7 (29.17)	2 (22.22)	5 (33.33)	
Age, y (mean ± SD)	51.75 ± 13.57	49.89 ± 15.93	52.87 ± 12.42	0.614[b]
Leukocytes, 10^3/μL (mean ± SD)	51.35 ± 51.08	64.47 ± 55.08	42.92 ± 48.51	0.335[b]
Cytogenetics (n, %)				0.057[a]
Favorable	3 (12.50)	0 (0)	3 (20.00)	
Intermediate	14 (58.33)	4 (44.44)	10 (66.67)	
Unfavorable	7 (29.17)	5 (55.56)	2 (13.33)	
Molecular risk (n, %)				
FLT3 ITD mutation	4 (16.67)	2 (22.22)	2 (13.33)	0.615[a]
NPM1 mutation	5 (20.83)	1 (11.11)	4 (26.67)	0.615[a]

[a]*Chi-squared.*
[b]t-*tests. All data are shown as means ± SD or n (%).*
CR, complete response; SD, standard deviation.

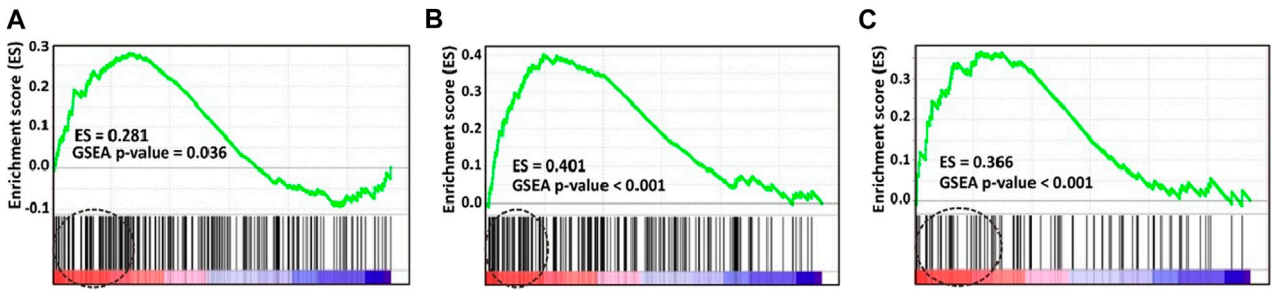

FIGURE 1 | Gene set enrichment analysis (GSEA) plots of three selected molecular signatures for Myc. Enrichment score (ES) generated by Myc signatures were **(A)** 0.281 (p = 0.036) **(B)** 0.401 (p < 0.001), and **(C)** 0.366 (p < 0.001). Molecular signature gene expression of Myc is significantly higher in patients without, than with CR. CR, complete remission.

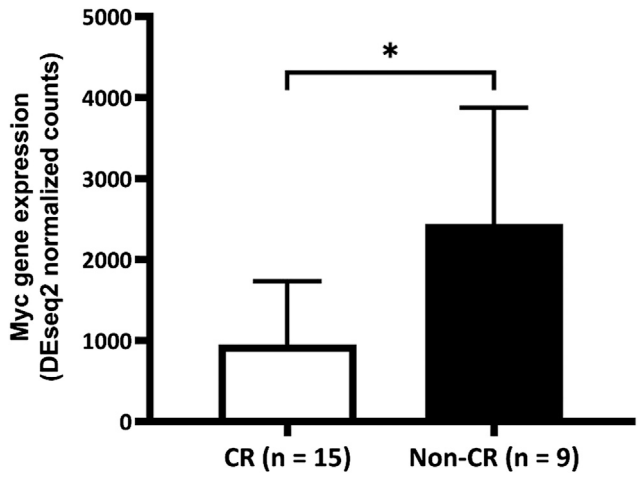

FIGURE 2 | Comparison of Myc gene expression between the complete remission (CR) and non-CR groups. Expression of Myc gene is significantly higher in the group without than with CR (2439.92 ± 1868.94 vs. 951.60 ± 780.68, p = 0.047). CR, complete remission.

laboratory features among patients with (n = 19) and without (n = 56) high c-Myc-immunopositivity. Sex (p = 0.849), cytogenetic (p = 0.193), and molecular (p = 0.307 for FLT3 ITD mutation; p = 0.751 for NPM1 mutation) risks did not significantly differ between these groups. However, AML patients high c-Myc-immunopositivity were younger (41.58 ± 14.88 vs. 44.37 ± 51.29 years; p = 0.031) and had more leukocytosis (90.10 ± 61.26 vs. 44.37 ± 51.29 (10^3/μL); p = 0.002) than those without high c-Myc-immunopositivity (**Table 2**). Notably, age, sex, leukocytes, cohort, high-risk cytogenetics, FLT3 ITD, and NPM1 mutations were not significantly associated with high c-Myc-immunopositivity in univariate and multivariate analyses, suggesting that c-Myc protein expression is independent of most clinical features of AML (**Table 3**).

High-Risk Cytogenetics and c-Myc-Immunopositivity as Biomarkers for "7 + 3" Induction Response Prediction

We examined whether c-Myc could be a potential surrogate marker to predict an induction response of AML to "7 + 3".

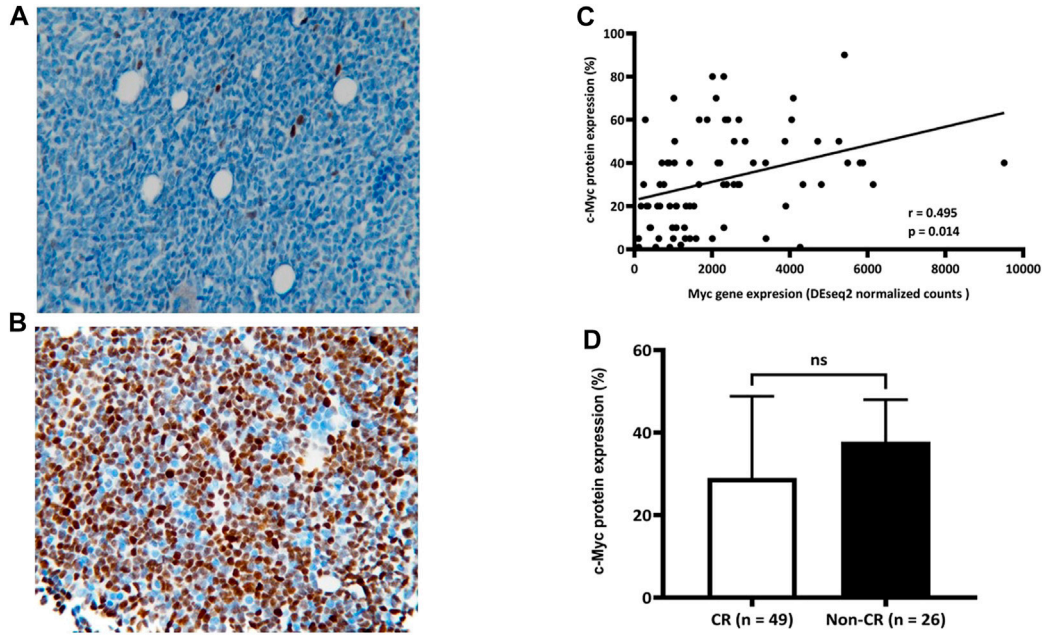

FIGURE 3 | Correlation between expression of c-Myc protein and Myc gene. Average ratio of c-Myc (+) bone marrow myeloblasts in combined cohort is 32.08% (range, < 1% **(A)** to >90% **(B)**; n = 75). Significant correlation **(C)** between c-Myc protein and Myc gene expression (r = 0.495; p = 0.014) **(D)** Ratios of c-Myc (+) bone marrow myeloblasts between groups with and without CR (29.04 ± 19.75 and 37.81 ± 25.13, respectively; p = 0.151). CR, complete remission.

TABLE 2 | Comparison of characteristics between patients with and without high[a] c-Myc-immunopositivity in combined cohort (n = 75).

Variable	High c-Myc (n = 19)	Without high c-Myc (n = 56)	P
Sex (n, %)			0.849[b]
Male	12 (63.16)	32 (57.14)	
Female	7 (36.84)	24 (42.86)	
Age, y (mean ± SD)	41.58 ± 14.88	49.84 ± 13.91	0.031[c]
Leukocytes, $10^3/\mu L$ (mean ± SD)	90.10 ± 61.26	44.37 ± 51.29	0.002[c]
Cytogenetics (n, %)			0.193[b]
Favorable	2 (10.53)	6 (10.71)	
Intermediate	10 (52.63)	33 (58.93)	
Unfavorable	7 (36.84)	10 (17.86)	
Undetermined	0 (0)	7 (12.50)	
Molecular risk (n, %)			
FLT3 ITD mutation	5 (26.32)	7 (12.50)	0.307[b]
NPM1 mutation	5 (26.32)	10 (17.86)	0.751[b]
Undetermined	2 (10.53)	15 (26.79)	0.209[b]

SD: standard deviation.
[a]*> 40% of myeloblasts in bone marrow are c-Myc (+).*
[b]*Chi-squared.*
[c]*t-tests.*

Because the presence of high-risk cytogenetics was significantly associated with "7 + 3" induction failure in the present cohort (data not shown), we also compared the predictive value of "7 + 3" induction response between high-risk cytogenetics and high c-Myc-immunopositivity. The results showed that the sensitivity of high c-Myc-immunopositivity and high-risk cytogenetics was respectively, 38.46 and 56.52%, and the specificity was 81.63 and 91.30%, respectively. High-risk cytogenetics was more accurate than high c-Myc-immunopositivity (79.71 vs. 66.67%). Notably, the specificity of high c-Myc-immunopositivity combined with high-risk cytogenetics reached 95.92%, suggesting that c-Myc could facilitate cytogenetics to identify AML patients who will respond to "7 + 3" induction chemotherapy more precisely than cytogenetics alone (**Table 4**).

TABLE 3 | Factors associated with high[a] c-Myc-immunopositivity in the combined cohort (n = 75).

	Univariate analysis			Multivariate analysis		
	OR	95% CI	P	OR	95% CI	p
Age (y)	1.00	0.97–1.03	0.979	1.01	0.96–1.05	0.769
Sex (female vs. male)	0.50	0.18–1.37	0.179	0.86	0.24–3.13	0.818
Leukocytes at diagnosis, $10^3/\mu L$	1.00	1.00–1.01	0.442	1.00	1.00–1.01	0.851
Prospective vs. retrospective cohort	1.20	0.44–3.30	0.724	1.93	0.54–6.93	0.311
High-risk cytogenetics (yes vs. no)	2.78	0.95–8.11	0.062	3.16	0.74–13.59	0.122
FLT3 ITD mutation (yes vs. no)	1.14	0.30–4.43	0.847	1.46	0.30–7.15	0.642
NPM1 mutation (yes vs. no)	0.45	0.11–1.85	0.268	0.42	0.08–2.12	0.295

[a]*> 40% of myeloblasts in bone marrow are c-Myc (+). CI, confidence interval; OR, odds ratio.*

TABLE 4 | Prediction of response to "7 + 3" induction based on high[a] c-Myc-immunopositivity and high-risk cytogenetics.

		Total (n)	Non-CR (n)	CR (n)	Sensitivity (%)	Specificity (%)	PPV (%)	NPV (%)	Accuracy (%)
High c-Myc-immunopositivity	Yes	19	10	9	38.46	81.63	52.63	71.43	66.67
	No	56	16	40					
High-risk cytogenetics	Yes	17	13	4	56.52	91.30	76.47	80.77	79.71
	No	52	10	42					
High c-Myc-immunopositivity + high-risk cytogenetics	Yes	7	5	2	19.23	95.92	71.43	69.12	69.33
	No	68	21	47					

[a]*> 40% of myeloblasts in bone marrow are c-Myc (+). CR, complete remission; NPV, negative predictive value; PPV, positive predictive value.*

DISCUSSION

We validated our previous finding of a higher Myc signature gene expression in patients with *de novo* AML who do not achieve CR under "7 + 3" induction therapy compared with those who achieve CR. The present findings also found higher Myc gene expression in patients without, than with CR. Furthermore, Myc gene expression positively correlated with ratios (%) of c-Myc (+) bone marrow myeloblasts. Therefore, the ratio (%) of c-Myc (+) bone marrow myeloblasts could be a feasible and timely approach with which to predict a chemoresponse of *de novo* AML to "7 + 3" induction. However, the ratio (%) of c-Myc (+) myeloblasts was not significantly higher in patients without, than with CR. Nonetheless, having >40% c-Myc (+) myeloblasts and high-risk cytogenetics could predict a response to "7 + 3" induction with 81.63 and 91.30% of specificity. Notably, adding high c-Myc-immunopositivity to the high-risk cytogenetics further increased the specificity to 95.92%. This result suggested that c-Myc expression could facilitate cytogenetics to more precisely identify AML patients who are likely to respond to "7 + 3" induction chemotherapy.

Various potential mechanisms of Myc-related chemoresistance in solid cancers have been suggested. Chemoresistance associated with TCRP1- can be transcriptionally regulated by c-Myc in tongue and lung cancers (Jia et al., 2017). In addition, Myc and MCL1 might cooperatively promote chemotherapy-resistant breast cancer stem cells by regulating mitochondrial oxidative phosphorylation (Lee et al., 2017). Moreover, the c-Myc/miR-27b-3p/ATG10 axis regulates chemoresistance in colorectal cancer (Sun et al., 2020). Among hematological malignancies, crosstalk between Myc and p53 proteins might result in an inferior outcome of B-cell lymphomas (Yu et al., 2019). Increased Myc copy numbers comprise a negative prognostic factor for diffuse large B cell lymphoma (Schieppati et al., 2020). The expression of NKG2D ligands is regulated by c-Myc in AML and AML cell lines rendered resistant to cytarabine express more of the NKG2D ligands ULBP1/2/3 (Nanbakhsh et al., 2014). Consequently, NKG2DL upregulation rendered the cell lines more sensitive to NK cell-mediated lysis.

Based on the possible mechanisms responsible for c-Myc-associated chemoresistance in AML, determining whether c-Myc protein can be a feasible and timely clinical parameter to predict induction response remains a clinical challenge. A bone marrow content of ≥5% Myc (+) myeloblasts is an independent poor prognostic factor for AML with myelodysplasia-related changes (Yun et al., 2019). Moreover, Myc immunopositivity >6% is significantly associated with inferior overall, event-free, and relapse-free survival (Ohanian et al., 2019). These results suggest that Myc-immunopositivity is a critical prognostic factor in untreated AML, particularly in patients at higher risk for relapse. Although c-Myc-immunopositivity > 40% was not more accurate than high-risk cytogenetics in identifying "7 + 3" responders, the present findings indicated that c-Myc-immunopositivity could enhance predictive specificity when combined with high-risk cytogenetics. We selected >40% c-Myc (+) myeloblasts as the cutoff in the present study by testing the sensitivity and specificity according to different ratios (%) of c-Myc (+) myeloblasts. However, the optimal cutoff of c-Myc-immunopositivity still needs further

validation. Notably, with a range from 0 to 100%, the average ratios of c-Myc-immunopositive myeloblasts were similar between the cohorts in the present study (32.08%) and that of Ohanian et al. (32%) (Ohanian et al., 2019), which indirectly validated our results.

The lack of a significant difference in c-Myc protein expression between the groups with and without CR remains unresolved. We did find a statistical correlation between Myc gene expression and the ratios (%) of c-Myc (+) myeloblasts ($r = 0.495$; $p = 0.014$). Ratios (%) of c-Myc (+) myeloblasts tended to be higher in the group without, than with CR (37.81 ± 25.13 vs. 29.04 ± 19.75), but the difference did not reach statistical significance. An insufficient number of patients might be the primary reason for this. The rapid degradation of Myc by the ubiquitin-proteasome system (Gregory and Hann, 2000) could be another explanation. In addition, many proteins are involved in the regulation of Myc protein stability and activity (Farrell and Sears, 2014), which might further interfere with c-Myc expression in myeloblasts in bone marrow specimens. The features of Myc have been further reflected in its potential clinical utilization. Direct c-Myc protein targeting does not seem to be an effective therapeutic approach. Conversely, targeting Myc transcription, disrupting Myc/Max dimerization, causing an interference in Myc protein stability, inhibiting Myc-associated cell cycle, and targeting metabolism through Myc target genes and cofactors are current anti-Myc strategies in cancer treatment (McAnulty and DiFeo, 2020).

The small patient cohort is a significant limitation of the present study. Because of this, we could not provide a validated model to predict a chemoresponse to "7 + 3" induction therapy. We are currently conducting a prospective observational study of more patients to develop a c-Myc protein-associated prediction model to overcome this clinical hurdle.

In summary, we showed that Myc and its related genes are responsible for chemoresistance in untreated *de novo* AML. The combination of cytogenetics and c-Myc-immunopositivity could be a feasible and timely approach with which to identify patients with *de novo* AML who are likely to achieve CR with "7 + 3" induction therapy. This therapy remains the standard of care for patients with *de novo* AML, especially for those without high c-Myc-immunopositivity and high-risk cytogenetics. However, other chemotherapeutic regimens (Fleischhack et al., 1998) or venetoclax-based induction (DiNardo et al., 2020) might be a solution for patients with high c-Myc-immunopositivity or high-risk cytogenetics. Prospective studies with more patients are needed to determine whether choosing different induction regimens based on this strategy can significantly improve the CR rates and overall survival among patients with recently diagnosed *de novo* AML.

DATA AVAILABILITY STATEMENT

The datasets presented in this study can be found in online repositories. The names of the repository/repositories and accession number(s) can be found below: https://www.ncbi.nlm.nih.gov/geo/, GSE164894.

ETHICS STATEMENT

The studies involving human participants were reviewed and approved by the IRB of Taichung Veterans General Hospital. The patients/participants provided their written informed consent to participate in this study.

AUTHOR CONTRIBUTIONS

TH designed the study and critically reviewed the manuscript. RW performed the research, analyzed the data. TL performed the research. CS performed the research and critically reviewed the manuscript. YS analyzed the data. JT analyzed the data. PJ performed the research. CL performed the research. HC performed the research. KC performed the statistics. CT designed the study, interpreted the data and wrote the paper. All authors gave final approval of the manuscript.

FUNDING

This study was partially supported by grants from TCVGH-1093703C and TCVGH-YM1100107.

SUPPLEMENTARY MATERIAL

The Supplementary Material for this article can be found online at: https://www.frontiersin.org/articles/10.3389/fphar.2021.649267/full#supplementary-material.

REFERENCES

Abdullah, L. N., and Chow, E. K. (2013). Mechanisms of chemoresistance in cancer stem cells. *Clin. Transl Med.* 2 (1), 3. doi:10.1186/2001-1326-2-3

Burnett, A., Wetzler, M., and Löwenberg, B. (2011). Therapeutic advances in acute myeloid leukemia. *J Clin Oncol.* 29 (5), 487–494. doi:10.1200/jco.2010.30.1820

Chen, H., Liu, H., and Qing, G. (2018). Targeting oncogenic Myc as a strategy for cancer treatment. *Signal. Transduct Target. Ther.* 3 (1), 5. doi:10.1038/s41392-018-0008-7

Chiu, Y. C., Hsiao, T. H., Tsai, J. R., Wang, L. J., Ho, T. C., Hsu, S. L., et al. (2019). Integrating resistance functions to predict response to induction chemotherapy in de novo acute myeloid leukemia. *Eur. J. Haematol.* 103 (4), 417–425. doi:10.1111/ejh.13301

De Kouchkovsky, I., and Abdul-Hay, M. (2016). 'Acute myeloid leukemia: a comprehensive review and 2016 update'. *Blood Cancer J.* 6 (7), e441. doi:10.1038/bcj.2016.50

Dinardo, C. D., Jonas, B. A., Pullarkat, V., Thirman, M. J., Garcia, J. S., Wei, A. H., et al. (2020). Azacitidine and venetoclax in previously untreated acute myeloid leukemia. *N. Engl. J. Med.* 383, 617–629. doi:10.1056/nejmoa2012971

Elbadawy, M., Usui, T., Yamawaki, H., and Sasaki, K. (2019). Emerging roles of C-Myc in cancer stem cell-related signaling and resistance to cancer chemotherapy: a potential therapeutic target against colorectal cancer. *Int. J. Mol. Sci.* 20 (9), 2340. doi:10.3390/ijms20092340

Farrell, A. S., and Sears, R. C. (2014). MYC degradation. *Cold Spring Harb Perspect. Med.* 4 (3), a014365. doi:10.1101/cshperspect.a014365

Fleischhack, G., Hasan, C., Graf, N., Mann, G., and Bode, U. (1998). IDA-FLAG (idarubicin, fludarabine, cytarabine, G-CSF), an effective remission-induction therapy for poor-prognosis AML of childhood prior to allogeneic or autologous bone marrow transplantation: experiences of a phase II trial. *Br. J. Haematol.* 102 (3), 647–655. doi:10.1046/j.1365-2141.1998.00836.x

Gregory, M. A., and Hann, S. R. (2000). c-Myc proteolysis by the ubiquitin-proteasome pathway: stabilization of c-Myc in Burkitt's lymphoma cells. *Mol. Cel. Biol.* 20 (7), 2423–2435. doi:10.1128/mcb.20.7.2423-2435.2000

Ho, T.-C., and Becker, M. W. (2013). Defining patient-specific risk in acute myeloid leukemia. *J. Clin. Oncol.* 31 (31), 3857–3859. doi:10.1200/jco.2013.51.4307

Jia, X., Zhang, Z., Luo, K., Zheng, G., Lu, M., Song, Y., et al. (2017). TCRP1 transcriptionally regulated by c-Myc confers cancer chemoresistance in tongue and lung cancer. *Sci. Rep.* 7 (1), 3744. doi:10.1038/s41598-017-03763-0

Kim, D., Paggi, J. M., Park, C., Bennett, C., and Salzberg, S. L. (2019). Graph-based genome alignment and genotyping with HISAT2 and HISAT-genotype. *Nat. Biotechnol.* 37 (8), 907–915. doi:10.1038/s41587-019-0201-4

Lee, K.-M., Giltnane, J. M., Balko, J. M., Schwarz, L. J., Guerrero-Zotano, A. L., Hutchinson, K. E., et al. (2017). MYC and MCL1 cooperatively promote chemotherapy-resistant breast cancer stem cells via regulation of mitochondrial oxidative phosphorylation. *Cel Metab.* 26 (4), 633–647.e7. doi:10.1016/j.cmet.2017.09.009

Liao, Y., Smyth, G. K., and Shi, W. (2014). featureCounts: an efficient general purpose program for assigning sequence reads to genomic features. *Bioinformatics* 30 (7), 923–930. doi:10.1093/bioinformatics/btt656

Liberzon, A., Subramanian, A., Pinchback, R., Thorvaldsdottir, H., Tamayo, P., and Mesirov, J. P. (2011). Molecular signatures database (MSigDB) 3.0. *Bioinformatics* 27 (12), 1739–1740. doi:10.1093/bioinformatics/btr260

Love, M. I., Huber, W., and Anders, S. (2014). Moderated estimation of fold change and dispersion for RNA-seq data with DESeq2. *Genome Biol.* 15 (12), 550. doi:10.1186/s13059-014-0550-8

Mcanulty, J., and Difeo, A. (2020). The molecular 'myc-anisms' behind myc-driven tumorigenesis and the relevant myc-directed therapeutics. *Int. J. Mol. Sci.* 21 (24), 9486. doi:10.3390/ijms21249486

Nanbakhsh, A., Pochon, C., Mallavialle, A., Amsellem, S., Bourhis, J. H., and Chouaib, S. (2014). c-Myc regulates expression of NKG2D ligands ULBP1/2/3 in AML and modulates their susceptibility to NK-mediated lysis. *Blood* 123 (23), 3585–3595. doi:10.1182/blood-2013-11-536219

Ng, S. W. K., Mitchell, A., Kennedy, J. A., Chen, W. C., Mcleod, J., Ibrahimova, N., et al. (2016). A 17-gene stemness score for rapid determination of risk in acute leukaemia. *Nature* 540 (7633), 433–437. doi:10.1038/nature20598

Ohanian, M., Rozovski, U., Kanagal-Shamanna, R., Abruzzo, L. V., Loghavi, S., Kadia, T., et al. (2019). MYC protein expression is an important prognostic factor in acute myeloid leukemia. *Leuk. Lymphoma* 60 (1), 37–48. doi:10.1080/10428194.2018.1464158

Sansom, O. J., Meniel, V. S., Muncan, V., Phesse, T. J., Wilkins, J. A., Reed, K. R., et al. (2007). Myc deletion rescues Apc deficiency in the small intestine. *Nature* 446 (7136), 676–679. doi:10.1038/nature05674

Schieppati, F., Balzarini, P., Fisogni, S., Re, A., Pagani, C., Bianchetti, N., et al. (2020). An increase in MYC copy number has a progressive negative prognostic impact in patients with diffuse large B-cell and high-grade lymphoma, who may benefit from intensified treatment regimens. *Haematologica* 105 (5), 1369–1378. doi:10.3324/haematol.2019.223891

Schlosser, I., Hölzel, M., Hoffmann, R., Burtscher, H., Kohlhuber, F., Schuhmacher, M., et al. (2005). Dissection of transcriptional programmes in response to serum and c-Myc in a human B-cell line. *Oncogene* 24 (3), 520–524. doi:10.1038/sj.onc.1208198

Sun, W., Li, J., Zhou, L., Han, J., Liu, R., Zhang, H., et al. (2020). The c-Myc/miR-27b-3p/ATG10 regulatory axis regulates chemoresistance in colorectal cancer. *Theranostics* 10 (5), 1981–1996. doi:10.7150/thno.37621

Vardiman, J. W., Thiele, J., Arber, D. A., Brunning, R. D., Borowitz, M. J., Porwit, A., et al. (2009). The 2008 revision of the World Health Organization (WHO) classification of myeloid neoplasms and acute leukemia: rationale and important changes. *Blood* 114 (5), 937–951. doi:10.1182/blood-2009-03-209262

Vidal, S. J., Rodriguez-Bravo, V., Galsky, M., Cordon-Cardo, C., and Domingo-Domenech, J. (2014). Targeting cancer stem cells to suppress acquired chemotherapy resistance. *Oncogene* 33 (36), 4451–4463. doi:10.1038/onc.2013.411

Walter, R. B., Othus, M., Burnett, A. K., Löwenberg, B., Kantarjian, H. M., Ossenkoppele, G. J., et al. (2015). Resistance prediction in AML: analysis of 4601 patients from MRC/NCRI, HOVON/SAKK, SWOG and MD anderson cancer center. *Leukemia* 29 (2), 312–320. doi:10.1038/leu.2014.242

Yu, L., Yu, T.-T., and Young, K. H. (2019). Cross-talk between Myc and p53 in B-cell lymphomas. *Chronic Dis. Translational Med.* 5 (3), 139–154. doi:10.1016/j.cdtm.2019.08.001

Yun, S., Sharma, R., Chan, O., Vincelette, N. D., Sallman, D. A., Sweet, K., et al. (2019). Prognostic significance of MYC oncoprotein expression on survival outcome in patients with acute myeloid leukemia with myelodysplasia related changes (AML-MRC). *Leuk. Res.* 84, 106194. doi:10.1016/j.leukres.2019.106194

Conflict of Interest: CT received an honorarium and consulting fees from Novartis, Roche, Takeda, Johnson and Johnson, Amgen, BMS Celgene, Kirin, AbbVie, and MSD.

The remaining authors declare that the research was conducted in the absence of any commercial or financial relationships that could be construed as a potential conflict of interest.

Copyright © 2021 Hsiao, Wang, Lu, Shih, Su, Tsai, Jhan, Lia, Chuang, Chang and Teng. This is an open-access article distributed under the terms of the Creative Commons Attribution License (CC BY). The use, distribution or reproduction in other forums is permitted, provided the original author(s) and the copyright owner(s) are credited and that the original publication in this journal is cited, in accordance with accepted academic practice. No use, distribution or reproduction is permitted which does not comply with these terms.

frontiers in Pharmacology

REVIEW
published: 06 May 2021
doi: 10.3389/fphar.2021.681320

Clinical Insights Into Novel Immune Checkpoint Inhibitors

Jii Bum Lee[1,2], *Sang-Jun Ha*[3]* *and Hye Ryun Kim*[2]*

[1]Division of Hemato-oncology, Wonju Severance Christian Hospital, Yonsei University Wonju College of Medicine, Wonju, South Korea, [2]Division of Medical Oncology, Department of Internal Medicine, Yonsei Cancer Center, Yonsei University College of Medicine, Seoul, South Korea, [3]Department of Biochemistry, College of Life Science & Biotechnology, Yonsei University, Seoul, South Korea

The success of immune checkpoint inhibitors (ICIs), notably anti-cytotoxic T lymphocyte associated antigen-4 (CTLA-4) as well as inhibitors of CTLA-4, programmed death 1 (PD-1), and programmed death ligand-1 (PD-L1), has revolutionized treatment options for solid tumors. However, the lack of response to treatment, in terms of *de novo* or acquired resistance, and immune related adverse events (IRAE) remain as hurdles. One mechanisms to overcome the limitations of ICIs is to target other immune checkpoints associated with tumor microenvironment. Immune checkpoints such as lymphocyte activation gene-3 (LAG-3), T cell immunoglobulin and ITIM domain (TIGIT), T cell immunoglobulin and mucin-domain containing-3 (TIM-3), V-domain immunoglobulin suppressor of T cell activation (VISTA), B7 homolog 3 protein (B7-H3), inducible T cell costimulatory (ICOS), and B and T lymphocyte attenuator (BTLA) are feasible and promising options for treating solid tumors, and clinical trials are currently under active investigation. This review aims to summarize the clinical aspects of the immune checkpoints and introduce novel agents targeting these checkpoints.

Keywords: immune checkpoint, LAG-3, TIGIT, TIM-3, B7-H3, VISTA, ICOS, BTLA

OPEN ACCESS

Edited by:
Claudia Cerella, Fondation de Recherche Cancer et Sang, Luxembourg

Reviewed by:
Carmen Stecher, Medical University of Vienna, Austria
Salman M Toor, Hamad bin Khalifa University, Qatar
Reem Saleh, Qatar Biomedical Research Institute, Qatar

***Correspondence:**
Hye Ryun Kim
nobelg@yuhs.ac
Sang-Jun Ha
sjha@yonsei.ac.kr

Specialty section:
This article was submitted to Pharmacology of Anti-Cancer Drugs, a section of the journal Frontiers in Pharmacology

Received: *16 March 2021*
Accepted: *22 April 2021*
Published: *06 May 2021*

Citation:
Lee JB, Ha S-J and Kim HR (2021) Clinical Insights Into Novel Immune Checkpoint Inhibitors. Front. Pharmacol. 12:681320. doi: 10.3389/fphar.2021.681320

BACKGROUND

Cancer cells have characteristics that allow diversification and sustenance of their neoplastic state (Hanahan and Weinberg, 2011). One of the hallmarks of cancer is immune evasion; cancer cells hamper immune activation by limiting T cell activation and expressing immune checkpoint proteins on T cells (Vinay et al., 2015). Blocking cytotoxic T lymphocyte associated antigen-4 (CTLA-4) and the interaction between programmed death 1 (PD-1) and programmed death ligand-1 (PD-L1) elicit activation of the host immune system through T cell responses (Pardoll, 2012). These findings have led to the development of immune checkpoint inhibitors (ICIs) to control one of the key mechanisms utilized by cancer cells (Pardoll, 2012). In 2011, ipilimumab, the first anti-CTLA-4 monoclonal antibody (mAb), was approved for treating metastatic melanoma (Cameron et al., 2011). Thereafter, anti-PD-1 mAbs such as pembrolizumab, nivolumab, cemiplimab and as well as anti-PD-L1 mAbs such as atezolizumab, avelumab, durvalumab, have been used to treat patients with cancer, especially

Abbreviations: adhesion molecule 1; BTLA, B and T-lymphocyte attenuator; HVEM, herpes-virus entry mediator; ICOS, Inducible T cell costimulator; ICOSL, Inducible T cell costimulatory ligand; LAG-3, lymphocyte-associated gene 3; mAb, monoclonal antibody; PtdSer, phosphatidyl serine; TIGIT, T cell immunoglobulin and ITIM domain; TIM-3, T-cell immunoglobulin and mucin domain-3; VISTA, V-domain immunoglobulin suppressor of T cell activation; VSIG-3, V-Set and Immunoglobulin domain containing 3.

in locally advanced and metastatic settings (Qin et al., 2019; Vaddepally et al., 2020). Besides PD-L1 expression, several emerging biomarkers have gained wide attention (Darvin et al., 2018). Pembrolizumab was approved in solid tumors harboring microsatellite instability-high (MSI-H) or mismatch repair deficient (dMMR), and high tumor mutation burden (TMB-H) defined as ≥10 mutations/megabase based on FoundationOneCDx assay (Foundation Medicine, Inc.) (Marcus et al., 2019; Marabelle et al., 2020).

Despite the feasibility and anti-tumor activity of ICIs, there remain several hurdles in immunotherapy for cancer. Only a subset of patients respond to treatment, and the majority of patients who have durable responses eventually experience disease progression (Trebeschi et al., 2019). Furthermore, patients experience IRAE, some of which are highly toxic (Boutros et al., 2016; Wang et al., 2018). To overcome these impediments, treatment strategies such as combination with chemotherapy, targeted agents, or radiotherapy have been implemented (Gandhi et al., 2018; Wang et al., 2018; Rini et al., 2019). Notably, treatment with a combination of different ICIs has resulted in increased clinical responses, as observed with the combination of nivolumab and ipilimumab in melanoma, non-small cell lung cancer (NSCLC), and renal cell carcinoma (RCC) (Rizvi et al., 2016; Hellmann et al., 2018; Motzer et al., 2018).

Promising results from the combination of anti-CTLA-4 and PD-L1 mAbs have resulted in the launch of several other ICI combinations with non-overlapping mechanisms of action that may increase efficacy and minimize toxicity (Barbari et al., 2020). Currently, approximately 2/3 of all oncology trials are dedicated to T cell-targeting immunomodulators, and there are more than 3,000 ongoing clinical trials (Xin Yu et al., 2019).

Resistance to immunotherapy is associated with loss of immunogenic neoantigens, increase of immunosuppressive cells, and upregulation of alternate immune checkpoint receptors (Sharma et al., 2017). This review provides an overview of the mechanisms and ongoing clinical trials specifically on novel emerging immune checkpoints, including lymphocyte activation gene-3 (LAG-3), T cell immunoglobulin and ITIM domain (TIGIT), T cell immunoglobulin and mucin-domain containing-3 (TIM-3), V-domain immunoglobulin suppressor of T cell activation (VISTA), B7 homolog 3 protein (B7-H3), inducible T cell costimulatory (ICOS), and B and T lymphocyte attenuator (BTLA) (Chapoval et al., 2001; Monney et al., 2002; Yu et al., 2009; Paulos and June, 2010; Wang et al., 2011; Andrews et al., 2017; Marinelli et al., 2018).

LAG-3

LAG-3 is a protein comprising four parts—the hydrophobic, extracellular, transmembrane, and cytoplasmic domains. LAG-3 shares structural similarity with CD4 in having four extracellular regions (Triebel et al., 1990; Huard et al., 1997). It is expressed mainly on activated $CD4^+$ and $CD8^+$ T cells, regulatory T cells (Tregs), and natural killer (NK) cells, as well as on B cells and plasmacytoid dendritic cells (DCs) (**Table 1**) (Huard et al., 1995; Andreae et al., 2002; Huang et al., 2004; Kisielow et al., 2005). LAG-3 binds its canonical ligand, major histocompatibility complex class II (MHC-II), as well as other ligands, including galectin-3, LSECtin, α-synuclein, and fibrinogen-like protein 1 (FGL1), thereby inducing exhaustion of immune cells and decreased cytokine secretion (Baixeras et al., 1992; Huard et al., 1994; Kouo et al., 2015; Anderson et al., 2016; Baumeister et al., 2016; Mao et al., 2016; Wang et al., 2019).

LAG-3 was found to be simultaneously co-expressed with other targets, such as PD-L1, TIGIT, and TIM-3, in preclinical settings (Woo et al., 2012; Baumeister et al., 2016). Blocking LAG-3 alone did not restore T cell exhaustion; however, the combination of LAG-3/PD-1 blockade resulted in reduced tumor volume (Woo et al., 2012). These findings were consistent across *in vivo* studies using murine models of other tumors, including melanoma, ovarian cancer, and lymphoma (Goding et al., 2013; Huang et al., 2015).

In humans, LAG-3 is expressed on $CD8^+$ tumor-infiltrating lymphocytes (TILs) and peripheral Tregs (Camisaschi et al., 2010; Matsuzaki et al., 2010; Li et al., 2013; Llosa et al., 2015; Taube et al., 2015). $CD8^+$ TILs isolated from tumors such as hepatocellular carcinoma (HCC), melanoma, ovarian cancer, and microsatellite instability high (MSI) colorectal cancer (CRC), have high levels of both PD-1 and LAG-3 (Matsuzaki et al., 2010; Li et al., 2013; Llosa et al., 2015; Taube et al., 2015). Peripheral Tregs have been observed in melanoma and CRC (Camisaschi et al., 2010). In patients with hormone receptor-positive breast cancer, treated with immunotherapy, soluble LAG-3 (sLAG-3) detected in the serum was correlated with better prognosis in terms of disease-free survival (DFS) and overall survival (OS) (Triebel et al., 2006). However, the mechanism of sLAG-3 has yet to be identified (Li et al., 2007).

Clinical Trials on LAG-3

Co-expression of LAG-3 with immune checkpoints, such as PD-1, and robust clinical data on the efficacy of LAG-3 and PD-1 dual blockade have prompted trials focusing on this combination as well as other immune checkpoint inhibitors. Currently, there are 17 agents targeting LAG-3 (**Table 2**), with multiple combinations of treatments across various tumors (**Table 3**). Eight of these agents have interim or final clinical results, and nine of the investigational agents are ongoing clinical trials.

A phase 1 study of eftilagimod alpha (IMP321), an antigen-presenting cell (APC) activator for LAG-3, in combination with pembrolizumab was conducted in 24 patients with metastatic melanoma (NCT02676869) (Atkinson et al., 2020). The primary endpoints were the recommended phase 2 dose (RP2D), safety, and tolerability of the combined agents. The study included cohort A of dose escalation and cohort B of extension, and the patients received subcutaneous pembrolizumab and eftilagimod alpha bi-weekly at doses of 1, 6, or 30 mg for up to 6 and 12 months for Cohorts A and B, respectively. There was no dose-limiting toxicity (DLT) and the treatment was well tolerated, with the injection site as the most common adverse event (AE). The response to treatment was encouraging, with an

TABLE 1 | Overview of novel immune checkpoints.

Immune checkpoints	LAG-3	TIGIT	TIM-3	B7-H3	VISTA	ICOS	BTLA
Other names	CD223	Vstm3, Vsig9, WUCAM	HAVCR2	CD276	Dies1, DD1α, Gi24, B7-H5, PD-1H	CD278	CD272
Function	Co-inhibition	Co-inhibition	Co-inhibition	Co-inhibition or co-stimulation	Co-inhibition	Co-inhibition or co-stimulation	Co-inhibition or co-stimulation
Cells that express the immune checkpoints	NK cells, DC, activated T cells, Tregs, B cells,	NK cells, T cells	NK cells, DCs, activated T cells, Tregs, B cells, monocytes, cancer cells	NK cells, DCs, activated T cells, monocytes, cancer cells	T cells, myeloid cells	Activated T cells	Mature T cells, Tregs, B cells, macrophages
Ligands or receptors	MHC-II, galectin-3, LSECtin, a-synuclein, FGL1	CD155, CD112	HMGB-1, galectin-9, ceacam-1, PtdSer	Unknown	VSIG-3	ICOSL	HVEM, LIGHT, lymphotoxin-α
Immune checkpoint agents	APC activator, anti-LAG3 mAb, LAG3 and PD1 DART protein, LAG3 fusion protein, bispecific Ab to both LAG3 and PD-L1	Anti-TIGIT mAb	Anti-TIM-3 mAb, anti-PD-1/TIM3 bispecific Ab	Anti-B7-H3 mAb, B7-H3-targeting ADC, radiolabeled anti-B7-H3 mAb, CAR T-cell therapy	Anti-VISTA mAb, small molecule VISTA	Anti-ICOS agonist, anti-ICOS antagonist	
No. of investigational agents	17	10	8	11	3	4	4
Clinical trials							
Phase 1	Completed (eftilagimod alpha, BI 754111, Sym022, INCAGN02385), ongoing	Ongoing	Completed (Sym023), ongoing	Completed (enoblituzumab), ongoing	Completed (CA-170), ongoing	Ongoing	Completed (JTX-2011), ongoing
Phase 2	Completed (eftilagimod alpha, LAG525), ongoing	Ongoing	Ongoing	Ongoing	NA	NA	NA
Phase 3	Ongoing (MGD013)	Ongoing (tiragolumab)	Ongoing (sabatolimab)	Ongoing	NA	NA	NA
Combination treatment	Yes	Yes	Yes	Yes	No	Yes	Yes
Other immune checkpoint inhibitors	Yes	Yes	Yes	Yes		Yes	Yes
Targeted agents	Yes	Yes	Yes	Yes		Yes	Yes
Chemotherapy	Yes	Yes	Yes	Yes		Yes	No
Radiotherapy	Yes	No	No	Yes		No	No

Abbreviations: *APC, antigen presenting cell; BTLA, B and T-lymphocyte attenuator; CAR-T, chimeric antigen receptor T cell; DART, dual-affinity re-targeting proteins; DCs, dendritic cells; Dies 1, differentiation of embryonic stem cells 1; HAVCR2, hepatitis A virus cellular receptor 2; HVEM, herpes-virus entry mediator; mAb, monoclonal antibody; ICOS, Inducible T cell costimulator; ICOSL, Inducible T cell costimulatory ligand; LAG-3, lymphocyte-associated gene 3; NK cells, natural killer cells; PD-1H, PD-1 homologue; PD-L1, programmed death-ligand 1; PtdSer, phosphatidyl serine; T regs, ceacam-1, carcinoembryonic antigen cell adhesion molecule 1; T regs, regulatory T cells; TIGIT, T cell immunoglobulin and ITIM domain; TIM-3, T-cell immunoglobulin and mucin domain-3; VISTA, V-domain immunoglobulin suppressor of T cell activation; VSIG-3, V-Set and Immunoglobulin domain containing 3; WUCAM, Washington University cell adhesion molecule.*

overall response rate (ORR) of 33 and 50% for pembrolizumab-refractory cohort A and PD-1 naive cohort B patients, respectively.

Similarly, the combination of eftilagimod alpha and pembrolizumab has been investigated in NSCLC and head and neck squamous cell carcinoma (HNSCC) (NCT03625323) (Peguero et al., 2019). The AIPAC study, a placebo-controlled randomized phase IIb study on eftilagimod alpha (or placebo) with paclitaxel as the first-line treatment in patients with metastatic breast cancer (MBC), is also under investigation (NCT02614833) (Dirix and Triebel, 2019). Preliminary results show that the agent could elicit durable immune responses. Clinical data, including progression-free survival (PFS), ORR, OS, and safety, are all awaiting results.

Relatlimab (BMS-986016), an IgG4 mAb targeting LAG-3, has been investigated in various settings and agents, notably with well-established immune checkpoint inhibitors such as nivolumab and ipilimumab and other novel agents such as indoleamine 2,3-dioxygenase-1 (IDO1) inhibitors, CCR2/5 dual antagonist, and anti-TIGIT. Notably, clinical trials are ongoing for phase II/III in previously untreated metastatic melanoma, in combination with or without nivolumab (NCT03470922), phase II of nivolumab and oxaliplatin-based chemotherapy with or without relatlimab in GC or gastroesophageal junction (GEJ) cancer (NCT03662659), and phase II of relatlimab with nivolumab in mismatch repair deficient (dMMR) cancers resistant to prior PD-1/PD-L1 inhibition (Lipson et al., 2018; Feeney et al., 2019; Bever et al.,

TABLE 2 | Emerging immune checkpoint inhibitors and their mechanisms.

Target	Name of agent	Company	Mechanism
LAG-3			
	Eftilagimod alpha (IMP321)	Immutep	APC activator
	Relatlimab (BMS-986016)	Bristol-Myers Squibb	IgG4 mAb
	LAG525	Norvatis	IgG4 mAb
	Cemiplimab (REGN3767)	Regeneron	mAb
	BI 754111	Bohringer Ingelheim	mAb
	Sym022	Symphogen	Fc-inert mAb
	MGD013	MacroGenics	LAG-3 and PD1 DART protein
	Mavezelimab (MK-4280)	Merck	IgG4 mAb
	TSR-033	Tesaro	IgG4 mAb
	INCAGN02385	Incyte	Fc engineered IgG1k antibody
	EOC202	EddingPharm Oncology	LAG-3 fusion protein
	89Zr-DFO-REGN3767	Memorial Sloan Kettering Cancer Center	Anti-LAG-3 antibody labeled with 89Zr
	XmAb®22,841	Xencor	Bispecific antibody to both LAG3 and CTLA-4
	LBL-007	Nanjing Leads Biolabs Co	AlphaLAG-3 mAb
	FS118	F-star	Bispecific antibody to both LAG3 and PD-L1
	RO7247669	Hoffmann-La Roche	Bispecific antibody to both LAG3 and PD-L1
	EMB-02	Shanghai EpimAb Biotherapeutics	Bispecific antibody to both LAG3 and PD-L1
TIGIT			
	Tiragolumab (MTIG7192A/RG-6058)	Genentech	Anti-TIGIT mAb
	Vibostolimab (MK-7684)	Merck	Anti-TIGIT mAb
	Etigilimab (OMP-313M32)	OncoMed	Anti-TIGIT mAb
	BMS-986207	Bristol-Myers Squibb	Anti-TIGIT mAb
	Domvanalimab (AB-154)	Arcus Biosciences	Anti-TIGIT mAb
	ASP-8374	Potenza	Anti-TIGIT mAb
	IBI939	Innovent Biologics	Anti-TIGIT mAb
	BGB-A1217	BeiGene	Anti-TIGIT mAb
	COM902	Compugen	Anti-TIGIT mAb
	M6223	EMD Serono	Anti-TIGIT mAb
TIM-3			
	Sym023	Symphogen	Anti-TIM-3 mAb
	LY3321367	Eli Lilly and Company	Anti-TIM-3 mAb
	Cobolimab (TSR-022)	Tesaro	Anti-TIM-3 mAb
	Sabatolimab (MBG453)	Novartis	Anti-TIM-3 mAb
	INCAGN2390	Incyte	Anti-TIM-3 mAb
	BMS-986258	Bristol-Myers Squibb	Anti-TIM-3 mAb
	SHR-1702	Jiangsu HengRui	Anti-TIM-3 mAb
	RO7121661	Roche	Anti-PD-1/TIM-33 bispecific Ab
B7-H3			
	Enoblituzumab (MGA271)	MacroGenetics	Anti-B7-H3 mAb
	DS-7300a	Daiichi Sankyo	B7-H3-targeting ADC
	Orlotamab (MGD009)	MacroGenetics	B7-H3 and CD3 DART protein
	131I-Omburtamab	Y-mAbs Therapeutics	Radiolabeled anti-B7-H3 mAb
	124I-Omburtamab	Y-mAbs Therapeutics	Radiolabeled anti-B7-H3 mAb
	177Lu-DTPA-Omburtamab	Y-mAbs Therapeutics	Radiolabeled anti-B7-H3 mAb
	4SCAR-276	Shenzhen Geno-Immune Medical Institute	CAR T-cell therapy
	SCRI-CARB7H3	Seattle Children's Hospital	CAR T-cell therapy
	B7-H3 CAR-T	BoYuan RunSheng Pharma	CAR T-cell therapy
	CAR.B7-H3	UNC Lineberger Comprehensive Cancer Center	CAR T-cell therapy
	Second-generation 4-1BBζ B7H3-EGFRt-DHFR	Seattle Children's Hospital	CAR T-cell therapy
VISTA			
	JNJ-61610588	Johnson & Johnson	Anti-VISTA mAb
	CI-8993	Curis	Anti-VISTA mAb
	CA-170	Curis	Small molecule targeting VISTA and PD-L1
ICOS			
	GSK3359609	GlaxoSmithKline	Anti-ICOS agonist
	JTX-2011	Jounce Therapeutics	Anti-ICOS agonist
	MEDI-570	National Cancer Institute	Anti-ICOS antagonist
	KY1044	Kymab Limited	Anti-ICOS antagonist
BTLA			
	INBRX-106	Inhibrx	Hexavalent OX40 agonist Ab
	PF-04518600	Pfizer	OX40 agonist
	Cudarolimab (IBI101)	Innovent Biologics	Anti-OX40 mAb
	TAB004 (JS004)	Shanghai Junshi Bioscience	Anti-BTLA mAb

Abbreviations: *ADC, antibody drug conjugate; APC, antigen-presenting cell; BTLA, B and T-lymphocyte attenuator; CAR, chimeric antigen receptor; CTLA-4, cytotoxic T-lymphocyte-associated protein; DART, dual-affinity re-targeting proteins; ICOS, inducible T-cell costimulator; LAG3, lymphocyte-associated gene 3; mAb, monoclonal antibody; PD-L1, programmed death-ligand 1; TIGIT, T cell immunoglobulin and ITIM domain; TIM, T-cell immunoglobulin and mucin domain-3; VISTA, V-domain immunoglobulin suppressor of T cell activation.*

2020). Relatlimab is being tested in a wide range of tumor types and settings as front- or second-line treatment, in resectable status, and in stage II/III.

An open label, phase 2 study including 72 patients treated with LAG-525, which is an IgG4 mAb for LAG-3, and spartalizumab (PDR001), an anti-PD-1, for advanced solid tumors and hematologic malignancies showed promising activity, especially in neuroendocrine tumors, small cell lung cancer (SCLC), and diffuse large B-cell lymphoma (DLBCL), with a clinical benefit rate at 24 weeks (CBR24) of 0.86, 0.27, and 0.804, respectively, meeting its primary endpoint (NCT03365791) (Uboha et al., 2019). In GEJ cancer, the CBR24 was 0.071, and enrollment was stopped for these subsets of patients. Other tumors such as triple-negative breast cancer (TNBC) (NCT03742349 and NCT03499899) and melanoma (NCT03484923) are ongoing trials in advanced and metastatic settings.

The preliminary results of a phase 1 study on cemiplimab (REGN3767), an mAb for LAG-3, as monotherapy (n = 27), and in combination with PD-1 mAb (n = 42) was conducted in advanced malignancies (NCT03005782) (Papadopoulos et al., 2019). No DLT was observed with in the monotherapy group, whereas the combination group, during treatment with R3767 3 mg/kg every 3 weeks (Q3W) + cemiplimab 3 mg/kg Q3W, experienced grade 4 elevated creatine phosphokinase levels in addition to grade 3 myasthenia gravis. Overall, both treatments were deemed tolerable; cemiplimab 20 mg/kg or 1600 mg as a fixed dose of Q3W is ongoing further evaluation as monotherapy and as a combination.

Similarly, BI 754111, an mAb for LAG-3, was also tested with BI 754091 (anti-PD-1) in treatment-refractory solid tumors, in a dose escalation phase 1 study, followed by an expansion phase in microsatellite stable (MSS) CRC and anti-PD1/PD-L1 refractory tumors including NSCLC (NCT03156114) (Johnson et al., 2020). The primary endpoints for dose escalation and dose expansion phase were DLT and the maximum tolerated dose (MTD) and ORR, respectively. Biomarker analysis was performed in MSS CRC refractory to immunotherapy; the patients who responded to these agents with a partial response (PR) or stable disease (SD) had increased treatment-associated IFN-γ gene signature scores (Bendell et al., 2020). Furthermore, patients with high PD-L1 gene expression in pre-treatment biopsy samples responded better to the treatment. Baseline immunohistochemistry of LAG-3 was not a predictive factor for this subset of patients.

Sym022 (anti-LAG-3) was evaluated as a single agent or in combination with sym021 (anti-PD-1) in phase 1 trials for solid tumors or lymphomas (NCT03311412, NCT03489369, and NCT03489343) (Lakhani et al., 2020). Interim analysis showed that 15 patients who were administered monotherapy and 20 patients under combination treatment, had one unconfirmed PR. Both treatment arms had tolerable safety profiles, with the combination treatment showing one grade 3–4 immune-related hypophysitis. Further assessments of the pharmacokinetic (PK) and pharmacodynamic (PD) markers and the anti-tumor activity of the monotherapy and combination are awaiting results.

MGD013 is a LAG-3 and PD-1 dual-affinity re-targeting (DART) protein; its safety, tolerability, DLT, MTD, PK/PD, and antitumor activity were analyzed in patients with unresectable and metastatic tumors in a phase 1 study (NCT03219268) (Luke et al., 2020). Fifty patients in the dose-escalation phase and 157 patients in the dose-expansion phase, with 46 and 32% of patients with prior exposure to immunotherapy, respectively, were enrolled. No MTD was reached, and the most common treatment-related adverse events (TRAE), which were fatigue and nausea, were well tolerated. Despite exposure to previous immunotherapy, both cohorts included patients with objective responses. More mature clinical data are awaiting results, and biomarker analysis of LAG-3 and PD-L1 is ongoing.

Other agents that are undergoing clinical trials are: 1) mavezelimab (MK-4280), an IgG4 mAb targeting LAG-3 (NCT03598608, NCT02720068, and NCT03516981); 2) TSR-033, an IgG4 mAb targeting LAG-3 (NCT03250832); 3) INCAGN02385, a Fc engineered IgG1k antibody for LAG-3 (NCT03538028, NCT04370704, and NCT03311412); 4) EOC202, a LAG-3 fusion protein (NCT03600090); 5) 89Zr-DFO-REGN3767, an anti-LAG-3 antibody labeled with 89Zr (NCT04566978); 6) XmAb®22841, a bispecific antibody to both LAG-3 and CTLA-4 (NCT03849469); 7) LBL-007, an alphaLAG-3 mAb (NCT04640545), and 8) bispecific antibody to both LAG-3 and PD-L1, which includes agents FS118 (NCT03440437), RO7247669 (NCT04140500), and EMB-02 (NCT04618393) treated as monotherapy or in combination for patients with treatment refractory solid and/or hematologic malignancies.

TIGIT

TIGIT, previously known as Vstm3, VSIG9, or Washington University cell adhesion molecule (WUCAM), is a protein comprising an extracellular IgV domain and an intracellular domain with a canonical ITIM and an immunoglobulin tyrosine tail (ITT) motif (**Table 1**) (Yu et al., 2009; Levin et al., 2011). TIGIT expression is tightly restricted to lymphocytes and is mainly observed in NK cells and T cell subsets, including effector and regulatory $CD4^+$ T cells, follicular helper $CD4^+$ T cells, and effector $CD8^+$ T cells (Boles et al., 2009; Yu et al., 2009; Lozano et al., 2012; Stengel et al., 2012; Johnston et al., 2014; Joller et al., 2014). Three ligands bind to TIGIT: 1) poliovirus receptor (PVR), also known as CD155, Necl5, and Tage4; 2) CD112, also called poliovirus receptor ligand2/nectin2 (PVRL2/nectin 2); and 3) PVRL3. PVR has a high affinity for TIGIT, whereas CD112 and PVRL3 bind to a lesser extent (Yu et al., 2009).

TIGIT plays multiple roles in the inhibition of cancer immunity. TIGIT inhibits NK cell-mediated tumor killing, induces immunosuppressive DCs, suppresses CD8 T cell priming and differentiation, and prevents CD8 T cell-mediated killing (Buisson and Triebel, 2005; Li et al., 2014; Fuhrman et al., 2015; Kurtulus et al., 2015; Liu et al., 2015; Kourepini et al., 2016). The interaction of TIGIT with other constituents of the tumor microenvironments (TMEs), such as cancer-associated fibroblasts and angiogenesis, remains to be elucidated (Manieri et al., 2017).

TABLE 3 | Clinical trials on novel immune checkpoint inhibitors.

Target	Drug	Clinical trial no.	Phase	Settings	Tumor types	Treatment arms	Status
LAG-3	Eftilagimod alpha (IMP321)	NCT03252938	1	Advanced/metastatic	Solid tumors	Eftilagimod alpha	Active, not recruiting
		NCT00351949	1	Advanced/metastatic	RCC	Eftilagimod alpha	Completed
		NCT00349934	1	First line	Breast cancer	Eftilagimod alpha	Completed
		NCT02614833	2	Advanced/metastatic	Breast cancer	Eftilagimod alpha	Active, not recruiting
		NCT00324623	1	Advanced/metastatic	Melanoma	Cyclophosphamide, fludarabine followed by melan-A VLP vaccine and eftilagimod alpha	Completed
		NCT00365937	1,2	Adjuvant	Melanoma	Eftilagimod alpha±HLA-A2 peptides	Terminated
		NCT01308294	1,2	Stage II-IV	Melanoma	Eftilagimod alpha+tumor antigenic peptides+monatide	Terminated
		NCT00732082	1	Advanced/metastatic	Pancreatic cancer	Eftilagimod alpha+gemcitabine	Terminated
		NCT02676869	1	Stage III-IV	Melanoma	Eftilagimod alpha+pembrolizumab	Completed
		NCT03625323	2	Advanced/metastatic	NSCLC and HNSCC	Eftilagimod alpha+pembrolizumab	Recruiting
	Relatlimab (BMS-986016)	NCT02966548	1	Advanced/metastatic	Solid tumors	Relatlimab±nivolumab	Recruiting
		NCT01968109	1,2	First, second line	Solid tumors	Relatlimab±nivolumab	Recruiting
		NCT03623854	2	Advanced/metastatic	Chordoma	Relatlimab+nivolumab	Recruiting
		NCT03743766	2	Advanced/metastatic	Melanoma	Relatlimab+nivolumab	Recruiting
		NCT03470922	2,3	Advanced/metastatic	Melanoma	Relatlimab±nivolumab	Recruiting
		NCT03642067	2	Advanced/metastatic	MSS CRC	Relatlimab+nivolumab	Recruiting
		NCT04658147	1	Resectable	HCC	Relatlimab±nivolumab	Not yet recruiting
		NCT02061761	1,2	Advanced/metastatic	Hematologic malignancies	Relatlimab+nivolumab	Active, not recruiting
		NCT04567615	2	Advanced/metastatic	HCC	Relatlimab+nivolumab	Not yet recruiting
		NCT03607890	2	Advanced, prior PD-(L)1 inhibitor	MSI-H solid tumors	Relatlimab+nivolumab	Recruiting
		NCT04326257	2	Advanced, prior PD-(L)1 inhibitor	HNSCC	Relatlimab+nivolumab or ipilimumab	Recruiting
		NCT03493932	1	Recurrent	Glioblastoma	Relatlimab+nivolumab	Recruiting
		NCT02658981	1	Recurrent	Glioblastoma	Relatlimab±nivolumab or urelumab (anti-CD137)	Active, not recruiting
		NCT03610711	1,2	Advanced/metastatic	GC, GEJ cancer	Relatlimab±nivolumab	Recruiting
		NCT03044613	1	Stage II/III	GC, GEJ cancer	Nivolumab, carboplatin, paclitaxel, radiation±relatlimab	Recruiting
		NCT03662659	2	Advanced/metastatic	GC, GEJ cancer	Relatlimab or nivolumab±investigator's choice of chemotherapy	Active, not recruiting
		NCT03335540	1,2	Advanced/metastatic	Solid tumors	Relatlimab+nivolumab or cabiralizumab or ipilimumab or IDO1 inhibitor or radiation therapy	Recruiting
		NCT04611126	1,2	Advanced/metastatic	Ovarian cancer	Relatlimab, nivolumab, cyclophosphamide, fludarabine phosphate, tumor infiltrating lymphocytes infusion ± ipilimumab	Not yet recruiting
		NCT02488759	1,2	Neoadjuvant and metastatic	Virus-associated tumors	Nivolumab±relatlimab or ipilimumab or daratumumab	Active, not recruiting
		NCT02519322	2	Neoadjuvant and adjuvant	Melanoma	Nivolumab±relatlimab or ipilimumab	Recruiting
		NCT03459222	2	Advanced/metastatic	Solid tumors	Relatlimab, nivolumab±ipilimumab	Recruiting
		NCT02996110	2	Advanced/metastatic	RCC	Nivolumab+ipilimumab or BMS-986205 (IDO1i) or BMS-813160 (CCR2/5 dual antagonist)	Recruiting
		NCT02935634	2	Advanced/metastatic	GC, GEJ cancer	Nivolumab±relatlimab or ipilimumab or rucaparib or BMS-986205; ipilimumab+ucaparib; nivolumab+ipilimumab+rucaparib	Recruiting

(Continued on following page)

TABLE 3 | (*Continued*) Clinical trials on novel immune checkpoint inhibitors.

Target	Drug	Clinical trial no.	Phase	Settings	Tumor types	Treatment arms	Status
		NCT02750514	2	Advanced/metastatic	NSCLC	Nivolumab± relatlimab or ipilimumab or BMS-986205 or dasatinib	Active, not recruiting
		NCT02060188	2	Advanced/metastatic	CRC	Nivolumab±relatimab or daratumumab or ipilimumab±cobimetinib	Active, not recruiting
		NCT04150965	1,2	Advanced/metastatic	Multiple myeloma	Relatlimab±pomalidromide and dexamethasone; BMS-986207 (anti-TIGIT)±pomalidromide and dexamethasone; elotuzumab	Recruiting
	LAG525	NCT02460224	1,2	Advanced/metastatic	Solid tumors	LAG525±spartalizumab (PDR001)	Active, not recruiting
		NCT03365791	2	Advanced/metastatic	Solid or hematologic malignancy	LAG525+spartalizumab	Completed
		NCT03742349	1	Advanced/metastatic	TNBC	LAG525+spartalizumab+NIR178 or capmatinib or lacnotuzumab (MCS110) or canakinumab	Recruiting
		NCT03499899	2	Advanced/metastatic	TNBC	LAG525±spartalizumab±carboplatin; LAG525+carboplatin	Active, not recruiting
		NCT03484923	2	Advanced/metastatic	Melanoma	Spartalizumab+lag525 or ribociclib or canakinumab or capmatinib	Recruiting
	Cemiplimab (REGN3767)	NCT03005782	1	Advanced/metastatic	Solid tumors or lymphomas	REGN3767±cemiplimab (REGN2810)	Recruiting
	BI 754111	NCT03433898	1	Advanced/metastatic	Solid tumors	BI 754111±BI 754091 (anti-PD-1)	Recruiting
		NCT03156114	1	Advanced/metastatic	Solid tumors	BI 754111+BI 754091	Active, not recruiting
		NCT03780725	1	Advanced/metastatic	NSCLC and HNSCC	BI 754111+BI 754091	Completed
		NCT03697304	2	Advanced/metastatic	Solid tumors	BI 754111 or BI 836880 (bispecific VEGF and Ang2 Ab)+BI 754091 (anti-PD-1)	Recruiting
		NCT03964233	1	Advanced/metastatic	Solid tumors	BI 754111+BI 754091±BI 907828 (MDM2-p53 antagonist)	Recruiting
	Sym022	NCT03489369	1	Advanced/metastatic	Solid tumors or lymphomas		Completed
	MGD013	NCT03219268	1	Advanced/metastatic	Solid or hematologic malignancy	MGD013+margetuximab (anti-HER2 monoclonal antibody)	Recruiting
		NCT04082364	2,3	Advanced/metastatic	GC, GEJ cancer	margetuximab+INCMGA00012 (anti-PD-1); margetuximab+chemotherapy±MGD013 or INCMGA00012; trastuzumab+chemotherapy (XELOX or mFOLFOX-6)	Recruiting
	Mavezelimab (MK-4280)	NCT03598608	1,2	Measurable disease	Hematologic malignancies	MK-4280+pembrolizumab	Recruiting
		NCT02720068	1	Advanced/metastatic	Solid tumors	MK4280+pembrolizumab±FOLFIRI or mFOLFOX7 or lenvatinib	Recruiting
		NCT03516981	2	First line	NSCLC	MK4280+pembrolizumab or lenvatinib or quavonlimab (MK-1308)	Recruiting
	TSR-033	NCT03250832	1	Advanced/metastatic	Solid tumors	TSR-033±dostarlimab (TSR-042)±mFOLFOX or FOLFIRI	Recruiting
	IN-CAGN02385	NCT03538028	1	Advanced/metastatic	Solid tumors		Completed
		NCT04370704	1,2	Advanced/metastatic	Solid tumors	INCAGN02385+INCAGN02390 (Anti-TIM-3)±INCMGA00012 (anti-PD-1)	Recruiting
		NCT03311412	1	Advanced/metastatic	Solid tumors or lymphomas	Sym022+Sym021 (anti-PD-1)±Sym023 (anti-TIM-3)	Recruiting
	ECO202	NCT03600090	1	Advanced/metastatic	Breast cancer	ECO202+paclitaxel	Recruiting
	89Zr-DFO-REGN3767	NCT04566978	1	Measurable disease by Lugano criteria	DLBCL		Recruiting
	XmAb®22,841	NCT03849469	1	Advanced/metastatic	Solid tumors	XmAb®22841±pembrolizumab	Recruiting
	LBL-007	NCT04640545	1	Advanced/metastatic	Melanoma	LBL-007+toripalimab (anti-PD-1)	Not yet recruiting
	FS118	NCT03440437	1	Advanced/metastatic	Solid or hematologic malignancy		Active, not recruiting
	RO7247669	NCT04140500	1	Advanced/metastatic	Solid tumors		Recruiting
	EMB-02	NCT04618393	1,2	Advanced/metastatic	Solid tumors		Not yet recruiting

(Continued on following page)

TABLE 3 | (*Continued*) Clinical trials on novel immune checkpoint inhibitors.

Target	Drug	Clinical trial no.	Phase	Settings	Tumor types	Treatment arms	Status
TIGIT	Tiragolumab (MTIG7192A/RG-6058)	NCT02794571	1	Locally advanced or metastatic	Solid tumors	Tiragolumab±atezolizumab±chemotherapy	Recruiting
		NCT03563716	2	Locally advanced or metastatic	NSCLC	Atezolizumab±tiragolumab	Active, not recruiting
		NCT04294810	3	Locally advanced or metastatic	NSCLC	Atezolizumab±tiragolumab	Recruiting
		NCT04256421	3	First line, extensive stage	SCLC	Atezolizumab+carboplatin+etoposide±tiragolumab	Recruiting
		NCT03281369	1,2	Advanced/metastatic	Esophageal cancer	Atezolizumab+tiragolumab; atezolizumab+cisplatin/5-FU±tiragolumab; cisplatin/5-FU	Recruiting
					GC, GEJ cancer	Atezolizumab+cobimetinib with mFOFLOX6; atezolizumab+cobimetinib or tiragolumab or mFOFLOX or linagliptin or PEGPH20 or BL-8040; pactliaxel+ramucirumab	Recruiting
	Vibostolimab (MK-7684)	NCT02964013	1	Advanced/metastatic	Solid tumors	Vibostolimab±pembrolizumab+pemetrexed/carboplatin; carboplatin+cisplatin+etoposide	Recruiting
		NCT04305054	1,2	First line	Melanoma	pembrolizumab±vibostolimab or quavonlimab (MK-1308)±lenvatinib	Recruiting
		NCT04305041	1,2	Stage III-IV	Melanoma	pembrolizumab+quavonlimab+ vibostolimab or lenvatinib	Recruiting
		NCT04303169	1,2	Stage III	Melanoma	pembrolizumab±vibostolimab or V937 (oncolytic virus)	Recruiting
	Etigilimab (OMP-313M32)	NCT03119428	1	Locally advanced or metastatic	Solid tumors	Etigilimab±nivolumab	Terminated
	BMS-986207	NCT02913313	1,2	Advanced/metastatic	Solid tumors	BMS-986207±nivolumab	Active, not recruiting
		NCT04570839	1,2	Advanced/metastatic	Solid tumors	Nivolumab±BMS-986207 with COM701 (anti-PVRIG Ab)	Recruiting
	Domvanalimab (AB-154)	NCT03628677	1	Advanced/metastatic	Solid tumors	Dombvanalimab+zimberelimab (AB122, anti-PD-1)	Recruiting
		NCT04262856	2	Locally advanced or metastatic	NSCLC	Zimberelimab±dombvanalimab±etrumadenant	Recruiting
	ASP-8374	NCT03945253	1	Advanced/metastatic	Solid tumors		Completed
		NCT03260322	1	Advanced/metastatic	Solid tumors	ASP-8374±pembrolizumab	Active, not recruiting
	IBI939	NCT04353830	1	Advanced/metastatic	Solid tumors	IBI939±sintilimab (anti-PD-1)	Recruiting
		NCT04672369	1	Advanced/metastatic	NSCLC	IBI939±sintilimab	Not yet recruiting
		NCT04672356	1	Advanced/metastatic	NSCLC and SCLC	IBI939±sintilimab	Not yet recruiting
	BGB-A1217	NCT04047862	1	Advanced/metastatic	Solid tumors	BGB-A1217+tiselizumab±chemotherapy	Recruiting
	COM902	NCT04354246	1	Advanced/metastatic	Solid tumors		Recruiting
	M6223	NCT04457778	1	Advanced/metastatic	Solid tumors	M6223±bintrafusp alfa (M7824)	Recruiting
TIM-3	Sym023	NCT03489343	1	Advanced/metastatic	Solid tumors or lymphomas		Completed
	LY3321367	NCT03099109	1	Advanced/metastatic	Solid tumors	LY3300054 (anti-PD-L1)+LY3321367	Active, not recruiting
		NCT02791334	1	Advanced/metastatic	Solid tumors	LY3300054±LY3321367 or abemaciclib or ramucirumab or merestinib	Active, not recruiting
	Cobolimab (TSR-022)	NCT02817633	1	Advanced/metastatic	Solid tumors	Cobolimab±nivolumab or TSR-042±TSR-033±docetaxel	Recruiting
		NCT03307785	1	Advanced/metastatic	Solid tumors	Dostarlimab (TSR-042)±TSR-022+chemotherapy[a]; dostarlimab+bevacizumab±niraparib or chemotherapy[a]	Active, not recruiting
		NCT03680508	2	BCLC stage B or C	HCC	Cobolimab+dostarlimab	Recruiting
		NCT04139902	2	Neoadjuvant	Melanoma	Cobolimab±dostarlimab	Recruiting
	Sabatolimab (MBG453)	NCT02608268	1,2	Advanced/metastatic	Solid tumors	Sabatolimab±spartalizumab; decitabine	Active, not recruiting

(Continued on following page)

TABLE 3 | (*Continued*) Clinical trials on novel immune checkpoint inhibitors.

Target	Drug	Clinical trial no.	Phase	Settings	Tumor types	Treatment arms	Status
		NCT03961971	1	Advanced/metastatic	GBM	Sabatolimab+spartalizumab	Recruiting
		NCT04623216	1,2	Received one prior aHSCT	AML	Sabatolimab±azacitidine	Not yet recruiting
		NCT03066648	1	Relapse/refractory	AML or high risk MDS	Sabatolimab±spartalizumab±decitabine	Recruiting
		NCT03940352	1	Relapse/refractory	AML or high risk MDS	HDM201 (p53-MDM2 inhibitor)+sabatolimab or venetoclax	Recruiting
		NCT03946670	2	IPSS-R intermediate, high, or very high risk	MDS	hypomethylating agents±sabatolimab	Active, not recruiting
		NCT04266301	3	IPSS-R intermediate, high, or very high risk for MDS	MDS or CML	Sabatolimab+azacitidine	Recruiting
	INCAGN2390	NCT03652077	1	Advanced/metastatic	Solid tumors		Active, not recruiting
	BMS-986258	NCT03446040	1,2	Advanced/metastatic	Solid tumors	BMS-986258+nivolumab or rHuPH20	Recruiting
	SHR-1702	NCT03871855	1	Advanced/metastatic	Solid tumors	SHR-1702±camrelizumab	Unknown
	RO7121661	NCT03708328	1	Advanced/metastatic	Solid tumors		Recruiting
B7-H3	Enoblituzumab (MGA271)	NCT01391143	1	Advanced/metastatic	Solid tumors		Completed
		NCT02982941	1	Advanced/metastatic	Pediatric solid tumors		Completed
		NCT02923180	2	Localized intermediate and high-risk	Prostate cancer		Active, not recruiting
		NCT04634825	2	Advanced/metastatic	HNSCC	Enoblituzumab+retifanlimab (anti-PD-1 antibody) or tebotelimab (PD-1 and LAG-3 bispecific DART molecule)	Not yet recruiting
		NCT02381314	1	Advanced/metastatic	Solid tumors	Enoblituzumab+ipilimumab	Completed
		NCT02475213	1	Advanced/metastatic	Solid tumors	Enoblituzumab+pembrolizumab or retifanlimab	Active, not recruiting
		NCT04129320	2,3	Advanced/metastatic	HNSCC	Enoblituzumab+retifanlimab or tebotelimab	Withdrawn
	DS-7300a	NCT04145622	1,2	Advanced/metastatic	Solid tumors		Recruiting
	Orlotamab (MGD009)	NCT02628535	1	Advanced/metastatic	solid tumors		Terminated
		NCT03406949	1	Advanced/metastatic	Solid tumors	Orlotamab+retifanlimab	Active, not recruiting
	131I-Omburtamab	NCT01099644	1	Peritoneal involvement	DSRCT		Active, not recruiting
		NCT00089245	1	Advanced/metastatic	CNS or leptomeningeal cancer		Active, not recruiting
		NCT03275402	2,3	Recurrent	Neuroblastoma, CNS, or leptomeningeal metastases		Recruiting
	124I-Omburtamab	NCT01502917	1	Prior external beam radiotherapy	Gliomas	124I-Omburtamab+external beam radiotherapy (prior to study entry)	Recruiting
	177Lu-DTPA-Omburtamab	NCT04167618	1,2	Recurrent	Medulloblastoma		Not yet recruiting
		NCT04315246	1,2	Advanced/metastatic	Leptomeningeal metastasis from solid tumors		Not yet recruiting
	4SCAR-276	NCT04432649	1	Advanced/metastatic	Solid tumors		Recruiting
	SCRI-CARB7H3	NCT04185038	1	Advanced/metastatic	Pediatric CNS tumors		Recruiting
	B7-H3 CAR-T	NCT04385173	1	Recurrent	GBM	B7-H3 CAR-T+temozolomide	Recruiting
		NCT04077866	1,2	Recurrent	GBM	B7-H3 CAR-T±temozolomide	Recruiting
	CAR.B7-H3	NCT04670068	1	Advanced/metastatic	Epithelial ovarian cancer	B7-H3 CAR-T+fludarabine+cyclophosphamide	Not yet recruiting
	Second generation 4-1BBζ B7H3-EGFRt-DHFR	NCT04483778	1	Recurrent	Non-primary CNS solid tumors	Second generation 4-1BBζ B7H3-EGFRt-DHFR±second generation 4-1BBζ CD19-Her2tG	Recruiting

(Continued on following page)

TABLE 3 | (*Continued*) Clinical trials on novel immune checkpoint inhibitors.

Target	Drug	Clinical trial no.	Phase	Settings	Tumor types	Treatment arms	Status
VISTA	JNJ-61610588	NCT02671955	1	Advanced/metastatic	Solid tumors		Terminated
	CI-8993	NCT04475523	1	Advanced/metastatic	Solid tumors		Recruiting
	CA-170	NCT02812875	1	Advanced/metastatic	Solid tumors or lymphomas		Completed
ICOS	GSK3359609	NCT04428333	1,2	Advanced/metastatic	HNSCC	GSK3359609±pembrolizumab+fluouracil-platinum based chemotherapy	Recruiting
		NCT04128696	3	Advanced/metastatic	HNSCC	GSK3359609+pembrolizumab	Recruiting
		NCT03693612	2	Advanced/metastatic	Solid tumors	GSK3359609+pembrolizumab; docetaxel+paclitaxel+cetuximab	Recruiting
	JTX-2011	NCT02904226	1,2	Advanced/metastatic	Solid tumors	JTX-2011+pembrolizumab or nivolumab or ipilimumab	Completed
	MEDI-570	NCT02520791	1	Advanced/metastatic	Lymphoma		Recruiting
	KY1044	NCT03829501	1,2	Advanced/metastatic	Solid tumors	KY1044±atezolizumab	Recruiting
BTLA	INBRX-106	NCT04198766	1	Locally advanced or metastatic	Solid tumors	INBRX-106+pembrolizumab	Recruiting
	Cudarolimab (IBI101)	NCT03758001	1	Advanced/metastatic	Solid tumors	Cudarolimab+sintilimab (anti-PD-1)	Recruiting
	PF-04518600	NCT02315066	1	Advanced/metastatic	Solid tumors	PF-04518600±utomilumab (PF-05082566, anti-TNFRSF9)	Completed
	TAB004 (JS004)	NCT04137900	1	Advanced/metastatic	Solid tumors or lymphomas		Recruiting
		NCT04278859	1	Advanced/metastatic	Solid tumors		Recruiting
		NCT04477772	1	Advanced/metastatic	Lymphoma		Recruiting

Abbreviations: *AML, acute myeloid leukemia; anti-PD-1, anti-programmed death-1; BCLC, Barcelona Clinic Liver Stage; BTLA, B and T-lymphocyte attenuator; CML, chronic myelogenous leukemia; CNS, central nervous system; CRC, colorectal cancer; DART, dual-affinity re-targeting proteins; DLBCL, diffuse large B cell lymphoma; DSRCT, desmoplastic small round cell tumor; GBM, glioblastoma multiforme; GC, gastric cancer; GEJ, gastroesophageal junction cancer; HCC, hepatocellular carcinoma; HNSCC, head and neck squamous cell carcinoma; ICOS, Inducible T cell costimulator; IDO1i, indoleamine 2,3-dioxygenase-1 inhibitor; IPSS-R, revised international prognostic scoring system; LAG3, lymphocyte-associated gene 3; MDM2, mouse double minute 2 homolog; MDS, myelodysplastic syndrome; MSI-H, microsatellite instability-high; MSS, microsatellite stable; NSCLC, non-small cell lung cancer; PEGPH20, pegylated recombinant human hyaluronidase; RCC, Renal cell carcinoma; rHuPH20, recombinant human hyaluronidase PH20 enzyme; SCLC, small cell lung carcinoma; TIGIT, T cell immunoglobulin and ITIM domain; TIM, T-cell immunoglobulin and mucin domain-3; TNBC, triple negative breast cancer; TNFRSF9, tumor necrosis factor receptor superfamily member 9; VEGF, vascular endothelial growth factor; VISTA, V-domain immunoglobulin suppressor of T cell activation.*

Regimens: *mFOLFOX, oxaliplatin 85 mg/m^2 intravenous (IV), leucovorin 400 mg/m^2 IV, and fluorouracil 2400 mg/m^2 IV over 46–48 h every 2 weeks (Q2W) FOLFIRI, irinotecan 180 mg/m^2 IV, leucovorin 400 mg/m^2 IV, and 5-FU 2400 mg/m^2 IV over 46–48 h (Q2W).*

[a]*Chemotherapy: carboplatin/pemetrexed, carboplatin/nab-paclitaxel, or carboplatin/paclitaxel.*

Recently, several studies have highlighted that TIGIT is co-expressed and associated with PD-1 expression (Johnston et al., 2014; Chauvin et al., 2015). Dual blockade of TIGIT and PD-1 resulted in the restoration of T-cell immunity in preclinical settings and provided a rationale for combination with these agents as a feasible anti-cancer therapeutic strategy (Johnston et al., 2014; Kurtulus et al., 2015; Zhang et al., 2018).

Clinical Trials on TIGIT

Among the 10 anti-TIGIT mAbs undergoing clinical trials, one of the most promising agents is tiragolumab (GO30103) (**Table 2**). In a randomized, double-blind, phase 2 trial, 135 treatment-naïve patients with unresectable and metastatic NSCLC, positive for PD-L1 expression, were treated with tiragolumab (or placebo) in combination with atezolizumab (anti-PD-L1) (NCT03563716) (Rodriguez-Abreu et al., 2020). Primary analysis of CITYSCAPE showed that the result was significant and durable, especially in patients with a PD-L1 tumor proportion score (TPS) ≥50% in the tiragolumab and atezolizumab groups, with an ORR of 31.3 vs. 16.2% and median PFS of 5.4 and 3.6 months in the combination treatment and atezolizumab monotherapy, respectively (hazard ratio 0.57, 95% confidence interval [CI] 0.37–0.90). The combination was well tolerated and had acceptable safety profiles. The positive and robust results of this trial prompted initiation of phase III in select patients with high PD-L1 expression (SKYSCRAPER-1, NCT04294810). Furthermore, the combination was supplemented with chemotherapy in chemotherapy-naive extensive stage SCLC (SKYSCRAPER-2, NCT04256421). Phase 1 and 2 clinical trials on tiragolumab are also ongoing for esophageal and gastric cancers (NCT03281369) in metastatic settings.

Vibostolimab (MK-7684) is also an anti-TIGIT mAb. The preliminary results of a phase 1 dose-finding study of vibostolimab (200 or 210 mg) with pembrolizumab (200 mg) on day 1 of each Q3W cycle administered to patients with advanced/metastatic solid tumors without prior anti-PD-1/PD-1, showed acceptable toxicity profiles (NCT02964013) (Niu et al., 2020). The ORR and median PFS were 29% and 5.4 months for all patients, and 46% and 8.4 months for 13 patients with TPS ≥1%, respectively. The effects of vibostolimab are also being investigated in melanoma, in combination with other agents (NCT04305054, NCT04305041, and NCT04303169).

Other anti-TIGIT mAbs under investigation include BMS-986207 (NCT02913313 and NCT04570839), domvanalimab (AB-154) (NCT03628677 and NCT04262856), ASP-8374 (NCT03945253 and NCT03260322), IBI939 (NCT04353830, NCT04672369, and NCT04672356), BGB-A1217 (NCT04047862), COM902 (NCT04354246), and M6223 (NCT04457778) as monotherapy or in combination with other agents in the treatment of refractory solid tumors. These agents are being tested in phase 1/2 trials and the results are awaited.

TIM-3

TIM-3, previously known as hepatitis A virus cellular receptor 2 (HAVCR2), is a member of the TIM gene family, encoding proteins such as TIM-1 and TIM-4 (**Table 1**) (Monney et al., 2002). It is structured with type-1 cell surface glycoproteins, an extracellular Ig variable region (IgV)-like domain, a mucin-like and transmembrane domain, and an intracellular cytoplasmic tail composed of five tyrosine residues (Monney et al., 2002). Once the two tyrosine residues, Y265 and 272, are phosphorylated by Src kinases or interleukin inducible T cell kinase, the downstream signaling of TIM-3 is activated (van de Weyer et al., 2006; Nagahara et al., 2008).

TIM-3 is expressed in tumor cells and immune cells, such as helper T cells (Th1), IL-17-producing $CD4^+$ effector cell lineage (Th17), $CD8^+$ T cells, Tregs, TILs, and innate immune cells (Monney et al., 2002; Huang et al., 2010; Jan et al., 2011; Anderson, 2012). Four ligands bind to TIM-3: two soluble ligands, high-mobility group protein B1 (HMGB1) and galectin-9, and two surface ligands, including carcinoembryonic antigen cell adhesion molecule 1 (ceacam-1) and phosphatidyl serine (PtdSer) (Zhu et al., 2005; Nakayama et al., 2009; Chiba et al., 2012; Huang et al., 2015; Kang et al., 2015). Interaction of TIM-3 with its ligands has been shown to induce T cell inhibition. TIM-3 is unique compared to other immune checkpoints in that its upregulation is initiated only by $CD4^+$ and $CD8^+$ cells that produce IFN-γ (Sakuishi et al., 2010; Gao et al., 2012).

Similar to PD-L1, TIM-3 is expressed in TILs is associated with disease progression in certain cancers (Ngiow et al., 2011). Meta-analysis of TIM-3 overexpression in solid tumors has shown that higher TIM-3 expression is associated with worse OS and may potentially be a prognostic marker (Zhang et al., 2017). Blocking TIM-3 expression results in T cell proliferation and cytokine production, thereby eliciting immune activation (Gao et al., 2012). In addition, targeting TIM-3 with PD-1 in preclinical settings has shown a synergistic effect by reinvigorating T cell function and increasing anti-tumor immunity (Sakuishi et al., 2010; Koyama et al., 2016). Thus, the dual blockade of PD-1 and TIM-3 is a feasible and promising therapeutic option.

Clinical Trials on TIM-3

There are seven anti-TIM-3 mAbs and one anti-PD-1 and TIM-3 bispecific Ab (RO7121661) undergoing clinical trials (**Table 2**). Sym021 (anti-PD-1), sym022 (anti-LAG-3), and sym023 (anti-TIM-3) were evaluated as single agents or combinations in phase 1 trials for solid tumors or lymphomas (NCT03311412, NCT03489369, and NCT03489343) (Lakhani et al., 2020). Sym023 monotherapy (n = 24) and in combination with Sym021 (n = 17) was administered; however, Sym023 and its combination did not reach their MTD. One patient in the monotherapy group had grade 3–4 immune-mediated arthritis. Overall, monotherapy and combination therapy were well tolerated, with two PRs observed in the combination group.

LY3321367 is also an anti-TIM-3 mAb; an interim analysis of a phase 1a/1b, dose-escalation and -expansion study showed that intravenous infusion of 3–1200 mg LY3321367 Q2W monotherapy (Arm A, 23 patients) or 70–1200 mg LY3321367

+ 200–700 mg LY3300054 (anti-PD-L1) Q2W combination therapy (Arm B, 18 patients) was well tolerated in the treatment of refractory solid tumors; further, no DLT was observed and most TRAEs observed were grade ≤2 (NCT03099109) (Harding et al., 2019). Two patients in arm A showed >20% tumor reduction. Overall, there was no effect on the pharmacokinetics, and the antidrug antibody titers were low; thus, Eli Lily dropped the agent from its pipeline.

Other investigational agents targeting TIM-3 include cobolimab (TSR-022), sabatolimab, INCAGN2390, BMS-986258, SHR-1702, and RO7121661, which are currently ongoing clinical trials. Cobolimab is administered in combination with chemotherapy, targeted agents, or immune checkpoints in solid tumors (NCT02817633, NCT03307785, NCT03680508, and NCT04139902). Sabatolimab (MBG453) is administered with other agents in solid tumors (NCT02608268 and NCT03961971) or in acute myeloid lymphoma (AML) (NCT04623216), high-risk myelodysplastic syndrome (MDS) (NCT03066648, NCT03940352, and NCT03946670), and chronic myelogenous leukemia (CML) (NCT04266301). In solid tumors, INCAGN2390 is administered as a monotherapy (NCT03652077), BMS-986258 is administered in combination with nivolumab or rHuPH20 (NCT03446040), SHR-1702 is administered with or without camrelizumab, an anti-PD-1 agent (NCT03871855), and RO7121661, a TIM-3 bispecific Ab, is administered as a monotherapy (NCT03708328).

B7-H3

B7-H3, also called CD276, is a member of the B7 family. It was initially recognized as a co-stimulatory molecule that activates T cells and IFN-γ production (**Table 1**) (Chapoval et al., 2001). B7-H3 is found in activated immune cells such as antigen-presenting cells (APCs), NK cells, T cells, and monocytes (Janakiram et al., 2017). In addition, B7-H3 is expressed in several tumors. Notably, high levels of B7-H3 expression in NSCLC, RCC, CRC, and prostate cancer are correlated with disease progression (Li et al., 2014; Jin et al., 2015; Benzon et al., 2017; Mao et al., 2017). In NSCLC, B7-H3 with Tregs was associated with poor prognosis, and co-expression of B7-H3 and CD14 was found to play a role in angiogenesis and tumor progression in RCC (Li et al., 2014; Jin et al., 2015). Patients with CRC, harboring B7-H3 and CD133 expression, have shorter survival (Castellanos et al., 2017). Similarly, high levels of B7-H3 are associated with higher Gleason grade, advanced stage, and poor outcomes in prostate cancer (Benzon et al., 2017).

Recently, the co-inhibitory function of B7-H3 in $CD4^+$ and $CD8^+$ T cells was discovered (Suh et al., 2003; Prasad et al., 2004). Studies are ongoing to identify the receptor for B7-H3, and the contradictory roles of B7-H3 in immune activity are yet to be fully elucidated (Yang et al., 2020). In addition to the immunological aspects of B7-H3, other signaling pathways, including PI3K/AKT/mTOR, JAK2/STAT3, and TLR4/NF-κB signaling, can activate B7-H3 expression (Kang et al., 2015; Zhang et al., 2015; Xie et al., 2016; Fan et al., 2017; Zhang et al., 2017). Other studies have highlighted that B7-H3 is associated with resistance to chemotherapy and targeted agents (Liu et al., 2011; Jiang et al., 2016; Flem-Karlsen et al., 2017; Flem-Karlsen et al., 2019).

Clinical Trials on B7-H3

Eleven agents targeting B7-H3 are currently under investigation in clinical trials (**Table 2**). Generally, patients harboring B7-H3 are enrolled in clinical trials. Enoblituzumab (MGA271), an anti-B7-H3 mAb with antibody-dependent cellular toxicity (ADCC) function, has been investigated in multiple solid tumors, including pediatric tumors. Interim analysis of enoblituzumab in refractory solid tumors revealed that it was well tolerated up to 15 mg/kg, with no DLT and MTD (Powderly et al., 2015). Although TRAEs, such as fatigue (30%) and infusion-related reactions (26%), occurred in 71% of the patients, most of these AEs were tolerated with adequate supportive care (NCT01391143). Enoblituzumab is currently being used as a monotherapy or in combination with anti-PD-1 antibody (retifanlimab or pembrolizumab), tebotelimab, a PD-1 and LAG-3 bispecific DART, or ipilimumab, as shown in **Table 3**.

DS-7300a is a B7-H3-targeting antibody drug conjugate (ADC) with DXd, a payload that is an exatecan derivative, which inhibits topoisomerase I (Bendell et al., 2020). The phase 1/II study is ongoing with patients enrolled in the dose-escalation part (NCT04145622). Orlotamab (MGD009) is a B7-H3 and CD3 DART protein, and its monotherapy (NCT02628535) and combination with retifanlimab (NCT03406949) are under investigation in heavily treated solid tumors. Orlotamab with radioactive labeling such as 131I-Omburtamab (NCT01099644, NCT00089245, and NCT03275402), 124I-Omburtamab (NCT01502917), and 177Lu-DTPA-Omburtamab (NCT04167618 and NCT04315246) are also ongoing trials. In patients with desmoplastic small round cell tumor (DSRCT), treatment with 131I-Omburtamab via intraperitoneal administration followed by external beam intensity-modulated whole-abdominopelvic radiotherapy (WAP-IMRT) to 3,000 cGy was tolerable with a satisfactory safety profile, and appeared to demonstrate micro-metastatic activity in a phase 1 trial (Modak et al., 2018). The biodistribution, organ, and whole-body exposure were measured with 124I-8H9-directed radioimmuno-PET, and the RP2D for 131I-Omburtamab was set at 80 mCi/m^2.

Other investigational agents include chimeric antigen receptor (CAR) T cell therapy targeting B7-H3: 4SCAR-276 in solid tumors (NCT04432649), SCRI-CARB7H3 in pediatric CNS tumors (NCT04185038), B7-H3 chimeric antigen receptor T cells (CAR-T) treated alone (NCT04385173) or with temozolamide (NCT04077866) in glioblastoma, CAR.B7-H3 with other agents in epithelial ovarian cancer (NCT04670068), and second-generation 4-1BBζ B7H3-EGFRt-DHFR in non-primary CNS solid tumors (NCT04483778).

VISTA

VISTA has several names such as differentiation of embryonic stem cells 1 (Dies1), DD1 α, Gi24, and B7H5 (**Table 1**). (Ceeraz

et al., 2013). Notably, it is also named PD-1 homologue (PD-1H), as its extracellular domain shows structural similarity to PD-1; however, it is different, as it lacks the classical ITIM or ITSM motif in the cytoplasmic domain (Flies et al., 2011). Furthermore, VISTA differs from PD-1, which functions in the effector stage, as VISTA is expressed on resting T cells, indicating its regulatory role in earlier stages (Kondo et al., 2016). Compared to that in peripheral lymph nodes, VISTA is more abundant in myeloid-derived suppressor cells (MDSCs) in the tumor microenvironment (TME) (Le Mercier et al., 2014).

High levels of VISTA are expressed by mature APCs with CD11b, whereas relatively low expression is found on Tregs, $CD8^+$, $CD4^+$, and TILs (Lines et al., 2014). Although the counter structures for VISTA have not been comprehensively elucidated, recent *in vitro* findings on V-Set and immunoglobulin domain containing 3 (VSIG-3) have shown that VISTA also acts as a co-inhibitory ligand on tumor cells (Wang et al., 2019). VISTA promotes Treg maturation and prevents T cell activation independent of PD-1 expression (Yoon et al., 2015; Torphy et al., 2017; Popovic et al., 2018). The non-overlapping mechanisms of VISTA and PD-L1 make their combination an ideal treatment strategy to overcome immune suppression. In mouse models, dual blockade of VISTA and PD-1, using monoclonal antibodies specific for these immune checkpoints, led to synergistic activity against T-cells with anti-tumor responses (Liu et al., 2015).

A wide array of tumors has been studied to determine the prognostic and predictive roles of VISTA. High-grade serous ovarian cancer patients with tumor cells expressing VISTA showed longer PFS and OS (Zong et al., 2020). Furthermore, VISTA expression on TILs in pT1/2 esophageal adenocarcinoma was associated with improved OS compared to the TILs negative for VISTA (Loeser et al., 2019). Similarly, $VISTA^+$ and $CD8^+$ TIL subtypes are associated with better OS in HCC (Zhang et al., 2018). Contrary to these findings, $VISTA^+$ and $CD8^+$ TIL subtypes were associated with worse prognosis in oral squamous cell carcinoma and cutaneous melanoma with VISTA expression, whereas VISTA had no correlation with survival outcome in GC expressing VISTA(Böger et al., 2017; Wu et al., 2017; Kuklinski et al., 2018).

Clinical Trials on VISTA

Ongoing clinical trials on VISTA include two anti-VISTA mAbs and one small-molecule antagonist of VISTA (**Table 2**). JNJ-61610588 (NCT02671955) and CI-8993 (NCT04475523) are anti-VISTA mAbs, currently under investigation in phase 1 trials for the treatment of refractory solid tumors. CA-170 is a small molecule that targets both VISTA and PD-L1 (Musielak et al., 2019). A phase 1 study in patients with advanced solid tumors or lymphomas showed no DLT during dose escalation in 19 patients treated across six dose levels (50–800 mg) (NCT02812875) (Powderly et al., 2017). Exploratory analysis showed an increased proportion of both circulating $CD8^+$ and $CD4^+$ cells after oral dosing with CA-170. Further data on dose escalation, the recommended phase 2 dose, and anti-tumor responses are awaiting results.

ICOS

ICOS, also known as cluster of differentiation 278 (CD278) in T cells, is a member of the CD28 coreceptor family, which includes costimulatory CD28 and coinhibitory receptor CTLA-4 (**Table 1**) (Hutloff et al., 1999). The ICOS ligand (ICOSL) is expressed in APCs such as macrophages, DCs, and B cells (Yoshinaga et al., 1999). In contrast to the expression of CD28 in both naive and memory T cells, the majority of ICOS is expressed only after the activation of memory T cells, with only small fractions expressed in resting memory T cells. Further, unlike CD28 and CTLA-4 ligands, which are expressed primarily on lymphoid tissues, ICOSL is expressed in non-lymphoid cells, such as endothelial cells, epithelial cells, mesenchymal cells, and fibroblasts, via the activation of tumor necrosis factor-α (Swallow et al., 1999; Khayyamian et al., 2002; Martin-Orozco et al., 2010). Activation of the ICOS pathway induces the production of cytokines, such as IL-4, IL-10, and IL-21, by $CD4^+$ Th cells, $CD4^+$ forkhead box P3 ($FoxP3^+$) Tregs, and $CD8^+$ cytotoxic T lymphocytes (CTL) (Hutloff et al., 1999; Gigoux et al., 2009; Solinas et al., 2020). ICOS interacts with its ligand (ICOSL) to increase anti-tumor effects via the regulation of memory and effector T cell development and humoral immune responses (Marinelli et al., 2018). The rationale for targeting the ICOS/ICOSL axis with agonists and antagonists is its capacity to trigger both anti-tumor T cell responses by Th1 and other effector T cells, as well as its protumor responses via Tregs (Solinas et al., 2020).

In preclinical studies, ICOS expression on $FoxP3^+$ Tregs and other Th subsets has been identified in multiple arrays of solid tumors, including melanoma, gastric, colorectal, and breast cancers (Strauss et al., 2008; Zhang et al., 2016; Gu-Trantien et al., 2017; Nagase et al., 2017). $ICOS^+$ Treg TILs have been found to be associated with worse survival in GC, whereas high levels of ICOS in Th1 TILs in colorectal cancer indicated better survival outcomes (Zhang et al., 2016; Nagase et al., 2017). Dual blockade of ICOS with anti-CTLA-4 has been effective in eliciting anti-tumor responses in ICOS knockout mice that were unresponsive to anti-CTLA-4 monotherapy (Fu et al., 2011; Fan et al., 2014). More importantly, the utilization of ICOS-targeted agents is gaining attention in hematological malignancies owing to the enhancement of co-stimulatory receptor 4-1BB in $CD4^+$ CAR T cells by ICOS (Guedan et al., 2018).

Clinical Trials on ICOS

Currently, both anti-ICOS agonists and anti-ICOS antagonists are under clinical investigation (**Table 2**). The phase 1 trial of GSK3359609 (INDUCE-1), a humanized anti-ICOS agonist monoclonal antibody, comprised two treatment groups: part 1 patients were treated with a monotherapy of GSK3359609, and part 2 patients were

administered a combination with pembrolizumab or other immunotherapy in the treatment of advanced solid tumors. The study is ongoing, with no dose-limiting toxicities from the first three dose-limiting cohorts (Angevin et al., 2017). In head and neck cancer, the efficacy of GSK3359609 and pembrolizumab with or without platinum-based chemotherapy is currently under investigation (NCT04428333 and NCT04128696).

Another investigational anti-ICOS agonist monoclonal antibody is JTX-2011, used in combination with either anti-PD1 (pembrolizumab or nivolumab) or anti-CTLA-4 (ipilimumab) in advanced solid tumors (NCT02904226) (Yap et al., 2018). In phase 1/II of the trial, anti-tumor activity was observed with JTX-2011 monotherapy and in combination with nivolumab, in heavily treated GC and TNBC with manageable toxicity profiles. Exploratory analysis showed that the peripheral blood CD4 $ICOS^{high}$ T cell subsets may be a potential biomarker for the response.

Further, agonistic antibodies such as MEDI-570 alone and KY1044 with atezolizumab are under investigation in phases 1 and phase 1/II, respectively (NCT02520791 and NCT03829501).

BTLA

BTLA (CD272) is also a member of the CD28 coreceptor family (**Table 1**) (Ceeraz et al., 2013). It is a co-inhibitory molecule with a structure and function similar to those of PD-1 and CTLA-4 (Paulos and June, 2010). When expressed on mature lymphocytes, such as B cells and T cells, macrophages, and DCs, BTLA binds to herpes virus entry mediator (HVEM), a member of the tumor necrosis factor receptor superfamily (TNFRSF), as well as to LIGHT and lymphotoxin-α, two members of the tumor necrosis factor (TNF) superfamily (Han et al., 2004; Sedy et al., 2005; Steinberg et al., 2011). Binding of BTLA to HVEM via CD160 transmits inhibitory signals to T cells, which are necessary for proliferation and cytokine production, whereas binding to LIGHT induces co-stimulatory signals (Sedy et al., 2005; Murphy et al., 2006; Cai et al., 2008). Thus, the complexity of the BTLA receptor and ligand activity poses a challenge for BTLA blockade treatment.

Recently, the possibility of BTLA as a potential therapeutic target in cancer immunotherapy has been established *in vivo,* wherein human melanoma tumor antigen-specific effector $CD8^+$ T cells expressing high levels of BTLA were downregulated with a vaccine formulated using CpG oligodeoxynucleotides, a toll-like receptor 9 (TLR9) agonist that triggers innate immunity, thereby proving that inhibition of BTLA may partially reverse the function of human $CD8^+$ cancer-specific T cells (Derré et al., 2010; Paulos and June, 2010).

Clinical Trials on BTLA

There are four agents targeting BTLA (**Table 2**): 1) INBRX-106, a hexavalent OX40 agonist Ab (NCT04198766), 2) PF-04518600 (NCT02315066), an OX40 agonist; 3) cudarolimab (IBI101) (NCT03758001), an anti-OX40 mAb, and 4) TAB004 (JS004) (NCT04278859), an anti-BTLA mAb. These agents target the OX40 receptor, also known as CD134 and tumor necrosis factor receptor superfamily member 4 (TNFRSF4), thereby preventing its interaction with BTLA (Croft et al., 2009). These phase 1 clinical trials are ongoing as monotherapy for patients with advanced/metastatic solid tumors and are awaiting results. TAB004 is also under investigation for the treatment of refractory lymphomas (NCT04137900 and NCT04477772).

CONCLUSION

Cancer immunotherapy is one of the major pillars in the field of medical oncology, especially for the treatment of unresectable, metastatic, and recurrent cancers. The success of ICIs, such as anti-CTLA-4 and anti-PD-1/PD-L1, in combination with chemotherapy, immunotherapy, and targeted agents, has changed the paradigm of cancer treatment. Nonetheless, the limited efficacy and IRAEs of ICIs have paved way for the discovery of novel checkpoints. Among the immune checkpoint inhibitors, anti-LAG-3 and anti-TIGIT are promising targets, and their efficacy in combination with anti-PD-1/PD-L1 may help overcome the limitations seen in prior treatments. More robust data are yet to follow on agents targeting TIM-3, B7-H3, VISTA, ICOS, and BTLA.

AUTHOR CONTRIBUTIONS

All authors listed have made a substantial, direct, and intellectual contribution to the work and approved it for publication.

FUNDING

This work was supported by National Research Foundation of Korea (NRF) grants funded by the Korean Government (MSIT) (NRF-2017M3A9E9072669, 2017M3A9E8029717, NRF-2019M3A9B6065231, 2019M3A9B6065221, 2018R1A2A1A05076997, 2017R1A5A1014560).

REFERENCES

Anderson, A. C., Joller, N., and Kuchroo, V. K. (2016). Lag-3, Tim-3, and TIGIT: Co-inhibitory Receptors with Specialized Functions in Immune Regulation. *Immunity* 44, 989–1004. doi:10.1016/j.immuni.2016.05.001

Anderson, A. C. (2012). Tim-3, a Negative Regulator of Anti-tumor Immunity. *Curr. Opin. Immunol.* 24, 213–216. doi:10.1016/j.coi.2011.12.005

Andreae, S., Piras, F., Burdin, N., and Triebel, F. (2002). Maturation and Activation of Dendritic Cells Induced by Lymphocyte Activation Gene-3 (CD223). *J. Immunol.* 168, 3874–3880. doi:10.4049/jimmunol.168.8.3874

Andrews, L. P., Marciscano, A. E., Drake, C. G., and Vignali, D. A. (2017). LAG3 (CD223) as a Cancer Immunotherapy Target. *Immunol. Rev.* 276, 80–96. doi:10.1111/imr.12519

Angevin, E., Barnette, M. S., Bauer, T. M., Cho, D. C., Ellis, C. E., Gan, H. K., et al. (2017). INDUCE-1: A Phase I Open-Label Study of GSK3359609, an ICOS Agonist Antibody, Administered Alone and in Combination with Pembrolizumab in Patients with Advanced Solid Tumors. *Jco* 35, TPS3113. doi:10.1200/JCO.2017.35.15_suppl.TPS3113

Atkinson, V., Khattak, A., Haydon, A., Eastgate, M., Roy, A., Prithviraj, P., et al. (2020). Eftilagimod Alpha, a Soluble Lymphocyte Activation Gene-3 (LAG-3) Protein Plus Pembrolizumab in Patients with Metastatic Melanoma. *J. Immunother. Cancer* 8, e001681. doi:10.1136/jitc-2020-001681

Baixeras, E., Huard, B., Miossec, C., Jitsukawa, S., Martin, M., Hercend, T., et al. (1992). Characterization of the Lymphocyte Activation Gene 3-encoded Protein. A New Ligand for Human Leukocyte Antigen Class II Antigens. *J. Exp. Med.* 176, 327–337. doi:10.1084/jem.176.2.327

Barbari, C., Fontaine, T., Parajuli, P., Lamichhane, N., Jakubski, S., Lamichhane, P., et al. (2020). Immunotherapies and Combination Strategies for Immuno-Oncology. *Ijms* 21, 5009. doi:10.3390/ijms21145009

Baumeister, S. H., Freeman, G. J., Dranoff, G., and Sharpe, A. H. (2016). Coinhibitory Pathways in Immunotherapy for *Cancer. Annu. Rev. Immunol.* 34, 539–573. doi:10.1146/annurev-immunol-032414-112049

Bendell, J. C., Doi, T., Patel, M. R., Piha-Paul, S. A., Sen, S., Shimizu, T., et al. (2020). A Phase I/II, Two-Part, Multicenter, First-In-Human Study of DS-7300a in Patients with Advanced Solid Malignant Tumors. *Jco* 38, TPS3646. doi:10.1200/JCO.2020.38.15_suppl.TPS3646

Bendell, J., Ulahannan, S. V., Chu, Q., Patel, M., George, B., Auguste, A., et al. (2020). Abstract 779: A Phase I Study of BI 754111, an Anti-LAG-3 Monoclonal Antibody (mAb), in Combination with BI 754091, an Anti-PD-1 mAb: Biomarker Analyses from the Microsatellite Stable Metastatic Colorectal Cancer (MSS mCRC) Cohort. *Cancer Res.* 80, 779. doi:10.1158/1538-7445.Am2020-779

Benzon, B., Zhao, S. G., Haffner, M. C., Takhar, M., Erho, N., Yousefi, K., et al. (2017). Correlation of B7-H3 with Androgen Receptor, Immune Pathways and Poor Outcome in Prostate Cancer: an Expression-Based Analysis. *Prostate Cancer Prostatic Dis.* 20, 28–35. doi:10.1038/pcan.2016.49

Bever, K. M., Wang, H., Durham, J. N., Petrie, S., Hoare, J., Wilt, C., et al. (2020). Phase II Study of Nivolumab and Relatlimab in Advanced Mismatch Repair Deficient (dMMR) Cancers Resistant to Prior PD-(L)1 Inhibition. *Jco* 38, TPS839. doi:10.1200/JCO.2020.38.4_suppl.TPS839

Böger, C., Behrens, H.-M., Krüger, S., and Röcken, C. (2017). The Novel Negative Checkpoint Regulator VISTA Is Expressed in Gastric Carcinoma and Associated with PD-L1/pd-1: A Future Perspective for a Combined Gastric Cancer Therapy? *Oncoimmunology* 6, e1293215. doi:10.1080/2162402X.2017.1293215

Boles, K. S., Vermi, W., Facchetti, F., Fuchs, A., Wilson, T. J., Diacovo, T. G., et al. (2009). A Novel Molecular Interaction for the Adhesion of Follicular CD4 T Cells to Follicular DC. *Eur. J. Immunol.* 39, 695–703. doi:10.1002/eji.200839116

Boutros, C., Tarhini, A., Routier, E., Lambotte, O., Ladurie, F. L., Carbonnel, F., et al. (2016). Safety Profiles of Anti-CTLA-4 and Anti-PD-1 Antibodies Alone and in Combination. *Nat. Rev. Clin. Oncol.* 13, 473–486. doi:10.1038/nrclinonc.2016.58

Buisson, S., and Triebel, F. (2005). LAG-3 (CD223) Reduces Macrophage and Dendritic Cell Differentiation from Monocyte Precursors. *Immunology* 114, 369–374. doi:10.1111/j.1365-2567.2004.02087.x

Cai, G., Anumanthan, A., Brown, J. A., Greenfield, E. A., Zhu, B., and Freeman, G. J. (2008). CD160 Inhibits Activation of Human CD4+ T Cells through Interaction with Herpesvirus Entry Mediator. *Nat. Immunol.* 9, 176–185. doi:10.1038/ni1554

Cameron, F., Whiteside, G., and Perry, C. (2011). Ipilimumab. *Drugs* 71, 1093–1104. doi:10.2165/11594010-000000000-00000

Camisaschi, C., Casati, C., Rini, F., Perego, M., De Filippo, A., Triebel, F., et al. (2010). LAG-3 Expression Defines a Subset of CD4+CD25highFoxp3+ Regulatory T Cells that Are Expanded at Tumor Sites. *J. Immunol.* 184, 6545–6551. doi:10.4049/jimmunol.0903879

Castellanos, J. R., Purvis, I. J., Labak, C. M., Guda, M. R., Tsung, A. J., Velpula, K. K., et al. (2017). B7-H3 Role in the Immune Landscape of Cancer. *Am. J. Clin. Exp. Immunol.* 6, 66–75.

Ceeraz, S., Nowak, E. C., and Noelle, R. J. (2013). B7 Family Checkpoint Regulators in Immune Regulation and Disease. *Trends Immunology* 34, 556–563. doi:10.1016/j.it.2013.07.003

Chapoval, A. I., Ni, J., Lau, J. S., Wilcox, R. A., Flies, D. B., Liu, D., et al. (2001). B7-H3: A Costimulatory Molecule for T Cell Activation and IFN-γ Production. *Nat. Immunol.* 2, 269–274. doi:10.1038/85339

Chauvin, J.-M., Pagliano, O., Fourcade, J., Sun, Z., Wang, H., Sander, C., et al. (2015). TIGIT and PD-1 Impair Tumor Antigen-specific CD8+ T Cells in Melanoma Patients. *J. Clin. Invest.* 125, 2046–2058. doi:10.1172/JCI80445

Chiba, S., Baghdadi, M., Akiba, H., Yoshiyama, H., Kinoshita, I., Dosaka-Akita, H., et al. (2012). Tumor-infiltrating DCs Suppress Nucleic Acid-Mediated Innate Immune Responses through Interactions between the Receptor TIM-3 and the Alarmin HMGB1. *Nat. Immunol.* 13, 832–842. doi:10.1038/ni.2376

Croft, M., So, T., Duan, W., and Soroosh, P. (2009). The Significance of OX40 and OX40L to T-Cell Biology and Immune Disease. *Immunological Rev.* 229, 173–191. doi:10.1111/j.1600-065X.2009.00766.x

Darvin, P., Toor, S. M., Sasidharan Nair, V., and Elkord, E. (2018). Immune Checkpoint Inhibitors: Recent Progress and Potential Biomarkers. *Exp. Mol. Med.* 50, 1–11. doi:10.1038/s12276-018-0191-1

Derré, L., Rivals, J.-P., Jandus, C., Pastor, S., Rimoldi, D., Romero, P., et al. (2010). BTLA Mediates Inhibition of Human Tumor-specific CD8+ T Cells that Can Be Partially Reversed by Vaccination. *J. Clin. Invest.* 120, 157–167. doi:10.1172/JCI40070

Dirix, L., and Triebel, F. (2019). AIPAC: a Phase IIb Study of Eftilagimod Alpha (IMP321 or LAG-3Ig) Added to Weekly Paclitaxel in Patients with Metastatic Breast Cancer. *Future Oncol.* 15, 1963–1973. doi:10.2217/fon-2018-0807

Fan, T.-F., Deng, W.-W., Bu, L.-L., Wu, T.-F., Zhang, W.-F., and Sun, Z.-J. (2017). B7-H3 Regulates Migration and Invasion in Salivary Gland Adenoid Cystic Carcinoma via the JAK2/STAT3 Signaling Pathway. *Am. J. Transl Res.* 9, 1369–1380.

Fan, X., Quezada, S. A., Sepulveda, M. A., Sharma, P., and Allison, J. P. (2014). Engagement of the ICOS Pathway Markedly Enhances Efficacy of CTLA-4 Blockade in Cancer Immunotherapy. *J. Exp. Med.* 211, 715–725. doi:10.1084/jem.20130590

Feeney, K., Kelly, R., Lipton, L. R., Chao, J., Acosta-Rivera, M., Earle, D., et al. (2019). CA224-060: A Randomized, Open Label, Phase II Trial of Relatlimab (Anti-LAG-3) and Nivolumab with Chemotherapy versus Nivolumab with Chemotherapy as First-Line Treatment in Patients with Gastric or Gastroesophageal Junction Adenocarcinoma. *Jco* 37, TPS4143. doi:10.1200/JCO.2019.37.15_suppl.TPS4143

Flem-Karlsen, K., Tekle, C., Andersson, Y., Flatmark, K., Fodstad, Ø., and Nunes-Xavier, C. E. (2017). Immunoregulatory Protein B7-H3 Promotes Growth and Decreases Sensitivity to Therapy in Metastatic Melanoma Cells. *Pigment Cel Melanoma Res.* 30, 467–476. doi:10.1111/pcmr.12599

Flem-Karlsen, K., Tekle, C., Øyjord, T., Flørenes, V. A., Mælandsmo, G. M., Fodstad, Ø., et al. (2019). p38 MAPK Activation through B7-H3-Mediated DUSP10 Repression Promotes Chemoresistance. *Sci. Rep.* 9, 5839. doi:10.1038/s41598-019-42303-w

Flies, D. B., Wang, S., Xu, H., and Chen, L. (2011). Cutting Edge: A Monoclonal Antibody Specific for the Programmed Death-1 Homolog Prevents Graft-Versus-Host Disease in Mouse Models. *J. Immunol.* 187, 1537–1541. doi:10.4049/jimmunol.1100660

Fu, T., He, Q., and Sharma, P. (2011). The ICOS/ICOSL Pathway Is Required for Optimal Antitumor Responses Mediated by Anti-CTLA-4 Therapy. *Cancer Res.* 71, 5445–5454. doi:10.1158/0008-5472.Can-11-1138

Fuhrman, C. A., Yeh, W.-I., Seay, H. R., Saikumar Lakshmi, P., Chopra, G., Zhang, L., et al. (2015). Divergent Phenotypes of Human Regulatory T Cells Expressing the Receptors TIGIT and CD226. *J. Immunol.* 195, 145–155. doi:10.4049/jimmunol.1402381

Gandhi, L., Rodríguez-Abreu, D., Gadgeel, S., Esteban, E., Felip, E., De Angelis, F., et al. (2018). Pembrolizumab Plus Chemotherapy in Metastatic Non-small-cell Lung *Cancer. N. Engl. J. Med.* 378, 2078–2092. doi:10.1056/NEJMoa1801005

Gao, X., Zhu, Y., Li, G., Huang, H., Zhang, G., Wang, F., et al. (2012). TIM-3 Expression Characterizes Regulatory T Cells in Tumor Tissues and Is Associated with Lung Cancer Progression. *PloS one* 7, e30676. doi:10.1371/journal.pone.0030676

Gigoux, M., Shang, J., Pak, Y., Xu, M., Choe, J., Mak, T. W., et al. (2009). Inducible Costimulator Promotes Helper T-Cell Differentiation through Phosphoinositide 3-kinase. *Proc. Natl. Acad. Sci.* 106, 20371–20376. doi:10.1073/pnas.0911573106

Goding, S. R., Wilson, K. A., Xie, Y., Harris, K. M., Baxi, A., Akpinarli, A., et al. (2013). Restoring Immune Function of Tumor-specific CD4+ T Cells during Recurrence of Melanoma. *J. Immunol.* 190, 4899–4909. doi:10.4049/jimmunol.1300271

Gu-Trantien, C., Migliori, E., Buisseret, L., de Wind, A., Brohée, S., Garaud, S., et al. (2017). CXCL13-producing TFH Cells Link Immune Suppression and Adaptive Memory in Human Breast Cancer. *JCI Insight* 2. doi:10.1172/jci.insight.91487

Guedan, S., Posey, A. D., Jr., Shaw, C., Wing, A., Da, T., Patel, P. R., et al. (2018). Enhancing CAR T Cell Persistence through ICOS and 4-1BB Costimulation. *JCI Insight* 3, e96976. doi:10.1172/jci.insight.96976

Han, P., Goularte, O. D., Rufner, K., Wilkinson, B., and Kaye, J. (2004). An Inhibitory Ig Superfamily Protein Expressed by Lymphocytes and APCs Is Also an Early Marker of Thymocyte Positive Selection. *J. Immunol.* 172, 5931–5939. doi:10.4049/jimmunol.172.10.5931

Hanahan, D., and Weinberg, R. A. (2011). Hallmarks of Cancer: the Next Generation. *Cell* 144, 646–674. doi:10.1016/j.cell.2011.02.013

Harding, J. J., Patnaik, A., Moreno, V., Stein, M., Jankowska, A. M., Velez de Mendizabal, N., et al. (2019). A Phase Ia/Ib Study of an Anti-TIM-3 Antibody (LY3321367) Monotherapy or in Combination with an Anti-PD-L1 Antibody (LY3300054): Interim Safety, Efficacy, and Pharmacokinetic Findings in Advanced Cancers. *Jco* 37, 12. doi:10.1200/JCO.2019.37.8_suppl.12

Hellmann, M. D., Ciuleanu, T.-E., Pluzanski, A., Lee, J. S., Otterson, G. A., Audigier-Valette, C., et al. (2018). Nivolumab Plus Ipilimumab in Lung *Cancer* with a High Tumor Mutational Burden. *N. Engl. J. Med.* 378, 2093–2104. doi:10.1056/NEJMoa1801946

Huang, C.-T., Workman, C. J., Flies, D., Pan, X., Marson, A. L., Zhou, G., et al. (2004). Role of LAG-3 in Regulatory T Cells. *Immunity* 21, 503–513. doi:10.1016/j.immuni.2004.08.010

Huang, R.-Y., Eppolito, C., Lele, S., Shrikant, P., Matsuzaki, J., and Odunsi, K. (2015). LAG3 and PD1 Co-inhibitory Molecules Collaborate to Limit CD8+ T Cell Signaling and Dampen Antitumor Immunity in a Murine Ovarian Cancer Model. *Oncotarget* 6, 27359–27377. doi:10.18632/oncotarget.4751

Huang, X., Bai, X., Cao, Y., Wu, J., Huang, M., Tang, D., et al. (2010). Lymphoma Endothelium Preferentially Expresses Tim-3 and Facilitates the Progression of Lymphoma by Mediating Immune Evasion. *J. Exp. Med.* 207, 505–520. doi:10.1084/jem.20090397

Huang, Y.-H., Zhu, C., Kondo, Y., Anderson, A. C., Gandhi, A., Russell, A., et al. (2015). CEACAM1 Regulates TIM-3-Mediated Tolerance and Exhaustion. *Nature* 517, 386–390. doi:10.1038/nature13848

Huard, B., Mastrangeli, R., Prigent, P., Bruniquel, D., Donini, S., El-Tayar, N., et al. (1997). Characterization of the Major Histocompatibility Complex Class II Binding Site on LAG-3 Protein. *Proc. Natl. Acad. Sci.* 94, 5744–5749. doi:10.1073/pnas.94.11.5744

Huard, B., Prigent, P., Tournier, M., Bruniquel, D., and Triebel, F. (1995). CD4/major Histocompatibility Complex Class II Interaction Analyzed with CD4- and Lymphocyte Activation Gene-3 (LAG-3)-Ig Fusion Proteins. *Eur. J. Immunol.* 25, 2718–2721. doi:10.1002/eji.1830250949

Huard, B., Tournier, M., Hercend, T., Triebel, F., and Faure, F. (1994). Lymphocyte-activation Gene 3/major Histocompatibility Complex Class II Interaction Modulates the Antigenic Response of CD4+ T Lymphocytes. *Eur. J. Immunol.* 24, 3216–3221. doi:10.1002/eji.1830241246

Hutloff, A., Dittrich, A. M., Beier, K. C., Eljaschewitsch, B., Kraft, R., Anagnostopoulos, I., et al. (1999). ICOS Is an Inducible T-Cell Co-stimulator Structurally and Functionally Related to CD28. *Nature* 397, 263–266. doi:10.1038/16717

Jan, M., Chao, M. P., Cha, A. C., Alizadeh, A. A., Gentles, A. J., Weissman, I. L., et al. (2011). Prospective Separation of Normal and Leukemic Stem Cells Based on Differential Expression of TIM3, a Human Acute Myeloid Leukemia Stem Cell Marker. *Proc. Natl. Acad. Sci.* 108, 5009–5014. doi:10.1073/pnas.1100551108

Janakiram, M., Shah, U. A., Liu, W., Zhao, A., Schoenberg, M. P., and Zang, X. (2017). The Third Group of the B7-CD28 Immune Checkpoint Family: HHLA2, TMIGD2, B7x, and B7-H3. *Immunol. Rev.* 276, 26–39. doi:10.1111/imr.12521

Jiang, B., Liu, F., Liu, Z., Zhang, T., and Hua, D. (2016). B7-H3 Increases Thymidylate Synthase Expression via the PI3k-Akt Pathway. *Tumor Biol.* 37, 9465–9472. doi:10.1007/s13277-015-4740-0

Jin, Y., Zhang, P., Li, J., Zhao, J., Liu, C., Yang, F., et al. (2015). B7-H3 in Combination with Regulatory T Cell Is Associated with Tumor Progression in Primary Human Non-small Cell Lung Cancer. *Int. J. Clin. Exp. Pathol.* 8, 13987–13995.

Johnson, M. L., Patel, M. R., Cherry, M., Kang, Y.-K., Yamaguchi, K., Oh, D.-Y., et al. (2020). Safety of BI 754111, an Anti-LAG-3 Monoclonal Antibody (mAb), in Combination with BI 754091, an Anti-PD-1 mAb, in Patients with Advanced Solid Tumors. *Jco* 38, 3063. doi:10.1200/JCO.2020.38.15_suppl.3063

Johnston, R. J., Comps-Agrar, L., Hackney, J., Yu, X., Huseni, M., Yang, Y., et al. (2014). The Immunoreceptor TIGIT Regulates Antitumor and Antiviral CD8 + T Cell Effector Function. *Cancer cell* 26, 923–937. doi:10.1016/j.ccell.2014.10.018

Joller, N., Lozano, E., Burkett, P. R., Patel, B., Xiao, S., Zhu, C., et al. (2014). Treg Cells Expressing the Coinhibitory Molecule TIGIT Selectively Inhibit Proinflammatory Th1 and Th17 Cell Responses. *Immunity* 40, 569–581. doi:10.1016/j.immuni.2014.02.012

Kang, C.-W., Dutta, A., Chang, L.-Y., Mahalingam, J., Lin, Y.-C., Chiang, J.-M., et al. (2015). Apoptosis of Tumor Infiltrating Effector TIM-3+CD8+ T Cells in Colon Cancer. *Sci. Rep.* 5, 15659. doi:10.1038/srep15659

Kang, F.-b., Wang, L., Jia, H.-c., Li, D., Li, H.-j., Zhang, Y.-g., et al. (2015). B7-H3 Promotes Aggression and Invasion of Hepatocellular Carcinoma by Targeting Epithelial-To-Mesenchymal Transition via JAK2/STAT3/Slug Signaling Pathway. *Cancer Cel Int*. 15, 45. doi:10.1186/s12935-015-0195-z

Khayyamian, S., Hutloff, A., Büchner, K., Gräfe, M., Henn, V., Kroczek, R. A., et al. (2002). ICOS-ligand, Expressed on Human Endothelial Cells, Costimulates Th1 and Th2 Cytokine Secretion by Memory CD4+ T Cells. *Proc. Natl. Acad. Sci.* 99, 6198–6203. doi:10.1073/pnas.092576699

Kisielow, M., Kisielow, J., Capoferri-Sollami, G., and Karjalainen, K. (2005). Expression of Lymphocyte Activation Gene 3 (LAG-3) on B Cells Is Induced by T Cells. *Eur. J. Immunol.* 35, 2081–2088. doi:10.1002/eji.200526090

Kondo, Y., Ohno, T., Nishii, N., Harada, K., Yagita, H., and Azuma, M. (2016). Differential Contribution of Three Immune Checkpoint (VISTA, CTLA-4, PD-1) Pathways to Antitumor Responses against Squamous Cell Carcinoma. *Oral Oncol.* 57, 54–60. doi:10.1016/j.oraloncology.2016.04.005

Kouo, T., Huang, L., Pucsek, A. B., Cao, M., Solt, S., Armstrong, T., et al. (2015). Galectin-3 Shapes Antitumor Immune Responses by Suppressing CD8+ T Cells via LAG-3 and Inhibiting Expansion of Plasmacytoid Dendritic Cells. *Cancer Immunol. Res.* 3, 412–423. doi:10.1158/2326-6066.Cir-14-0150

Kourepini, E., Paschalidis, N., Simoes, D. C., Aggelakopoulou, M., Grogan, J. L., and Panoutsakopoulou, V. (2016). TIGIT Enhances Antigen-specific Th2 Recall Responses and Allergic Disease. *J. Immunol.* 196, 3570–3580. doi:10.4049/jimmunol.1501591

Koyama, S., Akbay, E. A., Li, Y. Y., Herter-Sprie, G. S., Buczkowski, K. A., Richards, W. G., et al. (2016). Adaptive Resistance to Therapeutic PD-1 Blockade Is Associated with Upregulation of Alternative Immune Checkpoints. *Nat. Commun.* 7, 10501. doi:10.1038/ncomms10501

Kuklinski, L. F., Yan, S., Li, Z., Fisher, J. L., Cheng, C., Noelle, R. J., et al. (2018). VISTA Expression on Tumor-Infiltrating Inflammatory Cells in Primary Cutaneous Melanoma Correlates with Poor Disease-specific Survival. *Cancer Immunol. Immunother.* 67, 1113–1121. doi:10.1007/s00262-018-2169-1

Kurtulus, S., Sakuishi, K., Ngiow, S.-F., Joller, N., Tan, D. J., Teng, M. W. L., et al. (2015). TIGIT Predominantly Regulates the Immune Response via Regulatory T Cells. *J. Clin. Invest.* 125, 4053–4062. doi:10.1172/jci81187

Lakhani, N., Spreafico, A., Tolcher, A. W., Rodon, J., Janku, F., Chandana, S. R., et al. (2020). 1019O Phase I Studies of Sym021, an Anti-PD-1 Antibody, Alone and in Combination with Sym022 (Anti-LAG-3) or Sym023 (Anti-TIM-3). *Ann. Oncol.* 31, S704. doi:10.1016/j.annonc.2020.08.1139

Le Mercier, I., Chen, W., Lines, J. L., Day, M., Li, J., Sergent, P., et al. (2014). VISTA Regulates the Development of Protective Antitumor Immunity. *Cancer Res.* 74, 1933–1944. doi:10.1158/0008-5472.CAN-13-1506

Levin, S. D., Taft, D. W., Brandt, C. S., Bucher, C., Howard, E. D., Chadwick, E. M., et al. (2011). Vstm3 Is a Member of the CD28 Family and an Important Modulator of T-Cell Function. *Eur. J. Immunol.* 41, 902–915. doi:10.1002/eji.201041136

Li, F.-J., Zhang, Y., Jin, G.-X., Yao, L., and Wu, D.-Q. (2013). Expression of LAG-3 Is Coincident with the Impaired Effector Function of HBV-specific CD8+

T Cell in HCC Patients. *Immunol. Lett.* 150, 116–122. doi:10.1016/j.imlet.2012.12.004

Li, M., Xia, P., Du, Y., Liu, S., Huang, G., Chen, J., et al. (2014). T-cell Immunoglobulin and ITIM Domain (TIGIT) Receptor/Poliovirus Receptor (PVR) Ligand Engagement Suppresses Interferon-γ Production of Natural Killer Cells via β-Arrestin 2-mediated Negative Signaling. *J. Biol. Chem.* 289, 17647–17657. doi:10.1074/jbc.M114.572420

Li, M., Zhang, G., Zhang, X., Lv, G., Wei, X., Yuan, H., et al. (2014). Overexpression of B7-H3 in CD14+ Monocytes Is Associated with Renal Cell Carcinoma Progression. *Med. Oncol.* 31, 349. doi:10.1007/s12032-014-0349-1

Li, N., Wang, Y., Forbes, K., Vignali, K. M., Heale, B. S., Saftig, P., et al. (2007). Metalloproteases Regulate T-Cell Proliferation and Effector Function via LAG-3. *EMBO J.* 26, 494–504. doi:10.1038/sj.emboj.7601520

Lines, J. L., Sempere, L. F., Broughton, T., Wang, L., and Noelle, R. (2014). VISTA Is a Novel Broad-Spectrum Negative Checkpoint Regulator for Cancer Immunotherapy. *Cancer Immunol. Res.* 2, 510–517. doi:10.1158/2326-6066.Cir-14-0072

Lipson, E. J., Long, G. V., Tawbi, H., Schadendorf, D., Atkinson, V. G., Maurer, M., et al. (2018). CA224-047: A Randomized, Double-Blind, Phase II/III Study of Relatlimab (Anti-LAG-3) in Combination with Nivolumab (Anti-PD-1) versus Nivolumab Alone in Previously Untreated Metastatic or Unresectable Melanoma. *Ann. Oncol.* 29, viii464–viii465. doi:10.1093/annonc/mdy289.058

Liu, H., Tekle, C., Chen, Y.-W., Kristian, A., Zhao, Y., Zhou, M., et al. (2011). B7-H3 Silencing Increases Paclitaxel Sensitivity by Abrogating Jak2/Stat3 Phosphorylation. *Mol. Cancer Ther.* 10, 960–971. doi:10.1158/1535-7163.Mct-11-0072

Liu, J., Yuan, Y., Chen, W., Putra, J., Suriawinata, A. A., Schenk, A. D., et al. (2015). Immune-checkpoint Proteins VISTA and PD-1 Nonredundantly Regulate Murine T-Cell Responses. *Proc. Natl. Acad. Sci. USA* 112, 6682–6687. doi:10.1073/pnas.1420370112

Llosa, N. J., Cruise, M., Tam, A., Wicks, E. C., Hechenbleikner, E. M., Taube, J. M., et al. (2015). The Vigorous Immune Microenvironment of Microsatellite Instable Colon Cancer Is Balanced by Multiple Counter-inhibitory Checkpoints. *Cancer Discov.* 5, 43–51. doi:10.1158/2159-8290.Cd-14-0863

Loeser, H., Kraemer, M., Gebauer, F., Bruns, C., Schröder, W., Zander, T., et al. (2019). The Expression of the Immune Checkpoint Regulator VISTA Correlates with Improved Overall Survival in pT1/2 Tumor Stages in Esophageal Adenocarcinoma. *Oncoimmunology* 8, e1581546. doi:10.1080/2162402x.2019.1581546

Lozano, E., Dominguez-Villar, M., Kuchroo, V., and Hafler, D. A. (2012). The TIGIT/CD226 axis Regulates Human T Cell Function. *J. Immunol.* 188, 3869–3875. doi:10.4049/jimmunol.1103627

Luke, J. J., Patel, M. R., Hamilton, E. P., Chmielowski, B., Ulahannan, S. V., Kindler, H. L., et al. (2020). A Phase I, First-In-Human, Open-Label, Dose-Escalation Study of MGD013, a Bispecific DART Molecule Binding PD-1 and LAG-3, in Patients with Unresectable or Metastatic Neoplasms. *Jco* 38, 3004. doi:10.1200/JCO.2020.38.15_suppl.3004

Manieri, N. A., Chiang, E. Y., and Grogan, J. L. (2017). TIGIT: A Key Inhibitor of the *Cancer* Immunity Cycle. *Trends Immunology* 38, 20–28. doi:10.1016/j.it.2016.10.002

Mao, X., Ou, M. T., Karuppagounder, S. S., Kam, T.-I., Yin, X., Xiong, Y., et al. (2016). Pathological -synuclein Transmission Initiated by Binding Lymphocyte-Activation Gene 3. *Science* 353, aah3374. doi:10.1126/science.aah3374

Mao, Y., Chen, L., Wang, F., Zhu, D., Ge, X., Hua, D., et al. (2017). *Cancer* Cellexpressed B7H3 Regulates the Differentiation of Tumorassociated Macrophages in Human Colorectal Carcinoma. *Oncol. Lett.* 14, 6177–6183. doi:10.3892/ol.2017.6935

Marabelle, A., Fakih, M., Lopez, J., Shah, M., Shapira-Frommer, R., Nakagawa, K., et al. (2020). Association of Tumour Mutational Burden with Outcomes in Patients with Advanced Solid Tumours Treated with Pembrolizumab: Prospective Biomarker Analysis of the Multicohort, Open-Label, Phase 2 KEYNOTE-158 Study. *Lancet Oncol.* 21, 1353–1365. doi:10.1016/s1470-2045(20)30445-9

Marcus, L., Lemery, S. J., Keegan, P., and Pazdur, R. (2019). FDA Approval Summary: Pembrolizumab for the Treatment of Microsatellite Instability-High Solid Tumors. *Clin. Cancer Res.* 25, 3753–3758. doi:10.1158/1078-0432.Ccr-18-4070

Marinelli, O., Nabissi, M., Morelli, M. B., Torquati, L., Amantini, C., and Santoni, G. (2018). ICOS-L as a Potential Therapeutic Target for *Cancer* Immunotherapy. *Cpps* 19, 1107–1113. doi:10.2174/1389203719666180608093913

Martin-Orozco, N., Li, Y., Wang, Y., Liu, S., Hwu, P., Liu, Y.-J., et al. (2010). Melanoma Cells Express ICOS Ligand to Promote the Activation and Expansion of T-Regulatory Cells. *Cancer Res.* 70, 9581–9590. doi:10.1158/0008-5472.Can-10-1379

Matsuzaki, J., Gnjatic, S., Mhawech-Fauceglia, P., Beck, A., Miller, A., Tsuji, T., et al. (2010). Tumor-infiltrating NY-ESO-1-specific CD8+T Cells Are Negatively Regulated by LAG-3 and PD-1 in Human Ovarian Cancer. *Proc. Natl. Acad. Sci. USA* 107, 7875–7880. doi:10.1073/pnas.1003345107

Modak, S., Carrasquillo, J., LaQuaglia, M., Pat, Z., Heaton, T., Cheung, N.-K., et al. (2018). Abstract CT006: Intraperitoneal Radioimmunotherapy for Desmoplastic Small Round Cell Tumor: Results of a Phase I Study (NCT01099644). *Cancer Res.* 78, CT006. doi:10.1158/1538-7445.Am2018-ct006

Monney, L., Sabatos, C. A., Gaglia, J. L., Ryu, A., Waldner, H., Chernova, T., et al. (2002). Th1-specific Cell Surface Protein Tim-3 Regulates Macrophage Activation and Severity of an Autoimmune Disease. *Nature* 415, 536–541. doi:10.1038/415536a

Motzer, R. J., Tannir, N. M., McDermott, D. F., Arén Frontera, O., Melichar, B., Choueiri, T. K., et al. (2018). Nivolumab Plus Ipilimumab versus Sunitinib in Advanced Renal-Cell Carcinoma. *N. Engl. J. Med.* 378, 1277–1290. doi:10.1056/NEJMoa1712126

Murphy, K. M., Nelson, C. A., and Šedý, J. R. (2006). Balancing Co-stimulation and Inhibition with BTLA and HVEM. *Nat. Rev. Immunol.* 6, 671–681. doi:10.1038/nri1917

Musielak, B., Kocik, J., Skalniak, L., Magiera-Mularz, K., Sala, D., Czub, M., et al. (2019). CA-170 - a Potent Small-Molecule PD-L1 Inhibitor or Not? *Molecules* 24 (15), 2804. doi:10.3390/molecules24152804

Nagahara, K., Arikawa, T., Oomizu, S., Kontani, K., Nobumoto, A., Tateno, H., et al. (2008). Galectin-9 Increases Tim-3+ Dendritic Cells and CD8+ T Cells and Enhances Antitumor Immunity via Galectin-9-Tim-3 Interactions. *J. Immunol.* 181, 7660–7669. doi:10.4049/jimmunol.181.11.7660

Nagase, H., Takeoka, T., Urakawa, S., Morimoto-Okazawa, A., Kawashima, A., Iwahori, K., et al. (2017). ICOS+Foxp3+TILs in Gastric Cancer Are Prognostic Markers and Effector Regulatory T Cells Associated withHelicobacter Pylori. *Int. J. Cancer* 140, 686–695. doi:10.1002/ijc.30475

Nakayama, M., Akiba, H., Takeda, K., Kojima, Y., Hashiguchi, M., Azuma, M., et al. (2009). Tim-3 Mediates Phagocytosis of Apoptotic Cells and Cross-Presentation. *Blood* 113, 3821–3830. doi:10.1182/blood-2008-10-185884

Ngiow, S. F., von Scheidt, B., Akiba, H., Yagita, H., Teng, M. W. L., and Smyth, M. J. (2011). Anti-TIM3 Antibody Promotes T Cell IFN-γ-Mediated Antitumor Immunity and Suppresses Established Tumors. *Cancer Res.* 71, 3540–3551. doi:10.1158/0008-5472.Can-11-0096

Niu, J., Nagrial, A., Voskoboynik, M., Chung, H. C., Lee, D. H., Ahn, M.-J., et al. (2020). 1410P Safety and Efficacy of Vibostolimab, an Anti-TIGIT Antibody, Plus Pembrolizumab in Patients with Anti-PD-1/pd-L1-naive NSCLC. *Ann. Oncol.* 31, S891–S892. doi:10.1016/j.annonc.2020.08.1724

Papadopoulos, K. P., Lakhani, N. J., Johnson, M. L., Park, H., Wang, D., Yap, T. A., et al. (2019). First-in-human Study of REGN3767 (R3767), a Human LAG-3 Monoclonal Antibody (mAb), ± Cemiplimab in Patients (Pts) with Advanced Malignancies. *Jco* 37, 2508. doi:10.1200/JCO.2019.37.15_suppl.2508

Pardoll, D. M. (2012). The Blockade of Immune Checkpoints in Cancer Immunotherapy. *Nat. Rev. Cancer* 12, 252–264. doi:10.1038/nrc3239

Paulos, C. M., and June, C. H. (2010). Putting the Brakes on BTLA in T Cell-Mediated Cancer Immunotherapy. *J. Clin. Invest.* 120, 76–80. doi:10.1172/jci41811

Peguero, J. A., Bajaj, P., Carcereny, E., Clay, T. D., Doger, B., Felip, E., et al. (2019). A Multicenter, Phase II Study of Soluble LAG-3 (Eftilagimod Alpha) in Combination with Pembrolizumab (TACTI-002) in Patients with Advanced Non-small Cell Lung Cancer (NSCLC) or Head and Neck Squamous Cell Carcinoma (HNSCC). *Jco* 37, TPS2667. doi:10.1200/JCO.2019.37.15_suppl.TPS2667

Popovic, A., Jaffee, E. M., and Zaidi, N. (2018). Emerging Strategies for Combination Checkpoint Modulators in Cancer Immunotherapy. *J. Clin. Invest.* 128, 3209–3218. doi:10.1172/jci120775

Powderly, J., Cote, G., Flaherty, K., Szmulewitz, R. Z., Ribas, A., Weber, J., et al. (2015). Interim Results of an Ongoing Phase I, Dose Escalation Study of

MGA271 (Fc-Optimized Humanized Anti-B7-H3 Monoclonal Antibody) in Patients with Refractory B7-H3-Expressing Neoplasms or Neoplasms Whose Vasculature Expresses B7-H3. *J. Immunother. Cancer* 3, O8. doi:10.1186/2051-1426-3-S2-O8

Powderly, J., Patel, M. R., Lee, J. J., Brody, J., Meric-Bernstam, F., Hamilton, E., et al. (2017). CA-170, a First in Class Oral Small Molecule Dual Inhibitor of Immune Checkpoints PD-L1 and VISTA, Demonstrates Tumor Growth Inhibition in Pre-clinical Models and Promotes T Cell Activation in Phase 1 Study. *Ann. Oncol.* 28, v405–v406. doi:10.1093/annonc/mdx376.007

Prasad, D. V. R., Nguyen, T., Li, Z., Yang, Y., Duong, J., Wang, Y., et al. (2004). Murine B7-H3 Is a Negative Regulator of T Cells. *J. Immunol.* 173, 2500–2506. doi:10.4049/jimmunol.173.4.2500

Qin, S., Xu, L., Yi, M., Yu, S., Wu, K., and Luo, S. (2019). Novel Immune Checkpoint Targets: Moving beyond PD-1 and CTLA-4. *Mol. Cancer* 18, 155. doi:10.1186/s12943-019-1091-2

Rini, B. I., Plimack, E. R., Stus, V., Gafanov, R., Hawkins, R., Nosov, D., et al. (2019). Pembrolizumab Plus Axitinib versus Sunitinib for Advanced Renal-Cell Carcinoma. *N. Engl. J. Med.* 380, 1116–1127. doi:10.1056/NEJMoa1816714

Rizvi, N. A., Hellmann, M. D., Brahmer, J. R., Juergens, R. A., Borghaei, H., Gettinger, S., et al. (2016). Nivolumab in Combination with Platinum-Based Doublet Chemotherapy for First-Line Treatment of Advanced Non-small-cell Lung *Cancer*. *Jco* 34, 2969–2979. doi:10.1200/jco.2016.66.9861

Rodriguez-Abreu, D., Johnson, M. L., Hussein, M. A., Cobo, M., Patel, A. J., Secen, N. M., et al. (2020). Primary Analysis of a Randomized, Double-Blind, Phase II Study of the Anti-TIGIT Antibody Tiragolumab (Tira) Plus Atezolizumab (Atezo) versus Placebo Plus Atezo as First-Line (1L) Treatment in Patients with PD-L1-Selected NSCLC (CITYSCAPE). *Jco* 38, 9503. doi:10.1200/JCO.2020.38.15_suppl.9503

Sakuishi, K., Apetoh, L., Sullivan, J. M., Blazar, B. R., Kuchroo, V. K., and Anderson, A. C. (2010). Targeting Tim-3 and PD-1 Pathways to Reverse T Cell Exhaustion and Restore Anti-tumor Immunity. *J. Exp. Med.* 207, 2187–2194. doi:10.1084/jem.20100643

Sedy, J. R., Gavrieli, M., Potter, K. G., Hurchla, M. A., Lindsley, R. C., Hildner, K., et al. (2005). B and T Lymphocyte Attenuator Regulates T Cell Activation through Interaction with Herpesvirus Entry Mediator. *Nat. Immunol.* 6, 90–98. doi:10.1038/ni1144

Sharma, P., Hu-Lieskovan, S., Wargo, J. A., and Ribas, A. (2017). Primary, Adaptive, and Acquired Resistance to *Cancer* Immunotherapy. *Cell* 168, 707–723. doi:10.1016/j.cell.2017.01.017

Solinas, C., Gu-Trantien, C., and Willard-Gallo, K. (2020). The Rationale behind Targeting the ICOS-ICOS Ligand Costimulatory Pathway in Cancer Immunotherapy. *ESMO Open* 5, e000544. doi:10.1136/esmoopen-2019-000544

Steinberg, M. W., Cheung, T. C., and Ware, C. F. (2011). The Signaling Networks of the Herpesvirus Entry Mediator (TNFRSF14) in Immune Regulation. *Immunological Rev.* 244, 169–187. doi:10.1111/j.1600-065X.2011.01064.x

Stengel, K. F., Harden-Bowles, K., Yu, X., Rouge, L., Yin, J., Comps-Agrar, L., et al. (2012). Structure of TIGIT Immunoreceptor Bound to Poliovirus Receptor Reveals a Cell-Cell Adhesion and Signaling Mechanism that Requires Cis-Trans Receptor Clustering. *Proc. Natl. Acad. Sci.* 109, 5399–5404. doi:10.1073/pnas.1120606109

Strauss, L., Bergmann, C., Szczepanski, M. J., Lang, S., Kirkwood, J. M., and Whiteside, T. L. (2008). Expression of ICOS on Human Melanoma-Infiltrating CD4+CD25highFoxp3+ T Regulatory Cells: Implications and Impact on Tumor-Mediated Immune Suppression. *J. Immunol.* 180, 2967–2980. doi:10.4049/jimmunol.180.5.2967

Suh, W.-K., Gajewska, B. U., Okada, H., Gronski, M. A., Bertram, E. M., Dawicki, W., et al. (2003). The B7 Family Member B7-H3 Preferentially Down-Regulates T Helper Type 1-mediated Immune Responses. *Nat. Immunol.* 4, 899–906. doi:10.1038/ni967

Swallow, M. M., Wallin, J. J., and Sha, W. C. (1999). B7h, a Novel Costimulatory Homolog of B7.1 and B7.2, Is Induced by TNFα. *Immunity* 11, 423–432. doi:10.1016/s1074-7613(00)80117-x

Taube, J. M., Young, G. D., McMiller, T. L., Chen, S., Salas, J. T., Pritchard, T. S., et al. (2015). Differential Expression of Immune-Regulatory Genes Associated with PD-L1 Display in Melanoma: Implications for PD-1 Pathway Blockade. *Clin. Cancer Res.* 21, 3969–3976. doi:10.1158/1078-0432.Ccr-15-0244

Torphy, R., Schulick, R., and Zhu, Y. (2017). Newly Emerging Immune Checkpoints: Promises for Future *Cancer* Therapy. *Ijms* 18, 2642. doi:10.3390/ijms18122642

Trebeschi, S., Drago, S. G., Birkbak, N. J., Kurilova, I., Călin, A. M., Delli Pizzi, A., et al. (2019). Predicting Response to Cancer Immunotherapy Using Noninvasive Radiomic Biomarkers. *Ann. Oncol.* 30, 998–1004. doi:10.1093/annonc/mdz108

Triebel, F., Hacene, K., and Pichon, M.-F. (2006). A Soluble Lymphocyte Activation Gene-3 (sLAG-3) Protein as a Prognostic Factor in Human Breast Cancer Expressing Estrogen or Progesterone Receptors. *Cancer Lett.* 235, 147–153. doi:10.1016/j.canlet.2005.04.015

Triebel, F., Jitsukawa, S., Baixeras, E., Roman-Roman, S., Genevee, C., Viegas-Pequignot, E., et al. (1990). LAG-3, a Novel Lymphocyte Activation Gene Closely Related to CD4. *J. Exp. Med.* 171, 1393–1405. doi:10.1084/jem.171.5.1393

Uboha, N. V., Milhem, M. M., Kovacs, C., Amin, A., Magley, A., Purkayastha, D. D., et al. (2019). Phase II Study of Spartalizumab (PDR001) and LAG525 in Advanced Solid Tumors and Hematologic Malignancies. *Jco* 37, 2553. doi:10.1200/JCO.2019.37.15_suppl.2553

Vaddepally, R. K., Kharel, P., Pandey, R., Garje, R., and Chandra, A. B. (2020). Review of Indications of FDA-Approved Immune Checkpoint Inhibitors Per NCCN Guidelines with the Level of Evidence. *Cancers* 12, 738. doi:10.3390/cancers12030738

van de Weyer, P. S., Muehlfeit, M., Klose, C., Bonventre, J. V., Walz, G., and Kuehn, E. W. (2006). A Highly Conserved Tyrosine of Tim-3 Is Phosphorylated upon Stimulation by its Ligand Galectin-9. *Biochem. Biophysical Res. Commun.* 351, 571–576. doi:10.1016/j.bbrc.2006.10.079

Vinay, D. S., Ryan, E. P., Pawelec, G., Talib, W. H., Stagg, J., Elkord, E., et al. (2015). Immune Evasion in Cancer: Mechanistic Basis and Therapeutic Strategies. *Semin. Cancer Biol.* 35, S185–S198. doi:10.1016/j.semcancer.2015.03.004

Wang, D. Y., Salem, J.-E., Cohen, J. V., Chandra, S., Menzer, C., Ye, F., et al. (2018). Fatal Toxic Effects Associated with Immune Checkpoint Inhibitors. *JAMA Oncol.* 4, 1721–1728. doi:10.1001/jamaoncol.2018.3923

Wang, J., Sanmamed, M. F., Datar, I., Su, T. T., Ji, L., Sun, J., et al. (2019). Fibrinogen-like Protein 1 Is a Major Immune Inhibitory Ligand of LAG-3. *Cell* 176, 334–347. doi:10.1016/j.cell.2018.11.010

Wang, J., Wu, G., Manick, B., Hernandez, V., Renelt, M., Erickson, C., et al. (2019). VSIG-3 as a Ligand of VISTA Inhibits Human T-Cell Function. *Immunology* 156, 74–85. doi:10.1111/imm.13001

Wang, L., Rubinstein, R., Lines, J. L., Wasiuk, A., Ahonen, C., Guo, Y., et al. (2011). VISTA, a Novel Mouse Ig Superfamily Ligand that Negatively Regulates T Cell Responses. *J. Exp. Med.* 208, 577–592. doi:10.1084/jem.20100619

Wang, Y., Deng, W., Li, N., Neri, S., Sharma, A., Jiang, W., et al. (2018). Combining Immunotherapy and Radiotherapy for *Cancer* Treatment: Current Challenges and Future Directions. *Front. Pharmacol.* 9, 185. doi:10.3389/fphar.2018.00185

Woo, S.-R., Turnis, M. E., Goldberg, M. V., Bankoti, J., Selby, M., Nirschl, C. J., et al. (2012). Immune Inhibitory Molecules LAG-3 and PD-1 Synergistically Regulate T-Cell Function to Promote Tumoral Immune Escape. *Cancer Res.* 72, 917–927. doi:10.1158/0008-5472.Can-11-1620

Wu, L., Deng, W.-W., Huang, C.-F., Bu, L.-L., Yu, G.-T., Mao, L., et al. (2017). Expression of VISTA Correlated with Immunosuppression and Synergized with CD8 to Predict Survival in Human Oral Squamous Cell Carcinoma. *Cancer Immunol. Immunother.* 66, 627–636. doi:10.1007/s00262-017-1968-0

Xie, C., Liu, D., Chen, Q., Yang, C., Wang, B., and Wu, H. (2016). Soluble B7-H3 Promotes the Invasion and Metastasis of Pancreatic Carcinoma Cells through the TLR4/NF-Kb Pathway. *Sci. Rep.* 6, 27528. doi:10.1038/srep27528

Xin Yu, J., Hubbard-Lucey, V. M., and Tang, J. (2019). Immuno-oncology Drug Development Goes Global. *Nat. Rev. Drug Discov.* 18, 899–900. doi:10.1038/d41573-019-00167-9

Yang, S., Wei, W., and Zhao, Q. (2020). B7-H3, a Checkpoint Molecule, as a Target for Cancer Immunotherapy. *Int. J. Biol. Sci.* 16, 1767–1773. doi:10.7150/ijbs.41105

Yap, T. A., Burris, H. A., Kummar, S., Falchook, G. S., Pachynski, R. K., LoRusso, P., et al. (2018). ICONIC: Biologic and Clinical Activity of First in Class ICOS Agonist Antibody JTX-2011 +/- Nivolumab (Nivo) in Patients (Pts) with Advanced Cancers. *Jco* 36, 3000. doi:10.1200/JCO.2018.36.15_suppl.3000

Yoon, K. W., Byun, S., Kwon, E., Hwang, S.-Y., Chu, K., Hiraki, M., et al. (2015). Control of Signaling-Mediated Clearance of Apoptotic Cells by the Tumor Suppressor P53. *Science* 349, 1261669. doi:10.1126/science.1261669

Yoshinaga, S. K., Whoriskey, J. S., Khare, S. D., Sarmiento, U., Guo, J., Horan, T., et al. (1999). T-cell Co-stimulation through B7RP-1 and ICOS. *Nature* 402, 827–832. doi:10.1038/45582

Yu, X., Harden, K., C Gonzalez, L., Francesco, M., Chiang, E., Irving, B., et al. (2009). The Surface Protein TIGIT Suppresses T Cell Activation by Promoting the Generation of Mature Immunoregulatory Dendritic Cells. *Nat. Immunol.* 10, 48–57. doi:10.1038/ni.1674

Zhang, J., Liu, L., Han, S., Li, Y., Qian, Q., Zhang, Q., et al. (2017). B7-H3 Is Related to Tumor Progression in Ovarian Cancer. *Oncol. Rep.* 38, 2426–2434. doi:10.3892/or.2017.5858

Zhang, M., Pang, H.-J., Zhao, W., Li, Y.-F., Yan, L.-X., Dong, Z.-Y., et al. (2018). VISTA Expression Associated with CD8 Confers a Favorable Immune Microenvironment and Better Overall Survival in Hepatocellular Carcinoma. *BMC Cancer* 18, 511. doi:10.1186/s12885-018-4435-1

Zhang, P., Yu, S., Li, H., Liu, C., Li, J., Lin, W., et al. (2015). ILT4 Drives B7-H3 Expression via PI3K/AKT/mTOR Signalling and ILT4/B7-H3 Co-expression Correlates with Poor Prognosis in Non-small Cell Lung Cancer. *FEBS Lett.* 589, 2248–2256. doi:10.1016/j.febslet.2015.06.037

Zhang, Q., Bi, J., Zheng, X., Chen, Y., Wang, H., Wu, W., et al. (2018). Blockade of the Checkpoint Receptor TIGIT Prevents NK Cell Exhaustion and Elicits Potent Anti-tumor Immunity. *Nat. Immunol.* 19, 723–732. doi:10.1038/s41590-018-0132-0

Zhang, Y., Cai, P., Liang, T., Wang, L., and Hu, L. (2017). TIM-3 Is a Potential Prognostic Marker for Patients with Solid Tumors: A Systematic Review and Meta-Analysis. *Oncotarget* 8, 31705–31713. doi:10.18632/oncotarget.15954

Zhang, Y., Luo, Y., Qin, S.-L., Mu, Y.-F., Qi, Y., Yu, M.-H., et al. (2016). The Clinical Impact of ICOS Signal in Colorectal Cancer Patients. *Oncoimmunology* 5, e1141857. doi:10.1080/2162402X.2016.1141857

Zhu, C., Anderson, A. C., Schubart, A., Xiong, H., Imitola, J., Khoury, S. J., et al. (2005). The Tim-3 Ligand Galectin-9 Negatively Regulates T Helper Type 1 Immunity. *Nat. Immunol.* 6, 1245–1252. doi:10.1038/ni1271

Zong, L., Zhou, Y., Zhang, M., Chen, J., and Xiang, Y. (2020). VISTA Expression Is Associated with a Favorable Prognosis in Patients with High-Grade Serous Ovarian Cancer. *Cancer Immunol. Immunother.* 69, 33–42. doi:10.1007/s00262-019-02434-5

Conflict of Interest: The authors declare that the research was conducted in the absence of any commercial or financial relationships that could be construed as a potential conflict of interest.

Copyright © 2021 Lee, Ha and Kim. This is an open-access article distributed under the terms of the Creative Commons Attribution License (CC BY). The use, distribution or reproduction in other forums is permitted, provided the original author(s) and the copyright owner(s) are credited and that the original publication in this journal is cited, in accordance with accepted academic practice. No use, distribution or reproduction is permitted which does not comply with these terms.

frontiers in Pharmacology

ORIGINAL RESEARCH
published: 04 August 2021
doi: 10.3389/fphar.2021.696961

Targeting Fatty Acid Synthase Modulates Metabolic Pathways and Inhibits Cholangiocarcinoma Cell Progression

*Jittima Tomacha[1,2], Hasaya Dokduang[2], Sureerat Padthaisong[2], Nisana Namwat[1,2], Poramate Klanrit[1,2], Jutarop Phetcharaburanin[1,2], Arporn Wangwiwatsin[1,2], Tueanjit Khampitak[1], Supinda Koonmee[3,2], Attapol Titapun[4,2], Apiwat Jarearnrat[4,2], Narong Khuntikeo[4,2] and Watcharin Loilome[1,2]**

[1]Department of Biochemistry, Faculty of Medicine, Khon Kaen University, Khon Kaen, Thailand, [2]Cholangiocarcinoma Research Institute, Khon Kaen University, Khon Kaen, Thailand, [3]Department of Pathology, Faculty of Medicine, Khon Kaen University, Khon Kaen, Thailand, [4]Department of Surgery, Faculty of Medicine, Khon Kaen University, Khon Kaen, Thailand

OPEN ACCESS

Edited by:
Marc Diederich,
Seoul National University, South Korea

Reviewed by:
Feng Wang,
Affiliated Hospital of Nantong University, China
Susanne Müller,
Goethe University Frankfurt, Germany

***Correspondence:**
Watcharin Loilome
watclo@kku.ac.th

Specialty section:
This article was submitted to Pharmacology of Anti-Cancer Drugs, a section of the journal Frontiers in Pharmacology

Received: 18 April 2021
Accepted: 22 July 2021
Published: 04 August 2021

Citation:
Tomacha J, Dokduang H, Padthaisong S, Namwat N, Klanrit P, Phetcharaburanin J, Wangwiwatsin A, Khampitak T, Koonmee S, Titapun A, Jarearnrat A, Khuntikeo N and Loilome W (2021) Targeting Fatty Acid Synthase Modulates Metabolic Pathways and Inhibits Cholangiocarcinoma Cell Progression. Front. Pharmacol. 12:696961. doi: 10.3389/fphar.2021.696961

An aberrant regulation of lipid metabolism is involved in the pathogenesis and progression of cancer. Up-regulation of lipid biosynthesis enzymes, including acetyl-CoA carboxylase (ACC), fatty acid synthase (FASN) and HMG-CoA reductase (HMGCR), has been reported in many cancers. Therefore, elucidating lipid metabolism changes in cancer is essential for the development of novel therapeutic targets for various human cancers. The current study aimed to identify the abnormal expression of lipid-metabolizing enzymes in cholangiocarcinoma (CCA) and to evaluate whether they can be used as the targets for CCA treatment. Our study demonstrated that a high expression of FASN was significantly correlated with the advanced stage in CCA patients. In addition, survival analysis showed that high expression of FASN and HMGCR was correlated with shorter survival of CCA patients. Furthermore, FASN knockdown inhibited the growth, migration and invasion in CCA cell lines, KKU055 and KKU213, as well as induced cell cycle arrest and apoptosis in the CCA cell lines. In addition, metabolomics study further revealed that purine metabolism was the most relevant pathway involved in FASN knockdown. Adenosine diphosphate (ADP), glutamine and guanine levels significantly increased in KKU213 cells while guanine and xanthine levels remarkably increased in KKU055 cells showing a marked difference between the control and FASN knockdown groups. These findings provide new insights into the mechanisms associated with FASN knockdown in CCA cell lines and suggest that targeting FASN may serve as a novel CCA therapeutic strategy.

Keywords: lipid metabolism1, acetyl-CoA carboxylase2, fatty acid synthase3, HMG-CoA reductase4, metabolomics5, cholangiocarcinoma6

INTRODUCTION

Lipid metabolism is the biosynthesis and degradation processes of lipids in cells, relating to the storage or breakdown of fats for energy and the synthesis of functional and structural lipids. An aberrant regulation of lipid metabolism is involved in the pathogenesis and progression of cancer. Various evidence reported that an upregulation of lipid biosynthesis enzymes, including acetyl-CoA carboxylase (ACC), fatty acid synthase (FASN) and HMG-CoA reductase (HMGCR), can be found in many cancer types. For example, the upregulation of ACC contributes to the cell proliferation and migration of liver cancer. The overexpression of ACC in liver cancer tissues was correlated with a poorer prognosis and shorter survival for liver cancer patients. Moreover, down-regulation of ACC protein expression using siRNA leads to decreased liver cancer cell growth and migration (Ye et al., 2019). In addition, the up-regulation of FASN enhances colorectal cancer cell proliferation and metastasis. The high expression of FASN in colorectal cancer tissues was correlated with lymph node metastasis, the Tumor, Node, Metastases (TNM) stage and poor prognosis in colorectal cancer patients. Furthermore, FASN knockdown resulted in reduced colorectal cancer cell proliferation and migration while FASN overexpression had the opposite effects on colorectal cancer cells (Lu et al., 2019). The up-regulation of HMGCR can promote gastric cancer cell growth and migration. HMGCR overexpression is found in gastric cancer tissues and cell lines. In contrast, HMGCR knockdown can inhibited gastric cancer cell growth and migration both *in vitro* and *in vivo* (Chushi et al., 2016). These data demonstrate that ACC, FASN and HMGCR are promising potential targets for cancer treatment. Therefore, elucidating lipid metabolism changes in cancer is required to develop therapeutic targets for various human cancers.

Metabolomics is a systems biology tool for studying biochemical composition and investigating metabolic pathway alteration within an organism, cell or tissue. Metabolomics has been used widely in cancer research to explore potential biomarkers for early detection and diagnosis; for example in colorectal cancer (Zhang et al., 2014) and ovarian cancer (Gaul et al., 2015). It is also useful for providing better understanding of the molecular mechanisms (Griffin & Shockcor, 2004). In this study, liquid chromatography-mass spectrometry (LC-MS) was used to conduct metabolomics profiling. Because of its high sensitivity and selectivity, LC-MS is superior in secondary metabolite analysis at the detection level of picomole to femtomole (Emwas, 2015). The study of metabolomics provides new insights into the metabolic processes within cells and can be used to determine biomarkers for novel cancer therapeutic strategies.

Cholangiocarcinoma (CCA) is a bile duct cancer that is caused by malignant transformation of the cholangiocytes. CCA tumors are classified according to the position of tumor along the biliary tract and comprises intrahepatic CCA (iCCA), perihilar CCA (pCCA) and distal CCA (dCCA) (Alsaleh et al., 2019). Although CCA is a rare disease in many countries, the highest incidence has been reported in the northeast of Thailand (Khuntikeo et al., 2015). A major risk factor of CCA development in this area is related to chronic inflammation induced by liver fluke *Opisthorchis viverrini* infection, which leads to the alteration of genes, proteins and molecules such as increased proinflammatory cytokines levels and overproduction of reactive oxygen and nitrogen species (Yongvanit et al., 2012). Moreover, CCA is asymptomatic in its early stage and most patients are diagnosed when the disease becomes advanced resulting in short survival post-treatment and a poor prognosis (Banales et al., 2016). However, there is very limited information on lipid metabolism in CCA. Therefore, an in-depth study on lipid metabolism in CCA is required in order to improve patient survival and prognoses. In the present study, we aimed to identify the abnormal expression of lipid-metabolizing enzymes in CCA and to evaluate their potential as the targets for CCA treatment.

MATERIALS AND METHODS

Human Cholangiocarcinoma Tissues and Cell Lines

One hundred fifty-five formalin-fixed, paraffin-embedded CCA tissue samples were collected from CCA patients who had undergone surgery at Srinagarind Hospital, Khon Kaen University, from February 2007 to December 2016. These samples were kept by the Cholangiocarcinoma Research Institute (CARI), Faculty of Medicine, Khon Kaen University, under the ethics approval number HE571283. CCA cell lines, including KKU023, KKU055, KKU100, KKU156 and KKU213, were used for this study. The KKU023 cell line was established from the proven bile duct cancer of a patient living in the northeast region of Thailand with written consent from the patient. The KKU055, KKU100, KKU156 and KKU213 cell lines were obtained from the Japanese Collection of Research Bioresources (JCRB) Cell Bank, Osaka, Japan. These cells were cultured in Ham's F12 media supplemented with inactivated 10% fetal bovine serum (FBS) and 100 U/ml of penicillin-streptomycin, at 37°C with 5% CO_2.

Chemicals and Reagents

Monoclonal antibody against ACC (catalog Number: ab45174) and polyclonal antibody against FASN (catalog Number: ab22759) were purchased from Abcam, United Kingdom. Monoclonal antibody against HMGCR (catalog Number: SAB4200528) was purchased from Sigma-Aldrich, United States. Short hairpin RNA (shRNA) was purchased from Sigma-Aldrich, United States. The Annexin V/PI staining kit was purchased from Invitrogen, United States. High-performance liquid chromatography (HPLC)-grade methanol, chloroform and water were purchased from Merck, Germany.

Immunohistochemistry and Grading System

Immunohistochemical staining was performed in order to investigate lipid-metabolizing enzyme expression in human CCA tissues. Paraffin-embedded tissues were de-paraffinized and rehydrated with xylene followed by 100, 90, 80 and 70%

ethanol. Antigen retrieval was performed by microwave cooking with 10 mM sodium citrate buffer for 10 min. The tissue sections were treated for 30 min with 0.3% hydrogen peroxide to block the activity of endogenous hydrogen peroxide and 10% skim milk to block the non-specific binding. The tissue sections were incubated with primary antibodies at room temperature for 1 h followed by 4°C overnight, then incubated with secondary antibodies conjugated with horseradish peroxidase (HRP) for 3 h. The signal was developed using a 3,3′-diaminobenzidine tetrahydrochloride (DAB) substrate kit (Vector Laboratories, United States) for 5–10 min. Tissue sections were counterstained with Mayer's haematoxylin for 5 min and dehydrated with 70, 80, 90, 100% ethanol and xylene then mounted with permount. The stained tissue sections were observed under a microscope. The lipid-metabolizing enzyme expression was analyzed according to the staining frequency and intensity. The staining frequency of enzymes was semi-qualitatively scored based on the positive cells percentage, 0% = negative, 1–25% = +1, 26–50% = +2 and >50% = +3. The staining intensity of enzymes was scored as weak = 1, moderate = 2 and strong = 3. The lipid-metabolizing enzyme expression was divided into low or high expression group using median as the cut-off.

Western Blot Analysis

The cell pelltes were extracted with NP40 lysis buffer containing a cocktail of protease and phosphatase inhibitors. Protein concentration was determined using the Pierce BCA™ Protein Assay kit (Thermo Fisher Scientific, United States). Protein extracts were solubilized in sample buffer containing sodium dodecyl sulfate (SDS) and β-mercaptoethanol and boiled at 95°C for 5 min. Protein extracts were separated by 8% sodium dodecyl sulfate polyacrylamide gel electrophoresis (SDS-PAGE), transferred onto PVDF membranes and blocked by 5% skimmed milk for 1 h at room temperature. The membranes were probed with specific primary antibodies for 1 h at room temperature, incubated at 4°C with gentle shaking overnight, then probed with secondary antibodies. The membranes were exposed to ECL™ Prime Western Blotting Detection Reagent for chemiluminescent detection (GE Healthcare, United States). The band density on the membranes were quantified by ImageQuant™ Imager (GE Healthcare, United States). In this study, β-actin antibody (Sigma Aldrich, United States) was used as an internal loading control.

Fatty Acid Synthase Gene Knockdown

CCA cell lines (KKU055 and KKU213) were plated into 48-well plates. After 24 h, 100 µl of concentrated lentivirus was added to the medium containing 8 µg/ml polybrene. Two shRNAs (sh1 and sh2) targeting FASN were used, and control shRNA was used for the control cells. Cells were incubated at 37°C in a humidified atmosphere with 5% CO_2. Fresh medium was replaced 24 h post-transduction. FASN knockdown cells were selected with medium containing puromycin. The efficiency of shRNA transfection was determined using western blot analysis.

Cell Proliferation Assay

A sulforhodamine B (SRB) assay was used to determine the cell proliferation. The FASN-knockdown CCA cell lines were plated in triplicate in 96-well plates and incubated for 24, 48, and 72 h. Then, the cells were fixed with 10% trichloroacetic acid (TCA) at 4°C for 1 h and stained with 0.4% SRB for 30 min. The protein-bound stained cells were dissolved with 10 mM tris-base, pH 10.5 for 1 h on shaking plate. The absorbance was measured at 540 nm by microplate reader (TECAN Trading, Switzerland).

Cell Migration Assay

A wound-healing assay was used to evaluate the cell migration. The FASN-knockdown CCA cell lines were cultured in 24-well plates and incubated at 37°C in a humidified atmosphere with 5% CO_2 until the cells became more than 90% confluent. Cell monolayers were scratched using a sterile tip and then washed several times with 1X PBS to remove the cell debris. Cell migration in the wounded area was observed every 6 h and photographed under a microscope.

Cell Invasion Assay

A Boyden chamber assay was used to perform the cell invasion assay. The complete medium was added to the lower chamber while serum-free medium was added to the upper chamber. The FASN knockdown CCA cell lines were cultured in the upper chamber and incubated at 37°C in a humidified atmosphere with 5% CO_2 for 24 h. The cells attached to the filter were fixed with methanol for 30 min at room temperature and stained with hematoxylin overnight. After that, the filter was dried at 60°C for 30 min and mounted with permount, then observed under a microscope.

Cell Cycle Assay

The FASN knockdown CCA cell lines were plated into 6-well plates and incubated at 37°C in a humidified atmosphere with 5% CO_2 for 72 h. The cells were fixed with 70% ethanol and incubated at 4°C overnight. PI/RNase staining buffer was added to the fixed cells followed by incubation at 4°C in the dark for 30 min. The stained cells were detected using a flow cytometer (BD Bioscience, United States).

Apoptosis Assay

Apoptosis was detected using the Annexin V/PI staining kit. The FASN knockdown CCA cell lines were seeded into 6-well plates and incubated at 37°C in a humidified atmosphere with 5% CO_2 for 72 h. The cells were collected, washed with 1X PBS and resuspended in binding buffer, then annexin V and propidium iodide (PI) were added and incubated at room temperature for 15 min. The stained cells were measured using a flow cytometer (BD Bioscience, United States).

Liquid Chromatography-Mass Spectrometry-Based Metabolomics

Global metabolic profiles were acquired using LC-MS in the cell pellets from FASN knockdown CCA cell lines. The cells were quenched in ice-cold methanol and snap-frozen in liquid nitrogen, then sonicated (3 cycles of pulse at 30 s, off 5 s, at

amplitude of 40). Water (HPLC grade) and chloroform were added into the samples for dual-phase extraction followed by centrifugation at 4,000 g, 4°C for 20 min. Then, 450 µl of aqueous phase was collected into a microcentrifuge tube. The solvent contained in the aqueous phase was removed using speed vacuum concentrator (Labconco, United states). The aqueous phase sample was reconstituted in reconstitution buffer and transferred into a glass vial for LC-MS data acquisition. In addition, the samples were analyzed using a reverse-phase (RP) liquid chromatography platform. The separated part was analysed using the ultra-high performance liquid chromatography (UHPLC) system. A C18 column (2.1 × 100 mm, 2 µm) (Bruker, Germany) was used with the column temperature set at 40°C. Mobile phase A comprised water 100% mixed with 0.1% formic acid, and mobile phase B comprised acetonitrile 100% mixed with 0.1% formic acid. The elution gradient was set at a flow rate of 0.4 ml/min. Sodium formate (2 mM) was used as the calibrant. Mass spectrometry was performed on a compact electrospray ionization-quadrupole time-of-flight (ESI-Q-TOF) system (Bruker, Germany). The blank and quality control (QC) samples were randomly analyzed to reduce instrumentation artifacts.

Liquid Chromatography-Mass Spectrometry/MS Data Processing and Metabolite Identification

Following data acquisition, MetaboScape 4.0 (Bruker, Germany) software was used for feature extraction. The data file was subjected to MetaboAnalyst 5.0 (University of Alberta, Canada) software for statistical analysis (Pang et al., 2020). The Mann-Whitney *U*-test was used, and only features with an *p*-value less than 0.05 were selected for metabolite identification. The metabolite identification was performed by matching the m/z with online databases (Human Metabolome Database; HMDB and METLIN). Additionally, the fragmentation patterns of each feature were also investigated. The level of assignment was classified based on the previously published criteria (Vorkas et al., 2015) which were: 1) m/z matched to database, 2) m/z matched to database and fragmentation pattern matched to in silico fragmentation pattern, 3) fragmentation pattern matched to database or literature, 4) retention-time matched to standard compound, 5) fragmentation pattern matched to standard compound.

Statistical Analysis

The association between lipid-metabolizing enzyme expression with the clinicopathological characteristics of CCA patients was analzed using chi-square test. Survival analysis was performed by Kaplan-Meier (log-rank) analysis (Statistical Package for the Social Sciences; SPSS software v.19), statistical significance was considered if the *p*-value was less than 0.05. For functional analysis, the significant differences were determined using unpaired *t*-test (p-value < 0.05) on GraphPad Prism 5 (California, United states) software.

RESULTS

Correlation of Lipid-Metabolizing Enzyme Expression With Clinicopathological Features of Cholangiocarcinoma Patients

The expression levels of the lipid-metabolizing enzymes were investigated using immunohistochemical staining. The low and high expression of lipid-metabolizing enzymes, including ACC, FASN and HMGCR in human CCA tissues are represented in **Figure 1A**. To investigate the correlation between ACC, FASN and HMGCR expression and clinicopathological features of CCA patients, a total of 155 CCA patients were studied; 64 cases (41%) were females and 91 cases (59%) males. The ages ranged between 39 and 82 years (median = 61 years). Ninety seven cases (63%) were classified as iCCA while 58 cases (37%) were extrahepatic CCA (pCCA or dCCA). The histology typing resulted in 76 cases (49%) of the papillary type and 79 cases (51%) of other types. Fifty seven cases (37%) were classified as primary tumor (T) stage I or II whereas 98 cases (63%) were T stage III or IV. Among 155 patients, 64 (41%) had regional lymph node metastasis (N), and only 7 cases (5%) presented with distant metastases (M). In this study, 60 cases (39%) were divided into early stage (TNM stage I, II) while 95 cases (61%) were separated into late or advanced stage (TNM stage III, IV) and recurrence was detected after surgery in 60 cases (39%). The results demonstrated that high expression of FASN significantly correlated with advanced stage in CCA patients ($p = 0.041$, **Table 1**). Moreover, western blot analysis showed that ACC, FASN and HMGCR expression was observable in the five CCA cell lines - KKU023, KKU055, KKU100, KKU156 and KKU213 (**Figure 1B**).

Kaplan-Meier Survival Analysis of Lipid-Metabolizing Enzyme Expression in Cholangiocarcinoma Patients

To evaluate the prognostic role of lipid-metabolizing enzyme expression in CCA patients, the Kaplan-Meier survival curves showed that CCA patients with high expression of FASN and HMGCR were associated with shorter overall survival times ($p = 0.008$ and $p = 0.044$, respectively) (**Figure 1C**).

Western Blot Analysis of Fatty Acid Synthase Knockdown on Cholangiocarcinoma Cells

To examine the roles of FASN in CCA cell lines, lentiviral transduction was used to stably knockdown FASN expression in KKU055 and KKU213 cell lines. Western blot analysis was performed to ensure the knockdown efficiency; the expression of FASN was lowered at protein levels in cells transfected with shRNA against FASN (sh1 and sh2) ($p < 0.001$) compared with the control counterpart (**Figure 2**).

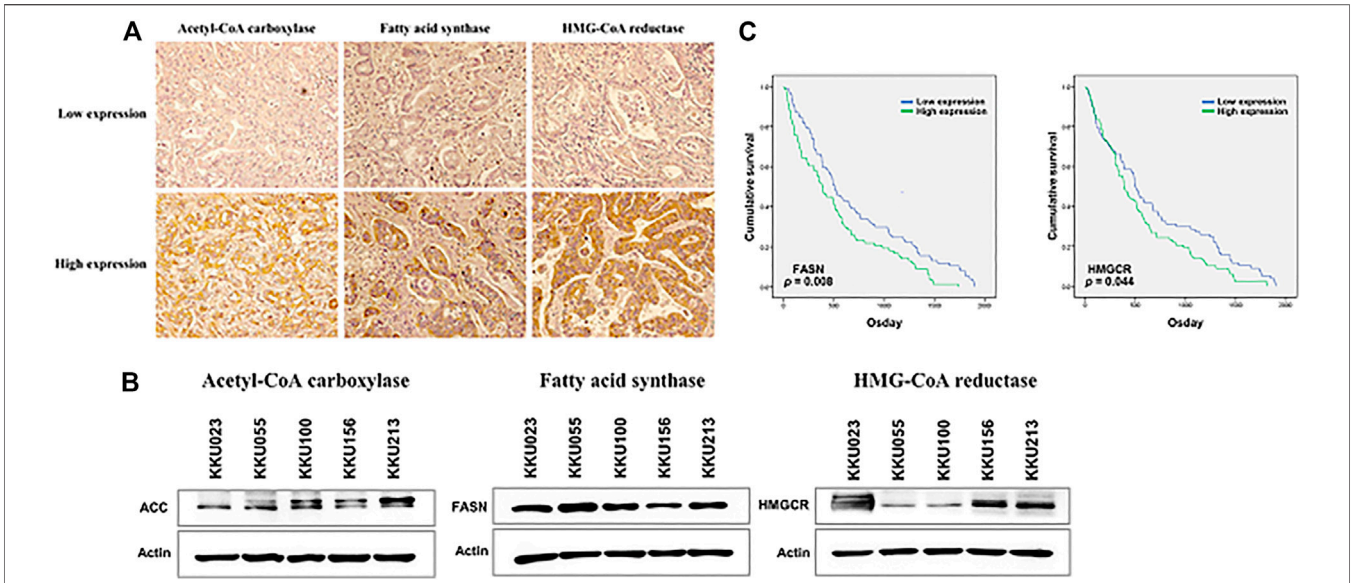

FIGURE 1 | The expression of lipid-metabolizing enzyme in CCA tissues and cell lines. **(A)** Immunohistochemical staining of ACC, FASN and HMGCR using a human CCA tissues microarray; low expression is shown in the upper panel and high expression in the lower panel. **(B)** ACC, FASN and HMGCR protein expression in five CCA cell lines using western blot analysis. **(C)** The Kaplan-Meier survival curves of CCA patients were examined according to lipid-metabolizing enzymes expression; the *p*-values were calculated by the log-rank test.

TABLE 1 | The correlation of lipid-metabolizing enzyme expression with the clinicopathological features of CCA patients.

Variable	ACC		*p*	FASN		*p*	HMGCR		*p*
	Low	High		Low	High		Low	High	
Sex			0.216			0.295			0.170
Female	28 (43.8)	36 (56.2)		35 (54.7)	29 (45.3)		36 (56.3)	28 (43.7)	
Male	49 (53.8)	42 (46.2)		42 (46.2)	49 (53.8)		41 (45.1)	50 (54.9)	
Age (year)			0.576			0.127			0.576
<61	39 (52.0)	36 (48.0)		42 (56.0)	33 (44.0)		39 (52.0)	36 (48.0)	
≥61	38 (47.5)	42 (52.5)		35 (43.8)	45 (56.2)		38 (47.5)	42 (52.5)	
Tumor location			0.950			0.085			0.206
Intrahepatic	48 (49.5)	49 (50.5)		43 (44.3)	54 (55.7)		52 (53.6)	45 (46.4)	
Extrahepatic	29 (50.0)	29 (50.0)		34 (58.6)	24 (41.4)		25 (43.1)	33 (56.9)	
Histology			0.689			0.471			0.573
Papillary	39 (51.3)	37 (48.7)		40 (52.6)	36 (47.4)		36 (47.4)	40 (52.6)	
Others	38 (48.1)	41 (51.9)		37 (46.8)	42 (53.2)		41 (51.9)	38 (48.1)	
Primary tumor (T)			0.440			0.220			0.440
I, II	26 (45.6)	31 (54.4)		32 (56.1)	25 (43.9)		26 (45.6)	31 (54.4)	
III, IV	51 (52.0)	47 (48.0)		45 (45.9)	53 (54.1)		51 (52.0)	47 (48.0)	
Lymph nodes metastasis (N)			0.694			0.796			0.694
No	44 (48.4)	47 (51.6)		46 (50.5)	45 (49.5)		44 (48.4)	47 (51.6)	
Yes	33 (51.6)	31 (48.4)		31 (48.4)	33 (51.6)		33 (51.6)	31 (48.4)	
Distant metastasis (M)			0.686			0.712			0.051
No	73 (49.3)	75 (50.7)		74 (50.0)	74 (50.0)		71 (48.0)	77 (52.0)	
Yes	4 (57.1)	3 (42.9)		3 (42.9)	4 (57.1)		6 (85.7)	1 (14.3)	
TNM stage			0.694			**0.041**			0.790
I, II	31 (51.7)	29 (48.3)		36 (60.0)	24 (40.0)		29 (48.3)	31 (51.7)	
III, IV	46 (48.4)	49 (51.6)		41 (43.2)	54 (56.8)		48 (50.5)	47 (49.5)	
Recurrence			0.209			0.167			0.949
No	51 (53.7)	44 (46.3)		43 (45.3)	52 (54.7)		47 (49.5)	48 (50.5)	
Yes	26 (43.3)	34 (56.7)		34 (56.7)	26 (43.3)		30 (50.0)	30 (50.0)	

ACC, Acetyl-CoA carboxylase; FASN, Fatty acid synthase; HMGCR, HMG-CoA reductase; Low, Low expression; High, High expression; TNM stage, Size of primary tumor-node metastasis-distant metastasis.

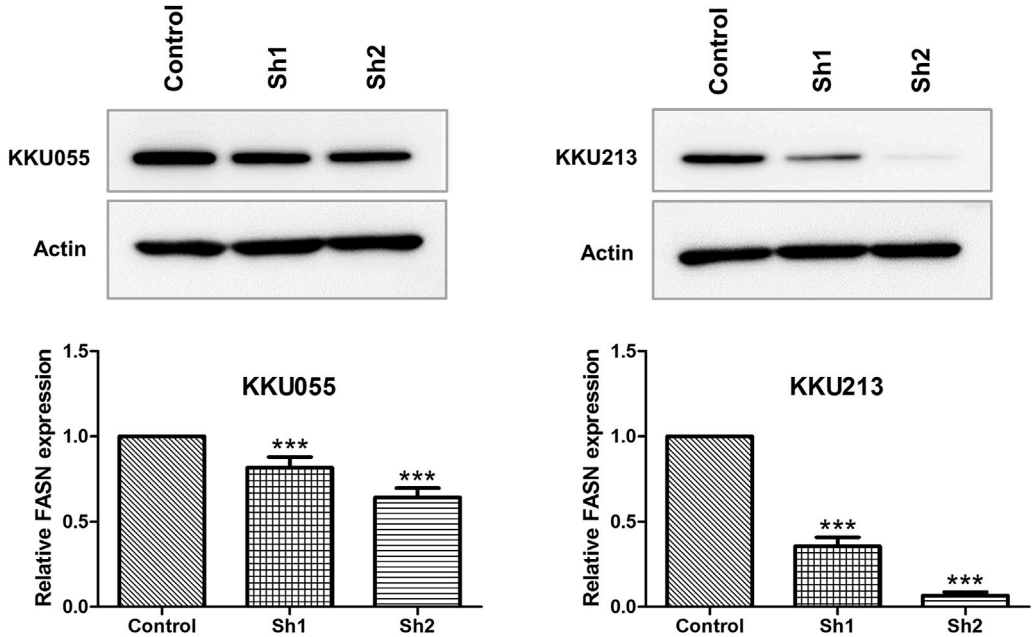

FIGURE 2 | Western blot analysis of FASN knockdown efficiency in CCA cell lines. The protein expressions of FASN in KKU055 and KKU213 cells stably transfected with control shRNA (control) or shRNA against FASN (sh1 and sh2) are shown at the top. The bands were quantified and shown at the bottom. The data are presented as the mean ± standard deviation (SD) of three independent experiments. Statistical significance was determined as ***$p < 0.001$.

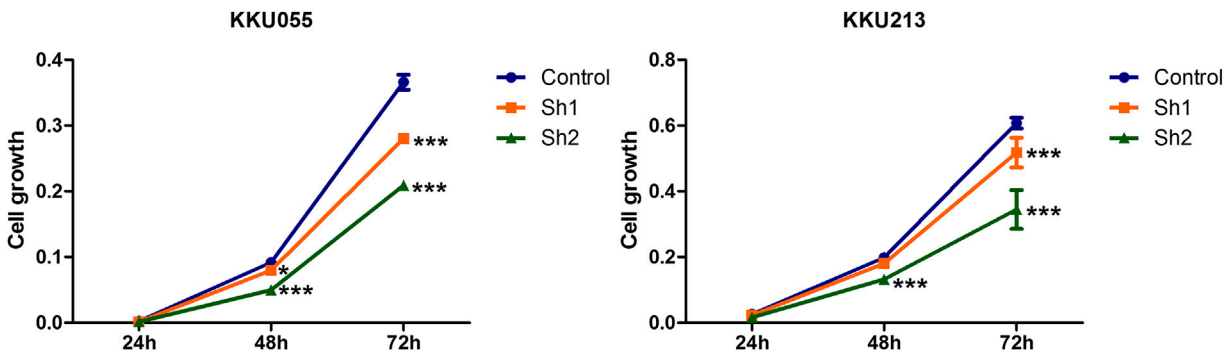

FIGURE 3 | The effect of FASN knockdown on CCA cell growth. The SRB assay was carried out for KKU055 and KKU213 cells at 24, 48 and 72 h post-transfection with shRNA targeting FASN. The data are presented as the mean ± standard deviation (SD) of three independent experiments. Statistical significance was determined as *$p < 0.05$ and ***$p < 0.001$, respectively.

Effect of Fatty Acid Synthase Knockdown on Cholangiocarcinoma Cell Growth

SRB assay was used to explore the effect of FASN knockdown on CCA cell growth (KKU055 and KKU213 cell lines) at 24, 48 and 72 h post-transfection with shRNA targeting FASN. The SRB assay showed a decrease in CCA cell growth in a time-dependent manner, resulting in a significant decrease in the sh1 group at 48 h ($p < 0.05$) and 72 h ($p < 0.001$), and in the sh2 group at 48 and 72 h ($p < 0.001$) in KKU055 cells compared with the control cells. Similarly, for the KKU213 cells, the cell growth was significantly decreased in the sh1 group at 72 h ($p < 0.001$), and in the sh2 group at 48 and 72 h ($p < 0.001$) (**Figure 3**).

Effect of Fatty Acid Synthase Knockdown on Cholangiocarcinoma Cell Migration

The wound-healing assay revealed that FASN knockdown in KKU055 and KKU213 significantly reduced their cell migration ability. Both the sh1 and sh2 groups showed significant reduction at 48 h ($p < 0.001$) in KKU055 cells compared with the control cells. For the KKU213 cells, the

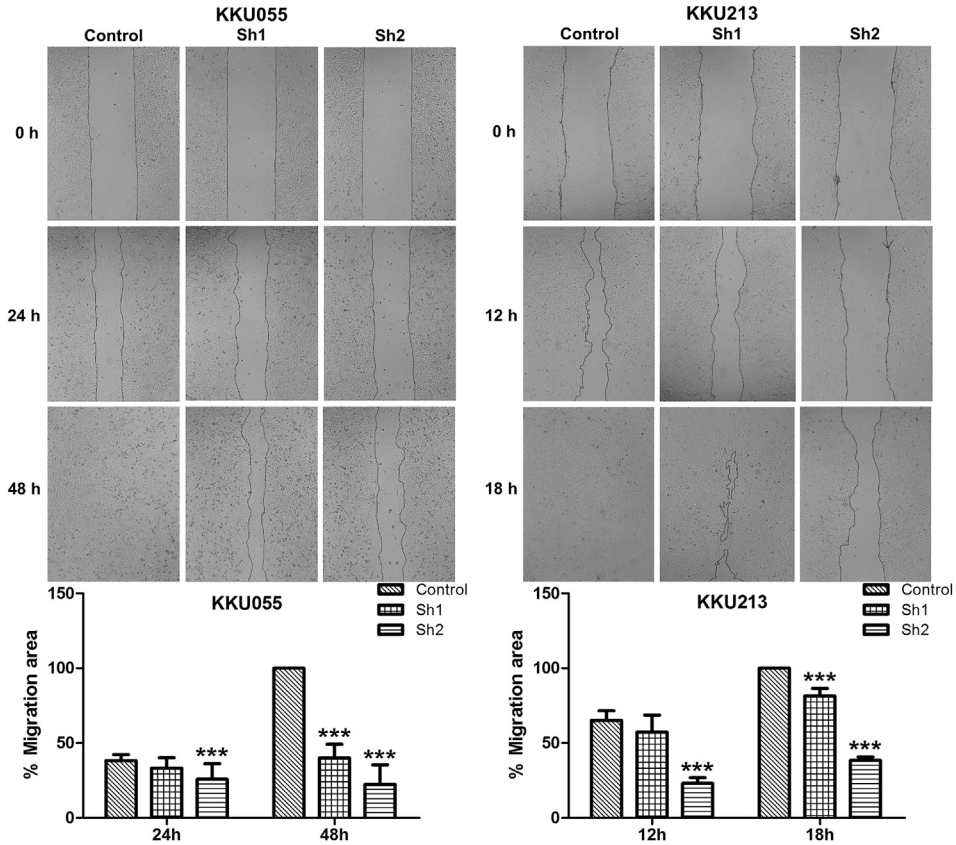

FIGURE 4 | The effect of FASN knockdown on CCA cell migration. The wound-healing assay was conducted on KKU055 and KKU213 cells as shown in the upper panels, respectively. The migration areas were calculated as shown in the lower graphs. The data are presented as the mean ± standard deviation (SD) of three independent experiments. Statistical significance was determined as ***$p < 0.001$.

migration ability of the sh1 and sh2 groups were significantly reduced at 18 h ($p < 0.001$) (**Figure 4**).

Effect of Fatty Acid Synthase Knockdown on Cholangiocarcinoma Cell Invasion

The Boyden chamber assay was used to study the effect of FASN knockdown on CCA cell invasion (KKU055 and KKU213 cell lines). The assay showed that FASN knockdown led to a significant reduction in the number of cells in the sh1 group ($p < 0.05$) and the sh2 group ($p < 0.01$) in KKU055 cells compared with the control cells. Similarly, FASN knockdown significantly reduced the number of cells in both sh1 and sh2 groups ($p < 0.001$) in KKU213 cells (**Figure 5**).

Effect of Fatty Acid Synthase Knockdown on the Cell Cycle of Cholangiocarcinoma Cells

Effect of FASN knockdown on the cell cycle was analyzed using flow cytometry with propidium iodide (PI) DNA staining to determine the cell cycle distribution of KKU055 and KKU213 cells. For KKU055 cells, the FASN knockdown yielded significantly decreased proportion of cells in the G1 phase of the sh1 and sh2 groups ($p < 0.001$) and a significant increase of cells in the G2M phase of the sh1 ($p < 0.05$) and sh2 ($p < 0.001$) groups compared with the control cells. For KKU213 cells, the proportion of cells in the G1 phase was significantly decreased, and G2M phase was elevated in the sh2 group ($p < 0.001$ and $p < 0.01$, respectively) (**Figure 6**).

Effect of Fatty Acid Synthase Knockdown on Apoptosis of Cholangiocarcinoma Cells

To investigate the effect of FASN knockdown on the apoptosis of CCA cells, flow cytometry with annexin V/PI staining was used to confirm programmed cell death in KKU055 and KKU213 cells. Knockdown of FASN expression significantly increased the number of apoptotic cells in the sh1 and sh2 groups ($p < 0.001$) for KKU055 cells, as well as significantly increased the apoptotic cells in the sh2 group ($p < 0.01$) for KKU213 cells compared with the control cells (**Figure 7**).

Metabolic Profiles of Fatty Acid Synthase Knockdown Cholangiocarcinoma Cells

The above results showed that FASN knockdown can inhibit the progression of CCA cells. In order to explore the mechanisms

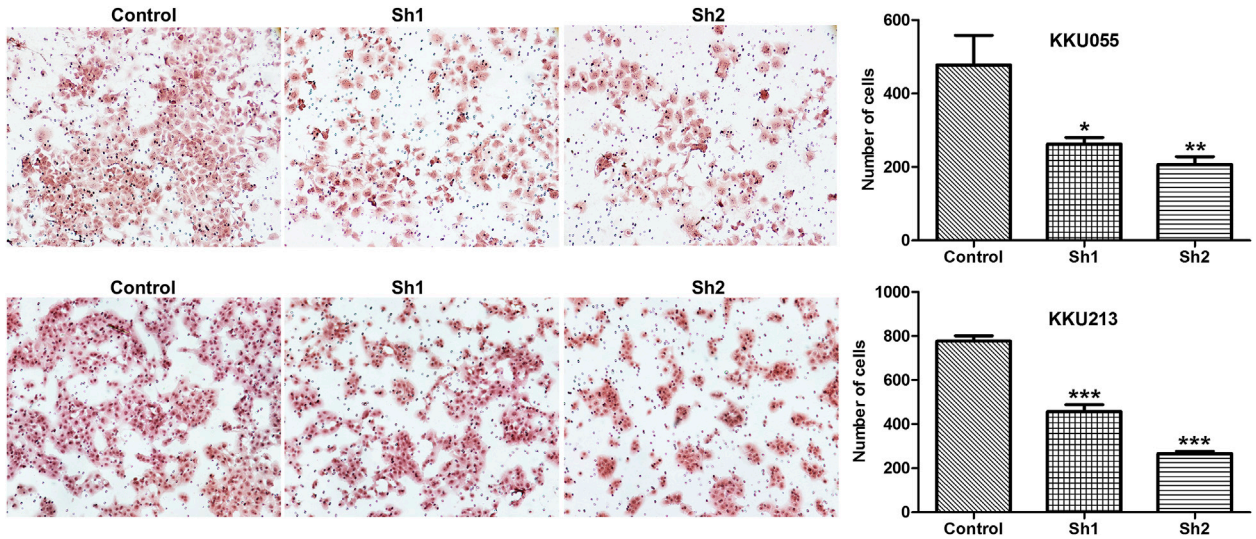

FIGURE 5 | The effect of FASN knockdown on CCA cell invasion. A Boyden chamber assay was evaluated in KKU055 and KKU213 cells as revealed on the left. The number of cells were counted as indicated on the right. The data are presented as the mean ± standard deviation (SD) of three independent experiments. Statistical significance was determined as $*p < 0.05$, $**p < 0.01$ and $***p < 0.001$, respectively.

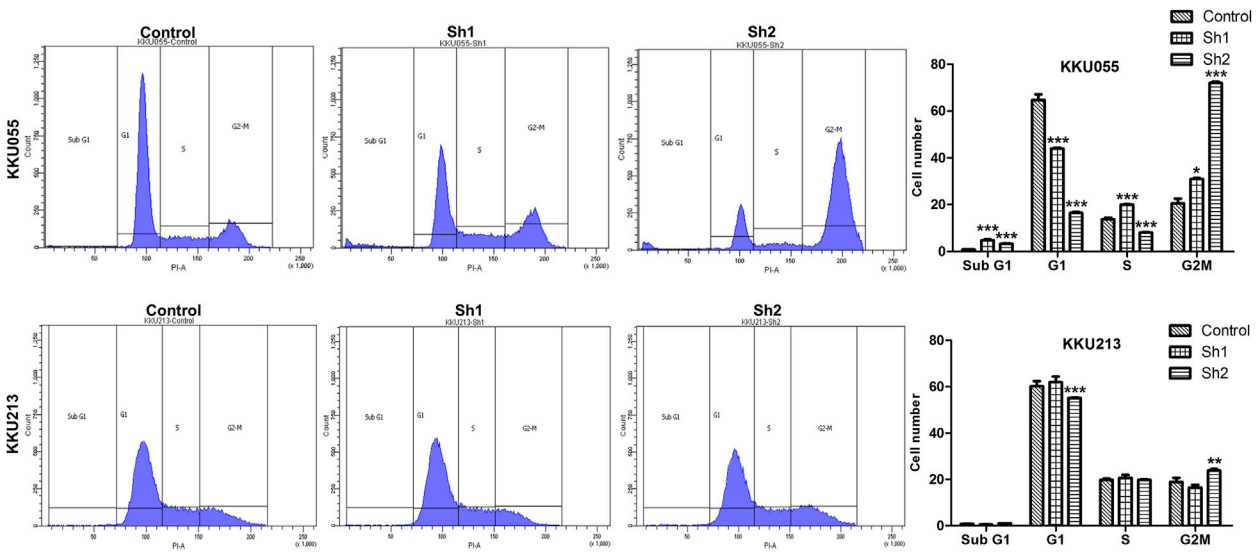

FIGURE 6 | The effect of FASN knockdown on the CCA cell cycle of KKU055 and KKU213 cells. The percentage of cells in each phase as measured by flow cytometry with PI staining is shown on the left. The cell numbers were calculated as shown on the right. The data are presented as the mean ± standard deviation (SD) of three independent experiments. Statistical significance was determined as $*p < 0.05$, $**p < 0.01$ and $***p < 0.001$.

underlying such effects, a metabolomics study was performed on cells transfected with control shRNA (control) and cells stably transfected with shRNA against FASN (FASN knockdown; sh2) in both KKU055 and KKU213 cells. Adenosine diphosphate (ADP), glutamine, guanine, Cer(d18:0/15:0) and peptides were significantly different between the control and FASN knockdown in KKU213 cells (**Figure 8A**). Guanine, xanthine, palmitic amide and PG (P-18:0) showed a significant difference in levels between the control and FASN knockdown KKU055 cells (**Figure 8B**). Moreover, the fold-change (FC) of each metabolite was examined. The result showed that ADP significantly increased in the FASN knockdown KKU213 cell line with an FC more than 1.5 (**Figure 8C**). Furthermore, PG (P-18:0) significantly increased in the FASN knockdown KKU055 cell line while palmitic amide significantly decreased in the FASN knockdown KKU055 cell line with an FC more than 1.5 (**Figure 8D**). In addition, a heatmap with hierarchical clustering was performed for selected metabolites, the results were shown in **Figures 8E,F**. To

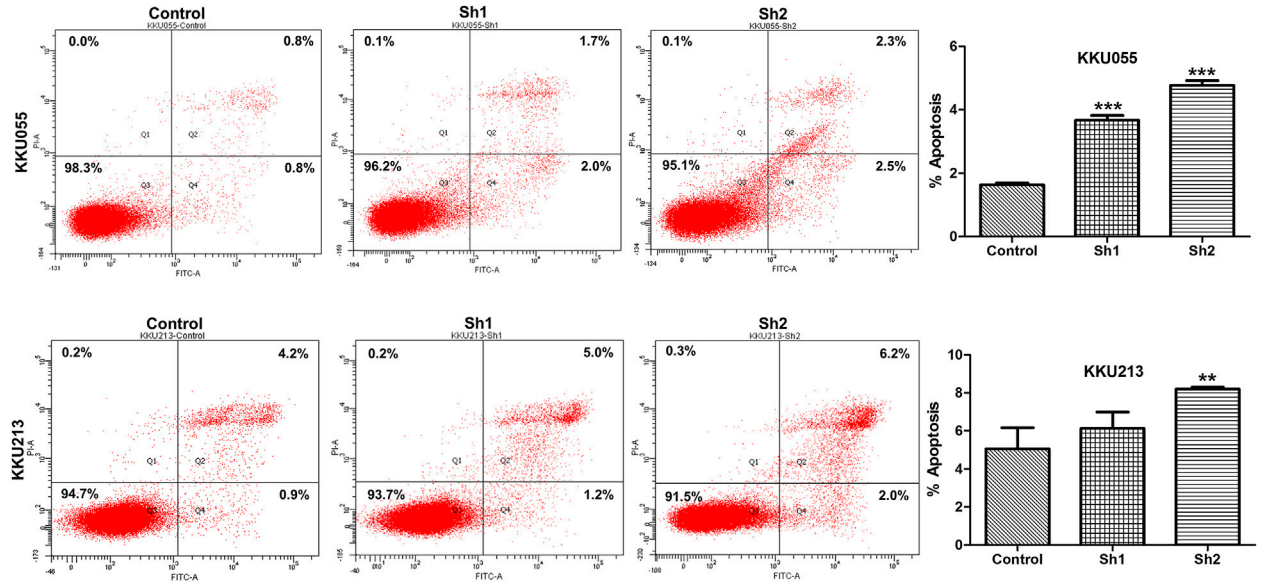

FIGURE 7 | The effect of FASN knockdown on cell apoptosis based on quantitative flow cytometry measurements in KKU055 and KKU213 cells. Apoptotic cells were detected by annexin V/PI staining as shown on the left. The percentages are shown on the right. The data are presented as the mean ± standard deviation (SD) of three independent experiments. Statistical significance was determined as $^{**}p < 0.01$ and $^{***}p < 0.001$.

explore the relevant pathways to the differential metabolites affected by FASN knockdown, enrichment analysis was performed using MetaboAnalyst 5.0 software. The result on KKU213 showed that purine metabolism was the most relevant pathway affected by the FASN knockdown (adjusted p-value < 0.05) (**Figure 9A**). A schematic diagram of the metabolic networks involved in FASN knockdown is depicted in **Figure 9B**.

DISCUSSION

It is commonly recognized that metabolic reprogramming is a hallmark of cancer, and cancer cells require certain changes in metabolism to assist their unrestricted proliferation and metastasis (Hanahan & Weinberg, 2011). Among all the metabolic shifts, activation of the *de novo* lipid biosynthesis pathway is essential for carcinogenesis. There is evidence that an up-regulation of lipid biosynthesis enzymes, including ACC, FASN and HMGCR, can be found in many cancer types. ACC is a major regulator of fatty acid metabolism that is involved in the conversion of acetyl-CoA into malonyl-CoA which is a critical substrate for fatty acid synthesis. Compared with normal cells, cancer cells have a higher synthesis of fatty acid. The factors involved in lipid synthesis are also detected in cell proliferation and viability of certain cancers. In non-small-cell lung cancer, ACC inhibition reduces *de novo* lipid synthesis and decreases cell growth and viability (Svensson et al., 2017). In human U87 EGFRvIII, ACC knockdown not only inhibits *de novo* lipogenesis, but also diminishes U87 EGFRvIII cellular proliferation and viability (Jones et al., 2017). In liver cancer, ACC overexpression is correlated with a poorer prognosis and shorter survival time in liver cancer patients. Moreover, ACC knockdown resulted in decreased liver cancer cell growth and migration. Additionally, ACC knockdown also decreases the mRNA and protein expression levels of the cell proliferation-associated genes; MYCN, JUN, cyclin D1 and cyclin A2 (Ye et al., 2019).

FASN, a crucial enzyme in *de novo* fatty acid synthesis, has been found overexpressed in cancers (Sun et al., 2018; Zielinska et al., 2018). Furthermore, studies showed that the overexpression of FASN is associated with cancer cell proliferation, metastasis, poor prognosis and a high risk of recurrence (Visca et al., 2000; Lu et al., 2019). In addition, FASN overexpression is correlated with lymph node metastasis, TNM stage and a poor prognosis in colorectal cancer patients. FASN knockdown resulted in reduced colorectal cancer cell proliferation and migration, while FASN overexpression exhibited the reverse phenomenon. Moreover, a potential mechanism through FASN-induced colorectal cancer proliferation and metastasis upon its regulation of the AMPK/mTOR pathway by increasing ATP production, resulted in inhibition of AMPK and activation of mTOR has been demostrated (Lu et al., 2019).

HMGCR, the target of statin, is the rate-limiting enzyme for the *in vivo* cholesterol synthesis (Sharpe & Brown, 2013). HMGCR is up-regulated in the gastric cancer tissues that was evident in the previous clinical study (Chushi et al., 2016). HMGCR overexpression promotes the growth and migration of gastric cancer cells, while HMGCR knockdown has the opposite effects both *in vitro* and *in vivo*. In addition, HMGCR activates Hedgehog/Gli1 signaling and promotes the expression of Gli1 target genes. Statin combined with the small molecular inhibitor for Hedgehog signaling might be effective for the gastric cancer treatment (Chushi et al., 2016). HMGCR has

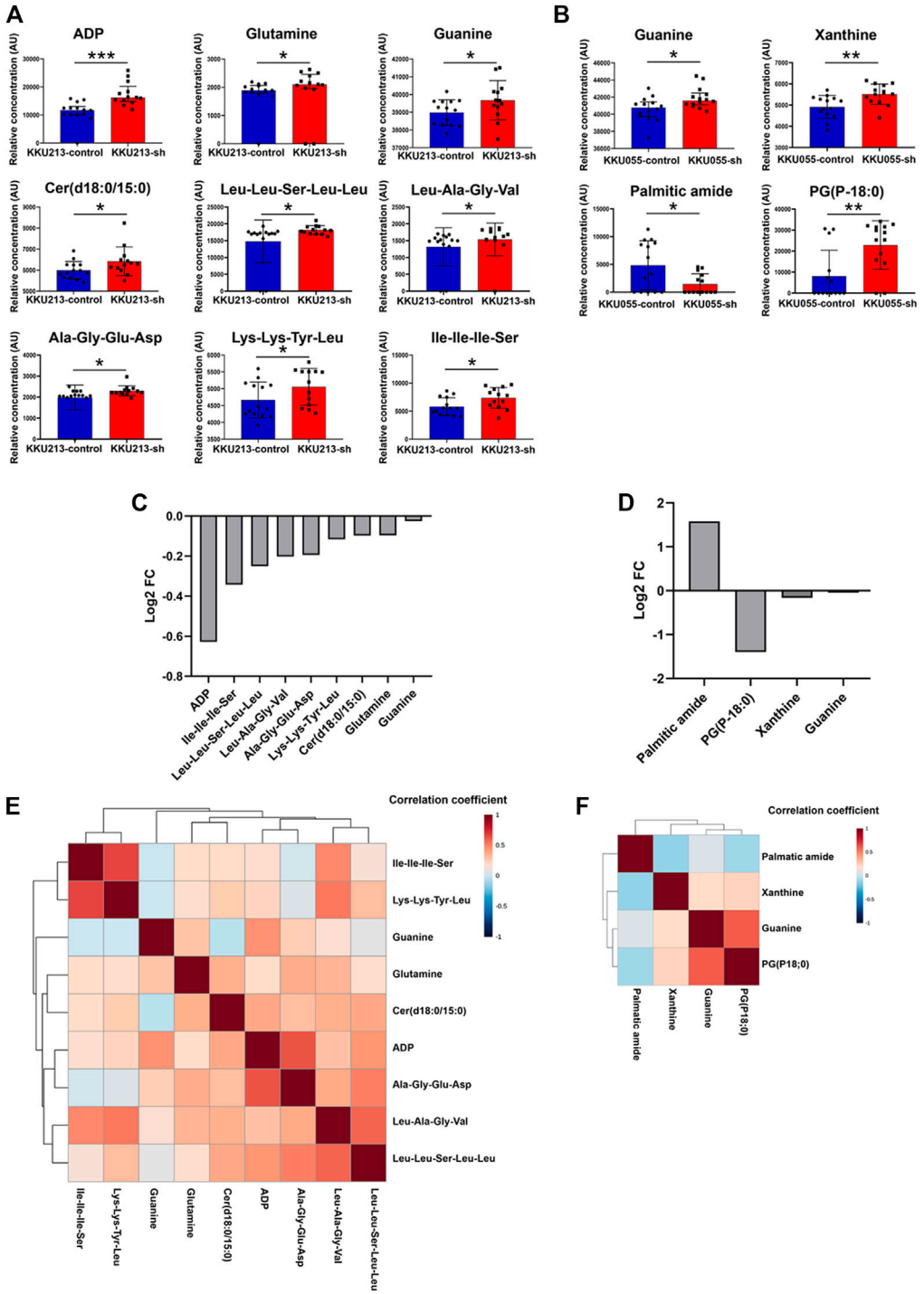

FIGURE 8 | The metabolic profiles of FASN knockdown CCA cells. **(A)** Relative concentrations of candidate metabolites in KKU213, and **(B)** in KKU055 cells; blue and red bar graphs indicate the control and FASN knockdown groups, respectively. Error bars represent the standard deviation (SD) of samples. **(C)** Log_2 of fold change (FC) of metabolites comparing the control and FASN knockdown groups in KKU213, and **(D)** in KKU055 cells. **(E)** Heatmap analysis with hierarchical clustering of all significant metabolites in KKU213, and **(F)** in KKU055 cells. The correlation coefficient from Spearman correlation is indicated in each colored cell on the map. The scale code is shown on the right (red and blue colors indicate positive and negative correlations, respectively). Statistical significance was determined as $^{*}p < 0.05$, $^{**}p < 0.01$ and $^{***}p < 0.001$, respectively.

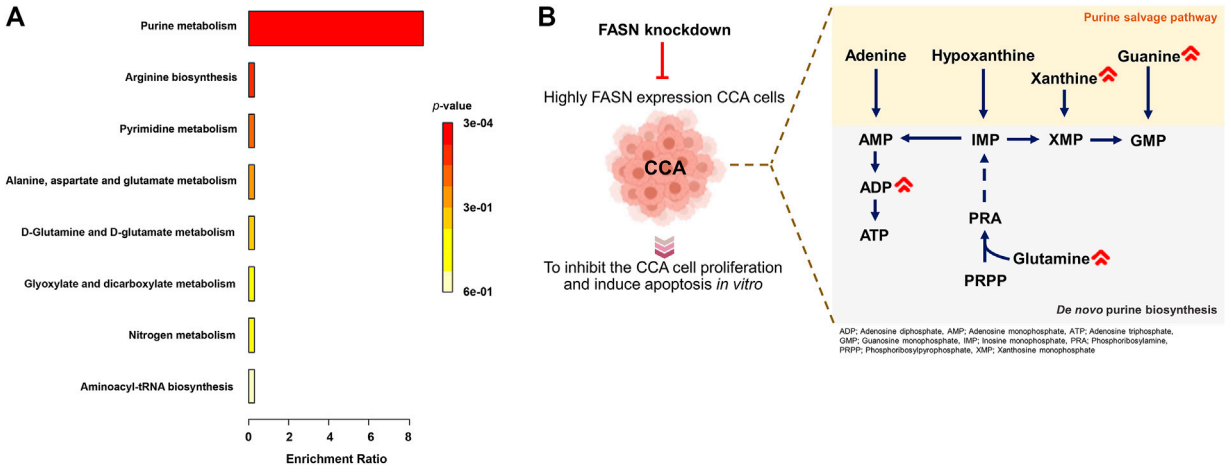

FIGURE 9 | Metabolic networks involved in FASN knockdown. **(A)** Enrichment analysis on identified metabolites from KKU213 cells. **(B)** A schematic diagram of the major metabolic networks involved in FASN knockdown.

been involved in the malignant transformation of normal breast cancer cells, and also in the early-stage tumorigenesis (Singh et al., 2015). Additionally, HMGCR has been reported to foster the growth and migration of the glioma cells (Qiu et al., 2015).

These data demonstrated that ACC, FASN and HMGCR are promising potential targets for cancer treatment. Therefore, the elucidation of changes in lipid metabolism in cancer is required to develop therapeutic targets for various human cancers. In the present study, lipid-metabolizing enzyme expression was higher in CCA tissues. Moreover, clinical data analyses demonstrated the significant association of high FASN expression with advanced-stage CCA. In addition, survival analysis showed that a high expression of FASN and HMGCR were correlated with a shorter survival for CCA patients. We also demonstrated that silencing FASN expression significantly inhibited CCA cell growth, migration, invasion, cell cycle and induced apoptosis *in vitro*.

Our findings reveal metabolic alterations in CCA cells in response to FASN knockdown, determined through an untargeted metabolomics analysis using the UHPLC-MS/MS technique. It demonstrates that global metabolomics is beneficial for study of cellular metabolism. Purines, one of the most abundant metabolic products, are vital biological components that provide the building blocks (adenine and guanine) of DNA and RNA (Pedley and Benkovic, 2018). Purines are also considered key components of several essential biomolecules including ATP, GTP, cAMP, NADH and coenzyme A. These biomolecules are involved in several pathways of biological machinery such as energy production, cellular signaling pathways, redox metabolism and fatty acid synthesis (Virgilio & Adinol, 2017). There are two main purine biosynthesis pathways in mammalian cells, namely the complementary salvage pathway and the purine *de novo* biosynthesis pathway (Yin et al., 2018). Rapidly proliferating cells and tumor cells require higher amount of purines, which are synthesized through the up-regulation of the purine *de novo* biosynthesis pathway (Su et al., 2021). Under normal physiological conditions, most of the cellular requirements for purine from the recycling of degraded bases *via* the salvage pathway. The salvage process uses hypoxanthine-guanine phosphoribosyl transferase (HPRT) to convert hypoxanthine and guanine to inosine monophosphate (IMP) and guanosine monophosphate (GMP), respectively. Adenine can also be combined with phosphoribosyl pyrophosphate (PRPP) to generate adenosine monophosphate (AMP) in a process catalyzed by adenine phosphoribosyl transferase (APRT) (Pedley and Benkovic, 2018). Under cellular conditions requiring higher purine levels, the intracellular purine demand by upregulating the *de novo* biosynthetic pathway, is a highly conserved, energy intensive pathway that generates IMP from PRPP. Purine nucleotide synthesis begins with PRPP and leads to the first fully formed nucleotide: IMP. Through a series of reactions utilizing ATP, tetrahydrofolate derivatives, glutamine, glycine and aspartate, this pathway yields IMP, which signifies a branch point for purine biosynthesis because of its conversion into either AMP or GMP through two distinct reaction pathways (Tolstikov et al., 2014).

Our findings collectively suggest the significant FASN knockdown-associated metabolic changes in purine metabolism of CCA cells that is in agreement with the previously reported mechanism of FASN knockdown DNA-targeting. Purine metabolism is essential for the production of DNA components required for CCA cell proliferation, and its inhibition can lead to apoptosis. In the present study, ADP, glutamine and guanine showed a significant difference between the control and FASN knockdown in KKU213 cells. ADP level decreased in the control group accompanied with lower levels of glutamine and guanine while FASN knockdown cells demonstrated the elevated level of ADP indicating the suppressed ATP content. Similarly, levels of guanine and xanthine were found to be significantly different between the control and FASN knockdown in KKU055 cells as can be evident by decreased levels of guanine and xanthine in the control group. In addition, purine metabolism is the most relevant pathway

involved in FASN knockdown. Glutamine, guanine and xanthine can be used to sustain high rates of cellular proliferation as a key nitrogen donor in purine nucleotide biosynthesis, and also serves as an essential substrate for key enzymes involved in the synthesis of purine nucleotides. The mechanism of FASN knockdown as a suppressor of purine metabolism leads to the inhibition of ATP production and less utilization of purine nucleotides substrate for DNA synthesis compared with control group, which in turn leads to the inhibition of CCA cell proliferation and induces apoptosis.

Based on our results, the two CCA cell lines behave differently with FASN knockdown, which reflect the fact that CCA is a heterogeneous group of malignancies based on histological and molecular characterization (Kendall et al., 2019). Moreover, CCA can emerge at different sites of the biliary tree and with different macroscopic or morphological features (Banales et al., 2016). Furthermore, CCA cells may have different characteristic that can affect pathogenesis and outcome; for example, Li et al. (2016) identified down-regulation of FASN in intrahepatic cholangiocarcinoma while up-regulation of FASN was reported to enhance tumor aggressiveness in various cancer types including CCA, which is consistent with our study (Hao et al., 2014; Li et al., 2014; Yasumoto et al., 2016; Zaytseva et al., 2015; Zhang et al., 2020).

Taken together, FASN may serve as a potential target for the development of a novel CCA therapeutic strategy. The association of genes related to lipid metabolism, cell proliferation and metastasis should be examined to increase our understanding of the functions and targets of FASN. In addition, the cellular functions of FASN *in vivo* and knockout of FASN *via* CRISPR-Cas9 technology should be the subject of further study. Furthermore, the novel drugs, which can inhibit those lipid metabolizing enzymes especially FASN should be further investigation.

CONCLUSION

The high expression of FASN was significantly correlated with advanced stage CCA, resulting in the shorter survival time of CCA patients. Furthermore, FASN knockdown inhibited the growth, migration, invasion, cell cycle and induced apoptosis in CCA cells. The study of metabolomics provides new insights into the mechanism associated with FASN knockdown in CCA cells and identified purine metabolism as the most relevant pathway. Targeting FASN may serve as a novel CCA therapeutic strategy.

DATA AVAILABILITY STATEMENT

The original contributions presented in the study are included in the article/supplementary material, further inquiries can be directed to the corresponding author.

ETHICS STATEMENT

The studies involving human participants were reviewed and approved by The Ethics Committee for Human Research, Khon Kaen University. The patients/participants provided their written informed consent to participate in this study.

AUTHOR CONTRIBUTIONS

WL provided the concept for the research; WL, JT and HD designed the experiments; JT performed the main experiments; JT and SP analyzed the metabolomics study; All authors contributed toward data discussion, manuscript review and editing.

FUNDING

This study was supported by the grant of the National Research Council of Thailand through Fluke Free Thailand Project and the Basic Research Fund of Khon Kaen University under Cholangiocarcinoma Research Institute to WL and a grant from Invitation Research Grant (IN64123) allocated to JT.

ACKNOWLEDGMENTS

The authors express gratitude to Professor Trevor N. Petney for editing the MS *via* the Publication Clinic KKU, Thailand.

REFERENCES

Alò, P. L., Visca, P., Framarino, M. L., Botti, C., Monaco, S., Sebastiani, V., et al. (2000). Immunohistochemical Study of Fatty Acid Synthase in Ovarian Neoplasms. *Oncol. Rep.* 7 (6), 1383–1388. doi:10.3892/or.7.6.1383

Alsaleh, M., Leftley, Z., Barbera, T. A., Sithithaworn, P., Khuntikeo, N., Loilome, W., et al. (2019). Cholangiocarcinoma: A Guide for the Nonspecialist. *Ijgm* 12, 13–23. doi:10.2147/IJGM.S186854

Banales, J. M., Cardinale, V., Carpino, G., Marzioni, M., Andersen, J. B., Invernizzi, P., et al. (2016). Cholangiocarcinoma: Current Knowledge and Future Perspectives Consensus Statement from the European Network for the Study of Cholangiocarcinoma (ENS-CCA). *Nat. Rev. Gastroenterol. Hepatol.* 13 (5), 261–280. doi:10.1038/nrgastro.2016.51

Chushi, L., Wei, W., Kangkang, X., Yongzeng, F., Ning, X., and Xiaolei, C. (2016). HMGCR Is Up-Regulated in Gastric Cancer and Promotes the Growth and Migration of the Cancer Cells. *Gene* 587 (1), 42–47. doi:10.1016/j.gene.2016.04.029

Emwas, A.-H. M. (2015). The Strengths and Weaknesses of NMR Spectroscopy and Mass Spectrometry with Particular Focus on Metabolomics Research. *Metabonomics* 1277, 161–193. doi:10.1007/978-1-4939-2377-9_13

Gaul, D. A., Mezencev, R., Long, T. Q., Jones, C. M., Benigno, B. B., Gray, A., et al. (2015). Highly-accurate Metabolomic Detection of Early-Stage Ovarian Cancer. *Sci. Rep.* 5, 1–7. doi:10.1038/srep16351

Griffin, J. L., and Shockcor, J. P. (2004). Metabolic Profiles of Cancer Cells. *Nat. Rev. Cancer* 4, 551–561. doi:10.1038/nrc1390

Hanahan, D., and Weinberg, R. A. (2011). Hallmarks of Cancer: The Next Generation. *Cell* 144 (5), 646–674. doi:10.1016/j.cell.2011.02.013

Hao, Q., Li, T., Zhang, X., Gao, P., Qiao, P., Li, S., and Geng, Z. (2014). Expression and Roles of Fatty Acid Synthase in Hepatocellular Carcinoma. *Oncol. Rep.* 32 (6), 2471–2476. doi:10.3892/or.2014.3484

Jones, J. E. C., Esler, W. P., Patel, R., Lanba, A., Vera, N. B., Pfefferkorn, J. A., et al. (2017). Inhibition of Acetyl-CoA Carboxylase 1 (ACC1) and 2 (ACC2) Reduces Proliferation and De Novo Lipogenesis of EGFRvIII Human Glioblastoma Cells. *PLoS ONE* 12 (1), e0169566–20. doi:10.1371/journal.pone.0169566

Kendall, T., Verheij, J., Gaudio, E., Evert, M., Guido, M., Goeppert, B., et al. (2019). Anatomical, Histomorphological and Molecular Classification of Cholangiocarcinoma. *Liver Internat.* 39 (S1), 7–18. doi:10.1111/liv.14093

Khuntikeo, N., Chamadol, N., Chamadol, N., Yongvanit, P., Loilome, W., Namwat, N., et al. (2015). Cohort Profile: Cholangiocarcinoma Screening and Care Program (CASCAP). *BMC Cancer* 15 (1), 1–8. doi:10.1186/s12885-015-1475-7

Li, J., Dong, L., Wei, D., Wang, X., Zhang, S., and Li, H. (2014). Fatty Acid Synthase Mediates the Epithelial-Mesenchymal Transition of Breast Cancer Cells. *Internat. J. Biol. Sci.* 10 (2), 171–180. doi:10.7150/ijbs.7357

Li, L., Che, L., Tharp, K. M., Park, H. M., Pilo, M. G., Cao, D., et al. (2016). Differential Requirement for de Novo Lipogenesis in Cholangiocarcinoma and Hepatocellular Carcinoma of Mice and Humans. *Hepatology* 63 (6), 1900–1913. doi:10.1002/hep.28508

Lu, T., Sun, L., Wang, Z., Zhang, Y., He, Z., and Xu, C. (2019). Fatty Acid Synthase Enhances Colorectal Cancer Cell Proliferation and Metastasis via Regulating AMPK/mTOR Pathway. *Ott* 12, 3339–3347. doi:10.2147/OTT.S199369

Pang, Z., Chong, J., Li, S., and Xia, J. (2020). MetaboAnalystR 3.0: Toward an Optimized Workflow for Global Metabolomics. *Metabolites* 10 (5), 186. doi:10.3390/metabo10050186

Pedley, A. M., and Benkovic, S. J. (2017). A New View into the Regulation of Purine Metabolism: The Purinosome. *Trends Biochem. Sci.* 42, 141–154. doi:10.1016/j.tibs.2016.09.009.A2

Qiu, Z., Yuan, W., Chen, T., Zhou, C., Liu, C., Huang, Y., et al. (2015). HMGCR Positively Regulated the Growth and Migration of Glioblastoma Cells. *Gene* 576 (1), 22–27. doi:10.1016/j.gene.2015.09.067

Sharpe, L. J., and Brown, A. J. (2013). Controlling Cholesterol Synthesis beyond 3-Hydroxy-3-Methylglutaryl-CoA Reductase (HMGCR). *J. Biol. Chem.* 288 (26), 18707–18715. doi:10.1074/jbc.R113.479808

Singh, R., Yadav, V., Kumar, S., and Saini, N. (2015). MicroRNA-195 Inhibits Proliferation, Invasion and Metastasis in Breast Cancer Cells by Targeting FASN, HMGCR, ACACA and CYP27B1. *Sci. Rep.* 5, 1–15. doi:10.1038/srep17454

Su, W. J., Lu, P. Z., Wu, Y., Kalpana, K., Yang, C. K., and Lu, G. D. (2021). Identification of Key Genes in Purine Metabolism as Prognostic Biomarker for Hepatocellular Carcinoma. *Front. Oncol.* 10, 1–13. doi:10.3389/fonc.2020.583053

Sun, L., Yao, Y., Pan, G., Zhan, S., Shi, W., Lu, T., et al. (2018). Small Interfering RNA mediated Knockdown of Fatty Acid Synthase Attenuates the Proliferation and Metastasis of Human Gastric Cancer Cells via the mTOR/Gli1 Signaling Pathway. *Oncol. Lett.* 16 (1), 594–602. doi:10.3892/ol.2018.8648

Svensson, R. U., Parker, S. J., Eichner, L. J., Kolar, M. J., Wallace, M., Brun, S. N., et al. (2016). Inhibition of Acetyl-CoA Carboxylase Suppresses Fatty Acid Synthesis and Tumor Growth of Non-small-cell Lung Cancer in Preclinical Models. *Nat. Med.* 22 (10), 1108–1119. doi:10.1038/nm.4181

Tolstikov, V., Nikolayev, A., Dong, S., Zhao, G., and Kuo, M. S. (2014). Metabolomics Analysis of Metabolic Effects of Nicotinamide Phosphoribosyltransferase (NAMPT) Inhibition on Human Cancer Cells. *PLoS ONE* 9 (12), e114019–24. doi:10.1371/journal.pone.0114019

Virgilio, F. Di., and Adinolfi, E. (2017). Extracellular Purines, Purinergic Receptors and Tumor Growth. *Oncogene* 36 (3), 293–303. doi:10.1038/onc.2016.206

Vorkas, P. A., Isaac, G., Anwar, M. A., Davies, A. H., Want, E. J., Nicholson, J. K., et al. (2015). Untargeted UPLC-MS Profiling Pipeline to Expand Tissue Metabolome Coverage: Application to Cardiovascular Disease. *Anal. Chem.* 87 (10), 4184–4193. doi:10.1021/ac50377510.1021/ac503775m

Yasumoto, Y., Miyazaki, H., Vaidyan, L. K., Kagawa, Y., Ebrahimi, M., Yamamoto, Y., et al. (2016). Inhibition of Fatty Acid Synthase Decreases Expression of Stemness Markers in Glioma Stem Cells. *PLoS ONE* 11 (1), 1–14. doi:10.1371/journal.pone.0147717

Ye, B., Yin, L., Wang, Q., and Xu, C. (2019). ACC1 Is Overexpressed in Liver Cancers and Contributes to the Proliferation of Human Hepatoma Hep G2 Cells and the Rat Liver Cell Line BRL 3A. *Mol. Med. Rep.* 49 (5), 3431–3440. doi:10.3892/mmr.2019.9994

Yin, J., Ren, W., Huang, X., Deng, J., Li, T., and Yin, Y. (2018). Potential Mechanisms Connecting Purine Metabolism and Cancer Therapy. *Front. Immunol.* 9, 1697–1698. doi:10.3389/fimmu.2018.01697

Yongvanit, P., Pinlaor, S., and Bartsch, H. (2012). Oxidative and Nitrative DNA Damage: Key Events in Opisthorchiasis-Induced Carcinogenesis. *Parasitol. Int.* 61 (1), 130–135. doi:10.1016/j.parint.2011.06.011

Zaytseva, Y. Y., Harris, J. W., Mitov, M. I., Kim, J. T., Allan Butterfield, D., Lee, E. Y., et al. (2015). Increased Expression of Fatty Acid Synthase Provides a Survival Advantage to Colorectal Cancer Cells via Upregulation of Cellular Respiration. *Oncotarget* 6 (22), 18891–18904. doi:10.18632/oncotarget.3783

Zhang, B., Zhou, B. H., Xiao, M., Li, H., Guo, L., and Wang, M. X. (2020). KDM5C Represses FASN-Mediated Lipid Metabolism to Exert Tumor Suppressor Activity in Intrahepatic Cholangiocarcinoma. *Front. Oncol.* 10, 1–13. doi:10.3389/fonc.2020.01025

Zhang, A., Sun, H., Yan, G., Wang, P., Han, Y., and Wang, X. (2014). Metabolomics in Diagnosis and Biomarker Discovery of Colorectal Cancer. *Cancer Lett.* 345 (1), 17–20. doi:10.1016/j.canlet.2013.11.011

Zielinska, H. A., Holly, J. M. P., Bahl, A., and Perks, C. M. (2018). Inhibition of FASN and ERα Signalling during Hyperglycaemia-Induced Matrix-specific EMT Promotes Breast Cancer Cell Invasion via a Caveolin-1-dependent Mechanism. *Cancer Lett.* 419, 187–202. doi:10.1016/j.canlet.2018.01.028

Conflict of Interest: The authors declare that the research was conducted in the absence of any commercial or financial relationships that could be construed as a potential conflict of interest.

Publisher's Note: All claims expressed in this article are solely those of the authors and do not necessarily represent those of their affiliated organizations, or those of the publisher, the editors and the reviewers. Any product that may be evaluated in this article, or claim that may be made by its manufacturer, is not guaranteed or endorsed by the publisher.

Copyright © 2021 Tomacha, Dokduang, Padthaisong, Namwat, Klanrit, Phetcharaburanin, Wangwiwatsin, Khampitak, Koonmee, Titapun, Jarearnrat, Khuntikeo and Loilome. This is an open-access article distributed under the terms of the Creative Commons Attribution License (CC BY). The use, distribution or reproduction in other forums is permitted, provided the original author(s) and the copyright owner(s) are credited and that the original publication in this journal is cited, in accordance with accepted academic practice. No use, distribution or reproduction is permitted which does not comply with these terms.

frontiers in Pharmacology

SYSTEMATIC REVIEW
published: 31 August 2021
doi: 10.3389/fphar.2021.747180

Absence of Biomarker-Driven Treatment Options in Small Cell Lung Cancer, and Selected Preclinical Candidates for Next Generation Combination Therapies

Nicholas R. Liguori[1,2], *Young Lee*[2], *William Borges*[2], *Lanlan Zhou*[2,3,4,5], *Christopher Azzoli*[4,5,6]* *and Wafik S. El-Deiry*[2,3,4,5,6]*

[1]Lewis Katz School of Medicine, Temple University, Philadelphia, PA, United States, [2]Laboratory of Translational Oncology and Experimental Cancer Therapeutics, Warren Alpert Medical School, Brown University, Providence, RI, United States, [3]Department of Pathology and Laboratory Medicine, Warren Alpert Medical School, Brown University, Providence, RI, United States, [4]Joint Program in Cancer Biology, Lifespan Health System and Brown University, Providence, RI, United States, [5]Cancer Center at Brown University, Thoracic Oncology, Providence, RI, United States, [6]Hematology/Oncology Division, Department of Medicine, Lifespan Health System and Brown University, Providence, RI, United States

OPEN ACCESS

Edited by:
Claudia Cerella,
Fondation de Recherche Cancer et Sang, Luxembourg

Reviewed by:
Xianda Zhao,
University of Minnesota, United States
Martin Früh,
Kantonsspital St. Gallen, Switzerland

***Correspondence:**
Wafik S. El-Deiry
wafik@brown.edu
Christopher Azzoli
christopher_azzoli@brown.edu

Specialty section:
This article was submitted to Pharmacology of Anti-Cancer Drugs, a section of the journal Frontiers in Pharmacology

Received: 25 July 2021
Accepted: 09 August 2021
Published: 31 August 2021

Citation:
Liguori NR, Lee Y, Borges W, Zhou L, Azzoli C and El-Deiry WS (2021) Absence of Biomarker-Driven Treatment Options in Small Cell Lung Cancer, and Selected Preclinical Candidates for Next Generation Combination Therapies. Front. Pharmacol. 12:747180. doi: 10.3389/fphar.2021.747180

Lung cancer is the second most common cancer in the United States, and small cell lung cancer (SCLC) accounts for about 15% of all lung cancers. In SCLC, more than other malignancies, the standard of care is based on clinical demonstration of efficacy, and less on a mechanistic understanding of why certain treatments work better than others. This is in large part due to the virulence of the disease, and lack of clinically or biologically relevant biomarkers beyond routine histopathology. While first line therapies work in the majority of patients with extensive stage disease, development of resistance is nearly universal. Although neuroendocrine features, Rb and p53 mutations are common, the current lack of actionable biomarkers has made it difficult to develop more effective treatments. Some progress has been made with the application of immune checkpoint inhibitors. There are new agents, such as lurbinectedin, that have completed late-phase clinical testing while other agents are still in the pre-clinical phase. ONC201/TIC10 is an imipridone with strong *in vivo* and *in vitro* antitumor properties and activity against neuroendocrine tumors in phase 1 clinical testing. ONC201 activates the cellular integrated stress response and induces the TRAIL pro-apoptotic pathway. Combination treatment of lurbinectedin with ONC201 are currently being investigated in preclinical studies that may facilitate translation into clinical trials for SCLC patients.

Keywords: SCLC, immunotherapys, chemotherapy, imipridones, genomics

INTRODUCTION

Lung cancer is the second most prevalent cancer diagnosis in the United States and has the highest mortality rate. SCLC comprises approximately 15% of all lung cancers. This is a man-made epidemic caused by cigarette smoking. Cigarette smoke contains polycyclic aromatic hydrocarbons, arsenic, and other potent carcinogens which cause the genetic changes which create SCLC (Govindan et al., 2006). The natural history of SCLC is to grow and spread quickly with a doubling time as short as

25–30 days and unique propensity to hematogenous spread (Pietanza et al., 2015). Patients with SCLC are typically diagnosed with a hilar mass or other bulky lymphadenopathy, frequently accompanied by symptoms of cough and dyspnea. It is uncommon for patients to present with solitary nodules or thoracic lymphadenopathy. Widespread metastatic disease often presents with weight loss, bone pain and neurologic problems. Without treatment, the median survival time for extensive disease is measured in weeks. Limited stage disease has a median survival time of 15–20 months, and the overall 5 years survival rate for SCLC is less than 7% (Byers and Rudin, 2015). The poor survival for patients with SCLC has not changed much in 4 decades (Weisenthal, 1981).

Other than categorizing the disease into limited or extensive stage, SCLC defies practical clinical or genomic categorization, and management decisions are stark. Often, patients are in an urgent or desperate situation upon initial presentation or at the time of recurrence of disease, e.g., superior vena cava syndrome (Chan et al., 1997; Brzezniak et al., 2017). Initial combination chemotherapy is typically, and dramatically effective, but responses are short-lived and recurrent disease is virulent. First-line, platinum-based chemotherapy, typically combined with etoposide, has been the foundation for SCLC treatment over the past half-century, with response rates up to 80% (Pietanza et al., 2015). These therapies also are toxic to patients, with many experiencing hair loss, high-grade fatigue, cytopenias, nausea, and diarrhea.

In response to the dismal prognosis of SCLC, innumerable drugs have been tested, several drugs have earned NCCN compendium listing, and some drugs are FDA-approved. Recent advances in SCLC treatment have been made with immune checkpoint inhibitor therapy (Esposito et al., 2020). Biomarkers such as PD-L1 protein expression, and tumor mutation burden, are not sufficiently robust to select which patients should receive it. Similarly, no biomarkers exist for treatment selection of other available drug treatments. In this complex disease, there exists a gap between preclinical efficacy in treatment and trial outcomes. This is due to the virulence mechanisms of the SCLC cells, as well as resistance to treatment that quickly develops in these patients.

Emerging therapies include novel immune therapies, as well as drugs with innovative mechanisms of action that target specific molecular pathways. Our review will detail some of the promising approaches emerging from a landscape which currently lacks molecular biomarkers for refinement of drug therapy selection.

IMMUNOTHERAPY INCREASES SURVIVAL IN SCLC

In recent years, immunotherapies have been used to increase overall survival in SCLC (Pavan et al., 2019; Saltos et al., 2020). Increasing tumor-specific T-cell immunity by inhibiting programmed death ligand 1 (PD-L1)–programmed death 1 (PD-1) signaling has shown promise in the treatment of small cell lung cancer, among many other malignancies, and are now routinely added to first-line therapy (Horn et al., 2018; Zhou et al., 2020). PD-1 inhibitors target PD-1 receptors on T-cells and prevent the interaction between PD-1 and its ligands, PD-L1 and PD-L2. PD-1 inhibition enhances T-lymphocyte function and increases cytokine crosstalk between the PD-1 positive T-cells and dendritic cells specialized in activation in the tumor microenvironment. A consequence of this interaction with PD-L1 and PD-L2 is the release of proinflammatory cytokines, such as TNF-α and IFN-γ, which enhance the stem-like properties of T-cells in the tumor microenvironment (Berraondo, 2019). PD-L1 inhibitors, such as atezolizumab, and durvalumab, target the interaction of PD-1 and B7, prevent protumor effects and restore antitumor T-cell function. Additionally, PD-L1 has been shown to exert non-immune proliferative effects on tumor cells (Han et al., 2020) providing an additional benefit to anti-PD-L1 therapies. An important difference between PD-1 inhibitors and PD-L1 inhibitors is that PD-L1 inhibitors still allow the interaction between PD-1 and PD-L2. The continued binding of PD-1 to PD-L2 weakens the immune and proinflammatory response, and, in theory, makes the therapy more tolerable for patients, decreasing the risk of adverse effects.

The CheckMate 032 trial evaluated the efficacy of PD-1 inhibitor nivolumab compared to the combination of nivolumab and ipilimumab, a CTLA-4 inhibitor in patients with previously-treated, extensive stage small cell lung cancer. The combination was shown to have a higher response rate than nivolumab alone (Antonia et al., 2016). In August 2018 the US FDA approved nivolumab for the treatment of patients with metastatic small cell lung cancer whose cancer has progressed after platinum-based chemotherapy and at least one other line of therapy based on the results of CheckMate 032. A subsequent phase 3 study (CheckMate 451), failed to demonstrate the efficacy of ipilimumab and nivolumab when started after initial response to chemotherapy, and off-label use of the combination has fallen out of favor (Owonikoko et al., 2021).

The KEYNOTE-028 study evaluated efficacy of the PD-1 inhibitor pembrolizumab in recurrent SCLC patients. The study showed an overall response rate of 18.7% (Chung et al., 2018). Patients with PD-L1 negative tumors had a median survival of 7.7 months, while PD-L1 positive patients had an impressive overall survival of 14.6 months (Chung et al., 2018), indicating pembrolizumab may have more benefit in patients with PD-L1 positive tumors. It should be noted that FDA approval was withdrawn from nivolumab and pembrolizumab in early 2021.

Atezolizumab, when added to first line carboplatin and etoposide, improves overall survival. The IMpower33 study showed that patients receiving atezolizumab, carboplatin and etoposide had a median overall survival of 12.3 months compared to 10.3 months in the control group (Mathieu et al., 2021). Progression free survival was also statistically improved, with a PFS of 5.2 months in the experimental arm compared to 4.3 months in the control arm (Mathieu et al., 2021). In March 2019, the US FDA approved atezolizumab in combination with carboplatin and etoposide for the first-line treatment of patients with extensive-stage small cell lung cancer.

The CASPIAN study tested another PD-L1 inhibitor, durvalumab, in combination with etoposide and platinum. In

this study, there was statistical benefit to adding durvalumab to first-line treatment, with patients receiving durvalumab, etoposide and platinum achieving an overall survival of 13.0 months compared to 10.3 months in the control arm (Mathieu et al., 2021). In March 2020, the US FDA approved durvalumab in combination with etoposide and either carboplatin or cisplatin as first-line treatment of patients with extensive-stage small cell lung cancer. A third study tested platinum-etoposide +/− the anti-PD-1 drug, pembrolizumab, with similar results, although the results in the pembrolizumab study were not statistically significant. (Rudin et al., 2020). There have been no head-to-head comparisons of atezolizumab, durvalumab, or pembrolizumab for this indication, although benefit is similar across studies.

While immunotherapies have had a fair amount of success relative to other treatment options in SCLC in the past 3 years, it is important to note that one of the many virulence factors that make SCLC difficult to target is their innate ability to avoid the surveillance of the host immune system. Compared to NSCLC cells, SCLC cells are less likely to be recognized by the host NK cells and induce an immune mediated response without pharmacological intervention. It has been reported that SCLC cells have a lower expression MHC-1 than their NSCLC counterparts (Zhu et al., 2021). Lack of MHC expression is what can drive reduced immunogenicity, despite SCLC's high tumor mutational burden (Zhu et al., 2021). Zhu et al. found that when innate immune cell interactions with SCLC were investigated, it was found that MICA/B and ULBP1,2,3 expression was considerably reduced when compared to NSCLC cells (George et al., 2015; Zhu et al., 2021). Similarly, SCLC NKG2DL levels were reduced and the protein expression of NKG2DLs in human SCLC-A lines showed undetectable levels of both MICA/B on their surface and soluble MICA/B (Zhu et al., 2021). These findings indicate that SCLC-A cells may have a diminished visibility to adaptive and innate immune responses. The lack of NKG2DL expression allows SCLC cells to evade the immune response and escape NK surveillance (Ni et al., 2017; Zhu et al., 2021).

This illustrates another important area of potentially beneficial therapy that requires further investigation as it relates to immune surveillance of cancer cells. Pharmacologic strategies of increasing NK-recognition of SCLC cells, including epigenetic regulators, could sensitize the tumor cells to therapeutic agents and to T-cell killing (Zhu et al., 2021). HDAC inhibitors are a promising option to suppress tumor growth and SCLC cell proliferation. These inhibitors also induce Notch signaling and induce cell-cycle arrest, and have been studied extensively *in vitro* (Zhu et al., 2015; Sun et al., 2018). A preclinical HDAC inhibitor showed potential to cause NK-dependent killing of the tumor cells, showing the NK-mediated antitumor effect of shHDAC6, though this model was not related to NKG2DL activity (Liu et al., 2018). Additional studies have shown that NKG2DL stimulating therapies have promoted responses in patients receiving NK-infusions (Cifaldi et al., 2017). This suggests that HDAC inhibitors may provide a synergistic benefit if added to an adoptive NK-cell transfer for patient treatment (Zhu et al., 2021). Lack of NKG2DLs can potentially be exploited by future studies to evaluate NK-cell activation therapies in SCLC treatment investigations (Zhu et al., 2021), especially those that monitor expression of NK activating ligands such as NKG2DLs.

These studies confirm that there is significant benefit to adding PD1/PD-L1 inhibitors to first-line chemotherapy in extensive stage SCLC, while also underscoring the importance of investigating epigenetic regulators in SCLC. It is important to note, that research to enhance the ability of the immune system to kill SCLC and its inherent properties are a major research effort. While advances in immunotherapy in SCLC patients are modest and there has not been an overwhelming breakthrough with these therapies, the effects of immunotherapies remain statistically significant and clinically relevant.

GENOMICS OF SMALL CELL LUNG CANCER

SCLC arises from stem cells that partially differentiate to have a neuroendocrine phenotype resulting in a unique appearance under the microscope. The histopathology of SCLC often shows dense sheets of small cells with neuroendocrine features (Bernhardt et al., 2016) that divide quickly and show frequent mitosis and high nuclear to cytoplasm ratio with little to no nucleoli (Bernhardt et al., 2016). These features contribute to SCLC cells' ability to proliferate, migrate, and form both local and metastatic tumors. The genetic profile of SCLC predisposes the cells to have an aggressive nature, and the multitude of mutations and high mutational burden in SCLC makes treating with chemotherapy a difficult task. It is essential to note that certain SCLC subsets will contain heterogeneity and contain non-small cell lung cancer features (Gazdar et al., 2017). Additionally, 15% of all SCLC do not express neuroendocrine markers at all (Gazdar et al., 2017) and may have protein expression patterns more similar to adenocarcinoma of the lung.

The arrival of combination chemotherapy has significantly improved pharmacologic effectiveness when treating SCLC. However, due to the complex genetic profile of SCLC, targeted chemotherapies remain elusive. Targeted therapies pursue specific genes and proteins that are involved with the growth and survival of tumor cells. These therapies can block the tumorigenic effects of specific abnormalities that make SCLC cells grow, survive, and metastasize. These therapies consist of small-molecule drugs that block angiogenesis and cell proliferation or monoclonal antibodies that block a specific target on the exterior of cancer cells. Other targeted therapies include apoptosis-inducing drugs, angiogenesis inhibitors and immunotherapies. Despite the diversity of actions of the drugs and the virulence mechanisms they target, targeted therapies in SCLC have yielded disappointing results.

Many prominent genomic features of small cell lung cancer currently lack drug therapy alternatives. For example, approximately 27% of SCLC has a SOX2 amplification (Gadgeel, 2018) SOX2, which encodes a transcriptional regulator of stem cells, promotes initiation and growth of SCLC (Gazdar et al., 2017) SOX2, located on chromosome 3q26.3-q27 is implicated in SCLC by a multiplication of the

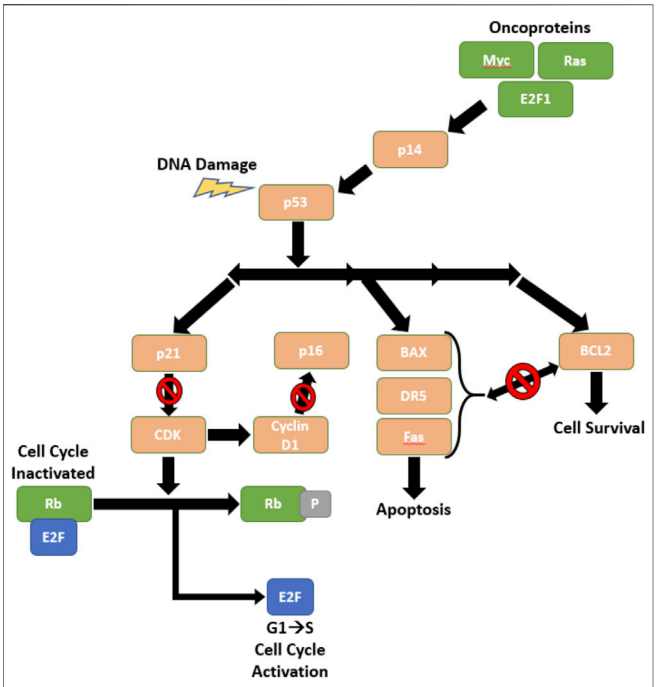

FIGURE 1 | The Role of p53 and Rb in Regulating Cell Cycle Progression.

3pq26.3 gene locus (Kaufhold et al., 2016). However, there are currently no therapies for combatting the effects of SOX2 amplification and its tumorigenic effect on initiating SCLC occurrence and growth.

Prominent phenotypic features of small cell lung cancer also lack drug therapy alternatives. For example, SCLC cells growing *in vitro* demonstrate that adhesion to extracellular matrix (ECM) increases tumorgenicity and resistance to chemotherapeutic agents. This is a result of B1 integrin-stimulated tyrosine kinase activating and inhibiting chemotherapy induced apoptosis (Sethi et al., 1999). The ECM protects SCLC cells from chemotherapy induced apoptosis. When the cells adhere to laminin (Ln), fibronectin (Fn) or collagen IV, there is substantial protection from chemotherapy-induced apoptosis, as was shown in H69, H345 and H510 cell lines (Sethi et al., 1999). Adhesion of the H69 cell line to Ln stimulates PTK activity and prevents chemotherapy induced caspase activation in the apoptosis pathway (Sethi et al., 1999). To target this phenotype, there has been great hope that matrix metalloproteinase inhibitors might hinder the virulent effects of the SCLC-ECM interaction. However, in two randomized trials: one with marimastat, the other with tanomastat, the results were disappointing, as neither survival nor quality of life improved (Shepherd et al., 2002; Zhang and He, 2013).

Tumor Suppressor Gene Loss

The loss of function of tumor protein 53 (P53) (Byers and Rudin, 2015) is almost universal in SCLC patients, as P53 is mutated in over 90% SCLC diagnoses (Wistuba et al., 2001). Additionally, Retinoblastoma 1 (RB1) (Helin et al., 1997) is frequently deleted in SCLC. Both P53 and RB1 are tumor suppressor genes that encode proteins that regulate the cell cycle and cell survival. **Figure 1** displays the mechanisms of p53 in response to DNA damage in SCLC cells. These are occasionally accompanied by a 3p deletion (Whang-Peng et al., 1982) and when they are deleted, the mechanism indicated in **Figure 1** is not able to inhibit cell growth or uncontrolled cell proliferation, and consequently there is tumor growth and disease progression. P53 and RB1 deficient SCLC tumors may also express increased cKit (Rao et al., 2020), MYC amplification (20% of patients (Pietanza et al., 2015)), and loss of phosphatase and tensin homolog (PTEN).

In the RB1 and P53 deficient SCLC cells, the Hedgehog pathway, a cell-intrinsic pathway, further promotes tumorigenicity. Activation of the Hedgehog signaling molecule promotes clonogenicity of SCLC *in vitro* and accelerates the initiation and progression of SCLC in mice *in vivo*. (Park et al., 2011). Further, suppression of Hedgehog signaling molecules inhibited growth of both mouse and human SCLC cells (Park et al., 2011). Hedgehog pathway inhibitors target certain Hedgehog activators and have been tested as an addition to combination chemotherapy. These inhibitors work by a mechanism of action that inhibits Smoothened, a Hedgehog pathway activator (Gadgeel, 2018) Vismodegib, a Smoothened inhibitor, was added to chemotherapy regimens in late-stage SCLC, but the combination did not show any overall benefit (Belani et al., 2016). Also of note, that, in the same study, cixutumumab, an IGF-1R inhibitor, was tested and likewise did not show any benefit when added to standard chemotherapy regimens for all tumor types.

In RB1 deficient tumor cells, apoptosis evasion mechanisms also add to the complexity of the SCLC genome. RB1 deficient cells can have overexpression of HIF-1α and aid cancer cells in evading apoptosis. HIF-1α over expression also aids in cell migration, increasing metastasis and promotion of angiogenesis *via* upregulation of VEGF (Forsythe et al., 1996). There has been significant progress in treating Rb-deficient tumors, as therapies targeting HIF-1α have shown preclinical antitumor efficacy (Zhao et al., 2020). In Rb deficient cells, such as many SCLC genotypes, there has been a significant benefit, *in vivo*, to dual inhibit CDK4/6 and HSP90 (Zhao et al., 2020). CDK4/6 and HSP90 inhibition suppress the tumorigenic traits of HIF-1α. This has been shown to significantly inhibit tumor cell viability in RB1 deficient colorectal cancer cell lines (Zhao et al., 2020), though the model is applicable in any RB1 deficient cancer cell.

Apoptosis/programmed cell death regulation also plays a significant role in SCLC virulence. Variations in the apoptosis cascade can increase SCLC progression and lead to worse prognosis for patients. SCLC has been further found to avoid chemotherapy-induced apoptosis by upregulation of BCL2, an anti-apoptotic gene (Gazdar et al., 2017). While BCL2 is an anti-apoptotic gene, BAX is its proapoptotic counterpart (Brambilla and Gazdar, 2009). SCLC cells are able to escape apoptosis *via* variations in the BCL2:BAX balance.

BCL2 inhibitors have been studied as an option to combat SCLC resistance. BCL2 inhibitors target the antiapoptotic characteristics of SCLC cells, as an elevated level of BCL2 is

an indicator of poor prognosis. (Lawson et al., 2010). However, despite early indications of success, Obatoclax, a BCL2 inhibitor, did not improve any clinical endpoints when combined with carboplatin and etoposide in a randomized study. (Langer et al., 2014). The oral BCL2 inhibitor, AT-101 also did not show any improvement in overall survival and the study was terminated at the first interim analysis. (Baggstrom et al., 2011). It is thought that these initial agents may lack potency in against BCL2, preventing a synergistic response when added to chemotherapy combinations and that they may be further studied at more potent dosages.

Oncogenic Drivers

All three members of the MYC family of genes, MYC, MYCL, MYCN are amplified in SCLC cell lines. Pulmonary neuroendocrine cells with deleted copies of RB1, P53, and P130 grow and express neuroendocrine marker genes but do not proliferate and become tumors. (Gazdar et al., 2017). Conversely, the addition of MYC family members, particularly MYCL, to the neuroendocrine cells with the previously mentioned deletions rapidly results in tumorgenicity (Gazdar et al., 2017).

Aberrant amplification of MYC family genes in SCLC can be explained by mechanisms including, promoter activation, attenuation of transcription, and control of gene copy number. In cells, each MYC family gene uses a different combination of these mechanisms to control mRNA transcription. In the context of SCLC, MYC has been shown to be regulated by both initiation and attenuation of transcription, MYCN appears to be regulated at the level of initiation of transcription, and MYCL has been shown to be regulated by attenuation of transcription (Krystal et al., 1988).

In normal cells, MYC expression is tightly regulated by transcription factors CNBP, FuBP1, and TCF as well as structural DNA elements (Brägelmann et al., 2017). It has been observed that phosphorylation of both MYC and MYCN affects polyubiquitination and by extension, proteasomal degradation, but no such regulatory mechanism has been reported for MYCL (Sjostrom et al., 2005; Malempati et al., 2006; Brockmann et al., 2013).

In mouse models, MYC withdrawal has led to tumor regression, indicating that MYC may be a valuable target in SCLC. This, however, has proven difficult, as MYC drivers are not due to intrinsic oncogenic mutations that could easily be targeted by therapeutic agents (Fletcher and Prochownik, 2015; Brägelmann et al., 2017). Rather, they are activated due to overamplification. This makes compound discovery aiming at kinase inhibition, such as agents that target mutated proteins only, extremely difficult (Brägelmann et al., 2017).

DNA Repair

Overexpression of DNA repair proteins such as PARP1, checkpoint kinase 1 (Chk1), and enhancer of zeste two polycomb repressive complex two subunit (EZH2) are independent of DNA-level mutations, but significantly contribute to tumor growth (Byers and Rudin, 2015). SCLC tumors also induce FGFR family alterations, and some have demonstrated sensitivity to FGFR inhibitors. However, the relationship between SCLC mutations and the family pathways is not currently known (Byers and Rudin, 2015).

SCLC relies on the ATR-CHK1 pathway to overcome cellular stress during the replication process that would otherwise cause DNA damage (Hsu et al., 2019). Due to the higher concentration of Chk1 gene expression and protein in SCLC compared to NSCLC, Chk1 inhibitors are a useful therapeutic agent in attempting to hinder this potent virulence mechanism in SCLC. Chk1 inhibitors such as prexasertib demonstrated effectiveness in SCLC cells *in vivo*, genetically engineered mice (GEM) and chemo-resistant mouse models (Sen et al., 2017). Chk1 showed synergistic effects when administered with cisplatin to induce mitotic cell death, combating resistance that may develop to first line therapies (Hsu et al., 2019).

PARP inhibitors such as Olaparib, Veliparib, Talazoparib et al. target PARP1 overexpression *via* the biomarker SLFN11 and work by two mechanisms. First, trapping PARP to the single strand DNA breaks and preventing repair. Second, PARP inhibitors inhibit poly ADP-ribosylation (PARylation) and binding of PARP to DNA (Murai et al., 2012), thus, preventing DNA repair and allowing for apoptosis pathways to begin their cascade and induce cell death. A phase I trial with Talazoparib showed some activity in decreasing chemotherapy resistance, including SCLC tumors (de Bono et al., 2017). These patients achieved an overall response rate of 9.0% with the duration of the response lasting up to 15 weeks. (de Bono et al., 2017).

The proteins of the Schlafen family are involved in regulation of cell proliferation and possibly helicase activity. EZH2 amplification increases resistance to chemotherapy by downregulation of Schlafen 11 (SLFN11) expression (Gazdar et al., 2017). EZH2 downregulates SLFN11 by histone modification and methylation in SCLC. EZH2 inhibition has become an important target for therapeutics as it was shown to decrease resistance in cells treated with cisplatin (Berns and Berns, 2017).

A 2015 study examined the efficacy of temozolomide and the PARP inhibitor, veliparib, in SCLC. In their phase II, double-blind trial, 4 month progression-free survival and overall survival did not differ between the treatment and placebo arms, though a significant overall response was found in the temozolomide/veliparib arm (Pietanza et al., 2018). Additionally, it was found that SLFN11 expression was associated with improved progression-free and overall survival in the temozolomide/veliparib arm (Pietanza et al., 2018).

DNA damage repair by cancer cells is another mechanism through which resistance occurs in SCLC cells. DNA repair can occur due to overexpression of repair proteins such as PARP1, wee-like protein kinase 1 (WEE1), Chk1, Rad3-related protein (ATR) and ataxia telangiectasia mutated (ATM) protein kinase (Pietanza et al., 2015; Berraondo, 2019).

SCLC resistance to the platinum series of drugs occurs, in part, due to the repair of DNA damage (Goldstein and Kastan, 2015) *via* glutathione (GSH). GSH is prevalent in SCLC

tumors and enhances the repair of DNA damage caused by drugs such as cisplatin, as well as increasing inactivation of the drug before it reaches the DNA (Chen et al., 2020). Various research studies have reinforced this relationship. In 1990, Meijer, Mulder et al. confirmed the relationship between GSH and cisplatin resistance in SCLC cells (Meijer et al., 1990).

Resistance in SCLC cells has also been indicated by abnormal DNA methylation. In 2017, Gardner et al. examined the mechanism of resistance by SCLC tumors to cisplatin and etoposide, a common chemotherapy combination, and revealed that histone H3 lysine 27 trimethylation (H3K27me3) resulted in resistance to the cisplatin and etoposide. (Gardner et al., 2017).

Cell Cycle and Differentiation Mechanisms

Notch signaling, while a powerful protumor effector in most cells, is uniquely diminished in the majority of SCLC cells. In SCLC, Notch acts as a tumor suppressor by negatively regulating neuroendocrine differentiation (Gazdar et al., 2017). SCLC cells express Notch inhibitors delta like non-canonical Notch ligand 1 (DLK1) and DLL3 (DLL3 is expressed as a neoantigen on the surface of some SCLC cells) or have inactivating mutations in the Notch pathways (Gazdar et al., 2017), leading to inactivation of the tumor suppression.

Inactivation of the Notch pathway in SCLC promotes tumor growth and metastases, and results in worse prognoses. In approximately 80% of SCLCs, Notch ligand Delta-like protein 3 (DLL3) is upregulated to act as an inhibitor of the pathway (Chapman et al., 2011). The TRINITY trial in 2018 evaluated the effectiveness of rovalpituzumab tesirine (ROVA-T), an antibody drug conjugate, in patients with recurrent SCLC with high DLL3 expression. There was a marginal benefit to patients receiving this drug (Carbone et al., 2018), though severe toxicities occurred in 40% of patients (Gadgeel, 2018), suggesting the modest benefit is outweighed by adverse reactions in a considerable portion of the studied patient population.

A significant portion of SCLC cells express the transcription factor achaete-scute homologue 1 (ASCL1), which enhances the survival and growth of these cells and ASCL1 amplified cells express the full set of neuroendocrine markers (Gazdar et al., 2017). Often associated with ASCL1, approximately 15% of SCLC cells express neurogenic differentiation factor 1 (NEUROD1) (Gazdar et al., 2017), a master regulator that enhances cell proliferation and growth.

This subgroup of SCLC, with mutated ASCL1, is characterized by having faster growth rates, MYC amplification, and oncogenic transcription regulation. Alisertib, an aurora kinase A/B inhibitor, has shown tumor suppression in SCLC cells with variant ASCL1 and MYC amplification in preclinical studies (Mollaoglu et al., 2017). Alisertib was added in clinical studies to regimens consisting of weekly paclitaxel in patients with recurrent SCLC. There was some improvement in overall survival for these patients but not enough to reach statistical significance (Gadgeel, 2018). However, in 46 patients whose tumors were analyzed *via* immunohistochemistry, patients with positive MYC expression had significant benefit in progression free survival, while the patients with MYC negative expression actually had worse outcomes when alisertib was added to paclitaxel (Gadgeel, 2018). It is important to note that these results have not been repeated or confirmed in prospective trials.

ONC201: A PROMISING NOVEL AGENT FOR SCLC

There are currently over 275 clinical trials registered with the FDA in SCLC that are active or recruiting patients for study. This large number is due, in part, to a rapid, trial-and-error approach which has evolved to apply any and all novel therapies to patients diagnosed with a highly prevalent and desperate disease. While there has been a disappointment in the availability of targeted therapies available to treat SCLC patients, there is optimism in the form of new therapies being tested.

ONC201 is an emerging imipridone therapy that has demonstrated strong antitumor properties *in vivo* and *in vitro* (Prabhu et al., 2020). It is entering an increasing number of clinical trials as it has effective tumor killing ability, while being well tolerated. ONC201 is administered weekly at a recommended phase two dose of 625 mg based on pharmacokinetics and pharmacodynamics in phase 1 testing, and preclinical dose intensification studies (Wagner et al., 2018). ONC201 activates the integrated stress response, (Kline et al., 2016), resulting in reduced proliferation of SCLC tumor cells (Lee et al., 2020). Currently being studied is the possibility of adding ONC201 to combination chemotherapy regimens, targeting the DNA of the tumor cells along in addition to activating the integrated stress response, thus, inducing higher levels of cleaved PARP, resulting in a synergistic pro-apoptotic effect.

Tests *in vivo* in SCLC and in clinical trials in additional solid tumors, show that ONC201 works by increasing cellular stress and inducing TRAIL-mediated apoptosis in the p53 pathway in several tumor cell lines. TRAIL is an endogenous protein that induces tumor cell apoptosis *via* its interaction with death receptors DR4 or DR5 (Ashkenazi, 2002). TRAIL is expressed in many human tissues, including lung tissue, as well as certain immune cells following cytokine activation (Fanger et al., 1999; Griffith et al., 1999; Allen et al., 2015).

ONC201 works by a unique mechanism of action, inhibition of dopamine receptors and direct activation of the enzyme ClpP (Prabhu et al., 2020). ClpP is allosterically modified by ONC201 to open substrate channel areas and alter the conformation of its active site (Prabhu et al., 2020). This allosteric modification causes hyperactivation of ClpP's proteolytic activity, leading to degradation of subunits in the electron transport chain, involved in cell respiration. This degradation results in impairment of oxidative phosphorylation and causes elevated cell stress levels, triggering apoptosis. While the mechanisms of the interaction between ClpP and the mitochondrial mechanics

TABLE 1 | Current FDA Trials involving ONC201 (clinicaltrials.gov).

Name of study	Phase	Disease	Status	ClinicalTrials.gov identifier
ONC201 in Relapsed/Refractory Acute Leukemias and High-Risk Myelodysplastic Syndromes (HR-MDS)	I/II	Leukemia	Active, not recruiting	NCT02392572
Oral ONC201 in Recurrent GBM, H3 K27M Glioma, and Midline Glioma	II	Various Gliomas	Recruiting	NCT02525692
Oral ONC201 in Relapsed/Refractory Multiple Myeloma	I/II	Multiple Myeloma	Active, not recruiting	NCT02863991
Phase 2 Study of ONC201 in Neuroendocrine Tumors	II	Recurrent/Metastatic Neuroendocrine Tumor	Recruiting	NCT03034200
ONC201 in Adults With Recurrent H3 K27M-mutant Glioma	II	Glioma	Recruiting	NCT03295396
ONC201 in Recurrent/Refractory Metastatic Breast Cancer and Advanced Endometrial Carcinoma	II	Triple Negative Breast Cancer, Endometrial Cancer, Hormone Receptor Positive, HER2 Negative Breast Cancer	Active, not recruiting	NCT03394027
ONC201 in Pediatric H3 K27M Gliomas	I	Glioma, Diffuse Intrinsic Pontine Glioma	Recruiting	NCT03416530
ONC201 in Recurrent or Metastatic Type II Endometrial Cancer Endometrial Cancer	II	Recurrent Endometrial Cancer	Recruiting	NCT03485729
BrUOG 379 phase Ib/II Trial ONC201 + nivolumab in MSS mCRC (379)	I/II	Metastatic Colorectal Cancer	Active, not recruiting	NCT03791398
ONC 201 Maintenance Therapy in Acute Myeloid Leukemia and Myelodysplastic Syndrome After Stem Cell Transplant	I	AML	Recruiting	NCT03932643

remain to be investigated, ClpP inactivation has made tumor cells at least partially resistant to ONC201 in AML, acute lymphoblastic leukemia (ALL) and breast cancer cells (Prabhu et al., 2020).

Two pathways are consistently impacted by ONC201 administration—activation of the ISR pathway (Kline et al., 2016; Prabhu et al., 2020) and Akt/ERK inactivation (Allen et al., 2013; Prabhu et al., 2020). The ISR pathway is also activated by proteasome inhibitors, but when activated by ONC201, causes upregulation of ATF-4 translation and CHOP transcription rapidly in tumor cells (Kline et al., 2016). While ISR activation happens rapidly, Akt/ERK inactivation happens over 2–3 days (Allen et al., 2013). These effects combine to produce a powerful upregulation of TRAIL, a proapoptotic ligand, *via* activation and nuclear translocation of Foxo3a and its receptor DR5 (Prabhu et al., 2020). It is noteworthy that DR5 is induced by activation of ATF4 and CHOP through the integrated stress response (Kline et al., 2016). An additional mechanism ONC201 may be effective in killing tumor cells is the degradation of MYC through a proteasomal pathway involving GSK3β mediated phosphorylation of threonine 58 (Ishida et al., 2018).

One of the most attractive aspects in the prospect of ONC201 as an emerging SCLC therapy is its low risk of toxicity when administered in both mice and humans (Prabhu et al., 2020). ONC201 displays a synchronization of unique anti-tumor mechanisms *via* early-stage ISR activation in the tumor cells that seemingly spares healthy epithelial and organ tissue cells (Allen et al., 2016). This remains the case in SCLC cells, ONC201 does not exhibit cytotoxic effects. While ONC201 was shown to effectively inhibit tumor cell survival in a dose-dependent experiment in the cell line H460 (Feng et al., 2016). ONC201 was also tested in patient derived human-cells and was found to inhibit tumor cell survival, while remaining nontoxic to healthy lung epithelial cells and healthy hepatocytes, indicating ONC201s specificity for tumor cells in lung tissue (Feng et al., 2016). ONC201 was also tested *in vitro* in mouse models and did not produce any significant toxicities in the mammals and did not induce DR5 or TRAIL in normal epithelial cells (Feng et al., 2016).This could potentially be related to the fact that Akt and Erk expression is low in healthy cells, therefore without any Akt and Erk inhibition, DR5 and TRAIL are not induced (Feng et al., 2016).

While approximately 10% of all SCLC patients present with brain metastases and 40% of all SCLC patients will experience brain metastases in their disease, it is crucial to consider which novel agents may cross into the central nervous system. (Schuette, 2004). The blood-brain barrier becomes less relevant in these patients, as it has most likely already been compromised due to the invasive nature of the disease (Schuette, 2004). ONC201 shows activity against tumors within the CNS. ONC201 has already shown its preclinical efficacy in brain tumors such as gliomas, and it is currently involved in clinical trials treating gliomas and various metastatic neuroendocrine tumors, where it has shown impressive clinical efficacy. These trials are displayed in **Table 1.** The small molecule therapy crosses the blood-brain barrier and has showed efficacy against glioblastomas, including those resistant to the standard of care temozolomide (Ralff et al., 2017). In addition to the clinical evidence with ONC201 that has accumulated since 2014, (Prabhu et al., 2020), mouse models have clearly displayed the efficacy of ONC201 crossing the blood-brain barrier and inhibiting tumor growth, due to dual inactivation of Akt and ERK and activation of the integrated stress response (Allen et al., 2013; Kline et al., 2016; Wagner et al., 2018). This further validates the investigation of ONC201 for SCLC cells, both primary and metastatic tumors, regardless of their location in the body.

TABLE 2 | Current FDA Trials involving Lurbinectedin in SCLC (clinicaltrials.gov).

Name of study	Phase	Status	ClinicalTrials.gov identifier
Study to Assess Safety, Tolerability, Efficacy of PM01183 and atezolizumab in Patients w/Advanced Small Cell Lung Cancer	I	Recruiting	NCT04253145
Lurbinectedin (PM01183) Combined With pembrolizumab in Small Cell Lung Cancer. (LUPER)	I/II	Recruiting	NCT04358237
Immune Checkpoint Inhibition With Lurbinectedin Relapsed/Recurrent SCLC	I/II	Recruiting	NCT04610658

ONC201 is particularly effective in SCLC due to the induction of TRAIL and DR5, as well as activated caspase-8, which induces extrinsic apoptosis (Prabhu et al., 2020). The drug also works as a selective competitive and competitive D2 receptor (DRD2) antagonist (Prabhu et al., 2020), which is overexpressed in SCLC patients who often have elevated plasma dopamine levels. Further, dopamine is a critical regulator in the innate and adaptive immune systems. Dopamine receptors are expressed by both T-cells and NK cells that can modulate the immune response to tumor formation and growth (Zhao et al., 2013; Wang et al., 2019), as dopamine is a negative regulator of NK response (Mikulak et al., 2014). DRD2 receptor inhibition has been shown to activate NK cells in the immune response to tumor cells (Mikulak et al., 2014), however, these mechanisms have not been evaluated in mouse or human models. ONC201 has been shown to activate NK cells (Wagner et al., 2018) and has clinical activity in neuroendocrine tumors such as pheochromocytoma and paraganglioma (Anderson and Gortz, 2021). This preclinical data is the basis for continued investigation, as ONC201 is under further review in a range of neuroendocrine and metastatic tumors (Anderson and Zahler, 2020). There is also evidence for synergy between ONC201 and EZH2 inhibitors in a variety of tumor types and this may be relevant to SCLC as discussed earlier (Zhang et al., 2021). **Table 1** displays current FDA approved clinical trials involving ONC201 (clinicaltrials.gov).

5 LURBINECTIDIN: A NOVEL AGENT IN CLINICAL USE IN SCLC

In June 2020, the FDA granted accelerated approval to lurbinectedin for patients with extensive stage SCLC with disease progression while receiving or after treatment with platinum-based chemotherapy. A phase two study treated 105 previously-treated patients, and demonstrated an overall response rate of 35% (95% CI 26–45%), which includes an impressive 22% response rate in 45 patients whose cancer started to grow <90 days since last dose of platinum (platinum-refractory disease), with a median duration of response of 5 months. Treatment was well tolerated, with the most common high-grade side effects being anemia (9%), neutropenia (46%), and thrombocytopenia (7%), and there were no treatment-related deaths (Trigo et al., 2020).

Lurbinectedin is an inhibitor of RNA polymerase II, an enzyme commonly hyperactivated in SCLC, and induces DNA breaks in cells that result in apoptosis (Markham, 2020). The drug covalently binds to central guanine in trinucleotide triplets in the minor groove of DNA, forming adducts capable of inducing DNA double-strand breaks (Markham, 2020). It may also induce immunogenic cell death and increase anti-tumor immunity. Lurbinectedin also has an impact on the tumor microenvironment as it is associated with a reduction in tumor associated macrophages (Markham, 2020). Lurbinectedin has been shown to downregulate ASCL1 and thus decrease the rapid growth rate that is characteristic of SCLC cells (Markham, 2020).

The recently completed phase III ATLANTIS trial, evaluating lurbinectedin + doxorubicin compared with cyclophosphamide + doxorubicin + vincristine (CAV) or topotecan enrolled 613 previously-treated patients and will add significant clinical evidence of lurbinectedin's effects. The ATLANTIS trial was terminated as it missed primary endpoints with patients. Though the combination of doxorubicin and lurbinectedin did not provide positive results, the study did confirm the tolerability and overall activity in patients.

Lurbinectedin is also under investigation for other solid tumors. **Table 2** shows currently active or recruiting clinical trials in SCLC, involving lurbinectedin (clinicaltrials.gov).

DISCUSSION

SCLC is a deadly and devastating disease for patients. Many patients present in the advanced stages of disease with distant metastasis. Another complication of SCLC, which makes it even harder to effectively treat, is the absence of targetable biomarkers. Due to the complex genomic profile of SCLC and its numerous virulence mechanisms, resistance to first line chemotherapies inevitably develops, leaving patients with dismal outlooks as the disease progresses and further metastasizes. Targeted therapies in SCLC have been largely unsuccessful.

In the past 3 years, the overall survival of patients with SCLC has been improved with routine, first-line use of anti-PD1/PD-L1 immunotherapy. With over 275 clinical trials either active or recruiting that focus on SCLC, there is optimism in emerging therapeutics. Interestingly, nonplatinum-based therapies that appear to have sufficient efficacy but are much less toxic to patients. ONC201 and lurbinectedin, while mechanistically

dissimilar, display effective anti-tumor characteristics while remaining tolerable when administered clinically. These therapies will be important to monitor going forward, as they are further evaluated in clinical trials, as well as *in vivo* and *in vitro*.

The p53 pathway is an important regulatory pathway that is often broken in SCLC. DNA damage or stimuli from oncoproteins can trigger p53 to induce cell cycle arrest, preventing cells from replicating with mutations or damaged DNA. This pathway also exerts influence over the TRAIL pathway *via* its control over DR5, which induces apoptosis (Brambilla and Gazdar, 2009). Figure adapted by way of Brambilla and Gazdar (2009).

DATA AVAILABILITY STATEMENT

The original contributions presented in the study are included in the article/Supplementary Material, further inquiries can be directed to the corresponding authors.

AUTHOR CONTRIBUTIONS

All authors listed have made a substantial, direct, and intellectual contribution to the work and approved it for publication.

FUNDING

This work was supported by an NIH grant (CA173453) to WSE-D. WSE-D is an American Cancer Society Research Professor and is supported by the Mencoff Family University Professorship at Brown University.

ACKNOWLEDGMENTS

The contents of this manuscript are solely the responsibility of the authors and do not necessarily represent the official views of the National Cancer Institute, the National Institutes of Health, or the American Cancer Society.

REFERENCES

Allen, J. E., Kline, C. L., Prabhu, V. V., Wagner, J., Ishizawa, J., Madhukar, N., et al. (2016). Discovery and Clinical Introduction of First-In-Class Imipridone ONC201. *Oncotarget* 7 (45), 74380–74392. doi:10.18632/oncotarget.11814

Allen, J. E., Krigsfeld, G., Mayes, P. A., Patel, L., Dicker, D. T., Patel, A. S., et al. (2013). Dual Inactivation of Akt and ERK by TIC10 Signals Foxo3a Nuclear Translocation, TRAIL Gene Induction, and Potent Antitumor Effects. *Sci. Transl Med.* 5 (171), 171ra17. doi:10.1126/scitranslmed.3004828

Allen, J. E., Krigsfeld, G., Patel, L., Mayes, P. A., Dicker, D. T., Wu, G. S., et al. (2015). Identification of TRAIL-Inducing Compounds Highlights Small Molecule ONC201/TIC10 as a Unique Anti-cancer Agent that Activates the TRAIL Pathway. *Mol. Cancer* 14 (1), 99. doi:10.1186/s12943-015-0346-9

Anderson, P. M., and Gortz, J. (2021). Phase 2 Study of DRD2 antagonist/ClpP Agonist ONC201 in Neuroendocrine Tumors. *Jco* 39 (15_Suppl. l), 3002. doi:10.1200/jco.2021.39.15_suppl.3002

Anderson, P. M., and Zahler, S. (2020). Phase II Study of ONC201 in Pheochromocytoma-Paragangliomas (PC-PG), Medullary Thyroid Carcinoma (MTC), and Other Neuroendocrine Tumors. *Jco* 38 (15_Suppl. l), e16703. doi:10.1200/jco.2020.38.15_suppl.e16703

Antonia, S. J., López-Martin, J. A., Bendell, J., Ott, P. A., Taylor, M., Eder, J. P., et al. (2016). Nivolumab Alone and Nivolumab Plus Ipilimumab in Recurrent Small-Cell Lung Cancer (CheckMate 032): a Multicentre, Open-Label, Phase 1/2 Trial. *Lancet Oncol.* 17 (7), 883–895. doi:10.1016/S1470-2045(16)30098-5

Ashkenazi, A. (2002). Targeting Death and Decoy Receptors of the Tumour-Necrosis Factor Superfamily. *Nat. Rev. Cancer* 2 (6), 420–430. doi:10.1038/nrc821

Baggstrom, M. Q., Qi, Y., Koczywas, M., Argiris, A., Johnson, E. A., Millward, M. J., et al. (2011). A Phase II Study of AT-101 (Gossypol) in Chemotherapy-Sensitive Recurrent Extensive-Stage Small Cell Lung Cancer. *J. Thorac. Oncol.* 6 (10), 1757–1760. doi:10.1097/JTO.0b013e31822e2941

Belani, C. P., Dahlberg, S. E., Rudin, C. M., Fleisher, M., Chen, H. X., Takebe, N., et al. (2016). Vismodegib or Cixutumumab in Combination with Standard Chemotherapy for Patients with Extensive-Stage Small Cell Lung Cancer: A Trial of the ECOG-ACRIN Cancer Research Group (E1508). *Cancer* 122 (15), 2371–2378. doi:10.1002/cncr.30062

Bernhardt, E. B., and Jalal, S. I. (2016). "Small Cell Lung Cancer," in *Lung Cancer: Treatment and Research*. Editor K. L. Reckamp (Cham: Springer International Publishing), 301–322. doi:10.1007/978-3-319-40389-2_14

Berns, K., and Berns, A. (2017). Awakening of "Schlafen11" to Tackle Chemotherapy Resistance in SCLC. *Cancer Cell* 31 (2), 169–171. doi:10.1016/j.ccell.2017.01.013

Berraondo, P. (2019). Mechanisms of Action for Different Checkpoint Inhibitors. *HemaSphere* 3 (S2). doi:10.1097/hs9.0000000000000244

Brägelmann, J., Böhm, S., Guthrie, M. R., Mollaoglu, G., Oliver, T. G., and Sos, M. L. (2017). Family Matters: How MYC Family Oncogenes Impact Small Cell Lung Cancer. *Cell Cycle* 16 (16), 1489–1498. doi:10.1080/15384101.2017.1339849

Brambilla, E., and Gazdar, A. (2009). Pathogenesis of Lung Cancer Signalling Pathways: Roadmap for Therapies. *Eur. Respir. J.* 33 (6), 1485–1497. doi:10.1183/09031936.00014009

Brockmann, M., Poon, E., Berry, T., Carstensen, A., Deubzer, H. E., Rycak, L., et al. (2013). Small Molecule Inhibitors of aurora-a Induce Proteasomal Degradation of N-Myc in Childhood Neuroblastoma. *Cancer Cell* 24 (1), 75–89. doi:10.1016/j.ccr.2013.05.005

Brzezniak, C., Oronsky, B., Carter, C. A., Thilagar, B., Caroen, S., and Zeman, K. (2017). Superior Vena Cava Syndrome in a Patient with Small-Cell Lung Cancer: A Case Report. *Case Rep. Oncol.* 10 (1), 252–257. doi:10.1159/000464278

Byers, L. A., and Rudin, C. M. (2015). Small Cell Lung Cancer: where Do We Go from Here?. *Cancer* 121 (5), 664–672. doi:10.1002/cncr.29098

Carbone, D. P., Morgensztern, D., Le Moulec, S., Santana-Davila, R., Ready, N., Hann, C. L., et al. (2018). Efficacy and Safety of Rovalpituzumab Tesirine in Patients with DLL3-Expressing, ≥ 3rd Line Small Cell Lung Cancer: Results from the Phase 2 TRINITY Study. *Jco* 36 (15_Suppl. l), 8507. doi:10.1200/jco.2018.36.15_suppl.8507

Chan, R. H., Dar, A. R., Yu, E., Stitt, L. W., Whiston, F., Truong, P., et al. (1997). Superior Vena Cava Obstruction in Small-Cell Lung Cancer. *Int. J. Radiat. Oncol. Biol. Phys.* 38 (3), 513–520. doi:10.1016/s0360-3016(97)00094-1

Chapman, G., Sparrow, D. B., Kremmer, E., and Dunwoodie, S. L. (2011). Notch Inhibition by the Ligand DELTA-LIKE 3 Defines the Mechanism of Abnormal Vertebral Segmentation in Spondylocostal Dysostosis. *Hum. Mol. Genet.* 20 (5), 905–916. doi:10.1093/hmg/ddq529

Chen, P., Kuang, P., Wang, L., Li, W., Chen, B., Liu, Y., et al. (2020). Mechanisms of Drugs-Resistance in Small Cell Lung Cancer: DNA-Related, RNA-Related, Apoptosis-Related, Drug Accumulation and Metabolism Procedure. *Transl Lung Cancer Res.* 9 (3), 768–786. doi:10.21037/tlcr-19-547

Chung, H. C., Lopez-Martin, J. A., Kao, S. C.-H., Miller, W. H., Ros, W., Gao, B., et al. (2018). Phase 2 Study of Pembrolizumab in Advanced Small-Cell Lung Cancer (SCLC): KEYNOTE-158. *Jco* 36 (15_Suppl. l), 8506. doi:10.1200/jco.2018.36.15_suppl.8506

Cifaldi, L., Locatelli, F., Marasco, E., Moretta, L., and Pistoia, V. (2017). Boosting Natural Killer Cell-Based Immunotherapy with Anticancer Drugs: a Perspective. *Trends Mol. Med.* 23 (12), 1156–1175. doi:10.1016/j.molmed.2017.10.002

de Bono, J., Ramanathan, R. K., Mina, L., Chugh, R., Glaspy, J., Rafii, S., et al. (2017). Phase I, Dose-Escalation, Two-Part Trial of the PARP Inhibitor Talazoparib in Patients with Advanced Germline BRCA1/2 Mutations and Selected Sporadic Cancers. *Cancer Discov.* 7 (6), 620–629. doi:10.1158/2159-8290.CD-16-1250

Esposito, G., Palumbo, G., Carillio, G., Manzo, A., Montanino, A., Sforza, V., et al. (2020). Immunotherapy in Small Cell Lung Cancer. *Cancers (Basel)* 12 (9). doi:10.3390/cancers12092522

Fanger, N. A., Maliszewski, C. R., Schooley, K., and Griffith, T. S. (1999). Human Dendritic Cells Mediate Cellular Apoptosis via Tumor Necrosis Factor-Related Apoptosis-Inducing Ligand (TRAIL). *J. Exp. Med.* 190 (8), 1155–1164. doi:10.1084/jem.190.8.1155

Feng, Y., Zhou, J., Li, Z., Jiang, Y., and Zhou, Y. (2016). Small Molecular TRAIL Inducer ONC201 Induces Death in Lung Cancer Cells: A Preclinical Study. *PLOS ONE* 11 (9), e0162133. doi:10.1371/journal.pone.0162133

Fletcher, S., and Prochownik, E. V. (2015). Small-molecule Inhibitors of the Myc Oncoprotein. *Biochim. Biophys. Acta* 1849 (5), 525–543. doi:10.1016/j.bbagrm.2014.03.005

Forsythe, J. A., Jiang, B. H., Iyer, N. V., Agani, F., Leung, S. W., Koos, R. D., et al. (1996). Activation of Vascular Endothelial Growth Factor Gene Transcription by Hypoxia-Inducible Factor 1. *Mol. Cel Biol* 16 (9), 4604–4613. doi:10.1128/mcb.16.9.4604

Gadgeel, S. M. (2018). Targeted Therapy and Immune Therapy for Small Cell Lung Cancer. *Curr. Treat. Options. Oncol.* 19 (11), 53. doi:10.1007/s11864-018-0568-3

Gardner, E. E., Lok, B. H., Schneeberger, V. E., Desmeules, P., Miles, L. A., Arnold, P. K., et al. (2017). Chemosensitive Relapse in Small Cell Lung Cancer Proceeds through an EZH2-SLFN11 Axis. *Cancer Cell* 31 (2), 286–299. doi:10.1016/j.ccell.2017.01.006

Gazdar, A. F., Bunn, P. A., and Minna, J. D. (2017). Small-cell Lung Cancer: what We Know, what We Need to Know and the Path Forward. *Nat. Rev. Cancer* 17 (12), 765–737. doi:10.1038/nrc.2017.106

George, J., Lim, J. S., Jang, S. J., Cun, Y., Ozretić, L., Kong, G., et al. (2015). Comprehensive Genomic Profiles of Small Cell Lung Cancer. *Nature* 524 (7563), 47–53. doi:10.1038/nature14664

Goldstein, M., and Kastan, M. B. (2015). The DNA Damage Response: Implications for Tumor Responses to Radiation and Chemotherapy. *Annu. Rev. Med.* 66, 129–143. doi:10.1146/annurev-med-081313-121208

Govindan, R., Page, N., Morgensztern, D., Read, W., Tierney, R., Vlahiotis, A., et al. (2006). Changing Epidemiology of Small-Cell Lung Cancer in the United States over the Last 30 years: Analysis of the Surveillance, Epidemiologic, and End Results Database. *J. Clin. Oncol.* 24 (28), 4539–4544. doi:10.1200/JCO.2005.04.4859

Griffith, T. S., Wiley, S. R., Kubin, M. Z., Sedger, L. M., Maliszewski, C. R., and Fanger, N. A. (1999). Monocyte-mediated Tumoricidal Activity via the Tumor Necrosis Factor-Related Cytokine, TRAIL. *J. Exp. Med.* 189 (8), 1343–1354. doi:10.1084/jem.189.8.1343

Han, Y., Liu, D., and Li, L. (2020). PD-1/PD-L1 Pathway: Current Researches in Cancer. *Am. J. Cancer Res.* 10 (3), 727–742.

Helin, K., Holm, K., Niebuhr, A., Eiberg, H., Tommerup, N., Hougaard, S., et al. (1997). Loss of the Retinoblastoma Protein-Related P130 Protein in Small Cell Lung Carcinoma. *Proc. Natl. Acad. Sci. U S A.* 94 (13), 6933–6938. doi:10.1073/pnas.94.13.6933

Horn, L., Mansfield, A. S., Szczęsna, A., Havel, L., Krzakowski, M., Hochmair, M. J., et al. (2018). First-Line Atezolizumab Plus Chemotherapy in Extensive-Stage Small-Cell Lung Cancer. *N. Engl. J. Med.* 379 (23), 2220–2229. doi:10.1056/NEJMoa1809064

Hsu, W. H., Zhao, X., Zhu, J., Kim, I. K., Rao, G., McCutcheon, J., et al. (2019). Checkpoint Kinase 1 Inhibition Enhances Cisplatin Cytotoxicity and Overcomes Cisplatin Resistance in SCLC by Promoting Mitotic Cell Death. *J. Thorac. Oncol.* 14 (6), 1032–1045. doi:10.1016/j.jtho.2019.01.028

Ishida, C. T., Zhang, Y., Bianchetti, E., Shu, C., Nguyen, T. T. T., Kleiner, G., et al. (2018). Metabolic Reprogramming by Dual AKT/ERK Inhibition through Imipridones Elicits Unique Vulnerabilities in Glioblastoma. *Clin. Cancer Res.* 24 (21), 5392–5406. doi:10.1158/1078-0432.CCR-18-1040

Kaufhold, S., Garbán, H., and Bonavida, B. (2016). Yin Yang 1 Is Associated with Cancer Stem Cell Transcription Factors (SOX2, OCT4, BMI1) and Clinical Implication. *J. Exp. Clin. Cancer Res.* 35, 84. doi:10.1186/s13046-016-0359-2

Kline, C. L., Van den Heuvel, A. P., Allen, J. E., Prabhu, V. V., Dicker, D. T., and El-Deiry, W. S. (2016). ONC201 Kills Solid Tumor Cells by Triggering an Integrated Stress Response Dependent on ATF4 Activation by Specific eIF2α Kinases. *Sci. Signal.* 9 (415), ra18. doi:10.1126/scisignal.aac4374

Krystal, G., Birrer, M., Way, J., Nau, M., Sausville, E., Thompson, C., et al. (1988). Multiple Mechanisms for Transcriptional Regulation of the Myc Gene Family in Small-Cell Lung Cancer. *Mol. Cel Biol* 8 (8), 3373–3381. doi:10.1128/mcb.8.8.3373

Langer, C. J., Albert, I., Ross, H. J., Kovacs, P., Blakely, L. J., Pajkos, G., et al. (2014). Randomized Phase II Study of Carboplatin and Etoposide with or without Obatoclax Mesylate in Extensive-Stage Small Cell Lung Cancer. *Lung Cancer* 85 (3), 420–428. doi:10.1016/j.lungcan.2014.05.003

Lawson, M. H., Cummings, N. M., Rassl, D. M., Vowler, S. L., Wickens, M., Howat, W. J., et al. (2010). Bcl-2 and β1-integrin Predict Survival in a Tissue Microarray of Small Cell Lung Cancer. *Br. J. Cancer* 103 (11), 1710–1715. doi:10.1038/sj.bjc.6605950

Lee, Y. S., Zhou, L., Azzoli, C., and El-Deiry, W. S. (2020). Abstract 5260: Preclinical Studies with ONC201 in Combination with Clinically Approved Chemotherapy as a Novel Treatment Strategy against Small Cell Lung Cancer (SCLC). *Cancer Res.* 80 (16 Suppl. ment), 5260. doi:10.1158/1538-7445.am2020-5260

Liu, Y., Li, Y., Liu, S., Adeegbe, D. O., Christensen, C. L., Quinn, M. M., et al. (2018). NK Cells Mediate Synergistic Antitumor Effects of Combined Inhibition of HDAC6 and BET in a SCLC Preclinical Model. *Cancer Res.* 78 (13), 3709–3717. doi:10.1158/0008-5472.CAN-18-0161

Malempati, S., Tibbitts, D., Cunningham, M., Akkari, Y., Olson, S., Fan, G., et al. (2006). Aberrant Stabilization of C-Myc Protein in Some Lymphoblastic Leukemias. *Leukemia* 20 (9), 1572–1581. doi:10.1038/sj.leu.2404317

Markham, A. (2020). Lurbinectedin: First Approval. *Drugs* 80 (13), 1345–1353. doi:10.1007/s40265-020-01374-0

Mathieu, L., Shah, S., Pai-Scherf, L., Larkins, E., Vallejo, J., Li, X., et al. (2021). FDA Approval Summary: Atezolizumab and Durvalumab in Combination with Platinum-Based Chemotherapy in Extensive Stage Small Cell Lung Cancer. *Oncologist* 26 (5), 433–438. doi:10.1002/onco.13752

Meijer, C., Mulder, N. H., Hospers, G. A., Uges, D. R., and de Vries, E. G. (1990). The Role of Glutathione in Resistance to Cisplatin in a Human Small Cell Lung Cancer Cell Line. *Br. J. Cancer* 62 (1), 72–77. doi:10.1038/bjc.1990.232

Mikulak, J., Bozzo, L., Roberto, A., Pontarini, E., Tentorio, P., Hudspeth, K., et al. (2014). Dopamine Inhibits the Effector Functions of Activated NK Cells via the Upregulation of the D5 Receptor. *J. Immunol.* 193 (6), 2792–2800. doi:10.4049/jimmunol.1401114

Mollaoglu, G., Guthrie, M. R., Böhm, S., Brägelmann, J., Can, I., Ballieu, P. M., et al. (2017). MYC Drives Progression of Small Cell Lung Cancer to a Variant Neuroendocrine Subtype with Vulnerability to Aurora Kinase Inhibition. *Cancer Cell* 31 (2), 270–285. doi:10.1016/j.ccell.2016.12.005

Murai, J., Huang, S. Y., Das, B. B., Renaud, A., Zhang, Y., Doroshow, J. H., et al. (2012). Trapping of PARP1 and PARP2 by Clinical PARP Inhibitors. *Cancer Res.* 72 (21), 5588–5599. doi:10.1158/0008-5472.CAN-12-2753

Ni, L., Wang, L., Yao, C., Ni, Z., Liu, F., Gong, C., et al. (2017). The Histone Deacetylase Inhibitor Valproic Acid Inhibits NKG2D Expression in Natural Killer Cells through Suppression of STAT3 and HDAC3. *Sci. Rep.* 7 (1), 45266–45269. doi:10.1038/srep45266

Owonikoko, T. K., Park, K., Govindan, R., Ready, N., Reck, M., Peters, S., et al. (2021). Nivolumab and Ipilimumab as Maintenance Therapy in Extensive-Disease Small-Cell Lung Cancer: CheckMate 451. *J. Clin. Oncol.* 39 (12), 1349–1359. doi:10.1200/JCO.20.02212

Park, K. S., Martelotto, L. G., Peifer, M., Sos, M. L., Karnezis, A. N., Mahjoub, M. R., et al. (2011). A Crucial Requirement for Hedgehog Signaling in Small Cell Lung Cancer. *Nat. Med.* 17 (11), 1504–1508. doi:10.1038/nm.2473

Pavan, A., Attili, I., Pasello, G., Guarneri, V., Conte, P. F., and Bonanno, L. (2019). Immunotherapy in Small-Cell Lung Cancer: from Molecular Promises to Clinical Challenges. *J. Immunother. Cancer* 7 (1), 205. doi:10.1186/s40425-019-0690-1

Pietanza, M. C., Byers, L. A., Minna, J. D., and Rudin, C. M. (2015). Small Cell Lung Cancer: Will Recent Progress lead to Improved Outcomes?. *Clin. Cancer Res.* 21 (10), 2244–2255. doi:10.1158/1078-0432.CCR-14-2958

Pietanza, M. C., Waqar, S. N., Krug, L. M., Dowlati, A., Hann, C. L., Chiappori, A., et al. (2018). Randomized, Double-Blind, Phase II Study of Temozolomide in

Combination with Either Veliparib or Placebo in Patients with Relapsed-Sensitive or Refractory Small-Cell Lung Cancer. *J. Clin. Oncol.* 36 (23), 2386–2394. doi:10.1200/JCO.2018.77.7672

Prabhu, V. V., Morrow, S., Rahman Kawakibi, A., Zhou, L., Ralff, M., Ray, J., et al. (2020). ONC201 and Imipridones: Anti-cancer Compounds with Clinical Efficacy. *Neoplasia* 22 (12), 725–744. doi:10.1016/j.neo.2020.09.005

Ralff, M. D., Kline, C. L. B., Küçükkase, O. C., Wagner, J., Lim, B., Dicker, D. T., et al. (2017). ONC201 Demonstrates Antitumor Effects in Both Triple-Negative and Non-triple-negative Breast Cancers through TRAIL-dependent and TRAIL-independent Mechanisms. *Mol. Cancer Ther.* 16 (7), 1290–1298. doi:10.1158/1535-7163.MCT-17-0121

Rao, S., Sclafani, F., Eng, C., Adams, R. A., Guren, M. G., Sebag-Montefiore, D., et al. (2020). International Rare Cancers Initiative Multicenter Randomized Phase II Trial of Cisplatin and Fluorouracil versus Carboplatin and Paclitaxel in Advanced Anal Cancer: InterAAct. *J. Clin. Oncol.* 38 (22), 2510–2518. doi:10.1200/JCO.19.03266

Rudin, C. M., Awad, M. M., Navarro, A., Gottfried, M., Peters, S., Csőszi, T., et al. (2020). Pembrolizumab or Placebo Plus Etoposide and Platinum as First-Line Therapy for Extensive-Stage Small-Cell Lung Cancer: Randomized, Double-Blind, Phase III KEYNOTE-604 Study. *J. Clin. Oncol.* 38 (21), 2369–2379. doi:10.1200/JCO.20.00793

Saltos, A., Shafique, M., and Chiappori, A. (2020). Update on the Biology, Management, and Treatment of Small Cell Lung Cancer (SCLC). *Front. Oncol.* 10 (1074), 1074. doi:10.3389/fonc.2020.01074

Schuette, W. (2004). Treatment of Brain Metastases from Lung Cancer: Chemotherapy. *Lung Cancer* 45 Suppl 2, S253–S257. doi:10.1016/j.lungcan.2004.07.967

Sen, T., Tong, P., Stewart, C. A., Cristea, S., Valliani, A., Shames, D. S., et al. (2017). CHK1 Inhibition in Small-Cell Lung Cancer Produces Single-Agent Activity in Biomarker-Defined Disease Subsets and Combination Activity with Cisplatin or Olaparib. *Cancer Res.* 77 (14), 3870–3884. doi:10.1158/0008-5472.CAN-16-3409

Sethi, T., Rintoul, R. C., Moore, S. M., MacKinnon, A. C., Salter, D., Choo, C., et al. (1999). Extracellular Matrix Proteins Protect Small Cell Lung Cancer Cells against Apoptosis: A Mechanism for Small Cell Lung Cancer Growth and Drug Resistance *In Vivo*. *Nat. Med.* 5 (6), 662–668. doi:10.1038/9511

Shepherd, F. A., Giaccone, G., Seymour, L., Debruyne, C., Bezjak, A., Hirsh, V., et al. (2002). Prospective, Randomized, Double-Blind, Placebo-Controlled Trial of Marimastat after Response to First-Line Chemotherapy in Patients with Small-Cell Lung Cancer: a Trial of the National Cancer Institute of Canada-Clinical Trials Group and the European Organization for Research and Treatment of Cancer. *J. Clin. Oncol.* 20 (22), 4434–4439. doi:10.1200/JCO.2002.02.108

Sjostrom, S. K., Finn, G., Hahn, W. C., Rowitch, D. H., and Kenney, A. M. (2005). The Cdk1 Complex Plays a Prime Role in Regulating N-Myc Phosphorylation and Turnover in Neural Precursors. *Dev. Cel* 9 (3), 327–338. doi:10.1016/j.devcel.2005.07.014

Sun, L., He, Q., Tsai, C., Lei, J., Chen, J., Vienna Makcey, L., et al. (2018). HDAC Inhibitors Suppressed Small Cell Lung Cancer Cell Growth and Enhanced the Suppressive Effects of Receptor-Targeting Cytotoxins via Upregulating Somatostatin Receptor II. *Am. J. Transl Res.* 10 (2), 545–553.

Trigo, J., Subbiah, V., Besse, B., Moreno, V., López, R., Sala, M. A., et al. (2020). Lurbinectedin as Second-Line Treatment for Patients with Small-Cell Lung Cancer: a Single-Arm, Open-Label, Phase 2 Basket Trial. *Lancet Oncol.* 21 (5), 645–654. doi:10.1016/S1470-2045(20)30068-1

Wagner, J., Kline, C. L., Zhou, L., Campbell, K. S., MacFarlane, A. W., Olszanski, A. J., et al. (2018). Dose Intensification of TRAIL-Inducing ONC201 Inhibits Metastasis and Promotes Intratumoral NK Cell Recruitment. *J. Clin. Invest.* 128 (6), 2325–2338. doi:10.1172/JCI96711

Wang, X., Wang, Z. B., Luo, C., Mao, X. Y., Li, X., Yin, J. Y., et al. (2019). The Prospective Value of Dopamine Receptors on Bio-Behavior of Tumor. *J. Cancer* 10 (7), 1622–1632. doi:10.7150/jca.27780

Weisenthal, L. M. (1981). Treatment of Small Cell Lung Cancer - 1981. *Arch. Intern. Med.* 141 (11), 1499–1501. doi:10.1001/archinte.141.11.1499

Whang-Peng, J., Kao-Shan, C. S., Lee, E. C., Bunn, P. A., Carney, D. N., Gazdar, A. F., et al. (1982). Specific Chromosome Defect Associated with Human Small-Cell Lung Cancer; Deletion 3p(14-23). *Science* 215 (4529), 181–182. doi:10.1126/science.6274023

Wistuba, I, Gazdar, A. F., and Minna, J. D. (2001). Molecular Genetics of Small Cell Lung Carcinoma. *Semin. Oncol.* 28 (2 Suppl. 4), 3–13. doi:10.1016/s0093-7754(01)90072-7

Zhang, Y., and He, J. (2013). The Development of Targeted Therapy in Small Cell Lung Cancer. *J. Thorac. Dis.* 5 (4), 538–548. doi:10.3978/j.issn.2072-1439.2013.07.04

Zhang, Y., Zhou, L., Safran, H., Borsuk, R., Lulla, R., Tapinos, N., et al. (2021). EZH2i EPZ-6438 and HDACi Vorinostat Synergize with ONC201/TIC10 to Activate Integrated Stress Response, DR5, Reduce H3K27 Methylation, ClpX and Promote Apoptosis of Multiple Tumor Types Including DIPG. *Neoplasia* 23 (8), 792–810. doi:10.1016/j.neo.2021.06.007

Zhao, S., Zhou, L., Dicker, D. T., Lev, A., Zhang, S., and El-Deiry, W. S., (2020). *HIF1α Inhibition by Dual Targeting of CDK4/6 and HSP90 Reduces Cancer Cell Viability Including Rb-Deficient Cells*.

Zhao, W., Huang, Y., Liu, Z., Cao, B. B., Peng, Y. P., and Qiu, Y. H. (2013). Dopamine Receptors Modulate Cytotoxicity of Natural Killer Cells via cAMP-PKA-CREB Signaling Pathway. *PLoS One* 8 (6), e65860. doi:10.1371/journal.pone.0065860

Zhou, T., Zhang, Z., Luo, F., Zhao, Y., Hou, X., Liu, T., et al. (2020). Comparison of First-Line Treatments for Patients with Extensive-Stage Small Cell Lung Cancer: A Systematic Review and Network Meta-Analysis. *JAMA Netw. Open* 3 (10), e2015748. doi:10.1001/jamanetworkopen.2020.15748

Zhu, M., Huang, Y., Bender, M. E., Girard, L., Kollipara, R., Eglenen-Polat, B., et al. (2021). Evasion of Innate Immunity Contributes to Small Cell Lung Cancer Progression and Metastasis. *Cancer Res.* 81 (7), 1813–1826. doi:10.1158/0008-5472.CAN-20-2808

Zhu, S., Denman, C. J., Cobanoglu, Z. S., Kiany, S., Lau, C. C., Gottschalk, S. M., et al. (2015). The Narrow-Spectrum HDAC Inhibitor Entinostat Enhances NKG2D Expression without NK Cell Toxicity, Leading to Enhanced Recognition of Cancer Cells. *Pharm. Res.* 32 (3), 779–792. doi:10.1007/s11095-013-1231-0

Conflict of Interest: WSE-D is a co-founder of Oncoceutics, Inc., a subsidiary of Chimerix. WSE-D has disclosed his relationship with Oncoceutics and potential conflict of interest to his academic institution/employer and is fully compliant with NIH and institutional policy that is managing this potential conflict of interest.

The remaining authors declare that the research was conducted in the absence of any commercial or financial relationships that could be construed as a potential conflict of interest.

Publisher's Note: All claims expressed in this article are solely those of the authors and do not necessarily represent those of their affiliated organizations, or those of the publisher, the editors and the reviewers. Any product that may be evaluated in this article, or claim that may be made by its manufacturer, is not guaranteed or endorsed by the publisher.

Copyright © 2021 Liguori, Lee, Borges, Zhou, Azzoli and El-Deiry. This is an open-access article distributed under the terms of the Creative Commons Attribution License (CC BY). The use, distribution or reproduction in other forums is permitted, provided the original author(s) and the copyright owner(s) are credited and that the original publication in this journal is cited, in accordance with accepted academic practice. No use, distribution or reproduction is permitted which does not comply with these terms.

frontiers in Pharmacology

ORIGINAL RESEARCH
published: 10 September 2021
doi: 10.3389/fphar.2021.715721

Global Pattern of CD8$^+$ T-Cell Infiltration and Exhaustion in Colorectal Cancer Predicts Cancer Immunotherapy Response

Sun Tian[1]*, *Fulong Wang*[2], *Rongxin Zhang*[2] and *Gong Chen*[2]*

[1]Carbon Logic Biotech (HK) Limited, Hongkong, China, [2]StateKey Laboratory of Oncology in South China, Department of Colorectal Surgery, Sun Yat-sen University Cancer Center, Collaborative Innovation Center for Cancer Medicine, Guangzhou, China

OPEN ACCESS

Edited by:
Marc Diederich,
Seoul National University, South Korea

Reviewed by:
Anne Jarry,
Institut National de la Santé et de la Recherche Médicale (INSERM), France
Veronica Aran,
Instituto Estadual do Cérebro Paulo Niemeyer (IECPN), Brazil

***Correspondence:**
Sun Tian
suntian.gw@gmail.com
Gong Chen
chengong@sysucc.org.cn

Specialty section:
This article was submitted to Pharmacology of Anti-Cancer Drugs, a section of the journal Frontiers in Pharmacology

Received: 27 May 2021
Accepted: 22 July 2021
Published: 10 September 2021

Citation:
Tian S, Wang F, Zhang R and Chen G (2021) Global Pattern of CD8$^+$ T-Cell Infiltration and Exhaustion in Colorectal Cancer Predicts Cancer Immunotherapy Response. Front. Pharmacol. 12:715721. doi: 10.3389/fphar.2021.715721

Background: The MSI/MSS status does not fully explain cancer immunotherapy response in colorectal cancer. Thus, we developed a colorectal cancer-specific method that predicts cancer immunotherapy response.

Methods: We used gene expression data of 454 samples (MSI = 131, MSI-L = 23, MSS = 284, and Unknown = 16) and developed a TMEPRE method that models signatures of CD8+ T-cell infiltration and CD8$^+$ T-cell exhaustion states in the tumor microenvironment of colorectal cancer. TMEPRE model was validated on three RNAseq datasets of melanoma patients who received pembrolizumab or nivolumab and one RNAseq dataset of purified CD8$^+$ T cells in different exhaustion states.

Results: TMEPRE showed predictive power in three datasets of anti-PD1-treated patients ($p = 0.056, 0.115, 0.003$). CD8$^+$ T-cell exhaustion component of TMEPRE model correlates with anti-PD1 responding progenitor exhausted CD8$^+$ T cells in both tumor and viral infection ($p = 0.048, 0.001$). The global pattern of TMEPRE on 454 colorectal cancer samples indicated that 10.6% of MSS patients and 67.2% of MSI patients show biological characteristics that can potentially benefit from anti-PD1 treatment. Within MSI nonresponders, approximately 50% showed insufficient tumor-infiltrating CD8$^+$ T cells and 50% showed terminal exhaustion of CD8$^+$ T cells. These terminally exhausted CD8$^+$ T cells coexisted with signatures of myeloid-derived suppressor cells in colorectal cancer.

Conclusion: TMEPRE is a colorectal cancer-specific method. It captures characteristics of CD8$^+$ T-cell infiltration and CD8$^+$ T-cell exhaustion state and predicts cancer immunotherapy response. A subset of MSS patients could potentially benefit from anti-PD1 treatment. Anti-PD1 resistance MSI patients with insufficient infiltration of CD8$^+$ T cells or terminal exhaustion of CD8$^+$ T cells need different treatment strategies.

Keywords: biomarker, prediction method, colorectal cancer, cancer immunotherapy response, anti-PD1

INTRODUCTION

Immune checkpoint inhibitors produce durable responses in some microsatellite instable (MSI) colorectal cancer patients. However, still, approximately 60% of MSI colorectal cancer patients do not respond to single immune checkpoint inhibitor treatment such as anti-PD1, and approximately 40% of MSI colorectal patients do not respond to combinations of immune checkpoint inhibitor treatment (Oliveira et al., 2019). The mechanism of resistance is unclear. In colorectal cancer, MSI/MSS status is widely used as an indication of whether a patient should receive immunotherapy. Therefore, most studies on colorectal cancer were focused on the comparison between MSI tumors and MSS tumors. Although these studies provide insights into the difference between these two colorectal cancer subtypes, they do not explain why resistance to immune checkpoint inhibitor treatment occurs within MSI colorectal tumors. In addition to MSI/MSS status, other biomarkers such as TMB, PDL1, POLE/POLD1 mutation, or MSI-like gene signature are also used in colorectal cancer (Tian et al., 2012; Havel et al., 2019). Essentially, PDL1 provides a direct indication of whether a tumor sample of a colorectal cancer patient has high $CD8^+$ T-cell infiltration, while MSI/MSS status, TMB, POLE/POLD1 mutation, and MSI-like gene signature characterize the likelihood of a tumor sample generating high neoantigen level, thus indirectly indicating whether a tumor sample of a colorectal cancer patient could potentially have high $CD8^+$ T-cell infiltration. However, it is already evident from the studies of anti-PD1 response in lung cancer and melanoma that the number of tumor-infiltrating $CD8^+$ T cells is not the only requirement of response to anti-PD1 treatment; the characteristics of exhaustion state of tumor-infiltrating $CD8^+$ T cells is also required (Thommen et al., 2015; Li et al., 2019; Sade-Feldman et al., 2019). Therefore, regardless of how technically robust biomarkers such as MSI/MSS status, TMB, PDL1, POLE/POLD1 mutation, and MSI-like gene signature, these biomarkers will only characterize the quantity of tumor-infiltrating $CD8^+$ T cells. However, the quantity of tumor-infiltrating $CD8^+$ T cells alone will not fully explain anti-PD1 resistance in colorectal cancer. There is a lack of prediction method of anti-PD1 response in colorectal cancer.

It is known that a tumor at least has two well documented immune escape mechanisms to become resistant to anti-PD1 treatment: lack of $CD8^+$ T-cell infiltration and $CD8^+$ T-cell dysfunction (Sharma et al., 2017; Sade-Feldman et al., 2019; Yost et al., 2019; Wu et al., 2020). Therefore, a colorectal tumor should meet at least two characteristics to become a responder to anti-PD1 treatment an anti-PD1 treatment responding tumors should have $CD8^+$ T-cell infiltration and at least a subset of tumor-infiltrating $CD8^+$ T cells display properties that can respond to anti-PD1. In this report, we develop a TMEPRE method that dissects the gene expression patterns of these two characteristics from the tumor microenvironment in colorectal cancer and predict anti-PD1 response.

MATERIALS AND METHODS

Data Used for the Development of the TMEPRE Model

Publicly available gene expression data with known MSI/MSS status of four colorectal cancer datasets [GSE13294 (Jorissen et al., 2008), GSE26682 (Vilar et al., 2011), GSE18088 (Gröne et al., 2011), and GSE39084 (Kirzin et al., 2014)] were downloaded from GEO database. All four datasets are from the same Affymetrix Human Genome U133 Plus 2.0 Array platform, and normalization was performed using the frozen RMA (fRMA) method in the *frma* package (McCall et al., 2010). The batch effects of samples in four datasets were removed using *ComBat* (Johnson et al., 2007). In total, gene expression data of 454 samples were collected (MSI = 131, MSI-L = 23, MSS = 284, Unknown = 16). The public or the patients were not involved in the design, conduct, reporting, or dissemination plans of our research.

Design of the TMEPRE Model

The score function of the TMEPRE model is comprised of two components: *TME*1.*TcellInfiltration* and *TME*2.*TcellResponse*.

1) *TME*1.*TcellInfiltration* scores tumor microenvironment that allows $CD8^+$ T-cell infiltration. To estimate the abundance of $CD8^+$ T cells, we use the expression level of CD8A. The cutoff of CD8A level is defined as 40% percentile of CD8A expression level in 131 MSI tumors. MSI tumors with a CD8A level higher than the cutoff are classified as tumors with high $CD8^+$ T-cell infiltration (n = 78); MSS tumors with a CD8A level lower than the cutoff are classified as tumors without high $CD8^+$ T-cell infiltration ($n = 211$). 200 rounds of 10-fold cross-validation between these two groups were performed. In each cross-validation round, a *t*-test for each gene was performed and p-values of genes were ranked. CD8A gene itself was excluded from the cross-validation procedure. Genes with p-values in the top 60 ranked genes in at least 80% of 200 rounds of cross-validations were selected as the signature of *TME*1.*TcellInfiltration*. The selected genes were used to construct the nearest centroid method. The inputs are expression values of these selected genes and the output is a *TME*1.*TcellInfiltration* score. To ensure that all potential anti-PD1 responders are selected sensitively, the cutoff was optimized to maximize the sensitivity and minimize the false-negative rate.

The relative range coverage ω of *TME*1.*TcellInfiltration* scores of MSS samples is defined as follows:

$$\omega = (\max . score_{mss} - \min . score_{mss}) / (\max . score_{all} - \min . score_{all}).$$

2) *TME*2.*TcellResponse* scores tumor microenvironment, that tumor-infiltrating $CD8^+$ T cells do not display a terminal exhaustion pattern and can still respond to checkpoint inhibitors. To define the terminal exhaustion pattern of tumor-infiltrating $CD8^+$ T cells, we use the co-expression

pattern of multiple inhibitory receptors of PD1 and TIM3 because TIM3 is an early acquired co-expressed inhibitor receptor among all co-expressed inhibitory receptors and using an early co-inhibitory receptor, TIM3, could sensitively capture more tumor samples with terminal exhausted $CD8^+$ T cells (Thommen et al., 2015). Within MSI tumors with high $CD8^+$ T-cell infiltration defined in the previous step (n = 78), the median of PD1 expression level is used as the cutoff of PD1 and the median of TIM3 expression level is used as the cutoff of TIM3. MSI tumors with high $CD8^+$ T-cell infiltration and both PD1 and TIM3 higher than cutoffs are defined as a tumor microenvironment of co-expression of multiple early inhibitory receptors. $CD8^+$ T cells in this type of tumor microenvironment become terminally exhausted and resist anti-PD1 treatment (n = 21). MSI tumors with high $CD8^+$ T-cell infiltration but both PD1 and TIM3 lower than cutoffs are defined as a tumor microenvironment in which $CD8^+$ T cells can still respond to anti-PD1 treatment (n = 21). 200 rounds of 10-fold cross-validation between these two groups were performed. In each cross-validation round, a t-test for each gene was performed and p-values of genes were ranked. Genes with p-values in the top 60 ranked genes in at least 80% of 200 rounds of cross-validations were selected as the signature of *TME2.TcellResponse*. The selected genes were used to construct the nearest centroid method. The inputs are expression values of these selected genes and outputs are a *TME2.TcellResponse* score. To ensure that all potential anti-PD1 responders are selected sensitively, the cutoff was optimized to maximize the sensitivity and minimize the false-negative rate.

Data Used for Testing Predictive Values of the Anti-PD1 Response of the TMEPRE Model

To test the predictive value of the anti-PD1 response, three RNAseq datasets were used. The first dataset includes normalized RNAseq data and clinical data of pretreatment samples of melanoma patients who received pembrolizumab or nivolumab. Patients in this cohort who received MAPK inhibitor were removed (n = 16, GSE78220) (Hugo et al., 2016). The second dataset includes normalized RNAseq data and clinical data of samples of melanoma patients who received nivolumab. Samples at the early treatment time point before cycle 1 day 29 and samples at the pretreatment time point before cycle 1 day 0 were analyzed separately. Patients who received *a priori* ipilimumab treatment or with incomplete overall survival data were removed (n = 21, GSE91061) (Riaz et al., 2017). The platform of these three anti-PD1-treated patients' datasets is different from the platform of the datasets used in the development of TMEPRE and the cutoff values can not be directly used. In three datasets of anti-PD1-treated patients, the median was therefore used as the default cutoff. TMEPRE comprises two components; the median was equally split as the cutoffs for each component. A colorectal tumor with either a low *TME1.TcellInfiltration* score (lowest 25%) or a high *TME1.TcellInfiltration* score (highest 25%) but a low *TME2.TcellResponse* score is considered as an anti-PD1 nonresponder. Survival analysis was performed using the R package survival (Therneau and Grambsch, 2000). The hazard ratio was calculated using the Cox proportional-hazards regression model and the p-value was calculated using the log-rank test. The combined p-value of three validation sets was calculated using the Z-transform method implemented in the R package survcomp (Whitlock, 2005; Haibe-Kains et al., 2008).

To read the *TME2.TcellResponse* score of the TMEPRE model on exhausted $CD8^+$ T cells**,** a dataset including normalized RNAseq data from progenitor exhausted and terminally exhausted $CD8^+$ T cells isolated from tumors and chronic viral infection (n = 20, GSE122713) was used (Miller et al., 2019). Because the *TME2.TcellResponse* signature is derived from the gene expression data of bulk tumor sample, the source of gene expressions originates from a mixture of $CD8^+$ T cells, tumor cells, and other tumor-infiltrating immune cell types in the tumor microenvironment, while the progenitor/terminal exhausted tumor-infiltrating $CD8^+$ T cells data are generated from isolated $CD8^+$ T cells. When *TME2.TcellResponse* scores were read, only genes in *TME2.TcellResponse* that primarily originated from $CD8^+$ T cells are used. For each gene in *TME2.TcellResponse*, median expression values in 16 purified main immune cell types were compared using BloodSpot with HemaExporer human hematopoiesis database (Bagger et al., 2019). A gene is considered as mainly expressed by $CD8^+$ T cells when $CD8^+$ T cell is among the top two immune cell types expressing this gene. The score function used for the read-out is the nearest centroid.

RESULTS

TMEPRE Model Predicts the Anti-PD1 Treatment Response

The TMEPRE model was developed using gene expression data of colorectal cancer patients and has two components: *TME1.TcellInfiltration* (28 genes, **Supplementary Table S1**) and *TME2.TcellResponse* (29 genes, **Supplementary Table 2**).

To date, melanoma is widely used as the main prototypic cancer type of immune hot tumor to study cancer immunotherapy response. Thus, most of the available gene expression datasets of anti-PD1 response were performed using melanoma as the model system. Because TMEPRE is a method that mainly measures characteristics of the tumor microenvironment and different cancer types have shared tumor microenvironment characteristics, in our study, we also used anti-PD1-treated melanoma datasets as a model system to test predictive values of TMEPRE. TMEPRE was validated on three datasets of melanoma patients who received anti-PD1 treatment. In the first dataset, the survival analysis of the TMEPRE prediction model resulted in a significant hazard ratio (n = 16, pretreatment samples, GSE78220, HR = 4.59, p-value = 0.056, **Figure 1A**). In the second dataset, although the p-value of the survival analysis of the TMEPRE prediction

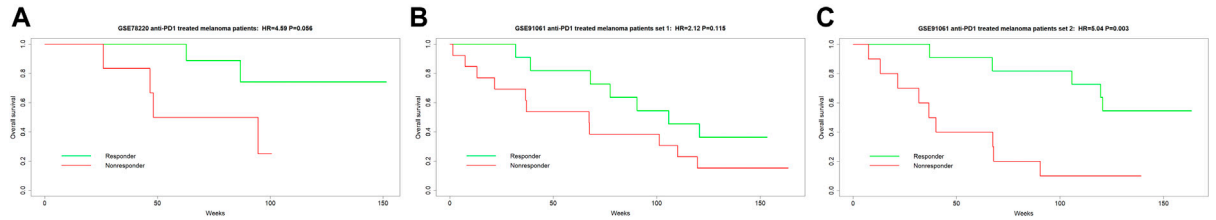

FIGURE 1 | TMEPRE was validated on three datasets of melanoma patients who received anti-PD1 treatment. **(1A)** n = 16, pretreatment samples, patients were treated with pembrolizumab or nivolumab, HR = 4.59, *p*-value = 0.056; **(1B)** n = 21, sampling before cycle 1 day 0, patients were treated with nivolumab, HR = 2.12, *p*-value = 0.115; **(1C)** n = 21, sampling at an early treatment time point before cycle 1 day 29, patients were treated with nivolumab, HR = 5.04, *p*-value = 0.003. Separation of overall survival between TMEPRE-predicted responder group and TMEPRE-predicted nonresponder group is clear in all three validations.

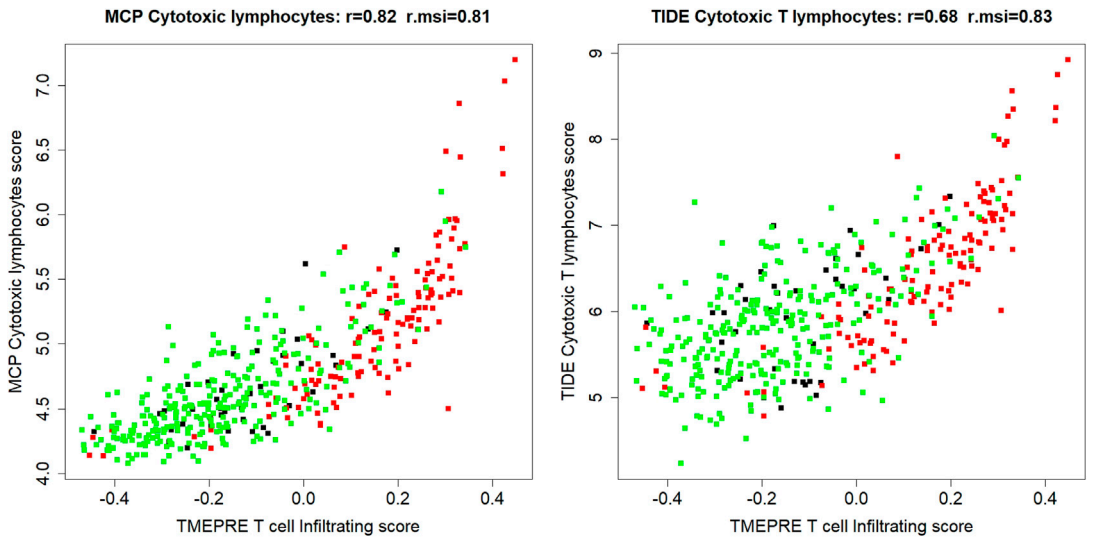

FIGURE 2 | In 454 colorectal cancer samples (MSI = 131, MSI-L = 23, MSS = 284, Unknown = 16), the first component of the TMEPRE model, *TME*1.*TcellInfiltration* score (*x*-axis), positively correlates with the counting of MCP-counter cytotoxic lymphocytes score (*y*-axis, left panel) and TIDE cytotoxic T lymphocytes score (*y*-axis, right panel). MSI tumors are shown in red; MSS tumors are shown in green; MSI-L and MSI-unknown tumors are shown in black. The relative range coverage of *TME*1.*TcellInfiltration* scores of MSS samples ($\omega_{MSS.TME1.TcellInfiltration}$=0.89) is the largest among all three methods.

model is large (n = 21, sampling before cycle 1 day 0, GSE91061, HR = 2.12, *p*-value = 0.115, **Figure 1B**), the separation of survival between the TMEPRE-predicted responder group and the TMEPRE-predicted nonresponder group is still clearly observed. In the third dataset, the survival analysis of the TMEPRE prediction model resulted in a significant hazard ratio (n = 21, sampling at an early treatment time point before cycle 1 day 29, GSE91061, HR = 5.04, *p*-value = 0.003, **Figure 1C**). The sample sizes of anti-PD1-treated samples in the current publicly available databases are small, and this small sample size artificially increased the *p*-values of each individual log-rank test (Ioannidis, 2019; Thiese et al., 2016). Still, the trend of separation of the responder group and the nonresponder group is clear in all three validation sets (**Figures 1A–C**). When three validation sets are combined together, the *Z*-transform combined probability test showed a significant *p*-value (*p*-value = 0.0007) (Whitlock, 2005). Taken together, the survival analysis indicated clinical significance, and the TMEPRE model showed predictive values for anti-PD1 treatment response.

The Underlying Biology of the TMEPRE Model Measures Amounts of Tumor-Infiltrating CD8$^+$ T Cells and Characteristics of Tumor-Infiltrating Terminally Exhausted CD8$^+$ T Cells

In the dataset of all 454 samples, the counts of tumor-infiltrating cytotoxic lymphocytes were read out using MCP-counter and TIDE cytotoxic T lymphocytes count (Becht et al., 2016; Jiang et al., 2018). The first component of the TMEPRE model, *TME*1.*TcellInfiltration* score, positively correlates with counting of MCP-counter cytotoxic lymphocytes (*r* = 0.82, r. msi = 0.81) and TIDE cytotoxic T lymphocytes (r = 0.68, r. msi = 0.83) (**Figure 2**). The relative range coverage of the

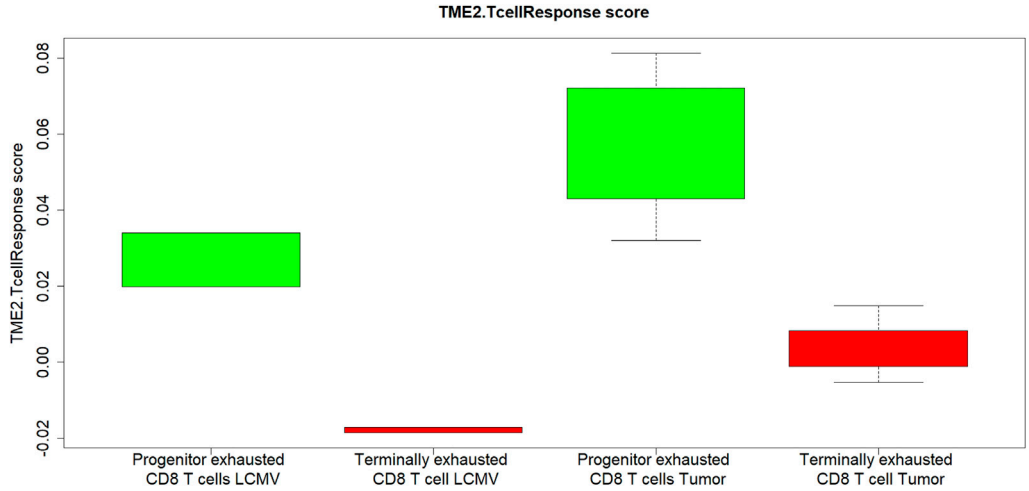

FIGURE 3 | In both tumor and chronic viral infection, $CD8^+$ T cells components of *TME2.TcellResponse* significantly correlates with anti-PD1 responding progenitor exhausted $CD8^+$ T cells (p = 0.048, 0.001, respectively). The *X*-axis is the groups of $CD8^+$ T cells. Green is the purified progenitor exhausted $CD8^+$ T cells; red is the purified terminally exhausted $CD8^+$ T cells. *Y*-axis is the *TME2.TcellResponse* score calculated using $CD8^+$ T cells components of *TME2.TcellResponse*.

TME1.TcellInfiltration scores of MSS samples is larger than the relative range coverage of MCP-counter score and TIDE score ($\omega_{MSS.TME1.TcellInfiltration}$=0.89, $\omega_{MSS.MCP.\text{Cytotoxiclymphocyte}}$ = 0.67, $\omega_{MSS.TIDE.\text{CytotoxicTlymphocyte}}$ = 0.81). These results suggested that counting of cytotoxic T lymphocytes by *TME1.TcellInfiltration* tends to agree with other counting methods, but in MSS colorectal tumors that harbor fewer tumor-infiltrating immune cells, *TME1.TcellInfiltration* might be a more sensitive measurement of tumor-infiltrating cytotoxic lymphocytes. The reason might be that *TME1.TcellInfiltration* is specifically designed for the tumor microenvironment of colorectal cancer.

The second component of the TMEPRE model, *TME2.TcellResponse* score, is designed to measure whether tumor-infiltrating $CD8^+$ T cells can respond to anti-PD1 treatment. To test whether *TME2.TcellResponse* indeed captures this characteristic of tumor-infiltrating $CD8^+$ T cells, we read out the scores of *TME2.TcellResponse* signature in two subgroups of dysfunction $CD8^+$ T cells isolated from tumors and chronic viral infection: terminally exhausted tumor-infiltrating $CD8^+$ T cells that can no longer respond to anti-PD-1 therapy and progenitor exhausted tumor-infiltrating $CD8^+$ T cells that can still respond to anti-PD-1 therapy (GSE122713) (Miller et al., 2019; Busselaar et al., 2020). Only genes in *TME2.TcellResponse* that likely primarily originated from $CD8^+$ T cells are used to read out scores on gene expression data generated from isolated $CD8^+$ cells. Seven genes (CCL5, CD2, CD48, CD84, FAM78A, HCST, and IL21R) in *TME2.TcellResponse* are considered as mainly expressed by $CD8^+$ T cells as $CD8^+$ T cell is among the top two immune cell types expressing them in the BloodSpot HemaExporer human hematopoiesis database (Bagger et al., 2019). Two genes in *TME2.TcellResponse* are inhibitor receptors on $CD8^+$ T cells used to define early terminal exhausted $CD8^+$ T cells (HAVCR2, PDCD1). These nine genes were used to read out *TME2.TcellResponse* scores in the isolated progenitor/terminal exhausted tumor-infiltrating $CD8^+$ T cells dataset. In both tumors and chronic viral infection, the scores of *TME2.TcellResponse* are significantly higher in the subgroup of progenitor exhausted tumor-infiltrating $CD8^+$ T cells ($pvalue_{tumor}$ <0.001, $pvalue_{viralinfection}$= 0.048, **Figure 3**). Therefore, the score of *TME2.TcellResponse* indeed captures the characteristics of progenitor exhausted tumor-infiltrating $CD8^+$ T cells that can still respond to anti-PD1.

Global Pattern of the TMEPRE Model in MSI and MSS Colorectal Tumors

The TMEPRE model was read out in 454 colorectal samples (MSI = 131, MSI-L = 23, MSS = 284, Unknown = 16). A splitted heatmap was plotted (Gu et al., 2016). Tumors displaying a pattern of sufficient $CD8^+$ T-cell infiltration but no pattern of $CD8^+$ T-cell terminal exhaustion are considered as potential responders to anti-PD1 therapy (**Figure 4**).

Within 284 MSS tumor samples, 10.6% (n = 30) are classified as responders and 89.4% (n = 254) as nonresponders. This predicted percentage of responders, 10.6% by TMEPRE, is consistent with the reported disease control rate, 11%, in pembrolizumab-treated metastatic MSS colorectal cancers (Le et al., 2015). Among MSS nonresponders, 86.6% (n = 246) showed insufficient tumor-infiltrating $CD8^+$ T cells and 2.8% (n = 8) showed sufficient tumor-infiltrating $CD8^+$ T cells; however, those $CD8^+$ T cells display patterns of terminally exhausted $CD8^+$ T cells. As expected, the anti-PD1 resistance mechanism of the majority of MSS tumors is an insufficient amount of tumor-infiltrating $CD8^+$ T cells.

Within 131 MSI tumor samples, 67.2% (n = 88) are classified as responders and 32.8% (n = 43) as nonresponders. This

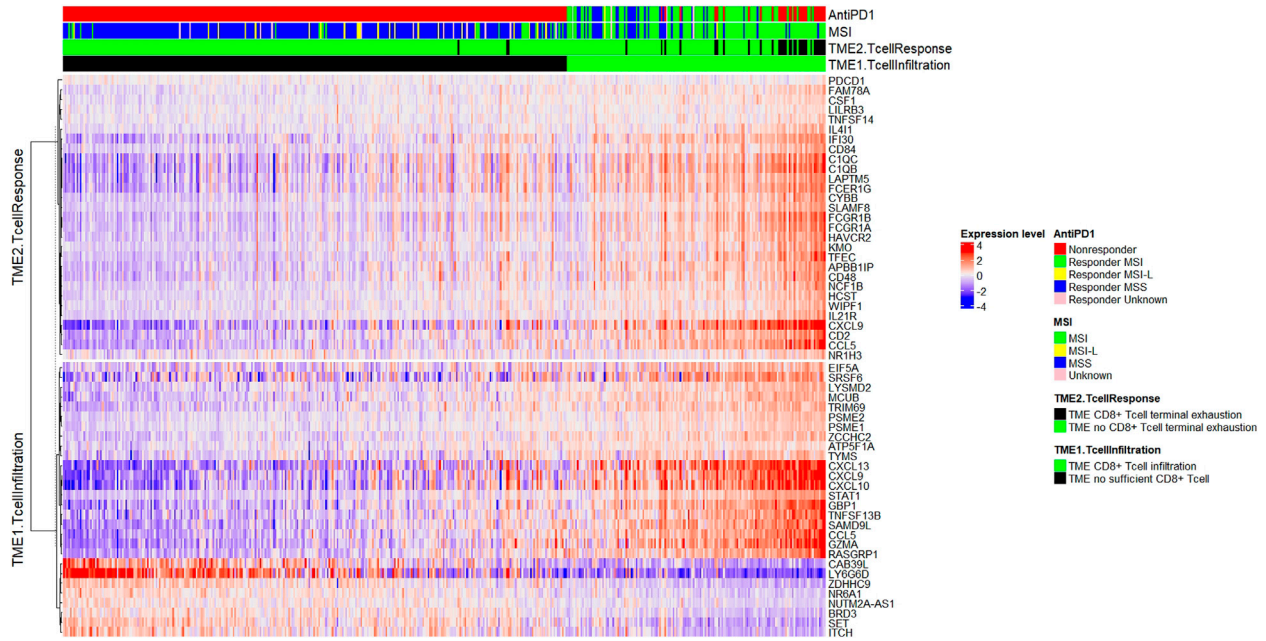

FIGURE 4 | Plot of TMEPRE over 454 colorectal cancer samples (MSI = 131, MSI-L = 23, MSS = 284, Unknown = 16). Samples were ranked according to scores of the TMEPRE model. Genes in *TME*1.*TcellInfiltration* were shown in the upper panel and genes in *TME*2.*TcellResponse* were shown in the lower panel. MSI row indicates MSI/MSS status. *TME*1.*TcellInfiltration* row indicates *TME*1.*TcellInfiltration* scores, green indicates sufficient $CD8^+$ T-cell infiltration, and black indicates insufficient $CD8^+$ T-cell infiltration. *TME*2.*TcellResponse* row indicates *TME*2.*TcellResponse* scores: green indicates that infiltrated $CD8^+$ T cells are not terminally exhausted if a tumor sample has $CD8^+$ T cells infiltration and black indicates infiltrated $CD8^+$ T cells are terminally exhausted if a tumor sample has $CD8^+$ T cells infiltration. AntiPD1 indicates whether the tumor microenvironment of a sample displays biological characteristics that can respond to anti-PD1 treatment (red: nonresponder; green: MSI responder; blue: MSS responder). 10.6% of MSS patients and 67.2% of MSI patients could potentially benefit from anti-PD1 treatment. Within MSI nonresponders, approximately 50% showed insufficient amount of tumor-infiltrating $CD8^+$ T cells and 50% showed terminal exhaustion of $CD8^+$ T cells.

predicted percentage of responders, 67.2% by TMEPRE, is between the range of the reported immune-related objective response rate, 40%, and the reported disease control rate, 78%, in pembrolizumab-treated metastatic MSI colorectal cancers (Le et al., 2015). Among the MSI nonresponders, 16.0% (n = 21) showed insufficient tumor-infiltrating $CD8^+$ T cells and 16.8% (n = 22) showed sufficient tumor-infiltrating $CD8^+$ T cells; however, those $CD8^+$ T cells display patterns of terminally exhausted $CD8^+$ T cells. Therefore, approximately 50% of MSI nonresponders are caused by terminal exhaustion of $CD8^+$ T cells in the tumor microenvironment, and the rest 50% of MSI nonresponders are caused by an insufficient amount of tumor-infiltrating $CD8^+$ T cells. Treatments of MSI nonresponders with insufficient infiltration of $CD8^+$ T cells and MSI nonresponders with terminal exhaustion of $CD8^+$ T cells need to be designed separately.

The TMEPRE model identified 10.6% of MSS and 67.2% of MSI colorectal cancer patients whose tumors show biological characteristics that can potentially benefit from anti-PD1 treatment. These predicted percentages of responders in MSS tumors and MSI tumors are consistent with the reported benefits of immune-related disease control rate at 20 weeks of a cohort of colorectal cancer patients treated with pembrolizumab (Le et al., 2015).

DISCUSSION

Drug resistance tumors in colorectal cancer often consist of heterogeneous subgroups of populations. A drug response prediction method needs first to identify different drug resistance patterns of subgroups and then reinforce the patterns later (Tian et al., 2013; Tian et al., 2020). Conceptually, a drug response prediction method must never consider the drug resistance tumors as a homogenous group. Current biomarkers for anti-PD1 in colorectal cancer, MSI/MSS, TMB, PDL1, and POLE/POLD1 mutation, share the same notion that anti-PD1 resistance is dominantly caused by one homogenous factor of an insufficient amount of $CD8^+$ T-cell infiltration. The quantity of tumor-infiltrating $CD8^+$ T cells needs to be supplemented by characteristics of tumor-infiltrating $CD8^+$ T cells to predict anti-PD1 response. In this report, we developed the computational method TMEPRE for colorectal cancer patients, which measures two factors of the tumor microenvironment that contribute to anti-PD1 resistance: $CD8^+$ T-cell infiltration (*TME*1.*TcellInfiltration*) and whether tumor-infiltrating $CD8^+$ T cells can respond to cancer immunotherapy (*TME*2.*TcellResponse*). TMEPRE was developed without using any anti-PD1 response data or survival data and was designed to reflect the biology of the

tumor microenvironment of colorectal cancer. The method was validated in three datasets of anti-PD1-treated patients.

Another example of a prediction method of anti-PD1 response using tumor microenvironment of $CD8^+$ T-cell exclusion and $CD8^+$ T-cell exhaustion is TIDE (Jiang et al., 2018). The TIDE method also has good validation performance in anti-PD1-treated melanoma data. It is difficult to directly compare TIDE and TMEPRE as these two methods are optimized for different tumor types. TIDE method was trained using survival data of melanoma and was specifically designed for five cancer types: melanoma, neuroblastoma, triple-negative breast cancer, endometrial cancer, and acute myeloid leukemia. On the contrary, the TMEPRE method is designed for colorectal cancer. Partially because the methods are optimized for different cancer types, the overlap between genes used in the TMEPRE model and genes used in the TIDE model is small (IL21R, GZMA). We expect that TMEPRE will be a more specific reflection of the tumor microenvironment of colorectal cancer.

The first component of TMEPRE, *TME1.TcellInfiltration*, measures the tumor microenvironment that allows $CD8^+$ T-cell infiltration. Approximately 50% of the MSI nonresponders have a low *TME1.TcellInfiltration* score. For those colorectal cancer patients, a combination of anti-PD1 with drugs inducing $CD8^+$ T-cell infiltration could be considered (Duan et al., 2020). The second component of TMEPRE, *TME2.TcellResponse*, measures the tumor microenvironment and whether tumor-infiltrating $CD8^+$ T cells can still respond to checkpoint inhibitors. It should be noted that because gene expression data were generated using bulk tumor samples, genes listed in *TME2.TcellResponse* are expressed on both $CD8^+$ T cells and other immune cell types in the tumor microenvironment. Among the genes in *TME2.TcellResponse*, two genes are known inhibitor receptors on $CD8^+$ T cells (HAVCR2, PDCD1) and seven genes (CCL5, CD2, CD48, CD84, FAM78A, HCST, and IL21R) have high expression levels in purified $CD8^+$ T cells. The expression values of these nine genes are higher in nonresponders, which correlates with the terminally exhausted type of $CD8^+$ T cells. Among the other genes in *TME2.TcellResponse*, CIQB, CIQC, KMO, FCGR1A, FCGR1B, and FCER1G show higher expression in nonresponders, and these are potential markers of the existence of myeloid-derived suppressor cells (Giorgini et al., 2013; Bournazos et al., 2016; Ryan et al., 2020). This pattern suggests that the reason why terminally exhausted $CD8^+$ T cells failed to respond to anti-PD1 therapy might be not only the co-expression of multiple inhibitors on $CD8^+$ T cells themselves but also the tumor microenvironment of colorectal tumor in which those terminally exhausted $CD8^+$ T cells may be infiltrated with myeloid-derived suppressor cells. Approximately 50% of the MSI nonresponders have a high *TME1.TcellInfiltration* score but a low *TME2.TcellResponse* score. For those colorectal cancer patients, a combination of anti-PD1 with drugs targeting myeloid-derived suppressor cells or a combination of drugs targeting other co-expressed inhibitors could be considered (Kuang et al., 2020; Lind et al., 2020; Zhang et al., 2020).

By only assessing the MSI/MSS status, it is not recommended that MSS colorectal cancer patients be treated with anti-PD1. However, data from clinical trials showed that the disease control rate in pembrolizumab-treated metastatic MSS colorectal cancers was 11%, and further, in a more recent clinical trial of neoadjuvant setting, the pathological response rate of ipilimumab + nivolumab–treated early-stage MSS colorectal cancers is 27% (Le et al., 2015; Chalabi et al., 2020). These results indicated that responders to anti-PD1 treatment exist within the MSS colorectal cancer population. In our analysis, approximately 10.6% of MSS tumor samples showed both high *TME1.TcellInfiltration* scores and high *TME2.TcellResponse* scores, suggesting the biological characteristics of tumor microenvironments in 10.6% of MSS patients can still potentially benefit from anti-PD1 treatment. This prediction agrees with the reported immune-related progression survival rate of MSS patients treated with pembrolizumab. As the number of MSS patients is much larger than MSI patients, in this dataset of 451 patients used for this study, 10.6% of MSS patients means that the percentage of patients who should be considered for anti-PD1 treatment would increase 23%. The limitation is that, at this moment, no dataset of colorectal cancer patients treated with anti-PD1 is publicly available. A clinical trial is proposed at our cancer center to further confirm the prediction of TMEPRE in colorectal cancer.

To conclude, we develop a colorectal cancer-specific method, TMEPRE, that predicts cancer immunotherapy response. The global patterns of TMEPRE in colorectal cancer patients explained the mechanism underlying the response of anti-PD1 in MSS patients and the resistance of anti-PD1 in MSI patients. A subset of MSS patients could potentially benefit from anti-PD1 treatment. Anti-PD1-resistant MSI patients could result from tumor microenvironment of insufficient infiltration of $CD8^+$ T-cell or tumor microenvironment of terminal exhaustion of $CD8^+$ T cells, and treatment strategies need to be different. TMEPRE will aid personalized medicine options of cancer immunotherapy for colorectal cancer patients.

DATA AVAILABILITY STATEMENT

The datasets presented in this study can be found in online repositories. The names of the repository/repositories and accession number(s) can be found in the article/ **Supplementary Material**.

ETHICS STATEMENT

The study uses publicly available dataset. Ethical review and approval were not required for the study on human participants in accordance with the local legislation and institutional requirements. Written informed consent for participation was not required for this study in accordance

with the national legislation and the institutional requirements.

AUTHOR CONTRIBUTIONS

ST was responsible for the conceptualization, methodology, and formal analysis and wrote the original draft; ST and GC investigated and interpreted the results; FW, RZ, and GC acquired the resources; ST, FW, RZ, and GC reviewed and edited the manuscript; ST and GC were responsible for project administration.

ACKNOWLEDGMENTS

This manuscript has been released as a pre-print at: https://www.researchsquare.com/article/rs-89397/v1.

SUPPLEMENTARY MATERIAL

The Supplementary Material for this article can be found online at: https://www.frontiersin.org/articles/10.3389/fphar.2021.715721/full#supplementary-material

REFERENCES

Bagger, F. O., Kinalis, S., and Rapin, N. (2019). BloodSpot: a Database of Healthy and Malignant Haematopoiesis Updated with Purified and Single Cell mRNA Sequencing Profiles. *Nucleic Acids Res.* 47, D881–D885. doi:10.1093/nar/gky1076

Becht, E., Giraldo, N. A., Lacroix, L., Buttard, B., Elarouci, N., Petitprez, F., et al. (2016). Estimating the Population Abundance of Tissue-Infiltrating Immune and Stromal Cell Populations Using Gene Expression. *Genome Biol.* 17, 218. doi:10.1186/s13059-016-1070-5

Bournazos, S., Wang, T. T., and Ravetch, J. V. (2016). The Role and Function of Fcγ Receptors on Myeloid Cells. *Microbiol. Spectr.* 4, 4. doi:10.1128/microbiolspec.MCHD-0045-2016

Busselaar, J., Tian, S., van Eenennaam, H., and Borst, J. (2020). Helpless Priming Sends CD8+ T Cells on the Road to Exhaustion. *Front. Immunol.* 11, 11. doi:10.3389/fimmu.2020.592569

Chalabi, M., Fanchi, L. F., Dijkstra, K. K., Van den Berg, J. G., Aalbers, A. G., Sikorska, K., et al. (2020). Neoadjuvant Immunotherapy Leads to Pathological Responses in MMR-Proficient and MMR-Deficient Early-Stage colon Cancers. *Nat. Med.* 26, 566–576. doi:10.1038/s41591-020-0805-8

Duan, Q., Zhang, H., Zheng, J., and Zhang, L. (2020). Turning Cold into Hot: Firing up the Tumor Microenvironment. *Trends Cancer.* 6, 605–618. doi:10.1016/j.trecan.2020.02.022

Giorgini, F., Huang, S.-Y., Sathyasaikumar, K. V., Notarangelo, F. M., Thomas, M. A. R., Tararina, M., et al. (2013). Targeted Deletion of Kynurenine 3-Monooxygenase in Mice. *J. Biol. Chem.* 288, 36554–36566. doi:10.1074/jbc.M113.503813

Gröne, J., Lenze, D., Jurinovic, V., Hummel, M., Seidel, H., Leder, G., et al. (2011). Molecular Profiles and Clinical Outcome of Stage UICC II Colon Cancer Patients. *Int. J. Colorectal Dis.* 26, 847–858. doi:10.1007/s00384-011-1176-x

Gu, Z., Eils, R., and Schlesner, M. (2016). Complex Heatmaps Reveal Patterns and Correlations in Multidimensional Genomic Data. *Bioinformatics.* 32, 2847–2849. doi:10.1093/bioinformatics/btw313

Haibe-Kains, B., Desmedt, C., Sotiriou, C., and Bontempi, G. (2008). A Comparative Study of Survival Models for Breast Cancer Prognostication Based on Microarray Data: Does a Single Gene Beat Them All? *Bioinformatics.* 24, 2200–2208. doi:10.1093/bioinformatics/btn374

Havel, J. J., Chowell, D., and Chan, T. A. (2019). The Evolving Landscape of Biomarkers for Checkpoint Inhibitor Immunotherapy. *Nat. Rev. Cancer.* 19, 133–150. doi:10.1038/s41568-019-0116-x

Hugo, W., Zaretsky, J. M., Sun, L., Song, C., Moreno, B. H., Hu-Lieskovan, S., et al. (2016). Genomic and Transcriptomic Features of Response to Anti-PD-1 Therapy in Metastatic Melanoma. *Cell.* 165, 35–44. doi:10.1016/j.cell.2016.02.065

Ioannidis, J. P. A. (2019). The Importance of Predefined Rules and Prespecified Statistical Analyses. *JAMA.* 321, 2067–2068. doi:10.1001/jama.2019.4582

Jiang, P., Gu, S., Pan, D., Fu, J., Sahu, A., Hu, X., et al. (2018). Signatures of T Cell Dysfunction and Exclusion Predict Cancer Immunotherapy Response. *Nat. Med.* 24, 1550–1558. doi:10.1038/s41591-018-0136-1

Johnson, W. E., Li, C., and Rabinovic, A. (2007). Adjusting Batch Effects in Microarray Expression Data Using Empirical Bayes Methods. *Biostat Oxf Engl.* 8, 118–127. doi:10.1093/biostatistics/kxj037

Jorissen, R. N., Lipton, L., Gibbs, P., Chapman, M., Desai, J., Jones, I. T., et al. (2008). DNA Copy-Number Alterations Underlie Gene Expression Differences between Microsatellite Stable and Unstable Colorectal Cancers. *Clin. Cancer Res.* 14, 8061–8069. doi:10.1158/1078-0432.ccr-08-1431

Kirzin, S., Marisa, L., Guimbaud, R., De Reynies, A., Legrain, M., Laurent-Puig, P., et al. (2014). Sporadic Early-Onset Colorectal Cancer Is a Specific Sub-type of Cancer: a Morphological, Molecular and Genetics Study. *PLoS One* 9, e103159. doi:10.1371/journal.pone.0103159

Kuang, Z., Li, L., Zhang, P., Chen, B., Wu, M., Ni, H., et al. (2020). A Novel Antibody Targeting TIM-3 Resulting in Receptor Internalization for Cancer Immunotherapy. *Antib Ther.* 3, 227–236. doi:10.1093/abt/tbaa022

Le, D. T., Uram, J. N., Wang, H., Bartlett, B. R., Kemberling, H., Eyring, A. D., et al. (2015). PD-1 Blockade in Tumors With Mismatch-Repair Deficiency. *N. Engl. J. Med.* 372, 2509–2520. doi:10.1056/NEJMoa1500596

Li, H., van der Leun, A. M., Yofe, I., Lubling, Y., Gelbard-Solodkin, D., van Akkooi, A. C. J., et al. (2019). Dysfunctional CD8 T Cells Form a Proliferative, Dynamically Regulated Compartment within Human Melanoma. *Cell.* 176, 775–789. doi:10.1016/j.cell.2018.11.043

Lind, H., Gameiro, S. R., Jochems, C., Donahue, R. N., Strauss, J., Gulley, J. L., et al. (2020). Dual Targeting of TGF-β and PD-L1 via a Bifunctional Anti-PD-l1/tgf-βrii Agent: Status of Preclinical and Clinical Advances. *J. Immunother. Cancer.* 8, e000433. doi:10.1136/jitc-2019-000433

McCall, M. N., Bolstad, B. M., and Irizarry, R. A. (2010). Frozen Robust Multiarray Analysis (fRMA). *Biostatistics.* 11, 242–253. doi:10.1093/biostatistics/kxp059

Miller, B. C., Sen, D. R., Al Abosy, R., Bi, K., Virkud, Y. V., LaFleur, M. W., et al. (2019). Subsets of Exhausted CD8+ T Cells Differentially Mediate Tumor Control and Respond to Checkpoint Blockade. *Nat. Immunol.* 20, 326–336. doi:10.1038/s41590-019-0312-6

Oliveira, A. F., Bretes, L., and Furtado, I. (2019). Review of PD-1/pd-L1 Inhibitors in Metastatic dMMR/MSI-H Colorectal Cancer. *Front. Oncol.* 9, 396. doi:10.3389/fonc.2019.00396

Riaz, N., Havel, J. J., Makarov, V., Desrichard, A., Urba, W. J., Sims, J. S., et al. (2017). Tumor and Microenvironment Evolution During Immunotherapy With Nivolumab. *Cell.* 171, 934–949. doi:10.1016/j.cell.2017.09.028

Ryan, A. F., Nasamran, C. A., Pak, K., Draf, C., Fisch, K. M., Webster, N., et al. (2020). Single-Cell Transcriptomes Reveal a Complex Cellular Landscape in the Middle Ear and Differential Capacities for Acute Response to Infection. *Front. Genet.* 11, 11. doi:10.3389/fgene.2020.00358

Sade-Feldman, M., Yizhak, K., Bjorgaard, S. L., Ray, J. P., de Boer, C. G., Jenkins, R. W., et al. (2019). Defining T Cell States Associated With Response to Checkpoint Immunotherapy in Melanoma. *Cell.* 176, 404. doi:10.1016/j.cell.2018.12.034

Sharma, P., Hu-Lieskovan, S., Wargo, J. A., and Ribas, A. (2017). Primary, Adaptive, and Acquired Resistance to Cancer Immunotherapy. *Cell* .168, 707–723. doi:10.1016/j.cell.2017.01.017

Therneau, T. M., and Grambsch, P. M. (2000). *Modeling Survival Data: Extending the Cox Model.* New York: Springer-Verlag.

Thiese, M. S., Ronna, B., and Ott, U. (2016). P Value Interpretations and Considerations. *J. Thorac. Dis.* 8, E928–E931. doi:10.21037/jtd.2016.08.16

Thommen, D. S., Schreiner, J., Müller, P., Herzig, P., Roller, A., Belousov, A., et al. (2015). Progression of Lung Cancer Is Associated With Increased Dysfunction of T Cells Defined by Coexpression of Multiple Inhibitory Receptors. *Cancer Immunol. Res.* 3, 1344–1355. doi:10.1158/2326-6066.CIR-15-0097

Tian, S., Roepman, P., Popovici, V., Michaut, M., Majewski, I., Salazar, R., et al. (2012). A Robust Genomic Signature for the Detection of Colorectal Cancer Patients with Microsatellite Instability Phenotype and High Mutation Frequency. *J. Pathol.* 4, 586–595. doi:10.1002/path.4092

Tian, S., Simon, I., Moreno, V., Roepman, P., Tabernero, J., Snel, M., et al. (2013). A Combined Oncogenic Pathway Signature ofBRAF,KRASandPI3KCAmutation Improves Colorectal Cancer Classification and Cetuximab Treatment Prediction. *Gut.* 62, 540–549. doi:10.1136/gutjnl-2012-302423

Tian, S., Wang, F., Lu, S., and Chen, G. (2020). Identification of Two Subgroups of FOLFOX Resistance Patterns and Prediction of FOLFOX Response in Colorectal Cancer Patients. *Cancer Invest.* 39, 62–72. doi:10.1080/07357907.2020.1843662

Vilar, E., Bartnik, C. M., Stenzel, S. L., Raskin, L., Ahn, J., Moreno, V., et al. (2011). MRE11 Deficiency Increases Sensitivity to Poly(ADP-Ribose) Polymerase Inhibition in Microsatellite Unstable Colorectal Cancers. *Cancer Res.* 71, 2632–2642. doi:10.1158/0008-5472.CAN-10-1120

Whitlock, M. C. (2005). Combining Probability from Independent Tests: the Weighted Z-Method Is superior to Fisher's Approach. *J. Evol. Biol.* 18, 1368–1373. doi:10.1111/j.1420-9101.2005.00917.x

Wu, T. D., Madireddi, S., de Almeida, P. E., Banchereau, R., Chen, Y.-J. J., Chitre, A. S., et al. (2020). Peripheral T Cell Expansion Predicts Tumour Infiltration and Clinical Response. *Nature.* 579, 274–278. doi:10.1038/s41586-020-2056-8

Yost, K. E., Satpathy, A. T., Wells, D. K., Qi, Y., Wang, C., Kageyama, R., et al. (2019). Clonal Replacement of Tumor-specific T Cells Following PD-1 Blockade. *Nat. Med.* 25, 1251–1259. doi:10.1038/s41591-019-0522-3

Zhang, L., Li, Z., Skrzypczynska, K. M., Fang, Q., Zhang, W., O'Brien, S. A., et al. (2020). Single-Cell Analyses Inform Mechanisms of Myeloid-Targeted Therapies in Colon Cancer. *Cell.* 181, 442–459. doi:10.1016/j.cell.2020.03.048

Conflict of Interest: ST has stocks and/or stock options in Carbon Logic Biotech. ST is a named inventor of a patent application.

The remaining authors declare that the research was conducted in the absence of any commercial or financial relationships that could be construed as a potential conflict of interest.

Publisher's Note: All claims expressed in this article are solely those of the authors and do not necessarily represent those of their affiliated organizations, or those of the publisher, the editors, and the reviewers. Any product that may be evaluated in this article, or claim that may be made by its manufacturer, is not guaranteed or endorsed by the publisher.

Copyright © 2021 Tian, Wang, Zhang and Chen. This is an open-access article distributed under the terms of the Creative Commons Attribution License (CC BY). The use, distribution or reproduction in other forums is permitted, provided the original author(s) and the copyright owner(s) are credited and that the original publication in this journal is cited, in accordance with accepted academic practice. No use, distribution or reproduction is permitted which does not comply with these terms.

frontiers in Pharmacology

ORIGINAL RESEARCH
published: 13 September 2021
doi: 10.3389/fphar.2021.733075

Adaptive NK Cell Therapy Modulated by Anti-PD-1 Antibody in Gastric Cancer Model

Shahrokh Abdolahi[1], Zeinab Ghazvinian[1], Samad Muhammadnejad[2], Mohammad Ahmadvand[3,4], Hamid Asadzadeh Aghdaei[5], Somayeh Ebrahimi-Barough[6], Jafar Ai[6], Mohammad Reza Zali[7], Javad Verdi[1] and Kaveh Baghaei[5,7]**

[1]Department of Applied Cell Sciences, School of Advanced Technologies in Medicine, Tehran University of Medical Sciences, Tehran, Iran, [2]Cell-Based Therapies Research Center, Digestive Diseases Research Institute, Tehran University of Medical Sciences, Tehran, Iran, [3]Hematology-Oncology and Stem Cell Transplantation Research Center, Tehran University of Medical Science, Tehran, Iran, [4]Department of Hematology and Applied Cell Sciences, Faculty of Medical Sciences, Tarbiat Modares University, Tehran, Iran, [5]Basic and Molecular Epidemiology of Gastrointestinal Disorders Research Center, Research Institute for Gastroenterology and Liver Diseases, Shahid Beheshti University of Medical Sciences, Tehran, Iran, [6]Department of Tissue Engineering, School of Advanced Technologies in Medicine, Tehran University of Medical Sciences, Tehran, Iran, [7]Gastrointestinal Disorders Research Center, Research Institute for Gastroenterology and Liver Diseases, Shahid Beheshti University of Medical Sciences, Tehran, Iran

OPEN ACCESS

Edited by:
Claudia Cerella, Fondation de Recherche Cancer et Sang, Luxembourg

Reviewed by:
Gabriele Multhoff, Technical University of Munich, Germany
Duck Cho, Sungkyunkwan University, South Korea

***Correspondence:**
Kaveh Baghaei
kavehbaghai@gmail.com
Javad Verdi
Javad0Verdi@gmail.com

Specialty section:
This article was submitted to Pharmacology of Anti-Cancer Drugs, a section of the journal Frontiers in Pharmacology

Received: *29 June 2021*
Accepted: *12 August 2021*
Published: *13 September 2021*

Citation:
Abdolahi S, Ghazvinian Z, Muhammadnejad S, Ahmadvand M, Aghdaei HA, Ebrahimi-Barough S, Ai J, Zali MR, Verdi J and Baghaei K (2021) Adaptive NK Cell Therapy Modulated by Anti-PD-1 Antibody in Gastric Cancer Model. Front. Pharmacol. 12:733075. doi: 10.3389/fphar.2021.733075

Recently, adaptive NK cell therapy has become a promising treatment but has limited efficacy as a monotherapy. The identification of immune checkpoint inhibitor (ICI) molecules has opened a new horizon of immunotherapy. Herein, we aimed to demonstrate the cytotoxic effects of a polytherapy consisting of *ex vivo* expanded IL-2-activated NK cells combined with human anti-PD-1 antibody as an important checkpoint molecule in a xenograft gastric cancer mouse model. EBV-LCL cell is used as a feeder to promote NK cell proliferation with a purity of 93.4%. Mice (NOG, female, 6–8 weeks old) with xenograft gastric tumors were treated with PBS, *ex vivo* IL-2-activated NK cells, IL-2-activated NK cell along with human anti-PD-1 (Nivolumab), and IL-2-activated pretreated NK cells with anti-PD-1 antibody. The cytotoxicity of *ex vivo* expanded NK cells against MKN-45 cells was assessed by a lactate dehydrogenase (LDH) assay. Tumor volume was evaluated for morphometric properties, and tumor-infiltrating NK cells were assessed by immunohistochemistry (IHC) and quantified by flow cytometry. Pathologic responses were considered by H and E staining. *Ex vivo* LDH evaluation showed the cytotoxic potential of treated NK cells against gastric cancer cell line. We indicated that the adoptive transfer of *ex vivo* IL-2-activated NK cells combined with anti-PD-1 resulted in tumor growth inhibition in a xenograft gastric cancer model. Mitotic count was significantly decreased ($*p < 0.05$), and the tumor was associated with improved infiltration of NK cells in the NK-anti-PD-1 pretreated group ($*p < 0.05$). In conclusion, the combination approach of activated NK cells and anti-PD-1 therapy results in tumor growth inhibition, accompanied by tumor immune cell infiltration in the gastric tumor model.

Keywords: anti-PD-1 antibody, NK cell therapy, immune checkpoint inhibitor, immunotherapy, gastric cancer

INTRODUCTION

Gastric cancer (GC) is the fifth leading cause of cancer and the third leading cause of death. (Thrift and El-Serag 2020). GC has low clinical symptoms, and it usually progresses at the time of diagnosis, making it challenging to treat patients. Various treatments can be considered, including surgery, chemotherapy, radiation therapy, and targeted therapies (Meza-Junco, Au et al., 2011; Wadhwa, Taketa et al., 2013). However, even after conventional treatments, many patients experience a recurrence of the disease and eventually, cancer metastasizes to other tissues (Enzinger and Mayer 2003). Therefore, consideration of innovative therapeutic approaches is of great importance. Indeed, there is an increasing investigation in establishing an effective immune cell-based therapy for GC by *ex vivo* activating and expanding immune cells. Multifarious studies have presented the therapeutic potential of effective immunotherapy of immune cells (Rezvani, Daher et al., 2020; Ingram, Madan et al., 2021).

Natural killer (NK) cells are promising approaches in treating solid tumors that recognize and lyse infected and malignant cells and exert their cytotoxicity effect without prior sensitization (Close 2016; Jung et al., 2018). NK cells are stimulated as anticancer agents by downregulating or lost MHC-I molecules, a process in which tumor cells can usually escape from cytotoxic T lymphocytes (CTLs) recognition (van Erp, van Kampen et al., 2019). Furthermore, NK cells activation is related to the balance between activating and inhibitor receptors and independent of antigen-presenting cells (APC) (Ljunggren and Malmberg 2007). Despite the advantages of NK therapy, there are major challenges in tumor infiltration or tumor site suppression (Li, Zhang et al., 2016; Melaiu, Lucarini et al., 2020). In an immunological response context, a tumor without infiltrating lymphocytes (TILs) is defined as a "non-inflamed" or "cold" tumor (Herbst, Soria et al., 2014; Mlecnik, Bindea et al., 2016). In contrast, "hot" tumors show a high number of TILs, making the TME more responsive to immunotherapeutic interventions (Kitano, Ono et al., 2017).

There are reasons for the tumor site suppression of adaptive NK cell monotherapy, including (i) myeloid-derived suppressor cells (MDSCs) and Tregs function (Pedroza-Pacheco, Shah et al., 2016; Liu, Wei et al., 2018); (ii) overexpression of MHC class I and MICA/B (Malmberg, Carlsten et al., 2017; Raneros, Puras et al., 2017); (iii) the expression level changes in activating and inhibitory receptors of NK cells (Pietra, Manzini et al., 2012; Davis, Vallera et al., 2017); (iv) marginal infiltration of NK cells (Uong, Lee et al., 2018). Therefore, any approaches to increase the efficacy of NK therapy should address the mentioned limitation. Among them, immune checkpoint inhibitors (ICI) have a crucial role in the cytotoxicity of NK cells.

PD-1 is a surface receptor known as an immunological checkpoint inhibitor for immune cells such as myeloid cells, thymocytes, activated T cells, and NK cells (Nishimura and Honjo 2001; Cheng, Veverka et al., 2013). PD-L1/2 ligands are expressed by various tumor cells, including liver cancer, breast, and GC (Engel, Honig et al., 2014; Jung, Jeong et al., 2017; Wu, Cao et al., 2017). By binding to its ligands, PD-1 plays a vital role in immunosuppressing by exhausting immune cells, increasing Tregs, reducing autoimmunity, and promoting tolerance (Keir, Butte et al., 2008; Francisco, Sage et al., 2010; Fife and Pauken 2011). Thus, blocking this inhibitory pathway is a promising approach to increase the efficacy of cancer immunotherapy (Topalian, Drake et al., 2012). These therapies can be well-tolerated compared with chemotherapy and provide long-term survival (Chiossone, Vienne et al., 2017). In addition, the PD-1 receptor can be targeted by a fully humanized IgG4 antibody (Nivolumab) and can attenuate the inhibitory signal of NK and T, responding to treatment in highly immunogenic tumors (Li, Shao et al., 2018; Havel, Chowell et al., 2019; Desai, Deva et al., 2020).

There have been limited studies on adaptive NK therapy on GC; however, it has been demonstrated that the infiltration and cytotoxicity effects of NK are major problems (Chen, Yang et al., 2014; Du and Wei 2019). Therefore, in the current study, to overcome the limitations, we surveyed the combination therapy of activated NK cells with Nivolumab as an anti-PD-1 inhibitor to enhance tumor infiltration and cytotoxicity of NK against gastric cancer tumors.

MATERIALS AND METHODS

Cell Lines and Culture Media

The MKN-45 cell line (human gastric cancer cell line) was purchased from the Iranian Biological Resource Center (Tehran, Iran). Epstein-Barr virus (EBV)–transformed lymphoblastoid cell line (LCL) as feeder cells was maintained in Roswell Park Memorial Institute-1640 (RPMI-1640) (Gibco, United States); media were supplemented with 10% FBS (Gibco, United States), 1% penicillin-streptomycin, and 1% L-glutamine.

Human NK Cell Isolation, *Ex Vivo* Expansion, and Activation

NK cells were isolated from healthy donors' buffy coats with Ficoll Paque Premium (GE Healthcare's, United States) gradient centrifugation. According to the manufacturer's instructions, NK cells were collected by negative selection using a human NK cell isolation kit (Miltenyi Biotech, Germany). The purity of NK cells was assessed by flow cytometry analysis of $CD3^-$ and $CD56^+$ markers (FACSCalibur Becton Dickinson, United States). EBV-LCL was applied for optimal NK cell expansion. EBV-LCL cell line was established by culturing peripheral blood mononuclear cells (PBMCs) in the presence of 100 μg/ml cyclosporin A with EBV supernatant harvested from the cell line B95-8 (Iranian Biological Research Center) (Igarashi, Wynberg et al., 2004). The procedure is based on an existing expansion protocol for *in vivo* studies (Berg, Lundqvist et al., 2009) that utilizes 100 Gy-irradiated EBV-LCL as feeder cells (at a ratio of 1:10) trigger NK cell proliferation and highly activated NK cells. In the first 5 days, NK cell colonies are formed, and every 3 days, a fresh medium enriched by IL-2 (500 IU/ml) (Miltenyi Biotech, Germany) is added to the cells for 21 days.

Cytotoxicity Assays

The cytotoxic effects of activated NK cells as an effector cell (E), whether alone and in combination with anti-PD-1, were defined in a co-culture of MKN-45 as a target cell (T). The ratios of 1:1, 1:

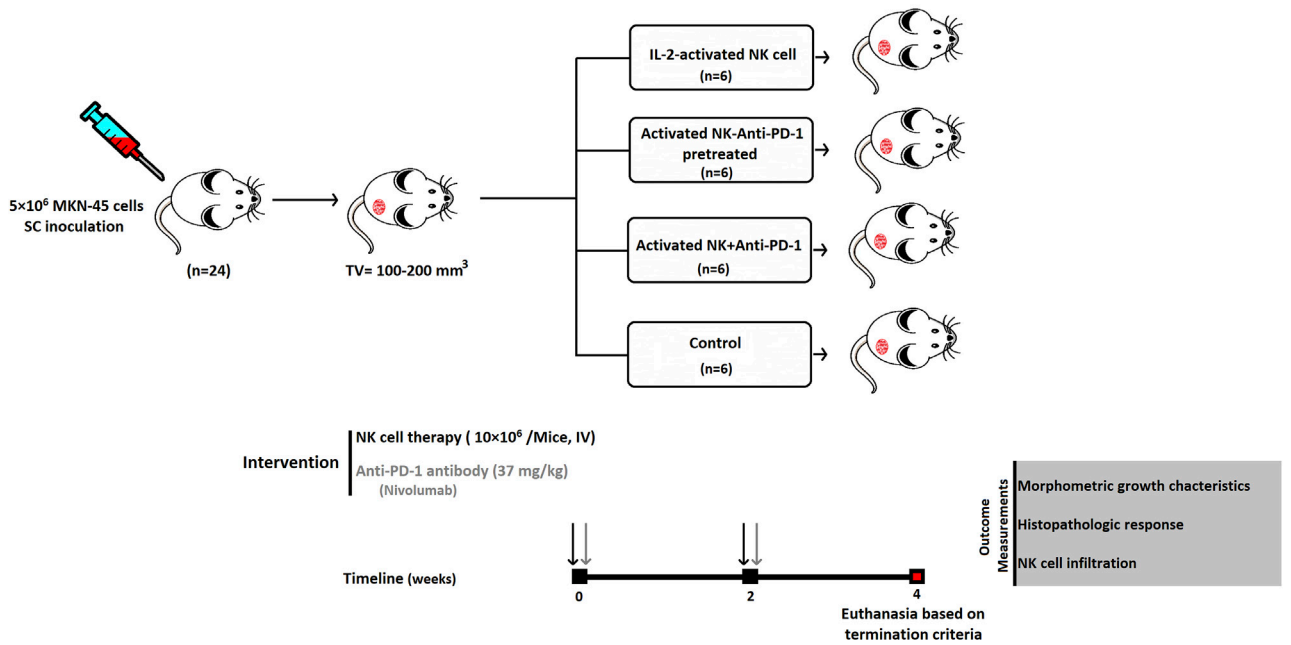

FIGURE 1 | Schematic diagram of anti-PD-1 antibody combined with NK-based immunotherapy in a gastric cancer xenograft model. SC, subcutaneous; IV, intravenous.

3, and 1:6 were studied. LDH assay was performed after 24 h of incubation as a necrosis marker in a cell culture medium (Chan, Moriwaki et al., 2013).

Heterotopic Gastric Cancer Mouse Model

All animals were housed in individually ventilated cages (IVC) for animal experiments. The center maintains standardized housing conditions and hygiene management according to the guidelines of the ethics committee. The animals are preserved under special conditions, e.g., a 12/12 h light-dark cycle, a humidity of 65%, and a temperature of 25°C. To assess the antitumor effect of NK cells in combination with Nivolumab (Bristol Myers Squibb, USA) *in vivo*, we used 6–8-week-old female NOD. Cg-Prkdcscid IL2rgtm1Sug (NOG) mice were obtained from the animal facility of the Digestive Disease Research Institute of Tehran University of Medical Sciences, which subcutaneously inoculated by 5×10^6 MKN-45 cells. Prior to euthanasia, animals are anesthetized with ketamine and xylazine and euthanized with CO_2. Tumor sizes and body weights were measured twice a week. Animals with a tumor volume ≥2000 mm^3, real bodyweight loss ≥20%, or BC = 1 (body condition) were humanely terminated. All animal experiments were authorized by the institutional ethics committee of the Tehran University of Medical Science (IR.TUMS.MEDICINE.REC.1399.644).

Sample Size, Dosages, and Schedule of Administration

Tumor median size of 100–200 mm^3 (day 0) was selected for dividing the animals randomly into four experimental groups, including IL-2-activated NK cells (NK cells), IL-2-activated NK cells along with anti-PD-1 antibody (Nivolumab) (NK + anti-PD-1), and IL-2-activated NK cells *ex vivo* pretreated with 20 μg/ml anti-PD-1 (NK-anti-PD-1 pretreated). Each mouse received 10×10^6 NK cells twice at 2-week intervals *via* the IV route (**Figure 1**). The dosage of anti-PD-1 (Nivolumab) was translated from human into murine setting based on body surface area using the following formula (Nair and Jacob 2016):

$$\text{Murine equivalent dosage (unit/kg)} = \text{pediatric dosage (unit/kg)} \times \frac{Human\ Km}{Mouse\ Km}.$$

The Km constant was 37 for adult humans 37 and 3 for mice (Reagan-Shaw et al., 2008). The NK + anti-PD-1 group was treated with 37 mg/kg anti-PD-1 antibody twice at 2-week intervals *via* the IV route. Control is the fourth group, which received phosphate-buffered saline (PBS).

Tumor Morphometric Outcomes

Tumor volume was measured by a caliper and calculated by the following formula: tumor volume = 1/2 (length × width 2). Relative tumor volume (RTV) was evaluated for morphometric growth kinetics of the tumors by dividing tumor volume on a measured day to tumor volume on day 0. Antitumor activity was presented by tumor growth inhibition (TGI) percentage using a formula by Tsukihara et al.: TGI (%) = [1 − (RTV of the treated group)/(RTV of the control group)] × 100 (%) (Tsukihara, Nakagawa et al., 2015).

Flow Cytometry

NK cells characterization by PE anti-human $CD56^+$ and FITC anti-human $CD3^-$ markers was quantitatively evaluated; the

TABLE 1 | Residual tumor (R) classification.

Classification	Description
R0	The entire tumor is destroyed in response to treatment
R1	More than 70% of the tumor is destroyed in response to treatment, and fibrosis and diffuse apoptosis (within the tumor) are observed
R2	30 and 70% of tumors in response to treatment have undergone fibrosis and apoptosis
R3	The response rate to treatment is very low or non-existent

TABLE 2 | The Allred score combined intensity and percent of immunoreactive cells.

Positive cells %	Proportion score	Intensity	Intensity score
No cells are immunoreactive	0	Negative	0
≤1%	1	Weak	1
1–10%	2	Intermediate	2
11–33%	3	Strong	3
34–66% o	4		
67–100%	5		
Aggregation of proportion and Intensity score			
0–1	Negative		
2–3	Weak positive		
4–6	Intermediate positive		
7–8	High positive		

infiltration of NK cells at the tumor site was performed using flow cytometry (FACSCalibur Becton Dickinson, United States). NKG2D and CD69 were evaluated before and after treatment of IL-2-stimulated NK cells by the anti-PD-1 antibody for further characterization. The whole tumor was collected and digested mechanically and enzymatically, and staining was done according to the manufacturer's instructions; then, flow cytometry was performed (Feng, Peng et al., 2009). Data were analyzed using the FlowJo 7 software (Tree Star, Inc.). Experiments were carried out in triplicate and quantified by GraphPad Prism 9 (GraphPad Software Inc., CA, United States).

Histopathology Assessments

The histopathologic response of tumors to the interventions was assessed based on the residual tumor (R) (Edge, Byrd et al., 2010) (**Table 1**). Hematoxylin and Eosin (H and E) stain slides were prepared to stratify the histopathologic responses. Proliferative activity changes assessed mitotic count on H and E slides. As previously described by Meuten and colleagues, mitotic cells are counted in areas and reported as an average over ten consecutive high power fields (HPF) (Meuten, Moore et al., 2016).

Immunohistochemistry (IHC) against human CD56 (Biolegend, United States) was performed as described previously (Kim et al., 2016) for NK cell infiltration evaluation. Furthermore, the active protein of caspase 3 for apoptosis induction evaluation was detected using a rabbit polyclonal antibody (Biolegend, United States). IHC was assessed based on the Allred score; this scoring combines the percentage of immunoreactive cells and the intensity score (Parvin et al., 2019) (**Table 2**). Following the euthanasia of the mice, tumor tissues were collected and processed for paraffin embedding. Briefly, paraffin-embedded tumors were cut by microtome to a thickness of 4 μm. After deparaffinization and hydration, the tumor tissues were incubated by primary and secondary antibodies (Adan, Alizada et al., 2017).

Statistical Analysis

All results are reported as the mean ± SEM and the data were analyzed by GraphPad Prism 9 software package (GraphPad Software, Inc., San Diego, United States). A p value of <0.05 represented statistical significance.

RESULTS

Ex Vivo Expansion and Immunophenotyping of NK Cells

NK cells isolated from peripheral blood were characterized by the presence of CD56 and the absence of CD3 as NK cell surface biomarkers. The purity was 93.4%, which included the $CD3^-$ $CD56^+$ cells based on flow cytometric analysis. Freshly isolated CD3- and CD56+ cells were cultured in the presence of IL-2 and feeder cells and expanded for 21 days. Expanded NK cells exhibited clonal growth and round shape morphology under cytokine-/feeder-enriched (IL-2/EBV-LCL cells) medium; finally, after 21 days, we reached 370 million cells with more than 95% viability, which were evaluated by trypan blue before injection (**Figures 2A,B**).

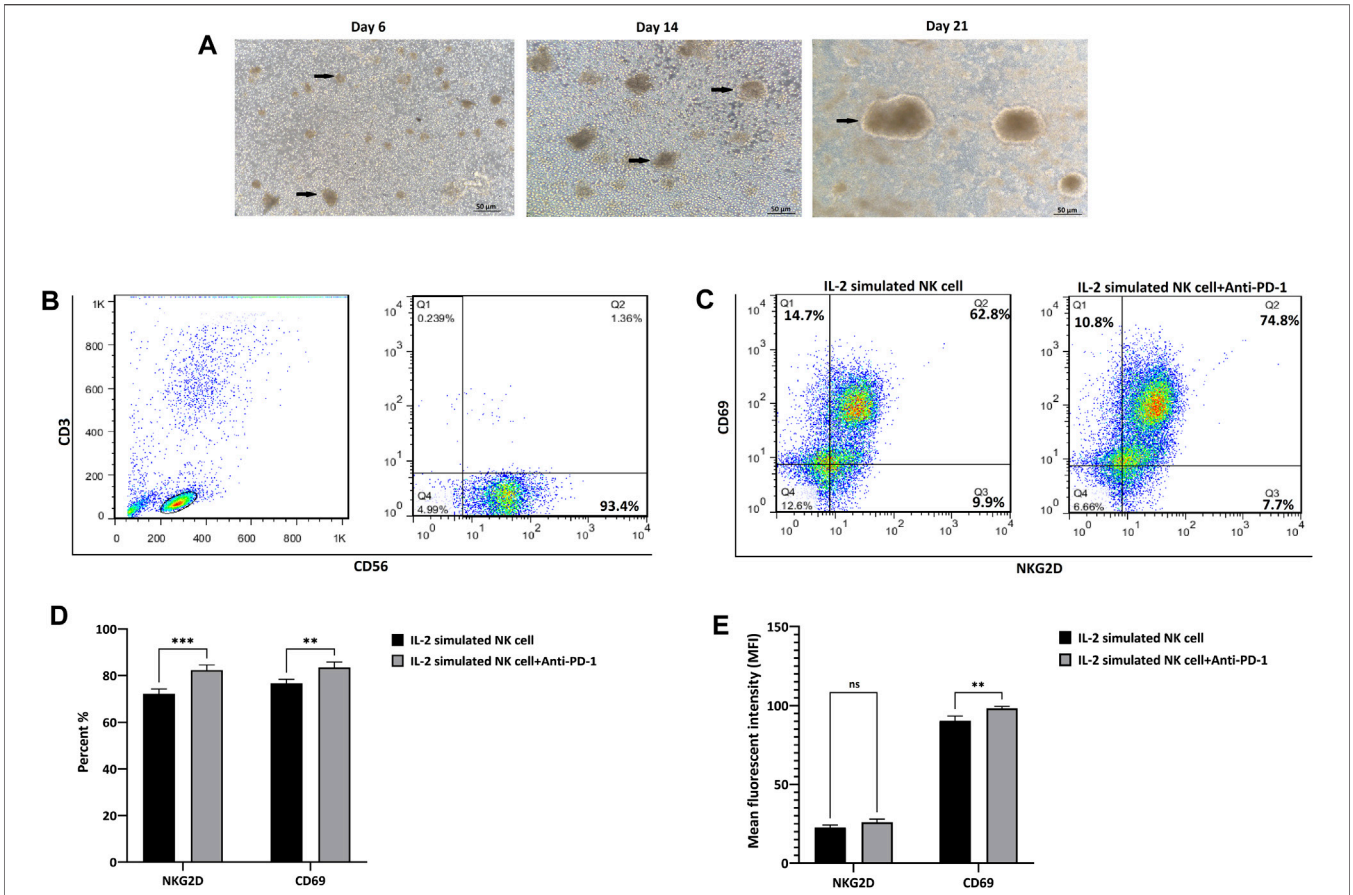

FIGURE 2 | Isolation, characterization, and expansion of NK cells. **(A)** The morphology of NK cells after 6, 14, and 21 days of round-shaped colony of NK cells is illustrated by arrows. **(B)** The frequency of CD56+CD3-NK cells in PBMC-derived NK cells, after MACS isolation with more than 93.4% purity. **(C)** The frequency of NKG2D and CD69 marker before and after treatment of IL-2-stimulated NK cells by anti-PD-1 antibody. **(D)** The quantification of positive cells for NKG2D and CD69 marker. **(E)** The quantification of mean fluorescence intensity for NKG2D and CD69 marker. Data presented as means ± standard error (M ± SE) for three independent experiments. Statistical significance was determined using one-way ANOVA with $^*p < 0.05$. Scale bar: 50 μm, magnification 200X. ns, not significant.

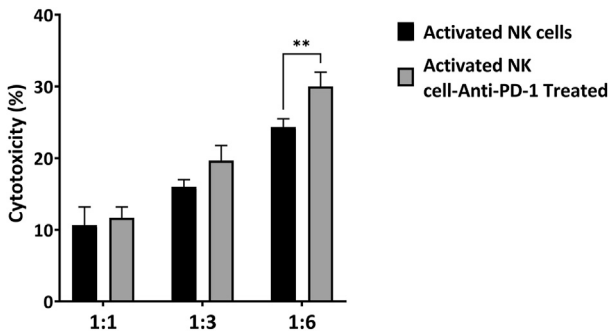

FIGURE 3 | Cytotoxicity of *ex vivo* activated NK cells and anti-PD1 antibody-treated NK cells toward MKN-45 cell at different E: T ratios. Data presented as means ± standard error (M ± SE) for three independent experiments. Statistical significance was determined using one-way ANOVA with $^*p < 0.05$.

Further investigation of NK + anti-PD-1 immunophenotyping NKG2D and CD69 was performed using flow cytometry. NK NKG2D$^+$ and CD69$^+$ cells increased 10 and 8 percent after treatment with IL-2-stimulated NK cells with anti-PD-1 antibody ($p < 0.0007$ and $p < 0.0085$, respectively). Moreover, quantification of mean fluorescence intensity (MFI) showed that anti-PD-1 treatment improved CD69 expression ($p < 0.002$), but no significant changes were observed in NKG2D marker after treatment with IL-2-stimulated NK cells with anti-PD-1 (**Figures 2**C,D,E).

Ex Vivo Cytotoxicity of IL-2-Activated NK Cells Combined With Anti-PD-1

To evaluate the effect of a combined strategy of IL-2-activated NK cells with anti-PD-1 antibody *in vitro,* MKN-45 cells were co-cultured with activated NK cells at three specific E: T ratios (1:1, 3:1, and 6:1). After a 24 h incubation, the NK-cell-mediated cytotoxicity against MKN-45 was detected by LDH assay. In the non-treated group, NK cells showed 11, 16, and 25 percent cytotoxicity at the following E: T ratios: 1:1, 3:1, and 6:1, respectively. In the anti-PD-1-treated group, the lysis percentages were 13, 19, and 30. The most prominent antitumor cytotoxicity of activated NK cells was achieved when PD-1 was inhibited with an anti-PD-1 antibody ($p < 0.006$) (**Figure 3**).

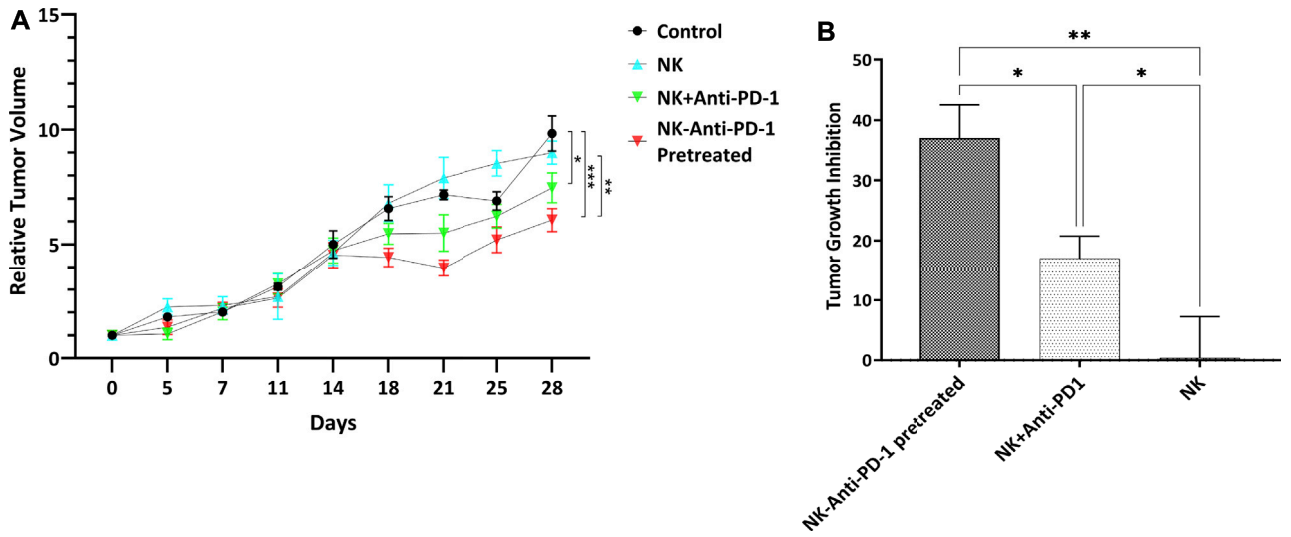

FIGURE 4 | Morphometric growth characteristics. **(A)** RTV versus the elapsed time curve showed tumor growth variations. **(B)** Tumor growth inhibition of interventions normalized with control tumor. Data presented as means ± standard error (M ± SE). Statistical significance was determined using 2-way ANOVA with $^{*}p < 0.05$.

The Therapeutic Effect of NK Cells Based on Morphometric Growth Characteristics in Gastric Cancer Xenograft Model

In order to explore the effect of adaptive NK cell therapy combined with Nivolumab in tumor growth *in vivo*, we further investigated the impact of interventions on the morphometric properties in the subcutaneous transplantation mouse model of gastric cancer using MKN-45 cell line.

The use of an Anti-PD-1 antibody confirms the hypothesis that PD-1/PDL-1 pathway inhibition can modulate the therapeutic cytotoxicity effect of NK cells. Ten days after cell line inoculation, tumors reached the desired size of 100–200 mm^3 for interventions. The sham-treated mice showed the most rapid tumor growth. Two IV injections of *ex vivo* IL-2-activated NK cells combined with an anti-PD-1 antibody caused a significant tumor growth delay. The morphometric growth curves of tumors are shown in **Figure 4A**. Optimal percent of TGI was observed 28 days after the beginning of treatment. The highest tumor growth inhibition was considered in the NK-anti-PD-1 pretreated group, with a median TGI of 38% (31–41). Also, the NK + anti-PD-1 therapy group showed an inhibitory effect with a median TGI of 18% (12–19); NK cells as monotherapy did not show an inhibitory effect on the gastric cancer model with a median TGI of -0.5%. NK-anti-PD-1 pretreated group significantly inhibited tumor growth more than NK + anti-PD-1 and NK cells ($p < 0.01$ and $p < 0.001$, respectively). Furthermore, NK + anti-PD-1 induces tumor inhibition compared to NK cells ($p < 0.03$). The best therapeutic outcome was observed after modulating NK cells by anti-PD-1 antibody (**Figure 4B**).

Effects of Experimental Interventions on Histopathologic Outcomes

PD-1 blockade was used to improve response to the immune-cell-based therapy approach. After implantation of 5×10^6 MKN-45 cells, the mice bearing tumor was intravenously injected with 10×10^6 NK cells, NK-anti-PD-1 pretreated, NK + anti-PD-1, and PBS (control).

NK-anti-PD-1 pretreated group based on residual tumor showed that in more than 30% of tumors, the fibrosis areas and apoptotic fragment were increased, R2 histologic response ($p < 0.0001$), in response to intervention. Furthermore, the NK + anti-PD-1 group showed a low response rate, R3 histologic response ($p < 0.02$). NK cells showed a degree of histopathologic response, which not statistically significant (**Figures 5A,B**).

Mitotic count was investigated to evaluate the effect of interventions on tumor proliferation intensity. NK cells anti-PD-1 pretreated showed the highest anti-proliferative effect; the mitotic count in this group was significantly lower than that in the control group (12 [8–15] vs. 21.5 [19–35] ($p < 0.002$). Furthermore, the mitotic count of the NK + anti-PD-1 group was significantly decreased compared to the control 14 [9–21] ($p < 0.03$), but NK cells did not show a difference in mitotic count (**Figure 5C**).

The cytotoxicity mechanism of different treated groups *via* apoptosis was evaluated by caspase 3 labeling. Our findings based on Allred score show that NK cells-anti-PD-1 pretreated and NK-Anti-PD-1 groups have intermediate level of caspase 3, while NK cell alone was weakly positive for caspase 3 (**Figure 6**).

In Vivo Treatment of NK-Anti-PD-1 Increased Lymphocyte Infiltration

In order to verify the NK cell permeation, human $CD56^+$ cells were evaluated. NK-anti-PD-1 pretreated cells were intermediate positive and the other treated groups that received NK cells were weakly positive for CD56 biomarker based on Allred score (**Figure 7A**). The infiltration percentage of the NK cells, NK +

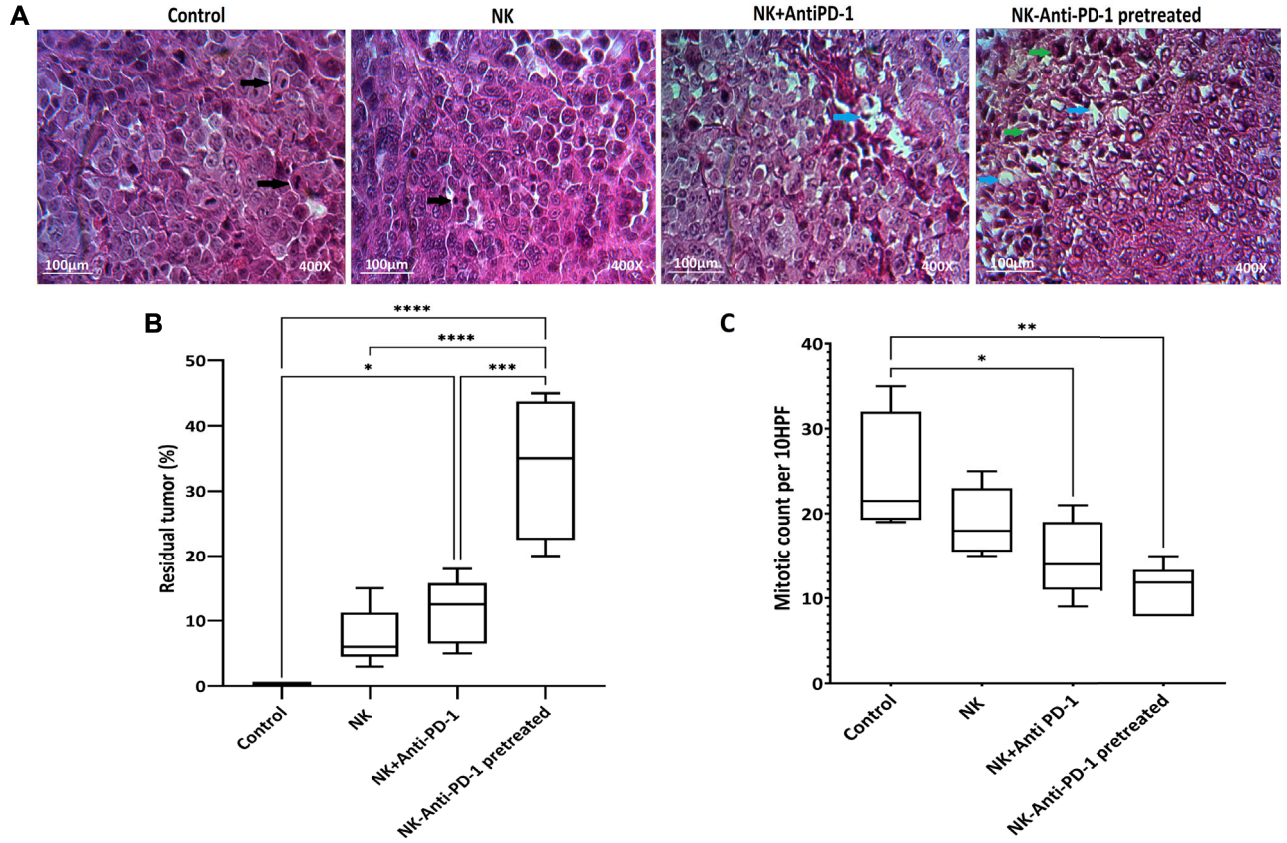

FIGURE 5 | Histopathological finding. **(A)** Representative Hematoxylin and Eosin (H and E). Black arrows showed mitosis, blue arrows showed fibrotic areas, and green arrows showed apoptotic bodies. **(B)** Boxplots showed tumor response based on the residual tumor. **(C)** Mitotic count as proliferation score assessed in 10HPF; anaphase cell division stage is visible in the control tissue sample. Data presented as means ± standard error (M ± SE). Statistical significance was determined using one-way ANOVA with $*p < 0.05$. Scale bar: 100 µm, 400X magnification.

anti-PD-1, and NK-anti-PD-1 pretreated cells groups were 3, 5, and 7%, respectively. Thus, this result indicated that NK-anti-PD-1 pretreated group showed the highest infiltration ($p < 0.008$) (**Figure 7B**).

DISCUSSION

The low number and infiltration of NK cells in the tumor area are challenging in GC patients (Li, Zhang et al., 2016; Peng, Zhang et al., 2017). PD-1 receptor as ICIs molecules negatively regulates T and NK cells. Therefore, GC tumors using PD-1 receptors inhibit the patient 's immune system. (Lesokhin, Callahan et al., 2015; Liu, Cheng et al., 2017). Accordingly, PD-1 inhibitor has been shown to enhance immunity in clinical trials of non-small cell lung cancer (NSCLC), colorectal cancer, gastric cancer, head, and neck squamous cell carcinoma (Brahmer, Rodríguez-Abreu et al., 2017; Kang, Boku et al., 2017; Overman, McDermott et al., 2017; Tahara, Muro et al., 2018). Recent advances in combination therapy targeting tumor microenvironment or immune checkpoint molecules seem advantageous for NK cell therapy.

In this study, anti-PD-1 antibodies were combined with NK cell-based therapy in gastric cancer xenograft mouse models. As reported in previous studies, a blockade of immune checkpoints can increase the efficiency of NK cell therapy by increasing cytotoxic activity. Bo Yuan Huang et al. and Shevtsov et al. (2019) have shown that PD-1 inhibited the increase in cytotoxic potency of NK cells by up to 10% (Huang, Zhan et al., 2015; Shevtsov, Pitkin et al., 2019). While the present study indicated *ex vivo* expanded IL-2-activated NK cells have therapeutic cytotoxic potential toward MKN-45 cells *in vitro*, anti-PD-1-treated IL-2-activated NK cells improved cytotoxicity of NK cells by 5%.

It has been confirmed that the mechanism underlying tumor recognition by NK cells was mainly through human lymphoid stress surveillance. These cells recognize and kill the cells that express NKG2D ligands (Shafi, Vantourout et al., 2011). NKG2D ligands were downregulated on normal tissues, whereas they were upregulated on the malignant cells (Groh, Bahram et al., 1996). Furthermore, the crucial role of NKG2D-mediated tumor surveillance is confirmed by the rapid elimination of the tumor cells that were transfected with NKG2D ligands by immune cells (Diefenbach, Jensen et al., 2001). In addition to NKG2D, the non-exclusive cytotoxic mechanism of NK cells and other molecules like CD69 might be implicated as a proliferative and cytotoxic marker (Borrego, Robertson et al., 1999). Our

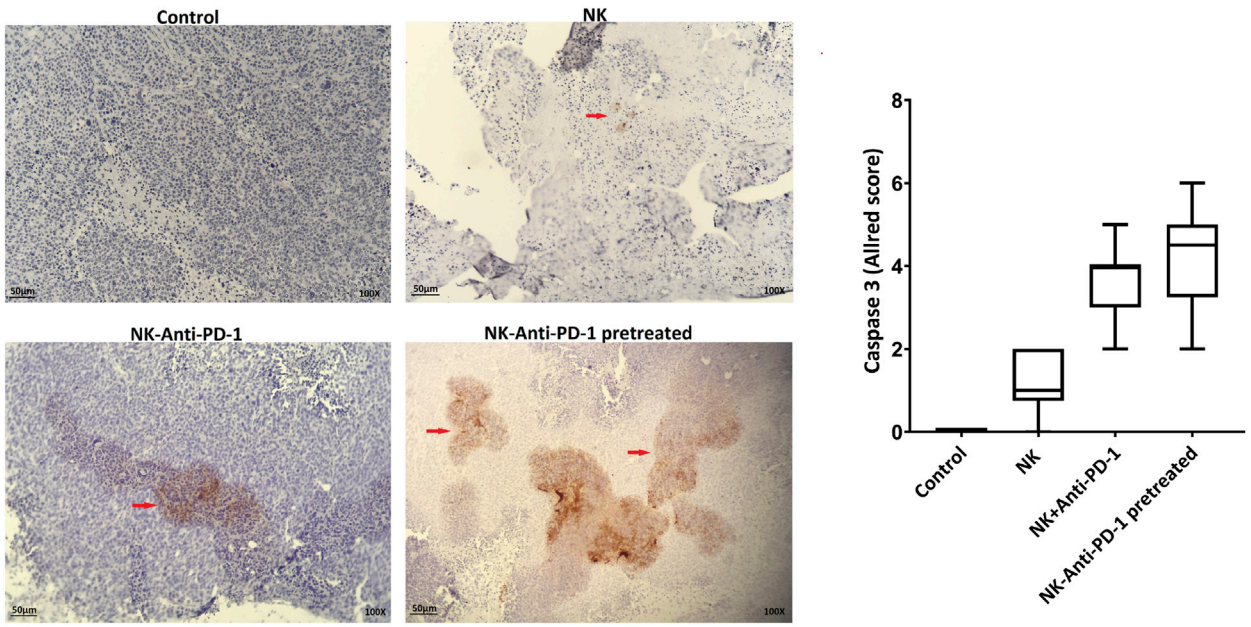

FIGURE 6 | Apoptosis induction by anti-PD-1 blockade NK cells. **(A)** Active caspase-3 was evaluated in the tumor section (red arrow, immunoreactive cells) and boxplots illustrate semi-quantitative analysis based on Allred score. Scale bar: 50 µm, 100X magnification.

results indicated that anti-PD-1 blockade could promote an elevation of NKG2D and CD69 expression levels, and this increase could be modulated by immune-promoting molecules (Marçais, Viel et al., 2013). In confirmation of our results, Dai et al. have shown that anti-PD-1 antibody increases NKG2D and other cytotoxic factors (Dai, Lin et al., 2016), demonstrating the synergistic effect of these therapeutic approaches. Our proof-of-principle study has illustrated the promising results of a combination therapy of *ex vivo* expanded IL-2-activated NK cells and anti-PD-1 antibody. The therapeutic efficacy observed in this experiment is in line with the previously reported effects (Janjigian, Bendell et al., 2018; Patel and Minn 2018). Furthermore, Chen et al. have performed a gastrointestinal (GI) cancer meta-analysis, which showed low responsiveness to ICIs molecules (Chen, Zhang et al., 2019). Therefore, the different cytotoxic improvements in these studies may be due to the different response rates of gastric cancer cells and different E: T ratios in this study.

In vivo interventions started at the 100–200 mm^3 of xenograft tumor volume, equivalent to the advanced stages of human tumors (Alley, Hollingshead et al., 2004). Combination groups improved TGI, leading to proliferative activity reduction linked to better survival rates and increasing apoptotic bodies and fibrotic areas. In accordance with the tumor mitotic counts and apoptosis results, the level of caspase 3 in NK-anti-PD-1 pretreated group was highly increased. Moreover, Yin et al. and Oyer et al. have indicated that cytotoxicity and antitumor efficacy of NK cells recovered when combined with anti-PD-1/PD-L1 blockade (Oyer, Gitto et al., 2018; Yin, Di et al., 2018). On the other hand, J Li et al. have shown that the knockdown of PD-L1 in human gastric cancer cells significantly improved the cytotoxic sensitivity to CIK (cytokine-induced killer cells) therapy (Li, Chen et al., 2017). These results showed that a combination strategy might be an effective and promising approach for GC immunotherapy.

Antitumor responses in immunodeficient mice were accompanied by an infiltration of the tumors; when PD-1 blockade was used, more infiltration induction was observed than that in the other groups. Although NK cell or PD-1 blockade therapies individually elicit an antitumor response, combination therapy is significantly more effective. Konrad Kokowski et al. have shown that the combination of NK cell transfer and radiochemotherapy with second-line PD-1 inhibition improved the overall survival of a patient with NSCLC stage IIIb and induced a massive NKG2D + immune cell infiltration (Kokowski, Stangl et al., 2019). The effect of the anti-PD-1 antibody on lymphocytes expressing the PD-1 receptor can cause this synergistic effect. This combination strategy also showed high NK cell infiltration in preclinical models of lung cancer and glioblastoma (Shevtsov, Pitkin et al., 2019). The moderate response obtained to the combined strategy *in vitro* compared to *in vivo* is probably due to differences in PD-1/PDL-1 expression and other stimuli of this ligand and receptor in 2- and 3-dimensional environments (Terme, Ullrich et al., 2011; Jung 2014; Abiko, Matsumura et al., 2015). Moreover, the mild antitumor effect achieved by monotherapy of NK cells resulted in a delayed tumor progression, which was not significant, that probably required continued therapy at higher doses.

In our study, we used the PD-1 inhibitor for improving adaptive NK cell therapy. However, other ICIs (e.g., anti-LAG3/PD-1, anti-NKG2A, anti–TIM-3 antibodies) have been reported to regulate antitumor functions of NK cells and thereby elevate their cytotoxic activity (André, Denis et al., 2018; Lanuza, Pesini et al., 2020; Zhang, Jiang et al., 2020). Thus, the

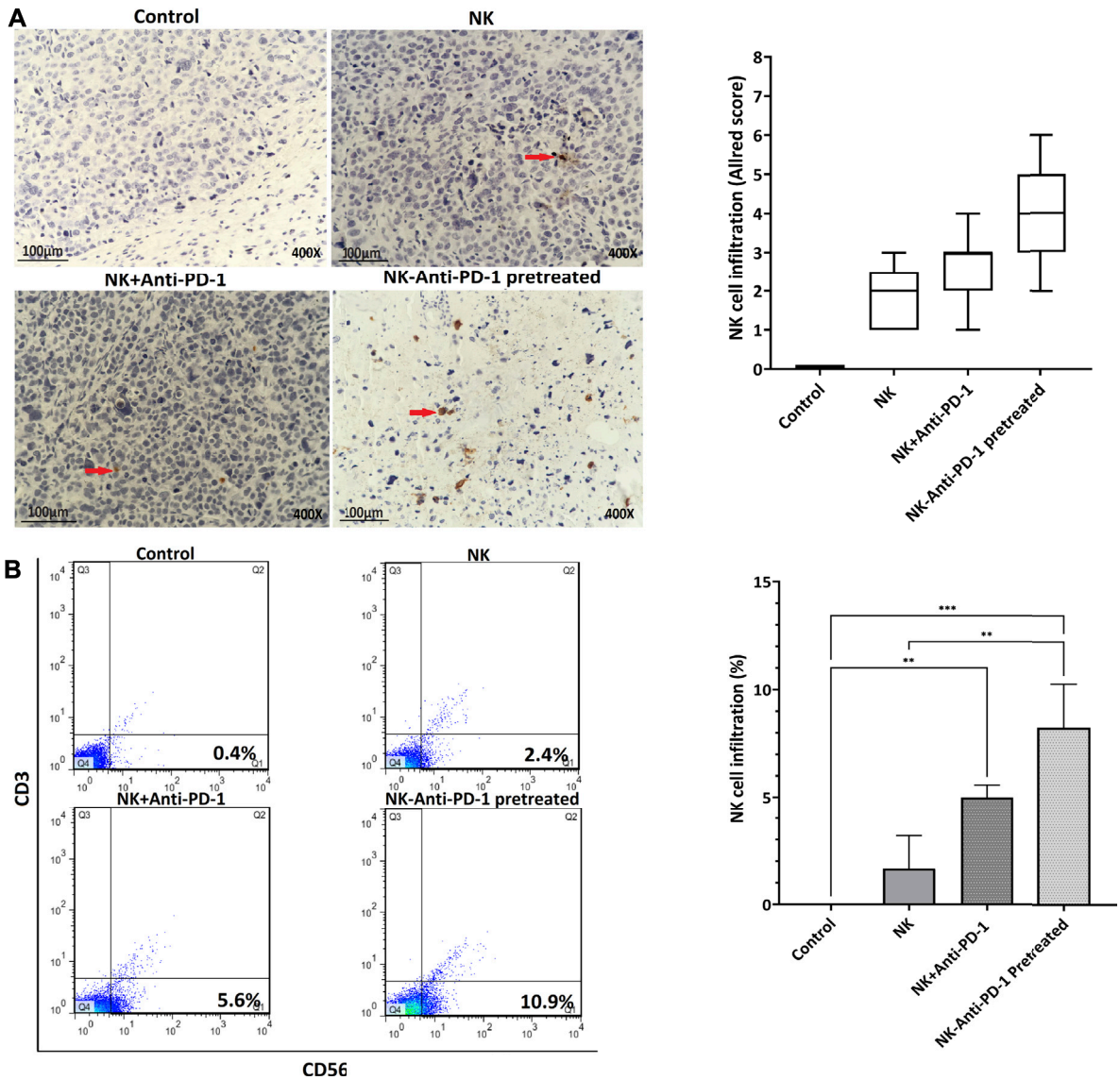

FIGURE 7 | *In vivo* treatment of NK cells increased lymphocyte infiltration. **(A)** Tumor microenvironment infiltrating NK cells were evaluated by IHC with anti-CD56 antibody in tumor masses (red arrow showed immunoreactive cells) and boxplots indicated semi-quantitative analysis based on Allred score. **(B)** Quantification of lymphocyte infiltration performed by whole tumor flow cytometry with anti-CD56 and anti-CD3 antibody, CD56+and CD3-cells showed infiltrating NK cells. Data presented as means ± standard error (M ± SE) for three independent experiments. Statistical significance was determined using one-way ANOVA with $^*p < 0.05$. Scale bar: 100 µm, 400X magnification.

combination therapy approach of IL-2-activated NK cells with several therapeutic antibodies can decrease exhaustion and enhance the cytotoxicity of NK cell-based immunotherapies.

The use of PD-1 blockade can cause other lymphocytes to accumulate in tumor sites such as cytotoxic T cells; NOG mice do not have immune cells (Shultz, Lyons et al., 2005). Therefore, the presence of other immune cells could not be assessed. However, the absence of an immune system confirms the antitumor function of NK cells, specifically with PD-1 blockade. Furthermore, a better clinical response is presumably observed in the presence of a complete immune system in clinical trials from this therapeutic approach.

CONCLUSION

Our results demonstrate the highest response of the combined strategy of NK and anti-PD1 in high T: E *in vitro,* and anti-PD-1 treatment improved proliferation and cytotoxic properties of NK cells. Furthermore, adaptive NK cells therapy with low efficacy in the monotherapy approach could be improved by adding an anti-PD-1 antibody, and the pretreated strategy was more effective against the gastric cancer animal model. Therefore, the combination approach of *ex vivo* expanded IL-2-activated NK cell and PD-1 blockade is promising, and its effectiveness could be evaluated in randomized clinical trials for gastric cancer.

DATA AVAILABILITY STATEMENT

The original contributions presented in the study are included in the article/supplementary material; further inquiries can be directed to the corresponding author/s.

ETHICS STATEMENT

The animal study was reviewed and approved by the Tehran University of Medical Science.

AUTHOR CONTRIBUTIONS

S Abdolahi, S Muhammadnejad, and K Baghaei contributed to the study design. S Abdolahi, S Muhammadnejad, K Baghaei, and M Ahmadvand developed the methodology. S Muhammadnejad, H A Aghdaei, and J Verdi were responsible for providing the facility and animals. S Abdolahi, S Muhammadnejad, S E Barough, and J Ai analyzed and interpreted the data. S Abdolahi, J Verdi, S Muhammadnejad, and K Baghaei wrote and reviewed the manuscript. J Verdi and K Baghaei supervised the study.

REFERENCES

Abiko, K., Matsumura, N., Hamanishi, J., Horikawa, N., Murakami, R., Yamaguchi, K., et al. (2015). IFN-γ from Lymphocytes Induces PD-L1 Expression and Promotes Progression of Ovarian Cancer. *Br. J. Cancer* 112 (9), 1501–1509. doi:10.1038/bjc.2015.101

Adan, A., Alizada, G., Kiraz, Y., Baran, Y., and Nalbant, A. (2017). Flow Cytometry: Basic Principles and Applications. *Crit. Rev. Biotechnol.* 37 (2), 163–176. doi:10.3109/07388551.2015.1128876

Alley, M. C., Hollingshead, M. G., Dykes, D. J., and Waud, W. R. (2004). "Human Tumor Xenograft Models in NCI Drug Development," in *Anticancer Drug Development Guide* (Springer), 125–152. doi:10.1007/978-1-59259-739-0_7

André, P., Denis, C., Soulas, C., Bourbon-Caillet, C., Lopez, J., Arnoux, T., et al. (2018). Anti-NKG2A mAb Is a Checkpoint Inhibitor that Promotes Anti-tumor Immunity by Unleashing Both T and NK Cells. *Cell* 175 (7), 1731–e13. e1713. doi:10.1016/j.cell.2018.10.014

Berg, M., Lundqvist, A., McCoy, P., Jr, Samsel, L., Fan, Y., Tawab, A., et al. (2009). Clinical-grade Ex Vivo-expanded Human Natural Killer Cells Up-Regulate Activating Receptors and Death Receptor Ligands and Have Enhanced Cytolytic Activity against Tumor Cells. *Cytotherapy* 11 (3), 341–355. doi:10.1080/14653240902807034

Borrego, F., Robertson, M. J., Ritz, J., Peña, J. R., and Solana, R. (1999). CD69 Is a Stimulatory Receptor for Natural Killer Cell and its Cytotoxic Effect Is Blocked by CD94 Inhibitory Receptor. *Immunology* 97 (1), 159–165. doi:10.1046/j.1365-2567.1999.00738.x

Brahmer, J. R., Rodríguez-Abreu, D., Robinson, A. G., Hui, R., Csőszi, T., Fülöp, A., et al. (2017). Health-related Quality-Of-Life Results for Pembrolizumab versus Chemotherapy in Advanced, PD-L1-Positive NSCLC (KEYNOTE-024): a Multicentre, International, Randomised, Open-Label Phase 3 Trial. *Lancet Oncol.* 18 (12), 1600–1609. doi:10.1016/S1470-2045(17)30690-3

Chan, F. K.-M., Moriwaki, K., and De Rosa, M. J. (2013). "Detection of Necrosis by Release of Lactate Dehydrogenase Activity," in *Immune Homeostasis* (Springer), 65–70. doi:10.1007/978-1-62703-290-2_7

Chen, C., Zhang, F., Zhou, N., Gu, Y. M., Zhang, Y. T., He, Y. D., et al. (2019). Efficacy and Safety of Immune Checkpoint Inhibitors in Advanced Gastric or Gastroesophageal junction Cancer: a Systematic Review and Meta-Analysis. *Oncoimmunology* 8 (5), e1581547. doi:10.1080/2162402X.2019.1581547

Chen, J., Yang, J., Jiang, J., Zhuang, Y., and He, W. (2014). Function and Subsets of Dendritic Cells and Natural Killer Cells Were Decreased in Gastric Cancer. *Int. J. Clin. Exp. Pathol.* 7 (11), 8304–8311.

Cheng, X., Veverka, V., Radhakrishnan, A., Waters, L. C., Muskett, F. W., Morgan, S. H., et al. (2013). Structure and Interactions of the Human Programmed Cell Death 1 Receptor. *J. Biol. Chem.* 288 (17), 11771–11785. doi:10.1074/jbc.M112.448126

Chiossone, L., Vienne, M., Kerdiles, Y. M., and Vivier, E. (2017). "Natural Killer Cell Immunotherapies against Cancer: Checkpoint Inhibitors and More," in *Seminars in Immunology* (Elsevier). doi:10.1016/j.smim.2017.08.003

Close, H. J. (2016). *Immune Evasion in Glioma*. Dissertation. (Leeds): University of Leeds.

Dai, C., Lin, F., Geng, R., Ge, X., Tang, W., Chang, J., et al. (2016). Implication of Combined PD-L1/pd-1 Blockade with Cytokine-Induced Killer Cells as a Synergistic Immunotherapy for Gastrointestinal Cancer. *Oncotarget* 7 (9), 10332–10344. doi:10.18632/oncotarget.7243

Davis, Z. B., Vallera, D. A., Miller, J. S., and Felices, M. (2017). "Natural Killer Cells Unleashed: Checkpoint Receptor Blockade and BiKE/TriKE Utilization in NK-Mediated Anti-tumor Immunotherapy," in *Seminars in Immunology* (Elsevier). doi:10.1016/j.smim.2017.07.011

Desai, J., Deva, S., Lee, J. S., Lin, C. C., Yen, C. J., Chao, Y., et al. (2020). Phase IA/IB Study of Single-Agent Tislelizumab, an Investigational Anti-PD-1 Antibody, in Solid Tumors. *J. Immunother. Cancer* 8 (1). doi:10.1136/jitc-2019-000453

Diefenbach, A., Jensen, E. R., Jamieson, A. M., and Raulet, D. H. (2001). Rae1 and H60 Ligands of the NKG2D Receptor Stimulate Tumour Immunity. *Nature* 413 (6852), 165–171. doi:10.1038/35093109

Du, Y., and Wei, Y. (2019). Therapeutic Potential of Natural Killer Cells in Gastric Cancer. *Front. Immunol.* 9, 3095. doi:10.3389/fimmu.2018.03095

Edge, S. B., Byrd, D. R., Carducci, M. A., Compton, C. C., Fritz, A., and Greene, F. (2010). *AJCC Cancer Staging Manual*. New York: Springer.

Engel, J. B., Honig, A., Kapp, M., Hahne, J. C., Meyer, S. R., Dietl, J., et al. (2014). Mechanisms of Tumor Immune Escape in Triple-Negative Breast Cancers (TNBC) with and without Mutated BRCA 1. *Arch. Gynecol. Obstet.* 289 (1), 141–147. doi:10.1007/s00404-013-2922-9

Enzinger, P. C., and Mayer, R. J. (2003). Esophageal Cancer. *N. Engl. J. Med.* 349 (23), 2241–2252. doi:10.1056/NEJMra035010

Feng, D., Peng, C., Li, C., Zhou, Y., Li, M., Ling, B., et al. (2009). Identification and Characterization of Cancer Stem-like Cells from Primary Carcinoma of the Cervix Uteri. *Oncol. Rep.* 22 (5), 1129–1134. doi:10.3892/or_00000545

Fife, B. T., and Pauken, K. E. (2011). The Role of the PD-1 Pathway in Autoimmunity and Peripheral Tolerance. *Ann. N. Y Acad. Sci.* 1217 (1), 45–59. doi:10.1111/j.1749-6632.2010.05919.x

Francisco, L. M., Sage, P. T., and Sharpe, A. H. (2010). The PD-1 Pathway in Tolerance and Autoimmunity. *Immunol. Rev.* 236 (1), 219–242. doi:10.1111/j.1600-065X.2010.00923.x

Groh, V., Bahram, S., Bauer, S., Herman, A., Beauchamp, M., and Spies, T. (1996). Cell Stress-Regulated Human Major Histocompatibility Complex Class I Gene Expressed in Gastrointestinal Epithelium. *Proc. Natl. Acad. Sci. U S A.* 93 (22), 12445–12450. doi:10.1073/pnas.93.22.12445

Havel, J. J., Chowell, D., and Chan, T. A. (2019). The Evolving Landscape of Biomarkers for Checkpoint Inhibitor Immunotherapy. *Nat. Rev. Cancer* 19 (3), 133–150. doi:10.1038/s41568-019-0116-x

Herbst, R. S., Soria, J. C., Kowanetz, M., Fine, G. D., Hamid, O., Gordon, M. S., et al. (2014). Predictive Correlates of Response to the Anti-PD-L1 Antibody MPDL3280A in Cancer Patients. *Nature* 515 (7528), 563–567. doi:10.1038/nature14011

Huang, B. Y., Zhan, Y. P., Zong, W. J., Yu, C. J., Li, J. F., Qu, Y. M., et al. (2015). The PD-1/b7-H1 Pathway Modulates the Natural Killer Cells versus Mouse Glioma Stem Cells. *PloS one* 10 (8), e0134715. doi:10.1371/journal.pone.0134715

Igarashi, T., Wynberg, J., Srinivasan, R., Becknell, B., McCoy, J. P., Jr, Takahashi, Y., et al. (2004). Enhanced Cytotoxicity of Allogeneic NK Cells with Killer Immunoglobulin-like Receptor Ligand Incompatibility against Melanoma and Renal Cell Carcinoma Cells. *Blood* 104 (1), 170–177. doi:10.1182/blood-2003-12-4438

Ingram, Z., Madan, S., Merchant, J., Carter, Z., Gordon, Z., Carey, G., et al. (2021). Targeting Natural Killer T Cells in Solid Malignancies. *Cells* 10 (6), 1329. doi:10.3390/cells10061329

Janjigian, Y. Y., Bendell, J., Calvo, E., Kim, J. W., Ascierto, P. A., Sharma, P., et al. (2018). CheckMate-032 Study: Efficacy and Safety of Nivolumab and Nivolumab Plus Ipilimumab in Patients with Metastatic Esophagogastric Cancer. *J. Clin. Oncol.* 36 (28), 2836–2844. doi:10.1200/JCO.2017.76.6212

Jung, H. I., Jeong, D., Ji, S., Ahn, T. S., Bae, S. H., Chin, S., et al. (2017). Overexpression of PD-L1 and PD-L2 Is Associated with Poor Prognosis in Patients with Hepatocellular Carcinoma. *Cancer Res. Treat.* 49 (1), 246–254. doi:10.4143/crt.2016.066

Jung, I. H., Kim, D. H., Yoo, D. K., Baek, S. Y., Jeong, S. H., Jung, D. E., et al. (2018). *In Vivo* study of Natural Killer (NK) Cell Cytotoxicity against Cholangiocarcinoma in a Nude Mouse Model. *In Vivo* 32 (4), 771–781. doi:10.21873/invivo.11307

Jung, J. (2014). Human Tumor Xenograft Models for Preclinical Assessment of Anticancer Drug Development. *Toxicol. Res.* 30 (1), 1–5. doi:10.5487/TR.2014.30.1.001

Kang, Y. K., Boku, N., Satoh, T., Ryu, M. H., Chao, Y., Kato, K., et al. (2017). Nivolumab in Patients with Advanced Gastric or Gastro-Oesophageal junction Cancer Refractory to, or Intolerant of, at Least Two Previous Chemotherapy Regimens (ONO-4538-12, ATTRACTION-2): a Randomised, Double-Blind, Placebo-Controlled, Phase 3 Trial. *Lancet* 390 (10111), 2461–2471. doi:10.1016/S0140-6736(17)31827-5

Keir, M. E., Butte, M. J., Freeman, G. J., and Sharpe, A. H. (2008). PD-1 and its Ligands in Tolerance and Immunity. *Annu. Rev. Immunol.* 26, 677–704. doi:10.1146/annurev.immunol.26.021607.090331

Kim, S.-W., Roh, J., and Park, C.-S. (2016). Immunohistochemistry For Pathologists: Protocols, Pitfalls, And Tips. *J. Pathol. Transl. Med.* 50 (6), 411.

Kitano, A., Ono, M., Yoshida, M., Noguchi, E., Shimomura, A., Shimoi, T., et al. (2017). Tumour-infiltrating Lymphocytes Are Correlated with Higher Expression Levels of PD-1 and PD-L1 in Early Breast Cancer. *ESMO open* 2 (2), e000150. doi:10.1136/esmoopen-2016-000150

Kokowski, K., Stangl, S., Seier, S., Hildebrandt, M., Vaupel, P., and Multhoff, G. (2019). Radiochemotherapy Combined with NK Cell Transfer Followed by Second-Line PD-1 Inhibition in a Patient with NSCLC Stage IIIb Inducing Long-Term Tumor Control: a Case Study. *Strahlenther Onkol* 195 (4), 352–361. doi:10.1007/s00066-019-01434-9

Lanuza, P. M., Pesini, C., Arias, M. A., Calvo, C., Ramirez-Labrada, A., and Pardo, J. (2020). Recalling the Biological Significance of Immune Checkpoints on NK Cells: a Chance to Overcome LAG3, PD1, and CTLA4 Inhibitory Pathways by Adoptive NK Cell Transfer?. *Front. Immunol.* 10, 3010. doi:10.3389/fimmu.2019.03010

Lesokhin, A. M., Callahan, M. K., Postow, M. A., and Wolchok, J. D. (2015). On Being Less Tolerant: Enhanced Cancer Immunosurveillance Enabled by Targeting Checkpoints and Agonists of T Cell Activation. *Sci. Transl Med.* 7 (280), 280sr1–281sr. doi:10.1126/scitranslmed.3010274

Li, J., Chen, L., Xiong, Y., Zheng, X., Xie, Q., Zhou, Q., et al. (2017). Knockdown of PD-L1 in Human Gastric Cancer Cells Inhibits Tumor Progression and Improves the Cytotoxic Sensitivity to CIK Therapy. *Cell Physiol Biochem* 41 (3), 907–920. doi:10.1159/000460504

Li, T., Zhang, Q., Jiang, Y., Yu, J., Hu, Y., Mou, T., et al. (2016). Gastric Cancer Cells Inhibit Natural Killer Cell Proliferation and Induce Apoptosis via Prostaglandin E2. *Oncoimmunology* 5 (2), e1069936. doi:10.1080/2162402X.2015.1069936

Li, X., Shao, C., Shi, Y., and Han, W. (2018). Lessons Learned from the Blockade of Immune Checkpoints in Cancer Immunotherapy. *J. Hematol. Oncol.* 11 (1), 31–26. doi:10.1186/s13045-018-0578-4

Liu, Y., Cheng, Y., Xu, Y., Wang, Z., Du, X., Li, C., et al. (2017). Increased Expression of Programmed Cell Death Protein 1 on NK Cells Inhibits NK-Cell-Mediated Anti-tumor Function and Indicates Poor Prognosis in Digestive Cancers. *Oncogene* 36 (44), 6143–6153. doi:10.1038/onc.2017.209

Liu, Y., Wei, G., Cheng, W. A., Dong, Z., Sun, H., Lee, V. Y., et al. (2018). Targeting Myeloid-Derived Suppressor Cells for Cancer Immunotherapy. *Cancer Immunol. Immunotherimmunotherapy* 67 (8), 1181–1195. doi:10.1007/s00262-018-2175-3

Ljunggren, H. G., and Malmberg, K. J. (2007). Prospects for the Use of NK Cells in Immunotherapy of Human Cancer. *Nat. Rev. Immunol.* 7 (5), 329–339. doi:10.1038/nri2073

Malmberg, K.-J., Carlsten, M., Björklund, A., Sohlberg, E., Bryceson, Y. T., and Ljunggren, H.-G. (2017). "Natural Killer Cell-Mediated Immunosurveillance of Human Cancer," in *Seminars in Immunology* (Elsevier). doi:10.1016/j.smim.2017.08.002

Marçais, A., Viel, S., Grau, M., Henry, T., Marvel, J., and Walzer, T. (2013). Regulation of Mouse NK Cell Development and Function by Cytokines. *Front. Immunol.* 4, 450. doi:10.3389/fimmu.2013.00450

Melaiu, O., Lucarini, V., Cifaldi, L., and Fruci, D. (2020). Influence of the Tumor Microenvironment on NK Cell Function in Solid Tumors. *Front. Immunol.* 10, 3038. doi:10.3389/fimmu.2019.03038

Meuten, D., Moore, F., and George, J. (2016). *Mitotic Count and the Field of View Area: Time to Standardize*. Los Angeles, CA: SAGE Publications Sage CA.

Meza-Junco, J., Au, H. J., and Sawyer, M. B. (2011). Critical Appraisal of Trastuzumab in Treatment of Advanced Stomach Cancer. *Cancer Manag. Res.* 3, 57–64. doi:10.2147/CMR.S12698

Mlecnik, B., Bindea, G., Angell, H. K., Maby, P., Angelova, M., Tougeron, D., et al. (2016). Integrative Analyses of Colorectal Cancer Show Immunoscore Is a Stronger Predictor of Patient Survival Than Microsatellite Instability. *Immunity* 44 (3), 698–711. doi:10.1016/j.immuni.2016.02.025

Nair, A. B., and Jacob, S. (2016). A Simple Practice Guide for Dose Conversion between Animals and Human. *J. Basic Clin. Pharm.* 7 (2), 27–31. doi:10.4103/0976-0105.177703

Nishimura, H., and Honjo, T. (2001). PD-1: an Inhibitory Immunoreceptor Involved in Peripheral Tolerance. *Trends Immunol.* 22 (5), 265–268. doi:10.1016/s1471-4906(01)01888-9

Overman, M. J., McDermott, R., Leach, J. L., Lonardi, S., Lenz, H. J., Morse, M. A., et al. (2017). Nivolumab in Patients with Metastatic DNA Mismatch Repair-Deficient or Microsatellite Instability-High Colorectal Cancer (CheckMate 142): an Open-Label, Multicentre, Phase 2 Study. *Lancet Oncol.* 18 (9), 1182–1191. doi:10.1016/S1470-2045(17)30422-9

Oyer, J. L., Gitto, S. B., Altomare, D. A., and Copik, A. J. (2018). PD-L1 Blockade Enhances Anti-tumor Efficacy of NK Cells. *Oncoimmunology* 7 (11), e1509819. doi:10.1080/2162402X.2018.1509819

Parvin, T., Das, C., Choudhury, M., Chattopadhyay, B. K., and Mukhopadhyay, M. (2019). Prognostic Utility of Cyclin D1 In Invasive Breast Carcinoma. *Indian J. Surg. Oncol.* 10 (1), 167–173.

Patel, S. A., and Minn, A. J. (2018). Combination Cancer Therapy with Immune Checkpoint Blockade: Mechanisms and Strategies. *Immunity* 48 (3), 417–433. doi:10.1016/j.immuni.2018.03.007

Pedroza-Pacheco, I., Shah, D., Domogala, A., Luevano, M., Blundell, M., Jackson, N., et al. (2016). Regulatory T Cells Inhibit CD34+ Cell Differentiation into NK Cells by Blocking Their Proliferation. *Sci. Rep.* 6 (1), 1–13. doi:10.1038/srep22097

Peng, L. S., Zhang, J. Y., Teng, Y. S., Zhao, Y. L., Wang, T. T., Mao, F. Y., et al. (2017). Tumor-Associated Monocytes/Macrophages Impair NK-Cell Function via TGFβ1 in Human Gastric Cancer. *Cancer Immunol. Res.* 5 (3), 248–256. doi:10.1158/2326-6066.CIR-16-0152

Pietra, G., Manzini, C., Rivara, S., Vitale, M., Cantoni, C., Petretto, A., et al. (2012). Melanoma Cells Inhibit Natural Killer Cell Function by Modulating the Expression of Activating Receptors and Cytolytic Activity. *Cancer Res.* 72 (6), 1407–1415. doi:10.1158/0008-5472.CAN-11-2544

Raneros, A. B., Minguela, A., Rodriguez, R. M., Colado, E., Bernal, T., Anguita, E., et al. (2017). Increasing TIMP3 Expression by Hypomethylating Agents Diminishes Soluble MICA, MICB and ULBP2 Shedding in Acute Myeloid Leukemia, Facilitating NK Cell-Mediated Immune Recognition. *Oncotarget* 8 (19), 31959–31976. doi:10.18632/oncotarget.16657

Reagan-Shaw, S., Nihal, M., and Ahmad, N. (2008). Dose Translation from Animal to Human Studies Revisited. *FASEB J.* 22 (3), 659–661. doi:10.2217/14750708.5.5.659

Rezvani, K., Daher, M., Basar, R., Gokdemir, E., Baran, N., Uprety, N., et al. (2020). *CIS Checkpoint Deletion Enhances the Fitness of Cord Blood Derived Natural Killer Cells Transduced with a Chimeric Antigen Receptor*. New York: bioRxiv.

Shafi, S., Vantourout, P., Wallace, G., Antoun, A., Vaughan, R., Stanford, M., et al. (2011). An NKG2D-Mediated Human Lymphoid Stress Surveillance Response with High Interindividual Variation. *Sci. Transl Med.* 3 (113), 113ra124. doi:10.1126/scitranslmed.3002922

Shevtsov, M., Pitkin, E., Ischenko, A., Stangl, S., Khachatryan, W., Galibin, O., et al. (2019). *Ex Vivo* Hsp70-activated NK Cells in Combination with PD-1 Inhibition Significantly Increase Overall Survival in Preclinical Models of Glioblastoma and Lung Cancer. *Front. Immunol.* 10, 454. doi:10.3389/fimmu.2019.00454

Shultz, L. D., Lyons, B. L., Burzenski, L. M., Gott, B., Chen, X., Chaleff, S., et al. (2005). Human Lymphoid and Myeloid Cell Development in NOD/LtSz-scid IL2R Gamma Null Mice Engrafted with Mobilized Human Hemopoietic Stem Cells. *J. Immunol.* 174 (10), 6477–6489. doi:10.4049/jimmunol.174.10.6477

Tahara, M., Muro, K., Hasegawa, Y., Chung, H. C., Lin, C. C., Keam, B., et al. (2018). Pembrolizumab in Asia-Pacific Patients with Advanced Head and Neck Squamous Cell Carcinoma: Analyses from KEYNOTE-012. *Cancer Sci.* 109 (3), 771–776. doi:10.1111/cas.13480

Terme, M., Ullrich, E., Aymeric, L., Meinhardt, K., Desbois, M., Delahaye, N., et al. (2011). IL-18 Induces PD-1-dependent Immunosuppression in Cancer. *Cancer Res.* 71 (16), 5393–5399. doi:10.1158/0008-5472.CAN-11-0993

Thrift, A. P., and El-Serag, H. B. (2020). Burden of Gastric Cancer. *Clin. Gastroenterol. Hepatol.* 18 (3), 534–542. doi:10.1016/j.cgh.2019.07.045

Topalian, S. L., Drake, C. G., and Pardoll, D. M. (2012). Targeting the PD-1/b7-H1(pd-L1) Pathway to Activate Anti-tumor Immunity. *Curr. Opin. Immunol.* 24 (2), 207–212. doi:10.1016/j.coi.2011.12.009

Tsukihara, H., Nakagawa, F., Sakamoto, K., Ishida, K., Tanaka, N., Okabe, H., et al. (2015). Efficacy of Combination Chemotherapy Using a Novel Oral Chemotherapeutic Agent, TAS-102, Together with Bevacizumab, Cetuximab, or Panitumumab on Human Colorectal Cancer Xenografts. *Oncol. Rep.* 33 (5), 2135–2142. doi:10.3892/or.2015.3876

Uong, T. N. T., Lee, K. H., Ahn, S. J., Kim, K. W., Min, J. J., Hyun, H., et al. (2018). Real-time Tracking of Ex Vivo-expanded Natural Killer Cells toward Human Triple-Negative Breast Cancers. *Front. Immunol.* 9, 825. doi:10.3389/fimmu.2018.00825

van Erp, E., van Kampen, M., van Kasteren, P., and de Wit, J. (2019). Viral Infection of Human Natural Killer Cells. *Viruses* 11 (3), 243. doi:10.3390/v11030243

Wadhwa, R., Taketa, T., Sudo, K., Blum, M. A., and Ajani, J. A. (2013). Modern Oncological Approaches to Gastric Adenocarcinoma. *Gastroenterol. Clin. North. Am.* 42 (2), 359–369. doi:10.1016/j.gtc.2013.01.011

Wu, Y., Cao, D., Qu, L., Cao, X., Jia, Z., Zhao, T., et al. (2017). PD-1 and PD-L1 Co-expression Predicts Favorable Prognosis in Gastric Cancer. *Oncotarget* 8 (38), 64066–64082. doi:10.18632/oncotarget.19318

Yin, M., Di, G., and Bian, M. (2018). Dysfunction of Natural Killer Cells Mediated by PD-1 and Tim-3 Pathway in Anaplastic Thyroid Cancer. *Int. Immunopharmacol* 64, 333–339. doi:10.1016/j.intimp.2018.09.016

Zhang, D., Jiang, F., Zaynagetdinov, R., Huang, H., Sood, V. D., Wang, H., et al. (2020). Identification and Characterization of M6903, an Antagonistic Anti-TIM-3 Monoclonal Antibody. *Oncoimmunology* 9 (1), 1744921. doi:10.1080/2162402X.2020.1744921

Conflict of Interest: The authors declare that the research was conducted in the absence of any commercial or financial relationships that could be construed as a potential conflict of interest.

Publisher's Note: All claims expressed in this article are solely those of the authors and do not necessarily represent those of their affiliated organizations, or those of the publisher, the editors and the reviewers. Any product that may be evaluated in this article, or claim that may be made by its manufacturer, is not guaranteed or endorsed by the publisher.

Copyright © 2021 Abdolahi, Ghazvinian, Muhammadnejad, Ahmadvand, Aghdaei, Ebrahimi-Barough, Ai, Zali, Verdi and Baghaei. This is an open-access article distributed under the terms of the Creative Commons Attribution License (CC BY). The use, distribution or reproduction in other forums is permitted, provided the original author(s) and the copyright owner(s) are credited and that the original publication in this journal is cited, in accordance with accepted academic practice. No use, distribution or reproduction is permitted which does not comply with these terms.

frontiers in Oncology

ORIGINAL RESEARCH
published: 16 September 2021
doi: 10.3389/fonc.2021.735820

Ex Vivo Drug Screening Informed Targeted Therapy for Metastatic Parotid Squamous Cell Carcinoma

Noora Nykänen[1], Rami Mäkelä[1], Antti Arjonen[1†], Ville Härmä[1,2], Laura Lewandowski[1†], Eileen Snowden[3], Rainer Blaesius[3], Ismo Jantunen[4], Teijo Kuopio[4,5], Juha Kononen[6] and Juha K. Rantala[1,2]*

[1] Misvik Biology Oy, Turku, Finland, [2] Department of Oncology and Metabolism, University of Sheffield, Sheffield, United Kingdom, [3] Genomic Sciences, BD Technologies, Research Triangle Park, Durham, NC, United States, [4] Central Finland Health Care District, Jyväskylä, Finland, [5] Department of Biological and Environmental Science, Jyväskylä, Finland, [6] Docrates Cancer Center, Helsinki, Finland

OPEN ACCESS

Edited by:
Claudia Cerella,
Fondation de Recherche Cancer et Sang, Luxembourg

Reviewed by:
Qigen Fang,
Henan Provincial Cancer Hospital, China
Ebrahim Mostafavi,
Stanford University, United States

***Correspondence:**
Juha K. Rantala
rantala@misvik.com

†Present address:
Antti Arjonen,
Brinter Ltd, Turku, Finland
Laura Lewandowski,
Forendo Pharma Ltd, Turku, Finland

Specialty section:
This article was submitted to Pharmacology of Anti-Cancer Drugs, a section of the journal Frontiers in Oncology

Received: 03 July 2021
Accepted: 23 August 2021
Published: 16 September 2021

Citation:
Nykänen N, Mäkelä R, Arjonen A, Härmä V, Lewandowski L, Snowden E, Blaesius R, Jantunen I, Kuopio T, Kononen J and Rantala JK (2021) Ex Vivo Drug Screening Informed Targeted Therapy for Metastatic Parotid Squamous Cell Carcinoma. Front. Oncol. 11:735820. doi: 10.3389/fonc.2021.735820

The purpose of *ex vivo* drug screening in the context of precision oncology is to serve as a functional diagnostic method for therapy efficacy modeling directly on patient-derived tumor cells. Here, we report a case study using integrated multiomics *ex vivo* drug screening approach to assess therapy efficacy in a rare metastatic squamous cell carcinoma of the parotid gland. Tumor cells isolated from lymph node metastasis and distal subcutaneous metastasis were used for imaging-based single-cell resolution drug screening and reverse-phase protein array-based drug screening assays to inform the treatment strategy after standard therapeutic options had been exhausted. The drug targets discovered on the basis of the *ex vivo* measured drug efficacy were validated with histopathology, genomic profiling, and *in vitro* cell biology methods, and targeted treatments with durable clinical responses were achieved. These results demonstrate the use of serial *ex vivo* drug screening to inform adjuvant therapy options prior to and during treatment and highlight HER2 as a potential therapy target also in metastatic squamous cell carcinoma of the salivary glands.

Keywords: *ex vivo* drug screening, precision oncology, HER2, T-DM1, trastuzumab, molecular profiling, parotid squamous cell carcinoma

INTRODUCTION

Ex vivo drug screening methods in the context of cancer research collectively refer to high-throughput screening (HTS) approaches that utilize vital patient-derived tumor cells as models for assessing drug efficacy. Similarly, as *in vitro* cell-based high-throughput drug screening, *ex vivo* drug screening methods allow assessment of cellular responses to up to thousands of drug perturbations in a single experiment (1–6). The utility of *ex vivo* drug screening has been pioneered in the context of hematological malignancies in which cancer cells can be collected and enriched for HTS directly from blood or bone marrow biopsies (7–10). These studies have demonstrated that the methods can be used to complement pathological cancer diagnostic procedures to track patient-specific drug sensitivity and guide treatment decisions on the most effective treatments or potential alternative therapies currently approved for other cancer indications. The first clinical trial utilizing *ex vivo* chemosensitivity profiling (NCT03096821) to inform treatments of patients with aggressive forms

of hematological cancers reported an 88% overall response rate (ORR) in patients matched to treatments on the basis of an *ex vivo* drug screening assay (11). By comparison, in recent clinical trials for genomics matched targeted therapies, the reported ORRs have varied from 11% to 36% (12–15). This suggests that the *ex vivo* drug screening methods could be used to improve the stratification of targeted cancer treatments and complement genomic oncology medicine approaches for personalized care of individual cancer patients. To improve the feasibility and accuracy of *ex vivo* drug screening techniques for solid cancers, especially without the need for invasive surgical tissue sampling, new assay strategies are needed. As an approach for diagnostic therapy efficacy testing in solid cancers, we devised a strategy integrating a phenotypic image-based assay method (1–4) with reverse-phase protein array (RPPA) drug screening to analyze patient-specific therapy efficacy for a rare metastatic parotid squamous cell carcinoma (SCC). Tumor cells isolated from a disease-affected lymph node were analyzed prior to treatment initiation and cells isolated from a distal metastatic lesion were analyzed to adjust treatment strategy after disease recurrence. Altogether, the efficacy of 193 anti-cancer compounds was evaluated to establish a comprehensive chemosensitivity profile. Parotic SCC is a rare, aggressive salivary gland malignancy to which a consensus regarding the use of adjuvant chemotherapy does not exist (16). Moreover, clinical development of novel treatments to this malignancy is limited by the low number of cases, which limits the use of conventional clinical study designs. Therefore, alternative approaches, such as the *ex vivo* screening, are needed to collect evidence on the efficacy of alternative targeted treatment strategies matched to the molecular characteristics of SCC tumors (17).

MATERIALS AND METHODS

Tumor Biopsy Samples

The patient, a 61-year-old male, was identified to the study by an oncologist at the Jyväskylä Medical Centre (Jyväskylä, Finland). The tissue biopsies (surgically resected lymph node, sample A and 3 × 18 gauge needle biopsies, sample B) were collected for the *ex vivo* drug screening with written informed consent from the patient and approval from the local Ethics Committee of the Central Finland Health Care District (KSSHP 3U/2015). All the experiments were undertaken with the understanding and written consent of the patient, and the study methodologies conformed to the standards set by the Declaration of Helsinki.

Image-Based *Ex Vivo* Drug Screening

The *ex vivo* drug screens were performed as previously described (3). Briefly, the therapeutic compound collection used in the drug screening consisted of 125 (sample A) and 193 (sample B) anti-cancer agents, purchased from commercial chemical vendors (Selleck Biochemical, Santa Cruz Biotechnology). To allow maximally broad characterization of different drug classes with the limited number of cells available from the tumor biopsies, each compound was tested in five different concentrations with twofold (sample A) and threefold (sample B) dilutions starting from 5 μM as the highest concentration. The single-cell milieu of freshly isolated tumor-derived cells (45 μl per well; 1,000 cells per well) was transferred to each well using a peristaltic MultiDrop Combi dispenser (ThermoScientific). The 384-well plates were incubated for 96 h in standard cell culture conditions, 37°C and 5% CO_2. Analysis of cell viability with cellular lineage separation was performed through high-content imaging. The cell cultures were fixed with 4% paraformaldehyde with 0.03% Triton-X100 and incubated overnight at +4°C with antibodies against epithelial cytokeratin-19 (KRT19, Abcam, Clone EP1580Y), stromal cell marker vimentin (VIM, Santa Cruz Biotechnology, Clone V9), and HER2 (DAKO, A0485). Secondary antibody staining was performed at room temperature for 1 h with AlexaFluor secondary antibodies against the primary host species (1:500, LifeTech) in 1% BSA. DAPI (4′,6- Diamidino-2-phenylindole nuclear counterstain, LifeTech) (1 μg/ml) was added to secondary staining buffers for DNA counterstaining. Cells were imaged using Olympus scan^R platform at 20× magnification. Nine frames were acquired from each 384-well to cover the whole well area. Images were analyzed with Olympus scan^R image analysis suite including integrated DNA staining-based primary object segmentation using a watershed algorithm. Primary objects (nuclei) were expanded a fixed 20-pixel distance, and mean fluorescence signal intensity for KRT19 and VIM was quantified from this expanded cellular region. Single-cell positivity for KRT19, VIM, and HER2 was determined by gating in the scan^R image analysis suite, using secondary antibody only stained cells for each marker as controls. Population separated cell count data were normalized using the GR method (18) (see Equation 1 in *Statistical Analysis*) to DMSO-only wells (negative control), 5 μM staurosporin-containing wells (positive control), and 2 μM aphidicolin-containing wells (cell growth control). Dose–response curves and growth rate normalized IC_{50} estimates were generated in GraphPad Prism software (V8, GraphPad Software). The *ex vivo* drug screening data (**Supplementary Figures S1–S3**) are deposited to Mendeley data (DOI: 10.17632/9t7gn926ry.1).

Targeted Genomic Sequencing

The genomic profiling was performed at the Jyväskylä Medical Centre molecular pathology core (Jyväskylä, Finland). Briefly, genomic DNA was extracted from the coarse needle tissue biopsy with QIAamp DNA Mini Kit (Qiagen) according to the protocol provided by the kit manufacturer. Qiaseq Human Comprehensive Cancer Panel (Qiagen, DHS-3501Z) including 275 cancer-related genes was used to prepare NGS amplicon gene library according to the protocol provided by the kit manufacturer. Unique molecular identifiers (UMIs) were used to tag individual DNA strands. Sequencing was performed with Illumina NextSeq500 instrument (Illumina) according to standard protocol. Data were de-multiplexed and fastq files were created with bcl2fastq software (Illumina). The data were processed in CLC Biomedical Genomics Workbench (Qiagen) with workflow provided by Qiagen and using Hg19 human

reference genome to call the gene variants. Gene annotations were performed according to the vcf files in OmnomicsNGS software (Euformatics, Espoo, Finland). The sequencing data files are deposited to NCBI Sequence Read Archive (SRA) under accession no. PRJNA760256.

Immunohistochemistry

Immunohistochemical stainings were performed by following standard procedures. Shortly, 2-µm FFPE sections were stained with Bond-III automated IHC stainer (Leica Biosystems) and Bond Polymer Refine Detection kit (DS9800, Leica Biosystems). For BLC-2, antigen retrieval was performed with Bond Epitope Retrieval Solution 2 (AR9640, Leica Biosystems) at 100°C for 20 min. The used antibody dilutions were 1:100 for KRT19 (clone A53-B/A2.26, ThermoScientific), VIM (clone V9, Novocastra/Leica), and HER2 (clone SP3, ThermoScientific). Thirty minutes incubation time was used for all antibodies. All stainings were interpreted by a pathologist.

HER2 Dual ISH Assay

HER2 amplification assay to formalin-fixed paraffin-embedded sections was done with fully automated Ventana BenchMark Xt slide stainer (Ventana Medical Systems). Shortly, dinitrophenyl (DNP)-labeled HER2 probe and digoxigenin-labeled chromosome 17 (Chr17) probes (INFORM HER2 Dual ISH DNA Probe Cocktail, Roche) were co-hybridized to their targets. HER2-DNP probe was visualized with UltraView SISH DNP detection kit (Roche) using HRP-driven silver metallographic detection. For Chr17-DIG probe, UltraView Red ISH DIG detection kit (Roche) was used to produce red signal in alkaline phosphatase-driven reaction. The copy number of HER2 was counted from minimum 20 representative nuclei. HER2 copy number ≥6 was determined as positive for amplification. If HER2 copy number was uncertain (between 4 and 6), the number of Chr17 centromeres was also counted. HER2/Chr17 ratios <2 were interpreted as non-amplified and ratios ≥2 were interpreted as amplified.

RPPA, Quantitation, and Analysis

For the RPPA, screening cells (1,000 per well) were treated in 384-microplate wells with 19 drugs in five concentrations with twofold dilutions starting from 5 µM as the highest concentration. Lysates were collected at the 48-h time point after drug treatment. To generate reverse-phase arrays, lysates were printed on nitrocellulose-coated glass slides (Grace Biolabs #305177) on a Genetix QArray Mini Arrayer (Molecular Devices). Primary antibodies used for RPPA experiments contained the following: p-AKT (Ser473) (Cell Signaling Technology Cat# 4060), AKT (Cell Signaling Technology Cat# 4691), p-ERK1/2 (Thr202/Tyr204) (Cell Signaling Technology Cat# 4370), p-S6 Ribosomal protein (Ser235/236) (Cell Signaling Technology Cat# 2211), Ki-67 (Abcam Cat# ab15580), HER2 (DAKO Cat# A0485), p-HER2 (Y1248) (R&D Systems Cat# AF1768), and p-cMET (Tyr1234/1235) (Cell Signaling Technology Cat# 3129). Secondary detection was performed with a goat anti-mouse IgG conjugated to DyLight 680 (Thermo Pierce Cat# 35518) and goat anti-rabbit IgG conjugated to DyLight 800 (Thermo Pierce Cat# 35571) antibodies. For total protein measurement, the arrays were stained with a Sypro Ruby Blot solution (Invitrogen) and an antibody for actin (Cell Signaling Technology Cat# 4970). The slides were scanned with a Tecan LSReloaded (Tecan) microarray scanner to detect the Sypro signals and Odyssey Licor IR-scanner (LI-COR Biosciences) to detect the antibody signals. Array-Pro Analyzer microarray analysis software (V6.3 Media Cybernetics) was used for analyzing the data. Antibody signals were normalized to the Sypro total protein, log transformed, and *z*-score standardized. *z*-scores < −2.0 or >2.0 (−/+ 2×standard deviation from the whole screen) were considered as significantly downregulated or upregulated, respectively. Box plots, heatmaps, and Pearson correlation analyses were created on GraphPad Prism software.

Flow Cytometry

MISB10 cells cultured in T75 flasks were treated with Accutase (BD Biosciences) and washed twice with PBS with 1% BSA. Suspensions were counted and measured for cell viability using the Vi-Cell XR cell counting and viability analyzer (Beckman Coulter). Cells were diluted in PBS to 1×10^6 cells/ml and stained for 30 min at RT with membrane viability dye (LIVE/DEAD Fixable Near-IR, Invitrogen). Cells were washed and distributed to a 96-well plate containing staining antibodies and Hoechst 33342 (Invitrogen). For characterization panels, immunophenotyping antibodies to the following targets were used: HER-2/neu, CD24, CD29, CD44, CD45, CD49f, CD90, CD166, CD326 (BD Biosciences), and CD133 (Miltenyi Biotec, Auburn, CA). Cells were incubated for 30 min at RT in the dark and then rinsed twice in PBS before acquisition with a BD LSRII flow cytometer. Analysis of results was performed using FACSDiva v6.1.3 and FlowJo analysis software (FlowJo).

MISB10 Cell Line

Approval to use the cells for culture and *in vitro* research was obtained from the patient and the local ethical committee prior to the study. The tumor tissue-derived cells were grown for 4 months in RPMI-1640 culture media supplemented with penicillin/streptomycin (100 units/100 mg), l-glutamine (2 mmol/L), fetal bovine serum (5%, Biowest), and 1× ITS-G (Insulin-Transferrin-Selenium, Gibco). The resulting cell line, designated MISB10, grew continuously when the culture medium was changed twice per week. Confluent cultures were dissociated for 2 min at +37°C using TrypLE Select enzyme (Gibco), and split into new cultures with ratios of 1:2 or 1:3. Cryopreservation was done in CellVation (MP Biomedicals) cryopreservation media. The MISB10 cell line will be available for non-profit research purposes through the corresponding author on reasonable request and in accordance to a specified MTA.

Statistical Analysis

The *ex vivo* drug screening data were analyzed using the normalized growth rate inhibition (GR) approach, which yields per-division metrics for drug potency and efficacy. The GR values were calculated from the raw image cytometry cell

count data with no plate normalization or other data pre-processing and used for comparison of drug potency between the epithelial and stromal sub-cell populations having a differential proliferation rate during the screening. GR values were calculated using:

- $x(c)$, the cell count value of a cell population per well following drug treatment at concentration c.
- x_{ctrl}, the average cell count value of a cell population in DMSO-treated control wells from the same plate; x_{ctrl} = mean({$x_i \in x$ | abs(log10(x_i)–log10(mean(x)))o1.5)}), where x are all DMSO-treated control values.
- x_0, the average cell count value of a cell population in 2 μM aphidicolin-treated control wells from the same plate; x_0 = mean({$x_i \in x$ | abs(log10(x_i)–log10(mean(x))) o1}), where x is the vector of treated values.

Supplementary Data 1, 2 comprise the GR values for each treated condition of the KRT19$^+$, VIM$^+$, and HER2$^+$ cell populations calculated as follows:

$$GR(c) = \frac{\log_2 (X(c)/X_0}{2^{\log_2\left(\frac{X_{ctrl}}{X_0}\right)} - 1} \quad (1)$$

Welch's *t*-test, Student's *t*-test, and Pearson correlation analyses as indicated in the figure legends were applied using GraphPad Prism V8 software according to assumptions on data normality.

RESULTS

Ex Vivo Drug Screen on Lymph Node Metastasis-Derived Tumor Cells

Our patient, a 61-year-old male, originally presented with facial nerve paresis and expansive mass in neck 3 years earlier to the study. Primary diagnostic studies revealed a mass in his left parotid gland. Following a lung CT, a radical parotidectomy and dissection of neck lymph nodes to regions I–V was performed. Histopathological diagnosis was poorly differentiated squamous cell cancer of the parotid gland and post-operative PET-CT scan revealed multiple lung metastases and residual activity in the tumor bed area. Treatment of the disease was initiated with cisplatin–5-fluorouracil chemotherapy regimen to reduce tumor burden. After two cycles of chemotherapy, concurrent chemoradiation therapy with weekly cisplatin was initiated and completed to 50 Gy dose to the residual tumor operation bed and left neck lymph node areas. Local control of the disease was achieved, but lung metastases remained, and residual lung lesions were considered inoperable. Following a 3-month treatment holiday, chemotherapy was changed to nab-paclitaxel (Abraxane). CT scan for response evaluation showed stable disease after 4 months. Response evaluation at 12 months showed progressive disease. At this time, as per discussion with the patient and with approval from the local Ethics Committee of the Central Finland Health Care District, a lymph node sample was retrieved from the left axilla area and processed for the *ex vivo* screening under written informed consent by the patient. The node was cut in half and one-half was processed for routine histopathology. The inner mass of the other half was drained from excess immune cells, cut into small fragments, and disaggregated enzymatically to achieve a single cell milieu of cells (1) (**Figure 1A**). The resulting cell suspension was diluted into cell culture medium and dispensed immediately onto drug containing 384-microwell plates (**Supplementary Figure S1**). Following 96-h exposure of the cells to 125 drugs in five concentrations, high-content imaging cytometry with immunofluorescent antibody staining of the cells with cytokeratin-19 (KRT19) as epithelial (19) and vimentin (VIM) as stromal (1, 3) cell marker was used to quantify the cell-type-specific drug efficacy (**Supplementary Figure S1A**). Dose responses were compared to the negative and positive assay controls to normalize the dose responses of the two cell populations separately to the measured growth rate (3, 18) of each population as described in Equation 1; 77.1% of all analyzed cells were KRT19$^+$ and 19.5% were VIM$^+$. The calculated cell doubling rate of the KRT19$^+$ cells was ~220 h and ~135 h for the VIM$^+$ cells, corresponding to 0.44 and 0.77 cell divisions over the course of the 96-h assay, respectively (18) (**Supplementary Figure S1B**). To identify the most potent tumor cell-targeted cytotoxic drugs, we compared the GR-corrected IC_{50} estimates of the drugs between the KRT19$^+$ and VIM$^+$ cells (**Figure 1C** and **Supplementary Figure S2A**). Topoisomerase inhibitors, HDAC inhibitors, alkaloid and taxane tubulin poisons, CDK inhibitor dinaciclib, and TKi dasatinib were collectively the most cytotoxic drugs on both cell types with an average IC_{50} below 1 μM (**Figure 1B** and **Supplementary Figure S2B**). Twenty-two drugs had a selective cytotoxic effect only on the KRT19$^+$ cells (**Figure 1C**). The EGFR-TKis afatinib, erlotinib, and neratinib, AKT-HER2 inhibitor lapatinib, and c-METi crizotinib were the most potent drugs with a selective cytotoxic effect only on the KRT19$^+$ cells (**Figures 1B–D**).

Ex Vivo Informed Treatment

Based on the *ex vivo* drug screening results, the patient's tumor cells were selectively most sensitive to EGFR/HER2 inhibitors as a class of drugs. Amplifications, high expression levels, and genomic aberrations of HER2 have been reported frequent in a subset of salivary duct carcinomas (17, 20) and several case studies using EGFR/HER2-TKi therapies including cetuximab, erlotinib, gefitinib, T-DM1, and trastuzumab on individual salivary gland cancer patients have been reported. However, at the time of diagnosis of the metastatic disease, checking HER2 status was not considered standard clinical practice in parotid carcinoma in Finland. To assess whether our patient's tumor cells' sensitivity to the EGFR/HER2 inhibitors was due to possible amplification of HER2, additional histopathological analysis including HER2 immunohistochemistry and dual ISH HER2 amplification assay was performed on the lymph node tissue from which the sample cells to the *ex vivo* assay were isolated. Immunohistochemistry results indicated complete, strong, membranous staining, compatible with 3+ HER2 (ASCO/CAP HER2 expression criteria) (**Figure 2A**) accompanied with a copy number gain confirmed with CISH analysis. Based on the *ex vivo* drug screening result, the

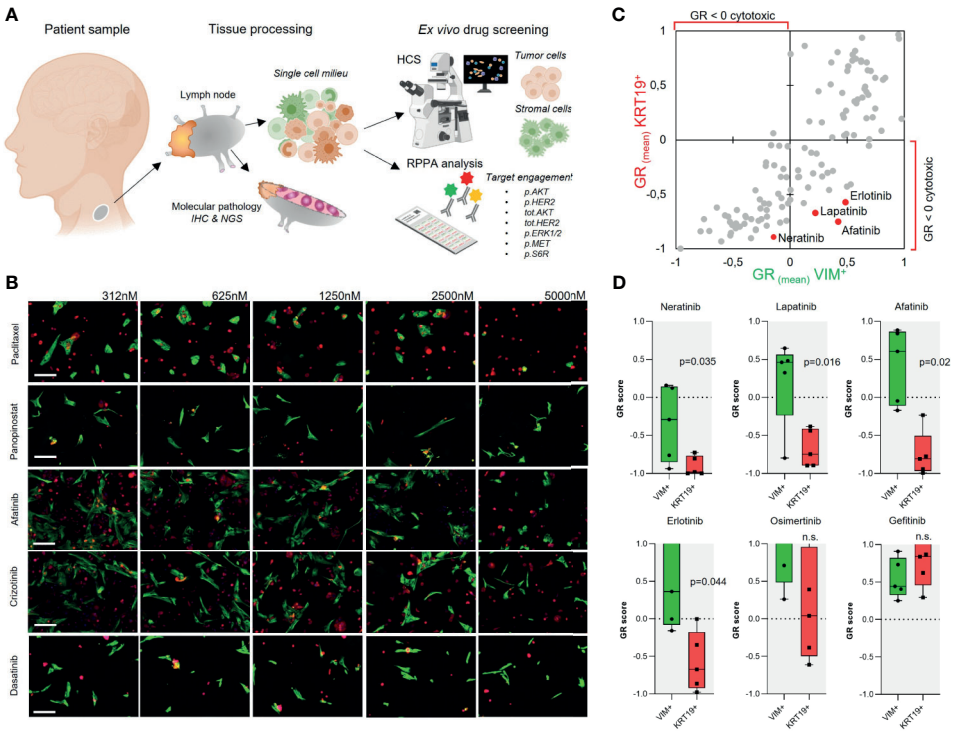

FIGURE 1 | *Ex vivo* drug screening in metastatic parotid duct carcinoma. **(A)** Schematic presentation of the study strategy. **(B)** Gallery view of representative 20× immunofluorescence microscopy images of the sample cells treated for 96 h with the indicated drugs in five different concentrations (nM). KRT19 staining shown in red and VIM staining in green. Bars: 50 µm. **(C)** Scatter plot showing correlation of the mean GR score of 125 drugs in five doses for the KRT19$^+$ and VIM$^+$ cells. **(D)** EGFR-TKis were identified as drugs with a selective cytotoxic effect on the KRT19$^+$ cells. Box plots showing the GR scores for the five doses of all EGFR-TKi included in the screen and compared using paired Student's *t*-test.

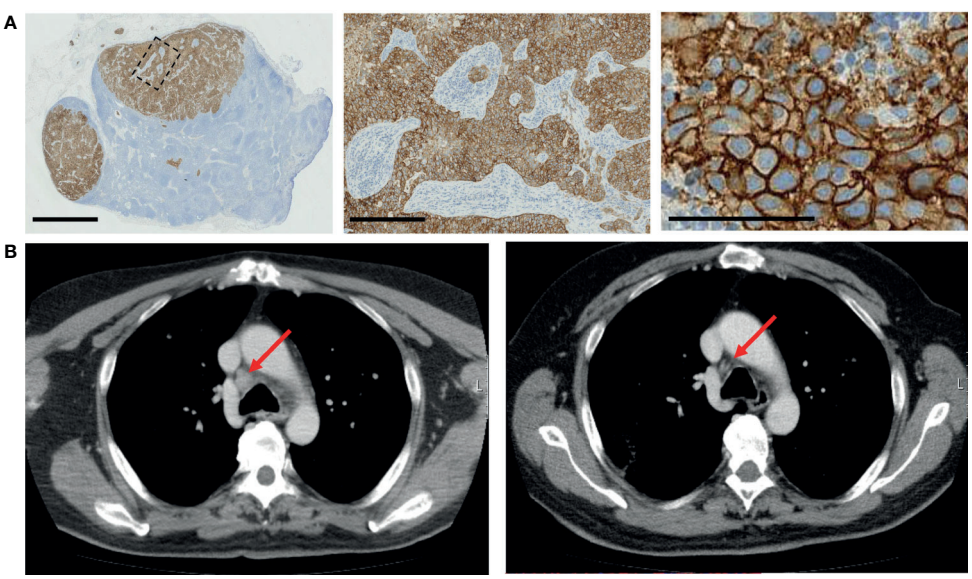

FIGURE 2 | Validation of HER2 status and targeted therapy. **(A)** Immunohistochemistry validation of HER2 staining in the affected lymph node. Scale bars: 2.5 mm, 250 µm, and 100 µm (left to right). **(B)** Radiologic response of patient. Left, prior to treatment, and right, after four cycles of treatment with T-DM1.

immunohistochemistry confirmation and an earlier case report describing sustained clinical response of two HER2$^+$ metastatic salivary gland cancer to ado-trastuzumab emtansine (T-DM1) (21, 22), the patient was considered for treatment with T-DM1. In Finland, HER2-directed therapies are still not reimbursed or generally available for salivary gland cancers. However, after clinical evaluation, treatment with T-DM1 was initiated with off-label use. After 4 months and four cycles of T-DM1, a partial response was confirmed with radiographic examination (**Figure 2B**). The patient was asymptomatic and tolerated the treatment well. After 6 months, the lung and lymph node lesions continued to shrink. Systemic treatment with T-DM1 was continued, and at 10 months of therapy, lung lesions remained stable, but a new 4-cm tumor lesion had appeared between the sixth and seventh rib and the lumbar spine (L1). A new biopsy sample for repeated *ex vivo* analysis was then retrieved from the lesion between the ribs (**Supplementary Figure S3**).

Repeat Analysis of Drug Efficacy in Recurrent Disease

To evaluate drug sensitivity of the new metastatic lesion and the recurrent disease, a repeat *ex vivo* drug screening was undertaken with cells isolated from the new lesion. A parallel tissue biopsy from the same lesion was subjected to targeted DNA sequencing. The image-based assay strategy as used with sample A was used again with staining of HER2 as a third marker for detection of HER2$^+$ cells (**Figure 3D**). Efficacy of 193 drugs in five doses was compared between the VIM$^+$, KRT19$^+$, and HER2$^+$ cells (**Supplementary Figures S1** and **S4A**). One hundred percent of the KRT19$^+$ cells were also HER2$^+$ (without treatments), and similarly as in sample A analysis, the EGFR-TKis afatinib and neratinib were among the most potent drugs with a selective cytotoxic effect on the KRT19$^+$ cells (**Figures 3A, B**). However, the cytotoxic effect of EGFR/HER2 targeted drugs erlotinib and lapatinib, as well as mTOR inhibitors everolimus and rapamycin varied significantly between samples A and B (**Figure 3C** and **Supplementary Figures S4B, C**). MTOR inhibitors AZD2014 and AZD8055, and PI3K inhibitors Buparlisib and AZD8835, on the other hand, showed higher efficacy in sample B (**Supplementary Figures S4B, C**).

To analyze the pathway inhibition efficacy of the most potent identified targeted inhibitors on downstream targets of the HER2/PI3K/AKT/mTOR and EGFR/RAS/MEK pathways, we performed a RPPA screen with the patient-derived cells. In the RPPA experiment, the cells were exposed for 48 h to 16 drugs selected from the *ex vivo* screen including all the EGFR-TKis and trastuzumab, T-DM1 (Kadcyla), and sapitinib (pan-EGFRi) as additional EGFR-TKis. Drugs were tested in five doses with twofold dilutions and eight markers; phospo-S6RP$^{S235/236}$, HER2, phospho-HER2^{Y1248}, AKT, phospho-AKT^{S473}, phospho-ERK1/2$^{T202/Y204}$, phospho-MET$^{Y1234/1235}$, and Ki-67 were used as the assay readout (**Figure 4A**). Analysis of the RPPA data (**Supplementary Figure S5A**) indicated strongest correlation between the proliferation of the cells (*z*-score Ki-67) and p.HER2 (Pearson correlation, r = .43), p.S6R (r = .48), and p.ERK1/2 (r = .68) (**Figure 4A**). EGFR-TKis including afatinib, sapitinib, and T-DM1 effectively blocked all of these markers, while the dual MTORC1/2 inhibitor AZD2014 (vistusertib) had the strongest dose-dependent effect on MTORC1/2 downstream effectors AKT and S6RP (**Supplementary Figure S5B**).

Supported by the RPPA results and the image-based screen results indicating that the HER2 expression was amplified in a dose-dependent manner by lapatinib and downregulated by the

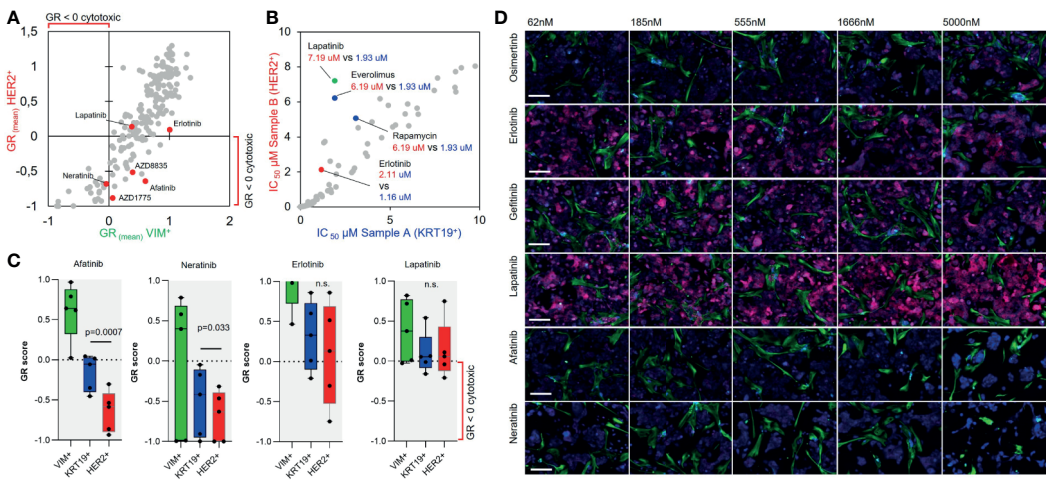

FIGURE 3 | Repeat *ex vivo* drug screen in recurrent disease. **(A)** Scatter plot showing correlation of the mean GR score of 193 drugs in five doses for the HER2$^+$ and VIM$^+$ cells. **(B)** Scatter plot showing correlation of the IC_{50} estimate of the analyzed drugs between the HER2$^+$ sample B cells and KRT19$^+$ sample A cells. **(C)** Box plots showing the GR scores for the five doses of afatinib, neratinib, erlotinib, and lapatinib in sample A and B KRT19$^+$ and HER$^+$ cells. Afatinib and neratinib displayed a statistically significant differential effect on the KRT19$^+$ and HER$^+$ cells from sample B as compared using paired Student's *t*-test. **(D)** Gallery view of representative 20× immunofluorescence microscopy images of the sample cells treated for 96 h with the different EGFR-TKis in five different concentrations (nM). KRT19 staining shown in blue, VIM staining in green and HER2 staining in red. Bars: 50 µm.

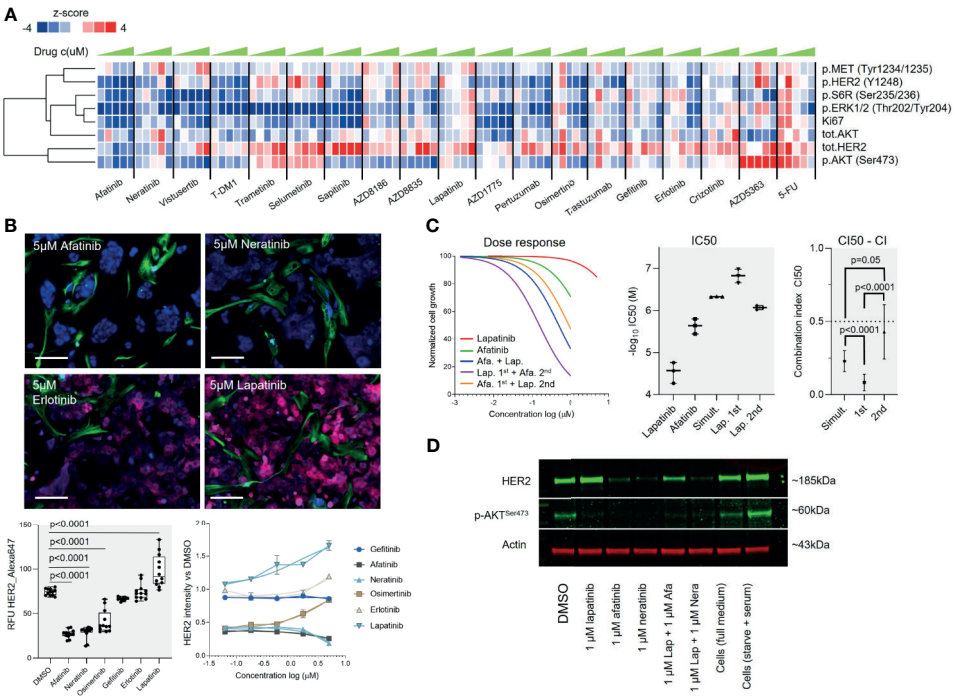

FIGURE 4 | A pathway perspective on targeted therapy responses. **(A)** Heat map visualization with one-dimensional (vertical) unsupervised clustering of the *z*-scores of the eight RPPA markers across 19 drugs in five concentrations (left to right, low to high, respectively). **(B)** Top: Representative microscope images of HER2 staining on sample B cells in the *ex vivo* screen following 96-h exposure to the indicated drugs at 5 µM concentration. KRT19 staining shown in blue, VIM staining in green, and HER2 staining in red. Bars: 50 µm. Bottom left: Box plot showing the mean and standard deviation of fluorescence intensity of HER2 staining (RFU) of the KRT19$^+$ cells in response to treatment with the different EGFR-TKis. Two biological replicate experiments were combined and compared using unpaired Welch's *t*-test. Bottom right: Comparison of the HER2 staining intensity to DMSO-treated cells. Signal shown as fold change. **(C)** Combination of lapatinib and afatanib shows a synergistic growth inhibitory effect. With all three different drug schedules tested, the combination resulted in significantly increased efficacy over the single agents as indicated by the lower IC_{50} (middle panel). On the basis of the CI_{50} combination index, lapatinib pre-treatment preceding afatinib treatment had the highest synergy (right panel). Comparison was made using unpaired Student's *t*-test. **(D)** The patient-derived tumor cells were treated with DMSO (–), 1000 nmol/L afatinib, lapatinib, neratinib, or combination of 1000 nmol/L afatinib+lapatinib, or neratinib+lapatinib for 48 h, and phosphorylation (p) AKT and total HER2 protein levels of indicated markers were assessed using Western blot. Actin was assessed as a loading control.

EGFR-TKis (**Figure 4B** and **Supplementary Figure S5A**), we rationalized that combination of lapatinib could potentiate the overall therapeutic efficacy of the EGFR-TKis as reported in several human cancers (23–25). We explored the effect of combining the highest-ranking EGFR-TKi afatinib with lapatinib to evaluate synergy between the two drugs. Three different drug combination schemes were compared with a fixed 1:5 molar ratio of the drugs (afatinib IC_{50} 1.64 µM, lapatinib IC_{50} 7.19): (1) 72-h simultaneous treatment, (2) 24-h lapatinib pre-treatment followed with 48 h addition of afatinib, and (3) 24-h afatinib pre-treatment followed with 48 h addition of lapatinib (**Figure 4C**). The combinations resulted in significant synergistic effects across all three treatment schedules with a mean CI50 combination index (26) of 0.47 with the simultaneous treatment, 0.15 with lapatinib pre-treatment, and 0.86 with afatinib pre-treatment (**Figure 4C**). The impact of the drug combination on HER2 protein level expression and phosphorylation of AKT was also confirmed with a Western blot analysis from the cells (**Figure 4D**). However, the synergistic effect was significantly more potent with lapatinib being administered first in comparison to simultaneous or reversed administration (p <.0001 both) (**Figure 4C**), suggesting that the order of administration of the two drugs could affect the overall combination efficacy.

Treatment of the Recurrent Disease

The targeted DNA sequencing performed from sample B identified a p53 p.R273C (allele frequency 69%) mutation, a CHEK2 p.I157T (freq. 40%) mutation, and a HER2 p.V747L mutation (freq. 93%), while HER2 CISH assay confirmed a HER2 copy number gain. Following relapse of the disease after treatment with T-DM1, the patient's treatment was continued with capecitabine as a single agent. After 2 months, the patient suffered a seizure and multiple brain metastases were detected in MRI. These lesions were not suitable for stereotactic radiotherapy and the patient received palliative whole-brain radiotherapy. The patient was then considered for a second cycle of experimental therapy based on the *ex vivo* drug screening and molecular pathology results. As the *ex vivo* experiments suggested that the patient's tumor cells continued

to respond to EGRF-TKis and that lapatinib potentiated these effects, trastuzumab–lapatinib regimen was initiated (27, 28) with five daily doses of lapatinib as a pre-treatment. Control CT scan performed after two cycles of trastuzumab and daily dosing of lapatinib showed that the lung metastases had remained stable. The soft tissue tumor component of the metastasis between the sixth and seventh rib had been completely resolved with only a sclerotic bony lesion remaining while the lytic, metabolically active metastatic lesion on the lumbar spine (L1) had been stabilized (**Figure 5**). The trastuzumab–lapatinib regimen was continued as therapy for 10 months until clear progressive disease was observed, and the patient started to receive the best palliative care. The patient succumbed to the disease 26 months after the initial *ex vivo* sample was obtained and 60 months from the primary diagnosis.

A New HER2$^+$ Parotid Carcinoma Model Cell Line

Many of the defined molecular subtypes of salivary gland malignancies represent a HER2$^+$ molecular background (20), yet no HER2$^+$ model cell lines have been described, and only two salivary gland cancer-derived model cell lines are altogether included in the CCLE collection of 1,739 human cancer cell lines (29). The patient-derived cells left over from the performed *ex vivo* analyses of sample B were kept in culture in standard cell culture conditions after the patient was started treatment with the trastuzumab–lapatinib regimen. After 4 months in culture, the cells started to show stable *in vitro* growth and a uniform morphology with no residual stromal cell contamination growing in the culture. The cells grew continuously as an adherent monolayer (**Figure 6B**) and reached confluence in 4 to 6 days with 1:3 ratio passaging in 10-cm culture dishes. After the cells had undergone ~20 passages, a comprehensive flow cytometry immunoprofiling was performed to establish an immunophenotypic profile of the cells and to assess clonal heterogeneity of the culture. Over 99% of the cells were found to be EpCAM$^+$ with >98% being HER2$^+$, CD24$^+$, CD44$^+$, CD29$^+$, CD49f$^+$, CD90$^-$, and CD184$^-$ (29) (**Figure 6A**). In addition to these epithelial cell lineage markers, the EpCAM$^+$ cells were also found to express CD47, a potential immune evasion marker (30), CD54 (31), CD64, CD73 (32), CD151, and c-MET (**Figure 6C**), which could explain the cells' responsiveness to the c-METi crizotinib (**Figure 1B** and **Supplementary Figure S2B**). Currently, subcultures of the cells devoted a cell line named MISB10, which have undergone an excess of 80 passages; they show continuous growth and can recover from repeated cryopreservation cycles; they show responsiveness to EGFR-TKi targeted therapies and form multicellular organotypic spheroids while grown in human tumor microenvironment mimicking 3D culture conditions (33) (**Supplementary Figure S6**).

DISCUSSION

Parotid squamous cell carcinoma is a rare, aggressive salivary gland malignancy, which often presents at an advanced stage with nodal metastases. While most salivary gland tumors in

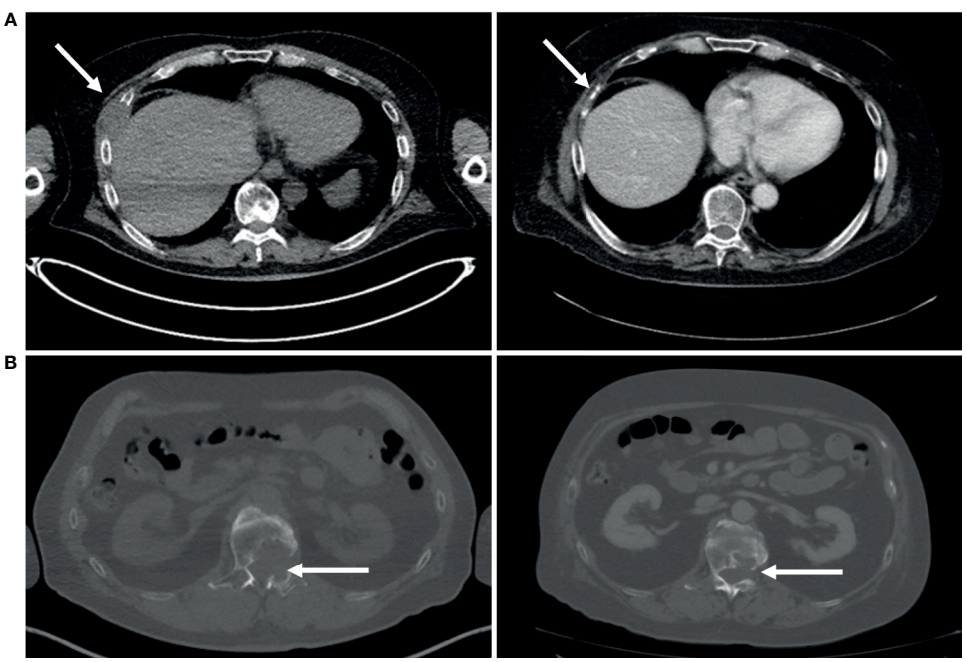

FIGURE 5 | Clinical response to dual inhibitor lapatinib (AKTi)–trastuzumab (HER2i) therapy. **(A)** Following 2 months of treatment, the soft tissue component of the metastasis lesion between the sixth and seventh rib was completely resolved**. (B)** The lytic lumbar spine (L1) lesion was stabilized following 2 months of treatment.

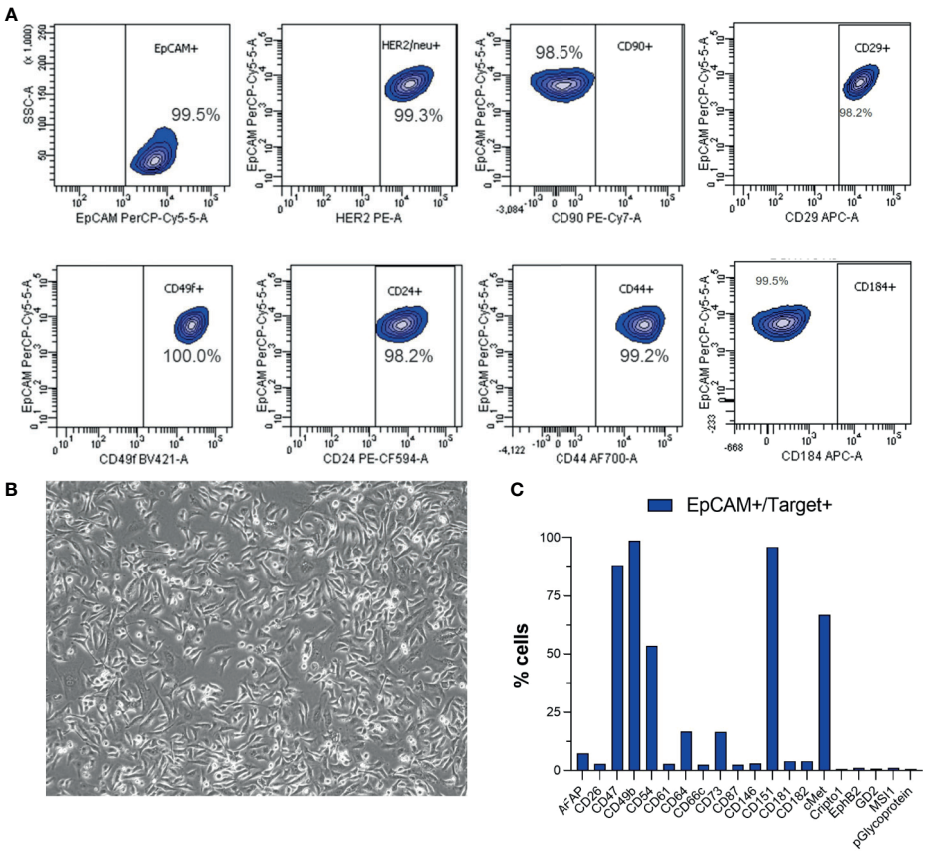

FIGURE 6 | Flow cytometry immunophenotyping of the MISB10B cells. **(A)** Analysis of expression of epithelial lineage markers and HER2 in the EpCAM$^+$ cells. **(B)** Representative bright-field microscopy image (10×) of the morphology of the MISB10B cells in near full confluent state. **(C)** Analysis of expression of additional immunophenotypic markers in the EpCAM$^+$ cells.

general are benign in nature, this tumor is highly aggressive and approximately 65% of patients die from progressive disease within 48 months (34). There are no standard treatment options for recurrent and metastatic disease, and the role of adjuvant chemotherapy on overall survival is not known due to the very low incidence rate. Surgical resection followed by radiation therapy thus remains the main management strategy for parotid squamous cell carcinomas with limited other therapeutic options for metastatic disease. While up to 44% of parotid duct carcinomas have been reported to have *HER2* amplifications or high protein or mRNA level expression of HER2 (20, 35), the number of HER2-positive parotid SCC cases is lower (36). This suggests that while less frequent in parotid SCC than parotic duct carcinomas, HER2 aberrations represent a significant target, biomarker, and opportunity for targeted treatment also in a subset of patients with parotid SCC tumors (17, 20, 33, 37). To improve outcomes and efficacy of treatment of primary and/or metastatic parotid SCC, systematic studies involving larger series of HER2$^+$ salivary gland cancers or stratification of patients to HER2-targeted therapies by alternative strategies are needed to determine the contribution of HER2 targeting on tumor response outcomes in parotid SCC and other salivary gland cancers (17).

In this study, we identified the sensitivity and HER2 positivity of the patient's cancer on the basis of drug sensitivity of the vital tumor cells to EGFR-TKi in an *ex vivo* drug screen. At time of the study, analysis of HER2 status was not considered standard clinical practice in parotid carcinoma in Finland. This shows that *ex vivo* drug screening can be used as a platform to complement molecular pathology information and quickly identify actionable drug sensitivities that can be matched with the molecular characteristics of the patient's tumor and thus motivate personalized medicine. By identifying the response of the patient-derived tumor cells to the EGFR-TKis, our results helped to guide our patient's treatment to include treatment options that are currently still not generally available for these patients, but which resulted in sustained clinical benefit. Molecular profiling of the patient's tumor also identified a novel *HER2* mutation affecting the protein tyrosine kinase domain and a *CHEK2* mutation previously identified as a cancer susceptibility gene in the Finnish population (38, 39). As *HER2* mutations have been shown to reduce the efficacy of therapies commonly used to

treat HER2-positive breast cancer, particularly in metastatic and previously HER2 inhibitor-treated patients (40), our data, even though limited by being an analysis only of one patient, provide novel insights into general and EGFR-TKi-specific drug efficacy in cancers bearing these aberrations. For further analyses of these aspects, the MISB10 cell established from the patient's tumor represents a unique new *in vitro* research resource as the first and only described *HER2*-amplified, *HER2* mutant salivary gland cancer cell line in the world (41).

In summary, we present here the first large-scale *ex vivo* drug screening in a metastatic parotid squamous cell carcinoma together with use of HER2-targeted therapies adding one more case example to the existing medical literature supporting the use of HER2-directed therapies for a subset of salivary gland tumors. Since parotic SCC is a rare tumor type, it is difficult to conduct prospective clinical studies to compare which of the existing HER2 directed agents is the most effective, but this case example suggests that antibody–chemotherapy conjugates seem to have promising activity. Future studies should also investigate trastuzumab–deruxtecan for this patient population as, currently, there are no adjuvant treatment options that affect the overall survival of metastatic parotid SCC patients (42). New treatment modalities are therefore urgently needed to improve the outcome of this aggressive disease.

DATA AVAILABILITY STATEMENT

The data presented in the study are deposited in the NCBI Sequencing Read Archive, accession number PRJNA760256 and Mendeley Data repository, accession number DOI: 10.17632/9t7gn926ry.1.

ETHICS STATEMENT

The studies involving human participants were reviewed and approved by Keski-Suomen sairaanhoitopiiri, Tutkimuseettinen toimikunta, Jyväskylä, Finland. The patients/participants provided their written informed consent to participate in this study.

AUTHOR CONTRIBUTIONS

Conception and design: RM, AA, JK, and JR. Clinical materials: IJ, TK, and JK. Development of methodology: RM, AA, and JR. Acquisition of data: NN, RM, AA, VH, and LL. Analysis and interpretation of data: LL, RM, IJ, TK, JK, and JR. Writing, review, and/or revision of the manuscript: NN, RM, TK, JK, and JR. Administrative, technical, or material support: TK, JK, and JR. Study supervision: JR. All authors contributed to the article and approved the submitted version.

FUNDING

This work has been supported in part by AZ-SLL-KI open innovation grant #18122013. The funding body had no input in the design of the study, collection, analysis, or interpretation of the data.

ACKNOWLEDGMENTS

We would like to thank the patient and the family with whom this study is connected and the personnel of the Central Finland Health Care District, Jyväskylä Medical Centre, Department of Oncology. The human myoma extract Myogel was a kind gift from Professor Tuula Salo, University of Oulu, Oulu, Finland.

SUPPLEMENTARY MATERIAL

The Supplementary Material for this article can be found online at: https://www.frontiersin.org/articles/10.3389/fonc.2021.735820/full#supplementary-material

REFERENCES

1. Arjonen A, Mäkelä R, Härmä V, Rintanen N, Kuopio T, Kononen J, et al. Image-Based *Ex Vivo* Drug Screen to Assess Targeted Therapies in Recurrent Thymoma. *Lung Cancer* (2020) 145:27–32. doi: 10.1016/j.lungcan.2020.04.036
2. Mäkelä R, Arjonen A, Härmä V, Rintanen N, Paasonen L, Paprotka T, et al. *Ex Vivo* Modelling of Drug Efficacy in a Rare Metastatic Urachal Carcinoma. *BMC Cancer* (2020) 20(1):590. doi: 10.1186/s12885-020-07092-w
3. Mäkelä R, Arjonen A, Suryo Rahmanto A, Härmä V, Lehtiö J, Kuopio T, et al. *Ex Vivo* Assessment of Targeted Therapies in a Rare Metastatic Epithelial-Myoepithelial Carcinoma. *Neoplasia* (2020) 22(9):390–8. doi: 10.1016/j.neo.2020.06.007
4. Arjonen A, Mäkelä R, Virtakoivu R, Härmä V, Kuopio T, Hakkarainen H, et al. *Ex Vivo* Modelling of Therapy Efficacy for Rare Krugenberg Tumors – A Report of Two Cases. *Clin Oncol Res* (2020) 3(7). doi: 10.31487/j.COR.2020.07.01
5. Kettunen K, Boström PJ, Lamminen T, Heinosalo T, West G, Saarinen I, et al. Personalized Drug Sensitivity Screening for Bladder Cancer Using Conditionally Reprogrammed Patient-Derived Cells. *Eur Urol* (2019) 76(4):430–4. doi: 10.1016/j.eururo.2019.06.016
6. Lehtomaki KI, Lahtinen LI, Rintanen N, Kuopio T, Kholova I, Makela R, et al. Clonal Evolution of MEK/MAPK Pathway Activating Mutations in a Metastatic Colorectal Cancer Case. *Anticancer Res* (2019) 39(11):5867–77. doi: 10.21873/anticanres.13791
7. Tyner JW, Yang WF, Bankhead A3rd, Fan G, Fletcher LB, Bryant J, et al. Kinase Pathway Dependence in Primary Human Leukemias Determined by Rapid Inhibitor Screening. *Cancer Res* (2013) 73:285–96. doi: 10.1158/0008-5472.CAN-12-1906
8. Pemovska T, Johnson E, Kontro M, Repasky GA, Chen J, Wells P, et al. Axitinib Effectively Inhibits BCR-ABL1(T315I) With a Distinct Binding Conformation. *Nature* (2015) 519:102–5. doi: 10.1038/nature14119
9. Kurtz SE, Eide CA, Kaempf A, Khanna V, Savage S, Rofelty A, et al. Molecularly Targeted Drug Combinations Demonstrate Selective Effectiveness for Myeloid- and Lymphoid-Derived Hematologic Malignancies. *Proc Natl Acad Sci USA* (2017) 114(36):E7554–63. doi: 10.1073/pnas.1703094114
10. Schmidl C, Vladimer GI, Rendeiro AF, Schnabl S, Krausgruber T, Taubert C, et al. Combined Chemosensitivity and Chromatin Profiling Prioritizes Drug Combinations in CLL. *Nat Chem Biol* (2019) 3:232–40. doi: 10.1038/s41589-018-0205-2

11. Snijder B, Vladimer GI, Krall N, Miura K, Schmolke AS, Kornauth C, et al. Image-Based *Ex Vivo* Drug Screening for Patients With Aggressive Haematological Malignancies: Interim Results From a Single-Arm, Open-Label, Pilot Study. *Lancet Haematol* (2017) 12:e595–606. doi: 10.1016/S2352-3026(17)30208-9
12. Massard C, Michiels S, Ferté C, Le Deley MC, Lacroix L, Hollebecque A, et al. High-Throughput Genomics and Clinical Outcome in Hard-to-Treat Advanced Cancers: Results of the MOSCATO 01 Trial. *Cancer Discov* (2017) 6:586–95. doi: 10.1158/2159-8290.CD-16-1396
13. Sicklick JK, Kato S, Okamura R, Schwaederle M, Hahn ME, Williams CB, et al. Molecular Profiling of Cancer Patients Enables Personalized Combination Therapy: The I-PREDICT Study. *Nat Med* (2019) 5:744–50. doi: 10.1038/s41591-019-0407-5
14. Rodon J, Soria JC, Berger R, Miller WH, Rubin E, Kugel A, et al. Genomic and Transcriptomic Profiling Expands Precision Cancer Medicine: The WINTHER Trial. *Nat Med* (2019) 5:751–8. doi: 10.1038/s41591-019-0424-4
15. Rothwell DG, Ayub M, Cook N, Thistlethwaite F, Carter L, Dean E, et al. Utility of ctDNA to Support Patient Selection for Early Phase Clinical Trials: The TARGET Study. *Nat Med* (2019) 5:738–43. doi: 10.1038/s41591-019-0380-z
16. Gargano SM, Senarathne W, Feldman R, Florento E, Stafford P, Swensen J, et al. Novel Therapeutic Targets in Salivary Duct Carcinoma Uncovered by Comprehensive Molecular Profiling. *Cancer Med* (2019) 8(17):7322–9. doi: 10.1002/cam4.2602
17. Kurzrock R, Bowles DW, Kang H, Meric-Bernstam F, Hainsworth J, Spigel DR, et al. Targeted Therapy for Advanced Salivary Gland Carcinoma Based on Molecular Profiling: Results From MyPathway, a Phase IIa Multiple Basket Study. *Ann Oncol* (2020) 3:412–21. doi: 10.1016/j.annonc.2019.11.018
18. Hafner M, Niepel M, Chung M, Sorger PK. Growth Rate Inhibition Metrics Correct for Confounders in Measuring Sensitivity to Cancer Drugs. *Nat Methods* (2016) 13:521–7. doi: 10.1038/nmeth.3853
19. Azevedo RS, de Almeida OP, Kowalski LP, Pires FR. Comparative Cytokeratin Expression in the Different Cell Types of Salivary Gland Mucoepidermoid Carcinoma. *Head Neck Pathol* (2008) 4:257–64. doi: 10.1007/s12105-008-0074-1
20. Alotaibi AM, Algarni MA, Alnobi A, Tarakji B. Human Epidermal Growth Factor Receptor 2 (HER2/neu) in Salivary Gland Carcinomas: A Review of Literature. *J Clin Diagn Res* (2015) 9:ZE04–08. doi: 10.7860/JCDR/2015/11289.5572
21. van Boxtel W, Boon E, Weijs WLJ, van den Hoogen FJA, Flucke UE, van Herpen CML. Combination of Docetaxel, Trastuzumab and Pertuzumab or Treatment With Trastuzumab-Emtansine for Metastatic Salivary Duct Carcinoma. *Oral Oncol* (2017) 72:198–200. doi: 10.1016/j.oraloncology.2017.06.023
22. Krop IE, Kim SB, Martin AG, LoRusso PM, Ferrero JM, Badovinac-Crnjevic T, et al. Trastuzumab Emtansine Versus Treatment of Physician's Choice in Patients With Previously Treated HER2-Positive Metastatic Breast Cancer (TH3RESA): Final Overall Survival Results From a Randomised Open-Label Phase 3 Trial. *Lancet Oncol* (2017) 18(6):743–54. doi: 10.1016/S1470-2045(17)30313-3
23. Scaltriti M, Verma C, Guzman M, Jimenez J, Parra JL, Pedersen K, et al. Lapatinib, A HER2 Tyrosine Kinase Inhibitor, Induces Stabilization and Accumulation of HER2 and Potentiates Trastuzumab-Dependent Cell Cytotoxicity. *Oncogene* (2009) 28(6):803–14. doi: 10.1038/onc.2008.432
24. Rimawi MF, Wiechmann LS, Wang YC, Huang C, Migliaccio I, Wu MF, et al. Reduced Dose and Intermittent Treatment With Lapatinib and Trastuzumab for Potent Blockade of the HER Pathway in HER2/neu-Overexpressing Breast Tumor Xenografts. *Clin Cancer Res* (2011) 17(6):1351–61. doi: 10.1158/1078-0432.CCR-10-1905
25. Okita R, Shimizu K, Nojima Y, Yukawa T, Maeda A, Saisho S, et al. Lapatinib Enhances Trastuzumab-Mediated Antibody-Dependent Cellular Cytotoxicity via Upregulation of HER2 in Malignant Mesothelioma Cells. *Oncol Rep* (2015) 34(6):2864–70. doi: 10.3892/or.2015.4314
26. Chou TC. Drug Combination Studies and Their Synergy Quantification Using the Chou–Talalay Method. *Cancer Res* (2010) 70:440–6. doi: 10.1158/0008-5472.CAN-09-1947
27. Scaltriti M, Chandarlapaty S, Prudkin L, Aura C, Jimenez J, Angelini PD, et al. Clinical Benefit of Lapatinib-Based Therapy in Patients With Human Epidermal Growth Factor Receptor 2-Positive Breast Tumors Coexpressing the Truncated P95her2 Receptor. *Clin Cancer Res* (2010) 16(9):2688–95. doi: 10.1158/1078-0432.CCR-09-3407
28. Rimawi MF, Mayer IA, Forero A, Nanda R, Goetz MP, Rodriguez AA, et al. Multicenter Phase II Study of Eoadjuvant Lapatinib and Trastuzumab With Hormonal Therapy and Without Chemotherapy in Patients With Human Epidermal Growth Factor Receptor 2-Overexpressing Breast Cancer: TBCRC 006. *J Clin Oncol* (2013) 31(14):1726–31. doi: 10.1200/JCO.2012.44.8027
29. Snowden E, Porter W, Hahn F, Ferguson M, Tong F, Parker JS, et al. Immunophenotyping and Transcriptomic Outcomes in PDX-Derived TNBC Tissue. *Mol Cancer Res* (2017) 15(4):429–38. doi: 10.1158/1541-7786.MCR-16-0286-T
30. Liu X, Kwon H, Li Z, Fu YX. Is CD47 an Innate Immune Checkpoint for Tumor Evasion? *J Hematol Oncol* (2017) 10(1):12. doi: 10.1186/s13045-016-0381-z
31. Wei W, Jiang D, Lee HJ, Li M, Kutyreff CJ, Engle JW, et al. Development and Characterization of CD54-Targeted immunoPET Imaging in Solid Tumors. *Eur J Nucl Med Mol Imaging* (2020) 47(12):2765–75. doi: 10.1007/s00259-020-04784-0
32. Chen Q, Pu N, Yin H, Zhang J, Zhao G, Lou W, et al. CD73 Acts as a Prognostic Biomarker and Promotes Progression and Immune Escape in Pancreatic Cancer. *J Cell Mol Med* (2020) 24(15):8674–86. doi: 10.1111/jcmm.15500
33. Tuomainen K, Al-Samadi A, Potdar S, Turunen L, Turunen M, Karhemo PR, et al. Human Tumor-Derived Matrix Improves the Predictability of Head and Neck Cancer Drug Testing. *Cancers (Basel)* (2019) 12(1):92. doi: 10.3390/cancers12010092
34. Schmitt NC, Kang H, Sharma A. Salivary Duct Carcinoma: An Aggressive Salivary Gland Malignancy With Opportunities for Targeted Therapy. *Oral Oncol* (2017) 74:40–8. doi: 10.1016/j.oraloncology.2017.09.008
35. Locati LD, Perrone F, Losa M, Mela M, Casieri P, Orsenigo M, et al. Treatment Relevant Target Immunophenotyping of 139 Salivary Gland Carcinomas (SGCs). *Oral Oncol* (2009) 45:986–90. doi: 10.1016/j.oraloncology.2009.05.635
36. Lee DS, Lee CG, Keum KC, Chung SY, Kim T, Wu HG, et al. Treatment Outcomes of Patients With Salivary Duct Carcinoma Undergoing Surgery and Postoperative Radiotherapy. *Acta Oncol* (2020) 59(5):565–8. doi: 10.1080/0284186X.2020.1730005
37. Jhaveri KL, Wang XV, Makker V, Luoh SW, Mitchell EP, Zwiebel JA, et al. Ado-Trastuzumab Emtansine (T-DM1) in Patients With HER2-Amplified Tumors Excluding Breast and Gastric/Gastroesophageal Junction (GEJ) Adenocarcinomas: Results From the NCI-MATCH Trial (EAY131) Subprotocol Q. *Ann Oncol* (2019) 30(11):1821–30. doi: 10.1093/annonc/mdz291
38. Vahteristo P, Bartkova J, Eerola H, Syrjäkoski K, Ojala S, Kilpivaara O, et al. A CHEK2 Genetic Variant Contributing to a Substantial Fraction of Familial Breast Cancer. *Am J Hum Genet* (2002) 71(2):432–8. doi: 10.1086/341943
39. Kuusisto KM, Bebel A, Vihinen M, Schleutker J, Sallinen SL. Screening for BRCA1, BRCA2, CHEK2, PALB2, BRIP1, RAD50, and CDH1 Mutations in High-Risk Finnish BRCA1/2-Founder Mutation-Negative Breast and/or Ovarian Cancer Individuals. *Breast Cancer Res* (2011) 13(1):R20. doi: 10.1186/bcr2832
40. Smyth LM, Piha-Paul SA, Won HH, Schram AM, Saura C, Loi S, et al. Efficacy and Determinants of Response to HER Kinase Inhibition in HER2-Mutant Metastatic Breast Cancer. *Cancer Discov* (2020) 10(2):198–213. doi: 10.1158/2159-8290.CD-19-0966
41. Ghandi M, Huang FW, Jané-Valbuena J, Kryukov GV, Lo CC, McDonald ER, et al. Next-Generation Characterization of the Cancer Cell Line Encyclopedia. *Nature* (2019) 569(7757):503–8. doi: 10.1038/s41586-019-1186-3
42. Osborn V, Givi B, Lee A, Sheth N, Roden D, Schwartz D, et al. Characterization, Treatment and Outcomes of Salivary Ductal Carcinoma Using the National Cancer Database. *Oral Oncol* (2017) 71:41–6. doi: 10.1016/j.oraloncology.2017.05.005

Conflict of Interest: Authors NN and JR are employed by Misvik Biology Oy. Authors RM, AA, VH, and LL were employed by Misvik Biology Oy. JR is the founder and owner of Misvik Biology Oy. Authors ES and RB were employed by BD Technologies.

The remaining authors declare that the research was conducted in the absence of any commercial or financial relationships that could be construed as a potential conflict of interest.

Publisher's Note: All claims expressed in this article are solely those of the authors and do not necessarily represent those of their affiliated organizations, or those of

the publisher, the editors and the reviewers. Any product that may be evaluated in this article, or claim that may be made by its manufacturer, is not guaranteed or endorsed by the publisher.

Copyright © 2021 Nykänen, Mäkelä, Arjonen, Härmä, Lewandowski, Snowden, Blaesius, Jantunen, Kuopio, Kononen and Rantala. This is an open-access article distributed under the terms of the Creative Commons Attribution License (CC BY). The use, distribution or reproduction in other forums is permitted, provided the original author(s) and the copyright owner(s) are credited and that the original publication in this journal is cited, in accordance with accepted academic practice. No use, distribution or reproduction is permitted which does not comply with these terms.

frontiers in Pharmacology

REVIEW
published: 24 September 2021
doi: 10.3389/fphar.2021.747837

Targeting the Integrated Stress Response in Cancer Therapy

Xiaobing Tian[1,2,3,4]*, Shengliang Zhang*[1,2,3,4], *Lanlan Zhou*[1,2,3,4], *Attila A. Seyhan*[1,2,3,4], *Liz Hernandez Borrero*[1], *Yiqun Zhang*[1] *and Wafik S. El-Deiry*[1,2,3,4,5]*

[1]Laboratory of Translational Oncology and Experimental Cancer Therapeutics, Warren Alpert Medical School, Brown University, Providence, RI, United States, [2]Department of Pathology and Laboratory Medicine, Warren Alpert Medical School, Brown University, Providence, RI, United States, [3]Joint Program in Cancer Biology, Lifespan Health System and Brown University, Providence, RI, United States, [4]Cancer Center at Brown University, Providence, RI, United States, [5]Hematology/Oncology Division, Department of Medicine, Lifespan Health System and Brown University, Providence, RI, United States

The integrated stress response (ISR) is an evolutionarily conserved intra-cellular signaling network which is activated in response to intrinsic and extrinsic stresses. Various stresses are sensed by four specialized kinases, PKR-like ER kinase (PERK), general control non-derepressible 2 (GCN2), double-stranded RNA-dependent protein kinase (PKR) and heme-regulated eIF2α kinase (HRI) that converge on phosphorylation of serine 51 of eIF2α. eIF2α phosphorylation causes a global reduction of protein synthesis and triggers the translation of specific mRNAs, including activating transcription factor 4 (ATF4). Although the ISR promotes cell survival and homeostasis, when stress is severe or prolonged the ISR signaling will shift to regulate cellular apoptosis. We review the ISR signaling pathway, regulation and importance in cancer therapy.

Keywords: integrated stress responses, ATF4, CHOP, apoptosis, cancer treatment

OPEN ACCESS

Edited by:
Anne Lorant, Laboratoire de Biologie Moléculaire et Cellulaire du Cancer (LBMCC), Luxembourg

Reviewed by:
Souvik Dey, Jadavpur University, India
Akihiro Tomida, Japanese Foundation For Cancer Research, Japan

***Correspondence:**
Xiaobing Tian
xiaobing_tian@brown.edu
Wafik S. El-Deiry
wafik@brown.edu

Specialty section:
This article was submitted to Pharmacology of Anti-Cancer Drugs, a section of the journal Frontiers in Pharmacology

Received: *26 July 2021*
Accepted: *10 September 2021*
Published: *24 September 2021*

Citation:
Tian X, Zhang S, Zhou L, Seyhan AA, Hernandez Borrero L, Zhang Y and El-Deiry WS (2021) Targeting the Integrated Stress Response in Cancer Therapy. Front. Pharmacol. 12:747837. doi: 10.3389/fphar.2021.747837

INTRODUCTION

ISR is an evolutionarily conserved intra-cellular signal network activated in response to various intrinsic and extrinsic factors (**Figure 1**). Extrinsic factors include amino acid depletion, glucose deprivation, viral infection, hypoxia, heme deficiency, ROS (reactive oxygen species) and DNA damage (Pakos-Zebrucka et al., 2016; Clementi et al., 2020; Akman et al., 2021). Cellular intrinsic stresses, such as ER (endoplasmic reticulum) stress, can also activate the ISR (Pakos-Zebrucka et al., 2016). In the context of cancer biology, oncogene activation, such as MYC overexpression, can trigger the ISR (Tameire et al., 2019). Cancer cells with enhanced proliferation have enhanced protein synthesis which leads to a high basal level of the ISR as compared to normal cells (McConkey, 2017; Tameire et al., 2019). This may explain why ISR inducers can selectively target cancer cells.

Various stresses are sensed by four specialized kinases (PERK, GCN2, PKR and HRI) that converge on phosphorylation of serine 51 of eIF2α (**Figure 1**) (Perkins and Barber, 2004; Wek et al., 2006; Donnelly et al., 2013). Although significant sequence homology exists between these four eIF2α kinases in their kinase catalytic domains, underlying their common role in phosphorylating eIF2α, each eIF2α kinase possesses distinct regulatory domains and additional unique features that determine the regulation of these four kinases by signals that activate them (Donnelly et al., 2013). Each kinase responds to distinct environmental and physiological stresses, which reflects their unique regulatory mechanisms (Donnelly et al., 2013). eIF2α phosphorylation causes global reduction of protein synthesis and triggers the translation of specific mRNAs, including ATF4 to help with cell survival and recovery. However, if the stress cannot be reduced, ATF4 regulates an apoptosis program to eliminate the damaged cells (Pakos-Zebrucka et al., 2016; Costa-Mattioli and Walter, 2020).

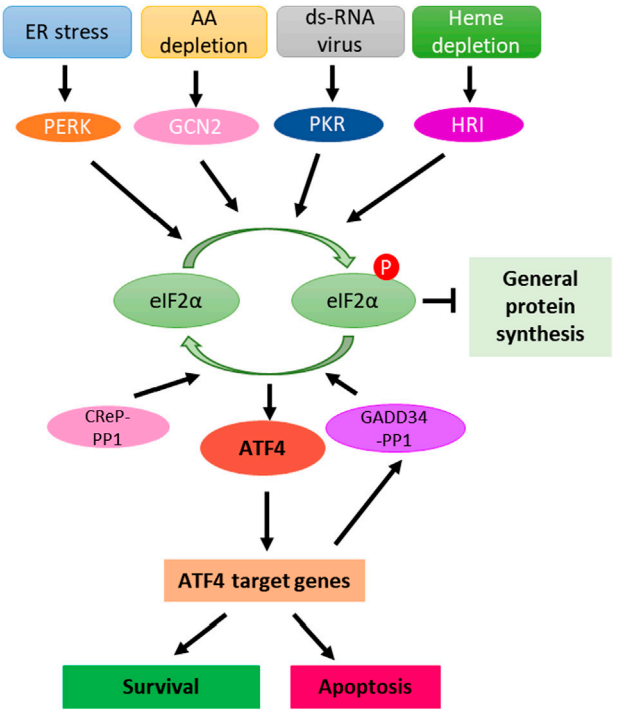

FIGURE 1 | Integrated stress responses signaling pathway**.** ER stress, mitochondria stress or heme depletion, amino acid deficiency and ds-RNA virus infection activate PERK, HRI, GCN2 and PKR sensor kinases, leading to phosphorylation of eIF2α. eIF2α phosphorylation causes global inhibition of protein synthesis but selective translation of ATF4 mRNA. ATF4 binds to DNA targets to regulate the expression of genes that promote cellular adaptation, survival and apoptosis. Feedback regulation of ISR is regulated by constitutively expressed phosphatase complex CReP-PP1 and inducible phosphatase GADD34-PP1, which dephosphorylate eIF2α and attenuate or terminate ISR. AA, Amino acid; ER, Endoplasmic reticulum.

ATF4 plays an important role in communicating pro-survival and pro-apoptotic signals. Once activated, ATF4 regulates transcriptional programs involved in cell survival (antioxidant response, amino acid biosynthesis and autophagy), senescence and apoptosis. The final outcome of ATF4 activation is dependent on the cell type, nature of stressors and duration of the stresses (**Figure 1**) (Wang et al., 2015; Wortel et al., 2017; Ojha et al., 2019; Tameire et al., 2019).

The Integrated Stress Response and Cell Survival

The ISR promotes cellular survival signaling by negative regulation of cell death pathways, such as apoptosis. For instance, as a consequence of ER stress, PERK-induced activation of the ISR results in the expression of cIAP1 and cIAP2 (cellular inhibitor of apoptosis proteins) in tumor and non-tumor cells (Hamanaka et al., 2009; Hu et al., 2004; Warnakulasuriyarachchi et al., 2004). Previously, it was demonstrated that restoration of the function of cIAP1 or cIAP2 in PERK$^{-/-}$ murine embryonic fibroblasts during ER stress delays the early onset of ER stress-induced caspase activation and apoptosis seen in these cells (**Figure 2**) (Hamanaka et al., 2009).

ATF4 has also been demonstrated to facilitate anti-neoplastic agent bortezomib-induced upregulation of anti-apoptotic myeloid cell leukemia-1 (Mcl-1) protein, which is an anti-apoptotic Bcl-2 family protein that plays essential roles in multiple myeloma survival and drug resistance in many tumor types (**Figure 2**) (Hu et al., 2012).

It has been shown that both MCL-1 and cIAPs can suppress apoptosis at different points in the apoptosis pathway that are upstream and downstream of the release of cytochrome c from the mitochondria. Mitochondrial cytochrome c plays a dual function in controlling both cellular energetic metabolism and apoptosis. It has been shown that, upon interacting with apoptotic protease activating factors (Apaf), cytochrome c can trigger the activation cascade of caspases once it is released from the mitochondria into the cytosol (Cai et al., 1998).

It has also been reported that miR-211 is a pro-survival microRNA that regulates CHOP expression in a PERK-dependent manner and thus PERK can mediate a pro-survival function by suppressing a stress-dependent expression of CHOP consequently leading to re-establishment of cellular homeostasis before the initiation of apoptosis (Chitnis et al., 2012). In addition to its beneficial roles in restoring homeostasis, these ISR mechanisms may also contribute to tumor development. For example, an increased miR-211 expression, found to be PERK-dependent, and was reported in mammary carcinoma and mouse models of human B-cell lymphoma (**Figure 2**) (Chitnis et al., 2012).

Cancer cells use multiple stress response pathways such as the integrated stress response (ISR), cytosolic heat shock response (HSR), and unfolded protein response (UPR) mediated by organelles such as the endoplasmic reticulum (ER) and mitochondria to respond exogenous and endogenous or environmental stresses to evade apoptosis, ensure survival, proliferation, metastatic potential, and maintain cellular homoeostasis (O'Malley et al., 2020). For example, to evade apoptosis and ensure survival, cancer cells may utilize the mitochondrial unfolded protein response (UPRmt) pathway and associated key proteins including chaperones HSP10, HSP60, and mtHSP70 and proteases ClpP and LONP1 to eliminate proteotoxic stress (**Figure 2**) (O'Malley et al., 2020). Notably, upregulation of HSP60 expression and its upstream regulator ATF5 has been shown to enhance the apoptotic threshold in cancer cells resulting in therapeutic resistance in many cancer types. ATF-5 has been reported to regulate expression of Egr-1, BCL-2, and MCL1 to mediate proliferation and survival in cancer (Dluzen et al., 2011; Liu et al., 2011; Karpel-Massler et al., 2016).

Moreover, in addition to the genes mentioned above many other genes activated in response to ISR (Costa-Mattioli and Walter, 2020), including those encoding ATF4, ATF5 (Zhou et al., 2008); CHOP (C/EBP-homologous protein) (Palam et al., 2011); GADD34 (Growth Arrest And DNA-Damage-Inducible 34) (Lee et al., 2009); and in neurons, OPHN1 (Oligophrenin-1) (Di Prisco et al., 2014), other genes such as IBTKα (the α isoform of inhibitor of Bruton's tyrosine kinase) (Baird et al., 2014) and NUPR1 (Nuclear protein-1), also play

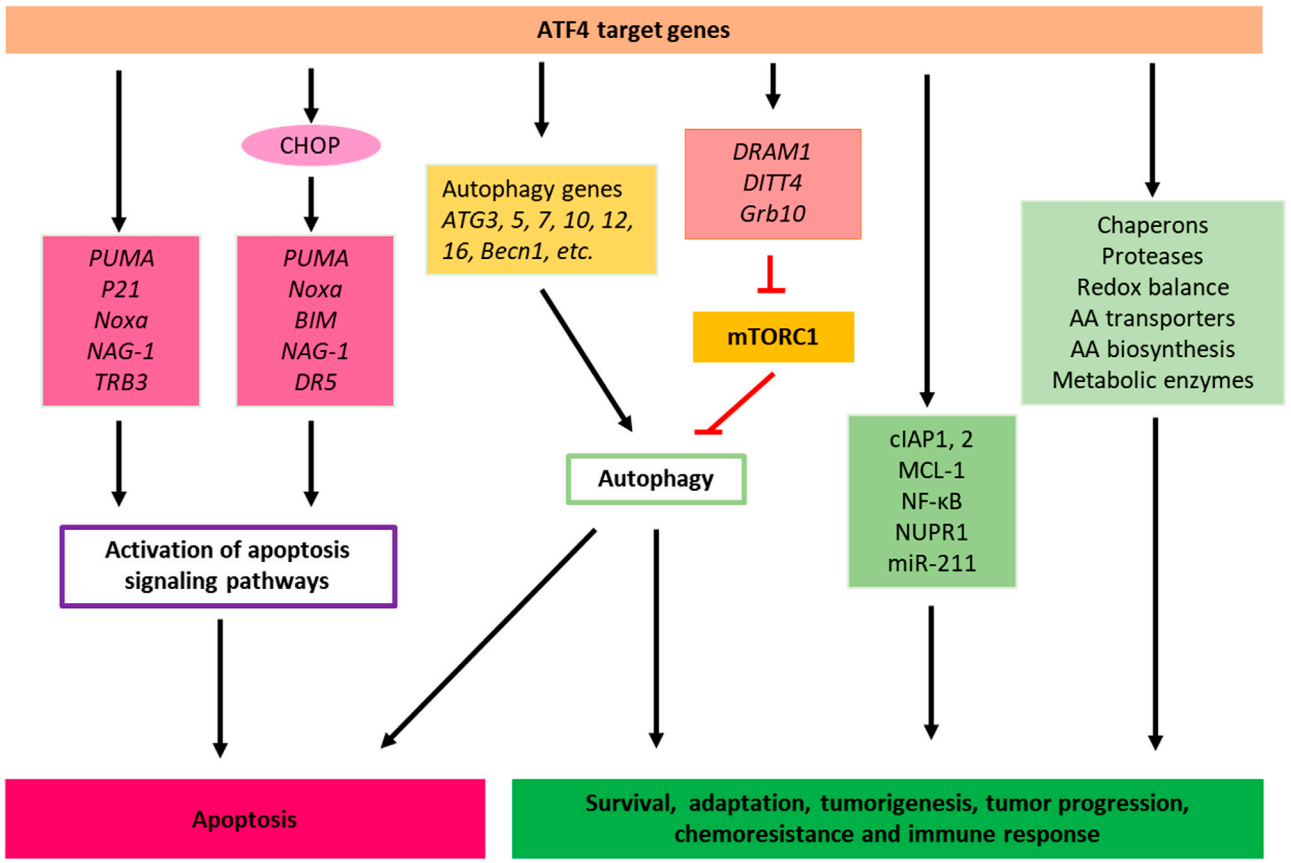

FIGURE 2 | Cell death, pro-survival, tumor progression and chemoresistance pathways of ISR. ATF4 directly or indirectly controls the transcription of apoptotic, adaptive, tumor progression and chemoresistance genes. When stress persists (for example, drug treatments) and cancer cells are unable to adapt to and reach homeostasis though the activation of ISR, ATF4 shifts this balance towards apoptosis by inducing apoptotic genes. AA, Amino acid.

important roles in cell survival. NUPR1 has been found to play an important role in cell stress and stress-related apoptosis (Martin et al., 2021) and inactivation of NUPR1 promotes cell death by coupling ER-stress responses with necrosis (Santofimia-Castaño et al., 2018). More evidences suggest that ATF4 initiates the activity of transcription factor NUPR1. NUPR1 regulates the expression of several metabolic stress-responsive genes, in particular, genes required in cell cycle regulation and DNA repair, as such, NUPR1 also is regarded as pro-survival factors (**Figure 2**) (Jin et al., 2009; Hamidi et al., 2012).

Another gene activated during the ISR is the IBTKα which is activated during ER stress. IBTKα is a major substrate adaptor for protein ubiquitination and is an essential pro-survival factor (Baird et al., 2014).

Likewise, eIF2α mediated translational repression has been suggested in activated B cell NF-κB pathway induction as a mechanism to protect cells against ER stress (Deng et al., 2004). In a recent study, a pharmacologically activable version of PERK was used to uncouple eIF2α phosphorylation from stress and it was determined that eIF2α phosphorylation is both required and adequate to activate both NF-κB DNA binding and an NF-κB reporter gene (Deng et al., 2004). Also, HRI has been shown to be involved in NF-κB activation (Abdel-Nour et al., 2019). This study found that the eIF2α kinase HRI controls NOD1 (Nucleotide-binding oligomerization domain-containing protein 1) signalosome folding and activation through a process requiring eIF2α, ATF4, and the heat shock protein HSPB8 (Abdel-Nour et al., 2019). Moreover, HRI/eIF2α signaling pathway was shown to be required for signaling downstream of the innate immune mediators including NOD2, MAVS (Mitochondrial antiviral-signaling protein), and TRIF (TIR-domain-containing adapter-inducing interferon-β) but dispensable for signaling pathways that rely on MyD88 (Myeloid differentiation primary response 88) or STING (Stimulator of interferon genes) (**Figure 2**) (Abdel-Nour et al., 2019).

The Integrated Stress Response and Activation of Autophagy

Autophagy is a highly regulated eukaryotic cellular pathway that plays a major role in the lysosomal degradation of cytoplasmic unfolded proteins, peptides, damaged organelles or cytosolic components while also serving as a means to replenish depleted amino acids for building proteins and to provide energy to a starved cell. Autophagy can be activated by a variety of cellular stresses such as nutrient or growth factor deprivation, hypoxia, reactive oxygen species, DNA damage, protein aggregates,

damaged organelles, or intracellular pathogens (Pakos-Zebrucka et al., 2016; Clementi et al., 2020; Akman et al., 2021). Autophagy can be activated both *via* specific, stimulus-dependent manner and more general, stimulus-independent signaling pathways to coordinate different phases of autophagy.

The ISR can modulate cell survival and cell death pathways through the activation of autophagy and the phosphorylation of eIF2α at S51 appears to be essential for stress-induced autophagy (Pakos-Zebrucka et al., 2016). Autophagy can be integrated with other cellular stress responses through parallel stimulation of autophagy and other stress responses by specific stress stimuli, through dual regulation of autophagy and other stress responses by multifunctional stress signaling molecules, and/or through mutual control of autophagy and other stress responses.

PERK Regulates Autophagy

Although mechanisms by which phosphorylated eIF2α induces autophagy are still not completely elucidated, specific extrinsic and intrinsic stresses that lead to the phosphorylation of eIF2α have been demonstrated to trigger autophagy. For instance, ER stress increases phosphorylation of eIF2α and ensuing upregulation of certain autophagy receptors including *SQSTM1, NBR1*, and *BNIP3L* through PERK (Deegan et al., 2015). Likewise, inhibition of PERK pharmacologically suppresses transcriptional upregulation of these autophagy receptors in mammalian cells (Deegan et al., 2015).

Furthermore, phosphorylation of eIF2α mediated by PERK increases the conversion of ATG12 and LC3 due to the expression of polyQ72 aggregates in C2C5 cells, which is an essential step for autophagy formation (Kouroku et al., 2007). This PERK-mediated Unfolded Protein Response (UPR) has been shown to regulate autophagy from induction, to vesicle nucleation, phagophore elongation, and maturation (Deegan et al., 2013).

Moreover, it was reported that ER stress due to bluetongue virus infection of cells leads to autophagy through the activation of the PERK-eIF2α pathway (Lv et al., 2015). The UPR which is initiated in response to the accumulation of misfolded proteins in the ER leading to stress is predominantly an adaptive response to the activation of the ISR. It was shown that UPR protects human tumor cells during hypoxia through regulation of the autophagy genes MAP1LC3B and ATG5 (Rouschop et al., 2010) and this was mediated by PERK phosphorylation of eIF2α. Conversely, abrogation of PERK signaling or expression of mutant eIF2α S51A which cannot be phosphorylated under the condition of hypoxia reduces the transcription of *MAP1LC3B* and *ATG5* (Rouschop et al., 2010).

IRS-induced autophagy also can lead to cell death. A recent paper reported that compound SH003 induces autophagy and autophagic cell death through a PERK-eIF2α-ATF4-CHOP signaling pathway in human gastric cancer cells (**Figure 2**) (Kim et al., 2020).

General Control Non-Derepressible 2 Regulates Autophagy

Similarly, amino acid deprivation in cancer cells leads to the phosphorylation of eIF2α mediated by GCN2 which is required for the activation of autophagy (Ye et al., 2010). Notably, while *GCN2* knockout cells exhibited decreased LC3 expression, cells with mutant the eIF2α S51A were not able to activate the processing of LC3 (Ye et al., 2010). Likewise, in the regulation of autophagy induced by amino acid starvation, phosphorylation of eIF2α at S51 was found to be required in yeast and mouse embryonic fibroblasts (MEFs) (Tallóczy et al., 2002). These findings suggest that eIF2α phosphorylation at S51 forms the central hub between different stresses and activation of autophagy.

Downstream of eIF2α phosphorylation, although ATF4 has been implicated to be essential for activation of autophagy, other mechanisms directed from eIF2α phosphorylation other than selective translation of ATF4 mRNA might also be involved in the activation of the autophagy process (Kroemer et al., 2010). It was previously suggested that phosphorylation of eIF2α might affect the ER in a manner that promotes the physical formation of the isolation membrane. Alternatively, eIF2α phosphorylation might stimulate autophagy through its effects on the transactivation of autophagy genes. eIF2α phosphorylation stimulates the selective translation of the ATF4 transcription factor, which stimulates LC3 expression which is essential for sustained autophagy (Milani et al., 2009; Kroemer et al., 2010). Furthermore, although autophagy interaction network components play important roles in vesicle trafficking, protein or lipid phosphorylation and protein ubiquitination and there are direct interactions between eIF2α subunits and core autophagy proteins, whether these interactions are biologically significant is not clearly understood (Behrends et al., 2010).

Under conditions of ER stress or amino acid deprivation, there is transcriptional upregulation of key autophagy genes mediated by ATF4 including *MAP1LC3B* and *ATG5* which are required for autophagosome biogenesis and function (Deegan et al., 2015; Rzymski et al., 2010; B'Chir et al., 2013). ATF4 can also upregulate the DITT4/REDD1 and DRAM1, which represses the activity of mTORC1, subsequently inducing autophagy (**Figure 2**) (Kazemi et al., 2007; Whitney et al., 2009; Dennis et al., 2013; Tian et al., 2021).

Furthermore, ATF4 activation in response to amino acid deprivation also directs an autophagy gene transcriptional program by upregulating several autophagy genes such as *Atg3, Atg5, Atg7, Atg10, Atg12, Atg16, Becn1, Gabarap, Gabarapl2, Map1lc3b,* and *Sqstm*1 (**Figure 2**) (B'Chir et al., 2013). Through the stimulation of key genes involved in autophagy, the ISR mediates the up-regulation of the autophagic process in an attempt to resolve the stress induced by amino acid deprivation. This is accomplished by the increased recycling of cytoplasmic components and sustaining the biosynthetic capacity of the cell and cellular ATP concentrations. The increased autophagic function leads to increased amino acid levels in ER required for *de novo* protein biosynthesis and similarly leads to increased levels of substrates including free fatty acids and amino acids for the tricarboxylic acid cycle (Rzymski et al., 2009; Ye et al., 2010).

However, it was also shown that a variety of autophagy genes can have a varying degree of reliance on ATF4 and CHOP signaling and that the transcriptional upregulation of such

genes is regulated by the ratio of ATF4 and CHOP proteins that are bound to a particular promoter, and thus fine-tuning the expression of autophagy genes depending on the needs of the cell (B'Chir et al., 2013).

Studies on the effect of proteasome inhibition on survival signaling by the ISR have revealed that suppression of proteasome function pharmacologically using antineoplastic agent bortezomib results in depletion of amino acids in the ER required for protein synthesis leading to the activation of the ISR *via* GCN2 stress sensor (Suraweera et al., 2012).

Amino acid depletion as a result of proteasome inhibition also activates autophagy through mTOR in an attempt to restore amino acid homeostasis (Suraweera et al., 2012). Conversely, exogenous supplementation of essential amino acids depleted by the inhibition of proteasome function inhibition attenuates the phosphorylation of eIF2α and down-regulates autophagy (Suraweera et al., 2012). As such, depletion of amino acids by proteasome inhibition establishes a link between ISR activation and induction of autophagy in an attempt to sustain the survival of the cell.

Heme-Regulated eIF2α Kinase Regulates Autophagy

Although the other eIF2α kinases are present across different tissues, eIF2α kinase HRI is more specific to erythroid cells and plays a major role in erythrocyte differentiation during erythropoiesis (Suraweera et al., 2012). eIF2α kinase HRI mediates the translation of globin mRNAs with the availability of heme for the production of hemoglobin. By doing so, HRI protects erythroid cells from the increase of toxic globin aggregates under conditions of iron deficiency (Bruns and London, 1965; Chefalo et al., 1998; Han et al., 2001; Suragani et al., 2012). Other stresses such as arsenite-induced oxidative stress, heat shock, osmotic stress, 26S proteasome inhibition, and nitric oxide also were shown to activate HRI (Han et al., 2001; Lu et al., 2001; McEwen et al., 2005; Yerlikaya et al., 2008; Ill-Raga et al., 2015) and activation of HRI by these stresses is independent of heme and heat shock proteins HSP90 and HSP70 facilitates this process; however, the exact mechanism of HRI activation is still being studied (Lu et al., 2001).

A recent report demonstrated that HRI controls autophagy to clear cytosolic protein aggregates (Mukherjee et al., 2021). In that study, researchers found that the eIF2α kinase HRI induced a cytosolic unfolded protein response to prevent aggregation of innate immune signalosomes. Furthermore, they demonstrated that HRI controls autophagy to clear cytosolic protein aggregates when the ubiquitin-proteasome system is inhibited (Mukherjee et al., 2021).

Growth factor receptor-bound protein 10 (Grb10) is regulated by ATF4 (Zhang et al., 2018). the HRI-eIF2αP-ATF4 pathway suppresses mTORC1 signaling through Grb10 specifically in the erythroid lineage (**Figure 2**) (Zhang et al., 2018). mTORC1 was shown to act as a master regulator of autophagy since inhibition of mTORC1 was required to initiate the autophagy process (Dossou and Basu, 2019). It was also shown that mTORC1 directly regulates the downstream steps of the autophagy process, such as the nucleation, autophagosome elongation, autophagosome maturation and termination (Dossou and Basu, 2019).

PKR Regulates Autophagy

Talloczy, Z. et al. report that PKR acts as a potent inducer of autophagy during viral infection (Tallóczy et al., 2006). Also, two papers indicate that PKR is very important for the autophagic degradation of herpes simplex virions both *in vitro* and *in vivo* (Tallóczy et al., 2006; Orvedahl et al., 2007). In these settings, PKR was shown to operate upstream of Beclin 1 (Tallóczy et al., 2006).

Shen, S. et al. report that STAT3 inhibitors (JSI-124, WP1066 and Stattic) caused the disruption of inhibitory STAT3-PKR interactions in human osteosarcoma U2OS cells, resulting in release and activation of PKR. PKR phosphorylates eIF2α, which regulates the activity of Beclin 1/Vps34 complex and facilitates autophagy induction (**Figure 3**) (Shen et al., 2012).

Pathogenic bacterium *Mycobacterium tuberculosis* (Mtb) infection induces the activation of PKR and PKR-mediated autophagy in macrophage. Sustained expression and activation of PKR reduced the intracellular survival of Mtb, which could be enhanced by Interferon gamma (IFNγ) treatment (Smyth et al., 2020).

The Integrated Stress Response and Cell Death

The cell death pathways are complex and can be exploited by cancer therapeutic agents (Carneiro and El-Deiry, 2020). When stress persists and cells are unable to reach homeostasis despite the activation of stress response pathways, ATF4 can induce the transcriptional activation of apoptotic genes encoding CHOP (DDIT3) (Harding et al., 2000), TRB3 (Tribbles homolog 3) (Ohoka et al., 2005), and pro-apoptotic BH3-only proteins including PUMA (p53 upregulated modulator of apoptosis), Noxa (Phorbol-12-myristate-13-acetate-induced protein 1) and BIM (Bcl-2 Interacting mediator of cell death), thus leading to cell death (Galehdar et al., 2010; Altman et al., 2009; Puthalakath et al., 2007). ATF4 has been shown to regulate Noxa at the transcriptional level and this leads to the induction of apoptosis (Sharma et al., 2018; Núñez-Vázquez et al., 2021). Overall, through the induction of ATF4, this transcription factor appears to mainly trigger the intrinsic apoptosis by modulating the expression of pro- and anti-apoptotic BCL-2 family members. Interestingly, in the case of CHOP activation, induction of DR5 (Death receptor 5) mediated apoptosis appeared to be DR5 ligand binding independent and involving the engagement of FADD (Fas-associated protein with death domain) and caspase-8 (**Figure 2**) (Lu et al., 2014; Li et al., 2015).

Additional stresses such as those resulting from decreased mitochondrial translation (Sasaki et al., 2020) as well as the generation of reactive oxygen species (Kasai et al., 2019) have been shown to induce ATF4 expression. In the case of sustained mitochondrial deficiency, ATF4 response has been reported to lead to p53-mediated apoptosis (Evstafieva et al., 2014). Reactive oxygen species generated by Fenretinide treatment in neuroblastoma cells activates ATF4 leading to the induction of Noxa ultimately leading to apoptosis (Nguyen et al., 2019). In multiple myeloma cells, sensitivity to bortezomib treatment was associated with higher expression of ATF4 and loss of its expression lead to lower levels of Noxa, CHOP and DR5

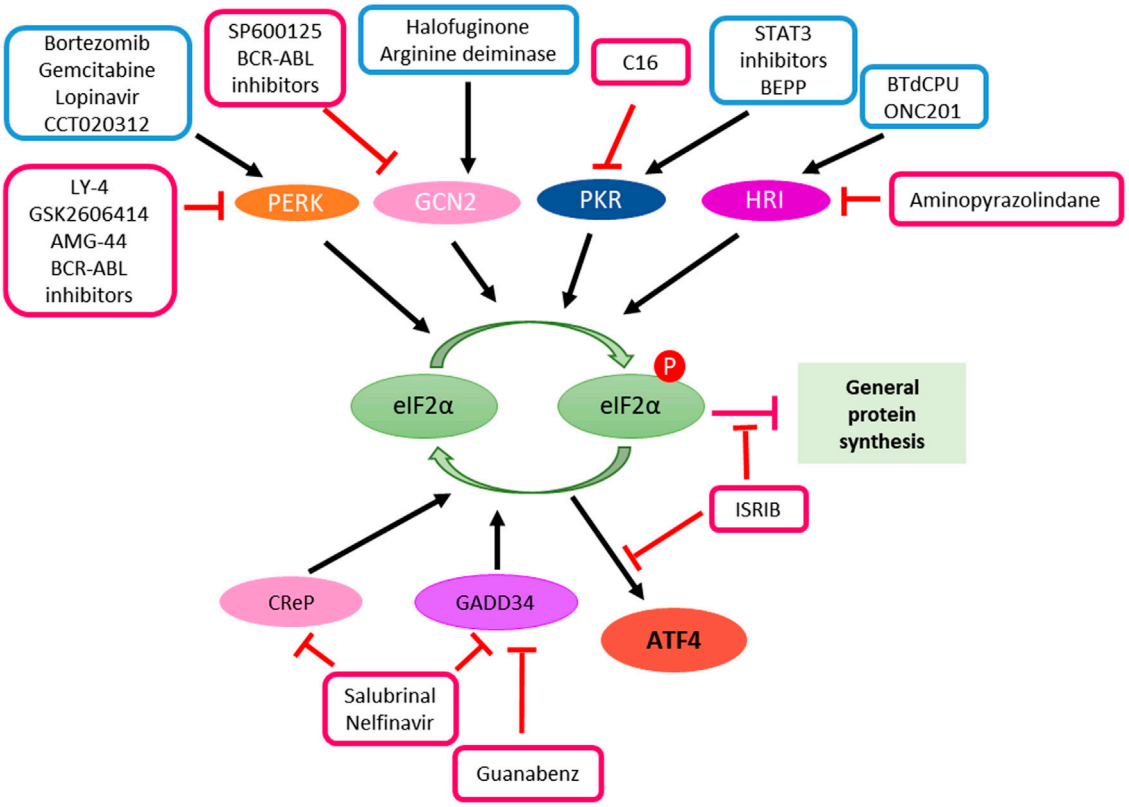

FIGURE 3 | Manipulation of ISR in cancer therapy. ATF4 induction can be achieved either through kinase activators such as bortezomib, gemcitabline, lopinavir, CCT020312, halofuginone, arginine deiminase, STAT3 inhibitors, BEPP, BTdCPU and ONC201 or the inhibitors of phosphatases such as salubrinal, guanabenz and nelfinavir. In the case of ISR promotes cancer cell survival and resistant to therapeutic treatments, inhibition of ATF4 can be achieved by kinase inhibitors such as LY-4, GSK2606414, AMG-44, BCR-ABL inhibitors, SP600125, C16 and aminopyranzolindane or compound ISRIB downstream of eIF2α phosphorylation.

(Narita et al., 2015). Recent work from our lab has also implicated ATF4 responsible for the induction of p53-target genes PUMA, Noxa, NAG-1(Nonsteroidal anti-inflammatory drug-activated gene-1)and DR5 upon treatment with prodigiosin analogue PG3-Oc (**Figure 2**) (Tian et al., 2021).

The aforementioned studies involve the induction of the ISR machinery in addition to distinct components of autophagy, cell cycle, and/or apoptosis pathway. This reflects the complexity of the interplay of these cellular pathways which remains underscored and likely to be context-dependent. Recent work has focused on post-translational modifications of ATF4 and how these affect the transcriptional control and cellular response. ATF4 has numerous sites that can be post-translationally modified including phosphorylation at various threonine and serine sites, methylation at arginine 239, and ubiquitination and acetylation at lysine residues (Wortel et al., 2017). These post-translational modifications affect ATF4 protein stability, activation and interaction with other proteins. In the case of apoptosis, methylation at arginine 239 by methyl transferase PRMT1 was found to be associated with the transcription of genes related to apoptosis (Yuniati et al., 2016). Further insight into ATF4 activation may shed light on understanding the context of how these transcription factors respond to stress and the biological outcome they ultimately trigger in both normal and cancer cells. Importantly, this will aid the intervention of novel therapies, the use of the ISR as potential biomarker for predicting therapy response and the combination of therapies that induce ATF4-mediated apoptosis. An example of therapy combination has been observed in *in vivo* neuroblastoma preclinical models with the BCL-2 inhibitor Venetoclax and Fenretinide (Nguyen et al., 2019). This studied combination highlighted the use of BCL-2 expression as a biomarker for neuroblastoma patients. A separate study in multiple myeloma suggested the use of ATF4 as a predictive therapy response biomarker for bortezomib and dexamethasone combination treatment (Narita et al., 2015). These studies exemplified the clinical translational applicability of exploiting the ISR in cancer therapy and highlight its warrant understanding to predict cancer types that will benefit from ISR modulating therapies.

Dual Roles of the Integrated Stress Response in Cancer

The ISR plays different roles in tumorigenesis and tumor progression in different types of tumors. Hypoxia is a common phenomenon in solid tumors. It may induce apoptosis of tumor cells or tumor cells may develop the ability to adapt to the hypoxia or anoxic environment. Hypoxia can induce ISR gene expression in transformed mouse embryonic fibroblasts and the activated ER stress response confers resistance

to apoptosis induced by hypoxia and thus facilitates tumor growth (Ameri et al., 2004). ISR mediator ATF4 is induced by anoxia in breast cancer cell lines (Ameri et al., 2004). The activated ISR plays an essential role in the adaptation to hypoxic stress allowing tumor cell survival under stress and is associated with resistance to therapy (Blais et al., 2004; Rouschop et al., 2013).

It was found that loss of extracellular matrix (ECM) attachment stimulates ISR signaling *in vitro*. And the activation of ISR further plays a critical role in resistance to anoikis and is required for metastasis (Dey et al., 2015). The ISR also has impact on the tumor microenvironment. Tumor cells undergoing ER stress can transmit ER stress to myeloid cells contributing to a pro-inflammatory tumor microenvironment, thus facilitating tumor progression (Mahadevan et al., 2011).

The role of ISR may be complex in tumors. In medulloblastoma, the ISR is activated, and the decreased ISR *via* gene manipulation attenuates medulloblastoma formation. Moderately enhanced ISR by gene manipulation noticeably increased the incidence of medulloblastoma, whereas a strongly enhanced ISR significantly decreased the incidence of medulloblastoma *in vivo*. Thus, the ISR plays dual roles in medulloblastoma formation (Stone et al., 2016).

Activation of the ISR is correlated with resistance to chemotherapy in pancreatic cancer and BRAF-mutated melanoma. Gemcitabine can induce ISR and the antiapoptotic pro-survival factors *via* the ISR pathway in pancreatic cancer cell line and the combination of gemcitabine + ISRIB which inhibits ISR induce more apoptosis *in vivo* (Palam et al., 2015). In BRAF-mutated melanoma, chronic ER stress involving induction of the ISR signaling pathway activates autophagy which contributes chemoresistance (Corazzari et al., 2015).

Triggering ISR can be a therapeutic strategy against cancer, since the ISR can induce apoptosis. ONC201 kills solid tumors by triggering ISR-dependent ATF4 activation and activation of the TRAIL-DR5 apoptotic pathway (Kline et al., 2016). In breast cancer, GBM and DMG cell lines, ONC201 induces ISR, TRAIL-DR5 and ultimately apoptosis (Zhang et al., 2021). The apoptosis increases with the enhancement of ISR induction by tazemetostat. The knockdown of ATF4 in GBM cell line reduced the apoptosis induced by ONC201 and the combination of ONC201 with tazemetostat or vorinostat remarkably. Therefore, induction of ISR can play an essential role in cell death of cancer cells. Apoptosis induced by ISR activation was also observed in AML cells (Ishizawa et al., 2016).

The combination of mitochondrial uncoupler niclosamide ethanolamine and dopamine receptor antagonist domperidone or TCAs induces ISR and leas to apoptosis in multiple cancer cell lines including CRC, GBM (Glioblastoma multiforme) and PDAC (Pancreatic ductal adenocarcinoma) cell lines (Hartleben et al., 2021). Even without inducing apoptosis, the ISR is induced by ONC201 in cancer cells exhibiting decreased cell proliferation (Kline et al., 2016).

The ISR contributes to drug sensitivity of cancer cells. Activation of the ISR in HER2+breast cancer contributes the sensitivity to Trastuzumab *in vivo*. Increased expression of the ISR mediator eIF2α-P predicts a better response of patients with HER2+ metastatic breast cancer to Trastuzumab therapy (Darini et al., 2019). Proteasome inhibitors are known to activate the ISR and lower expression of ISR markers thus implicating shorter progression-free survival in multiple myeloma (Obeng et al., 2006).

It was reported that ISR promotes the expression of potential target for immunotherapy (Obiedat et al., 2020). Thus, ISR may play a role in cancer immunotherapy.

On the one hand, activation of ISR plays a role in cancer therapy. On the other, Inhibition of ISR activation can increase the vulnerability of cancer cells. BCR-ABL inhibition prevents activation of ISR in K562 cell line derived from a chronic myeloid leukemia (CML) patient and makes the tumor cells more vulnerable to metabolic stress (Kato et al., 2018). Summaries of the mentioned cases and drugs can be found in the **Table 1**, **Table 2** and **Figure 3**.

Manipulation of Integrated Stress Response in Cancer Therapy

The ISR takes a dual role in cell survival and cell death. Enhance or inhibition of ISR signaling *via* targeting ISR components is a promising strategy for cancer therapy (**Figure 3**). Among the components in ISR signaling, eIF2α is a core component and an important focused for cancer therapy.

Enhanced Integrated Stress Response Signaling *via* Increased eIF2α Kinase

eIF2α is a core component of the ISR, and phosphorylation of eIF2α is regulated by upstream regulators. One of approaches is to phosphorylate eIF2α by increasing eIF2α kinases upstream of eIF2α, such as GCN2, PERK, and HRI (Pakos-Zebrucka et al., 2016; Chu et al., 2021). Most of eIF2α activators are small molecules. Halofuginone and arginine deiminase are GCN2 activators (Long et al., 2013; Castilho et al., 2014). BTdCPU and ONC201 activates HRI (Kline et al., 2016; Chen et al., 2011). Bortezomib, gemcitabine, lopinavir and CCT020312 selectively activates PERK (Narita et al., 2015; Palam et al., 2015; Obeng et al., 2006; Obiedat et al., 2020; Stockwell et al., 2012). BEPP works on PKR activation (**Figure 3**) (Hu et al., 2009). These elF2α kinase activators have been studied in cancer therapy. For example, Halofuginone and arginine deiminase were found to inhibit tumor growth, development and metastasis either as single agents or in combination with 5-FU or radiation (Abramovitch et al., 2004; Kim et al., 2009; Cook et al., 2010; Spector et al., 2010; Lamora et al., 2015; Brin et al., 2018; Singh et al., 2019; Wang et al., 2020; Huang and Hu, 2021). Our laboratory has identified two small molecules PG3-Oc (Tian et al., 2021) and ONC201 (Kline et al., 2016; Ishizawa et al., 2016) that suppress tumor growth through increased ISR signaling. These drugs enhance ISR signaling *via* activation of eIF2α kinases, and sequentially enhance or sustain eIF2α phosphorylation.

Another approach for eIF2α phosphorylation is to prevent eIF2α dephosphorylation from eIF2α phosphatase. GADD34 (PPP1R15A) and CReP recruit phosphatase PP1 to

TABLE 1 | The dual roles of ISR in various cancers.

Role of ISR in cancers	Cancer type
Mediator of ISR is up-regulated in anoxic tumor cells	Breast cancer Ishizawa et al. (2016)
Mediator of ISR is up-regulated in hypoxic tumor cells	Cervical cancer Hartleben et al. (2021)
Adaptation to hypoxia	Glioblastoma and colorectal cancer Darini et al. (2019)
Promotes survival of therapy-resistant hypoxic tumor cells	Glioblastoma Darini et al. (2019)
Contribute to the resistance to anoikis and promote metastasis	Fibrosarcoma Obeng et al. (2006)
ER stress is transmitted from tumor cells to myeloid cells and then facilitate tumor progression	Prostate cancer Obiedat et al. (2020)
Increase or decrease the incidence of tumor	Medulloblastoma Kato et al. (2018)
Contributes to chemoresistance	BRAF mutated melanoma Long et al. (2013)
Contributes drug sensitivity to Trastuzumab	HER2+ breast cancer Lamora et al. (2015)

TABLE 2 | Effects of ISR compounds in the treatments of cancers.

Compounds	Effect on ISR	Effects of ISR on tumor cells	Cancer type
Gemcitabine	Induce ISR	Contributes to chemoresistance	Pancreatic cancer Palam et al. (2015)
Bortezomib	Induce ISR	Contributes drug sensitivity	Multiple myeloma Obeng et al. (2006); Narita et al. (2015)
ONC201	Induce ISR	Reduce cell-viability	Lung cancer, thyroid cancer, prostate cancer Kline et al. (2016)
ONC201	Induce ISR	Induce apoptosis	Colorectal cancer, breast cancer, glioblastoma, diffuse midline glioblastoma, AML Kline et al. (2016); Ishizawa et al. (2016); Zhang et al. (2021)
Mitochondrial uncoupler niclosamide ethanolamine + dopamine receptor antagonist domperidone or tricyclic antidepressants (TCAs)	Induce ISR	Induce apoptosis	Colorectal cancer, glioblastoma and PDAC Hartleben et al. (2021)
Nelfinavir and lopinavir	Induce ISR	Promote the expression of potential target for immunotherapy	Melanoma Obiedat et al. (2020)
BCR-ABL inhibitors	Prevent ISR activation	Enhance apoptosis	CML Kato et al. (2018)

phosphorylated-eIF2α and this results in dephosphorylation of eIF2α. Salubrinal is the first small molecule discovered to inhibit eIF2α dephosphorylation *via* both GADD34 and CReP (Boyce et al., 2005). Inhibition of GADD34 activity by Guanabenz or its derivatives results in high levels of eIF2α Phosphorylation (Tsaytler et al., 2011). Different from Guanabenz, Nelfinavir increases phosphorylation of eIF2α by downregulating CReP in addition to it effect on GADD34 (De Gassart et al., 2016). Guanabenz has been found to sensitize glioblastoma cancer cells to sunitinib in combinatorial treatment (**Figure 3**) (Ho et al., 2021).

Inhibition of Integrated Stress Response Signaling by Reduction of eIF2α Kinase

Inhibition of ISR signaling may overcome drug resistance in cancer. One of the approaches is to inhibit eIF2α kinase upstream of eIF2α. Most of these kinase inhibitors compete with ATP to block their kinase domain. SP600125 and BCR-ABL inhibitors inactivate GCN2 (Kato et al., 2018; Robert et al., 2009). Amino-pyrazolindine inhibits HRI (Rosen et al., 2009). Imidazolo-oxindole PKR inhibitor C16 specifically inhibits PKR (Jammi et al., 2003). LY-4, AMG-44, BCR-ABL inhibitors and GSK2606414 inactivate PERK (Tameire et al., 2019; Kato et al., 2018; Axten et al., 2012; Mohamed et al., 2020). They bind to the eIF2α kinase in an ATP-competitive manner, result in inhibition of kinase activity, and reduce the phosphorylation of eIF2α. Another approach is to terminate eIF2α signaling downstream of eIF2α. Small-molecule ISRIB prevents the formation of stress granules caused by eIF2α phosphorylation, thus, impairing ATF4 synthesis (**Figure 3**) (Sidrauski et al., 2015).

Targeting Integrated Stress Response in Combination of Immunotherapy

High levels of PD-L1 on the cancer cell surface allows evasion from T cell attack by binding to the PD-1 receptor on T cells. Disruption of the PD-1/PD-L1 checkpoint can result in cytotoxic T cell killing of tumors. The ISR was found to increase PD-L1 translation in human cancers. Suresh et al. (2020) The increased PD-L1 suppress anti-tumor immune responses. PERK signaling was found to suppress immune responses by increasing tumor-myeloid-derived suppressor cells (MDSC). PERK blockade transforms MDSC's into myeloid cells that activate anti-tumor CD8+ T-cell immunity in the tumor microenvironment. AMG-44, a PERK inhibitor, in combination with Anti-PD-L1 showed a synergistic anti-tumor effect in B16 tumor-bearing mice model (**Figure 3**) (Mohamed et al., 2020). These studies suggest that PERK inhibitors enhance the antitumor efficacy of immune checkpoint inhibitors. Therefore, targeting ISR in combination

with immune checkpoint is an innovational strategy for cancer therapy.

CONCLUSION

The ISR is a double-edged sword with pro-survival and pro-death activities that may impact on tumor progression and response to therapy. Our approach for therapeutic targeting of cell death pathways has led us to uncover the ISR as a critical signaling component and target of drug candidates. The fact that the ISR can lead to alternative cell fates depending on cellular context suggests that greater efforts need to be directed at understanding its regulation and finding new ways for its modulation. The ISR holds promise for cancer therapy development.

AUTHOR CONTRIBUTIONS

All authors listed have made a substantial, direct, and intellectual contribution to the work and approved it for publication.

FUNDING

WE-D. is an American Cancer Society Research Professor and is supported by the Mencoff Family University Professorship at Brown University. This work was supported by an NIH grant (CA173453) and a grant from the Warren Alpert Foundation to WE-D. This work was supported by the Teymour Alireza P′98, P′00 Family Cancer Research Fund established by the Alireza Family.

REFERENCES

Abdel-Nour, M., Carneiro, L. A. M., Downey, J., Tsalikis, J., Outlioua, A., Prescott, D., et al. (2019). The Heme-Regulated Inhibitor Is a Cytosolic Sensor of Protein Misfolding that Controls Innate Immune Signaling. *Science* 365 (6448). doi:10.1126/science.aaw4144

Abramovitch, R., Itzik, A., Harel, H., Nagler, A., Vlodavsky, I., and Siegal, T. (2004). Halofuginone Inhibits Angiogenesis and Growth in Implanted Metastatic Rat Brain Tumor Model-Aan MRI Study. *Neoplasia* 6 (5), 480–489. doi:10.1593/neo.03520

Akman, M., Belisario, D. C., Salaroglio, I. C., Kopecka, J., Donadelli, M., De Smaele, E., et al. (2021). Hypoxia, Endoplasmic Reticulum Stress and Chemoresistance: Dangerous Liaisons. *J. Exp. Clin. Cancer Res.* 40 (1), 28. doi:10.1186/s13046-020-01824-3

Altman, B. J., Wofford, J. A., Zhao, Y., Coloff, J. L., Ferguson, E. C., Wieman, H. L., et al. (2009). Autophagy Provides Nutrients but Can lead to Chop-dependent Induction of Bim to Sensitize Growth Factor-Deprived Cells to Apoptosis. *Mol. Biol. Cel.* 20 (4), 1180–1191. doi:10.1091/mbc.e08-08-0829

Ameri, K., Lewis, C. E., Raida, M., Sowter, H., Hai, T., and Harris, A. L. (2004). Anoxic Induction of ATF-4 through HIF-1-independent Pathways of Protein Stabilization in Human Cancer Cells. *Blood* 103 (5), 1876–1882. doi:10.1182/blood-2003-06-1859

Axten, J. M., Medina, J. R., Feng, Y., Shu, A., Romeril, S. P., Grant, S. W., et al. (2012). Discovery of 7-Methyl-5-(1-{[3-(trifluoromethyl)phenyl]acetyl}-2,3-Dihydro-1h-Indol-5-Yl)-7h-Pyrrolo[2,3-D]pyrimidin-4-Amine (GSK2606414), a Potent and Selective First-In-Class Inhibitor of Protein Kinase R (PKR)-like Endoplasmic Reticulum Kinase (PERK). *J. Med. Chem.* 55 (16), 7193–7207. doi:10.1021/jm300713s

B'Chir, W., Maurin, A. C., Carraro, V., Averous, J., Jousse, C., Muranishi, Y., et al. (2013). The eIF2α/ATF4 Pathway Is Essential for Stress-Induced Autophagy Gene Expression. *Nucleic Acids Res.* 41 (16), 7683–7699. doi:10.1093/nar/gkt563

Baird, T. D., Palam, L. R., Fusakio, M. E., Willy, J. A., Davis, C. M., McClintick, J. N., et al. (2014). Selective mRNA Translation during eIF2 Phosphorylation Induces Expression of IBTKα. *Mol. Biol. Cel.* 25 (10), 1686–1697. doi:10.1091/mbc.E14-02-0704

Behrends, C., Sowa, M. E., Gygi, S. P., and Harper, J. W. (2010). Network Organization of the Human Autophagy System. *Nature* 466 (7302), 68–76. doi:10.1038/nature09204

Blais, J. D., Filipenko, V., Bi, M., Harding, H. P., Ron, D., Koumenis, C., et al. (2004). Activating Transcription Factor 4 Is Translationally Regulated by Hypoxic Stress. *Mol. Cel Biol.* 24 (17), 7469–7482. doi:10.1128/MCB.24.17.7469-7482.2004

Boyce, M., Bryant, K. F., Jousse, C., Long, K., Harding, H. P., Scheuner, D., et al. (2005). A Selective Inhibitor of eIF2alpha Dephosphorylation Protects Cells from ER Stress. *Science* 307 (5711), 935–939. doi:10.1126/science.1101902

Brin, E., Wu, K., Dagostino, E., Meng-Chiang Kuo, M., He, Y., Shia, W. J., et al. (2018). TRAIL Stabilization and Cancer Cell Sensitization to its Pro-apoptotic Activity Achieved through Genetic Fusion with Arginine Deiminase. *Oncotarget* 9 (97), 36914–36928. doi:10.18632/oncotarget.26398

Bruns, G. P., and London, I. M. (1965). The Effect of Hemin on the Synthesis of Globin. *Biochem. Biophys. Res. Commun.* 18, 236–242. doi:10.1016/0006-291x(65)90746-1

Cai, J., Yang, J., and Jones, D. P. (1998). Mitochondrial Control of Apoptosis: the Role of Cytochrome C. *Biochim. Biophys. Acta.* 1366 (1-2), 139–149. doi:10.1016/s0005-2728(98)00109-1

Carneiro, B. A., and El-Deiry, W. S. (2020). Targeting Apoptosis in Cancer Therapy. *Nat. Rev. Clin. Oncol.* 17 (7), 395–417. doi:10.1038/s41571-020-0341-y

Castilho, B. A., Shanmugam, R., Silva, R. C., Ramesh, R., Himme, B. M., and Sattlegger, E. (2014). Keeping the eIF2 Alpha Kinase Gcn2 in Check. *Biochim. Biophys. Acta.* 1843 (9), 1948–1968. doi:10.1016/j.bbamcr.2014.04.006

Chefalo, P. J., Oh, J., Rafie-Kolpin, M., Kan, B., and Chen, J. J. (1998). Heme-regulated eIF-2alpha Kinase Purifies as a Hemoprotein. *Eur. J. Biochem.* 258 (2), 820–830. doi:10.1046/j.1432-1327.1998.2580820.x

Chen, T., Ozel, D., Qiao, Y., Harbinski, F., Chen, L., Denoyelle, S., et al. (2011). Chemical Genetics Identify eIF2α Kinase Heme-Regulated Inhibitor as an Anticancer Target. *Nat. Chem. Biol.* 7 (9), 610–616. doi:10.1038/nchembio.613

Chitnis, N. S., Pytel, D., Bobrovnikova-Marjon, E., Pant, D., Zheng, H., Maas, N. L., et al. (2012). miR-211 Is a Prosurvival microRNA that Regulates Chop Expression in a PERK-dependent Manner. *Mol. Cel.* 48 (3), 353–364. doi:10.1016/j.molcel.2012.08.025

Chu, H. S., Peterson, C., Jun, A., and Foster, J. (2021). Targeting the Integrated Stress Response in Ophthalmology. *Curr. Eye Res.* 46 (8), 1075–1088. doi:10.1080/02713683.2020.1867748

Clementi, E., Inglin, L., Beebe, E., Gsell, C., Garajova, Z., and Markkanen, E. (2020). Persistent DNA Damage Triggers Activation of the Integrated Stress Response to Promote Cell Survival under Nutrient Restriction. *BMC Biol.* 18 (1), 36. doi:10.1186/s12915-020-00771-x

Cook, J. A., Choudhuri, R., Degraff, W., Gamson, J., and Mitchell, J. B. (2010). Halofuginone Enhances the Radiation Sensitivity of Human Tumor Cell Lines. *Cancer Lett.* 289 (1), 119–126. doi:10.1016/j.canlet.2009.08.009

Corazzari, M., Rapino, F., Ciccosanti, F., Giglio, P., Antonioli, M., Conti, B., et al. (2015). Oncogenic BRAF Induces Chronic ER Stress Condition Resulting in Increased Basal Autophagy and Apoptotic Resistance of Cutaneous Melanoma. *Cell Death Differ.* 22 (6), 946–958. doi:10.1038/cdd.2014.183

Costa-Mattioli, M., and Walter, P. (2020). The Integrated Stress Response: From Mechanism to Disease. *Science* 368 (6489). doi:10.1126/science.aat5314

Darini, C., Ghaddar, N., Chabot, C., Assaker, G., Sabri, S., Wang, S., et al. (2019). An Integrated Stress Response via PKR Suppresses HER2+ Cancers and Improves Trastuzumab Therapy. *Nat. Commun.* 10 (1), 2139. doi:10.1038/s41467-019-10138-8

De Gassart, A., Bujisic, B., Zaffalon, L., Decosterd, L. A., Di Micco, A., Frera, G., et al. (2016). An Inhibitor of HIV-1 Protease Modulates Constitutive eIF2α

Dephosphorylation to Trigger a Specific Integrated Stress Response. *Proc. Natl. Acad. Sci. U S A.* 113 (2), E117–E126. doi:10.1073/pnas.1514076113

Deegan, S., Koryga, I., Glynn, S. A., Gupta, S., Gorman, A. M., and Samali, A. (2015). A Close Connection between the PERK and IRE Arms of the UPR and the Transcriptional Regulation of Autophagy. *Biochem. Biophys. Res. Commun.* 456 (1), 305–311. doi:10.1016/j.bbrc.2014.11.076

Deegan, S., Saveljeva, S., Gorman, A. M., and Samali, A. (2013). Stress-induced Self-Cannibalism: on the Regulation of Autophagy by Endoplasmic Reticulum Stress. *Cell Mol Life Sci.* 70 (14), 2425–2441. doi:10.1007/s00018-012-1173-4

Deng, J., Lu, P. D., Zhang, Y., Scheuner, D., Kaufman, R. J., Sonenberg, N., et al. (2004). Translational Repression Mediates Activation of Nuclear Factor Kappa B by Phosphorylated Translation Initiation Factor 2. *Mol. Cel Biol.* 24 (23), 10161–10168. doi:10.1128/MCB.24.23.10161-10168.2004

Dennis, M. D., McGhee, N. K., Jefferson, L. S., and Kimball, S. R. (2013). Regulated in DNA Damage and Development 1 (REDD1) Promotes Cell Survival during Serum Deprivation by Sustaining Repression of Signaling through the Mechanistic Target of Rapamycin in Complex 1 (mTORC1). *Cell Signal.* 25 (12), 2709–2716. doi:10.1016/j.cellsig.2013.08.038

Dey, S., Sayers, C. M., Verginadis, I. I., Lehman, S. L., Cheng, Y., Cerniglia, G. J., et al. (2015). ATF4-dependent Induction of Heme Oxygenase 1 Prevents Anoikis and Promotes Metastasis. *J. Clin. Invest.* 125 (7), 2592–2608. doi:10.1172/JCI78031

Di Prisco, G. V., Huang, W., Buffington, S. A., Hsu, C. C., Bonnen, P. E., Placzek, A. N., et al. (2014). Translational Control of mGluR-dependent Long-Term Depression and Object-Place Learning by eIF2α. *Nat. Neurosci.* 17 (8), 1073–1082. doi:10.1038/nn.3754

Dluzen, D., Li, G., Tacelosky, D., Moreau, M., and Liu, D. X. (2011). BCL-2 Is a Downstream Target of ATF5 that Mediates the Prosurvival Function of ATF5 in a Cell Type-dependent Manner. *J. Biol. Chem.* 286 (9), 7705–7713. doi:10.1074/jbc.M110.207639

Donnelly, N., Gorman, A. M., Gupta, S., and Samali, A. (2013). The eIF2α Kinases: Their Structures and Functions. *Cel Mol Life Sci.* 70 (19), 3493–3511. doi:10.1007/s00018-012-1252-6

Dossou, A. S., and Basu, A. (2019). The Emerging Roles of mTORC1 in Macromanaging Autophagy. *Cancers (Basel)* 11 (10), 1422. doi:10.3390/cancers11101422

Evstafieva, A. G., Garaeva, A. A., Khutornenko, A. A., Klepikova, A. V., Logacheva, M. D., Penin, A. A., et al. (2014). A Sustained Deficiency of Mitochondrial Respiratory Complex III Induces an Apoptotic Cell Death through the P53-Mediated Inhibition of Pro-survival Activities of the Activating Transcription Factor 4. *Cell Death Dis.* 5, e1511. doi:10.1038/cddis.2014.469

Galehdar, Z., Swan, P., Fuerth, B., Callaghan, S. M., Park, D. S., and Cregan, S. P. (2010). Neuronal Apoptosis Induced by Endoplasmic Reticulum Stress Is Regulated by ATF4-CHOP-Mediated Induction of the Bcl-2 Homology 3-only Member PUMA. *J. Neurosci.* 30 (50), 16938–16948. doi:10.1523/JNEUROSCI.1598-10.2010

Hamanaka, R. B., Bobrovnikova-Marjon, E., Ji, X., Liebhaber, S. A., and Diehl, J. A. (2009). PERK-dependent Regulation of IAP Translation during ER Stress. *Oncogene* 28 (6), 910–920. doi:10.1038/onc.2008.428

Hamidi, T., Cano, C. E., Grasso, D., Garcia, M. N., Sandi, M. J., Calvo, E. L., et al. (2012). Nupr1-aurora Kinase A Pathway Provides protection against Metabolic Stress-Mediated Autophagic-Associated Cell Death. *Clin. Cancer Res.* 18 (19), 5234–5246. doi:10.1158/1078-0432.CCR-12-0026

Han, A. P., Yu, C., Lu, L., Fujiwara, Y., Browne, C., Chin, G., et al. (2001). Heme-regulated eIF2alpha Kinase (HRI) Is Required for Translational Regulation and Survival of Erythroid Precursors in Iron Deficiency. *EMBO J.* 20 (23), 6909–6918. doi:10.1093/emboj/20.23.6909

Harding, H. P., Novoa, I., Zhang, Y., Zeng, H., Wek, R., Schapira, M., et al. (2000). Regulated Translation Initiation Controls Stress-Induced Gene Expression in Mammalian Cells. *Mol. Cel.* 6 (5), 1099–1108. doi:10.1016/s1097-2765(00)00108-8

Hartleben, G., Schorpp, K., Kwon, Y., Betz, B., Tsokanos, F. F., Dantes, Z., et al. (2021). Combination Therapies Induce Cancer Cell Death through the Integrated Stress Response and Disturbed Pyrimidine Metabolism. *EMBO Mol. Med.* 13 (4), e12461. doi:10.15252/emmm.202012461

Ho, K. H., Lee, Y. T., Chen, P. H., Shih, C. M., Cheng, C. H., and Chen, K. C. (2021). Guanabenz Sensitizes Glioblastoma Cells to Sunitinib by Inhibiting GADD34-Mediated Autophagic Signaling. *Neurotherapeutics* 18, 1371–1392. doi:10.1007/s13311-020-00961-z

Hu, J., Dang, N., Menu, E., De Bruyne, E., De Bryune, E., Xu, D., et al. (2012). Activation of ATF4 Mediates Unwanted Mcl-1 Accumulation by Proteasome Inhibition. *Blood* 119 (3), 826–837. doi:10.1182/blood-2011-07-366492

Hu, P., Han, Z., Couvillon, A. D., and Exton, J. H. (2004). Critical Role of Endogenous Akt/IAPs and MEK1/ERK Pathways in Counteracting Endoplasmic Reticulum Stress-Induced Cell Death. *J. Biol. Chem.* 279 (47), 49420–49429. doi:10.1074/jbc.M407700200

Hu, W., Hofstetter, W., Wei, X., Guo, W., Zhou, Y., Pataer, A., et al. (2009). Double-stranded RNA-dependent Protein Kinase-dependent Apoptosis Induction by a Novel Small Compound. *J. Pharmacol. Exp. Ther.* 328 (3), 866–872. doi:10.1124/jpet.108.141754

Huang, Z., and Hu, H. (2021). Arginine Deiminase Induces Immunogenic Cell Death and Is Enhanced by N-Acetylcysteine in Murine MC38 Colorectal Cancer Cells and MDA-MB-231 Human Breast Cancer Cells *In Vitro*. *Molecules* 26 (2). doi:10.3390/molecules26020511

Ill-Raga, G., Tajes, M., Busquets-García, A., Ramos-Fernández, E., Vargas, L. M., Bosch-Morató, M., et al. (2015). Physiological Control of Nitric Oxide in Neuronal BACE1 Translation by Heme-Regulated eIF2α Kinase HRI Induces Synaptogenesis. *Antioxid. Redox Signal.* 22 (15), 1295–1307. doi:10.1089/ars.2014.6080

Ishizawa, J., Kojima, K., Chachad, D., Ruvolo, P., Ruvolo, V., Jacamo, R. O., et al. (2016). ATF4 Induction through an Atypical Integrated Stress Response to ONC201 Triggers P53-independent Apoptosis in Hematological Malignancies. *Sci. Signal.* 9 (415), ra17. doi:10.1126/scisignal.aac4380

Jammi, N. V., Whitby, L. R., and Beal, P. A. (2003). Small Molecule Inhibitors of the RNA-dependent Protein Kinase. *Biochem. Biophys. Res. Commun.* 308 (1), 50–57. doi:10.1016/s0006-291x(03)01318-4

Jin, H. O., Seo, S. K., Woo, S. H., Choe, T. B., Hong, S. I., Kim, J. I., et al. (2009). Nuclear Protein 1 Induced by ATF4 in Response to Various Stressors Acts as a Positive Regulator on the Transcriptional Activation of ATF4. *IUBMB Life.* 61 (12), 1153–1158. doi:10.1002/iub.271

Karpel-Massler, G., Horst, B. A., Shu, C., Chau, L., Tsujiuchi, T., Bruce, J. N., et al. (2016). A Synthetic Cell-Penetrating Dominant-Negative ATF5 Peptide Exerts Anticancer Activity against a Broad Spectrum of Treatment-Resistant Cancers. *Clin. Cancer Res.* 22 (18), 4698–4711. doi:10.1158/1078-0432.CCR-15-2827

Kasai, S., Yamazaki, H., Tanji, K., Engler, M. J., Matsumiya, T., and Itoh, K. (2019). Role of the ISR-ATF4 Pathway and its Cross Talk with Nrf2 in Mitochondrial Quality Control. *J. Clin. Biochem. Nutr.* 64 (1), 1–12. doi:10.3164/jcbn.18-37

Kato, Y., Kunimasa, K., Sugimoto, Y., and Tomida, A. (2018). BCR-ABL Tyrosine Kinase Inhibition Induces Metabolic Vulnerability by Preventing the Integrated Stress Response in K562 cells. *Biochem. Biophys. Res. Commun.* 504 (4), 721–726. doi:10.1016/j.bbrc.2018.09.032

Kazemi, S., Mounir, Z., Baltzis, D., Raven, J. F., Wang, S., Krishnamoorthy, J. L., et al. (2007). A Novel Function of eIF2alpha Kinases as Inducers of the Phosphoinositide-3 Kinase Signaling Pathway. *Mol. Biol. Cel.* 18 (9), 3635–3644. doi:10.1091/mbc.e07-01-0053

Kim, R. H., Coates, J. M., Bowles, T. L., McNerney, G. P., Sutcliffe, J., Jung, J. U., et al. (2009). Arginine Deiminase as a Novel Therapy for Prostate Cancer Induces Autophagy and Caspase-independent Apoptosis. *Cancer Res.* 69 (2), 700–708. doi:10.1158/0008-5472.CAN-08-3157

Kim, T. W., Cheon, C., and Ko, S. G. (2020). SH003 Activates Autophagic Cell Death by Activating ATF4 and Inhibiting G9a under Hypoxia in Gastric Cancer Cells. *Cel Death Dis.* 11 (8), 717. doi:10.1038/s41419-020-02924-w

Kline, C. L., Van den Heuvel, A. P., Allen, J. E., Prabhu, V. V., Dicker, D. T., and El-Deiry, W. S. (2016). ONC201 Kills Solid Tumor Cells by Triggering an Integrated Stress Response Dependent on ATF4 Activation by Specific eIF2α Kinases. *Sci. Signal.* 9 (415), ra18. doi:10.1126/scisignal.aac4374

Kouroku, Y., Fujita, E., Tanida, I., Ueno, T., Isoai, A., Kumagai, H., et al. (2007). ER Stress (PERK/eIF2alpha Phosphorylation) Mediates the Polyglutamine-Induced LC3 Conversion, an Essential Step for Autophagy Formation. *Cel Death Differ.* 14 (2), 230–239. doi:10.1038/sj.cdd.4401984

Kroemer, G., Mariño, G., and Levine, B. (2010). Autophagy and the Integrated Stress Response. *Mol. Cel.* 40 (2), 280–293. doi:10.1016/j.molcel.2010.09.023

Lamora, A., Mullard, M., Amiaud, J., Brion, R., Heymann, D., Redini, F., et al. (2015). Anticancer Activity of Halofuginone in a Preclinical Model of Osteosarcoma: Inhibition of Tumor Growth and Lung Metastases. *Oncotarget* 6 (16), 14413–14427. doi:10.18632/oncotarget.3891

Lee, Y. Y., Cevallos, R. C., and Jan, E. (2009). An Upstream Open reading Frame Regulates Translation of GADD34 during Cellular Stresses that Induce eIF2alpha Phosphorylation. *J. Biol. Chem.* 284 (11), 6661–6673. doi:10.1074/jbc.M806735200

Li, T., Su, L., Lei, Y., Liu, X., Zhang, Y., and Liu, X. (2015). DDIT3 and KAT2A Proteins Regulate TNFRSF10A and TNFRSF10B Expression in Endoplasmic Reticulum Stress-Mediated Apoptosis in Human Lung Cancer Cells. *J. Biol. Chem.* 290 (17), 11108–11118. doi:10.1074/jbc.M115.645333

Liu, D. X., Qian, D., Wang, B., Yang, J. M., and Lu, Z. (2011). p300-Dependent ATF5 Acetylation Is Essential for Egr-1 Gene Activation and Cell Proliferation and Survival. *Mol. Cel Biol.* 31 (18), 3906–3916. doi:10.1128/MCB.05887-11

Long, Y., Tsai, W. B., Wangpaichitr, M., Tsukamoto, T., Savaraj, N., Feun, L. G., et al. (2013). Arginine Deiminase Resistance in Melanoma Cells Is Associated with Metabolic Reprogramming, Glucose Dependence, and Glutamine Addiction. *Mol. Cancer Ther.* 12 (11), 2581–2590. doi:10.1158/1535-7163.MCT-13-0302

Lu, L., Han, A. P., and Chen, J. J. (2001). Translation Initiation Control by Heme-Regulated Eukaryotic Initiation Factor 2alpha Kinase in Erythroid Cells under Cytoplasmic Stresses. *Mol. Cel Biol.* 21 (23), 7971–7980. doi:10.1128/MCB.21.23.7971-7980.2001

Lu, M., Lawrence, D. A., Marsters, S., Acosta-Alvear, D., Kimmig, P., Mendez, A. S., et al. (2014). Opposing Unfolded-Protein-Response Signals Converge on Death Receptor 5 to Control Apoptosis. *Science* 345 (6192), 98–101. doi:10.1126/science.1254312

Lv, S., Sun, E. C., Xu, Q. Y., Zhang, J. K., and Wu, D. L. (2015). Endoplasmic Reticulum Stress-Mediated Autophagy Contributes to Bluetongue Virus Infection via the PERK-eIF2α Pathway. *Biochem. Biophys. Res. Commun.* 466 (3), 406–412. doi:10.1016/j.bbrc.2015.09.039

Mahadevan, N. R., Rodvold, J., Sepulveda, H., Rossi, S., Drew, A. F., and Zanetti, M. (2011). Transmission of Endoplasmic Reticulum Stress and Pro-inflammation from Tumor Cells to Myeloid Cells. *Proc. Natl. Acad. Sci. U S A.* 108 (16), 6561–6566. doi:10.1073/pnas.1008942108

Martin, T. A., Li, A. X., Sanders, A. J., Ye, L., Frewer, K., Hargest, R., et al. (2021). NUPR1 and its Potential Role in Cancer and Pathological Conditions (Review). *Int. J. Oncol.* 58 (5). doi:10.3892/ijo.2021.5201

McConkey, D. J. (2017). The Integrated Stress Response and Proteotoxicity in Cancer Therapy. *Biochem. Biophys. Res. Commun.* 482 (3), 450–453. doi:10.1016/j.bbrc.2016.11.047

McEwen, E., Kedersha, N., Song, B., Scheuner, D., Gilks, N., Han, A., et al. (2005). Heme-regulated Inhibitor Kinase-Mediated Phosphorylation of Eukaryotic Translation Initiation Factor 2 Inhibits Translation, Induces Stress Granule Formation, and Mediates Survival upon Arsenite Exposure. *J. Biol. Chem.* 280 (17), 16925–16933. doi:10.1074/jbc.M412882200

Milani, M., Rzymski, T., Mellor, H. R., Pike, L., Bottini, A., Generali, D., et al. (2009). The Role of ATF4 Stabilization and Autophagy in Resistance of Breast Cancer Cells Treated with Bortezomib. *Cancer Res.* 69 (10), 4415–4423. doi:10.1158/0008-5472.CAN-08-2839

Mohamed, E., Sierra, R. A., Trillo-Tinoco, J., Cao, Y., Innamarato, P., Payne, K. K., et al. (2020). The Unfolded Protein Response Mediator PERK Governs Myeloid Cell-Driven Immunosuppression in Tumors through Inhibition of STING Signaling. *Immunity* 52 (4), 668–e7. doi:10.1016/j.immuni.2020.03.004

Mukherjee, T., Ramaglia, V., Abdel-Nour, M., Bianchi, A. A., Tsalikis, J., Chau, H. N., et al. (2021). The eIF2α Kinase HRI Triggers the Autophagic Clearance of Cytosolic Protein Aggregates. *J. Biol. Chem.* 296, 100050. doi:10.1074/jbc.RA120.014415

Narita, T., Ri, M., Masaki, A., Mori, F., Ito, A., Kusumoto, S., et al. (2015). Lower Expression of Activating Transcription Factors 3 and 4 Correlates with Shorter Progression-free Survival in Multiple Myeloma Patients Receiving Bortezomib Plus Dexamethasone Therapy. *Blood Cancer J.* 5, e373. doi:10.1038/bcj.2015.98

Nguyen, T. H., Koneru, B., Wei, S. J., Chen, W. H., Makena, M. R., Urias, E., et al. (2019). Fenretinide via NOXA Induction, Enhanced Activity of the BCL-2 Inhibitor Venetoclax in High BCL-2-Expressing Neuroblastoma Preclinical Models. *Mol. Cancer Ther.* 18 (12), 2270–2282. doi:10.1158/1535-7163.MCT-19-0385

Núñez-Vázquez, S., Sánchez-Vera, I., Saura-Esteller, J., Cosialls, A. M., Noisier, A. F. M., Albericio, F., et al. (2021). NOXA Upregulation by the Prohibitin-Binding Compound Fluorizoline Is Transcriptionally Regulated by Integrated Stress Response-Induced ATF3 and ATF4. *FEBS J.* 288 (4), 1271–1285. doi:10.1111/febs.15480

O'Malley, J., Kumar, R., Inigo, J., Yadava, N., and Chandra, D. (2020). Mitochondrial Stress Response and Cancer. *Trends Cancer.* 6 (8), 688–701. doi:10.1016/j.trecan.2020.04.009

Obeng, E. A., Carlson, L. M., Gutman, D. M., Harrington, W. J., Lee, K. P., and Boise, L. H. (2006). Proteasome Inhibitors Induce a Terminal Unfolded Protein Response in Multiple Myeloma Cells. *Blood* 107 (12), 4907–4916. doi:10.1182/blood-2005-08-3531

Obiedat, A., Charpak-Amikam, Y., Tai-Schmiedel, J., Seidel, E., Mahameed, M., Avril, T., et al. (2020). The Integrated Stress Response Promotes B7H6 Expression. *J. Mol. Med. (Berl)* 98 (1), 135–148. doi:10.1007/s00109-019-01859-w

Ohoka, N., Yoshii, S., Hattori, T., Onozaki, K., and Hayashi, H. (2005). TRB3, a Novel ER Stress-Inducible Gene, Is Induced via ATF4-CHOP Pathway and Is Involved in Cell Death. *EMBO J.* 24 (6), 1243–1255. doi:10.1038/sj.emboj.7600596

Ojha, R., Leli, N. M., Onorati, A., Piao, S., Verginadis, I. I., Tameire, F., et al. (2019). ER Translocation of the MAPK Pathway Drives Therapy Resistance in BRAF-Mutant Melanoma. *Cancer Discov.* 9 (3), 396–415. doi:10.1158/2159-8290.CD-18-0348

Orvedahl, A., Alexander, D., Tallóczy, Z., Sun, Q., Wei, Y., Zhang, W., et al. (2007). HSV-1 ICP34.5 Confers Neurovirulence by Targeting the Beclin 1 Autophagy Protein. *Cell Host Microbe.* 1 (1), 23–35. doi:10.1016/j.chom.2006.12.001

Pakos-Zebrucka, K., Koryga, I., Mnich, K., Ljujic, M., Samali, A., and Gorman, A. M. (2016). The Integrated Stress Response. *EMBO Rep.* 17 (10), 1374–1395. doi:10.15252/embr.201642195

Palam, L. R., Baird, T. D., and Wek, R. C. (2011). Phosphorylation of eIF2 Facilitates Ribosomal Bypass of an Inhibitory Upstream ORF to Enhance CHOP Translation. *J. Biol. Chem.* 286 (13), 10939–10949. doi:10.1074/jbc.M110.216093

Palam, L. R., Gore, J., Craven, K. E., Wilson, J. L., and Korc, M. (2015). Integrated Stress Response Is Critical for Gemcitabine Resistance in Pancreatic Ductal Adenocarcinoma. *Cel Death Dis.* 6 (10), e1913. doi:10.1038/cddis.2015.264

Perkins, D. J., and Barber, G. N. (2004). Defects in Translational Regulation Mediated by the Alpha Subunit of Eukaryotic Initiation Factor 2 Inhibit Antiviral Activity and Facilitate the Malignant Transformation of Human Fibroblasts. *Mol. Cel Biol.* 24 (5), 2025–2040. doi:10.1128/mcb.24.5.2025-2040.2004

Puthalakath, H., O'Reilly, L. A., Gunn, P., Lee, L., Kelly, P. N., Huntington, N. D., et al. (2007). ER Stress Triggers Apoptosis by Activating BH3-Only Protein Bim. *Cell* 129 (7), 1337–1349. doi:10.1016/j.cell.2007.04.027

Robert, F., Williams, C., Yan, Y., Donohue, E., Cencic, R., Burley, S. K., et al. (2009). Blocking UV-Induced eIF2alpha Phosphorylation with Small Molecule Inhibitors of GCN2. *Chem. Biol. Drug Des.* 74 (1), 57–67. doi:10.1111/j.1747-0285.2009.00827.x

Rosen, M. D., Woods, C. R., Goldberg, S. D., Hack, M. D., Bounds, A. D., Yang, Y., et al. (2009). Discovery of the First Known Small-Molecule Inhibitors of Heme-Regulated Eukaryotic Initiation Factor 2alpha (HRI) Kinase. *Bioorg. Med. Chem. Lett.* 19 (23), 6548–6551. doi:10.1016/j.bmcl.2009.10.033

Rouschop, K. M., Dubois, L. J., Keulers, T. G., van den Beucken, T., Lambin, P., Bussink, J., et al. (2013). PERK/eIF2α Signaling Protects Therapy Resistant Hypoxic Cells through Induction of Glutathione Synthesis and protection against ROS. *Proc. Natl. Acad. Sci. U S A.* 110 (12), 4622–4627. doi:10.1073/pnas.1210633110

Rouschop, K. M., van den Beucken, T., Dubois, L., Niessen, H., Bussink, J., Savelkouls, K., et al. (2010). The Unfolded Protein Response Protects Human Tumor Cells during Hypoxia through Regulation of the Autophagy Genes MAP1LC3B and ATG5. *J. Clin. Invest.* 120 (1), 127–141. doi:10.1172/JCI40027

Rzymski, T., Milani, M., Pike, L., Buffa, F., Mellor, H. R., Winchester, L., et al. (2010). Regulation of Autophagy by ATF4 in Response to Severe Hypoxia. *Oncogene* 29 (31), 4424–4435. doi:10.1038/onc.2010.191

Rzymski, T., Milani, M., Singleton, D. C., and Harris, A. L. (2009). Role of ATF4 in Regulation of Autophagy and Resistance to Drugs and Hypoxia. *Cell Cycle.* 8 (23), 3838–3847. doi:10.4161/cc.8.23.10086

Santofimia-Castaño, P., Lan, W., Bintz, J., Gayet, O., Carrier, A., Lomberk, G., et al. (2018). Inactivation of NUPR1 Promotes Cell Death by Coupling ER-Stress Responses with Necrosis. *Sci. Rep.* 8 (1), 16999. doi:10.1038/s41598-018-35020-3

Sasaki, K., Uchiumi, T., Toshima, T., Yagi, M., Do, Y., Hirai, H., et al. (2020). Mitochondrial Translation Inhibition Triggers ATF4 Activation, Leading to Integrated Stress Response but Not to Mitochondrial Unfolded Protein Response. *Biosci. Rep.* 40 (11). doi:10.1042/BSR20201289

Sharma, K., Vu, T. T., Cook, W., Naseri, M., Zhan, K., Nakajima, W., et al. (2018). p53-independent Noxa Induction by Cisplatin Is Regulated by ATF3/ATF4 in Head and Neck Squamous Cell Carcinoma Cells. *Mol. Oncol.* 12 (6), 788–798. doi:10.1002/1878-0261.12172

Shen, S., Niso-Santano, M., Adjemian, S., Takehara, T., Malik, S. A., Minoux, H., et al. (2012). Cytoplasmic STAT3 Represses Autophagy by Inhibiting PKR Activity. *Mol. Cel.* 48 (5), 667–680. doi:10.1016/j.molcel.2012.09.013

Sidrauski, C., McGeachy, A. M., Ingolia, N. T., and Walter, P. (2015). The Small Molecule ISRIB Reverses the Effects of eIF2α Phosphorylation on Translation and Stress Granule Assembly. *Elife* 4. doi:10.7554/eLife.05033

Singh, P. K., Deorukhkar, A. A., Venkatesulu, B. P., Li, X., Tailor, R., Bomalaski, J. S., et al. (2019). Exploiting Arginine Auxotrophy with Pegylated Arginine Deiminase (ADI-PEG20) to Sensitize Pancreatic Cancer to Radiotherapy via Metabolic Dysregulation. *Mol. Cancer Ther.* 18 (12), 2381–2393. doi:10.1158/1535-7163.MCT-18-0708

Smyth, R., Berton, S., Rajabalee, N., Chan, T., and Sun, J. (2020). Protein Kinase R Restricts the Intracellular Survival of *Mycobacterium tuberculosis* by Promoting Selective Autophagy. *Front. Microbiol.* 11, 613963. doi:10.3389/fmicb.2020.613963

Spector, I., Honig, H., Kawada, N., Nagler, A., Genin, O., and Pines, M. (2010). Inhibition of Pancreatic Stellate Cell Activation by Halofuginone Prevents Pancreatic Xenograft Tumor Development. *Pancreas* 39 (7), 1008–1015. doi:10.1097/MPA.0b013e3181da8aa3

Stockwell, S. R., Platt, G., Barrie, S. E., Zoumpoulidou, G., Te Poele, R. H., Aherne, G. W., et al. (2012). Mechanism-based Screen for G1/S Checkpoint Activators Identifies a Selective Activator of EIF2AK3/PERK Signalling. *PLoS One* 7 (1), e28568. doi:10.1371/journal.pone.0028568

Stone, S., Ho, Y., Li, X., Jamison, S., Harding, H. P., Ron, D., et al. (2016). Dual Role of the Integrated Stress Response in Medulloblastoma Tumorigenesis. *Oncotarget* 7 (39), 64124–64135. doi:10.18632/oncotarget.11873

Suragani, R. N., Zachariah, R. S., Velazquez, J. G., Liu, S., Sun, C. W., Townes, T. M., et al. (2012). Heme-regulated eIF2α Kinase Activated Atf4 Signaling Pathway in Oxidative Stress and Erythropoiesis. *Blood* 119 (22), 5276–5284. doi:10.1182/blood-2011-10-388132

Suraweera, A., Münch, C., Hanssum, A., and Bertolotti, A. (2012). Failure of Amino Acid Homeostasis Causes Cell Death Following Proteasome Inhibition. *Mol. Cel.* 48 (2), 242–253. doi:10.1016/j.molcel.2012.08.003

Suresh, S., Chen, B., Zhu, J., Golden, R. J., Lu, C., Evers, B. M., et al. (2020). eIF5B Drives Integrated Stress Response-dependent Translation of PD-L1 in Lung Cancer. *Nat. Cancer.* 1 (5), 533–545. doi:10.1038/s43018-020-0056-0

Tallóczy, Z., Jiang, W., Virgin, H. W., Leib, D. A., Scheuner, D., Kaufman, R. J., et al. (2002). Regulation of Starvation- and Virus-Induced Autophagy by the eIF2alpha Kinase Signaling Pathway. *Proc. Natl. Acad. Sci. U S A.* 99 (1), 190–195. doi:10.1073/pnas.012485299

Tallóczy, Z., Virgin, H. W., and Levine, B. (2006). PKR-dependent Autophagic Degradation of Herpes Simplex Virus Type 1. *Autophagy* 2 (1), 24–29. doi:10.4161/auto.2176

Tameire, F., Verginadis, I. I., Leli, N. M., Polte, C., Conn, C. S., Ojha, R., et al. (2019). ATF4 Couples MYC-dependent Translational Activity to Bioenergetic Demands during Tumour Progression. *Nat. Cel Biol.* 21 (7), 889–899. doi:10.1038/s41556-019-0347-9

Tian, X., Ahsan, N., Lulla, A., Lev, A., Abbosh, P., Dicker, D. T., et al. (2021). P53-independent Partial Restoration of the P53 Pathway in Tumors with Mutated P53 through ATF4 Transcriptional Modulation by ERK1/2 and CDK9. *Neoplasia* 23 (3), 304–325. doi:10.1016/j.neo.2021.01.004

Tsaytler, P., Harding, H. P., Ron, D., and Bertolotti, A. (2011). Selective Inhibition of a Regulatory Subunit of Protein Phosphatase 1 Restores Proteostasis. *Science* 332 (6025), 91–94. doi:10.1126/science.1201396

Wang, C., Zhu, J. B., Yan, Y. Y., Zhang, W., Gong, X. J., Wang, X., et al. (2020). Halofuginone Inhibits Tumorigenic Progression of 5-FU-Resistant Human Colorectal Cancer HCT-15/FU Cells by Targeting miR-132-3p *In Vitro*. *Oncol. Lett.* 20 (6), 385. doi:10.3892/ol.2020.12248

Wang, S., Chen, X. A., Hu, J., Jiang, J. K., Li, Y., Chan-Salis, K. Y., et al. (2015). ATF4 Gene Network Mediates Cellular Response to the Anticancer PAD Inhibitor YW3-56 in Triple-Negative Breast Cancer Cells. *Mol. Cancer Ther.* 14 (4), 877–888. doi:10.1158/1535-7163.MCT-14-1093-T

Warnakulasuriyarachchi, D., Cerquozzi, S., Cheung, H. H., and Holcík, M. (2004). Translational Induction of the Inhibitor of Apoptosis Protein HIAP2 during Endoplasmic Reticulum Stress Attenuates Cell Death and Is Mediated via an Inducible Internal Ribosome Entry Site Element. *J. Biol. Chem.* 279 (17), 17148–17157. doi:10.1074/jbc.M308737200

Wek, R. C., Jiang, H. Y., and Anthony, T. G. (2006). Coping with Stress: eIF2 Kinases and Translational Control. *Biochem. Soc. Trans.* 34 (Pt 1), 7–11. doi:10.1042/BST20060007

Whitney, M. L., Jefferson, L. S., and Kimball, S. R. (2009). ATF4 Is Necessary and Sufficient for ER Stress-Induced Upregulation of REDD1 Expression. *Biochem. Biophys. Res. Commun.* 379 (2), 451–455. doi:10.1016/j.bbrc.2008.12.079

Wortel, I. M. N., van der Meer, L. T., Kilberg, M. S., and van Leeuwen, F. N. (2017). Surviving Stress: Modulation of ATF4-Mediated Stress Responses in Normal and Malignant Cells. *Trends Endocrinol. Metab.* 28 (11), 794–806. doi:10.1016/j.tem.2017.07.003

Ye, J., Kumanova, M., Hart, L. S., Sloane, K., Zhang, H., De Panis, D. N., et al. (2010). The GCN2-ATF4 Pathway Is Critical for Tumour Cell Survival and Proliferation in Response to Nutrient Deprivation. *EMBO J.* 29 (12), 2082–2096. doi:10.1038/emboj.2010.81

Yerlikaya, A., Kimball, S. R., and Stanley, B. A. (2008). Phosphorylation of eIF2alpha in Response to 26S Proteasome Inhibition Is Mediated by the Haem-Regulated Inhibitor (HRI) Kinase. *Biochem. J.* 412 (3), 579–588. doi:10.1042/BJ20080324

Yuniati, L., van der Meer, L. T., Tijchon, E., van Ingen Schenau, D., van Emst, L., Levers, M., et al. (2016). Tumor Suppressor BTG1 Promotes PRMT1-Mediated ATF4 Function in Response to Cellular Stress. *Oncotarget* 7 (3), 3128–3143. doi:10.18632/oncotarget.6519

Zhang, S., Macias-Garcia, A., Velazquez, J., Paltrinieri, E., Kaufman, R. J., and Chen, J. J. (2018). HRI Coordinates Translation by eIF2αP and mTORC1 to Mitigate Ineffective Erythropoiesis in Mice during Iron Deficiency. *Blood* 131 (4), 450–461. doi:10.1182/blood-2017-08-799908

Zhang, Y., Zhou, L., Safran, H., Borsuk, R., Lulla, R., Tapinos, N., et al. (2021). EZH2i EPZ-6438 and HDACi Vorinostat Synergize with ONC201/TIC10 to Activate Integrated Stress Response, DR5, Reduce H3K27 Methylation, ClpX and Promote Apoptosis of Multiple Tumor Types Including DIPG. *Neoplasia* 23 (8), 792–810. doi:10.1016/j.neo.2021.06.007

Zhou, D., Palam, L. R., Jiang, L., Narasimhan, J., Staschke, K. A., and Wek, R. C. (2008). Phosphorylation of eIF2 Directs ATF5 Translational Control in Response to Diverse Stress Conditions. *J. Biol. Chem.* 283 (11), 7064–7073. doi:10.1074/jbc.M708530200

Conflict of Interest: WE-D. is a co-founder of Oncoceutics, Inc., a subsidiary of Chimerix, and a Founder of p53-Therapeutics. WE-D has disclosed his relationship with these companies and potential conflict of interest to his academic institution/employer and is fully compliant with NIH and institutional policy that is managing this potential conflict of interest.

The remaining authors declare that the research was conducted in the absence of any commercial or financial relationships that could be construed as a potential conflict of interest.

Publisher's Note: All claims expressed in this article are solely those of the authors and do not necessarily represent those of their affiliated organizations, or those of the publisher, the editors and the reviewers. Any product that may be evaluated in this article, or claim that may be made by its manufacturer, is not guaranteed or endorsed by the publisher.

Copyright © 2021 Tian, Zhang, Zhou, Seyhan, Hernandez Borrero, Zhang and El-Deiry. This is an open-access article distributed under the terms of the Creative Commons Attribution License (CC BY). The use, distribution or reproduction in other forums is permitted, provided the original author(s) and the copyright owner(s) are credited and that the original publication in this journal is cited, in accordance with accepted academic practice. No use, distribution or reproduction is permitted which does not comply with these terms.

frontiers in Pharmacology

ORIGINAL RESEARCH
published: 13 October 2021
doi: 10.3389/fphar.2021.748867

Identification of Hub lncRNAs Along With lncRNA-miRNA-mRNA Network for Effective Diagnosis and Prognosis of Papillary Thyroid Cancer

Haiyan Li[1†], Feng Liu[2†], Xiaoyang Wang[1], Menglong Li[1], Zhihui Li[2,3], Yongmei Xie[2] and Yanzhi Guo[1]**

[1]College of Chemistry, Sichuan University, Chengdu, China, [2]Department of Thyroid Surgery, West China Hospital of Sichuan University, Chengdu, China, [3]Laboratory of Thyroid and Parathyroid Disease, Frontiers Science Center for Disease-Related Molecular Network, West China Hospital of Sichuan University, Chengdu, China

OPEN ACCESS

Edited by:
Claudia Cerella, Fondation de Recherche Cancer et Sang, Luxembourg

Reviewed by:
Weiru Liu, University of Pennsylvania, United States
Sheng Yang, Nanjing Medical University, China

***Correspondence:**
Zhihui Li
Rockoliver163@163.com
Yanzhi Guo
yzguo@scu.edu.cn

[†]These authors have contributed equally to this work and share first authorship

Specialty section:
This article was submitted to Pharmacology of Anti-Cancer Drugs, a section of the journal Frontiers in Pharmacology

Received: *28 July 2021*
Accepted: *22 September 2021*
Published: *13 October 2021*

Citation:
Li H, Liu F, Wang X, Li M, Li Z, Xie Y and Guo Y (2021) Identification of Hub lncRNAs Along With lncRNA-miRNA-mRNA Network for Effective Diagnosis and Prognosis of Papillary Thyroid Cancer. Front. Pharmacol. 12:748867. doi: 10.3389/fphar.2021.748867

Long noncoding RNAs (lncRNAs) play important roles in tumorigenesis and progression of different cancers and they have been potential biomarkers for cancer diagnosis and prognosis. As the most common endocrine malignancy, precise diagnosis and prognosis of papillary thyroid cancer (PTC) is of great clinical significance. Here, we aim to identify new hub lncRNAs for marking PTC and constructed prognostics signatures based on lncRNA-miRNA-mRNA competing endogenous RNAs (ceRNA) network to predict overall survival (OS) and disease-free survival (DFS) respectively. Five reliable hub lncRNAs were identified by integrating differential genes of four Gene Expression Omnibus (GEO) gene chips using the RobustRankAggreg (RRA) method. Based on differential analyses and interaction prediction, a lncRNA-mRNA co-expression network and a lncRNA-miRNA-mRNA ceRNA network were established. Then a comprehensive function characterization of the five hub lncRNAs was performed, including validation dataset testing, receiver operating characteristic (ROC) curve analysis, and functional analysis on two networks. All results suggest that these five hub lncRNAs could be potential biomarkers for marking PTC. The ceRNA network was used to identify RNAs which were associated with PTC prognosis. Two prognostic signatures were developed using univariate and step-wise multivariate Cox regression analyses and both of them were independent prognostic indicators for PTC OS and DFS. Tumor microenvironment difference analysis between high and low-risk patients showed that dendritic cells activated and macrophages M0 may be a possible target for immunotherapy of PTC. In addition, disclosing the potential drugs that may reverse the expression of hub genes may improve the prognosis of patients with PTC. Here, connectivity map (CMap) analysis indicates that three bioactive chemicals (pioglitazone, benserazide, and SB-203580) are promising therapeutic agents for PTC. So, the paper presents a comprehensive study on diagnosis, prognosis, and potential drug screening for PTC based on the five hub lncRNAs identified by us.

Keywords: papillary thyroid cancer, hub lncRNAs, lncRNA-miRNA-mRNA ceRNA network, diagnosis, prognosis signature, bioactive chemicals

INTRODUCTION

Thyroid cancer is the most common endocrine malignancy and the incidence has been rapidly increasing in the past 4 decades (Murugan et al., 2018). As the most common histological type of thyroid cancer, papillary thyroid cancer (PTC) accounts for approximately 85% of all cases (Fagin and Wells, 2016; Kitahara and Sosa, 2016). The incidence of PTC has also been increasing rapidly in most countries (La Vecchia et al., 2015). Generally it has an excellent prognosis but the recurrence to distant organs always threaten the patient's life (Ito et al., 2010). In the last few years, research has been performed to promote our understanding of molecular mechanisms of PTC (Nikiforov and Nikiforova, 2011; Fagin and Wells, 2016). Studies have suggested the crucial roles of lncRNAs, circRNAs, miRNAs, and mRNAs in PTC's diagnosis and prognosis (Chen et al., 2019; Huang et al., 2020; Xu and Jing, 2021). Discovering more biomarker genes and developing reliable prognostic signatures could remarkably promote the development of clinical treatment.

As we all know, human cancers are frequently correlated with the change of transcription pattern and the transcriptome is not only restricted to protein-coding RNAs but also refers to the multiple noncoding members (Liz and Esteller, 2016). The biological roles of RNAs in tumorigenesis and progression has become an interesting research hotpot. As the fundamental transcription regulators, lncRNAs could affect cellular functions including apoptosis, cycle regulation, proliferation, migration, and invasion by regulating expressions of many salient genes (Fang and Fullwood, 2016). Nowadays, competing endogenous RNAs (ceRNAs) have been proven to play a prominent role in cancer initiation and progression and might be explored as diagnostic markers or therapeutic targets (Qi et al., 2015).

Meanwhile, cancer biomarkers need to have a strong specificity for a particular disease condition and lncRNAs have been emerging as crucial players in the control of gene expression (Iaccarino and Klapper, 2021). Previous studies have shown the marked heterogeneity in lncRNA expression between individual cancer cells so that lncRNA have a much higher cell/tissue specificity of expression in comparison to other ncRNAs and mRNAs (Silva et al., 2015; Wu et al., 2021). Besides, lncRNAs are often stable in clinical samples and can easily be detected by common techniques, such as quantitative real-time PCR, sequencing, and microarray hybridization (Silva et al., 2015). The patterns of lncRNAs deregulation in primary tumor tissues have been found in bodily fluids, including plasma and urine (Silva et al., 2015), which presents an opportunity to develop lncRNA-based biomarker tools that are convenient, minimally invasive, and may be easily accepted by patients.

Studies have indicated that lncRNAs could play important roles as ceRNAs in certain cancers, such as breast cancer, colorectal cancer, pancreatic cancer, and so on (Liu et al., 2021; Rong et al., 2021; Zeng et al., 2021). They also could exert carcinogenic effects as ceRNAs in PTC. For example, Sui et al. have revealed that, as a ceRNA of miR-214-3p, small nucleolar RNA host gene 3 (SNHG3) is an oncogenic lncRNA in PTC by binding with miR-214-3p to regulate the expression of proteasome 26S subunit non-ATPase 10 (PSMD10) (Sui et al., 2020). Further, Zhang et al. have proven that the lncRNA of FOXD2-AS1 is highly up-regulated in PTC and acts as a ceRNA to promote the expression of KLK7 by sponging miR-485-5p, resulting in cell proliferation and migration (Zhang et al., 2019). Moreover, the expression levels of lncRNAs and miRNAs may be directly associated with the good/bad prognosis and could be involved in carcinogenic or tumor-suppressive pathways, which mark them as potential prognostic biomarkers (Murugan et al., 2018; Hanna et al., 2019). For example, Chen et al. identified lncRNA TTTY10 as prognostic markers for predicting tumor recurrence in PTC (Chen et al., 2019). Zhao et al. screened out three lncRNAs of LINC00284, RBMS3-AS1, and ZFX-AS1 by constructing lncRNA-miRNA-mRNA network, which were found to be associated with PTC progression and prognosis (Zhao et al., 2018). Recently, Sun et al. found five lncRNAs which were associated with PTC patient survival time but only based on one individual GEO data set (Sun et al., 2020). However, potential lncRNA biomarkers which are more reliable and convincing are yet to be found, because the existing studies always give different crucial lncRNAs based on different individual databases. Until now, the field still lacks integration of different databases for a comprehensive validation on PTC hub lncRNA genes and the regulation characteristics of them are not well revealed.

In this study, we integrated the data from four GEO databases with the most PTC samples and the Cancer Genome Atlas (TCGA) so as to screen crucial lncRNAs. Five hub lncRNAs were achieved by robust rank aggregation (RRA) method for data integration of different databases. To comprehensively validate five hub genes, their expression difference analysis and the receiver operating characteristic (ROC) diagnostic analysis were performed based on four GEO datasets, TCGA and Gene Expression Profiling Interactive Analysis (GEPIA) database, respectively. Meanwhile, lncRNA-mRNA co-expression network and lncRNA-miRNA-mRNA ceRNA network were also constructed. Functional analysis on mRNAs involved in the two networks along with the deep-literature exploring five hub lncRNAs and these mRNAs all indicate that they are all involved in cancer-related functions. So, the five hub lncRNAs give promising potentiality for diagnosing PTC.

We also established two prognostic risk models for PTC OS and DFS, namely PTC-mi1m4 and PTC-m3, respectively, by screening all genes in ceRNA network. To elucidate the potential pathogenesis of PTC, Gene Oncology (GO), Kyoto Encyclopedia of Genes and Genomes (KEGG), and Disease Ontology (DO) enrichment analyses were performed. The proportions of 22 immune cells of PTC were analyzed to estimate the tumor microenvironment in patients with PTC. Among them, two immune cells were demonstrated to be associated with the prognosis of PTC and they may be the potential target of immunotherapy.

Finally, connectivity map (CMap) analysis was performed based on five prognosis-related mRNAs to screen potential bioactive chemicals. Three promising drugs were predicted as compounds that play vital roles in PTC-related biological processes and may provide potential treatment of PTC.

MATERIALS AND METHODS

Data Collection and Pre-Processing

In this study, based on the same sequencing platform of Affymetrix Human Genome U133 Plus 2.0 Array from GEO database (http://www.ncbi.nlm.nih.gov/geo/query/acc.cdi), four gene chips with the most sample pairs were selected, including GSE29265 with 20 pairs of normal and PTC samples, GSE3678 with seven pairs, GSE3467 with nine pairs, and GSE33630 with 49 PTC samples and 45 normal samples. Furthermore, the RNA-Seq counts data of 501 PTC and 58 normal tissues were downloaded from TCGA data center (http://portal.gdc.cancer.gov/). Meanwhile, we obtained the clinical information of 496 PTC patients from cBioPortal for Cancer Genomics (http://www.cbioportal.org). After deleting PTC samples without either expression data or clinical information, 490 eligible PTC, and 58 normal tissues remained for the construction of PTC OS prediction model. Since 14 of 490 PTC samples lack clinical information about PTC DFS, the remaining 476 samples were used for DFS prediction.

In order to obtain lncRNA expression data, based on four GEO datasets, we only extracted genes annotated as "3prime_overlapping_ncRNA," "antisense," "sense_intronic," "sense_overlapping," "macro_lncRNA," "lincRNA," "non_coding," "bidirectional_promoter_lncRNA," and "misc_RNA." After deleting genes with no expression in more than four samples, in total 1038 lncRNAs remained from four gene chips. In addition, 743 miRNAs and 16160 mRNAs were achieved from TCGA. Finally, all the raw data from GEO were normalized by the Normalize Between Arrays method in R package "limma" and those from TCGA were normalized by Trimmed Mean of M values (TMM) in R package "edgeR."

Differential Expression Analysis and RobustRankAggreg Method

Firstly, each GEO dataset was normalized using the normalize Between Arrays function in R package "limma." Then, differential expression analysis was conducted on lncRNA expression data of four GEO individual datasets respectively also by R package "limma." Here, considering the limited number of lncRNAs in GEO datasets, those with $|\log FC|>1$ and adjusted $p < 0.05$ were selected as differentially expressed ones. However, different differential lncRNAs were extracted from different gene chips respectively. Here, in order to achieve more valid and representative differential lncRNAs as well as to remove the bath effect, RRA method in R package was employed to integrate the differentially expressed gene lists resulting from differential expression analysis of four individual datasets. The RRA method can detect genes that are ranked consistently better than expected and then assign a significance score for each gene. The significance scores provide a rigorous way to keep only the statistically relevant genes in the final list so that genes identified by this method will be robust, convincing, and significant (Kolde et al., 2012). Then, the significant differentially expressed lncRNAs selected by RRA method were considered as hub lncRNAs for further analysis.

Differential expression analysis with miRNA and mRNA expression data of TCGA database was performed using R software package "egdeR" with $|\log FC|>1$ and adjusted $p < 0.05$. Finally, the "ggplot2" package was used to make the volcano plot visualized, revealing the distributions of all differential genes.

Construction of lncRNA-mRNA Co-Expression Network

To establish the lncRNA-mRNA co-expression network, the Pearson correlation analysis was performed between expression levels of hub lncRNAs and differential mRNAs in TCGA so as to select co-expressed mRNAs that are correlated with hub lncRNAs with the coefficient value of $|\mathrm{Cor}|>0.5$ and $p < 0.05$. The network graph of lncRNA-mRNA co-expression network was built and visualized by Cytoscape (Version:3.7.1, https://cytoscape.org/).

Establishment of a lncRNA-miRNA-mRNA Network

For the purpose of constructing lncRNA-miRNA-mRNA ceRNA network, starBase v2.0 (http://starbase.sysu.edu.cn) was used to predict lncRNA-miRNA interactions. Those predicted miRNAs only proved to be differentially expressed by TCGA data are regarded as those which were used to construct the ceRNA network. mRNAs targeted by those miRNAs interacting with hub lncRNAs were predicted using miRTarbase (http://mirtarbase.cuhk.edu.cn/), miRDB (http://www.mirdb.org/), and TargetScan 7.2 (http://www.targetscan.org/vert_72/). Similarly, only those predicted target mRNAs that also differentially expressed TCGA can be involved in the ceRNA network. Finally, the lncRNA-miRNA-mRNA ceRNA network was established and visualized using Cytoscape (Version:3.7.1, https://cytoscape.org/).

Functional Analysis

To characterize the function of mRNAs in lncRNA-mRNA co-expression network and those in lncRNA-miRNA-mRNA ceRNA network respectively, GO, KEGG, and DO enrichment analyses were all performed with "clusterProfiler" package for investigating biological process, molecular function, pathways, and related diseases.

Development of Survival Signatures and Survival Analysis

Univariate Cox proportional hazards regression analysis was performed on all genes in lncRNA-miRNA-mRNA ceRNA network with $p < 0.05$ as the threshold to respectively identify OS-associated or DFS-associated lncRNAs, miRNAs, or mRNAs. Then, these genes were entered into the step-wise multivariate Cox regression analysis using R package "survminer" to screen out the key RNAs with great prognostic values. Finally, those

RNAs selected in the multivariate Cox regression were used to construct PTC OS-associated signature and DFS-associated signature. The prognostic signatures were constructed as follows:

$$Risk\ score = \sum_{i=1}^{n} \beta_i * Expression_i \quad (1)$$

where n is the number of candidate genes, β_i is the coefficient of gene i in multivariate regression analysis, and $Expression_i$ is the expression level of gene i that has been normalized by TMM.

Based on the risk score, the PTC patients were divided into high and low-risk groups by cut-off median. Time-dependent receiver operating characteristic (ROC) and Kaplan-Meier survival curve analyses were performed by R package of "survivalROC," "survival," and "survminer." Area under curve (AUC) value from the ROC curve and concordance index (C index) were calculated to determine the prognosis accuracy of the two signatures.

Using the other clinicopathological factors associated with PTC patients' OS or DFS time as confounding variables, clinical characteristics including age, gender (male/female), and stage (I, II, III, IV) were also analyzed using univariate and multivariate Cox regression. This stratified analysis was conducted to determine whether the prognostic signature is independent of these clinical factors.

Estimation of Tumor Microenvironment

In order to evaluate the proportions of all 22 immune cells in PTC tissues, CIBERSORT methods were used based on the gene expression profile by running CIBERSORT script from the website (http://rdrr.io/github/singha53/amritr/src/R/supportFunc_cibersort.R). The sums of immune cells of each PTC patient were equal to 1. The Wilcoxon test was used to test the prominent difference of immune cells' proportions between high and low-risk groups that was divided according to OS-associated signature and DFS-associated signature respectively. The Pearson correlation coefficient was calculated to study the correlations between 22 immune cells and key genes involved in two risk models with the cutoff values of $|Cor|>0.2$ and $p < 0.05$. So, the distinctive immune cells were identified that not only show significant differences between high and low-risk groups but are correlated with the expression levels of genes. Finally, univariate and multivariate Cox regression analyses were used to further identify those which may be associated with OS or DFS of patients.

CMap Analysis

The CMap online tool (http://broadinstitute.org/cmap) was used to predict the effect of drugs on the particular gene expression patterns in tumors. In order to study functional connections between the key genes associated with OS and DFS of PTC patients and bioactive chemicals, the up-regulated and down-regulated tags from the key genes were uploaded into the CMap online tool. How closely a compound is connected to the uploaded signature depends on the connectivity score with a range from −1 to 1. A positive connectivity score indicates that the compound promotes the query gene expression, whereas a negative connectivity score indicates that the compound represses the query gene expression.

RESULTS

Identification and Validation of Hub lncRNAs for Marking PTC

Four lncRNA gene chips (GSE29265, GSE3678, GSE33630, and GSE3467) based on the same sequencing platform were selected in this study. In total, eight differentially expressed lncRNAs were recognized in GSE29265 gene chip, including three lncRNAs with higher expression and five lncRNAs with lower expression (**Figure 1A**). A total of six differentially expressed lncRNAs were identified from GSE3678 gene chip, of which three are up-regulated and thre are down-regulated lncRNAs (**Figure 1B**). Moreover, there are nine differential lncRNAs in GSE33630 gene chip, containing five up-regulated and four down-regulated ones (**Figure 1C**). Only one down-regulated lncRNA was recognized in GSE3467 (**Figure 1D**). So, we can see that different gene chips give different differential lncRNAs. Then we used RRA method for integration and further screening so as to achieve more distinctive hub lncRNAs. Through rank analysis by RRA method among the four expression matrices, five hub lncRNAs were identified.

The five hub lncRNAs are SLC26A4-AS1, RNF157-AS1, NR2F1-AS1, ST7-AS1, and MIR31HG. Among them, RNA expressions of NR2F1-AS1 and MIR31HG in PTC tissues were significantly up-regulated compared with normal tissues, while expressions of the other three genes were significantly down-regulated in all four GEO datasets (**Figure 2**). In order to verify this observation, expression levels of these five hub genes were also analyzed based on two other validation datasets of GEPIA database and TCGA (**Supplementary Figures S1, S2**). Since RNF157-AS1 is not included in the GEPIA database, **Supplementary Figure S1** only gives differential analysis results of four other genes. We can see that all five hub lncRNAs are differentially expressed in all datasets. NR2F1-AS1 and MIR31HG are always up-regulated and the other three genes are down-regulated in all six or five datasets.

In order to further verify the potentiality of five hub lncRNAs for marking PTC, the diagnostic performance of these five hub lncRNAs were demonstrated by ROC curve analysis based on four GEO datasets and TCGA, as shown in **Figures 3A–E**. For each of them, the AUC value is higher than 0.90 in at least two datasets. SLC26A4-AS1 is the exception as it gives an AUC value of 0.753 in GSE29265, while all other 24 AUC values are higher than 0.80. ST7-AS1 yields the best diagnostic performance in all five databases with all five AUC values higher than 0.90 (**Figure 3B**) and those of SLC26A4-AS1, ST7-AS1, and RNF157-AS1 in GSE3678 are equal to 1. The results illustrate that the five hub genes screened out by us also yield excellent diagnostic efficiency between PTC and normal tissues. These validation tests suggest that the five hub lncRNAs are all reliable and potential biomarkers for marking PTC.

Finally, a deep literature-exploring was implemented and all five hub genes have been confirmed as having important roles in

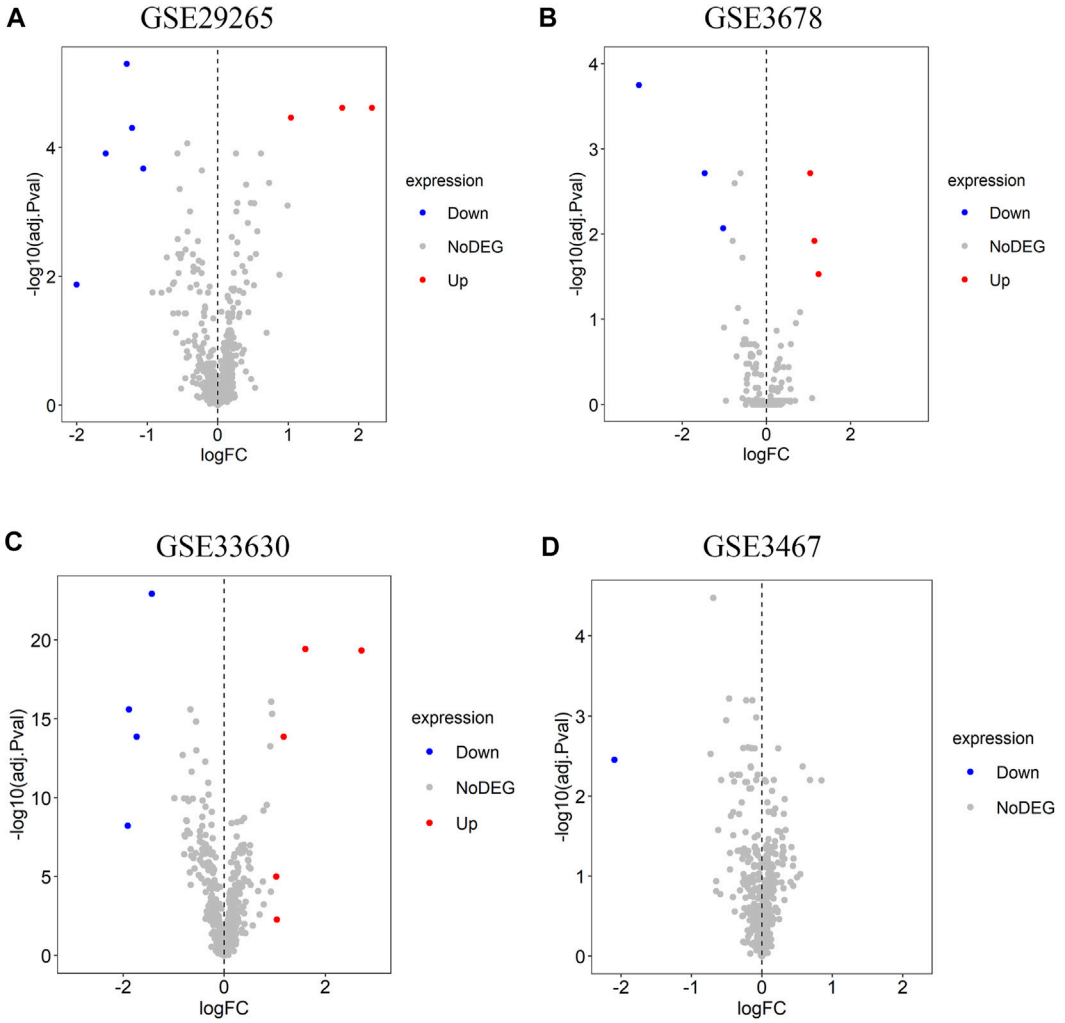

FIGURE 1 | Identification of differentially expressed lncRNAs in each dataset. **(A)** GSE29265, **(B)** GSE3678, **(C)** GSE33630, **(D)** GSE3467. The red pots represent the up-regulated lncRNAs and the blue pots represent the down-regulated ones with the cutoff criteria of |logFC| > 1 and adjusted $p < 0.05$. The grey pots represent lncRNAs with no prominent expression difference.

PTC and other cancers. The overexpression of SLC26A4-AS1 could decrease cell migration, invasion, and proliferation, and thus had anti-oncogenic effects in PTC (Wang DP. et al., 2020). But NR2F1-AS1 was reported to promote invasion and invasion of PTC (Yang et al., 2020). Besides, MIR31HG was observed to promote cell proliferation and cell cycle progression and inhibit cell apoptosis, and it could be a potential therapeutic target for head and neck squamous cell carcinoma in the study by Wang et al. (2018). As mentioned in previous research, up-regulated ST7-AS1 could expedite migration and invasion in gastric cancer and it promoted the oncogenicity of cervical cancer cells by ST7-AS1/miR-543/TPRM7 (Cai et al., 2020; Qi et al., 2020). Xu and Xu (2020) observed that the higher expression of RNF157-AS1 motivated the proliferation of ovarian cancer cells, while the overexpression of RNF157-AS1 decreased the chemoresistance; thus, ovarian cancer patients with overexpressed RNF157-AS1 have better prognosis.

lncRNA-mRNA Co-Expression Network

Further, functions of the co-expressed mRNAs with hub lncRNAs were investigated. By Pearson correlation analysis with the cutoff values of $|Cor| > 0.5$ and $p < 0.05$, the interactions between five lncRNAs and 2716 differential mRNAs in TCGA were researched. A total of 647 mRNAs were significantly related to the five hub lncRNAs, so the lncRNA-mRNA co-expression network was constructed. The network graph is shown in **Figure 4**. We can see that SLC26A4-AS1, RNF157-AS1, and ST7-AS1 share more interacting mRNAs, which may indicate that there are coordinated interactions among three lncRNAs by sharing common mRNAs. But NR2F1-AS1 individually has the most interacting mRNAs and MIR31HG has the least. So, we presented a further functional analysis on these co-expressed mRNAs using GO, KEGG pathway, and DO analysis.

Firstly, mRNAs involved in lncRNA-mRNA co-expression network were divided in to common or specific ones. If

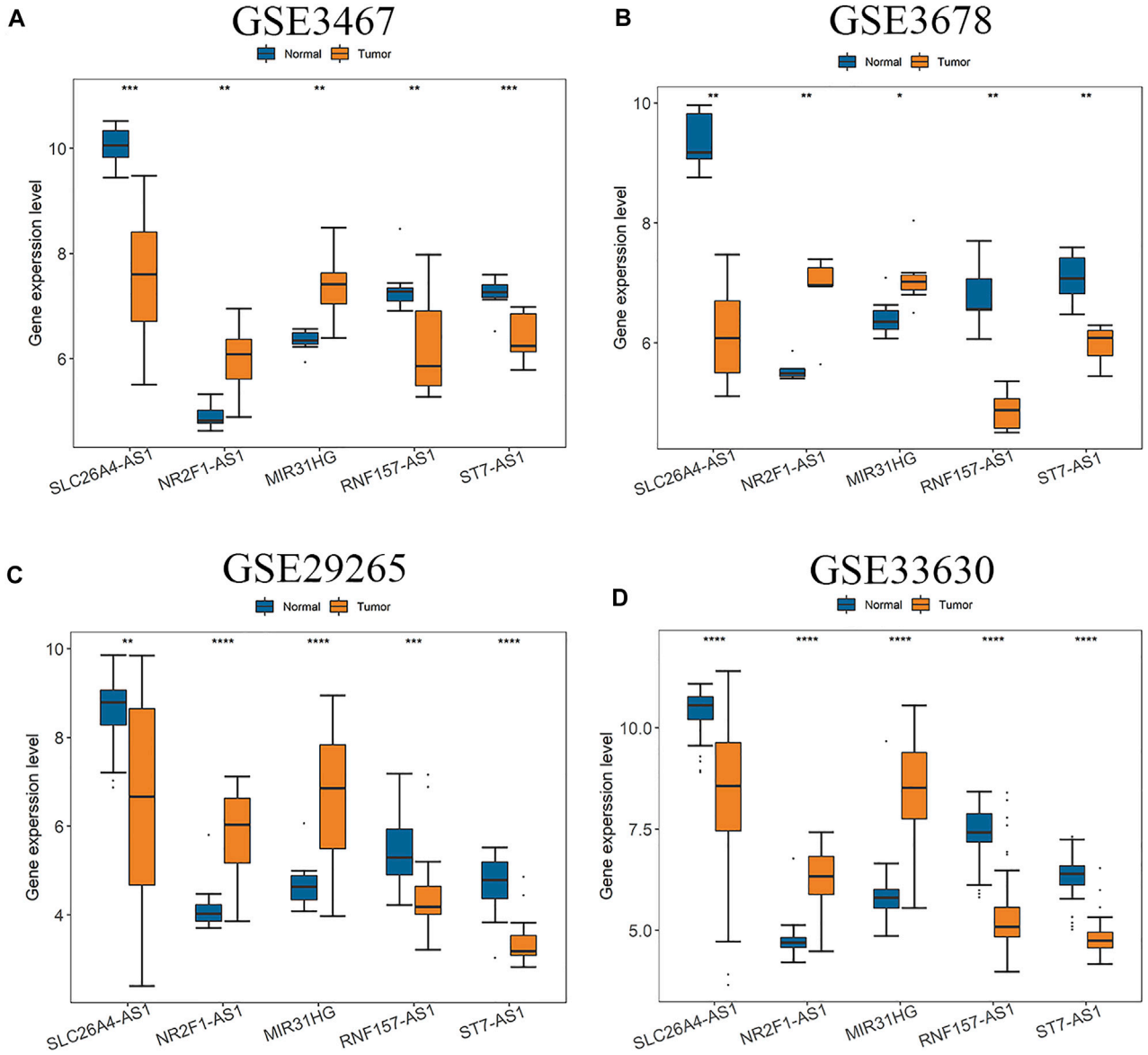

FIGURE 2 | Expressions of five hub lncRNAs in PTC compared with normal tissues in **(A)** GSE3467, **(B)** GSE3678, **(C)** GSE29265 and **(D)** GSE33630 dataset. (*: $p < 0.05$, **: $p < 0.01$, ***: $p < 0.001$).

mRNAs are related with two or more lncRNAs, they are defined as common and those that only connect with one lncRNA are specific mRNAs. As displayed in **Figure 5**, the common mRNAs are involved in the thyroid hormone generation (**Figure 5A**) and dynein intermediate chain binding function (**Figure 5B**). They are commonly associated with thyroid hormone synthesis (**Figure 5C**) and thyroid gland disease (**Figure 5D**). But specific mRNAs are most involved in axonogenesis (**Figure 5E**) and transmembrane receptor protein tyrosine kinase activity (**Figure 5F**). They may be related with p53 signaling pathway (**Figure 5G**) and papillary carcinoma (**Figure 5H**). So, the function analysis indicates that the co-expressed mRNAs that are common between five hub lncRNAs may have important roles in the development and progression of PTC.

lncRNA-miRNA-mRNA ceRNA Network

To construct lncRNA-miRNA-mRNA ceRNA network, the starBase v2.0 was used to predict the target miRNAs of five hub lncRNAs and 713 were identified. Then, 17 target miRNAs were determined by intersecting 167 differentially expressed miRNAs in TCGA and 713 predicted miRNAs. Consequently, miRDB, miRTarBase, and TargetScan 7.2 were used to predict probable target mRNAs of the above 17 miRNAs and extracted the intersections from the three online analysis tools. By overlapping the predicted mRNAs to 2716 differential derived

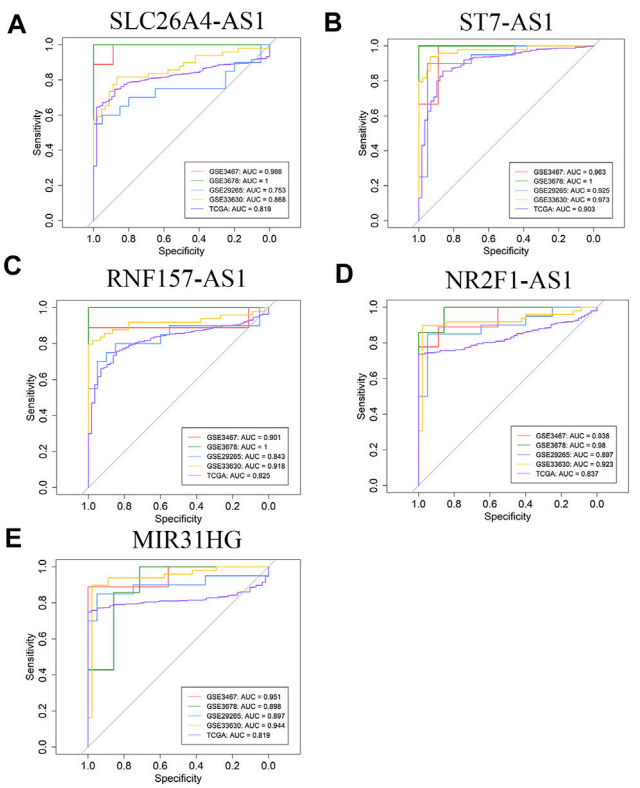

FIGURE 3 | ROC curve analysis of five hub lncRNAs diagnosis in GSE3467, GSE3678, GSE29265, GSE33630, and TCGA cohort. **(A)** SLC26A4-AS1 **(B)** ST7-AS1 **(C)** RNF157-AS1 **(D)** NR2FA-AS1 **(E)** MIR31HG.

constructed (**Figure 6A**). The potential functional characteristics of mRNAs in this ceRNA network were also interpreted by GO, KEGG pathway, and DO analysis respectively. The 68 differential target mRNAs are enriched in BP of skin morphogenesis and respond to corticosteroid (**Figure 6B**) as well as MF of platelet-derived growth factor binding and extracellular matrix (**Figure 6C**). Previous reports have been indicated that corticosteroid could alleviate cancer-related symptoms and play an indispensable role in cancer care (Drakaki et al., 2020). In addition, lymph node metastasis is important for the treatment and prognosis of PTC patients and some platelet-derived growth factors can promote lymph node metastasis by participating in lymphangiogenesis of rectal cancer (Liu et al., 2011). The extracellular matrix can also influence cancer progression and then significantly affect the matrix composition and structure (Malandrino et al., 2018). Among the enriched pathways (**Figure 6D**), PI3K-Akt signaling pathway plays an extensive role in thyroid tumorigenesis and focal adhesion is also a tumor-related pathway (Hou et al., 2007; Antoniades et al., 2021). In addition, mRNAs were observably associated with hyperparathyroidism and parathyroid gland disease (**Figure 6E**). The above analysis could indicate to some extent that these mRNAs may play important roles in PTC.

Construction of Prognostic Signatures and Survival Analysis

Initially, the five hub lncRNAs were used to establish the prognosis model. However, the univariate Cox analysis results

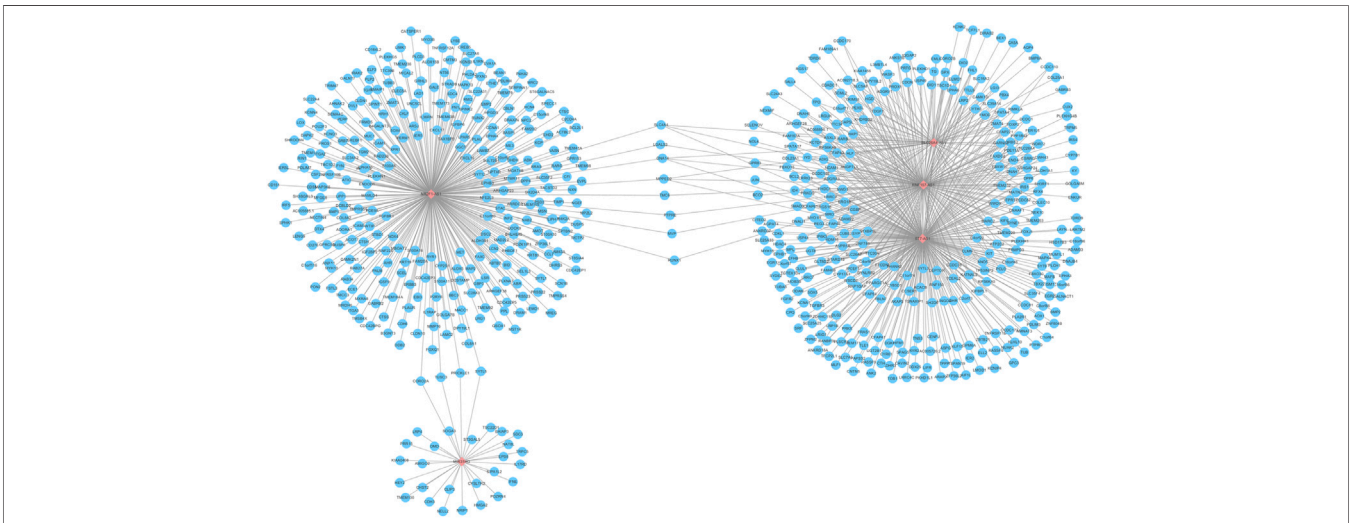

FIGURE 4 | lncRNA-mRNA co-expression network. The network includes the five hub lncRNAs (pink pots) and 650 mRNAs (blue pots).

from TCGA, 68 target mRNAs that may exert critical functions in PTC were discovered.

Based on the achieved lncRNA-miRNA pairs and miRNA-mRNA pairs, the lncRNA-miRNA-mRNA ceRNA network was

of five hub lncRNAs prove that the *p*-values of five hub lncRNAs are all much higher than 0.05, as shown in **Supplementary Figure S3**. So, these lncRNAs were not associated with PTC patients' OS and DFS, although they yield promising diagnostic performance.

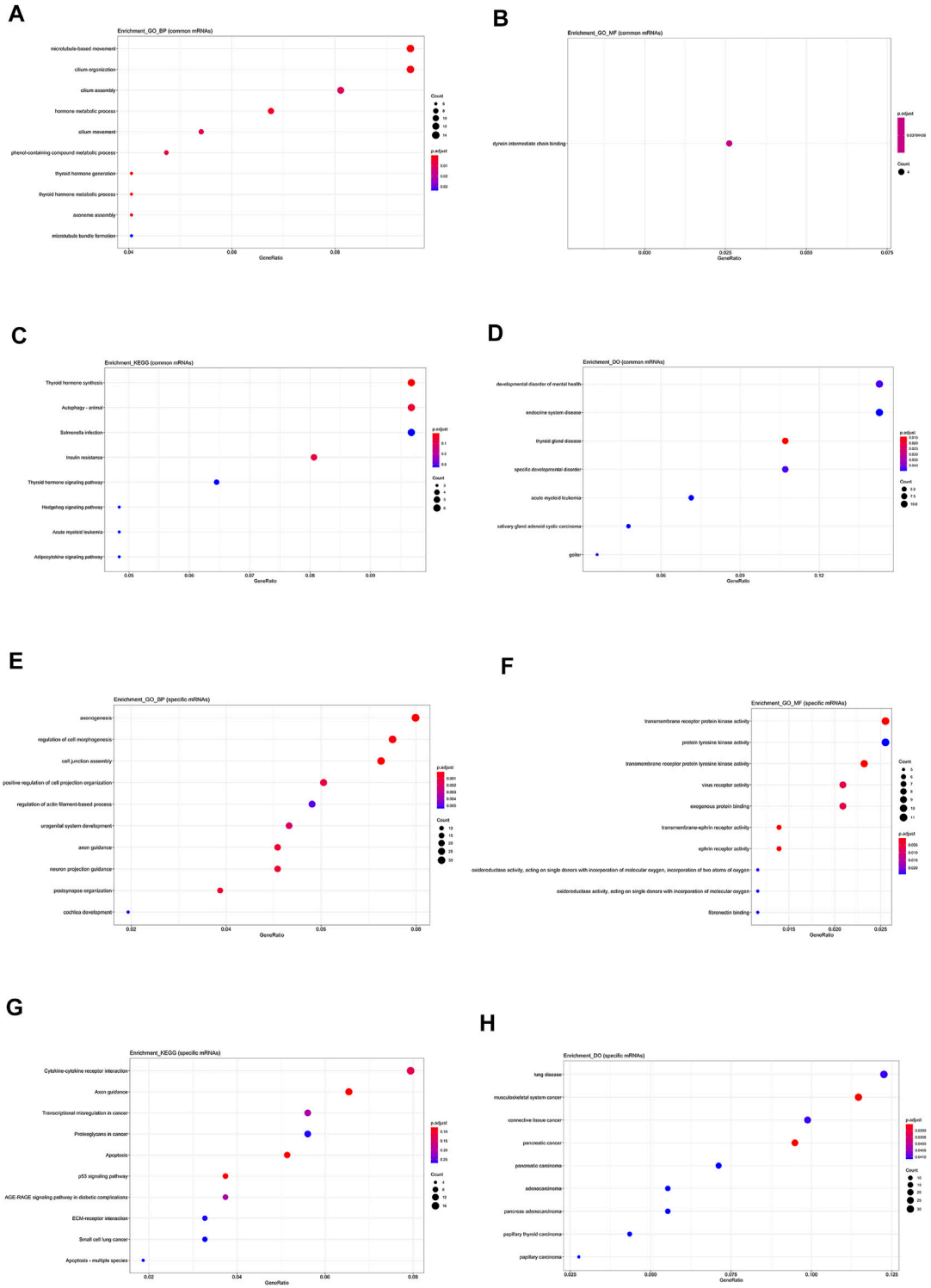

FIGURE 5 | Functional analysis on common and specific mRNAs in lncRNA-mRNA co-expression network. **(A)** The biological process items of common mRNAs by GO analysis. **(B)** The molecular function items of common mRNAs by GO analysis. **(C)** Functional enrichment analysis by KEGG for common mRNAs. **(D)** Functional enrichment analysis by DO for common mRNAs. **(E)** The biological process items of specific mRNAs by GO analysis. **(F)** The molecular function items of specific mRNAs by GO analysis. **(G)** Functional enrichment analysis of KEGG for specific mRNAs. **(H)** Functional enrichment analysis of DO of specific mRNAs.

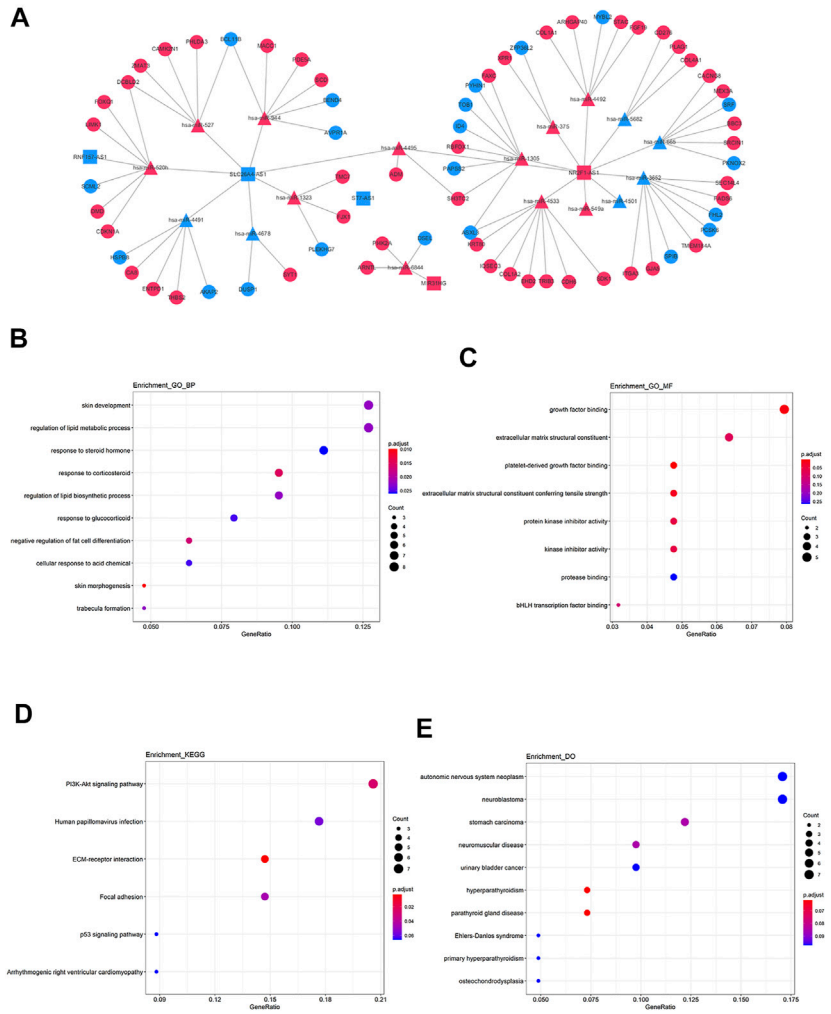

FIGURE 6 | | lncRNA-miRNA-mRNA ceRNA network and functional prediction of mRNAs in network. **(A)** The network consists of three lncRNAs (rectangles), 17miRNAs (triangles), and 68 mRNAs (circles). The red pots represent up-regulated RNAs and the blue pots represent down-regulated RNAs. **(B)** The biological process items by GO analysis. **(C)** The molecular function items by GO analysis. **(D, E)** Functional enrichment analysis of DO.

To identify the potential RNAs with prognostic characteristics, univariate Cox proportional hazards regression analysis was performed for five lncRNAs, 17 miRNAs, and 68 mRNA expression data and those related to patient OS or DFS were selected by using $p < 0.05$ as the criteria. As a result, nine mRNAs including TMEM184A, SRCIN1, PI4K2A, FADS6, ITGA3, KRT80, ADM, TOB1, and DCBLD2 were found to be correlated with PTC DFS. On the other hand, four miRNAs and nine mRNAs, namely hsa-miR-1305, hsa-miR-4501, hsa-miR-3652, hsa-miR-665, PASS2, SCD, THBS2, ID4, FHL2, MEX3A, DSEL, DCBLD2, and TMEM184A, were significantly associated with PTC OS. Then, in order to further screen out an optimal combination from these genes, stepwise multivariate Cox regression analysis was conducted and subsequently two predictive signatures named PTC-mi1m4 (hsa-miR-1305, PAPSS2, SCD, ID4, and DCBLD2) and PTC-m3 (TMEM184A, TOB1, and FADS6) were obtained for PTC OS and DFS respectively.

For the feature genes in the prognostic risk models, their cancer-related function roles were also investigated here. A previous study by Ng et al. (2015) has shown that hsa-miR-1305 may target the genes involved in cell cycle, cell junction, and cytoskeleton. In our study the target genes are PAPSS2, SCD, and ID4 which play significant roles in various cancers. PAPSS2 is downregulated in radiation-induced PTC and has been used as a potential biomarker for radiation-induced PTC (Stein et al., 2010). ID4 is a promising target in cancer therapy and it could be involved in thyroid tumorigenesis and prevent thyroid cancer invasion and metastasis (Amaral et al., 2019). Inhibiting SCD could result in tumor cell death including anaplastic thyroid carcinoma, colorectal adenocarcinoma, renal cell carcinoma, and non-small cell lung carcinoma (von Roemeling and Copland, 2016). DCBLD2 has been reported to play a positive role in lung cancer and glioblastomas but shows a negative role in gastric and neuroendocrine cancers (He et al., 2020). For the additional three mRNAs of TMEM184A, TOB1,

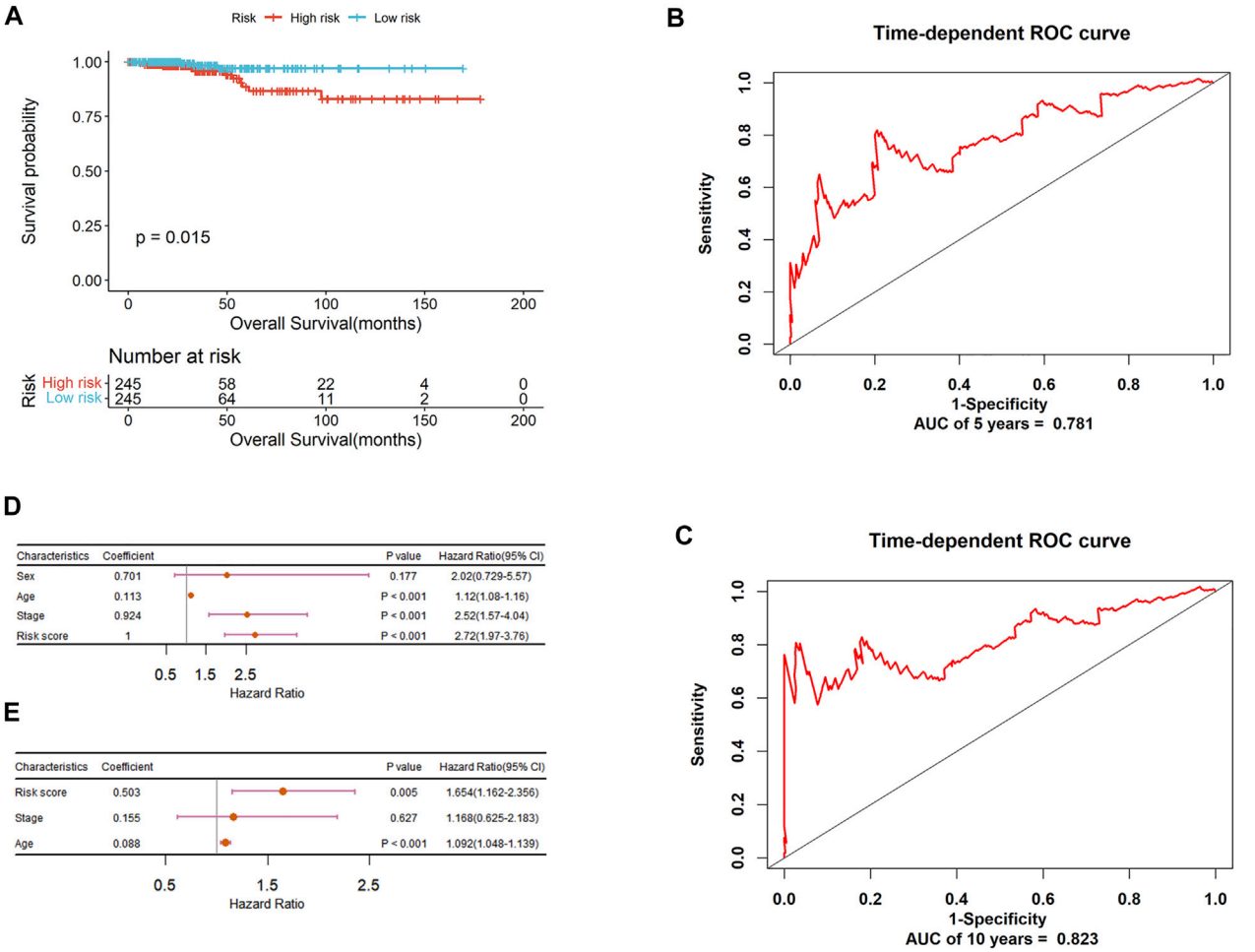

FIGURE 7 | The prognostic significance of PTC-mi1m4 signature to predict OS of PTC patients. **(A)** Kaplan-Meier curve analysis for OS. **(B)** ROC validation of prognostic value of PTC-mi1m4 signature for predicting 5-years survival of PTC patients. **(C)** ROC validation of prognostic value of PTC-mi1m4 signature for predicting 10-years survival of PTC patients. **(D)** Forest plot summary of univariable analysis of sex, age, stage, and risk score. **(E)** Forest plot summary of multivariable analysis of age, stage, and risk score.

and FADS6 in PTC DFS model, heparin binds specifically to TMEM184A and could induce anti-proliferative signaling *in vitro* (Farwell et al., 2017). As a Tob/BTG anti-proliferation protein family member, TOB1 acts as a tumor suppressor in many cancers. Tob phosphorylation also contributes to the progression of PTC (Ito et al., 2005) and NR2F1-AS1identified as a hub gene by us could suppress proliferation of colorectal cancer cells by regulating TOB1 (Wang J. et al., 2020). FADS6 was found to be mutated in Chinese Epstein-Barr virus-positive diffuse large B-cell lymphoma (Liu et al., 2018). Overall, these genes constructing two prognostic signatures are all involved in cancer-related functions.

The risk score of each patient was calculated and all patients were divided into high and low-risk groups using the median as the cutoff. For PTC-mi1m4, it can be seen from **Figure 7A** that the Kaplan-Meier analysis shows that patients with low-risk score have a higher survival rate compared to those in the high-risk group ($p = 0.015$). The time-dependent ROC analysis shows that the AUC values for predicting 5-years and 10-years OS rates are 0.781 and 0.823respectively with C index of 0.775 (**Figures 7B,C**), suggesting that this model yields a strong prognostic ability for predicting PTC OS. Then the stratification analysis was implemented based on risk score, age, gender, and tumor stage. As shown in **Figure 7D**, univariate Cox regression analysis reveals that risk score, age, and stage are associated with PTC patients' OS, but multivariate Cox regression analysis show that risk score and age are the independent prognostic indicators for PTC patients' OS (**Figure 7E**). Similarly, another prognostic signature (PTC-m3) for DFS prediction could also adequately classify PTC patients into low and high-risk groups. The survival analysis demonstrates that high-risk patients have shorter survival times than low-risk patients (**Figure 8A**). The AUC-ROC are 0.665 and 0.726 at five and 10 years respectively with C index of 0.676 (**Figures 8B,C**). After performing univariate and multivariate Cox

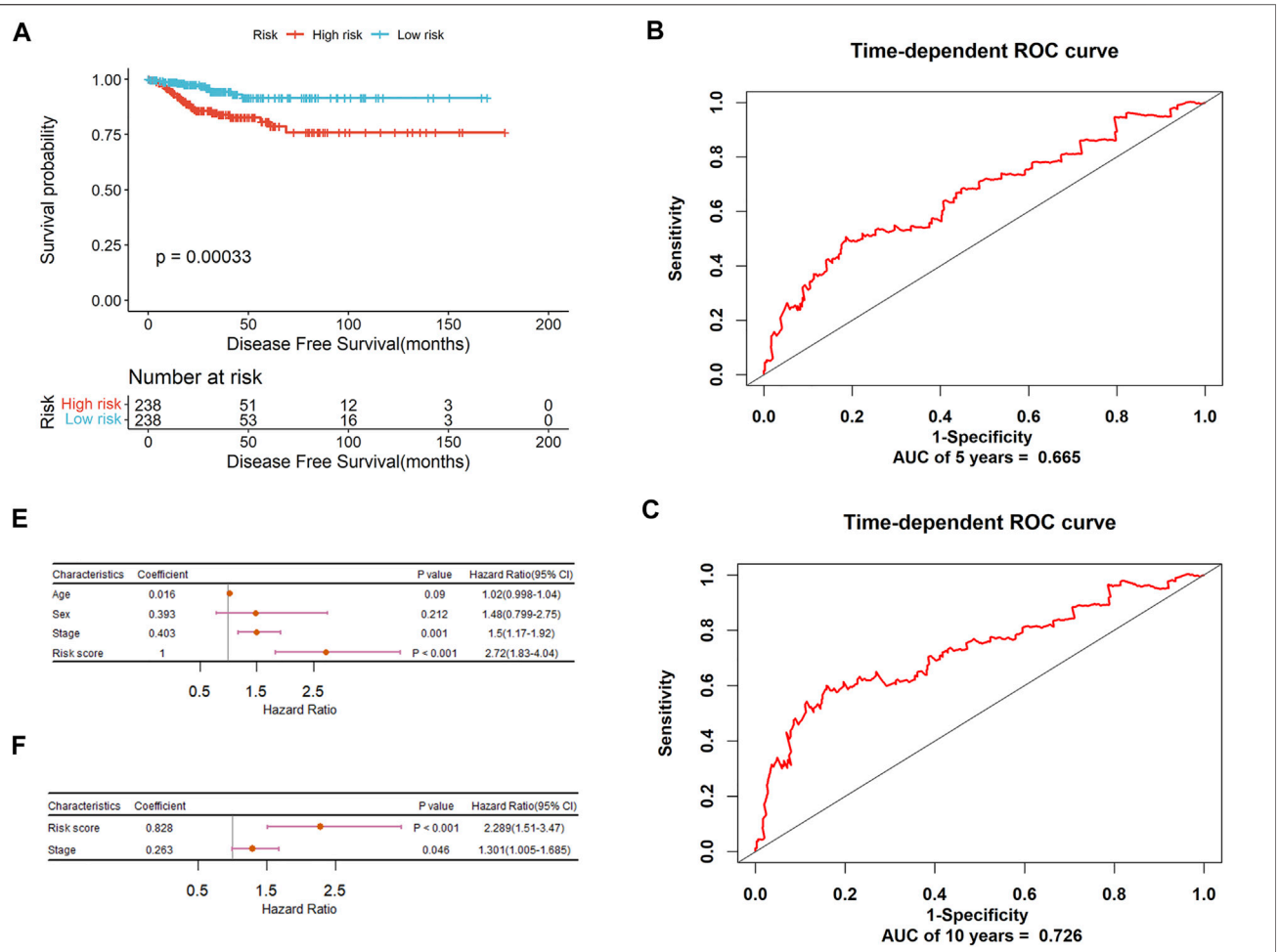

FIGURE 8 | The prognostic significance of PTC-m3 signature to predict DFS of PTC patients. **(A)** Kaplan-Meier curve analysis for DFS. **(B)** ROC validation of prognostic value of PTC-m3 signature for predicting 5-years survival of PTC patients. **(C)** ROC validation of prognostic value of PTC-m3 signature for predicting 10-years survival of PTC patients. **(D)** Forest plot summary of univariable analysis of sex, age, stage, and risk score. **(E)** Forest plot summary of multivariable analysis of stage and risk score.

regression analysis, the result also shows that this risk score could be an independent applicable prognostic indicator for predicting PTC patients' DFS (**Figures 8D,E**).

Immune Landscape in Patients With PTC

Understanding the tumor microenvironment (TME) is of practical significance for cancer diagnosis and treatments. The 22 immune cells form the major non-tumor constituents of tumor tissues, and can perturb the tumor signal and have an important role in cancer biology (Yoshihara et al., 2013). We know that differences in the proportion and level of tumor infiltrating immune cells may represent intrinsic characteristics of different individuals (Nie et al., 2020). In order to investigate the specific immune characteristics of PTC, the gene expression matrix of PTC dataset was used to estimate the portion of 22 immune cells by running CIBERSORT script. The proportion of immune cells in 490 PTC samples was shown in **Figure 9A**. We can see that the proportion of T cells CD4 memory resting is the highest, but the fraction of neutrophils is very low. It indicates that the two immune cells may play important roles in the development of PTC tumors.

Then the differences of immune cells' proportions between high and low-risk groups divided according to OS-associated signature and DFS-associated signature were further estimated by using Wilcoxon test and displayed in **Figures 9B,C**, respectively. As seen in **Figure 9B**, compared with low-risk patients, high-risk patients have significantly higher proportions of T cells CD4 memory resting, macrophages M0, and dendritic cells activated. Lower proportions of T cells CD8, T cells follicular helper, and T cells regulatory (Tregs) are observed in high-risk patients. Pearson correlation analysis indicates that macrophages M1, macrophages M0, eosinophils, NK cells activated, dendritic cells resting, Tregs, and dendritic cells activated are associated with mRNAs that are used to construct OS-associated signature. In summary, dendritic cells activated, macrophages M0, and Tregs not only have significant differences between high and low-risk groups but are closely related with the expression levels of four feature mRNAs in OS risk model. So univariate and

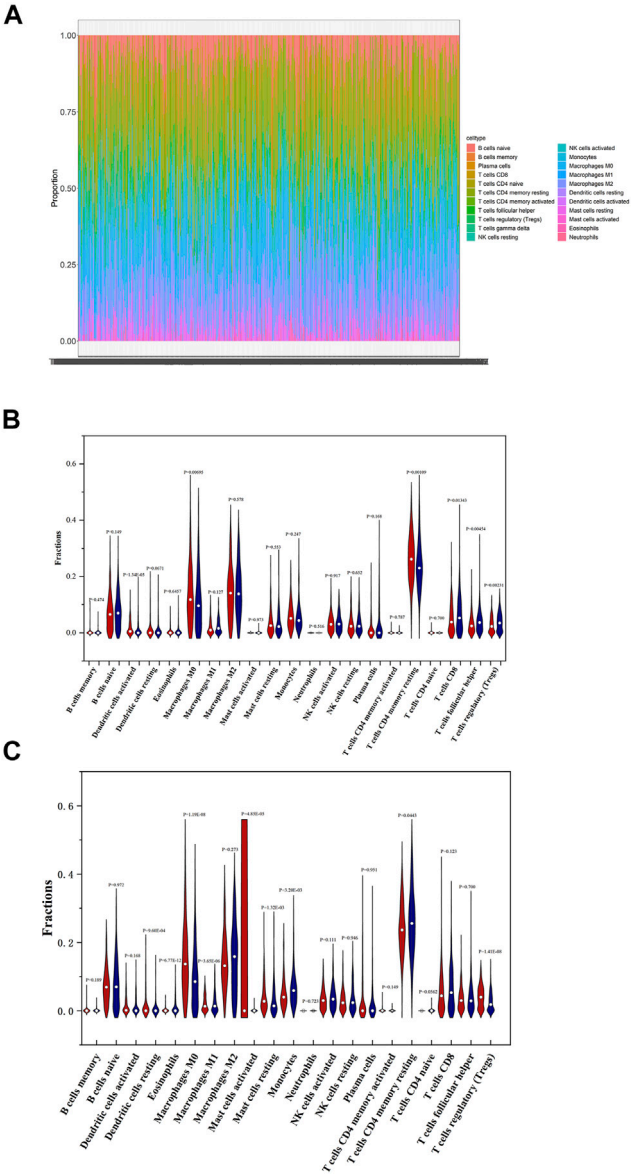

FIGURE 9 | Immune landscape in low and high-risk patients with PTC. **(A)** Proportions of 22 immune cells in PTC patients. **(B)** Comparisons on the proportions of immune infiltrating cells between low and high-risk patients based on OS-associated signature. **(C)** Comparisons on the proportions of immune infiltrating cells between low and high-risk patients based on DFS-associated signature.

multivariate Cox regression analyses were also performed on three immune cells. The results in **Table 1** shows that dendritic cells activated was associated with PTC OS. Moreover, it has a higher proportion in high-risk patients.

Figure 9C shows that the proportions of dendritic cells resting, macrophages M0, mast cells resting, and Tregs are higher and those of eosinophils, macrophages M1, mast cells activated, monocytes, and T cells CD4 memory resting are lower in high-risk patients compared to low-risk patients. Moreover, Pearson correlation analysis demonstrates that macrophages M0, eosinophils, dendritic cells activated, neutrophages, T cells CD4 naive, T cells CD8, T cells CD4 memory resting, and T cells regulatory (Tregs) are closely correlated with the three feature mRNAs in DFS-associated signature. So, macrophages M0, eosinophils, T cells CD4 memory resting, and Tregs not only have differences between high and low-risk groups but are related with the expression levels of mRNAs. Similarly, univariate and multivariate Cox regression analyses were also implemented, and **Table 2** indicates that macrophages M0 is related with PTC patients' DFS.

In general, the proportion of macrophages M0 is higher in high-risk patients either based on OS-associated signature or DFS-associated signature, which may indicate that macrophages M0 would be unfavorable to the prognosis of PTC, since it has been demonstrated by the study of Xie et al. that macrophages M0 as well as dendritic cells activated and Tregs were observed to play a tumor-promoting role in PTC (Xie et al., 2020).

Determination of Therapeutic Drugs by CMap Analysis

Discovering novel effective drugs may improve the prognosis of patients with PTC. In our two signatures, seven feature mRNAs related to the prognosis of PTC were achieved. It is expected that drugs targeted to them may be of great potential in the therapy of PTC. Except two without GPL96 probe ID, the remaining five mRNAs including PAPSS2, TOB1, ID4, SCD, and DCBLD2 were uploaded into the CMap web tool as down-regulated tags and up-regulated tags respectively to screen the compounds that can reverse the expression of these five hub genes. A negative connectivity score indicates that the compound represses the query gene expression. So, the top three bioactive compounds with connectivity scores close to -1 were determined as the potential therapeutic agents for PTC. The chemical structures of three compounds are shown in **Figure 10** and the detailed

TABLE 1 | | Univariate and multivariate Cox regression analyses of three immune cells and overall survival of PTC patients.

	Univariate cox regression			Multivariate cox regression		
	HR	95% CI	*p* value	HR	95% CI	*p* value
T cells regulatory (Tregs)	8.69E-05	1.52E-12-4970	0.305	0.00	0-6597.90	0.29
Mocrophages M0	30.1	0.619-1460	0.0858	121.89	1.86-7981.86	0.024
Dendritic cells activated	1.41E+07	439-4.55E+11	0.0019	3.31E+07	914.70-1.20E+12	0.0012

TABLE 2 | | Univariate and multivariate Cox regression analyses of four immune cells and disease-free survival of PTC patients.

	Univariate cox regression			Multivariate cox regression		
	HR	**95% CI**	***p* value**	**HR**	**95% CI**	***p* value**
Macrophages M0	90.4	8.59-952	<0.001	102.85	8.55-1236.73	<0.001
Eosinophils	0.0188	5.75E-10-615000	0.653	19.06	0-9.00E+08	0.744
T cells regulatory (Tregs)	6.92	7.62E-04-62800	0.677	0.51	0-16667	0.898
T cells CD4 memory resting	0.434	0.0181-10.4	0.607	0.954	0.0265-34.306	0.979

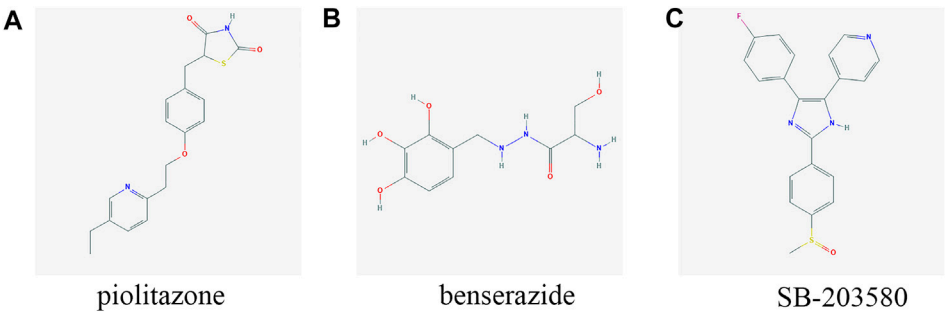

FIGURE 10 | Structures of the three most significant bioactive chemicals. **(A)** pioglitazone **(B)** benserazide **(C)** SB-203580.

TABLE 3 | | Three bioactive compounds with the top three negative connectivity scores in the CMap analysis.

Drug	**Dose, μM**	**Cell**	**Connectivity score**	**Up score**	**Down score**
Pioglitazone	10	MCF7	−1	−0.935	0.772
Benserazide	14	PC3	−0.99	−0.902	0.789
SB-203580	1	MCF7	−0.97	−0.876	0.779

information about them derived by CMap analysis are listed in **Table 3**.

Among the three compounds, it has been reported that pioglitazone may be the potential drug in patients with PAX8-PPARγfusion protein (PPFP) thyroid cancer and thyroid cancer. It can also promote apoptosis in human glioblastoma LN-18 cells (Giordano et al., 2018; Ozdemir Kutbay et al., 2020; Szoka and Palka, 2020). Benserazide has been used as a drug with low toxicity for the treatment of Parkinson's disease. It has been proven that it can suppress tumor growth by inhibiting HK2 so that it may be an antitumor agent (Li et al., 2017). SB-203580 is a p38 MAPK-specific inhibitor that could suppress IL-6-stimulated non-small cell lung cancer cells proliferation by inhibiting IL-6-induced p38 MAPK phosphorylating activity (Chang et al., 2005). Besides, p38 MAPK pathway has been reported to be activated in proliferation of PTC cells promoted by CXCL5 (Cui et al., 2019). Overall, the three compounds probably play vital roles in PTC-related biological processes and pathways, although their effects on PTC treatment remain to be explored.

DISCUSSION

Although the survival rate of PTC is relatively high, its recurrence rate is also high. Accurate diagnosis, prognosis for PTC patients, and discovering more potential drugs are of great significance in PTC clinical practice. lncRNAs have been indicated as an important biomarker for different cancers, such as colorectal cancer, gastric cancer, ovarian cancer, and so on (Luo and Xiang, 2021; Tan et al., 2021; Zhu and Mei, 2021). Moreover, lncRNAs could exert carcinogenic effects as ceRNAs in PTC (Zhang et al., 2019; Sui et al., 2020). In the present study, we systematically analyzed PTC-related genes and identified five hub lncRNAs for marking PTC tissues. By establishing lncRNA-miRNA-mRNA ceRNA network, two prognostic risk signatures were constructed for predicting OS and DFS of PTC respectively. Finally, three potential drugs were screened.

Firstly, five hub lncRNAs were identified by integrating four gene chips (GSE29265, GSE3678, GSE33630, and GSE3467) from GEO using differential expression analysis combined with RRA approach. The five lncRNAs of SLC26A4-AS1, NR2F1-AS1, MIR31HG, ST7-AS1, and RNF157-AS1 then underwent comprehensive validation tests. Significant expression difference could be observed between tumor and normal tissues in four GEO datasets, TCGA, and GEPIA databases, Moreover, ROC curve analysis shows that these five hub genes yield excellent diagnostic efficiency between tumor and normal tissues based on all four GEO datasets and TCGA and almost all AUC values higher than 0.8 in all five datasets. Actually, previous researchers have identified lncRNAs as prognostic markers of PTC, such as TTTY10

(Chen et al., 2019), LINC00284, RBMS3-AS1, and ZFX-AS1 (Zhao et al., 2018) and five lncRNAs of PPARG, E2F1, CCND1, JUN, and EZH2 (Sun et al., 2020) for predicting tumor recurrence in PTC. We have also performed ROC analysis for them in our four GEO datasets and TCGA. Among them, TTTY10 and LINC00284 both are included in the five datasets, but RBMS3-AS1 and ZFX-AS1 are only in TCGA. The five lncRNAs identified by Sun et al. (2020) are not in all datasets. So, the ROC analysis was performed on TTTY10, LINC00284, RBMS3-AS1, and ZFX-AS1 respectively, as shown in **Supplementary Figure S4**. It shows that only LINC00284 can give AUC values higher than 0.8 in three datasets and all others lower than 0.8. TTTY10 gives a poor performance with AUC values lower than 0.6.

In addition, lncRNA-mRNA co-expression network analysis shows that the common co-expressed mRNAs of the five hub lncRNAs are mainly involved in the cancer-related biological processes or pathways, which can indicate to some extent that these hub lncRNAs play crucial roles in PTC and other cancers. Finally, by deep literature-exploring, all of the five lncRNA genes have been confirmed as having important roles in cancers. All the above analysis proves that they would be potential biomarkers for PTC diagnosis.

However, the five hub lncRNA genes give poor correlation with the survival prognosis of PTC patients by univariate Cox regression analysis. So based on this, we aim to investigate the prognosis features from their interacting miRNAs and target mRNAs, since much more prognostic signatures have been constructed using miRNAs and mRNAs in cancers, such as gastric cancer, endometrial carcinoma, and so on (Cui et al., 2021; Deng et al., 2021). Among 713 target miRNAs identified by the starBase v2.0, 17 miRNAs are demonstrated to be differentially expressed in TCGA. And then miRDB, miRTarBase, and TargetScan 7.2 were used to give the reliable target mRNAs and 68 differentially expressed ones were identified in TCGA. Using five hub lncRNAs, 17 miRNAs, and 68 mRNAs, the lncRNA-miRNA-mRNA ceRNA network were constructed. Univariate and step-wise multivariate Cox regression analyses were performed and two prognostic signatures were achieved for effective prediction of PTC's OS and DFS respectively. Here, they are named as PTC-mi1m4 and PTC-m3. The Kaplan-Meier analyses suggest that both signatures could successfully divide PTC patients into high and low-risk groups. The low-risk patients always have longer survival times than high-risk patients by two risk scores. Moreover, the time-dependent ROC analysis manifest that both of them can better predict long-term survival than short-term survival of PTC patients. The stratification analysis shows that both signatures could be independent applicable prognostic indicators of PTC even after adjusting for clinical factors such as stage, age, and gender.

The immune cells are an essential part in the tumor microenvironment and the effects of them on therapy is simulative or impedimental. Meanwhile, the activation status of immune cells may be different in different cancer tumors (Wu and Dai, 2017). Therefore, we estimated the proportions of 22 immune cells in PTC and analyzed those with significant differences between high and low-risk groups. As a result, dendritic cells activated, macrophages M0, and Tregs were demonstrated to be associated with the four feature mRNAs in OS prognostic signature. And macrophages M0, eosinophils, T cells CD4 memory resting, and Tregs were demonstrated to also be associated with the three feature mRNAs in DFS prognostic signature. The previous study by Xie et al. has displayed that all the three immune cells, including dendritic cells activated macrophages M0 and Tregs, play a tumor-promoting role in PTC (Xie et al., 2020). In our study, dendritic cells activated and macrophages M0 are associated with OS and DFS respectively by the regression analysis. Specifically, dendritic cells activated and macrophages M0 give higher proportion in high-risk patients based on OS-associated signature. So, we can speculate that they may be possible targets for immunotherapy of PTC. Tregs has an antitumor effect between PTC OS and DFS; its role may need further analysis by using wet lab experiments.

Disclosing the potential drugs that may reverse the expression of hub genes may improve the prognosis of patients with PTC. Therefore, we performed CMap analysis on the five feature mRNAs derived from two risk models to screen the potential compounds for the therapy of PTC. Three compounds (pioglitazone, benserazide, and SB-203580) were identified. Through literature-searching, all three bioactive compounds were shown to regulate PTC-related biological processed or pathways by targeting to the five feature mRNAs, but the practical applicability of those drugs should be experimentally confirmed in future researches.

DATA AVAILABILITY STATEMENT

The original contributions presented in the study are included in the article/**Supplementary Material**, further inquiries can be directed to the corresponding authors.

AUTHOR CONTRIBUTIONS

HL: Acquisition of data; analysis and interpretation of data; drafting of the paper; statistical analysis. FL: Acquisition of data; study supervision; FL, HL, XW, YX, and ML: Technical and material support. ZL: Study concept and design; obtained funding; study supervision. YG: Study concept and design; drafting of the paper; study supervision; critical revision of the paper.

FUNDING

This work was financially supported by the Support Program for Science and Technology Department of Sichuan Province (2020YJ0237, 2018SZ0030) and the 1·3·5 Project for Disciplines of Excellence, West China Hospital, Sichuan University (ZYJC18025).

SUPPLEMENTARY MATERIAL

The Supplementary Material for this article can be found online at: https://www.frontiersin.org/articles/10.3389/fphar.2021.748867/full#supplementary-material

REFERENCE

Amaral, L. H. P., Bufalo, N. E., Peres, K. C., Barreto, I. S., Campos, A. H. J. F. M., and Ward, L. S. (2019). ID Proteins May Reduce Aggressiveness of Thyroid Tumors. *Endocr. Pathol.* 30, 24–30. doi:10.1007/s12022-018-9556-1

Antoniades, I., Kyriakou, M., Charalambous, A., Kalalidou, K., Christodoulou, A., Christoforou, M., et al. (2021). FAK Displacement from Focal Adhesions: a Promising Strategy to Target Processes Implicated in Cancer Progression and Metastasis. *Cell Commun Signal* 19, 3. doi:10.1186/s12964-020-00671-1

Cai, S., Weng, Y., Liu, P., and Miao, F. (2020). Knockdown of ST7-AS1 Inhibits Migration, Invasion, Cell Cycle Progression and Induces Apoptosis of Gastric Cancer. *Oncol. Lett.* 19, 777–782. doi:10.3892/ol.2019.11145

Chang, K. T., Tsai, C. M., Chiou, Y. C., Chiu, C. H., Jeng, K. S., and Huang, C. Y. (2005). IL-6 Induces Neuroendocrine Dedifferentiation and Cell Proliferation in Non-small Cell Lung Cancer Cells. *Am. J. Physiol. Lung Cell Mol Physiol* 289, L446–L453. doi:10.1152/ajplung.00089.2005

Chen, F., Li, Z., Deng, C., and Yan, H. (2019). Integrated Analysis Identifying New lncRNA Markers Revealed in ceRNA Network for Tumor Recurrence in Papillary Thyroid Carcinoma and Build of Nomogram. *J. Cell Biochem* 120, 19673–19683. doi:10.1002/jcb.29273

Cui, D., Zhao, Y., and Xu, J. (2019). Activation of CXCL5-CXCR2 axis Promotes Proliferation and Accelerates G1 to S Phase Transition of Papillary Thyroid Carcinoma Cells and Activates JNK and P38 Pathways. *Cancer Biol. Ther.* 20, 608–616. doi:10.1080/15384047.2018.1539289

Cui, L., Wang, P., Ning, D., Shao, J., Tan, G., Li, D., et al. (2021). Identification of a Novel Prognostic SIgnature for Gastric Cancer Based on Multiple Level Integration and Global Network Optimization. *Front Cell Dev Biol* 9, 631534. doi:10.3389/fcell.2021.631534

Deng, F., Mu, J., Qu, C., Yang, F., Liu, X., Zeng, X., et al. (2020). A Novel Prognostic Model of Endometrial Carcinoma Based on Clinical Variables and Oncogenomic Gene Signature. *Front. Mol. Biosci.* 7, 587822. doi:10.3389/fmolb.2020.587822

Drakaki, A., Dhillon, P. K., Wakelee, H., Chui, S. Y., Shim, J., Kent, M., et al. (2020). Association of Baseline Systemic Corticosteroid Use with Overall Survival and Time to Next Treatment in Patients Receiving Immune Checkpoint Inhibitor Therapy in Real-World US Oncology Practice for Advanced Non-small Cell Lung Cancer, Melanoma, or Urothelial Carcinoma. *OncoImmunology* 9, 1824645. doi:10.1080/2162402X.2020.1824645

Fagin, J. A., and Wells, S. A., Jr. (2016). Biologic and Clinical Perspectives on Thyroid Cancer. *N. Engl. J. Med.* 375, 1054–1067. doi:10.1056/NEJMra1501993

Fang, Y., and Fullwood, M. J. (2016). Roles, Functions, and Mechanisms of Long Non-coding RNAs in Cancer. *Genomics Proteomics Bioinformatics* 14, 42–54. doi:10.1016/j.gpb.2015.09.006

Farwell, S. L. N., Reylander, K. G., Iovine, M. K., and Lowe-Krentz, L. J. (2017). Novel Heparin Receptor Transmembrane Protein 184a Regulates Angiogenesis in the Adult Zebrafish Caudal Fin. *Front. Physiol.* 8, 671. doi:10.3389/fphys.2017.00671

Giordano, T. J., Haugen, B. R., Sherman, S. I., Shah, M. H., Caoili, E. M., and Koenig, R. J. (2018). Pioglitazone Therapy of PAX8-Pparγ Fusion Protein Thyroid Carcinoma. *J. Clin. Endocrinol. Metab.* 103, 1277–1281. doi:10.1210/jc.2017-02533

Hanna, J., Hossain, G. S., and Kocerha, J. (2019). The Potential for microRNA Therapeutics and Clinical Research. *Front. Genet.* 10, 478. doi:10.3389/fgene.2019.00478

He, J., Huang, H., Du, Y., Peng, D., Zhou, Y., Li, Y., et al. (2020). Association of DCBLD2 Upregulation with Tumor Progression and Poor Survival in Colorectal Cancer. *Cell Oncol (Dordr)* 43, 409–420. doi:10.1007/s13402-020-00495-8

Hou, P., Liu, D., Shan, Y., Hu, S., Studeman, K., Condouris, S., et al. (2007). Genetic Alterations and Their Relationship in the Phosphatidylinositol 3-Kinase/Akt Pathway in Thyroid Cancer. *Clin. Cancer Res.* 13, 1161–1170. doi:10.1158/1078-0432.CCR-06-1125

Huang, Y., Zhang, K., Li, Y., Dai, Y., and Zhao, H. (2020). The DLG1-AS1/miR-497/YAP1 axis Regulates Papillary Thyroid Cancer Progression. *Aging (Albany NY)* 12, 23326–23336. doi:10.18632/aging.104121

Iaccarino, I., and Klapper, W. (2021). "LncRNA as Cancer Biomarkers," in *Long Non-coding RNAs in Cancer*. Editor A. Navarro (New York, NY: Springer US), 27–41. doi:10.1007/978-1-0716-1581-2_2

Ito, Y., Higashiyama, T., Takamura, Y., Kobayashi, K., Miya, A., and Miyauchi, A. (2010). Clinical Outcomes of Patients with Papillary Thyroid Carcinoma after the Detection of Distant Recurrence. *World J. Surg.* 34, 2333–2337. doi:10.1007/s00268-010-0712-0

Ito, Y., Suzuki, T., Yoshida, H., Tomoda, C., Uruno, T., Takamura, Y., et al. (2005). Phosphorylation and Inactivation of Tob Contributes to the Progression of Papillary Carcinoma of the Thyroid. *Cancer Lett.* 220, 237–242. doi:10.1016/j.canlet.2004.08.017

Kitahara, C. M., and Sosa, J. A. (2016). The Changing Incidence of Thyroid Cancer. *Nat. Rev. Endocrinol.* 12, 646–653. doi:10.1038/nrendo.2016.110

Kolde, R., Laur, S., Adler, P., and Vilo, J. (2012). Robust Rank Aggregation for Gene List Integration and Meta-Analysis. *Bioinformatics* 28, 573–580. doi:10.1093/bioinformatics/btr709

La Vecchia, C., Malvezzi, M., Bosetti, C., Garavello, W., Bertuccio, P., Levi, F., et al. (2015). Thyroid Cancer Mortality and Incidence: A Global Overview. *Int. J. Cancer* 136, 2187–2195. doi:10.1002/ijc.29251

Li, W., Zheng, M., Wu, S., Gao, S., Yang, M., Li, Z., et al. (2017). Benserazide, a Dopadecarboxylase Inhibitor, Suppresses Tumor Growth by Targeting Hexokinase 2. *J. Exp. Clin. Cancer Res.* 36, 58. doi:10.1186/s13046-017-0530-4

Liu, F., Wang, Z., Zhou, X., Liu, Q., Chen, G., Xiao, H., et al. (2018). Genetic Heterogeneity and Mutational Signature in Chinese Epstein-Barr Virus-Positive Diffuse Large B-Cell Lymphoma. *PLoS One* 13, e0201546. doi:10.1371/journal.pone.0201546

Liu, K. W., Hu, B., and Cheng, S. Y. (2011). Platelet-derived Growth Factor Signaling in Human Malignancies. *Chin. J. Cancer* 30, 581–584. doi:10.5732/cjc.011.10300

Liu, Y., Xu, G., and Li, L. (2021). LncRNA GATA3-AS1-miR-30b-5p-Tex10 axis M-odulates T-umorigenesis in P-ancreatic C-ancer. *Oncol. Rep.* 45, 59. doi:10.3892/or.2021.8010

Liz, J., and Esteller, M. (2016). LncRNAs and microRNAs with a Role in Cancer Development. *Biochim. Biophys. Acta* 1859, 169–176. doi:10.1016/j.bbagrm.2015.06.015

Luo, J., and Xiang, H. (2021). LncRNA MYLK-AS1 Acts as an Oncogene by Epigenetically Silencing Large Tumor Suppressor 2 (LATS2) in Gastric Cancer. *Bioengineered* 12, 3101–3112. doi:10.1080/21655979.2021.1944019

Malandrino, A., Mak, M., Kamm, R. D., and Moeendarbary, E. (2018). Complex Mechanics of the Heterogeneous Extracellular Matrix in Cancer. *Extreme Mech. Lett.* 21, 25–34. doi:10.1016/j.eml.2018.02.003

Murugan, A. K., Munirajan, A. K., and Alzahrani, A. S. (2018). Long Noncoding RNAs: Emerging Players in Thyroid Cancer Pathogenesis. *Endocr. Relat. Cancer* 25, R59–R82. doi:10.1530/ERC-17-0188

Ng, T. K., Huang, L., Cao, D., Yip, Y. W., Tsang, W. M., Yam, G. H., et al. (2015). Cigarette Smoking Hinders Human Periodontal Ligament-Derived Stem Cell Proliferation, Migration and Differentiation Potentials. *Sci. Rep.* 5, 7828. doi:10.1038/srep07828

Nie, K., Zheng, Z., Wen, Y., Shi, L., Xu, S., Wang, X., et al. (2020). Construction and Validation of a TP53-Associated Immune Prognostic Model for Gastric Cancer. *Genomics* 112, 4788–4795. doi:10.1016/j.ygeno.2020.08.026

Nikiforov, Y. E., and Nikiforova, M. N. (2011). Molecular Genetics and Diagnosis of Thyroid Cancer. *Nat. Rev. Endocrinol.* 7, 569–580. doi:10.1038/nrendo.2011.142

Ozdemir Kutbay, N., Biray Avci, C., Sarer Yurekli, B., Caliskan Kurt, C., Shademan, B., Gunduz, C., et al. (2020). Effects of Metformin and Pioglitazone Combination on Apoptosis and AMPK/mTOR Signaling Pathway in Human Anaplastic Thyroid Cancer Cells. *J. Biochem. Mol. Toxicol.* 34, e22547. doi:10.1002/jbt.22547

Qi, H., Lu, L., and Wang, L. (2020). Long Noncoding RNA ST7-AS1 Upregulates TRPM7 Expression by Sponging microRNA-543 to Promote Cervical Cancer Progression. *Onco Targets Ther.* 13, 7257–7269. doi:10.2147/OTT.S253868

Qi, X., Zhang, D. H., Wu, N., Xiao, J. H., Wang, X., and Ma, W. (2015). ceRNA in Cancer: Possible Functions and Clinical Implications. *J. Med. Genet.* 52, 710–718. doi:10.1136/jmedgenet-2015-103334

Rong, D., Dong, Q., Qu, H., Deng, X., Gao, F., Li, Q., et al. (2021). m6A-induced LINC00958 Promotes Breast Cancer Tumorigenesis via the miR-378a-3p/YY1 axis. *Cell Death Discov* 7, 27. doi:10.1038/s41420-020-00382-z

Silva, A., Bullock, M., and Calin, G. (2015). The Clinical Relevance of Long Non-coding RNAs in Cancer. *Cancers (Basel)* 7, 2169–2182. doi:10.3390/cancers7040884

Stein, L., Rothschild, J., Luce, J., Cowell, J. K., Thomas, G., Bogdanova, T. I., et al. (2010). Copy Number and Gene Expression Alterations in Radiation-Induced Papillary Thyroid Carcinoma from Chernobyl Pediatric Patients. *Thyroid* 20, 475–487. doi:10.1089/thy.2009.0008

Sui, G., Zhang, B., Fei, D., Wang, H., Guo, F., and Luo, Q. (2020). The lncRNA SNHG3 Accelerates Papillary Thyroid Carcinoma Progression via the miR-214-3p/PSMD10 axis. *J. Cell Physiol* 235, 6615–6624. doi:10.1002/jcp.29557

Sun, Y., Dai, W. R., and Xia, N. (2020). Comprehensive Analysis of lncRNA-Mediated ceRNA Network in Papillary Thyroid Cancer. *Eur. Rev. Med. Pharmacol. Sci.* 24, 10003–10014. doi:10.26355/eurrev_202010_23214

Szoka, L., and Palka, J. (2020). Capsaicin Up-Regulates Pro-apoptotic Activity of Thiazolidinediones in Glioblastoma Cell Line. *Biomed. Pharmacother.* 132, 110741. doi:10.1016/j.biopha.2020.110741

Tan, X., Mao, L., Huang, C., Yang, W., Guo, J., Chen, Z., et al. (2021). Comprehensive Analysis of lncRNA-miRNA-mRNA Regulatory Networks for Microbiota-Mediated Colorectal Cancer Associated with Immune Cell Infiltration. *Bioengineered* 12, 3410–3425. doi:10.1080/21655979.2021.1940614

Von Roemeling, C. A., and Copland, J. A. (2016). Targeting Lipid Metabolism for the Treatment of Anaplastic Thyroid Carcinoma. *Expert Opin. Ther. Targets* 20, 159–166. doi:10.1517/14728222.2016.1086341

Wang, D. P., Tang, X. Z., Liang, Q. K., Zeng, X. J., Yang, J. B., and Xu, J. (2020a). Overexpression of Long Noncoding RNA SLC26A4-AS1 Inhibits the Epithelial-Mesenchymal Transition via the MAPK Pathway in Papillary Thyroid Carcinoma. *J. Cell Physiol* 235, 2403–2413. doi:10.1002/jcp.29145

Wang, J., Dong, S., Zhang, J., Jing, D., Wang, W., Dong, L., et al. (2020b). LncRNA NR2F1-AS1 Regulates miR-371a-3p/TOB1 Axis to Suppress the Proliferation of Colorectal Cancer Cells. *Cancer Biother. Radiopharm.* 35, 760–764. doi:10.1089/cbr.2019.3237

Wang, R., Ma, Z., Feng, L., Yang, Y., Tan, C., Shi, Q., et al. (2018). LncRNA MIR31HG Targets HIF1A and P21 to Facilitate Head and Neck Cancer Cell Proliferation and Tumorigenesis by Promoting Cell-Cycle Progression. *Mol. Cancer* 17, 162. doi:10.1186/s12943-018-0916-8

Wu, M., Zhang, X., Han, X., Pandey, V., Lobie, P. E., and Zhu, T. (2021). The Potential of Long Noncoding RNAs for Precision Medicine in Human Cancer. *Cancer Lett.* 501, 12–19. doi:10.1016/j.canlet.2020.11.040

Wu, T., and Dai, Y. (2017). Tumor Microenvironment and Therapeutic Response. *Cancer Lett.* 387, 61–68. doi:10.1016/j.canlet.2016.01.043

Xie, Z., Li, X., He, Y., Wu, S., Wang, S., Sun, J., et al. (2020). Immune Cell Confrontation in the Papillary Thyroid Carcinoma Microenvironment. *Front. Endocrinol. (Lausanne)* 11, 570604. doi:10.3389/fendo.2020.570604

Xu, S., and Xu, P. (2020). LncRNA RNF157-AS1 Inhibits Autophagy in Ovarian Cancer Cells by Downregulating ARHI: The Different Role in Proliferation and Drug Resistance. *Cancer Res.* 80, 3717.

Xu, X., and Jing, J. (2020). Advances on circRNAs Contribute to Carcinogenesis and Progression in Papillary Thyroid Carcinoma. *Front. Endocrinol. (Lausanne)* 11, 555243. doi:10.3389/fendo.2020.555243

Yang, C., Liu, Z., Chang, X., Xu, W., Gong, J., Chai, F., et al. (2020). NR2F1-AS1 Regulated miR-423-5p/SOX12 to Promote Proliferation and Invasion of Papillary Thyroid Carcinoma. *J. Cell Biochem* 121, 2009–2018. doi:10.1002/jcb.29435

Yoshihara, K., Shahmoradgoli, M., Martínez, E., Vegesna, R., Kim, H., Torres-Garcia, W., et al. (2013). Inferring Tumour Purity and Stromal and Immune Cell Admixture from Expression Data. *Nat. Commun.* 4, 2612. doi:10.1038/ncomms3612

Zeng, Z. L., Lu, J. H., Wang, Y., Sheng, H., Wang, Y. N., Chen, Z. H., et al. (2021). The lncRNA XIST/miR-125b-2-3p axis Modulates Cell Proliferation and Chemotherapeutic Sensitivity via Targeting Wee1 in Colorectal Cancer. *Cancer Med.* 10, 2423–2441. doi:10.1002/cam4.3777

Zhang, Y., Hu, J., Zhou, W., and Gao, H. (2019). LncRNA FOXD2-AS1 Accelerates the Papillary Thyroid Cancer Progression through Regulating the miR-485-5p/KLK7 axis. *J. Cell Biochem* 120, 7952–7961. doi:10.1002/jcb.28072

Zhao, Y., Wang, H., Wu, C., Yan, M., Wu, H., Wang, J., et al. (2018). Construction and Investigation of lncRNA-Associated ceRNA Regulatory Network in Papillary Thyroid Cancer. *Oncol. Rep.* 39, 1197–1206. doi:10.3892/or.2018.6207

Zhu, L., and Mei, M. (2021). Interference of Long Non-coding RNA HAGLROS Inhibits the Proliferation and Promotes the Apoptosis of Ovarian Cancer Cells by Targeting miR-26b-5p. *Exp. Ther. Med.* 22, 879. doi:10.3892/etm.2021.10311

Conflict of Interest: The authors declare that the research was conducted in the absence of any commercial or financial relationships that could be construed as a potential conflict of interest.

Publisher's Note: All claims expressed in this article are solely those of the authors and do not necessarily represent those of their affiliated organizations, or those of the publisher, the editors and the reviewers. Any product that may be evaluated in this article, or claim that may be made by its manufacturer, is not guaranteed or endorsed by the publisher.

Copyright © 2021 Li, Liu, Wang, Li, Li, Xie and Guo. This is an open-access article distributed under the terms of the Creative Commons Attribution License (CC BY). The use, distribution or reproduction in other forums is permitted, provided the original author(s) and the copyright owner(s) are credited and that the original publication in this journal is cited, in accordance with accepted academic practice. No use, distribution or reproduction is permitted which does not comply with these terms.

frontiers in Pharmacology

REVIEW
published: 19 October 2021
doi: 10.3389/fphar.2021.747194

Integrating Molecular Biomarker Inputs Into Development and Use of Clinical Cancer Therapeutics

Anna D. Louie[1,2], *Kelsey Huntington*[1,3], *Lindsey Carlsen*[1,3], *Lanlan Zhou*[1,4,5,6] *and Wafik S. El-Deiry*[1,3,4,5,6,7]*

[1]*Laboratory of Translational Oncology and Experimental Cancer Therapeutics, Warren Alpert Medical School, Brown University, Providence, RI, United States,* [2]*Department of Surgery, Lifespan Health System and Brown University, Providence, RI, United States,* [3]*Pathobiology Graduate Program, Warren Alpert Medical School, Brown University, Providence, RI, United States,* [4]*Department of Pathology and Laboratory Medicine, Warren Alpert Medical School, Brown University, Providence, RI, United States,* [5]*Joint Program in Cancer Biology, Lifespan Health System and Brown University, Providence, RI, United States,* [6]*Cancer Center at Brown University, Providence, RI, United States,* [7]*Hematology/Oncology Division, Department of Medicine, Lifespan Health System and Brown University, Providence, RI, United States*

Biomarkers can contribute to clinical cancer therapeutics at multiple points along the patient's diagnostic and treatment course. Diagnostic biomarkers can screen or classify patients, while prognostic biomarkers predict their survival. Biomarkers can also predict treatment efficacy or toxicity and are increasingly important in development of novel cancer therapeutics. Strategies for biomarker identification have involved large-scale genomic and proteomic analyses. Pathway-specific biomarkers are already in use to assess the potential efficacy of immunotherapy and targeted cancer therapies. Judicious application of machine learning techniques can identify disease-relevant features from large data sets and improve predictive models. The future of biomarkers likely involves increasing utilization of liquid biopsy and multiple samplings to better understand tumor heterogeneity and identify drug resistance.

Keywords: biomarkers, cancer therapeutics, genomics, machine learning, liquid biopsy

OPEN ACCESS

Edited by:
Anne Lorant,
Laboratoire de Biologie Moléculaire et Cellulaire du Cancer (LBMCC), Luxembourg

Reviewed by:
Maha Mohamed Saber-Ayad, University of Sharjah, United Arab Emirates
Leena Latonen, University of Eastern Finland, Finland

***Correspondence:**
Wafik S. El-Deiry
wafik@brown.edu

Specialty section:
This article was submitted to Pharmacology of Anti-Cancer Drugs, a section of the journal Frontiers in Pharmacology

Received: *25 July 2021*
Accepted: *30 September 2021*
Published: *19 October 2021*

Citation:
Louie AD, Huntington K, Carlsen L, Zhou L and El-Deiry WS (2021) Integrating Molecular Biomarker Inputs Into Development and Use of Clinical Cancer Therapeutics. Front. Pharmacol. 12:747194. doi: 10.3389/fphar.2021.747194

INTRODUCTION

A biomarker is a measurable indicator that predicts disease presence, severity, or response to treatment. Levels of biomarkers can be clinically useful by guiding disease diagnosis, or by revealing the pharmacodynamics of drug treatment. **Figure 1** depicts various types of biomarkers and their potential for clinical utility.

Approved and experimental biomarkers can be classified based on their clinical uses. These clinical uses parallel the progressive utilization of biomarkers during the development of cancer therapeutics. **Figure 2** gives an overview of biomarker development strategies and potential uses. Biomarkers are divided into categories including diagnostic, prognostic, pharmacodynamic, and predictive, with some falling into several categories. This review briefly summarizes some current clinical uses of biomarkers and their effect on development and application of cancer therapeutics. It also addresses promising strategies for biomarker discovery such as genomics, proteomics and machine learning, and discusses the increased clinical accessibility and potential applications of liquid biopsies.

Types of Biomarkers and Their Clinical Utility

	Diagnostic	
Predicts:	Presence of a disease	
Time of Measurement:	Before diagnosis	At diagnosis
Clinical Utility:	Allows screening of healthy patients	Distinguish benign vs. malignant; classify into subtypes

	Prognostic	
	Overall patient survival, independent of therapy	
	At diagnosis	After diagnosis
	Estimate risk of disease	Allows monitoring of disease status; detects recurrence

	Predictive
Predicts:	Response to treatment (efficacy and/or toxicity)
Time of Measurement:	Before treatment selection
Clinical Utility:	Identify treatments likely to be effective; guides initial treatment decision making.

	Pharmacodynamic
	Drug interaction with its target
	During or post-treatment
	Determines degree of drug response; guides treatment decision making in real-time.

FIGURE 1 | Clinical uses of biomarkers. Diagnostic, prognostic, predictive, and pharmacodynamic biomarkers are shown along with what each predicts, and the clinical setting in which they can be used.

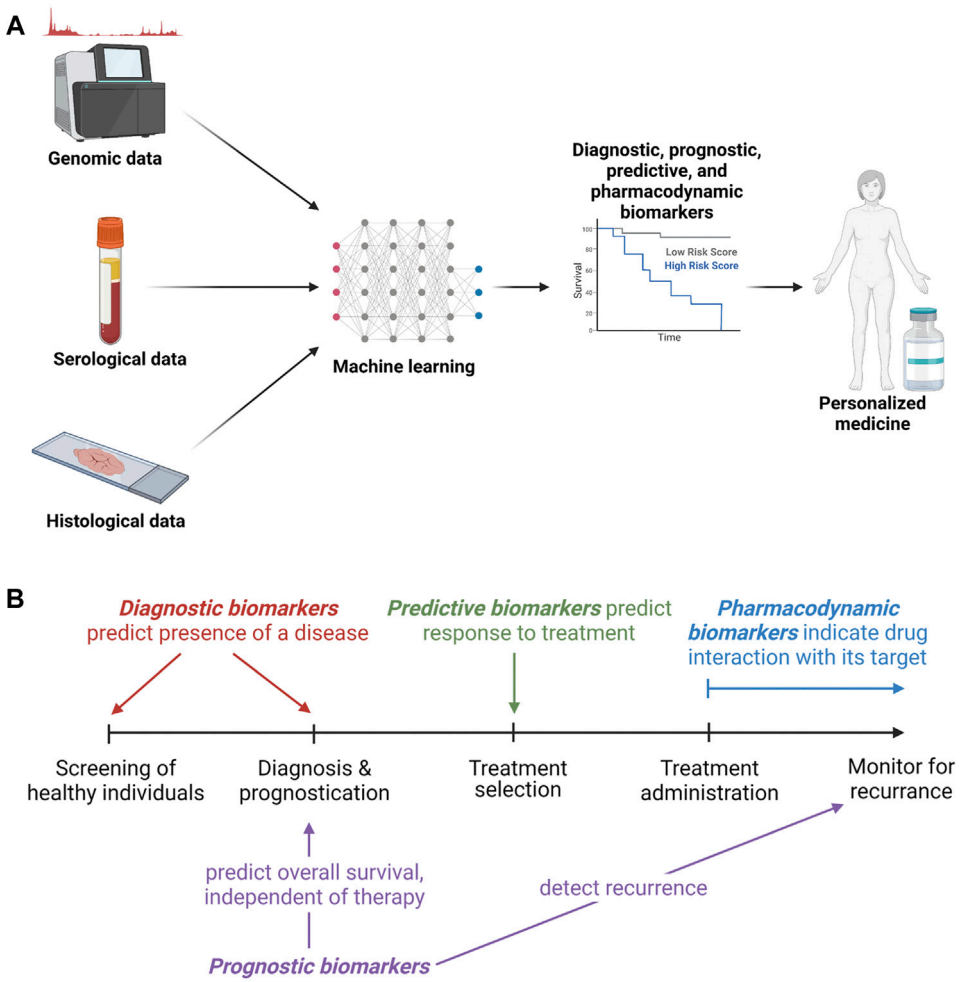

FIGURE 2 | Biomarker development and clinical utility. **(A)**. Overview of methods of biomarker development, testing and clinical utilization. **(B)**. Types of biomarkers with a timeline of opportunities for utilization.

Companion Diagnostics

Companion diagnostics is the development of predictive biomarkers in conjunction with novel therapeutics. It identifies patients who are likely to respond to the treatment or to experience severe toxicity. An early example is estrogen receptor assays which are implemented in the prescription of the estrogen receptor modulator tamoxifen. Since then, others have been developed including measurement of HER2 levels prior to treatment of breast cancer with the anti-HER2 antibody pertuzumab, and measurement of PD-L1 levels prior to treatment with the anti-PD-L1 antibody pembrolizumab (Jørgensen et al., 2016). Companion diagnostics increasingly subdivide patients based on molecular biomarkers, which may be required to direct prescription of targeted therapies. This codependence is reflected in FDA approvals of companion biomarkers in conjunction with novel therapeutics, such as the simultaneous approval of vemurafenib and an assay to detect the V600E mutation it targets (Scheerens et al., 2017). Companion diagnostics allow improved patient selection for drug trials and quicker identification of clinically effective drugs for personalized treatments.

Diagnostic Biomarkers

While companion diagnostics focuses on predictive biomarkers, all types are utilized in both patient care and the phases of drug development. Diagnostic biomarkers suggest the presence of a disease or can classify patients into subtypes. Elevated levels of these diagnostic biomarkers may suggest the presence of cancer, and thus can be used as a screening tool in healthy individuals or can support other diagnostic measures such as imaging and biopsy. Several long-used cancer diagnostic biomarkers include prostate-specific antigen (PSA), used for diagnosis of prostate cancer (Welch and Albertsen 2009); cancer antigen 19-9 (CA 19-9), the gold standard serum biomarker for diagnosis of pancreatic ductal adenocarcinoma (PDAC) (Poruk et al., 2013); and CA 125, a classical biomarker in ovarian cancer (Felder et al., 2014). Evidence supporting the utility of cytokines as diagnostic biomarkers is evolving, including data demonstrating IL-6 and VEGF as possible diagnostic biomarkers in ovarian and gastric cancer (Monastero and Srinivas, 2017). Further validation of these cytokines is needed to uncover their diagnostic utility, either as independent biomarkers or in conjunction with classical biomarkers to increase sensitivity and specificity. While diagnostic biomarkers are often used for subtyping a known malignancy, such as in leukemia (Jiang et al., 2016), many lack the specificity needed for cancer diagnosis in the general population (Califf 2018).

Prognostic Biomarkers

Prognostic biomarkers predict the patient's overall survival, independent of therapy. Examples of diagnostic biomarkers with prognostic value include CA 19-9 and CA 125, which can predict overall survival in PDAC and ovarian cancer, respectively (Poruk et al., 2013; Felder et al., 2014). Carcinoembryonic antigen (CEA) indicates poor overall survival in colorectal, breast, and lung cancer patients, though it is only regularly used for prognostication in colorectal cancer (CRC) (Dixon et al., 2003). Other types of biomarkers can also have prognostic value, such as miRNA-155 in hepatocellular carcinoma, which increases Wnt signaling pathway activity and is suggestive of a poor clinical prognosis (Nalejska et al., 2014). Even the presence of circulating tumor cells is correlated with metastasis and can serve as a marker of poor prognosis in non-metastatic breast cancer (Lucci et al., 2012). The prognostic information of biomarkers can guide treatment decision-making, monitor disease progression, and detect recurrence.

Pharmacodynamic Biomarkers

Pharmacodynamic biomarkers suggest whether a drug has reached its target and exerted a cellular response (Jackson 2012). For example, measurement of Mitogen-Activated Protein Kinase (MAPK) pathway inhibition (*via* measurement of pERK) in non-small-cell lung cancer (NSCLC) patients receiving BRAF inhibitors can indicate direct drug-target interaction (Gainor et al., 2014). Such pathway-specific measurements can be taken simultaneously with markers of tumor cell proliferation (cyclin D1, Ki67) or tumor growth [*via* fludeoxyglucose (18F) measured by PET/CT] to determine first if the drug is hitting its primary target and second if the drug is mediating tumor suppression (Kelloff et al., 2005; Gainor et al., 2014). These measurements can determine the degree of response to the drug in clinical trials and guide treatment decision making in real-time. Most pharmacodynamic biomarkers are measured with tumor biopsies, but recently there has been increasing interest in less invasive blood-based biomarker development (Jackson 2012). Further study of pharmacodynamic biomarkers could personalize treatment doses for patients and provide a method to both minimize toxicity and avoid subtherapeutic dosing.

Predictive Biomarkers and An Example of Biomarker Application

Predictive biomarkers indicate how patients are likely to respond to treatment, either in terms of efficacy or toxicity (Alves et al., 2019). They can be measured before first-line treatment or to choose a salvage therapy. Well-established predictive biomarkers include HER2 overexpression which predicts breast cancer response to anti-HER2 therapies like trastuzumab and KRAS, NRAS and BRAF mutations which predict resistance to Epithelial Growth Factor Receptor (EGFR) inhibitors in CRC (Jørgensen et al., 2016). Using EGFR therapy in CRC may lead to shorter survival in patients with certain mutations in these MAPK pathway genes, making them biomarkers of resistance to cetuximab (Boussios et al., 2019). More recent developments indicate that high circulating levels of IFN-γ predict response to immunotherapies such as immune checkpoint blockade (Karachaliou et al., 2018). Other predictive biomarkers forecast pharmacodynamic resistance or toxicity. Examples include genetic alterations in dihydropyrimidine dehydrogenase (DPD) and of UDP glucuronosyltransferase family one member A1 (UGT1A1), the enzymes responsible for inactivation of 5-FU and irinotecan, respectively. Genetic alterations that reduce the activity of these enzymes result in severe toxicity after treatment

with the compound. Additionally, enhanced expression of excision repair cross-complementation group 1 (ERCC1) enhances DNA excision repair and leads to resistance to platinum-based drugs (Chung 2021). These predictive biomarkers guide initial treatment decisions by identifying potentially successful drugs and minimizing toxicity.

The clinical application of disease-related biomarkers can parallel their integration into drug development. For example, the use of biomarkers in breast cancer evolved to include diagnostic, prognostic, pharmacodynamic, and predictive biomarkers as the treatments and understanding of the disease progressed. Diagnostic biomarkers such as hormone receptor (HR) status are used to differentiate molecular subtypes of breast cancer. HR status was found to be associated with survival, making it also a prognostic biomarker (American Cancer Society Inc, 2019). Prognostic markers such as hormonal status, HER2 expression, and the 21-gene expression assay Oncotype DX have all been integrated into care and treatment decisions for breast cancer patients. Oncotype DX can predict chances of recurrence and this prediction is used clinically to evaluate the risks and benefits of adjuvant chemotherapy in patients with early stage HR positive breast cancer (Wang et al., 2019). The American Society of Clinical Oncology recommends the use of Oncotype Dx to guide the use of chemotherapy after surgery for patients with HR positive, HER2 negative early stage breast cancer, showing integration of multiple gene and protein expression biomarkers into clinical best practice recommendations for selection of therapeutics (Andre et al., 2019). As estrogen receptor modulators and aromatase inhibitors became available, HR status was also used as a predictive biomarker for endocrine therapy (Duffy et al., 2017). Ki67 is a marker of cell proliferation, and a pharmacodynamic response in Ki67 expression after treatment with endocrine therapy is an indication of on-target drug effects (Freelander et al., 2021). Mutations in the ESR1 gene encoding the estrogen receptor serve as a predictive biomarker of resistance to endocrine therapy (Dustin et al., 2019). This example shows how the development and clinical application of diagnostic, prognostic, pharmacodynamic, and predictive biomarkers can all be important in the development and application of targeted therapeutics.

GENOMICS, PROTEOMICS, AND MACHINE LEARNING

Cancer-specific mutations are an appealing source of potential biomarkers. Genomic analyses have been applied to biomarker identification in both inherited and sporadic cancers. Early applications of gene mutations involved the identification of germline mutations that serve as prognostic biomarkers of elevated cancer risk, such as p53 mutations in Li-Fraumeni syndrome or BRCA mutations in hereditary breast cancer (Olivier et al., 2019). These tests expanded the role of genetic counselors and still guide screening and treatment recommendations (Weil, 2002). Other -omics applications have sought to further characterize tumor cells. Transcriptomics, epigenomics, metabolomics, and proteomics can all contribute information on tumor state. While integrated multi-omic approaches have not yet been fully integrated into therapeutic decision-making, new drug trials may incorporate this information into patient selection. For example, in PDAC, an immune profile combining whole-exome sequencing, RNA transcriptomics, and cell-surface protein expression has been developed to identify patients who are more likely to respond to immunotherapy (Lenzo et al., 2021).

Genomics

The convoluted mutational profile of most sporadic cancers increases the complexity of genomic analysis. Advances in sequencing technologies including single-cell sequencing have further underscored tumor heterogeneity and provided insight into the variation in patient responses to therapy. Predictive biomarkers when combined with targeted therapies have shifted treatment decisions from a focus on tumor type to gene-directed individualized treatment plans. For instance, FDA-approved biomarkers such as activating mutations in EGFR predict effectiveness of EGFR inhibitors like gefitinib (Tsimberidou et al., 2020). Patients selected by EGFR mutation biomarker for gefitinib treatment have a 65% response rate, compared to 20–30% in unselected patients (Feng et al., 2021). Improvements in the accuracy and standardization of sequencing and reporting have increased the clinical utilization of large multi-gene panels and whole genome analysis.

Proteomics

Proteomics attempts to directly analyze the main mediators of cellular function by quantifying protein activity and location (Olivier et al., 2019). The dynamic nature of the proteome may allow for better biomarkers of response to treatment and cancer surveillance. Proteomics can clarify the role of the tumor microenvironment (TME). Cell surface urokinase plasminogen activator receptor is an example of a prognostic biomarker that emerged from proteomic analyses. Mass spectrometry methods have also been FDA approved for analysis of the human microbiome, and are being assessed for relevance to colorectal and lung cancers (Su et al., 2021).

Machine Learning

Many genomic and proteomic datasets are large, nonlinear, and multidimensional. The high number of variables measured for each clinical sample can require sophisticated data analysis strategies to differentiate signal from noise and adjust for multiple comparisons. Machine learning can be used to make predictions that incorporate and simplify multivariate information and can determine which variables (e.g., genetic mutations) are relevant biomarkers. The methods to select disease-relevant features while eliminating redundancy and noise range from linear models to neural networks (Feng et al., 2021). In selecting relevant features, machine learning models can work solely from information within the annotated data set or can incorporate known biologic relationships such as in gene set variation analysis.

There are many existing web servers and bioinformatic analysis tools. Among pan-cancer human—omics datasets, web servers aggregating patient data are available for DNA mutation, methylation, mRNA, micro-RNA, long non-coding RNA, and protein information. DNA mutation servers include cBioPortal (its 102,589 samples include The Cancer Genome Atlas data), GSCALite and CaPSSA. DNA methylation is available at MEXPRESS, GSCALite, and MethSurv. There are many databases of mRNA data including GENT2, PROGgeneV2, LOGpc, SurvExpress, PRECOG, and Oncomine which all have more than 15,000 patient samples. OncoLnc combines mRNA micro-RNA and long-noncoding RNA data. Proteomics patient datasets are available through CPTAC, TCPAv3.0, and TRGAted (Zheng et al., 2020).

Model development typically involves separate training and testing data. The quality of a model is determined by how much more effectively it classifies test data than would be expected by other available means. Validation can be achieved through independent datasets, but ideally also involves animal experiments or clinical trials (Deo, 2015). Clinical applications of machine learning analyses include the Oncotype Dx scoring in breast cancer (Wang et al., 2019), and clinical trials of personalized combination therapies chosen based on predicted response (Boichard et al., 2020). The application of machine learning can identify novel biomarkers from relationships not readily apparent within large data sets and will be increasingly important in new multi-omic approaches.

LIQUID BIOPSY

Biomarkers can be derived from tumor tissue, blood, other biologic fluids, and even imaging. Blood-based biomarkers, or liquid biopsies, have become increasingly attractive in patient care (Michela 2021). Liquid biopsies have advantages over traditional solid biopsies as they are non-invasive, cost-effective, and expedite time to diagnosis. The most studied cancer biomarkers in plasma or serum samples are circulating tumor cells (CTCs), circulating tumor DNA (ctDNA), and exosomes.

Circulating Tumor Cells

CTCs are a rare, migratory cell population shed from a tumor and believed to play a role in metastasis. CTCs have both diagnostic and prognostic value across several tumor types including PDAC (Ankeny et al., 2016b), breast cancer (Cristofanilli et al., 2004), ovarian cancer (Poveda et al., 2011), colon cancer (Romiti et al., 2014), and metastatic castration-resistant prostate cancer (CRPC) (Bono et al., 2008). In PDAC, CTCs can be a biomarker at diagnosis and a marker of disease progression, though they are not yet part of general clinical practice (Ankeny et al., 2016a). In breast cancer, the number of CTCs before treatment and at the first follow-up visit are independent predictors of progression free survival (PFS) and overall survival (OS) (Cristofanilli et al., 2004). Moreover, in ovarian and colorectal cancers, elevated CTC numbers are correlated with a higher risk of progression and worse OS (Poveda et al., 2011; Romiti et al., 2014). Finally, in CRPC, CTC counts were more predictive of OS than the classical biomarker PSA (Bono et al., 2008).

Circulating Tumor DNA

ctDNA is tumor-released single- or double-stranded DNA that enters the bloodstream and can be detected for diagnosis, guidance of treatment, and monitoring of disease progression. Recently, ctDNA has been used to guide clinical decision-making in several tumor types including CRC (Chen et al., 2021), NSCLC (Song et al., 2020), and metastatic breast cancer (MBC) (Darrigues et al., 2021). In CRC, postoperative serial ctDNA detection identified recurrence before radiological imaging and was predictive of high relapse risk (Chen et al., 2021). ctDNA has suggested a novel therapeutic rechallenge strategy for CRC based on evidence that resistance mechanisms to anti-EGFR therapy extinguish over time off of that therapy (Misale et al., 2014; Parseghian et al., 2019; Sartore-Bianchi et al., 2021). Moreover, in a prospective real-world study of NSCLC, ctDNA clearance during treatment was correlated with better OS (Song et al., 2020). The FDA has approved the use of liquid biopsy for analysis of sensitizing and resistance mutations in NSCLC due to multiple studies where the application of biomarkers derived from liquid biopsy successfully guided treatment decisions (Saarenheimo et al., 2019). In MBC, ctDNA was a prognostic factor of PFS and efficacy of treatment was effectively monitored by serial ctDNA analyses before radiological evaluation (Darrigues et al., 2021). Analysis of ctDNA has been employed to differentiate between the clinical scenarios of pseudoprogression and hyperprogression following treatment of patients with immune checkpoint blockade therapy (Jia et al., 2019; Ma et al., 2019). Pseudoprogression is transient enlargement of lesions followed by partial response, and hyperprogression is unexpectedly rapid disease progression during treatment (Frelaut et al., 2020). Distinguishing between pseudoprogression and hyperprogression determines whether patients should remain on therapy or discontinue therapy. The speed of ctDNA analyses is ideal as tumors accelerate their rate of growth during hyperprogression.

Exosomes

Exosomes are small cell-derived vesicles that are shed from myriad cell types into biological fluids under normal and pathological conditions. They carry molecular constituents of their host cells, including proteins, lipids, mRNAs, and miRNAS (Zhou et al., 2020). They have been implicated in tumor development and metastasis, making them potential diagnostic biomarkers for several tumor types including gastrointestinal, breast, and lung cancers. In a gastrointestinal meta-analysis, a change in exosome expression was significantly correlated with poor OS (Zhang et al., 2021). Furthermore, circulating exosomal miRNAs were indicative of breast cancer (Hannafon et al., 2016) while exosomal proteins were indicative of lung cancer (Sandfeld-Paulsen et al., 2016).

BIOMARKERS OF IMMUNOTHERAPY

Biomarkers are particularly important in immunotherapy as immune checkpoint inhibitors have demonstrated impressive

responses across multiple tumor types. However, most patients do not benefit from this therapy and there is a growing need for biomarkers that can predict patient response.

Tumor and Immune Cell Phenotype

Some patients with PD-L1 positive tumors have improved clinical outcomes. However, the utility of this biomarker is inconsistent across tumor types (Doroshow et al., 2021). Increased circulating levels of sPD-L1 have also been correlated with poor response to immunotherapy, and may be more predictive than tumor cell expression of PD-L1 in soft tissue sarcomas (Asanuma et al., 2020). Diversity of immune cell repertoires could also function as a biomarker of response, as effective T cell responses require a diversity in T-cell receptor (TCR) clonality. In NSCLC, patients with increased CD8+ TCR clonality after immunotherapy had improved PFS compared to those with decreased clonality (Han et al., 2020).

Tumor Microenvironment

Immune status of the TME, including tumor-infiltrating immune cells and cytokine profiles, can be predictive biomarkers for immunotherapy. In melanoma, tumor-infiltrating immune cell subsets such as CD4+, CD8+, and FOXP3+ T cells correlate with improved treatment efficacy and disease outcome (Balatoni et al., 2018). An increased presence of cytotoxic T cells is generally predictive of clinical benefit from immunotherapy (Wei et al., 2021). In contrast, immunodepleted or immunodeficient tumors are less likely to respond. Furthermore, immunostimulatory TMEs characterized by inflamed IFN-γ profiles are predicted to respond better to immunotherapy (Gibney et al., 2016).

Tumor Genomic Biomarkers

Genomic biomarkers such as tumor mutational burden (TMB), neoantigen load, and microsatellite status are all clinically relevant biomarkers of immunotherapy. Tumors with high TMB are thought to have increased neoantigen burden making them immunogenic and more responsive to immunotherapy. High TMB is correlated with response to immunotherapy in several cancer types including NSCLC (Hellmann et al., 2018b), melanoma (Goodman et al., 2017), and CRC (Schrock et al., 2019). Similarly, microsatellite status is significantly associated with response to immunotherapy, where mismatch repair deficient or microsatellite instability high tumors are associated with durable responses to immunotherapy and improved prognosis. This correlation has been shown in cancers like NSCLC (Hellmann et al., 2018a), melanoma (Kubecek et al., 2016), and CRC (Andr et al., 2020).

DISCUSSION AND CONCLUSION

As the use of biomarkers in clinical cancer therapeutics advances, more frequent screening to evaluate drug efficacy and the development of resistance will be desirable. For patients undergoing these repeated screenings, the noninvasive nature of liquid biopsy is advantageous. ctDNA has been applied in detecting resistance to EGFR tyrosine kinase inhibitors and can replace a tumor biopsy in the decision to transition to third-generation EGFR tyrosine kinase inhibitors (Kilgour et al., 2020). While sequential targeting of the predominant mutation can prolong treatment responses, intratumoral heterogeneity can be a source of persistent residual disease and eventual drug resistance and recurrence. Multiregional sequencing, single-cell methods and sequential liquid biopsies allow more detailed evaluation of tumor heterogeneity with the potential to contribute multiple sub-population biomarkers and guide combinatorial treatment strategies (Lim and Ma 2019).

The complexities of tumor biology, its evolution over time and heterogeneity both between patients, and within a single tumor all add challenge to the development of biomarkers that meaningfully impact clinical cancer therapeutics. Biomarkers have the most clinical relevance when they are reproducibly and accurately measurable, clinically feasible, and prospectively validated in randomized clinical trials. Biomarkers are increasingly available at all phases of patient care, from screening and prevention to evaluations of drug efficacy and tumor response. Some biomarkers, such as those related to the EGFR pathway have already become approved decision-making tools for selecting cancer therapeutics. More are under development and may add insights to important areas of research such as tumor immune modulators and the tumor microenvironment. Blood-based biomarkers promise to reduce the potential for biopsy complications and make it easier to test repeatedly for tumor evolution. Many new trials are utilizing companion diagnostics where biomarker assays guide the use of targeted cancer drugs (Jørgensen et al., 2016). As the types of biomarkers expand, the information contained in published datasets also grows. Cross-validation among the increasing number of existing datasets will increase the power of machine learning algorithms and improve their clinical predictions (Shukla et al., 2015). While there are still many treatment decisions made without the aid of biomarkers, the future may yield more tools to guide the development and utilization of clinical cancer therapeutics.

AUTHOR CONTRIBUTIONS

All authors were involved in drafting and editing the manuscript.

FUNDING

This work was supported by an NIH grant (CA173453) and a grant from the Warren Alpert Foundation to W.S.E-D. This work was supported by the Teymour Alireza P'98, P'00 Family Cancer Research Fund established by the Alireza Family.

REFERENCES

Alves, M., Augusto, B., de Bulhões, G. F., Cavalcanti, I. N., Martins, M. M., de Oliveira, P. G., et al. (2019). Biomarkers in Colorectal Cancer: The Role of Translational Proteomics Research. *Front. Oncol.* 9, 1284. doi:10.3389/fonc.2019.01284

Andre, F., Ismaila, N., and Stearns, V. (2019). Use of Biomarkers to Guide Decisions on Adjuvant Systemic Therapy for Women with Early-Stage Invasive Breast Cancer: ASCO Clinical Practice Guideline Update Summary. *Jop* 15 (9), 495–497. doi:10.1200/JOP.19.00264

André, T., Shiu, K. K., Kim, T. W., Jensen, B. V., Jensen, L. H., Punt, C., et al. (2020). Pembrolizumab in Microsatellite-Instability-High Advanced Colorectal Cancer. *N. Engl. J. Med.* 383 (23), 2207–2218. doi:10.1056/NEJMoa2017699

Ankeny, J. S., Court, C. M., Hou, S., Li, Q., Song, M., Wu, D., et al. (2016a). Circulating Tumour Cells as a Biomarker for Diagnosis and Staging in Pancreatic Cancer. *Br. J. Cancer* 114 (12), 1367–1375. doi:10.1038/bjc.2016.121

Ankeny, J. S., Court, C. M., Hou, S., Li, Q., Song, M., Wu, D., et al. (2016b). Circulating Tumour Cells as a Biomarker for Diagnosis and Staging in Pancreatic Cancer. *Br. J. Cancer* 114 (12), 1367–1375. doi:10.1038/bjc.2016.121

Asanuma, K., Nakamura, T., Hayashi, A., Okamoto, T., Iino, T., Asanuma, Y., et al. (2020). Soluble Programmed Death-Ligand 1 rather Than PD-L1 on Tumor Cells Effectively Predicts Metastasis and Prognosis in Soft Tissue Sarcomas. *Sci. Rep.* 10 (1), 9077. doi:10.1038/s41598-020-65895-0

Balatoni, T., Mohos, A., Papp, E., Sebestyén, T., Liszkay, G., Oláh, J., et al. (2018). Tumor-Infiltrating Immune Cells as Potential Biomarkers Predicting Response to Treatment and Survival in Patients with Metastatic Melanoma Receiving Ipilimumab Therapy. *Cancer Immunol. Immunother.* 67 (1), 141–151. doi:10.1007/s00262-017-2072-1

Boichard, A., Richard, S. B., and Kurzrock, R. (2020). The Crossroads of Precision Medicine and Therapeutic Decision-Making: Use of an Analytical Computational Platform to Predict Response to Cancer Treatments. *Cancers (Basel)* 12 (1), E166. doi:10.3390/cancers12010166

Boussios, S., Ozturk, M. A., Moschetta, M., Karathanasi, A., Zakynthinakis-Kyriakou, N., Katsanos, K. H., et al. (2019). The Developing Story of Predictive Biomarkers in Colorectal Cancer. *J. Pers Med.* 9 (1), E12. doi:10.3390/jpm9010012

Califf, R. M. (2018). Biomarker Definitions and Their Applications. *Exp. Biol. Med. (Maywood)* 243 (3), 213–221. doi:10.1177/1535370217750088

Chen, G., Peng, J., Xiao, Q., Wu, H.-X., Wu, X., Wang, F., et al. (2021). Postoperative Circulating Tumor DNA as Markers of Recurrence Risk in Stages II to III Colorectal Cancer. *J. Hematol. Oncol.* 14 (1), 80. doi:10.1186/s13045-021-01089-z

Chung, C. (2021). Predictive and Prognostic Biomarkers with Therapeutic Targets in Colorectal Cancer: A 2021 Update on Current Development, Evidence, and Recommendation. *J. Oncol. Pharm. Pract.* 3, 107815522110055. doi:10.1177/10781552211005525

Cristofanilli, M., Budd, G. T., Ellis, M. J., Stopeck, A., Matera, J., Miller, M. C., et al. (2004). Circulating Tumor Cells, Disease Progression, and Survival in Metastatic Breast Cancer. *N. Engl. J. Med.* 351 (8), 781–791. doi:10.1056/NEJMoa040766

Darrigues, L., Pierga, J. Y., Bernard-Tessier, A., Bièche, I., Silveira, A. B., Michel, M., et al. (2021). Circulating Tumor DNA as a Dynamic Biomarker of Response to Palbociclib and Fulvestrant in Metastatic Breast Cancer Patients. *Breast Cancer Res.* 23 (1), 31. doi:10.1186/s13058-021-01411-0

de Bono, J. S., Scher, H. I., Montgomery, R. B., Parker, C., Miller, M. C., Tissing, H., et al. (2008). Circulating Tumor Cells Predict Survival Benefit from Treatment in Metastatic Castration-Resistant Prostate Cancer. *Clin. Cancer Res.* 14 (19), 6302–6309. doi:10.1158/1078-0432.CCR-08-0872

Deo, R. C. (2015). Machine Learning in Medicine. *Circulation* 132 (20), 1920–1930. doi:10.1161/CIRCULATIONAHA.115.001593

Dixon, M. R. (2003). Carcinoembryonic Antigen and Albumin Predict Survival in Patients with Advanced Colon and Rectal Cancer. *Arch. Surg.* 138 (9), 962–966. doi:10.1001/archsurg.138.9.962

Doroshow, D. B., Bhalla, S., Beasley, M. B., Sholl, L. M., Kerr, K. M., Gnjatic, S., et al. (2021). PD-L1 as a Biomarker of Response to Immune-Checkpoint Inhibitors. *Nat. Rev. Clin. Oncol.* 18 (6), 345–362. doi:10.1038/s41571-021-00473-5

Duffy, M. J., Harbeck, N., Nap, M., Molina, R., Nicolini, A., Senkus, E., et al. (2017). Clinical Use of Biomarkers in Breast Cancer: Updated Guidelines from the European Group on Tumor Markers (EGTM). *Eur. J. Cancer* 75 (April), 284–298. doi:10.1016/j.ejca.2017.01.017

Dustin, D., Gu, G., and Fuqua, S. A. W. (2019). ESR1 Mutations in Breast Cancer. *Cancer* 125 (21), 3714–3728. doi:10.1002/cncr.32345

Felder, M., Kapur, A., Gonzalez-Bosquet, J., Horibata, S., Heintz, J., Albrecht, R., et al. (2014). MUC16 (CA125): Tumor Biomarker to Cancer Therapy, a Work in Progress. *Mol. Cancer* 13 (May), 129. doi:10.1186/1476-4598-13-129

Feng, F., Shen, B., Mou, X., Li, Y., and Li, H. (2021). Large-Scale Pharmacogenomic Studies and Drug Response Prediction for Personalized Cancer Medicine. *J. Genet. Genomics* 48, 540–551. doi:10.1016/j.jgg.2021.03.007

Freelander, A., Brown, L. J., Parker, A., Segara, D., Portman, N., Lau, B., et al. (2021). Molecular Biomarkers for Contemporary Therapies in Hormone Receptor-Positive Breast Cancer. *Genes (Basel)* 12 (2), 285. doi:10.3390/genes12020285

Frelaut, M., du Rusquec, P., de Moura, A., Le Tourneau, C., and Borcoman, E. (2020). Pseudoprogression and Hyperprogression as New Forms of Response to Immunotherapy. *BioDrugs* 34 (4), 463–476. doi:10.1007/s40259-020-00425-y

Gainor, J. F., Longo, D. L., and Chabner, B. A. (2014). Pharmacodynamic Biomarkers: Falling Short of the Mark? *Clin. Cancer Res.* 20 (10), 2587–2594. doi:10.1158/1078-0432.CCR-13-3132

Gibney, G. T., Weiner, L. M., and Atkins, M. B. (2016). Predictive Biomarkers for Checkpoint Inhibitor-Based Immunotherapy. *Lancet Oncol.* 17 (12), e542–51. doi:10.1016/S1470-2045(16)30406-5

Goodman, A. M., Kato, S., Bazhenova, L., Patel, S. P., Frampton, G. M., Miller, V., et al. (2017). Tumor Mutational Burden as an Independent Predictor of Response to Immunotherapy in Diverse Cancers. *Mol. Cancer Ther.* 16 (11), 2598–2608. doi:10.1158/1535-7163.MCT-17-0386

Han, J., Duan, J., Bai, H., Wang, Y., Wan, R., Wang, X., et al. (2020). TCR Repertoire Diversity of Peripheral PD-1+CD8+ T Cells Predicts Clinical Outcomes after Immunotherapy in Patients with Non-small Cell Lung Cancer. *Cancer Immunol. Res.* 8 (1), 146–154. doi:10.1158/2326-6066.CIR-19-0398

Hannafon, B. N., Trigoso, Y. D., Calloway, C. L., Zhao, Y. D., Lum, D. H, Welm, A. L., et al. (2016). Plasma Exosome MicroRNAs Are Indicative of Breast Cancer. *Breast Cancer Res.* 18 (1), 90. doi:10.1186/s13058-016-0753-x

Hellmann, M. D., Ciuleanu, T. E., PluzanskiOtterson, A., Lee, J. S., Otterson, G. A., Audigier-Valette, C., et al. (2018a). Nivolumab Plus Ipilimumab in Lung Cancer with a High Tumor Mutational Burden. *N. Engl. J. Med.* 378 (22), 2093–2104. doi:10.1056/NEJMoa1801946

Hellmann, M. D., Nathanson, T., Rizvi, H., Creelan, B. C., Sanchez-Vega, F., Ahuja, A., et al. (2018b). Genomic Features of Response to Combination Immunotherapy in Patients with Advanced Non-small-cell Lung Cancer. *Cancer Cell* 33 (5), 791–793. doi:10.1016/j.ccell.2018.04.005

Jackson, R. C. (2012). Pharmacodynamic Modelling of Biomarker Data in Oncology. *ISRN Pharmacol.* 2012 (February), 590626. doi:10.5402/2012/590626

Jia, W., Gao, Q., Han, A., Zhu, H., and Yu, J. (2019). The Potential Mechanism, Recognition and Clinical Significance of Tumor Pseudoprogression after Immunotherapy. *Cancer Biol. Med.* 16 (4), 655–670. doi:10.20892/j.issn.2095-3941.2019.0144

Jiang, Z., Wu, D., Lin, S., and Li, P. (2016). CD34 and CD38 Are Prognostic Biomarkers for Acute B Lymphoblastic Leukemia. *Biomark Res.* 4 (1), 23. doi:10.1186/s40364-016-0080-5

Jørgensen, J. T., Hersom, M., and Hersom, M. (2016). Companion Diagnostics-A Tool to Improve Pharmacotherapy. *Ann. Transl. Med.* 4 (24), 482. doi:10.21037/atm.2016.12.26

Karachaliou, N., Gonzalez-Cao, M., Crespo, G., Drozdowskyj, A., Aldeguer, E., Gimenez-Capitan, A., et al. (2018). Interferon Gamma, an Important Marker of Response to Immune Checkpoint Blockade in Non-small Cell Lung Cancer and Melanoma Patients. *Ther. Adv. Med. Oncol.* 10, 1758834017749748. doi:10.1177/1758834017749748

Kelloff, G. J., Hoffman, J. M., Johnson, B., Scher, H. I., Siegel, B. A., Cheng, E. Y., et al. (2005). Progress and Promise of FDG-PET Imaging for Cancer Patient Management and Oncologic Drug Development. *Clin. Cancer Res.* 11 (8), 2785–2808. doi:10.1158/1078-0432.CCR-04-2626

Kilgour, E., Rothwell, D. G., Brady, G., and Dive, C. (2020). Liquid Biopsy-Based Biomarkers of Treatment Response and Resistance. *Cancer Cell* 37 (4), 485–495. doi:10.1016/j.ccell.2020.03.012

Kubecek, O., Trojanova, P., Molnarova, V., and Kopecky, J. (2016). Microsatellite Instability as a Predictive Factor for Immunotherapy in Malignant Melanoma. *Med. Hypotheses* 93 (August), 74–76. doi:10.1016/j.mehy.2016.05.023

Lenzo, F. L., Kato, S., Pabla, S., DePietro, P., Nesline, M. K., Conroy, J. M., et al. (2021). Immune Profiling and Immunotherapeutic Targets in Pancreatic Cancer. *Ann. Transl Med.* 9 (2), 119. doi:10.21037/atm-20-1076

Lim, Z.-F., and Ma, P. C. (2019). Emerging Insights of Tumor Heterogeneity and Drug Resistance Mechanisms in Lung Cancer Targeted Therapy. *J. Hematol. Oncol.* 12 (1), 134. doi:10.1186/s13045-019-0818-2

Lucci, A., Hall, C. S., Lodhi, A. K., Anderson, A. E., Xiao, L., Bedrosian, I., et al. (2012). Circulating Tumour Cells in Non-metastatic Breast Cancer: a Prospective Study. *Lancet Oncol.* 13 (7), 688–695. doi:10.1016/S1470-2045(12)70209-7

Ma, Y., Wang, Q., Dong, Q., Zhan, L., and Zhang, J. (2019). How to Differentiate Pseudoprogression from True Progression in Cancer Patients Treated with Immunotherapy. *Am. J. Cancer Res.* 9 (8), 1546–1553.

Michela, B. (2021). Liquid Biopsy: A Family of Possible Diagnostic Tools. *Diagnostics (Basel)* 11 (8), 1391. doi:10.3390/diagnostics11081391

Misale, S., Di Nicolantonio, F., Sartore-Bianchi, A., Siena, S., and Bardelli, A. (2014). Resistance to Anti-EGFR Therapy in Colorectal Cancer: From Heterogeneity to Convergent Evolution. *Cancer Discov.* 4 (11), 1269–1280. doi:10.1158/2159-8290.CD-14-0462

Monastero, R. N., and Pentyala, S. (2017). Cytokines as Biomarkers and Their Respective Clinical Cutoff Levels. *Int. J. Inflam* 2017, 4309485. doi:10.1155/2017/4309485

Nalejska, E., Mączyńska, E., and Lewandowska, M. A. (2014). Prognostic and Predictive Biomarkers: Tools in Personalized Oncology. *Mol. Diagn. Ther.* 18 (3), 273–284. doi:10.1007/s40291-013-0077-9

Olivier, M., Asmis, R., Hawkins, G. A., Howard, T. D., and Cox, L. A. (2019). The Need for Multi-Omics Biomarker Signatures in Precision Medicine. *Int. J. Mol. Sci.* 20 (19), 4781. doi:10.3390/ijms20194781

Parseghian, C. M., Loree, J. M., Morris, V. K., Liu, X., Clifton, K. K., Napolitano, S., et al. (2019). Anti-EGFR-Resistant Clones Decay Exponentially after Progression: Implications for Anti-EGFR Re-Challenge. *Ann. Oncol.* 30 (2), 243–249. doi:10.1093/annonc/mdy509

Poruk, K. E., Gay, D. Z., Brown, K., Mulvihill, J. D., Boucher, K. M., Scaife, C. L., et al. (2013). The Clinical Utility of CA 19-9 in Pancreatic Adenocarcinoma: Diagnostic and Prognostic Updates. *Curr. Mol. Med.* 13 (3), 340–351. doi:10.2174/1566524011313030003

Poveda, A., Kaye, S. B., McCormack, R., Wang, S., Parekh, T., Ricci, D., et al. (2011). Circulating Tumor Cells Predict Progression Free Survival and Overall Survival in Patients with Relapsed/Recurrent Advanced Ovarian Cancer. *Gynecol. Oncol.* 122 (3), 567–572. doi:10.1016/j.ygyno.2011.05.028

Romiti, A., Raffa, S., Di Rocco, R., Roberto, M., Milano, A., Zullo, A., et al. (2014). Circulating Tumor Cells Count Predicts Survival in Colorectal Cancer Patients. *J. Gastrointestin Liver Dis.* 23 (3), 279–284. doi:10.15403/jgld.2014.1121.233.arom1

Saarenheimo, J., Eigeliene, N., Andersen, H., Tiirola, M., and Jekunen, A. (2019). The Value of Liquid Biopsies for Guiding Therapy Decisions in Non-small Cell Lung Cancer. *Front. Oncol.* 9 (March), 129. doi:10.3389/fonc.2019.00129

Sandfeld-Paulsen, B., Jakobsen, K. R., Bæk, R., Folkersen, B. H., Rasmussen, T. R., Meldgaard, P., et al. (2016). Exosomal Proteins as Diagnostic Biomarkers in Lung Cancer. *J. Thorac. Oncol.* 11 (10), 1701–1710. doi:10.1016/j.jtho.2016.05.034

Sartore-Bianchi, A., Pietrantonio, F., Lonardi, S., Mussolin, B., Rua, F., Fenocchio, E., et al. (2021). Phase II Study of Anti-EGFR Rechallenge Therapy with Panitumumab Driven by Circulating Tumor DNA Molecular Selection in Metastatic Colorectal Cancer: The CHRONOS Trial. *Jco* 39 (15_Suppl. l), 3506. doi:10.1200/JCO.2021.39.15_suppl.3506

Scheerens, H., Malong, A., Bassett, K., Boyd, Z., Gupta, V., Harris, J., et al. (2017). Current Status of Companion and Complementary Diagnostics: Strategic Considerations for Development and Launch. *Clin. Transl Sci.* 10 (2), 84–92. doi:10.1111/cts.12455

Schrock, A. B., Ouyang, C., Sandhu, J., Sokol, E., Jin, D., Ross, J. S., et al. (2019). Tumor Mutational Burden Is Predictive of Response to Immune Checkpoint Inhibitors in MSI-High Metastatic Colorectal Cancer. *Ann. Oncol.* 30 (7), 1096–1103. doi:10.1093/annonc/mdz134

Shukla, H. D., Mahmood, J., and Vujaskovic, Z. (2015). Integrated Proteo-Genomic Approach for Early Diagnosis and Prognosis of Cancer. *Cancer Lett.* 369 (1), 28–36. doi:10.1016/j.canlet.2015.08.003

Song, Y., Hu, C., Xie, Z., Wu, L., Zhu, Z., Rao, C., et al. (2020). Circulating Tumor DNA Clearance Predicts Prognosis across Treatment Regimen in a Large Real-World Longitudinally Monitored Advanced Non-small Cell Lung Cancer Cohort. *Transl Lung Cancer Res.* 9 (2), 269–279. doi:10.21037/tlcr.2020.03.17

American Cancer Society Inc, (2019) *Breast Cancer Facts & Figures 2019-2020*. Atlanta, Georgia, US: American Cancer Society, 44.

Su, M., Zhang, Z., Zhou, L., Han, C., Huang, C., and Nice, E. C. (2021). Proteomics, Personalized Medicine and Cancer. *Cancers (Basel)* 13 (11), 2512. doi:10.3390/cancers13112512

Tsimberidou, A. M., Fountzilas, E., Nikanjam, M., and Kurzrock, R. (2020). Review of Precision Cancer Medicine: Evolution of the Treatment Paradigm. *Cancer Treat. Rev.* 86 (June), 102019. doi:10.1016/j.ctrv.2020.102019

Wang, M., Wu, K., Zhang, P., Zhang, M., Ding, A., and Chen, H. (2019). The Prognostic Significance of the Oncotype DX Recurrence Score in T1-2N1M0 Estrogen Receptor-Positive HER2-Negative Breast Cancer Based on the Prognostic Stage in the Updated AJCC 8th Edition. *Ann. Surg. Oncol.* 26 (5), 1227–1235. doi:10.1245/s10434-018-7068-3

Wei, X., Gu, L., and Heng, W. (2021). T Lymphocytes Related Biomarkers for Predicting Immunotherapy Efficacy in Non-small Cell Lung Cancer. *Oncol. Lett.* 21 (2), 89. doi:10.3892/ol.2020.12350

Weil, J. (2002). Genetic Counselling in the Era of Genomic Medicine. As We Move towards Personalized Medicine, it Becomes More Important to Help Patients Understand Genetic Tests and Make Complex Decisions about Their Health. *EMBO Rep.* 3 (7), 590–593. doi:10.1093/embo-reports/kvf144

Welch, H. G., and Albertsen, P. C. (2009). Prostate Cancer Diagnosis and Treatment after the Introduction of Prostate-specific Antigen Screening: 1986-2005. *J. Natl. Cancer Inst.* 101 (19), 1325–1329. doi:10.1093/jnci/djp278

Zhang, J., Fu, S., Chen, W., and Chen, H. (2021). Exosome as Potential Biomarkers for Gastrointestinal Tumors. *Medicine* 100 (6), e24509. doi:10.1097/MD.0000000000024509

Zheng, H., Zhang, G., Zhang, L., Wang, Q., Li, H., Han, Y., et al. (2020). Comprehensive Review of Web Servers and Bioinformatics Tools for Cancer Prognosis Analysis. *Front. Oncol.* 10 (February), 68. doi:10.3389/fonc.2020.00068

Zhou, B., Xu, K., Zheng, X., Chen, T., Wang, J., Song, Y., et al. (2020). Application of Exosomes as Liquid Biopsy in Clinical Diagnosis. *Signal. Transduct Target. Ther.* 5 (1), 144. doi:10.1038/s41392-020-00258-9

Conflict of Interest: The authors declare that the research was conducted in the absence of any commercial or financial relationships that could be construed as a potential conflict of interest.

Publisher's Note: All claims expressed in this article are solely those of the authors and do not necessarily represent those of their affiliated organizations, or those of the publisher, the editors and the reviewers. Any product that may be evaluated in this article, or claim that may be made by its manufacturer, is not guaranteed or endorsed by the publisher.

Copyright © 2021 Louie, Huntington, Carlsen, Zhou and El-Deiry. This is an open-access article distributed under the terms of the Creative Commons Attribution License (CC BY). The use, distribution or reproduction in other forums is permitted, provided the original author(s) and the copyright owner(s) are credited and that the original publication in this journal is cited, in accordance with accepted academic practice. No use, distribution or reproduction is permitted which does not comply with these terms.

frontiers in Pharmacology

REVIEW
published: 30 November 2021
doi: 10.3389/fphar.2021.751568

Therapeutic Targeting of Autophagy in Pancreatic Ductal Adenocarcinoma

Alexander G. Raufi[1,2,3,4], Nicholas R. Liguori[1,5], Lindsey Carlsen[1,3,4,6], Cassandra Parker[1,7], Liz Hernandez Borrero[1,6], Shengliang Zhang[1,3,4,8], Xiaobing Tian[1,3,4,8], Anna Louie[1,7], Lanlan Zhou[1,3,4,8], Attila A. Seyhan[1,3,4,8] and Wafik S. El-Deiry[1,2,3,4,6,8]**

[1]*Laboratory of Translational Oncology and Experimental Cancer Therapeutics, Warren Alpert Medical School, Brown University, Providence, RI, United States,* [2]*Hematology/Oncology Division, Department of Medicine, Lifespan Health System and Brown University, Providence, RI, United States,* [3]*Joint Program in Cancer Biology, Lifespan Health System and Brown University, Providence, RI, United States,* [4]*Cancer Center at Brown University, Providence, RI, United States,* [5]*Temple University, Lewis Katz School of Medicine, Philadelphia, PA, United States,* [6]*Pathobiology Graduate Program, Warren Alpert Medical School, Brown University, Providence, RI, United States,* [7]*Department of Surgery, Warren Alpert Medical School, Brown University, Providence, RI, United States,* [8]*Department of Pathology and Laboratory Medicine, Warren Alpert Medical School, Brown University, Providence, RI, United States*

OPEN ACCESS

Edited by:
Anne Lorant, Laboratoire de Biologie Moléculaire et Cellulaire du Cancer (LBMCC), Luxembourg

Reviewed by:
Carmela Spagnuolo, National Research Council (CNR), Italy
Claudio Daniel Gonzalez, Centro de Educación Médica e Investigaciones Clínicas Norberto Quirno (CEMIC), Argentina

***Correspondence:**
Wafik S. El-Deiry
wafik@brown.edu
Alexander G. Raufi
alexander_raufi@brown.edu

Specialty section:
This article was submitted to Pharmacology of Anti-Cancer Drugs, a section of the journal Frontiers in Pharmacology

Received: *01 August 2021*
Accepted: *25 October 2021*
Published: *30 November 2021*

Citation:
Raufi AG, Liguori NR, Carlsen L, Parker C, Hernandez Borrero L, Zhang S, Tian X, Louie A, Zhou L, Seyhan AA and El-Deiry WS (2021) Therapeutic Targeting of Autophagy in Pancreatic Ductal Adenocarcinoma. Front. Pharmacol. 12:751568. doi: 10.3389/fphar.2021.751568

Pancreatic ductal adenocarcinoma (PDAC) is an aggressive disease characterized by early metastasis, late detection, and poor prognosis. Progress towards effective therapy has been slow despite significant efforts. Novel treatment approaches are desperately needed and autophagy, an evolutionary conserved process through which proteins and organelles are recycled for use as alternative energy sources, may represent one such target. Although incompletely understood, there is growing evidence suggesting that autophagy may play a role in PDAC carcinogenesis, metastasis, and survival. Early clinical trials involving autophagy inhibiting agents, either alone or in combination with chemotherapy, have been disappointing. Recently, evidence has demonstrated synergy between the MAPK pathway and autophagy inhibitors in PDAC, suggesting a promising therapeutic intervention. In addition, novel agents, such as ONC212, have preclinical activity in pancreatic cancer, in part through autophagy inhibition. We discuss autophagy in PDAC tumorigenesis, metabolism, modulation of the immune response, and preclinical and clinical data with selected autophagy modulators as therapeutics.

Keywords: autophagy, pancreatic cancer, MEK inhibitors, ONC212, chloroquine, Atg5, LC3, beclin 1

PANCREATIC CANCER

Pancreatic ductal adenocarcinoma (PDAC) is an aggressive disease characterized by early metastasis, late detection, and little progress towards effective treatment or cure. The vast majority of patients present with incurable unresectable or metastatic disease. Even in the 15–20% of patients who are candidates for, and ultimately undergo resection, recurrence ultimately occurs in 80%. Presently, the mortality-to-incidence ratio for PDAC remains amongst the highest of all malignancies and by 2030 PDAC is projected to be the second leading cause of cancer-related death in the United States (Miller et al., 2016). For individuals diagnosed with unresectable or metastatic PDAC, combination chemotherapy with mFOLFIRINOX or gemcitabine/nab-paclitaxel remains the standard of care. These regimens provide modest benefit, improving quality of life and median overall survival by several months, however, the 5-years overall survival is only 10% (Siegel et al., 2021). In light of this, identifying novel therapeutic agents to treat PDAC has become a major focus of research.

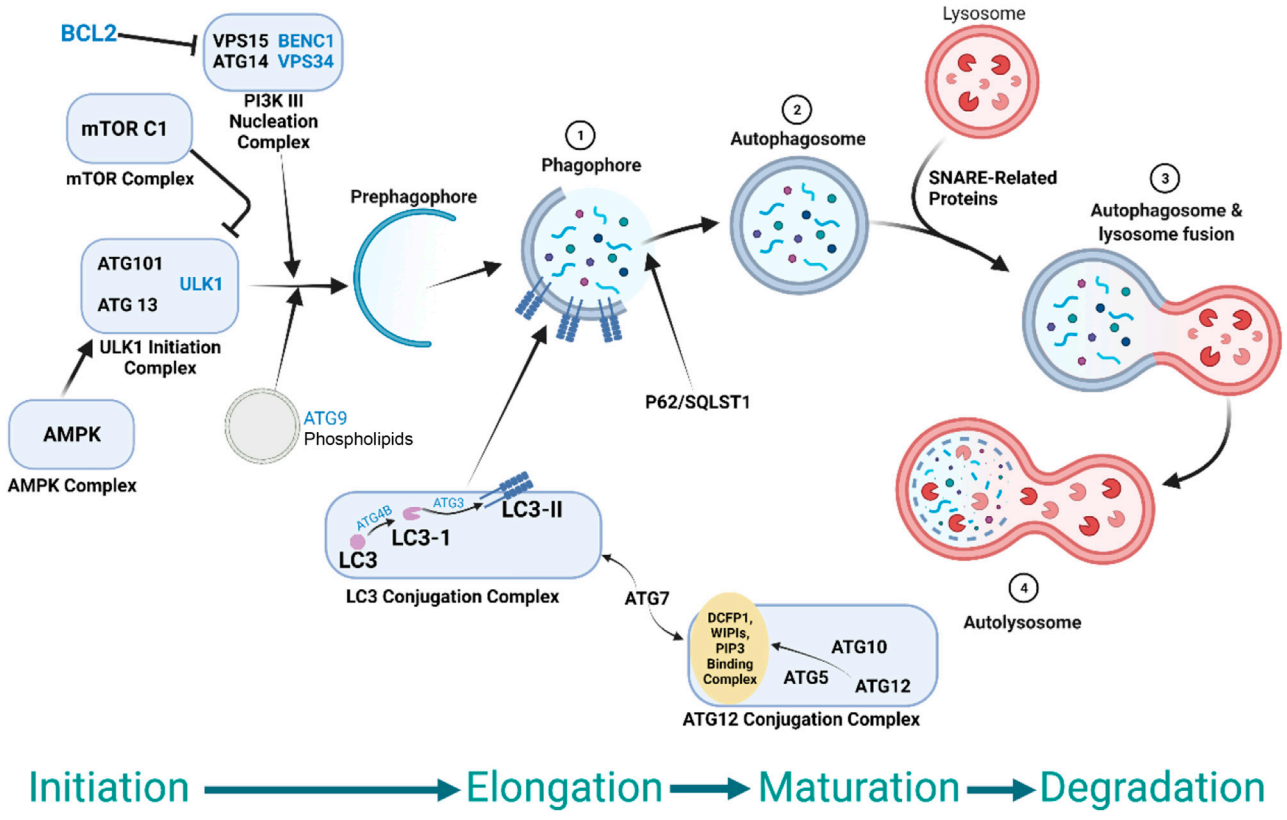

FIGURE 1 | Schematic depiction of the autophagy pathway and its regulation by various signaling molecules, autophagosomes, and lysosomes in cell biology. Autophagosome formation is a complex process that involves several phases: Autophagosome initiation which involves ULK1 complex and the class III phosphatidylinositol 3-kinase (PI3K) complex and other protein complexes. The elongation step involves the action of two ubiquitin-like conjugation systems and requires the conjugation of LC3 to the phosphatidylethanolamine, a form called LC3-II, allowing the expansion of the initial membrane and confining a portion of the cytosol. The maturation and degradation step involve autophagosome closure, the fusion of the autophagosome with the lysosome to form the autolysosome, and degradation step mediated by lysosomal enzymes which degrade the proteins and other substrates in the autolysosome. More information on autophagosomes and autophagy process can be found in the literature (Reggiori and Ungermann, 2017).

Although several mutations (e.g., *KRAS, TP53, SMAD4, CDKN2A*) are commonly identified in PDAC, the disease is genetically complex and development of targeted therapy has been slow. Only two targeted therapies have been approved to date: erlotinib, an EGFR inhibitor which improves in overall survival by approximately 2 weeks, and olaparib, a PARP inhibitor, which improves progression free survival by several months in germline BRCA2-mutated metastatic PDAC that has not progressed after 4 months of platinum containing chemotherapy (Moore et al., 2007; Golan et al., 2019). Unfortunately, aside from rare cases of microsatellite instability, immune checkpoint blockade has also had little to no impact on outcomes for patients diagnosed with PDAC. The lack of effective therapies has served as an impetus to further improve our understanding of pancreatic tumor biology in order to identify alternative treatment strategies.

Autophagy is a complex, evolutionarily conserved process through which proteins and organelles are recycled for use as alternative energy sources. Although typically upregulated during states of cellular stress or starvation, tumor cells can also take advantage of this process to maintain homeostasis. In this review we will focus on macro-autophagy, which refers to the removal of cytoplasmic components through autophagosome-delivery of organelles to lysosomes for degradation (**Figure 1**) (Mizushima et al., 2011). This process is required for cell survival, homeostasis, and can be upregulated through multiple cell signaling pathways. In cancer, it is thought to play a role in tumor cell survival and resistance to chemotherapy, and hence represents an area of therapeutic development.

We will discuss the role autophagy plays in PDAC tumorigenesis and metabolism, modulation of the immune response, as well as both preclinical and clinical data with select autophagy modulators.

AUTOPHAGY IS UPREGULATED IN PDAC

Although the precise role of autophagy in PDAC is incompletely understood, increased basal levels of autophagy have been reported. Using GFP-LC3 puncta as an indicator of cells undergoing autophagy, Yang et al. demonstrated increased

autophagic flux in eight PDAC cell lines (Yang et al., 2011). The authors further supported these findings by measuring levels of microtubule-associated protein 1 light chain 3 (LC3), more specifically the conversion of LC3-I to LC3-II. Previous work established an interaction between LC3 and autophagosome membranes, notably in PDAC (Fujii et al., 2008). Yang et al. noted increased levels of LC3-II in PDAC cells lines, relative to control normal pancreatic ductal cells, a finding that was not reproducible in select lung or breast cancer cell lines, suggesting that this may be a unique feature of PDAC. Given that autophagy is a dynamic process, elevations in LC3-II could suggest a block in later stages of autophagy, such as impaired autophagosome degradation, and not exclusively upregulation. Therefore, an analysis of long-term protein degradation using a GFP-Neo fusion protein was performed (Klionsky et al., 2008). Over a 2-day period, 8988T PDAC cells were examined and were noted to have a significant reduction in levels, further supporting increased autophagic flux. The authors were also able to restore GFP-Neo levels with the autophagy inhibitor chloroquine. Finally, they showed that chloroquine also reduces PDAC cell proliferation *in vitro*, suggesting a possible novel approach to therapy.

Several additional components of the autophagy pathway have been identified as key mediators in governing PDAC cell proliferation. ATG5, for example, is a ubiquitin-related protein shown to be necessary for autophagosome expansion and completion (**Figure 1**) (Levine and Kroemer, 2008). Selective siRNA-mediated knockdown of ATG5 notably reduced 8988T PDAC cell proliferation by greater than 50% (Yang et al., 2011). The MiTF family of transcription factors (MiTF, TFE3, and TFEB) have also been implicated as drivers of autophagy in PDAC cells (Rouschop et al., 2010). Upon nuclear import, these transcription factors drive increased expression of catabolic lysosomal genes and gene set enrichment analyses indicate a strong relationship between expression of MiT/TFE factors and autophagy in PDAC (Rouschop et al., 2010). Furthermore, MITF, TFE3, or TFEB knockout leads to downregulation of CLEAR (Coordinated Lysosomal Expression and Regulation)-carrying genes in PDAC cells, leading to reduction in proliferation and growth of PDAC tumor cells (Rouschop et al., 2010).

In the setting of amino acid starvation, unc5-like autophagy activating kinase 1 (ULK1) is known to play an indispensable role in driving autophagy. It is primarily regulated by nutrient-sensing kinases such as mammalian target of rapamycin (mTOR) complex-1 (mTORC1) and AMPK (Kim et al., 2011; Shang et al., 2011; Wong et al., 2015). When starvation-levels of amino acids are detected, mTORC1 is suppressed and ULK1 is phosphorylated inducing autophagy (Kim et al., 2011; Shang et al., 2011; Wong et al., 2015). Interestingly, starvation appears to be a more profound driver of autophagy than direct inhibition of mTORC1, suggesting that alternative pathways also play a role (Wong et al., 2015). Furthermore, cells with high levels of autophagy also have increased phosphatase activity, including phosphatase PPA2. This enzyme dephosphorylates ULK1 at S637 reducing levels of autophagy (Wong et al., 2015).

Given that the vast majority of PDAC cases have constitutive activation of KRAS, the effects of the MAPK pathway on autophagic flux is of particular interest. Although poorly defined, it is unlikely that constitutive MAPK signaling is solely responsible for driving increased basal levels of autophagy in PDAC. In fact, several studies have reported that inhibition of the MAPK cascade leads to increased autophagy which will be described in further detail later (Bryant et al., 2019; Kinsey et al., 2019). As described above, activation of the MAPK pathway is expected to promote phosphorylation and cytoplasmic retention of the transcription factors TFEB and TFE3, and hence a reduce expression of autophagy promoting genes.

In summary, high rates of basal autophagy in PDAC is regulated by multiple mechanisms and each of these processes represents a unique target for further investigation.

AUTOPHAGY AND PDAC CARCINOGENESIS

The precise role autophagy plays in PDAC tumorigenesis is complicated by several conflicting studies that have shown that autophagy can lead to both promotion and inhibition of tumor development. A tumor-promoting mechanism of autophagy has been described in mice with heterozygous deletions of mammalian Beclin1. Deletion of this key autophagy promoting enzyme results in the development of malignant neoplasms in various organs in mice (Qu et al., 2003; Yue et al., 2003). Another partial autophagy phenotype, $ATG5^{+/-}$, leads to increased tumor formation and metastasis but this is not observed in mice completely deficient of autophagy ($ATG^{-/-}$) which spontaneously developed only benign liver tumors and increased acinar-to-ductal metaplasia (Takamura et al., 2011; Görgülü et al., 2019). It has been suggested that autophagy is a relatively weak tumor suppressor yet at the same time it is necessary for the progression of benign tumors to malignancy (Takamura et al., 2011). There is also evidence suggesting that defects in autophagy lead to increased dysfunctional or damaged mitochondria in tumor cells and impaired tumorigenesis (White, 2015). This implies that autophagy may induce tumorigenesis and disease by preserving the integrity and quality of mitochondria and also by supplementing essential substrates for mitochondrial metabolism (White, 2015). Autophagy may also promote tumorigenesis by suppressing induction of the p53 tumor suppressor protein and maintaining metabolic function of mitochondria, enabling cancer cells to survive environmental stresses (White, 2015). Further study is required to bring clarity to our understanding of autphagic recycling of substrates, the identity of specific substrates, and the metabolic pathways and functions that they are used for.

Using a KRAS-driven lung cancer model, Guo et al. found that homozygous deletion of ATG7 reduced tumor burden and proliferation of tumor cells (Guo et al., 2016). ATG5, another member of the ATG family, was shown to increase PanIN but not PDAC formation in a genetically engineered PDAC mouse model

with mutant KRAS and a single Trp53 allele. Chloroquine or hydroxychloroquine treated PDAC cell lines and patient derived xenograft models led to decreased proliferation, increased DNA damage and apoptosis (Yang et al., 2014). Interestingly, ATG7 deletion in a similar KRAS mutant/Trp53null model of lung cancer showed reduced tumor burden (Karsli-Uzunbas et al., 2014). These studies support the role that autophagy plays in carcinogenesis and in maintaining tumor growth and proliferation.

AUTOPHAGY AND METABOLOMICS

As discussed in a recent review, cellular metabolism and autophagy are two interconnected cellular processes (Piffoux et al., 2021). A hallmark of tumor metabolism is the preferred use of aerobic glycolysis over oxidation of glycolytic pyruvate to produce both energy and lactate, the latter of which serves as a substrate for nucleic acid, protein, and lipid production. While aerobic glycolysis is inefficient in terms of energetics, it serves as a mechanism to promote growth, survival, and proliferation in tumor cells. This phenomenon of increased glucose uptake and fermentation of glucose to lactate is observed even in the presence of completely functioning mitochondria and is known as the Warburg Effect (Vander Heiden et al., 2009; Liberti and Locasale, 2016). Because autophagy degrades proteins and organelles to create new substrates it is integrally connected with tumor metabolism (Vander Heiden et al., 2009). It has been reported that oncogene ablation-resistant pancreatic cancer cells depend on mitochondrial function and that resistance to KRAS-targeted therapy might be mediated by a subset of tumor cells that depend on oxidative phosphorylation for survival instead of the classic Warburg effect (Viale et al., 2014). Oxidative phosphorylation is highly dependent on mitochondrial respiration, and genes involved in this process, as well as autophagy- and lysosome-related genes, were found to be upregulated in surviving cells. However, upregulation of autophagy in surviving cells is likely only one side of a transcriptional program which supplies tumor cells with nutrients (Perera et al., 2015). Collectively, autophagy has a role in maintaining sufficient supplies of energy and nutrient to tumors *via* tumor-cell-autonomous, stromal and systemic autophagy.

Autophagy induction is not only triggered by nutrient deficiency but also by low oxygen levels. Cellular adaptation to hypoxic conditions involves multiple mechanisms, such as upregulation of the unfolded protein response (UPR) (Rouschop et al., 2010). Hypoxia has been shown to increase transcription of the essential autophagy genes MAP1LC3B and ATG5 *via* the transcription factors ATF4 and CHOP, respectively. Notably, MAP1LC3B and ATG5 are not required for initiation of autophagy but are involved in phagophore expansion and autophagosome formation. Furthermore, autophagy and MAP1LC3B induction have been shown to mostly occur in hypoxic regions of tumor xenografts. Pharmacological inhibition of autophagy sensitizes human tumor cells to hypoxia and decreases the proportion of viable hypoxic tumor cells and sensitizes tumor xenografts to irradiation. Collectively, these data suggest that the UPR is an important mediator of the hypoxic tumor microenvironment and that it contributes to resistance to treatment through its ability to facilitate autophagy.

Hypoxia is involved in tumorigenesis, associated with altered metabolism, abnormal vascularization, resistance to chemo/radiotherapy, and increased cancer cell stemness and may even promote metastasis (Wilson and Hay, 2011; Yun and Lin, 2014; Horsman and Overgaard, 2016; Minassian et al., 2019). In response to hypoxia, the transcription factor hypoxia-inducible factor 1α (HIF1α), activates a variety of target genes that are involved in altered metabolism, cell survival and tumor progression (Kaelin, 2011; Masson and Ratcliffe, 2014; Chen and Sang, 2016). Both hypoxia and anoxia, with oxygen concentrations <3% and <0.1%, respectively, cause autophagy through a variety of different mechanisms (Kroemer et al., 2010). Hypoxia-induced autophagy depends on hypoxia-inducible factor, HIF, while anoxia-induced autophagy is HIF-independent (Majmundar et al., 2010; Mazure and Pouysségur, 2010). HIF is a heterodimer of a constitutive ß subunit and an oxygen-regulated α subunit that only becomes stabilized (and hence expressed) when oxygen concentration declines below a threshold of ~5%. Under moderate hypoxia (1–3% oxygen), HIF activates the transcription of *BNIP3* and *BNIP3L* (NIX), two BH3-only proteins that can disrupt the inhibitory interaction between Beclin 1 and Bcl-2 (Bellot et al., 2009). Moreover, BNIP3L, which often is present at the outer surface of mitochondria, possesses a WXXL motif that binds to LC3 and its homolog GABARAP (Novak et al., 2010), thereby targeting mitochondria for autophagic destruction. The transcription of *BNIP3* is also upregulated by the transcription factor FOXO3, on condition that it is deacetylated by Sirt1 (Kume et al., 2010).

Under severe hypoxia or anoxia, additional pathways including the protein DJ-1, the autocrine stimulation of a PDGFR-dependent pathway, the stimulation of AMPK through metabolic stress, and the UPR of the ER have been demonstrated to play role in hypoxia-induced autophagy (Mazure and Pouysségur, 2010). Hypoxia-mediated upregulation of autophagy also requires phosphorylation of eIF2α mediated by PERK (see below), further highlighting the significance of the phosphorylation of eIF2α as a universal autophagy regulator (Rouschop et al., 2010). Lastly, hypoxia has been shown to upregulate the transcription of the key autophagy genes, *LC3* and *Atg5*, *via* ATF4 and CHOP transcription factors, respectively, which are both regulated by PERK (Rouschop et al., 2010).

AUTOPHAGY AND THE INTEGRATED STRESS RESPONSE

The integrated stress response (ISR) is an evolutionarily conserved cellular stress response in eukaryotic organisms that inhibits global protein biosynthesis and activates the expression of specific genes in response to extrinsic environmental factors and intrinsic pathophysiological stresses (Pakos-Zebrucka et al.,

2016). Extrinsic stress factors include hypoxia, starvation (e.g., amino acid deprivation, glucose deprivation), viral infection, and presence of oxidants. One of the primary intrinsic factors is endoplasmic reticulum (ER) stress which results from increased levels of unfolded proteins and polypeptides in the ER. It is now well established that oncogene activation can also activate the ISR. Activation of the ISR will either stimulate the expression of specific genes to restore cellular homeostasis by resolving cellular damage caused by these stressors, or, if unable to restore homeostasis, activate programmed cell death (apoptosis) (Pakos-Zebrucka et al., 2016).

Many of the stress signaling pathways converge on eIF2α. Phosphorylation of this transcription factor subsequently initiates the ISR, but outcome of ISR activation can be quite different and depends not only by the type of the stressor but also its extent and severity. This influences the duration of the phosphorylation of eIF2α as well as translation of *ATF4* and other bZIP transcription factors (Dey et al., 2010; Guan et al., 2014). For example, a short duration of ISR activity appears to be an adaptive, pro-survival response to various stresses aimed at overcoming the stress and restoring homeostasis, whereas activation of ISR for an extended period can induce the cell to programmed cell death (Rutkowski et al., 2006). However, this dual action of eIF2α phosphorylation requires further elucidation.

It has been widely accepted that the ISR can regulate cell survival and cell death pathway *via* induction of autophagy which facilitates the degradation of unfolded proteins, polypeptides or protein aggregates, and damaged organelles. As a result, autophagy restores depleted amino acids pool for protein synthesis and reenergizes a starved cell restoring homeostasis. Although mechanisms by which phosphorylated eIF2α induces autophagy are still being explored, similar extrinsic and intrinsic stress signals leading to phosphorylation of eIF2α have been shown to activate autophagy. For example, ER stress-induced phosphorylation of eIF2α phosphorylation has been shown to upregulate a number of autophagy receptors such as *SQSTM1, NBR1*, and *BNIP3L via* PERK (Deegan et al., 2013). Furthermore, pharmacologic suppression of PERK represses transcriptional upregulation of these autophagy receptors (Deegan et al., 2015). Likewise, eIF2α phosphorylation-mediated by PERK upregulates the conversion of ATG12 and LC3 as a result of expression of polyQ72 aggregates, which is an important phase for the formation of autophagy (Kouroku et al., 2007). Consequently, the PERK-driven Unfolded Protein Response (UPR) regulates autophagy process from induction, to vesicle nucleation, phagophore elongation, and maturation (Deegan et al., 2013). The UPR, which is initiated in the setting of accumulation of misfolded proteins in the ER, is predominantly an adaptive response to the activation of the ISR. UPR protects cancer cells during hypoxia through regulation of the autophagy genes MAP1LC3B and ATG5 (Rouschop et al., 2010) and this is facilitated by PERK phosphorylation of eIF2α. On the other hand, elimination of PERK signaling or expression of mutant eIF2α S51A which cannot be phosphorylated under hypoxia decreases the transcription of *MAP1LC3B* and *ATG5* (Rouschop et al., 2010).

Amino acid deprivation in cancer cells also promotes the phosphorylation of eIF2α *via* GCN2, a protein essential for the activation of autophagy (Ye et al., 2010). GCN2 knockout cells exhibit decreased LC3 expression, whereas cells with mutant the eIF2α S51A cannot induce LC3 processing (Ye et al., 2010). Similarly, phosphorylation of eIF2α at S51 was found to be essential for regulation of autophagy induced by amino acid starvation in yeast and mouse embryonic fibroblasts (MEFs) (Tallóczy et al., 2002).

Critically, ATF4, which is essential for activation of autophagy, is downstream of eIF2α (Kroemer et al., 2010). ATF4 activation in response to stress signals induced by amino acid deprivation upregulates several autophagy genes transcriptionally including *Atg3, Atg5, Atg7, Atg10, Atg12, Atg16, Becn1, Gabarap, Gabarapl2, Map1lc3b,* and *Sqstm1* (B'Chir et al., 2013). In addition, ATF4 medicates REDD1, which represses the activity of mTORC1 under conditions of ER stress or amino acid deprivation, subsequently inducing autophagy (Whitney et al., 2009; Rzymski et al., 2010; B'Chir et al., 2013; Dennis et al., 2013; Deegan et al., 2015). Notably, several autophagy genes may have a varying magnitude of dependence on ATF4 and CHOP signaling and the transcriptional activation of these genes is controlled by the ratio of ATF4 and CHOP proteins that are bound to a particular promoter suggesting that the level of expression of autophagy genes depend on the needs of the cell (B'Chir et al., 2013).

Notably, a conditionally active form of the eIF2α kinase PKR functions upstream of PI3K and activates the Akt/PKB-FRAP/mTOR pathway leading to the phosphorylation of ribosomal protein S6 kinase 1 (S6K1) and eukaryotic initiation factor 4E binding protein 1 (4E-BP1) and that stimulation of PI3K signaling antagonizes the apoptotic and protein synthesis suppressive effects of the conditionally active PKR (Kazemi et al., 2007; Showkat et al., 2014). Furthermore, pharmacologic suppression of proteasome function with antineoplastic agent bortezomib results in depletion of amino acids in the ER required for protein synthesis leading to the activation of the ISR *via* GCN2 stress sensor (Suraweera et al., 2012). These findings suggest that proteasome inhibition has a role on survival signaling by the ISR. Moreover, amino acid depletion mediated by proteasome inhibition also induces autophagy through mTOR in an attempt to restore amino acid homeostasis (Suraweera et al., 2012), whereas, supplementation of essential amino acids depleted by the inhibition of proteasome function inhibition impairs the phosphorylation of eIF2α and down-regulates autophagy (Suraweera et al., 2012). Thus, depletion of amino acids by proteosome inhibition forms a connection between ISR activation and activation of autophagy to sustain cell survival.

Therefore, PERK, which facilitates the phosphorylation of eIF2α and inducing the ISR, acts alongside the different components of the UPR, IRE1, and ATF6 to suppress proteotoxicity induced by misfolded proteins and polypeptides. This is accomplished by upregulating the transcription of genes that stimulate proper protein folding and increase degradation of misfolded or aggregated proteins (Harding et al., 2000; Liu et al., 2000), as such, the cross talk between the various components of

the UPR regulates the cellular outcome (Szegezdi et al., 2006). The ISR-mediated cell survival during ER stress indicates that ATF4 acts as a hub connecting PERK-mediated translational control with IRE1- and ATF6-mediated gene expression (Ron, 2002). Strikingly, the relative extent of PERK and IRE1 signaling appears to be critical for determining the cell fate, with the constant stimulation of PERK leading to activation of programmed cell death (i.e., apoptosis) and extended duration of activation of IRE1 leading to cell survival (Lin et al., 2007; Lin et al., 2009).

AUTOPHAGY AS A MECHANISM OF RESISTANCE TO ANTICANCER THERAPY

Tumor cell activation of autophagy has been described as a potential mechanism of resistance to anticancer therapy. This is supported by several *in vitro* studies demonstrating that further augmentation of autophagic flux results in increased resistance to chemotherapy, resistance that can be overcome with inhibition of autophagy (Sotelo et al., 2006; Carew et al., 2007; Firat et al., 2012; Hu et al., 2012; Zou et al., 2012). In pancreatic cancer, inducing autophagy through upregulation of receptor for advanced glycation end products (RAGE) increases resistance to chemotherapy *in vivo* (Kang et al., 2010). Although further studies are necessary to elucidate precise mechanisms of resistance, autophagy-induced activation of several common cell signaling pathways have been described. These include epidermal growth factor receptor (EGFR), PI3K/AKT/mTOR, MAPK, and p53 pathways. Han et al. demonstrated that inhibiting EGFR with either gefitinib or erlotinib not only activates autophagy but also serves as a cytoprotective mechanism in human lung cancer. They further combined these tyrosine kinase inhibitors with various autophagy inhibitors or siRNAs targeting ATG5/7 and demonstrated enhanced cell killing (Han et al., 2011). As described earlier in this review, inhibition of the MAPK pathway also leads to up-regulation of autophagy and has been proposed as a mechanism of drug resistance. Furthermore, PI3K/mTOR inhibitors have been shown to induce protective autophagy in malignant peripheral nerve sheath tumor (MPNST) cells; however, pretreatment with chloroquine or bafilomycin consistently reverses this, potentially representing a treatment strategy in this difficult to treat sarcoma subtype (Ghadimi et al., 2012). The reciprocal interaction between autophagy and p53 may also have important implications for cancer therapy. Autophagic flux increases suppression of p53 while p53 activates autophagy (White, 2016). Autophagy inhibition alone is unlikely sufficient to overcome autophagy-induced resistance to anticancer therapy, however, a deeper understanding of autophagy in this setting may lead to new therapeutic approaches.

ONC212, AUTOPHAGY AND PDAC

Our work unraveling cell death pathways (Carneiro and El-Deiry, 2020) as an approach to understand and therapeutically target human cancer led us to discover TRAIL receptor DR5 as a p53 target gene (Wu et al., 1997). We discovered that the Tumor Necrosis Factor-Related Apoptosis-Inducing Ligand (TRAIL), the ligand for DR5 in the extrinsic cell death pathway is also a p53-regulated gene (Kuribayashi et al., 2008). We performed screening for TRAIL-inducing compounds in 2007 and discovered TRAIL-Inducing Compound #10 (TIC10), later published in 2013 (Allen et al., 2013). TIC10 activated the TRAIL gene in a p53-independent manner that involved dual inhibition of ERK and Akt and nuclear translocation of Foxo3a to bind and transactivate the TRAIL gene (Allen et al., 2013). TIC10 was advanced to clinical trials as ONC201 (Stein et al., 2017). We discovered that ONC201/TIC10 activates the integrated stress response (ISR) through kinases HRI and PKR leading to eIF2-alpha phosphorylation, activation of ATF4, CHOP, and DR5 (Kline et al., 2016). We found that ONC201 targets cancer stem cells (Prabhu et al., 2015) and activates an immune response involving natural killer (NK) cells (Wagner et al., 2018). We collaborated with Provid and Oncoceutics to synthesize and test ONC201/TIC10 analogues and uncovered ONC212 as a potent analogue (Wagner et al., 2017).

ONC212 appeared to have efficacy against PDAC cells and xenografted tumors *in vivo* (Lev et al., 2017). ONC212 was found to target the integrated stress response and activate the TRAIL pathway. Moreover, the compound appears to act through a mechanism involving mitochondrial caseinolytic protease ClpP which targets degradation of multiple mitochondrial proteins including respiratory chain proteins involved in oxidative phosphorylation (Ferrarini, 2021). The mitochondrial stress signals the integrated tress response leading to cell death and also inhibits autophagy in pancreatic cancer (Ferrarini, 2021). As efforts are underway to bring ONC212 to clinical trials, we have been exploring combinations with ONC212 in pancreatic cancer (Jhaveri, 2020; Raufi, 2021). In particular, ONC212 appears to synergize with MEK inhibitors against PDAC cell lines, in part through effects involving autophagy inhibition (Raufi, 2021).

AUTOPHAGY, IMMUNE CELL FUNCTION AND RESPONSE TO IMMUNE CHECKPOINT BLOCKADE

PDAC is characterized by a unique and complex tumor immune microenvironment comprised of distinct stromal and tumor compartments. The stromal compartment contains cancer associated fibroblasts (CAFs), as well as both innate and adaptive immune cells. Autophagy is necessary for immune cell function, differentiation, and survival and therefore a thorough understanding of the impact of autophagy modulating agents on these cells is essential to developing new therapies.

Autophagy is required for pluripotent hematopoietic stem cell (HSC) survival and differentiation (Mortensen et al., 2011). HSCs give rise to monocytes, which differentiate into macrophages with phagocytic and cytokine production capabilities. Autophagy has been shown to be essential for monocyte survival as well as their differentiation into macrophages (Jacquel et al., 2012; Zhang et al., 2012). In mature macrophages, autophagy plays a role

in LC3-mediated phagocytosis, a form of non-canonical autophagy that promotes immune tolerance (Cunha et al., 2018). The breakdown of biomolecules during autophagy also mediates antigen presentation by dendritic cells (Li et al., 2012; Germic et al., 2019). Interestingly, autophagy inhibition-mediated tumor regression can be hindered by macrophage depletion in an autochthonous mouse model of PDAC, suggesting an essential role of the innate immune system in tumor cell killing (Yang et al., 2018).

Autophagy is also essential for adaptive immune cell function, as it supports T cell renewal, differentiation, and homeostasis. In the thymus, negative selection of $CD4^+$ T cells is at least partially directed by autophagy and the transition of $CD4^-CD8^-$cells to $CD4^+CD8^+$ cells is associated with maximum activation of autophagy, though its explicit role in this transition is incompletely understood. Autophagy also mediates T cell survival and differentiation outside the thymus. Upon autophagy inhibition, T cells accumulate organelles and shift their metabolism from oxidative phosphorylation to glycolysis. Cells that generate energy predominantly through oxidative phosphorylation [memory T cells, T regulatory cells (T-regs)] are particularly vulnerable to autophagy inhibition. The vulnerability of T-regs to autophagy inhibition is further enhanced due to their dependence on high levels of autophagy (Clarke and Simon, 2019). However, autophagy inhibition also degrades extracellular ATP and attracts T-regs. This mechanism likely plays an important role *in vivo*, as triggering autophagy in lung tumor-bearing mice improved the efficacy of chemotherapy and this was at least partially mediated by a reduction of tumor-infiltrating T-regs (Pietrocola et al., 2016).

Interest in immune checkpoint blockade (ICB) has increased in recent years following clinical success in treating various malignancies. Single agent ICB has had little to no impact on outcomes in patients with PDAC. This may be partly due to the immunosuppressive components of the tumor immune microenvironment therefore there is much interest in identifying combination treatments that improve responses to ICB (Bian and Almhanna, 2021). A recent compelling study reported that autophagy promotes immune evasion of PDAC *via* MHC-I degradation, and that autophagy inhibition and ICB synergize in mice to reduce tumor burden (Yamamoto et al., 2020). Similar observations in other cancer types support these findings. For example, mice with metastatic liver tumors experience an enhanced response to high dose IL-2 when combined with an autophagy inhibitor (Liang et al., 2012), and impairment of autophagy in mice with colon or breast tumors improved response to ICB therapy (Young et al., 2020). Together, these findings suggest a role of autophagy in limiting the response of immunotherapies such as ICB across cancer types and provide an exciting new direction for investigating combination treatments for PDAC and other cancers.

PRECLINICAL STUDIES IN PDAC

The relationship between autophagy and tumor progression is complex. First, autophagy has been shown to suppress cancer initiation in many models. As described above, Rosenthal et al. showed that genetically modified mice with loss of autophagy genes Atg5 or Atg7 showed increased benign pancreatic cell tumor formation, but with lack of progression to malignant disease. Other genetically-modified mouse models have shown similar results in liver (Takamura et al., 2011) and lung (Strohecker et al., 2013) tumors. Additionally, there is evidence that once the growth of a malignant tumor has been initiated, autophagy promotes tumor progression. Degenhardt et al. explored the impact of autophagy on the tumor immune microenvironment and showed that autophagic activity is increased in the hypoxic tumor microenvironment, which ultimately leads to increased degradation of waste products resulting in decreased inflammation and increased tumor cell survival. This was further supported by Guo et al. who found that autophagy knock-out xenografts in a KRAS-activated mouse model showed reduced tumor growth and also exhibited an increased immune response, leading to the development of immune-driven pathologies, such as pneumonia (Guo et al., 2013). Levy et al. explored the potential role of this hyperactivated immune response in reduced tumor induction and growth in an autophagy knock-out model, and postulated that reduced induced autophagy in T cells may lead to more T cell-induced tumor cell killing (Mulcahy Levy and Thorburn, 2020). Lastly, evidence suggesting that autophagy is important for malignant cell growth can also be found at the genetic level. Transcriptome analysis has shown that core autophagy proteins highly conserved in cancer (Lebovitz et al., 2015) and that many of the transcription factors that promote autophagy are oncogenes (Roczniak-Ferguson et al., 2012).

Early pre-clinical investigations focused on the use of hydroxychloroquine and chloroquine, which act through inhibiting lysosomes, which in part leads to degradation of autophagosomes and endosomes (Dolgin, 2019). PDAC is an attractive solid tumor for autophagy inhibition, as autophagy is known to be increased in pancreatic cancer, and has been shown to correlate to poorer patient outcomes (Fujii et al., 2008). Friboes et al. showed that treatment of a malignant pancreatic cancer line with chloroquine lead to decreased cell viability and decreased levels of autophagy (Frieboes et al., 2014). Yang et al. showed decreased tumor progression in an *in vitro* model when cells grown from pancreatic cancer tumors grown in genetically modified mice were treated with chloroquine (Yang and Kimmelman, 2014). Because the mechanism of action of chloroquine and hydroxychloroquine is targeted at lysosomes, and therefore not specific to the inhibition of autophagy, it is difficult to determine to what degree autophagy inhibition actually contributes to their overall mechanism of action in cancer therapy. In 2014 Maes et al. examined the use of hydroxychloroquine and chloroquine against melanoma tumor cells in an *in vivo* model and showed that treatment with these drugs leads to a normalization of the organization of tumor vessel and function, thereby decreasing hypoxia and increasing delivery of other drugs, which could certainly contribute to their antitumor effect (Maes et al., 2014). Another small molecule target for autophagy inhibition is the molecule of the PI3K class III that is known to be important in the promotion of autophagy,

and has been shown to be effective at blocking autophagy *in vivo* (Dowdle et al., 2014). Ronan et al. developed an inhibitor specific to this molecule that was shown to act synergistically with everolimus in lung and renal cancer *in vitro* (Ronan et al., 2014), and Honda et al. discovered an inhibitor shown to be effective against colorectal cancer as monotherapy in an *in vivo* model (Honda et al., 2016). This molecule also has issues with specificity. In addition to contributing to the activation of autophagosomes, it is also involved in endocytic and vesicular function, and therefore has produced concern for toxic off-target effects (Dolgin, 2019). Alternatively, many investigators are focusing in on the autophagy activating kinase ULK1. Lazarus et al. performed a structural activity relationship analysis of ULK1 in order to identify binding sites of the molecule most ideal structure of a drug to bind to and inhibit these sites (Lazarus et al., 2015; Lazarus and Shokat, 2015). Egan et al. went further to discover a specific substrate that exhibits potent and highly selective inhibition of ULK1 in an *in vitro* model, and showed that it induced increased cell death in glioblastoma and lung cancer cells when used in concert with mTOR inhibition (Tang et al., 2017).

As autophagy has been shown to be important in both blocking the initiation of tumor formation as well as potentiating the spread of tumors when growth has already been initiated, there has been interest in studying autophagy-activating drugs to treat PDAC. mTOR inhibitors have therefore been studied in several but have been shown to only lead to a cytostatic effect. In a review from 2019, Tian et al. (2019) postulate that this result is due to the ability of mTOR inhibitors to lead to optimization of the tumor microenvironment, and that this could be inhibited with the addition of an autophagy inhibitor, which could explain synergy seen in pre-clinical models that have examined dual therapy with mTOR inhibitors and autophagy inhibitors, such as the results that Ronan et al. saw when combining everolimus with and VSP34 inhibitor.

As previously mentioned, ONC212 is a novel potent imipridone analogue with preclinical activity against PDAC in multiple *in vivo* models, biochemical evidence of autophagy inhibition, and synergistic activity when combined with MEK inhibitors (Lev et al., 2017; Wagner et al., 2017; Ferrarini, 2021; Raufi, 2021). As p53 mutations are common in human cancer, including PDAC, we have pursued therapeutic targeting of tumors with mutant p53 (Wang et al., 2006; Bassett et al., 2008; Hernández Borrero and El-Deiry, 2021). We previously reported that a p53 pathway restoring small molecule, CB002, induces morphological changes of autophagy and modulates LC3B expression in a manner that requires pro-apoptotic Noxa induction (Richardson et al., 2017; Hernandez-Borrero et al., 2018). Our recent results suggest that in addition to partial restoration of a p53 transcriptome, CB002 and other xanthine analogues impact on an S-phase cell cycle checkpoint (Hernandez Borrero et al., 2021). These small molecular weight compounds and others such as PG3-Oc and NSC59984 that restore p53 pathway responses merit further investigation as potential therapeutics in PDAC (Zhang et al., 2015; Prabhu et al., 2016; Zhang, 2017a; Zhang, 2017b; Zhang, 2018; Hernandez Borrero et al., 2021; Tian et al., 2021).

Mutations of the oncoprotein KRAS are very common in pancreatic cancer, and therefore there has always been a great deal of interest in targeting the MAPK pathway in the treatment of pancreatic cancer, but while there have been some promising pre-clinical results, KRAS inhibitors have shown to be relatively ineffective at treating pancreatic cancer in humans. Kinsey et al. established that inhibition of the MAPK pathway also leads to up-regulation of autophagy, which has been postulated as serving as a mechanism of drug resistance (Kinsey et al., 2019). Therefore, dual inhibition of the MAPK pathway and autophagy could theoretically lead to synergistic cell death. The combination proved synergistic in PDAC cell lines *in vitro* as well as in patient-derived xenografts grown in a murine model, as well as in melanoma and colorectal cancer models. Bryant et al. also examined the relationship between the MAPK pathway and autophagy and showed not only that dual inhibition of these pathways leads to increased cell death in PDAC cell lines, but also shed light on the mechanism of this synergy (Bryant et al., 2019) by showing that inhibition of two key members of the MAPK pathway—KRAS and ERK—lead to decreased metabolic functions, and would therefore lead to an increased dependence on autophagy to avoid cell death.

In summary, there is a breadth of literature examining the impact of autophagy on cancer initiation and growth. These studies have shown that the relationship between tumorigenesis and metastasis is complex, providing both pro- and anti-tumor effects. With this knowledge, various researchers have focused on both the inhibition and activation of autophagy. Harnessing the anti-tumor effect of autophagy inhibition has been attempted both *via* the use of existing drugs with broad mechanisms of action, such as chloroquine or hydroxychloroquine, as well as through the development of new targets to inhibit autophagy, such as VSP34 and ULK1 inhibitors. Likewise, other researchers have focused on promoters of autophagy, and have shown good effect with dual therapy with autophagy inhibitors. Lastly, it has been shown that dual targeting of the MAP kinase pathway and the autophagy pathway—especially in cancer with a high prevalence of KRAS mutation, such as pancreatic cancer—may result in increased tumor killing by inhibitors of the MAP kinase pathway by blocking autophagy, which could serve as a key mechanism of resistance.

A diagrammatic representation depicting modulation of the autophagy pathway by small molecules is shown in **Figure 2**. A list of compounds with activity as autophagy inhibitors is shown in **Table 1**.

Clinical Trials in PDAC

Various modulators of autophagy have been tested either alone or in combination with other agents in clinical trials for patients with PDAC. Chloroquine, and its less toxic derivative, hydroxychloroquine, are the among the best studied inhibitors of autophagy.

Hydroxychloroquine has been evaluated as a single agent in a phase II study published in 2014. In this study, 20 patients with previously treated metastatic PDAC received twice daily hydroxychloroquine, either 400 mg or 600 mg. Unfortunately,

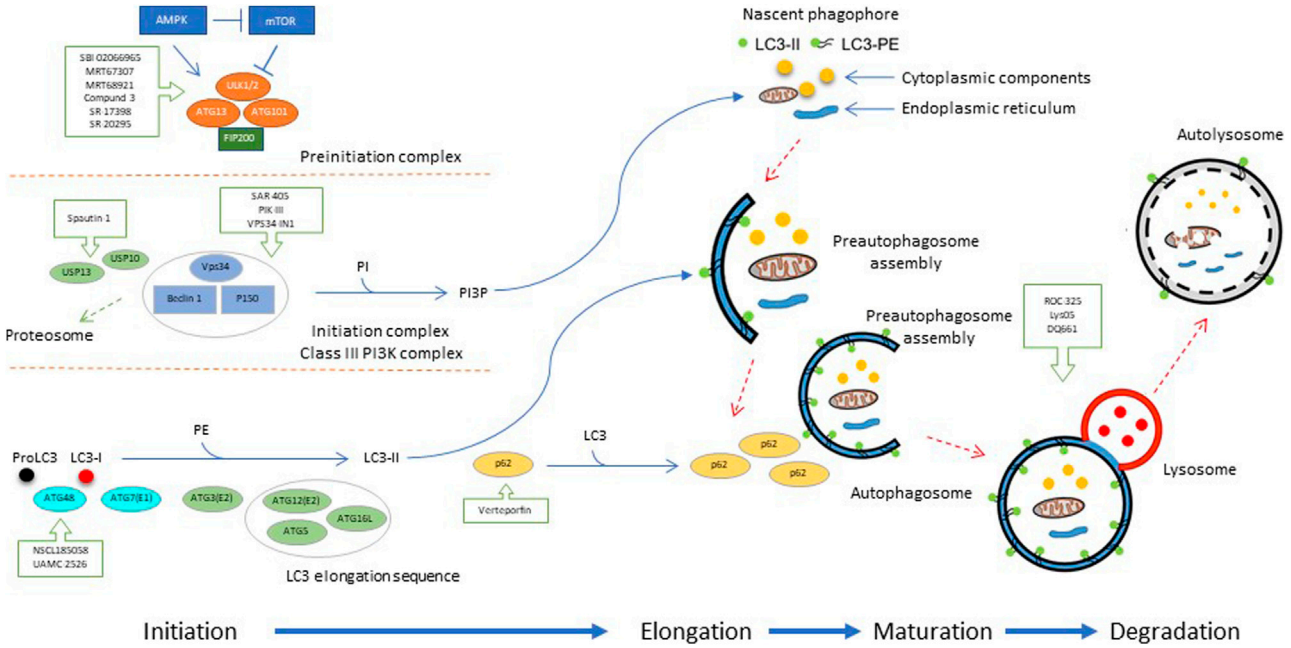

FIGURE 2 | Modulation of multiple stages of autophagy process by small molecules. As illustrated in the schema, autophagy is a process where cells recycle proteins and other essential substrates and macromolecules including whole organelles such as mitochondria by forming an autophagosome. Autophagosomes confine and distribute their cargo for a highly regulated autophagy process which involves the fusion of autophagosomes with lysosomes. Therefore, each of the key complexes formed throughout the autophagy process involving preinitiation, initiation, elongation, maturation and degradation steps provide opportunities for therapeutic interventions by the small molecules that can modulate autophagic pathways. Under nutrient deprivation, mTOR is inactivated and AMPK is activated leading to phosphorylation of negative and positive regulatory sites on ULK1/2 within the preinitiation complex which subsequently activates the initiation complex or the class III PI-IIIK complex *via* phosphorylation of VPS34 and Beclin-1. The initiation complex involves the production of PI3P from the precursor PI needed for nucleation of the isolation of the autophagosome initiation membrane. Cellular concentrations of the initiation complex are regulated by a ubiquitination cascade which is regulated by USP10 and USP13 deubiquitination peptidases. Expansion of nascent precursor vesicles depends on the autophagosome LC3 protein which then conjugates with PE forming LC3-II protein which is derived from the LC3 elongation sequence of modifying enzymes. LC3-I is generated by proteolytic cleavage of proLC3 by the ATG4B. LC3-I is subsequently conjugated with lipids by a series of conjugating enzymes to form the LC3-II which then forms a stable complex with the membranes of autophagosomes. The p62 scaffold protein also plays an important role in the trafficking of proteins to the autophagosome by stably binding to the LC3-II protein. p62 also plays a role in apoptosis pathways. **Abbreviations:** mTOR, mammalian target of rapamycin; AMPK, 5′-AMP-activated protein kinase; ULK1/2, Unc-51-like autophagy activating kinase 1/2; VPS34, vacuolar protein sorting protein 34; PI3P, phosphatidylinositol-3-phosphate, PI: phosphatidylinositol, USP10 and USP13: deubiquitination peptidases, LC3: microtubule-associated protein 1A/1B light chain 3B, PE, phosphatidylethanolamine; LC3-II, conjugated form of the LC3 protein, ATG4B: protease autophagy-related protein 4B, p62, p62 is a receptor for cargo destined to be degraded by autophagy. Adapted from (Limpert et al., 2018).

no patient demonstrated a response (Wolpin et al., 2014). In 2017, the results of a phase I trial combining chloroquine with standard of care gemcitabine were published. Although three out of nine enrolled patients had partial responses and a median overall survival (OS) of 7.6 months was reported, this did not outperform historical data with gemcitabine alone (Samaras et al., 2017). More recently, the results of a randomized phase II study of the combination of standard of care gemcitabine and nab-paclitaxel with or without hydroxychloroquine were published in 2019. In total, 112 patients with previously untreated metastatic or advanced PDAC were enrolled and were randomized 1:1. The primary endpoint was OS at 1 year. The addition of hydroxychloroquine resulted in a 12 months OS rate of 41% (95% CI, 27–53%) compared with 49% (95% CI, 35–61%) with chemotherapy alone. Furthermore, the authors reported no increase in progression free survival and there was a higher rate of toxicity, visual and gastrointestinal, in the hydroxychloroquine treatment group. Interestingly, the authors did report an improvement in overall response rate, 38.2% (n = 21) in the hydroxychloroquine group versus 21.1% (n = 12) in the non-hydroxychloroquine group, which was statically significant (p = 0.047) (Karasic et al., 2019).

Several studies have also investigated the role of autophagy promoting agents. The oral mTOR inhibitor everolimus has been studied in a phase II study in patients with gemcitabine-refractory metastatic pancreatic cancer. No complete or partial treatment responses were noted in this trial and the median progression-free survival and OS were 1.8 and 4.5 months, respectively. One patient (3%) had a biochemical response, defined as greater than or equal to 50% reduction in serum CA19-9 (Wolpin et al., 2009). Additional studies investigating single agent mTOR inhibitors have also been disappointing (Javle et al., 2010).

There are a number of ongoing clinical trials investigating novel autophagy-modulating agents and novel combinations of agents. For example, one trial is currently investigating newer combinations of chemotherapy (e.g., paclitaxel protein bound plus gemcitabine plus cisplatin) together with hydrochloroquine (NCT04669197). Hydroxychloroquine is also being combined

TABLE 1 | Selected compounds that modulate different phases of autophagy. Adapted from (Limpert et al., 2018).

Compound	Target	Novel features	Potency/Selectivity	Refs
SBI-0206965	ULK1 and ULK2	Selective inhibitor Pyrimidine scaffold Suppresses ULK1 downstream phosphorylation of VPS34 and Beclin-1 Induces apoptosis in NSCLC cells by destabilizing Bcl2 and Bclxl	ULK1: IC_{50} of 108 nM; ULK2: IC_{50} of 711 nM	Egan et al. (2015); Tang et al. (2017)
MRT67307	ULK1 and ULK2	*In vitro* inhibitor Pyrimidine scaffold Also targets TBK1 and AMPK-related kinases	ULK1: IC_{50} of 45 nM; ULK2: IC_{50} of 38 nM	Petherick et al. (2015)
MRT68921	ULK1 and ULK2	*In vitro* inhibitor Pyrimidine scaffold Also targets TBK1 and AMPK-related kinases	ULK1: IC_{50} of 2.9 nM; ULK2: IC_{50} of 1.1 nM	Petherick et al. (2015)
Compound 1	ULK1 and ULK2	Inhibitor Pyrazole amino quinazoline scaffold Crystal structure obtained with ULK1	ULK1: IC_{50} of 5.3 nM; ULK2: IC_{50} of 13 nM; PDPK1: IC_{50} of 420 nM	Lazarus and Shokat, (2015)
BX-795	PDK1	Inhibitor of PDK1 Also shown to inhibit ULK1, ULK2 and IKKε Pyrimidine scaffold	ULK1: IC_{50} of 87 nM; ULK2: IC_{50} of 310 nM; PDPK1: IC_{50} of 65 nM	Lazarus and Shokat, (2015)
Compound 3	ULK1	Inhibitor Pyrimidine scaffold Crystal structure obtained with ULK1	ULK1: IC_{50} of 120 nM; ULK2: IC_{50} of 360 nM; PDPK1: IC_{50} of 710 nM	Lazarus and Shokat, (2015)
SR-17398	ULK1	Indazole-derived inhibitor Mixture of four stereoisomers	ULK1: IC_{50} of 22 μM	Wood et al. (2017)
SR-20295	ULK1	Indazole-derived inhibitor	ULK1: IC_{50} of 45 nM *In vitro* microsome stability half-life of 225 min	Wood et al. (2017)
NSC185058	ATG4B	Inhibitor/antagonist Targets autophagosome formation, and suppresses activation and lipidation of LC3	ATG4B IC_{50} of 51 μM	Akin et al. (2014); Huang et al. (2017)
UAMC-2526	ATG4B	Inhibitor Benzotropolone scaffold Targets autophagosome formation Inhibits starvation-induced autophagy *in vivo*	Plasma half-life of 126 min, and 70% metabolization after 30 min	Kurdi et al. (2017)
SAR405	VPS34	Selective inhibitor Tetrahydropyrimido-pyrimidinone scaffold Dose-dependent inhibition Targets autophagosome formation Crystal structure obtained with VPS34	VPS34: IC_{50} of 1.2 nM and K_D of 1.5 nM	Ronan et al. (2014); Young et al. (2015); Hong et al. (2017)
PIK-III	VPS34	Selective and orally bioavailable inhibitor of VPS34 Pyrimidine scaffold Inhibits autophagy and LC3 lipidation	VPS34: IC_{50} of 18 nM; mTOR: IC_{50} of >9.1 μM	Dowdle et al. (2014); Honda et al. (2016)
VPS34-IN1	VPS34	Selective cell-permeable inhibitor Pyrimidine scaffold Selectively inhibits class III PI3K	VPS34: IC_{50} of 25 nM *in vitro*	Bago et al. (2014)
Verteporfin	ATG	Concentration-dependent inhibition Benzoporphyrin scaffold Targets autophagosome formation and accumulation when co-treated with CQ Targets p62: prevents autophagy-induced degradation of p62 in nutrient-deprived conditions	CQ-verteporfin EGFP-LC3 cell IC_{50} of 1 μM Plasma concentrations after single intraperitoneal dose of 45 mg/kg: 122 μM at 2 h, 3.9 μM at 24 h	Donohue et al. (2011); Donohue et al. (2013); Donohue et al. (2014)
Spautin-1	ATG	Autophagy inhibitor Fluoroquinazoline scaffold USP10 and USP13 inhibitor: promotes ubiquitination and decreases levels of Beclin-1 Targets autophagosome formation when co-treated with imatinib mesylate Spautin-1 alone has no activity	Co-treatment with Spautin-1 improved imatinib mesylate-induced cytotoxicity of K562 leukemia cells: IC_{50} from 1.03 to 0.45 μM	Shao et al. (2014)
ROC-325	ATG	Orally bioavailable inhibitor Chloroquinoline scaffold Targets lysosomal function and autophagosome accumulation ~10-fold more potent than HCQ Exhibits significant anticancer activity against range of tumor types	Acute myeloid leukemia cell IC_{50} range: 0.7–2.2 μM; A498 renal cell: IC_{50} of 4.9 μM	Nawrocki et al. (2016); Carew et al. (2017); Carew and Nawrocki, (2017)

(Continued on following page)

TABLE 1 | (*Continued*) Selected compounds that modulate different phases of autophagy. Adapted from (Limpert et al., 2018).

Compound	Target	Novel features	Potency/Selectivity	Refs
Lys05	ATG	Autophagy inhibitor Dimeric chloroquinoline scaffold Targets lysosomal function	LN229 (glioma), 1205Lu (melanoma), c8161 (melanoma), HT-29 (colon) cell: IC_{50} range 4–8 μM	Amaravadi and Winkler, (2012); McAfee et al. (2012)
DQ661	ATG	Inhibitor of autophagy and mTOR by targeting PPT1 Dimeric quinacrine scaffold *In vivo* activity against melanoma, pancreatic cancer, and colorectal cancer tumor growth in mice Can be used in combination with chemotherapy	Estimated A375P melanoma cell IC_{50} of ~0.1 μM	Rebecca et al. (2017); Nicastri et al. (2018)

TABLE 2 | Clinical trials of autophagy inhibitors of pancreatic cancer. Source: clinicaltrials.gov.

Title	Status	Interventions	Url	NCT number
A phase I/II/Pharmacodynamic Study of Hydroxychloroquine in Combination With Gemcitabine/Abraxane to Inhibit Autophagy in Pancreatic Cancer	Active, not recruiting	Drug: Hydroxychloroquine (HCQ)|Drug: Gemcitabine|Drug: Abraxane	https://clinicaltrials.gov/ct2/show/NCT01506973	NCT01506973
LY3214996$^{+/-}$HCQ in Pancreatic Cancer	Recruiting	Drug: Hydroxychloroquine Sulfate|Drug: LY3214996	https://clinicaltrials.gov/ct2/show/NCT04386057	NCT04386057
Binimetinib and Hydroxychloroquine in Treating Patients With KRAS Mutant Metastatic Pancreatic Cancer	Recruiting	Drug: binimetinib|Drug: Hydroxychloroquine	https://clinicaltrials.gov/ct2/show/NCT04132505	NCT04132505
Paricalcitol and Hydroxychloroquine in Combination With Gemcitabine and Nab-Paclitaxel for the Treatment of Advanced or Metastatic Pancreatic Cancer	Recruiting	Drug: Gemcitabine|Drug: Hydroxychloroquine| Drug: Nab-paclitaxel|Drug: Paricalcitol	https://clinicaltrials.gov/ct2/show/NCT04524702	NCT04524702
Randomized phase II Trial of Pre-Operative Gemcitabine and Nab Paclitacel With or With Out Hydroxychloroquine	Completed	Drug: gemcitabine|Drug: abraxane|Drug: hydroxychloroquine	https://clinicaltrials.gov/ct2/show/NCT01978184	NCT01978184
Short Course Radiation Therapy With Proton or Photon Beam Capecitabine and Hydroxychloroquine for Resectable Pancreatic Cancer	Active, not recruiting	Drug: Capecitabine| Drug: Hydroxychloroquine| Radiation: Proton or Photon Radiation Therapy	https://clinicaltrials.gov/ct2/show/NCT01494155	NCT01494155
Study of Combination Therapy With the MEK Inhibitor, cobimetinib, Immune Checkpoint Blockade, atezolizumab, and the AUTOphagy Inhibitor, Hydroxychloroquine in KRAS-mutated Advanced Malignancies	Recruiting	Drug: cobimetinib| Drug: Hydroxychloroquine|Drug: atezolizumab| Drug: Hydroxychloroquine| Drug: atezolizumab	https://clinicaltrials.gov/ct2/show/NCT04214418	NCT04214418
Trametinib and Hydroxychloroquine in Treating Patients With Pancreatic Cancer	Recruiting	Drug: Hydroxychloroquine|Drug: trametinib	https://clinicaltrials.gov/ct2/show/NCT03825289	NCT03825289
Phase II Study of Paclitaxel Protein Bound + Gemcitabine + Cisplatin + Hydrochloroquine as Treatment in Untreated Pancreas Cancer	Recruiting	Drug: Paclitaxel protein bound|Drug: Gemcitabine| Drug: Cisplatin|Drug: Hydroxychloroquine	https://clinicaltrials.gov/ct2/show/NCT04669197	NCT04669197

with the vitamin D analogue, paricalcitol, and chemotherapy in a phase II trial (NCT04524702).

As discussed above, there is also interest in combining autophagy inhibitors with agents targeting the MAPK pathway. For example, two ongoing trials with two different MEK inhibitors, trametinib or binimetinib, combined with hydroxychloroquine are currently being tested in patients with PDAC (NCT03825289, NCT04132505). LY3214996, an ERK inhibitor, is currently being tested alone and in combination with hydroxychloroquine in a small phase two study (NCT04386057). The combination of the MEK inhibitor cobimetinib and hydroxychloroquine are also being tested in combination with immune checkpoint blockade in a phase I/II trial KRAS-mutated PDAC (NCT04214418).

A listing of clinical trials employing autophagy inhibitors is listed in **Table 2**.

DISCUSSION

Recent advances in our understanding of autophagy and evidence suggesting that it may be necessary for PDAC tumorigenesis,

maintenance, and metastasis has rekindled enthusiasm to target this process for therapeutic benefit. Development of effective therapies has been slow, in part due to the tremendous complexity and dynamic roles autophagy plays in both cell survival and cell death. No agent to date has demonstrated clear clinical benefit but ongoing trials will hopefully shed light on biological effects and emerging resistance pathways.

Traditionally, autophagy has been described as an adaptive mechanism through which cells facing stress or starvation are able to maintain viability. The role of autophagy in tumorigenesis is less clear, but we do know that established PDAC tumors rely on chronically elevated levels of basal autophagy. Furthermore, there is evidence that autophagy may also be required for metastasis. The unique PDAC tumor immune microenvironment represents a hypoxic, acidic, nutrient-poor setting in which autophagy has been repeatedly demonstrated to be upregulated. Adding further complexity is the fact that autophagy also plays a role in immune cell function and therefore, it is possible that modulating this process may impact immune response to cancer.

Several potential predictive biomarkers, such as ATG5 and LC3-II, are currently being studied and may help to ensure adequate dosing of autophagy targeting agents. Incorporation of biomarker studies into future clinical trials will be necessary to confirm utility.

With the identification of novel autophagy pathway components and the development of more specific pharmacologic agents, future trials will likely hold more promise. Recent preclinical data supporting combinatory therapy with MAPK pathway and autophagy inhibition with chloroquine has led to the activation of multiple clinical trials with these agents. Additional novel agents with preclinical activity such as ONC212, with the ability to inhibit autophagy, may be well-suited for further study in combination with MEK inhibitors or other agents in pancreatic cancer. Therapeutics targeting other molecular drivers in PDAC, such as mutant p53, may have future use in this disease. Further investigation with improved preclinical models and biomarker directed clinical trials is warranted to further our understanding of autophagy modulation and ultimately improve outcomes in PDAC.

DATA AVAILABILITY STATEMENT

The original contributions presented in the study are included in the article/Supplementary Material, further inquiries can be directed to the corresponding authors.

AUTHOR CONTRIBUTIONS

All authors listed have made a substantial, direct, and intellectual contribution to the work and approved it for publication.

FUNDING

WE-D. is an American Cancer Society Research Professor and is supported by the Mencoff Family University Professorship at Brown University. This work was supported by an NIH grant (CA173453), a Warren Alpert Foundation grant and by the Teymour Alireza P′98, P′00 Family Cancer Research Fund established by the Alireza Family. The contents of this manuscript are solely the responsibility of the authors and do not necessarily represent the official views of the National Cancer Institute, the National Institutes of Health, the Warren Alpert Foundation, or the American Cancer Society.

ACKNOWLEDGMENTS

Figure 1 created with BioRender.com.

REFERENCES

Akin, D., Wang, S. K., Habibzadegah-Tari, P., Law, B., Ostrov, D., Li, M., et al. (2014). A Novel ATG4B Antagonist Inhibits Autophagy and Has a Negative Impact on Osteosarcoma Tumors. *Autophagy* 10 (11), 2021–2035. doi:10.4161/auto.32229

Allen, J. E., Krigsfeld, G., Mayes, P. A., Patel, L., Dicker, D. T., Patel, A. S., et al. (2013). Dual Inactivation of Akt and ERK by TIC10 Signals Foxo3a Nuclear Translocation, TRAIL Gene Induction, and Potent Antitumor Effects. *Sci. Transl. Med.* 5 (171), 171ra17. doi:10.1126/scitranslmed.3004828

Amaravadi, R. K., and Winkler, J. D. (2012). Lys05: a New Lysosomal Autophagy Inhibitor. *Autophagy* 8 (9), 1383–1384. doi:10.4161/auto.20958

B'Chir, W., Maurin, A. C., Carraro, V., Averous, J., Jousse, C., Muranishi, Y., et al. (2013). The eIF2α/ATF4 Pathway Is Essential for Stress-Induced Autophagy Gene Expression. *Nucleic Acids Res.* 41 (16), 7683–7699. doi:10.1093/nar/gkt563

Bago, R., Malik, N., Munson, M. J., Prescott, A. R., Davies, P., Sommer, E., et al. (2014). Characterization of VPS34-IN1, a Selective Inhibitor of Vps34, Reveals that the Phosphatidylinositol 3-Phosphate-Binding SGK3 Protein Kinase Is a Downstream Target of Class III Phosphoinositide 3-kinase. *Biochem. J.* 463 (3), 413–427. doi:10.1042/BJ20140889

Bassett, E. A., Wang, W., Rastinejad, F., and El-Deiry, W. S. (2008). Structural and Functional Basis for Therapeutic Modulation of P53 Signaling. *Clin. Cancer Res.* 14 (20), 6376–6386. doi:10.1158/1078-0432.CCR-08-1526

Bellot, G., Garcia-Medina, R., Gounon, P., Chiche, J., Roux, D., Pouysségur, J., et al. (2009). Hypoxia-induced Autophagy Is Mediated through Hypoxia-Inducible Factor Induction of BNIP3 and BNIP3L via Their BH3 Domains. *Mol. Cel. Biol.* 29 (10), 2570–2581. doi:10.1128/MCB.00166-09

Bian, J., and Almhanna, K. (2021). Pancreatic Cancer and Immune Checkpoint Inhibitors-Still a Long Way to Go. *Transl. Gastroenterol. Hepatol.* 6, 6. doi:10.21037/tgh.2020.04.03

Bryant, K. L., Stalnecker, C. A., Zeitouni, D., Klomp, J. E., Peng, S., Tikunov, A. P., et al. (2019). Combination of ERK and Autophagy Inhibition as a Treatment Approach for Pancreatic Cancer. *Nat. Med.* 25 (4), 628–640. doi:10.1038/s41591-019-0368-8

Carew, J. S., Espitia, C. M., Zhao, W., Han, Y., Visconte, V., Phillips, J., et al. (2017). Disruption of Autophagic Degradation with ROC-325 Antagonizes Renal Cell Carcinoma Pathogenesis. *Clin. Cancer Res.* 23 (11), 2869–2879. doi:10.1158/1078-0432.CCR-16-1742

Carew, J. S., and Nawrocki, S. T. (2017). Drain the Lysosome: Development of the Novel Orally Available Autophagy Inhibitor ROC-325. *Autophagy* 13 (4), 765–766. doi:10.1080/15548627.2017.1280222

Carew, J. S., Nawrocki, S. T., Kahue, C. N., Zhang, H., Yang, C., Chung, L., et al. (2007). Targeting Autophagy Augments the Anticancer Activity of the Histone

Deacetylase Inhibitor SAHA to Overcome Bcr-Abl-Mediated Drug Resistance. *Blood* 110 (1), 313–322. doi:10.1182/blood-2006-10-050260

Carneiro, B. A., and El-Deiry, W. S. (2020). Targeting Apoptosis in Cancer Therapy. *Nat. Rev. Clin. Oncol.* 17 (7), 395–417. doi:10.1038/s41571-020-0341-y

Chen, S., and Sang, N. (2016). Hypoxia-Inducible Factor-1: A Critical Player in the Survival Strategy of Stressed Cells. *J. Cel. Biochem.* 117 (2), 267–278. doi:10.1002/jcb.25283

Clarke, A. J., and Simon, A. K. (2019). Autophagy in the Renewal, Differentiation and Homeostasis of Immune Cells. *Nat. Rev. Immunol.* 19 (3), 170–183. doi:10.1038/s41577-018-0095-2

Cunha, L. D., Yang, M., Carter, R., Guy, C., Harris, L., Crawford, J. C., et al. (2018). LC3-Associated Phagocytosis in Myeloid Cells Promotes Tumor Immune Tolerance. *Cell* 175 (2), 429–e16. doi:10.1016/j.cell.2018.08.061

Deegan, S., Koryga, I., Glynn, S. A., Gupta, S., Gorman, A. M., and Samali, A. (2015). A Close Connection between the PERK and IRE Arms of the UPR and the Transcriptional Regulation of Autophagy. *Biochem. Biophys. Res. Commun.* 456 (1), 305–311. doi:10.1016/j.bbrc.2014.11.076

Deegan, S., Saveljeva, S., Gorman, A. M., and Samali, A. (2013). Stress-induced Self-Cannibalism: on the Regulation of Autophagy by Endoplasmic Reticulum Stress. *Cell. Mol. Life Sci.* 70 (14), 2425–2441. doi:10.1007/s00018-012-1173-4

Dennis, M. D., McGhee, N. K., Jefferson, L. S., and Kimball, S. R. (2013). Regulated in DNA Damage and Development 1 (REDD1) Promotes Cell Survival during Serum Deprivation by Sustaining Repression of Signaling through the Mechanistic Target of Rapamycin in Complex 1 (mTORC1). *Cell. Signal.* 25 (12), 2709–2716. doi:10.1016/j.cellsig.2013.08.038

Dey, S., Baird, T. D., Zhou, D., Palam, L. R., Spandau, D. F., and Wek, R. C. (2010). Both transcriptional Regulation and Translational Control of ATF4 Are central to the Integrated Stress Response. *J. Biol. Chem.* 285 (43), 33165–33174. doi:10.1074/jbc.M110.167213

Dolgin, E. (2019). Anticancer Autophagy Inhibitors Attract 'resurgent' Interest. *Nat. Rev. Drug Discov.* 18 (6), 408–410. doi:10.1038/d41573-019-00072-1

Donohue, E., Balgi, A. D., Komatsu, M., and Roberge, M. (2014). Induction of Covalently Crosslinked P62 Oligomers with Reduced Binding to Polyubiquitinated Proteins by the Autophagy Inhibitor Verteporfin. *PLoS One* 9, e114964. doi:10.1371/journal.pone.0114964

Donohue, E., Thomas, A., Maurer, N., Manisali, I., Zeisser-Labouebe, M., Zisman, N., et al. (2013). The Autophagy Inhibitor Verteporfin Moderately Enhances the Antitumor Activity of Gemcitabine in a Pancreatic Ductal Adenocarcinoma Model. *J. Cancer* 4 (7), 585–596. doi:10.7150/jca.7030

Donohue, E., Tovey, A., Vogl, A. W., Arns, S., Sternberg, E., Young, R. N., et al. (2011). Inhibition of Autophagosome Formation by the Benzoporphyrin Derivative Verteporfin. *J. Biol. Chem.* 286 (9), 7290–7300. doi:10.1074/jbc.M110.139915

Dowdle, W. E., Nyfeler, B., Nagel, J., Elling, R. A., Liu, S., Triantafellow, E., et al. (2014). Selective VPS34 Inhibitor Blocks Autophagy and Uncovers a Role for NCOA4 in Ferritin Degradation and Iron Homeostasis *In Vivo*. *Nat. Cel. Biol.* 16 (11), 1069–1079. doi:10.1038/ncb3053

Egan, D. F., Chun, M. G., Vamos, M., Zou, H., Rong, J., Miller, C. J., et al. (2015). Small Molecule Inhibition of the Autophagy Kinase ULK1 and Identification of ULK1 Substrates. *Mol. Cel* 59 (2), 285–297. doi:10.1016/j.molcel.2015.05.031

Ferrarini, I. (2021). ONC212 Is a Novel Mitocan Acting Synergistically with Glycolysis Inhibition in Pancreatic Cancer. *Mol. Cancer Ther.*. p. molcanther.MCT-20-0962-A.2020.

Firat, E., Weyerbrock, A., Gaedicke, S., Grosu, A. L., and Niedermann, G. (2012). Chloroquine or Chloroquine-PI3K/Akt Pathway Inhibitor Combinations Strongly Promote γ-irradiation-induced Cell Death in Primary Stem-like Glioma Cells. *PLoS One* 7, e47357. doi:10.1371/journal.pone.0047357

Frieboes, H. B., Huang, J. S., Yin, W. C., and McNally, L. R. (2014). Chloroquine-mediated Cell Death in Metastatic Pancreatic Adenocarcinoma through Inhibition of Autophagy. *Jop* 15 (2), 189–197. doi:10.6092/1590-8577/1900

Fujii, S., Mitsunaga, S., Yamazaki, M., Hasebe, T., Ishii, G., Kojima, M., et al. (2008). Autophagy Is Activated in Pancreatic Cancer Cells and Correlates with Poor Patient Outcome. *Cancer Sci.* 99 (9), 1813–1819. doi:10.1111/j.1349-7006.2008.00893.x

Germic, N., Frangez, Z., Yousefi, S., and Simon, H. U. (2019). Regulation of the Innate Immune System by Autophagy: Monocytes, Macrophages, Dendritic Cells and Antigen Presentation. *Cell Death Differ.* 26 (4), 715–727. doi:10.1038/s41418-019-0297-6

Ghadimi, M. P., Lopez, G., Torres, K. E., Belousov, R., Young, E. D., Liu, J., et al. (2012). Targeting the PI3K/mTOR axis, Alone and in Combination with Autophagy Blockade, for the Treatment of Malignant Peripheral Nerve Sheath Tumors. *Mol. Cancer Ther.* 11 (8), 1758–1769. doi:10.1158/1535-7163.MCT-12-0015

Golan, T., Hammel, P., Reni, M., Van Cutsem, E., Macarulla, T., Hall, M. J., et al. (2019). Maintenance Olaparib for Germline BRCA-Mutated Metastatic Pancreatic Cancer. *N. Engl. J. Med.* 381 (4), 317–327. doi:10.1056/NEJMoa1903387

Görgülü, K., Diakopoulos, K. N., Ai, J., Schoeps, B., Kabacaoglu, D., Karpathaki, A. F., et al. (2019). Levels of the Autophagy-Related 5 Protein Affect Progression and Metastasis of Pancreatic Tumors in Mice. *Gastroenterology* 156 (1), 203–e20. doi:10.1053/j.gastro.2018.09.053

Guan, B. J., Krokowski, D., Majumder, M., Schmotzer, C. L., Kimball, S. R., Merrick, W. C., et al. (2014). Translational Control during Endoplasmic Reticulum Stress beyond Phosphorylation of the Translation Initiation Factor eIF2α. *J. Biol. Chem.* 289 (18), 12593–12611. doi:10.1074/jbc.M113.543215

Guo, J. Y., Karsli-Uzunbas, G., Mathew, R., Aisner, S. C., Kamphorst, J. J., Strohecker, A. M., et al. (2013). Autophagy Suppresses Progression of K-Ras-Induced Lung Tumors to Oncocytomas and Maintains Lipid Homeostasis. *Genes Dev.* 27 (13), 1447–1461. doi:10.1101/gad.219642.113

Guo, J. Y., Teng, X., Laddha, S. V., Ma, S., Van Nostrand, S. C., Yang, Y., et al. (2016). Autophagy Provides Metabolic Substrates to Maintain Energy Charge and Nucleotide Pools in Ras-Driven Lung Cancer Cells. *Genes Dev.* 30 (15), 1704–1717. doi:10.1101/gad.283416.116

Han, W., Pan, H., Chen, Y., Sun, J., Wang, Y., Li, J., et al. (2011). EGFR Tyrosine Kinase Inhibitors Activate Autophagy as a Cytoprotective Response in Human Lung Cancer Cells. *PLoS One* 6, e18691. doi:10.1371/journal.pone.0018691

Harding, H. P., Zhang, Y., Bertolotti, A., Zeng, H., and Ron, D. (2000). Perk Is Essential for Translational Regulation and Cell Survival during the Unfolded Protein Response. *Mol. Cel.* 5 (5), 897–904. doi:10.1016/s1097-2765(00)80330-5

Hernandez Borrero, L., Dicker, D. T., Santiago, J., Sanders, J., Tian, X., Ahsan, N., et al. (2021). A Subset of CB002 Xanthine Analogs Bypass P53-Signaling to Restore a P53 Transcriptome and Target an S-phase Cell Cycle Checkpoint in Tumors with Mutated-P53. *Elife* 10, 10. doi:10.7554/eLife.70429

Hernández Borrero, L. J., and El-Deiry, W. S. (2021). Tumor Suppressor P53: Biology, Signaling Pathways, and Therapeutic Targeting. *Biochim. Biophys. Acta (Bba) - Rev. Cancer* 1876 (1), 188556. doi:10.1016/j.bbcan.2021.188556

Hernandez-Borrero, L. J., Zhang, S., Lulla, A., Dicker, D. T., and El-Deiry, W. S. (2018). CB002, a Novel P53 Tumor Suppressor Pathway-Restoring Small Molecule Induces Tumor Cell Death through the Pro-apoptotic Protein NOXA. *Cell Cycle* 17 (5), 557–567. doi:10.1080/15384101.2017.1346762

Honda, A., Harrington, E., Cornella-Taracido, I., Furet, P., Knapp, M. S., Glick, M., et al. (2016). Potent, Selective, and Orally Bioavailable Inhibitors of VPS34 Provide Chemical Tools to Modulate Autophagy *In Vivo*. *ACS Med. Chem. Lett.* 7 (1), 72–76. doi:10.1021/acsmedchemlett.5b00335

Hong, Z., Pedersen, N. M., Wang, L., Torgersen, M. L., Stenmark, H., and Raiborg, C. (2017). PtdIns3P Controls mTORC1 Signaling through Lysosomal Positioning. *J. Cel. Biol.* 216 (12), 4217–4233. doi:10.1083/jcb.201611073

Horsman, M. R., and Overgaard, J. (2016). The Impact of Hypoxia and its Modification of the Outcome of Radiotherapy. *J. Radiat. Res.* 57 (Suppl. 1), i90. doi:10.1093/jrr/rrw007

Hu, Y. L., Jahangiri, A., Delay, M., and Aghi, M. K. (2012). Tumor Cell Autophagy as an Adaptive Response Mediating Resistance to Treatments Such as Antiangiogenic Therapy. *Cancer Res.* 72 (17), 4294–4299. doi:10.1158/0008-5472.CAN-12-1076

Huang, T., Kim, C. K., Alvarez, A. A., Pangeni, R. P., Wan, X., Song, X., et al. (2017). MST4 Phosphorylation of ATG4B Regulates Autophagic Activity, Tumorigenicity, and Radioresistance in Glioblastoma. *Cancer Cell* 32 (6), 840–e8. doi:10.1016/j.ccell.2017.11.005

Jacquel, A., Obba, S., Boyer, L., Dufies, M., Robert, G., Gounon, P., et al. (2012). Autophagy Is Required for CSF-1-Induced Macrophagic Differentiation and Acquisition of Phagocytic Functions. *Blood* 119 (19), 4527–4531. doi:10.1182/blood-2011-11-392167

Javle, M. M., Shroff, R. T., Xiong, H., Varadhachary, G. A., Fogelman, D., Reddy, S. A., et al. (2010). Inhibition of the Mammalian Target of Rapamycin (mTOR) in Advanced Pancreatic Cancer: Results of Two Phase II Studies. *BMC Cancer* 10, 368. doi:10.1186/1471-2407-10-368

Jhaveri, A. V. (2020). Abstract 6225: Addition of TRAIL Receptor Agonists after Treatment with ONC201 or ONC212 Converts Pancreatic Cancer Cells from Anti-proliferative to Apoptotic *In Vitro*. *Cancer Res.* 80 (16 Suppl. ment), 6225.

Kaelin, W. G., Jr. (2011). Cancer and Altered Metabolism: Potential Importance of Hypoxia-Inducible Factor and 2-oxoglutarate-dependent Dioxygenases. *Cold Spring Harb. Symp. Quant. Biol.* 76, 335–345. doi:10.1101/sqb.2011.76.010975

Kang, R., Tang, D., Schapiro, N. E., Livesey, K. M., Farkas, A., Loughran, P., et al. (2010). The Receptor for Advanced Glycation End Products (RAGE) Sustains Autophagy and Limits Apoptosis, Promoting Pancreatic Tumor Cell Survival. *Cel. Death Differ.* 17 (4), 666–676. doi:10.1038/cdd.2009.149

Karasic, T. B., O'Hara, M. H., Loaiza-Bonilla, A., Reiss, K. A., Teitelbaum, U. R., Borazanci, E., et al. (2019). Effect of Gemcitabine and Nab-Paclitaxel with or without Hydroxychloroquine on Patients with Advanced Pancreatic Cancer: A Phase 2 Randomized Clinical Trial. *JAMA Oncol.* 5 (7), 993–998. doi:10.1001/jamaoncol.2019.0684

Karsli-Uzunbas, G., Guo, J. Y., Price, S., Teng, X., Laddha, S. V., Khor, S., et al. (2014). Autophagy Is Required for Glucose Homeostasis and Lung Tumor Maintenance. *Cancer Discov.* 4 (8), 914–927. doi:10.1158/2159-8290.CD-14-0363

Kazemi, S., Mounir, Z., Baltzis, D., Raven, J. F., Wang, S., Krishnamoorthy, J. L., et al. (2007). A Novel Function of eIF2alpha Kinases as Inducers of the Phosphoinositide-3 Kinase Signaling Pathway. *Mol. Biol. Cel.* 18 (9), 3635–3644. doi:10.1091/mbc.e07-01-0053

Kim, J., Kundu, M., Viollet, B., and Guan, K. L. (2011). AMPK and mTOR Regulate Autophagy through Direct Phosphorylation of Ulk1. *Nat. Cel. Biol.* 13 (2), 132–141. doi:10.1038/ncb2152

Kinsey, C. G., Camolotto, S. A., Boespflug, A. M., Guillen, K. P., Foth, M., Truong, A., et al. (2019). Protective Autophagy Elicited by RAF→MEK→ERK Inhibition Suggests a Treatment Strategy for RAS-Driven Cancers. *Nat. Med.* 25 (4), 620–627. doi:10.1038/s41591-019-0367-9

Kline, C. L., Van den Heuvel, A. P., Allen, J. E., Prabhu, V. V., Dicker, D. T., and El-Deiry, W. S. (2016). ONC201 Kills Solid Tumor Cells by Triggering an Integrated Stress Response Dependent on ATF4 Activation by Specific eIF2α Kinases. *Sci. Signal.* 9, ra18. doi:10.1126/scisignal.aac4374

Klionsky, D. J., Abeliovich, H., Agostinis, P., Agrawal, D. K., Aliev, G., Askew, D. S., et al. (2008). Guidelines for the Use and Interpretation of Assays for Monitoring Autophagy in Higher Eukaryotes. *Autophagy* 4 (2), 151–175. doi:10.4161/auto.5338

Kouroku, Y., Fujita, E., Tanida, I., Ueno, T., Isoai, A., Kumagai, H., et al. (2007). ER Stress (PERK/eIF2alpha Phosphorylation) Mediates the Polyglutamine-Induced LC3 Conversion, an Essential Step for Autophagy Formation. *Cel. Death Differ.* 14 (2), 230–239. doi:10.1038/sj.cdd.4401984

Kroemer, G., Mariño, G., and Levine, B. (2010). Autophagy and the Integrated Stress Response. *Mol. Cel.* 40 (2), 280–293. doi:10.1016/j.molcel.2010.09.023

Kume, S., Uzu, T., Horiike, K., Chin-Kanasaki, M., Isshiki, K., Araki, S., et al. (2010). Calorie Restriction Enhances Cell Adaptation to Hypoxia through Sirt1-dependent Mitochondrial Autophagy in Mouse Aged Kidney. *J. Clin. Invest.* 120 (4), 1043–1055. doi:10.1172/JCI41376

Kurdi, A., Cleenewerck, M., Vangestel, C., Lyssens, S., Declercq, W., Timmermans, J. P., et al. (2017). ATG4B Inhibitors with a Benzotropolone Core Structure Block Autophagy and Augment Efficiency of Chemotherapy in Mice. *Biochem. Pharmacol.* 138, 150–162. doi:10.1016/j.bcp.2017.06.119

Kuribayashi, K., Krigsfeld, G., Wang, W., Xu, J., Mayes, P. A., Dicker, D. T., et al. (2008). TNFSF10 (TRAIL), a P53 Target Gene that Mediates P53-dependent Cell Death. *Cancer Biol. Ther.* 7 (12), 2034–2038. doi:10.4161/cbt.7.12.7460

Lazarus, M. B., Novotny, C. J., and Shokat, K. M. (2015). Structure of the Human Autophagy Initiating Kinase ULK1 in Complex with Potent Inhibitors. *ACS Chem. Biol.* 10 (1), 257–261. doi:10.1021/cb500835z

Lazarus, M. B., and Shokat, K. M. (2015). Discovery and Structure of a New Inhibitor Scaffold of the Autophagy Initiating Kinase ULK1. *Bioorg. Med. Chem.* 23 (17), 5483–5488. doi:10.1016/j.bmc.2015.07.034

Lebovitz, C. B., Robertson, A. G., Goya, R., Jones, S. J., Morin, R. D., Marra, M. A., et al. (2015). Cross-cancer Profiling of Molecular Alterations within the Human Autophagy Interaction Network. *Autophagy* 11 (9), 1668–1687. doi:10.1080/15548627.2015.1067362

Lev, A., Lulla, A. R., Wagner, J., Ralff, M. D., Kiehl, J. B., Zhou, Y., et al. (2017). Anti-pancreatic Cancer Activity of ONC212 Involves the Unfolded Protein Response (UPR) and Is Reduced by IGF1-R and GRP78/BIP. *Oncotarget* 8 (47), 81776–81793. doi:10.18632/oncotarget.20819

Levine, B., and Kroemer, G. (2008). Autophagy in the Pathogenesis of Disease. *Cell* 132 (1), 27–42. doi:10.1016/j.cell.2007.12.018

Li, Y., Hahn, T., Garrison, K., Cui, Z. H., Thorburn, A., Thorburn, J., et al. (2012). The Vitamin E Analogue α-TEA Stimulates Tumor Autophagy and Enhances Antigen Cross-Presentation. *Cancer Res.* 72 (14), 3535–3545. doi:10.1158/0008-5472.CAN-11-3103

Liang, X., De Vera, M. E., Buchser, W. J., Romo de Vivar Chavez, A., Loughran, P., Beer Stolz, D., et al. (2012). Inhibiting Systemic Autophagy during Interleukin 2 Immunotherapy Promotes Long-Term Tumor Regression. *Cancer Res.* 72 (11), 2791–2801. doi:10.1158/0008-5472.CAN-12-0320

Liberti, M. V., and Locasale, J. W. (2016). The Warburg Effect: How Does it Benefit Cancer Cells. *Trends Biochem. Sci.* 41 (3), 211–218. doi:10.1016/j.tibs.2015.12.001

Limpert, A. S., Lambert, L. J., Bakas, N. A., Bata, N., Brun, S. N., Shaw, R. J., et al. (2018). Autophagy in Cancer: Regulation by Small Molecules. *Trends Pharmacol. Sci.* 39 (12), 1021–1032. doi:10.1016/j.tips.2018.10.004

Lin, J. H., Li, H., Yasumura, D., Cohen, H. R., Zhang, C., Panning, B., et al. (2007). IRE1 Signaling Affects Cell Fate during the Unfolded Protein Response. *Science* 318 (5852), 944–949. doi:10.1126/science.1146361

Lin, J. H., Li, H., Zhang, Y., Ron, D., and Walter, P. (2009). Divergent Effects of PERK and IRE1 Signaling on Cell Viability. *PLoS One* 4, e4170. doi:10.1371/journal.pone.0004170

Liu, C. Y., Schröder, M., and Kaufman, R. J. (2000). Ligand-independent Dimerization Activates the Stress Response Kinases IRE1 and PERK in the Lumen of the Endoplasmic Reticulum. *J. Biol. Chem.* 275 (32), 24881–24885. doi:10.1074/jbc.M004454200

Maes, H., Kuchnio, A., Peric, A., Moens, S., Nys, K., De Bock, K., et al. (2014). Tumor Vessel Normalization by Chloroquine Independent of Autophagy. *Cancer Cell* 26 (2), 190–206. doi:10.1016/j.ccr.2014.06.025

Majmundar, A. J., Wong, W. J., and Simon, M. C. (2010). Hypoxia-inducible Factors and the Response to Hypoxic Stress. *Mol. Cel.* 40 (2), 294–309. doi:10.1016/j.molcel.2010.09.022

Masson, N., and Ratcliffe, P. J. (2014). Hypoxia Signaling Pathways in Cancer Metabolism: the Importance of Co-selecting Interconnected Physiological Pathways. *Cancer Metab.* 2 (1), 3. doi:10.1186/2049-3002-2-3

Mazure, N. M., and Pouysségur, J. (2010). Hypoxia-induced Autophagy: Cell Death or Cell Survival. *Curr. Opin. Cel. Biol.* 22 (2), 177–180. doi:10.1016/j.ceb.2009.11.015

McAfee, Q., Zhang, Z., Samanta, A., Levi, S. M., Ma, X. H., Piao, S., et al. (2012). Autophagy Inhibitor Lys05 Has Single-Agent Antitumor Activity and Reproduces the Phenotype of a Genetic Autophagy Deficiency. *Proc. Natl. Acad. Sci. U S A.* 109 (21), 8253–8258. doi:10.1073/pnas.1118193109

Miller, K. D., Siegel, R. L., Lin, C. C., Mariotto, A. B., Kramer, J. L., Rowland, J. H., et al. (2016). Cancer Treatment and Survivorship Statistics, 2016. *CA Cancer J. Clin.* 66 (1), 271–289. doi:10.3322/caac.21349

Minassian, L. M., Cotechini, T., Huitema, E., and Graham, C. H. (2019). Hypoxia-Induced Resistance to Chemotherapy in Cancer. *Adv. Exp. Med. Biol.* 1136, 123–139. doi:10.1007/978-3-030-12734-3_9

Mizushima, N., Yoshimori, T., and Ohsumi, Y. (2011). The Role of Atg Proteins in Autophagosome Formation. *Annu. Rev. Cel. Dev. Biol.* 27, 107–132. doi:10.1146/annurev-cellbio-092910-154005

Moore, M. J., Goldstein, D., Hamm, J., Figer, A., Hecht, J. R., Gallinger, S., et al. (2007). Erlotinib Plus Gemcitabine Compared with Gemcitabine Alone in Patients with Advanced Pancreatic Cancer: A Phase III Trial of the National Cancer Institute of Canada Clinical Trials Group. *J. Clin. Oncol.* 25 (15), 1960–1966. doi:10.1200/JCO.2006.07.9525

Mortensen, M., Soilleux, E. J., Djordjevic, G., Tripp, R., Lutteropp, M., Sadighi-Akha, E., et al. (2011). The Autophagy Protein Atg7 Is Essential for Hematopoietic Stem Cell Maintenance. *J. Exp. Med.* 208 (3), 455–467. doi:10.1084/jem.20101145

Mulcahy Levy, J. M., and Thorburn, A. (2020). Autophagy in Cancer: Moving from Understanding Mechanism to Improving Therapy Responses in Patients. *Cel. Death Differ.* 27 (3), 843–857. doi:10.1038/s41418-019-0474-7

Nawrocki, S. T., Han, Y., Visconte, V., Phillips, J. G., Przychodzen, B. P., Maciejewski, J. P., et al. (2016). Development of ROC-325: A Novel Small Molecule Inhibitor of Autophagy with Promising Anti-leukemic Activity. 128 (22), p. 525. doi:10.1182/blood.v128.22.525.525

Nicastri, M. C., Rebecca, V. W., Amaravadi, R. K., and Winkler, J. D. (2018). Dimeric Quinacrines as Chemical Tools to Identify PPT1, a New Regulator of Autophagy in Cancer Cells. *Mol. Cel. Oncol.* 5, e1395504. doi:10.1080/23723556.2017.1395504

Novak, I., Kirkin, V., McEwan, D. G., Zhang, J., Wild, P., Rozenknop, A., et al. (2010). Nix Is a Selective Autophagy Receptor for Mitochondrial Clearance. *EMBO Rep.* 11 (1), 45–51. doi:10.1038/embor.2009.256

Pakos-Zebrucka, K., Koryga, I., Mnich, K., Ljujic, M., Samali, A., and Gorman, A. M. (2016). The Integrated Stress Response. *EMBO Rep.* 17 (10), 1374–1395. doi:10.15252/embr.201642195

Perera, R. M., Stoykova, S., Nicolay, B. N., Ross, K. N., Fitamant, J., Boukhali, M., et al. (2015). Transcriptional Control of Autophagy-Lysosome Function Drives Pancreatic Cancer Metabolism. *Nature* 524 (7565), 361–365. doi:10.1038/nature14587

Petherick, K. J., Conway, O. J., Mpamhanga, C., Osborne, S. A., Kamal, A., Saxty, B., et al. (2015). Pharmacological Inhibition of ULK1 Kinase Blocks Mammalian Target of Rapamycin (mTOR)-dependent Autophagy. *J. Biol. Chem.* 290 (48), 28726. doi:10.1074/jbc.A114.627778

Pietrocola, F., Pol, J., Vacchelli, E., Rao, S., Enot, D. P., Baracco, E. E., et al. (2016). Caloric Restriction Mimetics Enhance Anticancer Immunosurveillance. *Cancer Cell* 30 (1), 147–160. doi:10.1016/j.ccell.2016.05.016

Piffoux, M., Eriau, E., and Cassier, P. A. (2021). Autophagy as a Therapeutic Target in Pancreatic Cancer. *Br. J. Cancer* 124 (2), 333–344. doi:10.1038/s41416-020-01039-5

Prabhu, V. V., Allen, J. E., Dicker, D. T., and El-Deiry, W. S. (2015). Small-Molecule ONC201/TIC10 Targets Chemotherapy-Resistant Colorectal Cancer Stem-like Cells in an Akt/Foxo3a/TRAIL-dependent Manner. *Cancer Res.* 75 (7), 1423–1432. doi:10.1158/0008-5472.CAN-13-3451

Prabhu, V. V., Hong, B., Allen, J. E., Zhang, S., Lulla, A. R., Dicker, D. T., et al. (2016). Small-Molecule Prodigiosin Restores P53 Tumor Suppressor Activity in Chemoresistant Colorectal Cancer Stem Cells via C-Jun-Mediated ΔNp73 Inhibition and P73 Activation. *Cancer Res.* 76 (7), 1989–1999. doi:10.1158/0008-5472.CAN-14-2430

Qu, X., Yu, J., Bhagat, G., Furuya, N., Hibshoosh, H., Troxel, A., et al. (2003). Promotion of Tumorigenesis by Heterozygous Disruption of the Beclin 1 Autophagy Gene. *J. Clin. Invest.* 112 (12), 1809–1820. doi:10.1172/JCI20039

Raufi, A. G. (2021). Abstract 1006: Combination Therapy with MEK Inhibitors and a Novel Anti-neoplastic Drug, Imipridone ONC212, Demonstrates Synergy in Pancreatic Ductal Adenocarcinoma Cell Lines. *Cancer Res.* 81 (13 Suppl. ment), 1006.

Rebecca, V. W., Nicastri, M. C., McLaughlin, N., Fennelly, C., McAfee, Q., Ronghe, A., et al. (2017). A Unified Approach to Targeting the Lysosome's Degradative and Growth Signaling Roles. *Cancer Discov.* 7 (11), 1266–1283. doi:10.1158/2159-8290.CD-17-0741

Reggiori, F., and Ungermann, C. (2017). Autophagosome Maturation and Fusion. *J. Mol. Biol.* 429 (4), 486–496. doi:10.1016/j.jmb.2017.01.002

Richardson, C., Zhang, S., Hernandez Borrero, L. J., and El-Deiry, W. S. (2017). Small-molecule CB002 Restores P53 Pathway Signaling and Represses Colorectal Cancer Cell Growth. *Cell Cycle* 16 (18), 1719–1725. doi:10.1080/15384101.2017.1356514

Roczniak-Ferguson, A., Petit, C. S., Froehlich, F., Qian, S., Ky, J., Angarola, B., et al. (2012). The Transcription Factor TFEB Links mTORC1 Signaling to Transcriptional Control of Lysosome Homeostasis. *Sci. Signal.* 5, ra42. doi:10.1126/scisignal.2002790

Ron, D. (2002). Translational Control in the Endoplasmic Reticulum Stress Response. *J. Clin. Invest.* 110 (10), 1383–1388. doi:10.1172/JCI16784

Ronan, B., Flamand, O., Vescovi, L., Dureuil, C., Durand, L., Fassy, F., et al. (2014). A Highly Potent and Selective Vps34 Inhibitor Alters Vesicle Trafficking and Autophagy. *Nat. Chem. Biol.* 10 (12), 1013–1019. doi:10.1038/nchembio.1681

Rouschop, K. M., van den Beucken, T., Dubois, L., Niessen, H., Bussink, J., Savelkouls, K., et al. (2010). The Unfolded Protein Response Protects Human Tumor Cells during Hypoxia through Regulation of the Autophagy Genes MAP1LC3B and ATG5. *J. Clin. Invest.* 120 (1), 127–141. doi:10.1172/JCI40027

Rutkowski, D. T., Arnold, S. M., Miller, C. N., Wu, J., Li, J., Gunnison, K. M., et al. (2006). Adaptation to ER Stress Is Mediated by Differential Stabilities of Pro-survival and Pro-apoptotic mRNAs and Proteins. *Plos Biol.* 4, e374. doi:10.1371/journal.pbio.0040374

Rzymski, T., Milani, M., Pike, L., Buffa, F., Mellor, H. R., Winchester, L., et al. (2010). Regulation of Autophagy by ATF4 in Response to Severe Hypoxia. *Oncogene* 29 (31), 4424–4435. doi:10.1038/onc.2010.191

Samaras, P., Tusup, M., Nguyen-Kim, T. D. L., Seifert, B., Bachmann, H., von Moos, R., et al. (2017). Phase I Study of a Chloroquine-Gemcitabine Combination in Patients with Metastatic or Unresectable Pancreatic Cancer. *Cancer Chemother. Pharmacol.* 80 (5), 1005–1012. doi:10.1007/s00280-017-3446-y

Shang, L., Chen, S., Du, F., Li, S., Zhao, L., and Wang, X. (2011). Nutrient Starvation Elicits an Acute Autophagic Response Mediated by Ulk1 Dephosphorylation and its Subsequent Dissociation from AMPK. *Proc. Natl. Acad. Sci. U S A.* 108 (12), 4788–4793. doi:10.1073/pnas.1100844108

Shao, S., Li, S., Qin, Y., Wang, X., Yang, Y., Bai, H., et al. (2014). Spautin-1, a Novel Autophagy Inhibitor, Enhances Imatinib-Induced Apoptosis in Chronic Myeloid Leukemia. *Int. J. Oncol.* 44 (5), 1661–1668. doi:10.3892/ijo.2014.2313

Showkat, M., Beigh, M. A., Bhat, B. B., Batool, A., and Andrabi, K. I. (2014). Phosphorylation Dynamics of Eukaryotic Initiation Factor 4E Binding Protein 1 (4E-BP1) Is Discordant with its Potential to Interact with Eukaryotic Initiation Factor 4E (eIF4E). *Cel. Signal.* 26 (10), 2117–2121. doi:10.1016/j.cellsig.2014.06.008

Siegel, R. L., Miller, K. D., Fuchs, H. E., and Jemal, A. (2021). Cancer Statistics, 2021. *CA A. Cancer J. Clin.* 71 (1), 7–33. doi:10.3322/caac.21654

Sotelo, J., Briceño, E., and López-González, M. A. (2006). Adding Chloroquine to Conventional Treatment for Glioblastoma Multiforme: a Randomized, Double-Blind, Placebo-Controlled Trial. *Ann. Intern. Med.* 144 (5), 337–343. doi:10.7326/0003-4819-144-5-200603070-00008

Stein, M. N., Bertino, J. R., Kaufman, H. L., Mayer, T., Moss, R., Silk, A., et al. (2017). First-in-Human Clinical Trial of Oral ONC201 in Patients with Refractory Solid Tumors. *Clin. Cancer Res.* 23 (15), 4163–4169. doi:10.1158/1078-0432.CCR-16-2658

Strohecker, A. M., Guo, J. Y., Karsli-Uzunbas, G., Price, S. M., Chen, G. J., Mathew, R., et al. (2013). Autophagy Sustains Mitochondrial Glutamine Metabolism and Growth of BrafV600E-Driven Lung Tumors. *Cancer Discov.* 3 (11), 1272–1285. doi:10.1158/2159-8290.CD-13-0397

Suraweera, A., Münch, C., Hanssum, A., and Bertolotti, A. (2012). Failure of Amino Acid Homeostasis Causes Cell Death Following Proteasome Inhibition. *Mol. Cel.* 48 (2), 242–253. doi:10.1016/j.molcel.2012.08.003

Szegezdi, E., Logue, S. E., Gorman, A. M., and Samali, A. (2006). Mediators of Endoplasmic Reticulum Stress-Induced Apoptosis. *EMBO Rep.* 7 (9), 880–885. doi:10.1038/sj.embor.7400779

Takamura, A., Komatsu, M., Hara, T., Sakamoto, A., Kishi, C., Waguri, S., et al. (2011). Autophagy-deficient Mice Develop Multiple Liver Tumors. *Genes Dev.* 25 (8), 795–800. doi:10.1101/gad.2016211

Tallóczy, Z., Jiang, W., Virgin, H. W., Leib, D. A., Scheuner, D., Kaufman, R. J., et al. (2002). Regulation of Starvation- and Virus-Induced Autophagy by the eIF2alpha Kinase Signaling Pathway. *Proc. Natl. Acad. Sci. U S A.* 99 (1), 190–195. doi:10.1073/pnas.012485299

Tang, F., Hu, P., Yang, Z., Xue, C., Gong, J., Sun, S., et al. (2017). SBI0206965, a Novel Inhibitor of Ulk1, Suppresses Non-small Cell Lung Cancer Cell Growth by Modulating Both Autophagy and Apoptosis Pathways. *Oncol. Rep.* 37 (6), 3449–3458. doi:10.3892/or.2017.5635

Tian, T., Li, X., and Zhang, J. (2019). mTOR Signaling in Cancer and mTOR Inhibitors in Solid Tumor Targeting Therapy. *Int. J. Mol. Sci.* 20, 20. doi:10.3390/ijms20030755

Tian, X., Ahsan, N., Lulla, A., Lev, A., Abbosh, P., Dicker, D. T., et al. (2021). P53-independent Partial Restoration of the P53 Pathway in Tumors with Mutated P53 through ATF4 Transcriptional Modulation by ERK1/2 and CDK9. *Neoplasia* 23 (3), 304–325. doi:10.1016/j.neo.2021.01.004

Vander Heiden, M. G., Cantley, L. C., and Thompson, C. B. (2009). Understanding the Warburg Effect: the Metabolic Requirements of Cell Proliferation. *Science* 324 (5930), 1029–1033. doi:10.1126/science.1160809

Viale, A., Pettazzoni, P., Lyssiotis, C. A., Ying, H., Sánchez, N., Marchesini, M., et al. (2014). Oncogene Ablation-Resistant Pancreatic Cancer Cells Depend on Mitochondrial Function. *Nature* 514 (7524), 628–632. doi:10.1038/nature13611

Wagner, J., Kline, C. L., Ralff, M. D., Lev, A., Lulla, A., Zhou, L., et al. (2017). Preclinical Evaluation of the Imipridone Family, Analogs of Clinical Stage Anti-cancer Small Molecule ONC201, Reveals Potent Anti-cancer Effects of ONC212. *Cell Cycle* 16 (19), 1790–1799. doi:10.1080/15384101.2017.1325046

Wagner, J., Kline, C. L., Zhou, L., Campbell, K. S., MacFarlane, A. W., Olszanski, A. J., et al. (2018). Dose Intensification of TRAIL-Inducing ONC201 Inhibits Metastasis and Promotes Intratumoral NK Cell Recruitment. *J. Clin. Invest.* 128 (6), 2325–2338. doi:10.1172/JCI96711

Wang, W., Kim, S. H., and El-Deiry, W. S. (2006). Small-molecule Modulators of P53 Family Signaling and Antitumor Effects in P53-Deficient Human colon Tumor Xenografts. *Proc. Natl. Acad. Sci. U S A.* 103 (29), 11003–11008. doi:10.1073/pnas.0604507103

White, E. (2016). Autophagy and P53. *Cold Spring Harb. Perspect. Med.* 6, a026120. doi:10.1101/cshperspect.a026120

White, E. (2015). The Role for Autophagy in Cancer. *J. Clin. Invest.* 125 (1), 42–46. doi:10.1172/jci73941

Whitney, M. L., Jefferson, L. S., and Kimball, S. R. (2009). ATF4 Is Necessary and Sufficient for ER Stress-Induced Upregulation of REDD1 Expression. *Biochem. Biophys. Res. Commun.* 379 (2), 451–455. doi:10.1016/j.bbrc.2008.12.079

Wilson, W. R., and Hay, M. P. (2011). Targeting Hypoxia in Cancer Therapy. *Nat. Rev. Cancer* 11 (6), 393–410. doi:10.1038/nrc3064

Wolpin, B. M., Hezel, A. F., Abrams, T., Blaszkowsky, L. S., Meyerhardt, J. A., Chan, J. A., et al. (2009). Oral mTOR Inhibitor Everolimus in Patients with Gemcitabine-Refractory Metastatic Pancreatic Cancer. *J. Clin. Oncol.* 27 (2), 193–198. doi:10.1200/JCO.2008.18.9514

Wolpin, B. M., Rubinson, D. A., Wang, X., Chan, J. A., Cleary, J. M., Enzinger, P. C., et al. (2014). Phase II and Pharmacodynamic Study of Autophagy Inhibition Using Hydroxychloroquine in Patients with Metastatic Pancreatic Adenocarcinoma. *Oncologist* 19 (6), 637–638. doi:10.1634/theoncologist.2014-0086

Wong, P. M., Feng, Y., Wang, J., Shi, R., and Jiang, X. (2015). Regulation of Autophagy by Coordinated Action of mTORC1 and Protein Phosphatase 2A. *Nat. Commun.* 6, 8048. doi:10.1038/ncomms9048

Wood, S. D., Grant, W., Adrados, I., Choi, J. Y., Alburger, J. M., Duckett, D. R., et al. (2017). In Silico HTS and Structure Based Optimization of Indazole-Derived ULK1 Inhibitors. *ACS Med. Chem. Lett.* 8 (12), 1258–1263. doi:10.1021/acsmedchemlett.7b00344

Wu, G. S., Burns, T. F., McDonald, E. R., Jiang, W., Meng, R., Krantz, I. D., et al. (1997). KILLER/DR5 Is a DNA Damage-Inducible P53-Regulated Death Receptor Gene. *Nat. Genet.* 17 (2), 141–143. doi:10.1038/ng1097-141

Yamamoto, K., Venida, A., Yano, J., Biancur, D. E., Kakiuchi, M., Gupta, S., et al. (2020). Autophagy Promotes Immune Evasion of Pancreatic Cancer by Degrading MHC-I. *Nature* 581 (7806), 100–105. doi:10.1038/s41586-020-2229-5

Yang, A., Herter-Sprie, G., Zhang, H., Lin, E. Y., Biancur, D., Wang, X., et al. (2018). Autophagy Sustains Pancreatic Cancer Growth through Both Cell-Autonomous and Nonautonomous Mechanisms. *Cancer Discov.* 8 (3), 276–287. doi:10.1158/2159-8290.CD-17-0952

Yang, A., and Kimmelman, A. C. (2014). Inhibition of Autophagy Attenuates Pancreatic Cancer Growth Independent of TP53/TRP53 Status. *Autophagy* 10 (9), 1683–1684. doi:10.4161/auto.29961

Yang, A., Rajeshkumar, N. V., Wang, X., Yabuuchi, S., Alexander, B. M., Chu, G. C., et al. (2014). Autophagy Is Critical for Pancreatic Tumor Growth and Progression in Tumors with P53 Alterations. *Cancer Discov.* 4 (8), 905–913. doi:10.1158/2159-8290.CD-14-0362

Yang, S., Wang, X., Contino, G., Liesa, M., Sahin, E., Ying, H., et al. (2011). Pancreatic Cancers Require Autophagy for Tumor Growth. *Genes Dev.* 25 (7), 717–729. doi:10.1101/gad.2016111

Ye, J., Kumanova, M., Hart, L. S., Sloane, K., Zhang, H., De Panis, D. N., et al. (2010). The GCN2-ATF4 Pathway Is Critical for Tumour Cell Survival and Proliferation in Response to Nutrient Deprivation. *EMBO J.* 29 (12), 2082–2096. doi:10.1038/emboj.2010.81

Young, C. D., Arteaga, C. L., and Cook, R. S. (2015). Dual Inhibition of Type I and Type III PI3 Kinases Increases Tumor Cell Apoptosis in HER2+ Breast Cancers. *Breast Cancer Res.* 17, 148. doi:10.1186/s13058-015-0656-2

Young, T. M., Reyes, C., Pasnikowski, E., Castanaro, C., Wong, C., Decker, C. E., et al. (2020). Autophagy Protects Tumors from T Cell-Mediated Cytotoxicity via Inhibition of TNFα-Induced Apoptosis. *Sci. Immunol.* 5, 5. doi:10.1126/sciimmunol.abb9561

Yue, Z., Jin, S., Yang, C., Levine, A. J., and Heintz, N. (2003). Beclin 1, an Autophagy Gene Essential for Early Embryonic Development, Is a Haploinsufficient Tumor Suppressor. *Proc. Natl. Acad. Sci. U S A.* 100 (25), 15077–15082. doi:10.1073/pnas.2436255100

Yun, Z., and Lin, Q. (2014). Hypoxia and Regulation of Cancer Cell Stemness. *Adv. Exp. Med. Biol.* 772, 41–53. doi:10.1007/978-1-4614-5915-6_2

Zhang, S., Zhou, L., Hong, B., van den Heuvel, A. P., Prabhu, V. V., Warfel, N. A., et al. (2015). Small-Molecule NSC59984 Restores P53 Pathway Signaling and Antitumor Effects against Colorectal Cancer via P73 Activation and Degradation of Mutant P53. *Cancer Res.* 75 (18), 3842–3852. doi:10.1158/0008-5472.CAN-13-1079

Zhang, S. (2018). Abstract 1866: Small Molecule NSC59984 Is a Radio-Sensitizer Dependent on ERK2 and DDR but Independent of Wild-type P53. *Cancer Res.* 78 (13 Suppl. ment), 1866.

Zhang, S. (2017). Abstract 1892: Small Molecule NSC59984 Prevents Cancer Cell Migration and Invasion. *Cancer Res.* 77 (13 Suppl. ment), 1892.

Zhang, S. (2017). Abstract 2156: NSC59984 Induces Mutant P53 Degradation via Activating ERK2 Pathway-MDM2 axis. *Cancer Res.* 77 (13 Suppl. ment), 2156.

Zhang, Y., Morgan, M. J., Chen, K., Choksi, S., and Liu, Z. G. (2012). Induction of Autophagy Is Essential for Monocyte-Macrophage Differentiation. *Blood* 119 (12), 2895–2905. doi:10.1182/blood-2011-08-372383

Zou, Z., Yuan, Z., Zhang, Q., Long, Z., Chen, J., Tang, Z., et al. (2012). Aurora Kinase A Inhibition-Induced Autophagy Triggers Drug Resistance in Breast Cancer Cells. *Autophagy* 8 (12), 1798–1810. doi:10.4161/auto.22110

Conflict of Interest: WE-D is a co-founder of Oncoceutics, Inc., a subsidiary of Chimerix, and a Founder of p53-Therapeutics. WE-D has disclosed his relationship with these companies and potential conflict of interest to his academic institution/employer and is fully compliant with NIH and institutional policy that is managing this potential conflict of interest.

The remaining authors declare that the research was conducted in the absence of any commercial or financial relationships that could be construed as a potential conflict of interest

Publisher's Note: All claims expressed in this article are solely those of the authors and do not necessarily represent those of their affiliated organizations, or those of the publisher, the editors and the reviewers. Any product that may be evaluated in this article, or claim that may be made by its manufacturer, is not guaranteed or endorsed by the publisher.

Copyright © 2021 Raufi, Liguori, Carlsen, Parker, Hernandez Borrero, Zhang, Tian, Louie, Zhou, Seyhan and El-Deiry. This is an open-access article distributed under the terms of the Creative Commons Attribution License (CC BY). The use, distribution or reproduction in other forums is permitted, provided the original author(s) and the copyright owner(s) are credited and that the original publication in this journal is cited, in accordance with accepted academic practice. No use, distribution or reproduction is permitted which does not comply with these terms.

frontiers in Pharmacology

REVIEW
published: 20 January 2022
doi: 10.3389/fphar.2021.753387

Evolution of a Paradigm Switch in Diagnosis and Treatment of HPV-Driven Head and Neck Cancer—Striking the Balance Between Toxicity and Cure

Bouchra Tawk[1,2,3,4]*, *Jürgen Debus*[1,2,3,4] and *Amir Abdollahi*[1,2,3,4]

[1]German Cancer Consortium (DKTK) Core Center Heidelberg, German Cancer Research Center (DKFZ), Heidelberg, Germany, [2]Clinical Cooperation Units (CCU) Translational Radiation Oncology and Radiation Oncology, National Center for Tumor Diseases (NCT), German Cancer Research Center (DKFZ), Heidelberg University Hospital (UKHD), Heidelberg, Germany, [3]Division of Molecular and Translational Radiation Oncology, Heidelberg Ion-Beam Therapy Center (HIT), Heidelberg Faculty of Medicine (MFHD), Heidelberg University Hospital (UKHD), Heidelberg, Germany, [4]Heidelberg Institute of Radiation Oncology (HIRO), National Center for Radiation Research in Oncology (NCRO), German Cancer Research Center (DKFZ), Heidelberg University Hospital (UKHD), Heidelberg, Germany

OPEN ACCESS

Edited by:
Claudia Cerella, Fondation de Recherche Cancer et Sang, Luxembourg

Reviewed by:
Thorsten Rieckmann, University Medical Center Hamburg-Eppendorf, Germany
Lennox Chitsike, Loma Linda University, United States
Arshin Sheybani, UnityPoint Health, United States

***Correspondence:**
Bouchra Tawk
bouchra.tawk@med.uni-heidelberg.de

Specialty section:
This article was submitted to Pharmacology of Anti-Cancer Drugs, a section of the journal Frontiers in Pharmacology

Received: *04 August 2021*
Accepted: *09 December 2021*
Published: *20 January 2022*

Citation:
Tawk B, Debus J and Abdollahi A (2022) Evolution of a Paradigm Switch in Diagnosis and Treatment of HPV-Driven Head and Neck Cancer—Striking the Balance Between Toxicity and Cure. Front. Pharmacol. 12:753387. doi: 10.3389/fphar.2021.753387

More than a decade after the discovery of p16 immunohistochemistry (IHC) as a surrogate for human papilloma virus (HPV)-driven head and neck squamous cell carcinoma (HNSCC), p16-IHC has become a routinely evaluated biomarker to stratify oropharyngeal squamous cell carcinoma (OPSCC) into a molecularly distinct subtype with favorable clinical prognosis. Clinical trials of treatment de-escalation frequently use combinations of biomarkers (p16-IHC, HPV-RNA *in situ* hybridization, and amplification of HPV-DNA by PCR) to further improve molecular stratification. Implementation of these methods into clinical routine may be limited in the case of RNA by the low RNA quality of formalin-fixed paraffin-embedded tissue blocks (FFPE) or in the case of DNA by cross contamination with HPV-DNA and false PCR amplification errors. Advanced technological developments such as investigation of tumor mutational landscape (NGS), liquid-biopsies (LBx and cell-free cfDNA), and other blood-based HPV immunity surrogates (antibodies in serum) may provide novel venues to further improve diagnostic uncertainties. Moreover, the value of HPV/p16-IHC outside the oropharynx in HNSCC patients needs to be clarified. With regards to therapy, postoperative (adjuvant) or definitive (primary) radiochemotherapy constitutes cornerstones for curative treatment of HNSCC. Side effects of chemotherapy such as bone-marrow suppression could lead to radiotherapy interruption and may compromise the therapy outcome. Therefore, reduction of chemotherapy or its replacement with targeted anticancer agents holds the promise to further optimize the toxicity profile of systemic treatment. Modern radiotherapy gradually adapts the dose. Higher doses are administered to the visible tumor bulk and positive lymph nodes, while a lower dose is prescribed to locoregional volumes empirically suspected to be invaded by tumor cells. Further attempts for radiotherapy de-escalation may improve acute toxicities, for example, the rates for dysphagia and feeding tube requirement, or ameliorate late toxicities like tissue scars (fibrosis) or dry mouth. The main objective of current de-

intensification trials is therefore to reduce acute and/or late treatment-associated toxicity while preserving the favorable clinical outcomes. Deep molecular characterization of HPV-driven HNSCC and radiotherapy interactions with the tumor immune microenvironment may be instructive for the development of next-generation de-escalation strategies.

Keywords: head and neck (H&N) cancer, human papilloma virus—HPV, radiotherapy, oropharyngeal cancer (OPC), precision medicine, de-intensification trials, patient stratification strategy

1 INTRODUCTION

Human papilloma virus (HPV)-driven oropharyngeal squamous cell carcinoma (OPSCC) is a subtype of head and neck squamous cell carcinoma (HNSCC) with improved clinical outcomes (Ragin and Taioli, 2007; Ang et al., 2010; Dayyani et al., 2010; Rischin et al., 2010). While the incidence of HNSCCs attributable to tobacco and alcohol (known as "HPV-negative HNSCC") continues to decrease, the worldwide prevalence of HPV-driven HNSCC has increased to 47.7% since 2005, accounting for ~73 and ~72% of oropharyngeal tumors in Europe and the United States (United States), respectively (Mehanna et al., 2013). In the United States, HPV-driven OPSCC has overtaken cervical cancer as the most frequent HPV-driven cancer (Senkomago et al., 2019). HPV type 16, the most prevalent viral driver of carcinogenesis in HPV-driven OPSCC (Dayyani et al., 2010), is the culprit behind 95–100% of this cancer type (Herrero et al., 2003; Ragin et al., 2007; Ragin and Taioli, 2007; Mehanna et al., 2013).

Individuals affected are likely to present at a younger age (less than 60 years) with a history of no or little tobacco consumption and high nodal tumor burden (Fakhry et al., 2008; Ang et al., 2010; Huang et al., 2012; Psyrri et al., 2014). The improved survival outcome has been demonstrated in case series, meta-analyses, and prospective randomized clinical trials (RCTs) (Ragin and Taioli, 2007; Fakhry et al., 2008; Shi et al., 2009; Ang et al., 2010; Dayyani et al., 2010; Rischin et al., 2010; Mehanna et al., 2013), regardless of therapy as long as it conformed to the standard of care (Mirghani et al., 2015a). Similarly, cancer survivorship studies showed a statistically significant difference in survivorship rates between survivors with OPSCC cancers vs. oral cancers (an HPV-negative HNSCC surrogate) (115 individuals per 100,000 per year vs. 16 per 100,000 per year, respectively, $p < 0.0001$) (Patel et al., 2016). In an RCT conducted by the Radiation Therapy Oncology Group (RTOG; RTOG0129), patients with HPV-driven OPSCC had a 58% reduction in the risk of death (HR 0.42, 95% CI 0.27–0.66) and a 51% reduction in risk of disease progression or death (HR 0.49, 95% CI 0.33–0.74) compared to HPV-negative OPSCC (Ang et al., 2010).

To this day, the biological basis of the heightened sensitivity of HPV-driven OPSCC toward treatment is not completely elucidated. To which extent does the interplay between intrinsic properties of the tumor cells vs. the tumor microenvironment affect this radiosensitivity is also an active area of research. Some studies have postulated that expression of wild-type p53 (though inactivated by E6 oncoprotein) persists at low levels and is activated after radiation-induced DNA damage, resulting in cell cycle arrest and death (Kimple et al., 2013). Another study postulated that p16 overexpression leads to an increase in misrepair of DNA double-strand breaks (DSBs) because it inhibits the binding of RAD51, a factor essential for homologous recombination (Dok et al., 2014). This results in a shift toward the non-homologous end-joining pathway (NHEJ) and increased misrepair of DSBs. Cell line experiments have also implicated the cell cycle redistribution of HPV-positive vs. HPV-negative cell lines. HPV + cells lines showed an extensive cell cycle arrest in G2, which could be associated with higher radiosensitivity (Busch et al., 2013; Rieckmann et al., 2013). Additionally, tumor hypoxia is not an inverse prognosticator in HPV + OPSCC(Lassen et al., 2010), although studies have shown no significant difference in tumor hypoxia between HPV + OPSCC and HPV-negative tumors, whether by immunohistochemical staining (Kong et al., 2009), gene signatures (Toustrup et al., 2012), or PET-scans (Mortensen et al., 2012). Finally, the tumor immune microenvironment may play a crucial role in mediating this radiosensitivity. HPV-driven OPSCCs show higher levels of tumor-infiltrating lymphocytes (TILs CD8 T cells) (Balermpas et al., 2016). Radiation therapy causes cellular damage, releasing viral and tumor antigens, which may synergistically activate the immune antitumor response.

The standard of care is based on data from trials conducted irrespective of tumor HPV status, and treatment of advanced stage HNSCC is multimodal par excellence. Non-resectable advanced stage HNSCC is treated with definitive radiochemotherapy (CRT), the standard conventional fractionation scheme being 70 Gray (Gy) in 2 Gy fractions (Fx) with concurrent cisplatin (100 mg/m2) on days 1, 22, and 43 (Pignon et al., 2009). In surgically operable disease, surgery (including reconstruction) is followed by postoperative RT up to 66 Gy (Gregoire et al., 2010). Patients with extracapsular extension (ECE) in the involved lymph nodes (LNs) or positive surgical margins (R) benefit from the addition of cisplatin (100 mg/m2) on days 1, 22, and 43 (Bernier et al., 2005; Gregoire et al., 2010).

The toxicity profile accrued per treatment modality (surgery, RT, or chemotherapy) is significant and increases whenever they are combined (summarized in **Figure 1A**) (Nguyen et al., 2002; Parsons et al., 2002; Pignon et al., 2009; Kelly et al., 2016). Given that patients with HPV-driven OPSCC are younger and will continue to live longer, de-escalation trials were conceived with the aim of decreasing treatment toxicity. Selection of appropriate candidates for treatment de-intensification is crucial to avoid compromising favorable survival outcomes.

This article will briefly discuss the morbidity of treatment modalities in HNSCC. Then, the newest paradigms for diagnosis, risk stratification, and staging of HPV-driven OPSCC will be discussed. Finally, strategic principles behind current de-escalation trials will be summarized, and data emerging from trials that have finished reporting will be discussed.

2 TOXICITY OF TREATMENT

Toxicity of treatment in HNSCC may be local (to the anatomical region) or systemic as a consequence of cancer burden or administration of chemotherapy. Interruptions or delays in completion of therapy are associated with worsened local control (LC) due to accelerated tumor repopulation (Bese et al., 2007).

Broadly speaking, toxicity can be conceptualized on several domains. Temporally, acute vs. late toxicities are defined as those occurring within 90 days vs. beyond 90 days of treatment completion (Trotti, 2000). Qualitatively, adverse events may be functional or emotional in nature (Trotti, 2000). Quantitatively, the landscape of toxicities (related to surgery, chemotherapy, or RT) can be graded using the Common Terminology Criteria for Adverse Events (CTCAE) (Bentzen and Trotti, 2007). Toxicities are organized according to System Organ Class (SOC) and vary in severity between grade 1 (mild, asymptomatic, and no intervention required), grade 2 (moderate, requiring minimal, local, or non-invasive intervention), grade 3 (severe or medically significant, significantly impairing Activities of Daily Living (ADL), and necessitating hospitalization), and grade 4 (life-threatening and requiring urgent intervention). Grade 5 is death-causing toxicity (Bentzen and Trotti, 2007). Additionally, quality of life questionnaires (QoL) such as the European Organization for Research and Treatment of Cancer—Quality of Life core questionnaire (EORTC-QLQ-C30) or the head and neck–specific module (EORTC-QLQ-HN35) assess the impact of treatment on four domains: psychological, occupational, physical, and social.

As an example of toxicity profiles in the pre–Intensity Modulated Radiotherapy (IMRT) era, in the Intergroup trial, patients randomized to receive RT alone (70 Gy in 2 Gy Fx) had a 51% rate of all grade 3–5 toxicities, the bulk of which was mucositis/dysphagia (32%), followed by dermatitis (13%) and nausea/vomiting (6%). 39% of patients necessitated the use of a feeding tube (Adelstein et al., 2003). Comparatively, in RT with the concurrent cisplatin (100 mg/m2 weekly) arm, grade 3–5 toxicities were significantly increased with an 85% rate of overall toxicities ($p < 0.0001$), 43% mucositis/dysphagia ($p < 0.08$), 40% leukopenia ($p < 0.001$), 18% anemia ($p < 0.001$), 15% rates of nausea/vomiting ($p < 0.03$), and an 8% rate of renal toxicity ($p < 0.01$) (Adelstein et al., 2003).

The patterns of acute symptom burden have been recently described for patients receiving IMRT alone vs. concurrent CRT (Rosenthal et al., 2014). Toxicities were evaluated using the MD Anderson Symptom Inventory—Head and Neck Module (MDASI—HN). For patients receiving IMRT only, in weeks 1–2, the top three most severe symptoms were fatigue, dry mouth, and drowsiness, in decreasing order of severity (Rosenthal et al., 2014). During weeks 6–7, the top three most severe symptoms were problem tasting food, problems with mouth/throat mucus, and difficulty swallowing/chewing. For patients receiving concurrent CRT, there was a statistically significant increase in the overall severity of these symptoms ($p < 0.001$) (Rosenthal et al., 2014).

Most acute side effects usually resolve within months of treatment completion. Conversely, late complications may be milder at onset but can progress over time and be detrimental to the patient's quality of life (Bentzen and Trotti, 2007). The chronic side effects of RT are dose and volume dependent. Dysphagia rates increase per each 10-Gy increment of the radiation dose to the superior and middle pharyngeal constrictors above 55 Gy (Eisbruch et al., 2004). Risk of aspiration approximates 50% following around 65-Gy dose delivery (Levendag et al., 2007; Feng et al., 2010; Christianen et al., 2015). One-year and 4-year feeding tube dependency rates have been reported to be as high as 41 and 16.7% at 72 Gy, respectively (Garden et al., 2008). Other side effects include tissue fibrosis (Levendag et al., 2007; Feng et al., 2010; Eisbruch et al., 2011), xerostomia, swallowing dysfunction (Langendijk et al., 2009), and development of second primary cancers (Eisbruch et al., 2004, 2011; Nguyen et al., 2006; Machtay et al., 2008; Langendijk et al., 2009; Ramaekers et al., 2011; Mirghani et al., 2015a; Kelly et al., 2016).

With the development of transoral robotic surgery (TORS), surgeons can resect oropharyngeal tumors through the open mouth. According to a case series of 121 patients, 18% of patients experienced Clavien–Dindo grade 3–5 complications (Hay et al., 2017). The most common TORS-related complication was hemorrhage (minor 5.29% vs. major 2.9%) according to a recent meta-analysis (Stokes et al., 2021). Other toxicities included pain at the local site, aspiration-related infections, and dysphagia (Hay et al., 2017). In a case series of 257 patients with HPV-driven OPSCC, post-TORS, moderate and acute dysphagia rates were 14.7 and 8.0%, respectively (Hutcheson et al., 2019). By 3–6 months, moderate–severe dysphagia rates were 0 vs. 13.6% vs. 13.3% in patients treated with TORS alone, TORS + RT, and TORS + CRT, respectively. Gastrotomy tube dependence also increased in patients with increasing treatment intensity. For instance, in a cohort series of 111 patients, addition of adjuvant postoperative RT and CRT increased rates of gastrotomy tube use from 0/13 (0%) to 10/31 (32.3%) and 39/67 (58.2%), respectively ($p < 0.0002$). At 12 months, rates of gastrotomy tubes were 0/13 (0%), 2/31 (6.4%), and 15.9% (10/67) in the TORS alone, TORT + RT, and TORS + CRT groups, respectively, $p < 0.007$ (Sethia et al., 2018).

3 DIAGNOSIS AND RISK STRATIFICATION OF HPV-DRIVEN OPSCC

3.1 Diagnosis of HPV-Driven Tumors

The first step in managing a patient presenting with a newly diagnosed OPSCC is establishing the presence of an HPV-driven tumor. A crucial distinction must be made between tumors harboring a passenger HPV infection versus those with a

transcriptionally active virus. In an HPV-driven tumor, oncoproteins E6 and E7 are transcribed from the virus DNA and expressed in the tumor cells, leading to an interaction with growth regulatory proteins such as tumor suppressors *TP53* (p53) and retinoblastoma (*RB1*), progression into the cell cycle, and acquisition of genomic instability (Münger et al., 2004; Doorbar et al., 2015).

Broadly speaking, there are two classes of HPV testing. Direct tests detect the presence of HPV DNA or RNA, whereas indirect tests establish the presence of HPV *via* molecular surrogates. In clinical settings, the most frequently used direct tests are performed on routine formalin-fixed paraffin-embedded (FFPE) tissue. *In situ* hybridization (ISH) or polymerase chain reaction (PCR) tests detect HPV DNA or RNA (Venuti and Paolini, 2012). Due to the low quality of RNA in FFPE material, detection of HPV E6 and E7 mRNA *via* reverse-transcriptase PCR is infrequently utilized in clinical routines. This method is favored for fresh frozen tissue (Venuti and Paolini, 2012). A promising ISH-based assay (HPV RNAscope) has shown optimal sensitivity and specificity in FFPE tissue but is still not broadly used in clinical practice (Mirghani et al., 2015b).

The most widely used indirect test is p16 immunohistochemistry (p16-IHC), performed on FFPE material (Venuti and Paolini, 2012). Increased expression of p16 (encoded by *CDKN2A* gene) occurs following E7-mediated phospho-RB1 inactivation, allowing p16-expressing tumor cells to bypass cell cycle arrest (Doorbar et al., 2015). The prognostic utility of p16-IHC has been investigated in RCTs (Fakhry and Gillison, 2006; Ang et al., 2010; Rischin et al., 2010; Gillison et al., 2012; Lassen et al., 2013; Fakhry et al., 2014; Masterson et al., 2014), and it is considered an independent prognostic marker for OS in a meta-analysis by the College of American Pathologists (CAP) (Lewis et al., 2018).

However, p16-IHC may represent other physiological or pathophysiological states such as cellular senescence (Rayess et al., 2012). Approximately 10–20% of tumors testing positive for p16-IHC may lack a transcriptionally active HPV infection (Rischin et al., 2010; Singhi and Westra, 2010; Schache et al., 2011; Rietbergen et al., 2013; Rietbergen et al., 2014; Mirghani et al., 2015b; Craig et al., 2019). Patients with p16-IHC+ and HPVDNA-tumors had significantly reduced 5-year OS compared to patients with p16-IHC+ and HPVDNA + tumors (Rietbergen et al., 2013; Rietbergen et al., 2014; Craig et al., 2019) and showed clinical outcomes similar to HPV-negative patients. For instance, in a cohort of 231 patients with OPSCC, 20 patients' tumors (9%) tested positive for p16-IHC and negative by HPVDNA ISH and HPVRNA PCR (Craig et al., 2019). The 5-year OS in this group was 33 vs. 77% in patients with p16-IHC+ and HPVDNA ISH + tumors ($p < 0.05$) (Craig et al., 2019). A recent meta-analysis compared the performance of standalone p16-IHC, HPVDNA PCR, HPVDNA ISH, and various combinatory testing against the performance of HPVRNA PCR testing (Prigge et al., 2017). The best sensitivity and specificity were achieved with a combination of p16-IHC and HPVDNA PCR testing {sensitivity: 93%, [95% confidence interval (CI) 87–97%], specificity; 96% (95%CI 89–100%) (Prigge et al., 2017)}. The specificity of combining both tests was significantly better than either on its own ($p < 0.05$) (Prigge et al., 2017).

Currently, CAP, the American Joint Committee on Cancer (AJCC), and the Union for International Cancer Control (UICC) eighth-edition TNM staging systems recommend using p16-IHC as a standalone surrogate test for an HPV-driven OPSCC (Lewis et al., 2018). However, the 10–20% false-positive rate of p16-IHC may result in enrolling this patient group into de-escalation trials and undertreating them. Of note, the Eastern Cooperative Oncology Group (ECOG) 1,308 trial, a phase II de-escalation trial of RT based on response to induction chemotherapy (ICT), reported 15/80 (19%) of patients with p16-IHC+ and HPVDNA ISH- tumors (Marur et al., 2017). Compared to patients with p16-IHC+/HPVDNA ISH+, at the 2-year follow-up, these patients had lower PFS rates [0.57 (95%CI 0.28–0.78) vs. 0.83 (95%CI 0.71–0.91)] and OS [0.67 (95%CI 0.05–0.95) vs. 0.98 (95% 0.83–0.97)] (Marur et al., 2017). Additionally, within this de-escalated protocol using ICT (**Table 1**), there were eight local recurrences (LR) and 1 case of distant metastasis (DM) at the 2-year follow-up. These results warrant further follow-up, given previous reports that most treatment failures in HPV-driven OPSCC occur after 2 years of follow-up and are distant metastases in nature (Huang et al., 2013).

Most recently, Shinn et al. has retrospectively analyzed the concordance between p16-IHC and HPV-mRNA and its impact on the clinical outcome of 467 patients with oropharyngeal tumors (Shinn et al., 2021). They found a rate of 4.9% discordance between p16-IHC and HPV mRNA (3.4% p16-IHC-/HPV mRNA+ and 1.5% p16 IHC+/HPV mRNA-). Both patient groups had an inferior clinical outcome to double positives. When stratified by HPV mRNA status alone, patients who were p16 negative but HPV mRNA positive had a better outcome than their p16-positive but HPV mRNA–negative counterparts (Shinn et al., 2021).

3.2 Not All HPV-Driven OPSCC Are Equal: Risk Stratification in HPV OPSCC.

RCTs (Ang et al., 2010) and large collaborative cohorts (O'Sullivan et al., 2016) identified negative prognostic factors in HPV-related OPSCC.

Post hoc analysis of RTOG0129 classified patients with HPV tumors into low or intermediate risk groups based on the N-stage and pack-years of smoking:

- Patients with ≤10py were categorized as the low-risk group regardless of TN staging (Ang et al., 2010).
- Patients with >10py and N0-N2a nodes were also low risk, with 3-year OS rates of 93% (95%CI 88.3–97.7%).
- By contrast, patients with >10py and N2b-N3 tumors were considered intermediate risk with OS rates of 70.8% (95%CI 60.7–80.8%) (Ang et al., 2010).

Additionally, clinical studies revealed that the staging system for HNSCC was not suitable for prognosticating the outcome of HPV-driven tumors as it could not discriminate hazards (Huang et al., 2015; Dahlstrom et al., 2016). In the International Collaboration on Oropharyngeal Cancer Network for Staging (ICON-S), a multi-centric study on 1907 patients in North

America, after stratification by the seventh AJCC, patients with Stage I, II, III, and IVa had similar 5-year OS rates of 88, 82, 84, and 81%, respectively. Patients with stage IVb OPSCC had a 5-year OS rate of 60% (O'Sullivan et al., 2016).

Using RPA and adjusted hazard ratios (AHRs), the novel eighth AJCC staging edition was derived (O'Sullivan et al., 2016). In this staging system, p16-IHC is the test for diagnosing an HPV-driven tumor. The T stage remains largely unmodified, and the main consequence is that there are differences between clinical and pathologic N staging, as the N stage was the strongest correlate of OS (Lydiatt et al., 2018). For clinically palpable or radiographically visible disease, the main difference was location of LNs and size (≥6 cm) (Lydiatt et al., 2018). Patients with unilateral LNs smaller than 6 cm are staged cN1 and those with contralateral or bilateral LNs <6 cm are cN2 and any LN ≥ 6 cm confers a cN3 stage (Lydiatt et al., 2018). For surgically resected tumors, the number of LNs (≥5) was the main prognostic factor (Lydiatt et al., 2018). Patients with 1–4 affected LNs and ≥5 LNs were pN1 and pN2, respectively (Lydiatt et al., 2018). ECE was not a prognostic factor in HPV-driven OPSCC and, therefore, is not considered in the updated eighth AJCC staging system (Lydiatt et al., 2018).

This staging system was first developed in patients who received primary CRT and later validated in patients who received surgery followed by adjuvant therapy (Huang et al., 2015; O'Sullivan et al., 2016; Lydiatt et al., 2018).

On this basis, the eighth AJCC staging system for HPV-driven OPSCC was adopted (Lydiatt et al., 2018):

- Stage I: T1-T2 N0-N1 (seventh AJCC equivalent is T1-T2 N0-N2b)
- Stage II: T1-T2 N2 or T3 N0-N2 (seventh AJCC equivalent is T1-2 N2c or T3 N0-N2c)
- Stage III: T4 or N3
- Stage IV: M1

Based on the eighth AJCC, 48% of patients who would have been staged as Stage III or IV according to the seventh AJCC edition migrate to stage I (Lydiatt et al., 2018). Retrospective appraisal of hazard discrimination for the eighth AJCC staging system was conducted in the National Cancer Database (NCDB) for 3,745 patients (Zhan et al., 2017), revealing 4-year OS rates of Stage I (92%), II (81%), and III (63%) (Zhan et al., 2017).

In discussing the eighth AJCC system, it is important to keep in mind that tobacco consumption is not included. Beyond the smoking history, patients with seventh AJCC stage I and stage II OPSCC were candidates for single-modality treatment with excellent outcomes. Patients with stage III–IV 7th AJCC received multimodal therapy (surgery followed by adjuvant CRT or primary CRT). The eighth AJCC staging system was developed based on survival outcomes using retrospectively collected data. The patients with stage III–IVa seventh AJCC who migrated to stage I and II 8th AJCC received more intense therapy compared to patients who were stage I–II in the seventh AJCC and migrated to stage I in the eighth AJCC system.

Consequently, several questions remain to be elucidated. Are the favorable clinical outcomes of these patients related to multimodal therapies reserved for advanced stage OPSCC? Are all stage I HPV OPSCC eligible for treatment de-intensification? Who should receive multimodal therapy? Taken together, several parameters are relevant for evaluation and interpretation of currently completed and ongoing de-escalation trials. First, is the de-escalation arm compared with a "standard of care" arm? What is the primary endpoint? Is the study statistically powered to detect differences in clinical outcomes? Which risk group is this trial targeting (low versus intermediate risk)? How is HPV diagnosis defined? How is the response monitored (clinical/radiographic vs. pathological)? In trials of surgery and adjuvant therapy, what constitutes a negative margin? Finally, questions of cost-effectiveness should be kept in mind when evaluating these trials.

4 PRINCIPLES OF DE-ESCALATION TREATMENT

The overarching aim is the identification of appropriate treatment intensity that minimizes morbidity of cancer survivors without compromising their survival prospects, as seen in **Figures 1B**, **2** below.

De-escalation trials follow one or a combination of the following strategies. In the primary RT/CRT treatment setting, strategies followed include the following:

- Reduction of chemotherapy toxicity by replacing cisplatin with targeted agents (e.g., anti-EGFR treatment with cetuximab)
- Reduction of chemotherapy and or RT dose/volume
- Omission or modification of chemotherapy dose or RT dose/volume depending on clinical or pathologic response to ICT
- Omission of chemotherapy

In the surgical and adjuvant treatment setting, the strategy includes reduction or omission of RT, chemotherapy, or CRT after surgery. Additionally, emerging clinical trials are evaluating the combination of immunotherapy with radiotherapy (sequential or concomitant) (NCT02764593, 2016; Spreafico et al., 2018) and the use of particle therapy with protons instead of conventional photon radiotherapy to reduce toxicity to the surrounding tissue (Gunn et al., 2016).

4.1 De-Escalation Trials in Primary (Chemo) Radiotherapy

4.1.1 Combining Radiotherapy With Cetuximab

Cetuximab is a monoclonal antibody targeting the epidermal growth factor receptor (EGFR), which mediates the activation of oncogenic pathways in HNSCC. In 2006, the Bonner RCT prospectively evaluated the impact of adding cetuximab to RT in patients with advanced-stage HNSCC (Bonner et al., 2006). Compared to patients who received RT alone, there was a statistically significant survival advantage without a concomitant increase in radiation-induced toxicity (median OS 29.3 vs. 40 months, respectively) (Bonner et al., 2006). The survival advantage was strongest among patients with clinical

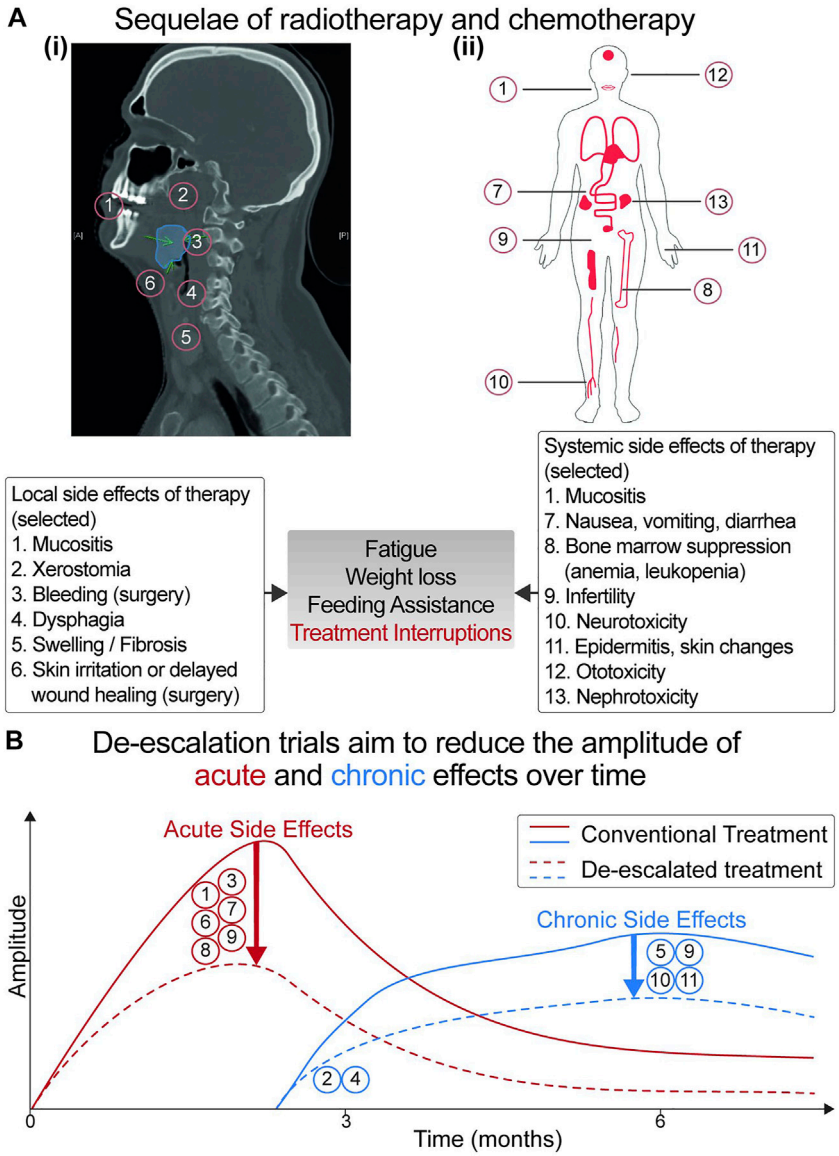

FIGURE 1 | (A) Acute and late toxicity profile of local and systemic chemotherapy. **(i)** Sagittal view of a CT-scan shows the patient's tumor (in blue). Local therapy (surgery and radiotherapy) and systemic treatment can result in acute side effects (occurring within the first 90 days of treatment) or chronic side effects (lasting beyond 90 days). Local side effects include dermatitis, mucositis, xerostomia (dry mouth), dysphagia (difficulty swallowing), bleeding, wound healing swelling, and fibrosis. **(ii)** Systemic side effects are related to the cytotoxic properties of chemotherapy. Increased rates of adverse events (occurring synergistically due to the combination of radiotherapy/chemotherapy) may lead to treatment interruptions, jeopardizing patient outcomes. **(B)** Kinetics of adverse events over time. The aim of de-escalation trials is to flatten the curve of adverse effects [whether acute (in red) or chronic (in blue)], thereby improving the quality of life of patients with HNSCC and cancer survivors.

features suggestive of HPV-driven HNSCC, namely, young patients with oropharyngeal tumors, smaller primaries, and higher nodal involvement (Bonner et al., 2006), a finding subsequently confirmed upon secondary analysis based on p16-IHC status (Rosenthal et al., 2016).

At the present date, three prospective clinical trials, RTOG1016, De-ESCALaTE HPV, and TROG12.01, have evaluated the impact of adding cetuximab to primary RT of 70 Gy. In these trials, non-inferiority of cetuximab was not achieved and cisplatin-based CRT consequently remained the standard of care in HPV-driven OPSCC treated with primary RT (Gillison et al., 2019; Mehanna et al., 2019). The findings are summarized in **Table 1** below.

In the De-ESCALaTE HPV trial (NCT01874171), 304 patients with T3T4-N0 and T1T4-N1N3 (seventh AJCC) p16-IHC + OPSCC and <10py smoking received 70 Gy RT with cisplatin (100 mg/m2 every 3 weeks) or cetuximab. The primary endpoint was overall (acute and late) grade 3–5 toxicities. The study was powered to detect a 25% reduction in overall toxicities in the cetuximab arm. No significant differences in the overall mean number of grade 3–5 toxicity events per patient (cetuximab 4.82 vs. cisplatin 4.81, $p = 0.98$), acute severe toxicities (both arms

TABLE 1 | Selection of de-escalation trials with reported outcomes: primary chemoradiation: substitution of cisplatin (cis) with cetuximab (cetux).

Study name, ID	AJCC, HPV, smoking	Design and primary endpoint	Adverse events	Survival outcomes
De-ESCALATE NCT01874171 (n = 334) Phase III	7th AJCC: T3T4-N0; T1N1-T4N3 8th AJCC:I, II, III HPV testing p16-IHC HPVDNA ISHSmoking<10py	Design: 70 Gy RT + cetuximab vs. cisplatin (100 mg/m^2). Primary endpoint: overall acute and late severe toxicity	Cetux vs. cis: 2 years number of grade 3–5 events per patient: 4.82 vs. 4.81 (p = 0.98)	Cetux vs. cis: 2 years OS: 89.4 vs. 97.5%, p = 0.0007 2 year LR: 12 vs. 3%, p = 0.0026 2 yearr DM: 9 vs. 3% p = 0.0092
RTOG 1016 Phase III, n = 987	7th AJCC: T3N0-T4N0; T1T2-N2aN3 8th AJCCI, II, III HPV testing: p16-IHC Smoking<10py	Design: 70 Gy accelerated RT + cetuximab vs cisplatin (100 mg/m^2). Primary endpoint: 5-year OS (non-inferiority)	Cetuximab vs. cisplatin: no difference in overall rates of acute events (p = 0.16); lower mean number of events per patient (2.35 vs. 3.19, p < 0.001); no difference in overall rates of late events (p = 0.19) or mean number (p = 0.12)	Cetux vs. cis: 5 years OS: 77.% vs. 84.6%, p = 0.016 5 years LR: 17.3 vs. 9.9%, p = 0.0005 5 years DM: 11.7 vs. 8.7%, p = 0.09

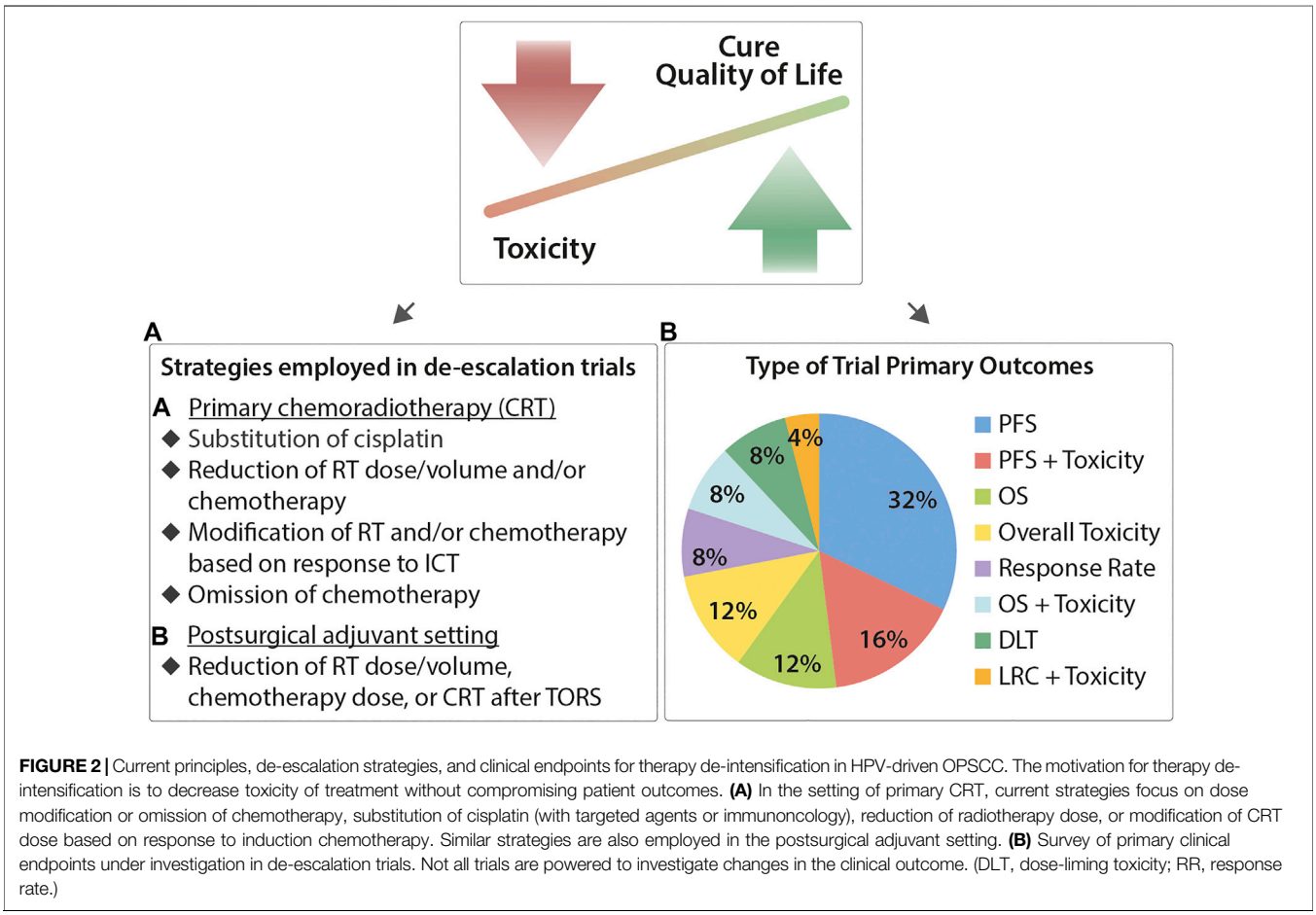

FIGURE 2 | Current principles, de-escalation strategies, and clinical endpoints for therapy de-intensification in HPV-driven OPSCC. The motivation for therapy de-intensification is to decrease toxicity of treatment without compromising patient outcomes. **(A)** In the setting of primary CRT, current strategies focus on dose modification or omission of chemotherapy, substitution of cisplatin (with targeted agents or immunoncology), reduction of radiotherapy dose, or modification of CRT dose based on response to induction chemotherapy. Similar strategies are also employed in the postsurgical adjuvant setting. **(B)** Survey of primary clinical endpoints under investigation in de-escalation trials. Not all trials are powered to investigate changes in the clinical outcome. (DLT, dose-liming toxicity; RR, response rate.)

scored 4.4, p = 0.84), and severe late toxicities (cetuximab: 0.5 vs. cisplatin 0.4, p = 0.53) were detected. Similarly, there was no difference measured in the global QoL score at 2 years (p = 0.99), as measured by EORTC-QLQ-C30. Additionally, there was no difference in QoL scores or dysphagia (as measured by the MD Anderson Dysphagia Index [MDADI]). Nevertheless, a lower number of serious adverse events (SAE) were observed in the cetuximab arm (95 vs. 162 with cisplatin, p < 0.0001). Finally, at the 2-year follow-up, OS was significantly inferior in the cetuximab arm vs. the cisplatin arm (89.4 vs. 97.5%, p = 0.0007), with increased rates of LR (12 vs 3%, p = 0.0026) and DM (9 vs 3%, p = 0.0092).

RTOG1016 (NCT01302834) was a non-inferiority RCT randomizing 987 patients with p16-IHC + OPSCC to cisplatin (100mg/m2 every 3 weeks) or cetuximab with accelerated RT (70Gy in 35 fx, six fx per week). The primary endpoint was the 5-year OS. The trial revealed worsened rates of OS in the cetuximab arm [77.9% (95%CI 73.4–82.5) vs. 84.6% (95%CI 80.6–88.6), p = 0.016], worsened PFS (67.3 vs. 78.5%, p = 0.0002), increased rates of LR (17.3 vs. 9.9%, p = 0.0005), and a non-significant trend

toward increased DM (11.7 vs. 8.6%, $p = 0.09$) (Gillison et al., 2019). Consequently, non-inferiority of cetuximab was not achieved and cisplatin-based CRT remains the standard of care in HPV-driven OPSCC treated with primary RT (Gillison et al., 2019; Mehanna et al., 2019). The findings are summarized in **Table 1** below.

A third trial, TROG12.01 (NCT01855451), randomized 182 patients with p16-IHC + OPSCC (seventh AJCC) (T1T2-N2c or T3-N0N2c) to receive RT 70 Gy in 35Fx with cisplatin weekly (dose-reduced, 40 mg/m2) or cetuximab (Rischin et al., 2021). The primary endpoint was toxicity (acute and at 2 years), measured by the MDADI and MDASI-HN. There was no difference in toxicities between both arms (Rischin et al., 2021). However, there was a significant decrease in the 3-year failure-free survival rates in the cetuximab arm (80%) versus the cisplatin arm (93%) [HR = 3.0 (95% CI: 1.2–7.7); $p = 0.015$] (Rischin et al., 2021).

For all de-escalation trials, the biomarkers used for selection of HPV-driven tumors, the AJCC staging (seventh and corresponding eighth when applicable), and the smoking status of patients enrolled will be described in the adjacent tables.

4.1.2 Reduction of Radiotherapy/Chemoradiotherapy Dose

NCT01530997 is a phase II trial, where patients with tumor stages T0-T3, N0-2c, and M0 (seventh AJCC) and <10py smoking history were treated with 60 Gy IMRT over a 6-week period with concurrent dose-reduced weekly cisplatin (dose-reduced, 30 mg/m2). The primary endpoint was pathologic complete response (pCR). Toxicity was measured using physician-reported outcomes and Patient-Reported Outcomes CTCAE (PRO-CTCAE). QoL was evaluated using the EORTC-QLQ-HN35. At a 10-Gy total dose reduction, the pathologic complete remission (pCR) rate was 86% (37/43). The 2-year OS, LC, disease-free survival (DFS), and PFS were 95, 100, 100, and 100%, respectively (Chera et al., 2017). 15/43 (39%) of patients required a feeding tube for a median of up to 15 weeks following treatment, but none permanently. Moreover, there were no grade 3 late adverse effects (Chera et al., 2017).

Consequently, a larger trial with 114 patients (NCT02281955) was planned with 2-year PFS as the primary endpoint (Chera et al., 2019). The study was powered to detect a 2-year PFS of 87% or greater, with the alternate hypothesis that the PFS was 80% or less. Patients with eighth AJCC stage I tumors (T1–T2 and N0–N1) received standalone RT (60 Gy/2 Gy Fx), and patients with stage II–III tumors received 60 Gy RT with concurrent weekly cisplatin (30 mg/m^2) (Chera et al., 2019). Clinical response was assessed using positron emitted tomography (PET) and computed tomography (CT) imaging at 10–16 weeks, omitting post-treatment biopsies and selective neck dissection (Chera et al., 2019). The PET/CT complete response rate was 93 and 80% at the primary tumor site and the neck, respectively (Chera et al., 2019). The 2-year PFS and OS were 86 and 97%, respectively. 34% of patients required feeding tubes acutely, with none developing feeding tube dependence (Chera et al., 2019). There were no grade 3 or higher late adverse events reported (Chera et al., 2019). Mouth dryness was the greatest symptom burden, with no return of function to the baseline after 1 year (Chera et al., 2019).

NRG-HN002 is another trial where 316 patients, classified as Ang low risk (Ang et al., 2010) (i.e., seventh AJCC T1T2-N1N2b or T3-N0N2b, <10py), were randomized to either IMRT (60 Gy/2 Gy Fx) with concomitant weekly cisplatin (40 mg/m2) or accelerated standalone IMRT 60 Gy in 5 weeks (Yom et al., 2021). For either arm to progress into a phase III trial, the co-primary endpoint was a 2-year PFS rate more than the historic control of 85% and an acceptable dysphagia toxicity measured by

TABLE 2 | Selection of de-escalation trials with reported outcomes: primary chemoradiation: de-escalation of chemoradiotherapy dose.

Study name, ID	AJCC, HPV, smoking	Design and primary endpoint	Adverse events	Survival data
NCT01530997 *n* = 43	7th AJCC T0T3-N0N2c 8th AJCC I, II, III HPV testing: p16 IHC or HPV ISH Smoking:<10py	Design: Stage I: RT 60 Gy. All others: 60 Gy RT + weekly cisplatin (30 mg/m2). Response monitoring: pathologic. Primary endpoint: pathologic complete response	Feeding tube: during treatment: 39%, 0% permanent; EORTC QLQ QLO–C30: pre and 2 years post global 80/82 (lower worse); CTCAE: 0% grade 3–4 adverse events at 36 months	pCR: 86% 2 years OS: 95% 2 yearS PFS: 100% 2 years: LC: 100% 2 years DM: 100%
NCT02281955 *n* = 114	7th AJCC: T0T3 N0N2c 8th AJCC I, II, III HPV testing: p16 IHC or HPV ISH Smoking: 80% with <10 py 20%with >10 py	Design: Stage I: RT 60 Gy. All others: 60 Gy RT + weekly cisplatin (30 mg/m2). Response monitoring: post-treatment PET and CT. Primary endpoint: 2-year PFS	Feeding tube during treatment: 34%, 0% permanent; EORTC QLQ QOL–C30: pre and 2 years post global 79/84 (lower worse); CTCAE: 0% grade 3–4 adverse events at 36 months	2 years PFS: 86% 2 years OS: 95% 2 years LR: 95% 2 years DM-free survival (DMFS): 91%
NRG HN002 NCT02254278 *n* = 316	7th AJCC: T1T2-N1N2b T3-N0N2b 8th AJCC I, II HPV testing: p16 IHC Smoking: <10py	Design: Arm 1: IMRT 60 Gy in 6 weeks + cisplatin (40 mg/m2). Arm B: IMRT alone 60 Gy in 5 weeks. Primary endpoint: 2-year PFS acceptability >85% with an MDADI threshold of >60% (α = 0.05)	IMRT + Cis vs. IMRT 1 year MDADI 85.3 vs. 81.76%; CTCAE: acute toxicity; Grade 4: 15.1 vs. 2.0%; Grade 3: 65.5 vs. 50.3%. Late toxicity: Grade 4: 1.3 vs. 1.4%; Grade 3: 20.0 vs. 16.7%	IMRT + Cis vs IMRT alone: 2 years PFS: 90.5 vs. 87.6% IMRT arm did not meet acceptability criterion (>85%, $p = 0.228$) 2 years OS: 96.7 vs. 97.3% 2 years LRF: 3.3 vs 9.5% ($p = 0.02$)

an MDADI score ≥60. Patients in the IMRT + Cisplatin arm had a PFS of 90.5% ($p = 0.035$) and an acceptable 1-year MDADI mean score of 85.3% (Yom et al., 2021). By contrast, the IMRT alone arm failed to meet the acceptability criterion for non-inferiority with a PFS of 87.6% ($p = 0.228$). The 1-year MDADI mean score was adequate with 81.76%. Strikingly, patients in the IMRT alone arm had a higher rate of locoregional failures (LRF: 9.5 vs. 3.3%) [HR = 0.39 (95% CI, 0.17 to 0.90), $p = 0.02$], with most failures occurring at the primary tumor site (Yom et al., 2021). Toxicities were higher for the IMRT + Cisplatin arm than the IMRT alone arm, but 2-year late toxicities were comparable (grade 4: 1.3 vs. 1.4%, grade 3: 20.0 vs. 16.7%) (Yom et al., 2021). The 2-year OS was 96.7% in the IMRT + Cisplatin arm and 97.3% in the IMRT alone arm (Yom et al., 2021). The trial has currently advanced to phase III, where de-intensified IMRT [60 Gy/2GFx) + weekly Cisplatin (40 mg/m2)], de-intensified IMRT (60 Gy/2Fx) + nivolumab, and 70 Gy IMRT + weekly Cisplatin (40 mg/m2) will be directly compared. The co-primary endpoints are PFS and the MDADI QoL score (Yom et al., 2021).

Data from these trials (summarized in **Table 2** below) are in agreement with De-ESCALaTE HPV and RTOG1016 regarding the importance of concurrent cisplatin in primary CRT. Nevertheless, with a 10Gy reduction in the RT dose and 20–40% reductions of the cisplatin dose (from 300 mg/m2 to 180–240 mg/m2), clinical and functional outcomes were encouraging. The main limitation is the short follow-up duration, given that distant metastases are detected in this patient population from 2 years on after treatment (Huang et al., 2013).

4.1.3 Modulation of Treatment According to Response to Induction Chemotherapy (ICT)

Historically, response to cisplatin-based ICT was considered a good predictor of radiation sensitivity (Mirghani et al., 2015a). The first trial exploring ICT in HPV-driven OPSCC was ECOG 2399 (Fakhry et al., 2008)[79], whereby patients with oropharyngeal or laryngeal tumors (seventh AJCC T2-N1N3 or T3T4-N0N3) received two cycles of induction, paclitaxel and carboplatin, followed by CRT (70Gy RT with paclitaxel) (Fakhry et al., 2008). The primary endpoint was organ preservation, defined as freedom from primary site salvage surgery or primary tumor recurrence. For the subset of patients with HPV-driven OPSCC, 2-year OS and PFS were 95% and 86%, respectively (Fakhry et al., 2008). Nevertheless, high toxicity rates were observed, with 54–53% grade 3 or worse rates of dysphagia and mucositis (Cmelak et al., 2007). 26% of patients required gastrotomy tube placement during treatment, and 17% were dependent on tube feedings at 6 months (Cmelak et al., 2007).

Therefore, ICT-based de-escalation trials utilize the principle of monitoring tumor response after ICT to guide the decision toward a decrease in RT or CRT doses (selected trials in **Table 3**). In ECOG 1308 (NCT01084083), patients with resecteable OPSCC (seventh AJCC T3-T4b, N0-N3) received three cycles of ICT with cisplatin, paclitaxel, and cetuximab (Marur et al., 2017). Their next treatment was selected based on their clinical response to ICT. Patients with clinical complete response (CR was assessed by clinical examination using endoscopy and CT or magnetic resonance imaging (MRI)) received de-escalated RT 54Gy with concurrent cetuximab. Partial responders received 69.3 Gy with concurrent cetuximab (Marur et al., 2017). The 2-year OS and 2-year PFS were 94% (95%CI 82–98) and 80% (95%CI 65–89) for patients who achieved a primary site CR and were treated with 54 Gy of radiation. For all evaluated patients, the 2-year OS and PFS rates were 91% (95%CI 82–96) and 78% (95% CI 67–86), respectively (Marur et al., 2017). Additionally, this trial reported significantly lower rates of difficulties swallowing solids in patients receiving 54 vs. 69 Gy (40 vs. 89%, $p = 0.01$) and impaired nutrition (10 vs. 44%, $p = 0.025$), as measured by the Vanderbilt Head and Neck Symptom Survey-version 2 (VHNSSv2) (Marur et al., 2017). Nonetheless, 13/80 patients (16%) had strong protocol deviations in this trial (Marur et al., 2017), and several patients had dose reduction of cisplatin (17.5%), cetuximab (22.5%), and carboplatin (2.5%), respectively, due to grade 3 or more toxicity (CTCAE) during induction, raising the question of whether addition of ICT-associated toxicity for patient selection should not be considered to assess the net benefit of treatment de-escalation (Marur et al., 2017; Mirghani and Blanchard, 2018; Wirth et al., 2019). Finally, a *post hoc* analysis of this trial suggested worsened outcomes for patients with >10 py of smoking (Marur et al., 2017).

The Optima non-inferiority trial stratified 62 patients with oropharyngeal tumors based on risk factors (low risk: seventh AJCC ≤ T3 ≤N2b ≤ 10py, high risk: T4 or ≥ N2c or >10py) and pathological response to three cycles of ICT with nab-paclitaxel and carboplatin (≥50% response vs. 30 to <50% response vs. <30%) (Seiwert et al., 2019). Low-risk patients with ≥50% response after ICT received standalone RT (50Gy in 2Gy over 5 weeks) (Seiwert et al., 2019). Low-risk patients with 30 to <50% response and high-risk patients with ≥50% response received CRT 45 Gy in 1.5 Gy Fx twice daily with concurrent paclitaxel, 5-Fluorouracil, and hydroxyurea (THFX) (Seiwert et al., 2019). All other patients (low risk with <30% response and high risk with <50% response) received CRT 75 Gy in 1.5 Gy Fx twice daily and concurrent THFX (Seiwert et al., 2019). The primary endpoint was 2-year overall PFS, with the study powered to allow 11% difference from the historical control of 85%. At 2 years, PFS was 94.5%, proving non-inferiority. There were 28 low-risk and 34 high-risk patients in this trial, respectively (Seiwert et al., 2019). Toxicities increased significantly as regiments increased in intensity (RT50Gy < CRT45Gy < CRT75Gy) with acute grade 3–4 mucositis rates of 30, 63, and 91%, respectively ($p = 0.004$), and gastrotomy tube requirements of 0, 20, and 55%, respectively ($p = 0.004$) (Seiwert et al., 2019). 82% of patients received de-escalated treatment (RT50Gy or CRT45Gy), with 2-year PFS being 100% in the low-risk group and 92% in the high-risk group (Seiwert et al., 2019). In a similar vein, 2-year OS was 100% in the low-risk group and 97% in the high-risk group (Seiwert et al., 2019).

The Quarterback trial was a planned prospective randomized control trial, where patients received three cycles of induction with docetaxel, cisplatin, and 5-Fluorouracil (TPF) (Misiukiewicz et al., 2019). Complete or partial responders (as monitored by PET-CT or biopsies) would be randomized to 56 Gy IMRT or 70 Gy IMRT with weekly carboplatin (Misiukiewicz et al., 2019). Non-responders would receive the standard 70 Gy CRT arm (Misiukiewicz et al., 2019). The primary endpoint was non-

TABLE 3 | Modulation of radiotherapy or chemoradiotherapy dose according to response to induction chemotherapy (ICT).

Study name, ID	AJCC, HPV, smoking	Design and primary endpoint	Adverse events	Survival data
ECOG 1308 Marur et al. (2017) NCT01084083 *N* = 80	7th AJCC: T3T4N0, T1N1-T4N3 8th AJCC: I, II, III HPV testing: p16 IHC or HPV ISH Smoking: 39% pts >10py	Design: ICT: 3 cycles of cisplatin, paclitaxel, and cetuximab; then cCR: RT 54Gy + cetuximab; no cCR: 69.3 Gy + cetuximab. Response monitoring: clinical. Primary endpoint: 2-year PFS (powered to expect 85% in patients with cCR after induction and 54 Gy)	54 vs. 69.3 Gy: 1 year swallowing dysfunction: (40 vs. 89%, p = 0.011); 1 year impaired nutrition (10 vs. 44%, p = 0.025); 18/80 (22.5%) patients with ICT protocol deviation	cCR group treated with 54 Gy, (n = 51): 2 years PFS 80%, 2 years OS 94% No cCR with 69 Gy (n = 15): 2 years PFS 67%, 2 years OS 87% p16IHC+and HPVISH+: 2 years PFS HR = 0.83, OS HR = 0.93 p16IHC + but HPVISH-2 years PFS = 0.57, OS 0.87
CCRO-022 Chen et al. (2017) NCT01716195 NCT02048020 N = 45	7th AJCC: III-IV 8th AJCC: I-II-III HPV testing: p16 IHC Smoking: 24.4% > 10py	Design: 2 cycles of ICT paclitaxel–carboplatin; then, responders: RT 54 Gy + weekly paclitaxel. Non-responders: RT 60 Gy + weekly paclitaxel. Response: clinical radiography. Primary endpoint: 2-year PFS (72 vs. 86% as thresholds for inefficacy vs. efficacy of trial α = 0.09)	FACT- H&N During ICT: 39% grade III adverse events including 39% leukopenia. During CRT: grade III dysphagia (20%) 2 years grade III + mucosal–esophageal toxicity: no difference in 54 vs. 60 Gy (p = 0.47)	2 years PFS: 92% 2 years OS: 98% 2 years LR: 95% 2 years DM: 98%
OPTIMA NCT02258659 *N* = 62	7th AJCC: T1T4-N2N3 T3T4-anyN 8th AJCC: I-II-III stratified into: low risk n = 28, ≤T3 and ≤N2b and ≤10py High Risk n = 34, T4 or ≥ N2c or >10py HPV testing: p16-IHC or HPVDNA PCR or HPVRNA ISH Smoking: 35% > 10py	Design: ICT with nab-paclitaxel + carboplatin; then, low risk + >50% pCR after ICT: 50 Gy RT low risk + 30–50% pCR OR high risk + >50% pCR: CRT 45 Gy (THFX). All others: CRT 75 Gy (THFX) Response monitoring: pathologic response. Primary endpoint: 2-year PFS to detect non-inferiority to historical control (85%)	Toxicities (CTCAE) for RT50 < CRT45 < CRT75; acute grade III + mucositis (30, 63, 91%, p = 0.004); acute grade III + dermatitis (0, 20, 55%, p < 0.00001); PEG-tube requirement (0, 31,82%, p < 0.001)	Non-inferiority demonstrated: 2 years overall PFS: 94.5% 2 years PFS: 100% in low risk, 92% for high risk 2 years OS: 100% low risk, 97% in high risk 2 years LC: 100% low risk, 97% in high risk 2 years DM: 100% low risk, 100% high risk
Quarterback trial NCT01706939 (n = 23) Misiukiewicz et al. (2019)	7th AJCC: T3T4-N0 T1N1-T4N3 OPSCC, Nasopharynx or CUP 8th AJCC: I-II-III HPV testing: p16-IHC and HPVDNA PCR Smoking: <20 py	Design: ICT TPF followed by complete or partial remission randomized to - RT 56 Gy + weekly carboplatin - RT 70 Gy + weekly carboplatin. None responders: RT70 Gy + weekly carboplatin. Primary endpoint: 3-year non-inferior PFS, LC	Trial ended early	56 vs. 70 Gy 3 years PFS 83.3 vs. 87.5% 3 years OS: 83.3 vs. 87.5%. Non-inferiority could not be determined

inferiority with 3-year PFS. The trial closed early with 23 patients enrolled (Misiukiewicz et al., 2019). Although 20 patients developed significant response to ICT and were randomized, non-inferiority could not be demonstrated (p = 0.8) (Misiukiewicz et al., 2019).

4.2 De-Escalation of Post-Surgical Treatment

4.2.1 De-Escalation of Adjuvant Radiochemotherapy

Stratification of patients after surgery based on their pathological results aims to identify patients who can benefit from the complete omission of postoperative radiation and chemotherapy (Kelly et al., 2016), (see **Table 4**).

ECOG3311 is a phase II trial where 445 patients with intermediate risk OPSCC (seventh AJCC T1T2-N1N2b p16-IHC + OPSCC) were randomized into four clinical arms based on the presence/absence of pathological risk factors after TORS resection of the primary tumor and neck dissection (NCT01898494, 2013). Patients with 0-1 LNs, no ECE, and negative margins did not receive subsequent adjuvant treatment (arm A) (Ferris et al., 2021). Patients with R0, N2 disease, or ECE <1 mm received de-escalated RT (in one of two possible arms: Arm B 50 Gy or Arm C 60 Gy). Arm D consisted of patients with R1, >4 involved LNs, or ECE who received CRT (66Gy RT + weekly cisplatin 40mg/m2) (Ferris et al., 2020; Ferris et al., 2021) Co-primary outcomes were 2-year PFS>85%, accrual rate, grade 3–4 bleeding events during surgery, and positive resection margins (Ferris et al., 2020). The positive margin rate was 3.3 and 5.9% grade III or IV oropharyngeal bleeding (Ferris et al., 2021). This trial also met its primary endpoint for PFS: 2-year PFS for Arms A, B, C, and D were 96.9, 94.9, 96, and 90.7%, respectively (Ferris et al., 2021).

MC1273 is a trial which enrolled patients with intermediate-risk HPV-driven OPSCC and R0 surgeries to receive de-escalated adjuvant CRT (Ma et al., 2019). Intermediate risk criteria were defined as seventh AJCC stage III–IV and high-risk features such as ECE, lymphovascular invasion (LVI) or perineural invasion

TABLE 4 | Surgical approaches: de-escalation of adjuvant radiotherapy or chemoradiotherapy.

Study name, ID	AJCC, HPV, smoking	Design and primary endpoint	Adverse events	Survival data
MC1273 Ma et al. (2019) NCT01932697 *N* = 80	7th AJCC: III-IV with high risk features: ECE or LVI, PNI ≥2 LN, any LN > 3 cm or ≥ T3) 8th AJCC: I-II-III HPV testing: p16-IHC Smoking: <10 py	Design: surgery (R0) + neck dissection. Cohort A: ECE-: 30 Gy/1.5 Gy twice daily + 15 mg/m2 docetaxel. Cohort B: ECE+: 36 Gy/1.8 Gy twice daily + docetaxel. Primary endpoint: 2-year LRC rate of 20% or less (with 2-sided 85% CI) and <20% rate of acute grade 3 or worse toxicity, α = 0.06	2-year grade III toxicity (CTCAE): 0%	2 years LC: cohort A; 100%, cohort B: 93% 2 years DM: cohort A: 97.2%, cohort B 79% 2 years PFS: 91.1% 2 years OS: 98.7%
NCT02760667 Sadeghi et al. (2019) *n* = 54	7th AJCC: T1T2-N1N2cT3-N0N2c T4-N0N2c 8th AJCC: I-II-III HPV testing: p16-IHC Smoking: Unknown	Design: 3 cycles of ICT (cisplatin + docetaxel) and then TORS + ND. Primary endpoint: pathologic response	—	Complete pathologic response: primary tumor: 72%; nodal site: 57%; both: 44%
ECOG3311 NCT01898494 *N* = 511 Ferris et al. (2020)	7th AJCC: T1T2-N1N2b 8th AJCC: I-II HPV testing: p16-IHC Smoking: Unknown	Design: low risk: Arm A: TORS only; intermediate risk (R0, N2, ECE<1 mm): Arm B: TORS +50 Gy IMRT Arm C: TORS + 60 Gy IMRT; high risk (R1, ECE+) into Arm D: TORS + 66 Gy IMRT + cisplatin (40 mg/m2). Primary endpoint: 2-year PFS, grade 3–4 bleeding events during surgery, and positive margins	—	2-year PFS: Arm A: 96.9%; Arm B: 94.9%; Arm C: 96.0%; Arm D: 90.7%
DART-HPV NCT02908477 *N* = 194	7th AJCC: ≥T3, ≥N2, LVI, PNI and R0 HPV testing: p16-IHC 8th AJCC: II-III Smoking: <10py	Design: TORS and then intermediate risk: ECE-Twice daily RT30 Gy/1.5 Gy + Docetaxel; high risk: ECE + Twice daily RT36 Gy/1.8 Gy + Docetaxel. Standard arm: RT 60 + cisplatin weekly (40 mg/m2)	2-year grade III AES (CTCAE): 1.6% for the experimental arm and 7.1% for the standard p = 0.058	2 years PFS 86.9 vs. 95.8% for experimental vs. standard pN2 and ECE: 2 years PFS 42.9% for experimental arm vs. standard

(PNI), ≥2LN, any LN > 3 cm, or ≥ T3 (Ma et al., 2019). Patients with >10py history were excluded (Ma et al., 2019). ECE was the stratifying factor whereby patients with no ECE (cohort A) received 30 Gy RT in 1.5 Gy twice daily fractions and concurrent docetaxel (Ma et al., 2019). Cohort B consisted of patients with ECE, who received 36 Gy in 1.8 Gy twice daily fractions and concurrent docetaxel (Ma et al., 2019). The primary endpoint was 2-year LC with rates of 100 and 93% in cohorts A and B, respectively (Ma et al., 2019). 2-year PFS and OS for all patients were 91.1 and 98.7%, respectively (Ma et al., 2019). No patient required a gastrotomy tube by 1 month after treatment (Ma et al., 2019). A subsequent phase III trial, DART-HPV, has been designed, where patients were randomized to RT (twice daily, 30 Gy/1.5 Gy or 36/Gy in 1.8 Gy with concomitant docetaxel) or RT 60Gy/2Gy once daily and cisplatin weekly (40 mg/m2) (NCT02908477, 2016; Ma et al., 2019) The primary endpoint was grade 3 AE preliminary results that were presented at the annual 2021 American Society of Radiation Oncology (ASTRO) meeting. Grade 3 AEs were 1.6% for the experimental arm vs. 7.1% for the standard of care (p = 0.058). However, 2-year PFS was 86.9 vs. 95.8%. Particularly, patients with pN2 disease and ECE had the worst outcomes after de-escalation, with 42.9% PFS rates compared to 100% in the standard of care arm.

Taken together, the outcomes of ECOG3311 and MC1675 provide an encouraging basis for de-escalation of therapy in the adjuvant setting. However, patients with ECE + pN2 disease may not be suitable for treatment de-escalation. In MC167, the 2-year PFS was 42.9% for these patients who were in the de-escalation arm of the trial, with 77% LRC and 59.4% DMFS rates. By contrast, those patients had a 100% 2-year PFS in the standard of care arm. Similar results were seen in ECOG3311, whereby patients with either ECE or >4LNs received a standard dose CRT (66 Gy) with weekly cisplatin and had a 2-year PFS of 90.7%. This once again highlights the importance of adequate patient selection.

Further data are also awaited from two prospective trials, PATHOS and DELPHI. The PATHOS trial stratifies 242 patients with OPSCC seventh AJCC T1T3-N0N2b disease into four arms as well, depending on pathological results after TORS (Owadally et al., 2015). Patients with no risk factors go into an observational alone arm, patients with intermediate risk factors (seventh AJCC T3 stage, pN2a-N2b, LVI, pNI, or close margins) receive RT only (50 Gy or 60 Gy), high-risk patients with R1 resections receive 60 Gy RT, and patients with ECE receive CRT 60 Gy with cisplatin (100 mg/m2) (Owadally et al., 2015). Co-primary outcomes are 1-year MDADI and 1-year OS (Owadally et al., 2015).

The ongoing DELPHI trial (NCT03396718, 2018) aims to enroll 384 patients into two clinical arms of radiation dose de-escalation based on pathological risk factors. In the first level of the DELPHI trial, patients with intermediate risk (pT3, R0 margins, ≤ involved LNs, and no ECE) receive a 10% reduction of standalone RT (54 Gy to the tumor bed) and 45 Gy to the cervical LNs. Patients with at least one high-risk feature (R1 status, pT4, ≥4LNs, or ECE) will receive 59.4 Gy for the tumor bed, 45Gy to the cervical LNs, and additional chemotherapy. The primary endpoint is 2-year locoregional recurrence. If no more than three tumor recurrences in 30 patients occur in the first 2 years, further de-escalation of the RT dose will ensue, whereby patients with no high-risk features will receive 48.4 and 39.6 Gy to the tumor bed and cervical LNs, respectively. Patients with high-risk features will receive 55 and 39.6 Gy to the tumor bed and cervical LNs, respectively (NCT03396718, 2018).

The ADEPT trial (NCT01687413, 2012) was comparing 60 Gy RT alone vs. 60 Gy RT + weekly cisplatin 40 mg/m2 in stage I–III HPV-driven OPSCC with ECE. However, this trial has terminated due to slow accrual.

4.3 Comparison of Primary Radio(Chemotherapy) Versus Postoperative Adjuvant Radio(Chemo) Therapy

Between 2004 and 2013, the percentage of patients with T1-T2 OPSCC undergoing surgery increased from 56 to 82% in the US, with a meta-analysis suggesting decreased toxicity associated with surgery compared to definitive CRT (Nichols et al., 2019). Although not a de-escalation trial, ORATOR evaluated QoL outcomes in primary RT/CRT vs. surgical intervention (Nichols et al., 2019) (**Supplementary Table S1**). In the surgical arm, 34 patients underwent TORS + neck dissection (ND), with 47% receiving adjuvant RT up to 64 Gy and 23.5% receiving CRT (RT + cisplatin 100 mg/m2 every 3 weeks). In the primary arm, 26.5% received RT up to 70 Gy and 67.6% received CRT. The primary outcome was powered to detect a 10-point difference in MDADI total mean scores at 1 year (higher is better). 1-year scores were 86.9 in the primary CRT arm vs. 80.1 in the surgical arm ($p = 0.042$). Grade 2 or higher adverse event rates (CTCAE) were similar in both arms, with preponderance for oral bleeding and trismus in the surgical arm and for neutropenia, hearing loss, tinnitus, and constipation in the primary CRT arm. TORS and ND were not associated with a superior QoL, and 3-year OS and PFS were 93 and 93.1%, respectively, with no differences between both arms ($p = 0.89$ and $p = 0.63$) (Nichols et al., 2019).

A follow-up prospective trial, ORATOR2, was planned to randomize patients to de-escalated CRT vs. de-escalating adjuvant treatment, the primary outcome being 2-year OS (Nichols et al., 2020). The results of a direct comparison between TORS and definitive CRT were eagerly awaited. Unfortunately, the trial was terminated due to unacceptable toxicity in the TORS + ND arm (two treatment-related deaths) (Palma et al., 2021), establishing primary CRT as a safe approach for treatment de-escalation. 61 patients were randomized in total. The 2-year OS was 100% for the RT arm vs. 83.5% in the TORS + ND arm (Palma et al., 2021). The findings of E3311, MC1765, and ORATOR are encouraging. Nonetheless, the data from ORATOR2 suggest that further studies will be needed to answer the question of surgery versus primary radiochemotherapy.

4.4 De-Intensification Schemes Using Immune Therapy

An emerging strategy is the combination of primary or adjuvant RT with modulators of the immune response, predominantly immune-checkpoint blockers (ICB, **Supplementary Table S2**).

HCC 18-034 (NCT03715946, 2018) is evaluating the addition of postoperative adjuvant reduced dose, moderately accelerated RT (45 or 50 Gy, in daily dose fx, six fx per week), and nivolumab (monoclonal antibody against Programmed cell Death protein 1 (PD-1)) in patients with advanced stage p16-IHC + OPSCC (seventh AJCC: T0, T3 + >2Nb and <10py or T0, T3 with >N1 and >10py) with intermediate risk features (ECE or positive margins). Nivolumab will be administered in two doses of 240 mg/m2 during weeks two and four of RT, and up to six doses afterward, of 480 mg/m2. The primary outcome is PFS at 3 years and gastrotomy tube dependence at 1 year (NCT03715946, 2018).

For definitive RT/CRT, NRG-HN005 is a prospective trial aiming to randomize 711 patients with p16-IHC + OPSCC, eighth AJCC stage I–II, and less than 10py to reduced dose RT (60 Gy in five fx, 6 weeks) with cisplatin, reduced dose RT (60 Gy in six fx, 5 weeks) with nivolumab, or standard of care (70 Gy RT in six fx, 5 weeks + cisplatin) (NCT03952585, 2019). The primary endpoint is 6-year PFS (NCT03952585, 2019).

NCT03799445 will evaluate the impact of upfront dual ICB with nivolumab and ipilimumab [monoclonal antibody against cytotoxic T-lymphocyte–associated protein 4 (CTLA4)], followed by RT (50–66 Gy) in patients with the eighth AJCC (stage I–II). In this trial, patients' tumors must test positive for both p16-IHC and HPVDNA or RNA by ISH (NCT03799445, 2019). Primary endpoints include dose-limiting toxicity [DLT, defined as any ≥ grade III toxicity (CTCAE) related to immunotherapy not resolving within 28 days after treatment], complete response rate at 6 months, and 2-year PFS (NCT03799445, 2019).

The Canadian Cancers Trial Group CCTG HN.9 (NCT03410615) will randomize patients with p16-IHC + OPSCC and intermediate risk features (T1-2N1 smokers, T3N0-N1 smokers, and T1-3N2 any smoking history) in CRT 70 Gy/35 with cisplatin 100 mg/m^2 or RT70Gy/35 with concurrent durvalumab 1500 mg (days 7 and 22), followed by durvalumab maintenance for six doses (Spreafico et al., 2018). The primary endpoint is event-free survival (EFS). A translational program including immunophenotyping, radiomic imaging, circulating tumor DNA (ctDNA), and microbiome analyses will be conducted in parallel (Spreafico et al., 2018).

The results of these trials are eagerly awaited, in light of the negative results from the Javelin Head and Neck 100 (.NCT02952586) and GORTEC 2017-01 (REACH,

NCT02999087.) phase III trials. Javelin Head and Neck 100 compared the combination of avelumab, a PD-L1 inhibitor, + standard-of-care CRT (RT70Gy/2Gy + cisplatin 100 mg/m^2 every 3 weeks) against standalone CRT in locally advanced HNSCC (Lee et al., 2021). The trial included HPV-positive and HPV-negative disease. The primary endpoint of PFS prolongation was not met, and there was no benefit seen upon stratification in HPV-positive disease (Lee et al., 2021). Similarly, in the GORTEC 2017-01-Reach trial, the combination of avelumab and cetuximab-based chemoradiotherapy did not improve PFS, further cementing the role of cisplatin-based radiochemotherapy as the standard of care in the treatment of locally advanced HNSCC (Bourhis et al., 2021).

Beyond ICB combinations, exploration of radiotherapy-induced immune activation and unmasking of HPV-associated neoepitope may, together with the growing arsenal of immunoncology (IO) drugs, facilitate the development of effective antitumor specific vaccines.

5 MOLECULAR STRATIFICATION OF HPV-DRIVEN OPSCC

Beyond p16-IHC, direct HPV testing, and tobacco smoking, de-escalation trials can also contribute to a deeper understanding of the biology of HPV-driven OPSCC.

In one approach, PET imaging (18F-MISO PET detecting tumoral hypoxia) was used in a pilot study from the Memorial Sloan Kettering Cancer Center (MSKCC) to modulate the RT dose to the LNs in patients with p16-IHC + OPSCC receiving CRT (Lee et al., 2016). Patients with no baseline tumor hypoxia or with resolution of hypoxia after week 1 (per 18F-MISO PET scans) were candidates for 10-Gy dose de-escalation to the LNs (Lee et al., 2016). The primary tumor site received the standard RT dose (70 Gy). 10 patients (30%) were eligible for dose de-escalation (Lee et al., 2016). The 2-year clinical outcomes were as follows: 100% LC, 97% DM, and 100% for OS (Lee et al., 2016).

Additionally, targeting hypoxic HPV-driven tumors with heavy charged particles that are less dependent on the oxygen enhancement ratio (OER) (Klein et al., 2017; Chiblak et al., 2019) may provide another attractive venue to specifically escalate the dose while sparing normal tissue in this subgroup.

The association between the mutational landscape of HPV-driven OPSCC and patient outcomes is still under investigation. Beaty et al. performed next generation sequencing (NGS) of tumor samples from 78 patients enrolled in de-escalation trials of primary RT to investigate the prognostic role of PIK3CA mutations (Beaty B. T. et al., 2019). PIK3CA was the most significantly mutated gene in 21.8% of patients (Beaty B. T. et al., 2019; Beaty B. et al., 2019.). Patients with mutated PIK3CA had significantly lower 3-year DFS (65%) compared to patients with wild-type PIK3CA (93%, p = 0.0009), suggesting that this patient population is not suitable for de-escalation trials (Beaty B. T. et al., 2019; Beaty B. et al., 2019). However, conflicting data emerged from studies of patients with metastastic HPV-driven OPSCC where mutations in the PI3K pathway (PI3KCA, PIK3CA2B, and PIK3R1) were associated with an improved overall survival outcome at 5 years (Hanna et al., 2018).

Another biomarker trial approach is based on monitoring of circulating free DNA (cfDNA) or circulating tumor HPVDNA (ctHPVDNA) detected in patients' blood. In NCT0316182, 115 patients were prospectively followed up for a median duration of 23 months after being treated with curative intent chemoradiotherapy (Chera et al., 2020). The trial estimated the positive predictive value (PPV) and negative predictive value (NPV) of ctHPV-DNA for determining disease recurrence (Chera et al., 2020). Undetectable levels of ctHPVDNA at post-treatment time points had an NPV of 100%. Conversely, two consecutively positive ctHPVDNA blood tests had a PPV of 94%. The median time from ctHPVDNA positivity to biopsy-proven recurrence was 3.9 months (Chera et al., 2020). cfHPV-DNA was confirmed as a highly specific biomarker of surveillance in a recent meta-analysis of 11 studies (Hanna et al., 2018). cfHPV-DNA had a pooled sensitivity of 0.81 (95% CI 0.78-0.84) and 0.98 (95%CI 0.96–0.99) at the first diagnosis. At follow-up, it had a sensitivity of 0.73 (95%CI 0.57–0.86) and a specificity of 1 (Hanna et al., 2018). Interestingly, one study found a significant association between levels of cfHPV-DNA and N status, as well as the extent of disease involvement (Tanaka et al., 2022). Levels of cfHPV-DNA increased as function of involvement, with the lowest in locally advanced disease, followed by locoregional spread, and the highest for distant metastases (Tanaka et al., 2022).

Similarly, HPVDNA may be detected from oral rinses. Patients with persistent oral HPVDNA after the end of therapy had a decreased 2-year OS (HR = 1.86, p = 0.003) compared to patients without detectable DNA in a prospective phase II clinical trial (Fakhry et al., 2019). Finally, the association between seropositivity to HPV16 antigens and clinical outcomes has been demonstrated in several studies (Dahlstrom et al., 2015; Nelson et al., 2017). Furthermore, a recent study investigated differential patterns of antibody response to cancer antigens in HPV-driven versus HPV-negative HNSCC: antibodies against IMP-1 (found in n = 9/153, 6% of patients) were adversely prognostic only in HPV-driven OPSCC (HR = 3.28, p < 0.001) (Laban et al., 2019). Detecting relevant tumor immune microenvironment (TIME) parameters may also assist in stratifying risk for recurrence and inferior OS in HPV-driven HNSCC. A multicentric retrospective study from the German Cancer Consortium (DKTK) identified enrichment in CD8$^+$ infiltrating immune cells as an independent prognostic factor both in p16-IHC+/HPVDNA + OPSCC tumors and HPV-negative tumors, in a cohort of 161 patients treated with surgery and postoperative CRT (Balermpas et al., 2016). Disappointingly, high levels of PD-L1 were not prognostic in the Javelin 100 Head and Neck trial, although this finding was not stratified by HPV status (Lee et al., 2021).

Taken together, these findings reaffirm the importance of validating all biomarkers in prospective phase III clinical trials.

6 CONCLUSION

The identification of HPV as a protoypic predictive marker for molecular stratification of patients has paved the way for the

development of several avenues of treatment de-intensification. Individualized therapy may be tailored by de-escalation or adaption of local radiotherapy and de-intensification/replacement of systemic therapy. This field is evolving at a rapid pace. In this dynamic era, deeper understanding of the biology of HPV-driven tumors shapes physicians' approach toward improved diagnosis, staging, risk stratification, and management of this disease. With a steadily increasing complexity and a plethora of opportunities, a consensus is needed to assure better comparability, for example, homogenizing inclusion criteria, exclusion criteria, risk stratification (most noteworthy, the impact of smoking), staging, and diagnosis of an HPV-driven tumor, replacing the single p16-immunohistochemistry test with a combination of direct HPV tests or including more advanced molecular methods that better assist in stratifying patients at low risk for locoregional or distant recurrence.

In postoperative adjuvant treatment of OPSCC, the design of current trials accounts for extracapsular extension, although it was not included as an adverse prognosis factor in the eighth AJCC staging system. In primary definitive CRT treatment, data from phase III trials, where substitution of cisplatin with cetuximab leads to inferior survival outcomes, have established cisplatin-based radiochemotherapy as the standard of care. Similarly, results from NRG-HN002 consolidated the role of cisplatin, whereby a higher rate of locoregional recurrence was found in patients treated with moderately accelerated radiotherapy alone (60 Gy in 5 weeks) and complete omission of cisplatin. Nevertheless, numerous other strategies are ongoing, with promising data emerging from phase II clinical trials. Confirmation in randomized phase III clinical trials is awaited. Maturity of follow-up will be an issue to address in these trials, given the main pattern of distant relapse after 2 years in HPV-driven OPSCC.

Multiparametric tumor characterization may be needed for accurate patient selection to avoid de-escalating patients at high risk of recurrence. In parallel, broadening the therapeutic window with targeted tumor-specific agents, a growing immunoncology arsenal, and novel radiation dose/quality painting *via* heavy charged particles may navigate the therapy of HPV-driven HNSCC toward high-precision oncology.

AUTHOR CONTRIBUTIONS

Conceptualization, BT and AA; writing—original draft preparation, BT; writing—review and editing, JD and AA. All authors have read and agreed to the published version of the manuscript.

FUNDING

This work was supported by intramural funds of the National Center for Tumor Diseases Personalized Radiation Oncology Program (NCT PRO-2015.21) and the German Cancer Consortium (DKTK).

ACKNOWLEDGMENTS

We would like to thank Katrin Rein and Yara Falakha for their editorial assistance and help with the preparation of the graphical presentations.

SUPPLEMENTARY MATERIAL

The Supplementary Material for this article can be found online at: https://www.frontiersin.org/articles/10.3389/fphar.2021.753387/full#supplementary-material

REFERENCES

Adelstein, D. J., Li, Y., Adams, G. L., Wagner, H., Kish, J. A., Ensley, J. F., et al. (2003). An Intergroup Phase III Comparison of Standard Radiation Therapy and Two Schedules of Concurrent Chemoradiotherapy in Patients with Unresectable Squamous Cell Head and Neck Cancer. *J. Clin. Oncol.* 21, 92–98. doi:10.1200/JCO.2003.01.008

Ang, K. K., Harris, J., Wheeler, R., Weber, R., Rosenthal, D. I., Nguyen-Tân, P. F., et al. (2010). Human Papillomavirus and Survival of Patients with Oropharyngeal Cancer. *N. Engl. J. Med.* 363, 24–35. doi:10.1056/NEJMoa0912217

Balermpas, P., Rödel, F., Rödel, C., Krause, M., Linge, A., Lohaus, F., et al. (2016). CD8+ Tumour-Infiltrating Lymphocytes in Relation to HPV Status and Clinical Outcome in Patients with Head and Neck Cancer after Postoperative Chemoradiotherapy: A Multicentre Study of the German Cancer Consortium Radiation Oncology Group (DKTK-ROG). *Int. J. Cancer* 138, 171–181. doi:10.1002/ijc.29683

Beaty, B., Gupta, G. P., Shen, C., Amdur, R. J., Weiss, J., Grilley-Olson, J., et al. (2019). PIK3CA Mutation Is an Adverse Prognostic Factor in HPV-Associated Oropharynx Cancer. *J Natl Cancer Inst.* 105, S215. doi:10.1016/j.ijrobp.2019.06.295

Beaty, B. T., Moon, D. H., Shen, C. J., Amdur, R. J., Weiss, J., Grilley-Olson, J., et al. (2019). PIK3CA Mutation in HPV-Associated OPSCC Patients Receiving Deintensified Chemoradiation. *JNCI J. Natl. Cancer Inst.* 112, 855–858. doi:10.1093/jnci/djz224

Bentzen, S. M., and Trotti, A. (2007). Evaluation of Early and Late Toxicities in Chemoradiation Trials. *J. Clin. Oncol.* 25, 4096–4103. doi:10.1200/JCO.2007.13.3983

Bernier, J., Cooper, J. S., Pajak, T. F., van Glabbeke, M., Bourhis, J., Forastiere, A., et al. (2005). Defining Risk Levels in Locally Advanced Head and Neck Cancers: A Comparative Analysis of Concurrent Postoperative Radiation Plus Chemotherapy Trials of the EORTC (#22931) and RTOG (# 9501). *Head Neck* 27, 843–850. doi:10.1002/hed.20279

Bese, N. S., Hendry, J., and Jeremic, B. (2007). Effects of Prolongation of Overall Treatment Time Due to Unplanned Interruptions during Radiotherapy of Different Tumor Sites and Practical Methods for Compensation. *Int. J. Radiat. Oncol. Biol. Phys.* 68, 654–661. doi:10.1016/j.ijrobp.2007.03.010

Bonner, J. A., Harari, P. M., Giralt, J., Azarnia, N., Shin, D. M., Cohen, R. B., et al. (2006). Radiotherapy Plus Cetuximab for Squamous-Cell Carcinoma of the Head and Neck. *N. Engl. J. Med.* 354, 567–578. doi:10.1056/NEJMoa053422

Bourhis, J., Tao, Y., Sun, X., Sire, C., Martin, L., Liem, A., et al. (2021). Avelumab-cetuximab-radiotherapy versus Standards of Care in Patients with Locally Advanced Squamous Cell Carcinoma of Head and Neck (LA-SCCHN): Ran. OncologyPRO. *Ann. Oncol.* 32, S1283–S1346. Available at: https://oncologypro.esmo.org/meeting-resources/esmo-congress-2021/avelumab-cetuximab-radiotherapy-versus-standards-of-care-in-patients-with-locally-

advanced-squamous-cell-carcinoma-of-head-and-neck-la-scchn-ran (Accessed November 25, 2021). doi:10.1016/annonc/annonc741

Busch, C. J., Kriegs, M., Laban, S., Tribius, S., Knecht, R., Petersen, C., et al. (2013). HPV-positive HNSCC Cell Lines but Not Primary Human Fibroblasts Are Radiosensitized by the Inhibition of Chk1. *Radiother. Oncol.* 108, 495–499. doi:10.1016/J.RADONC.2013.06.035

Chen, A. M., Felix, C., Wang, P. C., Hsu, S., Basehart, V., Garst, J., et al. (2017). Reduced-dose Radiotherapy for Human Papillomavirus-Associated Squamous-Cell Carcinoma of the Oropharynx: a Single-Arm, Phase 2 Study. *Lancet Oncol.* 18, 803–811. doi:10.1016/S1470-2045(17)30246-2

Chera, B. S., Amdur, R. J., Green, R., Shen, C., Gupta, G., Tan, X., et al. (2019). Phase II Trial of De-intensified Chemoradiotherapy for Human Papillomavirus-Associated Oropharyngeal Squamous Cell Carcinoma. *J. Clin. Oncol.* 37, 2661–2669. doi:10.1200/JCO.19.01007

Chera, B. S., Kumar, S., Shen, C., Amdur, R., Dagan, R., Green, R., et al. (2020). Plasma Circulating Tumor HPV DNA for the Surveillance of Cancer Recurrence in HPV-Associated Oropharyngeal Cancer. *J. Clin. Oncol.* 38, 1050–1058. doi:10.1200/JCO.19.02444

Chera, B. S., Amdur, R. J., Tepper, J. E., Qaqish, B. F., Hayes, D. N., Weiss, J., et al. (2017). Two-year Clinical Outcomes of De-intensified Chemoradiotherapy for Low-Risk HPV-Associated Oropharyngeal Squamous Cell Carcinoma. *Jco* 35, 6044. doi:10.1200/JCO.2017.35.15_suppl.6044

Chiblak, S., Tang, Z., Lemke, D., Knoll, M., Dokic, I., Warta, R., et al. (2019). Carbon Irradiation Overcomes Glioma Radioresistance by Eradicating Stem Cells and Forming an Antiangiogenic and Immunopermissive Niche. *JCI Insight* 4, e123837. doi:10.1172/JCI.INSIGHT.123837

Christianen, M. E., Verdonck-de Leeuw, I. M., Doornaert, P., Chouvalova, O., Steenbakkers, R. J., Koken, P. W., et al. (2015). Patterns of Long-Term Swallowing Dysfunction after Definitive Radiotherapy or Chemoradiation. *Radiother. Oncol.* 117, 139–144. doi:10.1016/J.RADONC.2015.07.042

Cmelak, A. J., Li, S., Goldwasser, M. A., Murphy, B., Cannon, M., Pinto, H., et al. (2007). Phase II Trial of Chemoradiation for Organ Preservation in Resectable Stage III or IV Squamous Cell Carcinomas of the Larynx or Oropharynx: Results of Eastern Cooperative Oncology Group Study E2399. *J. Clin. Oncol.* 25, 3971–3977. doi:10.1200/JCO.2007.10.8951

Craig, S. G., Anderson, L. A., Schache, A. G., Moran, M., Graham, L., Currie, K., et al. (2019). Recommendations for Determining HPV Status in Patients with Oropharyngeal Cancers under TNM8 Guidelines: a Two-Tier Approach. *Br. J. Cancer* 120, 827–833. doi:10.1038/s41416-019-0414-9

Dahlstrom, K. R., Anderson, K. S., Cheng, J. N., Chowell, D., Li, G., Posner, M., et al. (2015). HPV Serum Antibodies as Predictors of Survival and Disease Progression in Patients with HPV-Positive Squamous Cell Carcinoma of the Oropharynx. *Clin. Cancer Res.* 21, 2861–2869. doi:10.1158/1078-0432.CCR-14-3323

Dahlstrom, K. R., Garden, A. S., William, W. N., Lim, M. Y., and Sturgis, E. M. (2016). Proposed Staging System for Patients with HPV-Related Oropharyngeal Cancer Based on Nasopharyngeal Cancer N Categories. *J. Clin. Oncol.* 34, 1848–1854. doi:10.1200/JCO.2015.64.6448

Dayyani, F., Etzel, C. J., Liu, M., Ho, C. H., Lippman, S. M., and Tsao, A. S. (2010). Meta-analysis of the Impact of Human Papillomavirus (HPV) on Cancer Risk and Overall Survival in Head and Neck Squamous Cell Carcinomas (HNSCC). *Head Neck Oncol.* 2, 15. doi:10.1186/1758-3284-2-15

Dok, R., Kalev, P., Van Limbergen, E. J., Asbagh, L. A., Vázquez, I., Hauben, E., et al. (2014). p16INK4a Impairs Homologous Recombination-Mediated DNA Repair in Human Papillomavirus-Positive Head and Neck Tumors. *Cancer Res.* 74, 1739–1751. doi:10.1158/0008-5472.CAN-13-2479

Doorbar, J., Egawa, N., Griffin, H., Kranjec, C., and Murakami, I. (2015). Human Papillomavirus Molecular Biology and Disease Association. *Rev. Med. Virol.* 25 Suppl 1 (Suppl. 1), 2–23. doi:10.1002/rmv.1822

Eisbruch, A., Kim, H. M., Feng, F. Y., Lyden, T. H., Haxer, M. J., Feng, M., et al. (2011). Chemo-IMRT of Oropharyngeal Cancer Aiming to Reduce Dysphagia: Swallowing Organs Late Complication Probabilities and Dosimetric Correlates. *Int. J. Radiat. Oncol. Biol. Phys.* 81, e93–9. doi:10.1016/J.IJROBP.2010.12.067

Eisbruch, A., Schwartz, M., Rasch, C., Vineberg, K., Damen, E., Van As, C. J., et al. (2004). Dysphagia and Aspiration after Chemoradiotherapy for Head-And-Neck Cancer: Which Anatomic Structures Are Affected and Can They Be Spared by IMRT. *Int. J. Radiat. Oncol. Biol. Phys.* 60, 1425–1439. doi:10.1016/j.ijrobp.2004.05.050

Fakhry, C., and Gillison, M. L. (2006). Clinical Implications of Human Papillomavirus in Head and Neck Cancers. *J. Clin. Oncol.* 24, 2606–2611. doi:10.1200/JCO.2006.06.1291

Fakhry, C., Westra, W. H., Li, S., Cmelak, A., Ridge, J. A., Pinto, H., et al. (2008). Improved Survival of Patients with Human Papillomavirus-Positive Head and Neck Squamous Cell Carcinoma in a Prospective Clinical Trial. *J. Natl. Cancer Inst.* 100, 261–269. doi:10.1093/jnci/djn011

Fakhry, C., Zhang, Q., Nguyen-Tan, P. F., Rosenthal, D., El-Naggar, A., Garden, A. S., et al. (2014). Human Papillomavirus and Overall Survival after Progression of Oropharyngeal Squamous Cell Carcinoma. *J. Clin. Oncol.* 32, 3365–3373. doi:10.1200/JCO.2014.55.1937

Fakhry, C., Blackford, A. L., Neuner, G., Xiao, W., Jiang, B., Agrawal, A., et al. (2019). Association of Oral Human Papillomavirus DNA Persistence with Cancer Progression after Primary Treatment for Oral Cavity and Oropharyngeal Squamous Cell Carcinoma. *JAMA Oncol.* 5, 985. doi:10.1001/jamaoncol.2019.0439

Feng, F. Y., Kim, H. M., Lyden, T. H., Haxer, M. J., Worden, F. P., Feng, M., et al. (2010). Intensity-modulated Chemoradiotherapy Aiming to Reduce Dysphagia in Patients with Oropharyngeal Cancer: Clinical and Functional Results. *J. Clin. Oncol.* 28, 2732–2738. doi:10.1200/JCO.2009.24.6199

Ferris, R. L., Flamand, Y., Weinstein, G. S., Li, S., Quon, H., Mehra, R., et al. (2021). Phase II Randomized Trial of Transoral Surgery and Low-Dose Intensity Modulated Radiation Therapy in Resectable P16+ Locally Advanced Oropharynx Cancer: An ECOG-ACRIN Cancer Research Group Trial (E3311). *J. Clin. Oncol.*, JCO2101752. doi:10.1200/JCO.21.01752

Ferris, R. L., Flamand, Y., Weinstein, G. S., Li, S., Quon, H., Mehra, R., et al. (2020). Transoral Robotic Surgical Resection Followed by Randomization to Low- or Standard-Dose IMRT in Resectable P16+ Locally Advanced Oropharynx Cancer: A Trial of the ECOG-ACRIN Cancer Research Group (E3311). *Jco* 38, 6500. doi:10.1200/jco.2020.38.15_suppl.6500

Garden, A. S., Harris, J., Trotti, A., Jones, C. U., Carrascosa, L., Cheng, J. D., et al. (2008). Long-Term Results of Concomitant Boost Radiation Plus Concurrent Cisplatin for Advanced Head and Neck Carcinomas: A Phase II Trial of the Radiation Therapy Oncology Group (RTOG 99-14). *Int. J. Radiat. Biol. Phys.* 71, 1351–1355. doi:10.1016/J.IJROBP.2008.04.006

Gillison, M. L., Trotti, A. M., Harris, J., Eisbruch, A., Harari, P. M., Adelstein, D. J., et al. (2019). Radiotherapy Plus Cetuximab or Cisplatin in Human Papillomavirus-Positive Oropharyngeal Cancer (NRG Oncology RTOG 1016): a Randomised, Multicentre, Non-inferiority Trial. *Lancet* 393, 40–50. doi:10.1016/S0140-6736(18)32779-X

Gillison, M. L., Zhang, Q., Jordan, R., Xiao, W., Westra, W. H., Trotti, A., et al. (2012). Tobacco Smoking and Increased Risk of Death and Progression for Patients with P16-Positive and P16-Negative Oropharyngeal Cancer. *J. Clin. Oncol.* 30, 2102–2111. doi:10.1200/JCO.2011.38.4099

Grégoire, V., Lefebvre, J. L., Licitra, L., and Felip, E.EHNS-ESMO-ESTRO Guidelines Working Group (2010). Squamous Cell Carcinoma of the Head and Neck: EHNS-ESMO-ESTRO Clinical Practice Guidelines for Diagnosis, Treatment and Follow-Up. *Ann. Oncol.* 21 Suppl. 5, v184–6. doi:10.1093/annonc/mdq185

Gunn, G. B., Blanchard, P., Garden, A. S., Zhu, X. R., Fuller, C. D., Mohamed, A. S., et al. (2016). Clinical Outcomes and Patterns of Disease Recurrence after Intensity Modulated Proton Therapy for Oropharyngeal Squamous Carcinoma. *Int. J. Radiat. Oncol. Biol. Phys.* 95, 360–367. doi:10.1016/j.ijrobp.2016.02.021

Hanna, G. J., Kacew, A., Chau, N. G., Shivdasani, P., Lorch, J. H., Uppaluri, R., et al. (2018). Improved Outcomes in PI3K-Pathway-Altered Metastatic HPV Oropharyngeal Cancer. *JCI Insight* 3, e12279. doi:10.1172/JCI.INSIGHT.122799

Hay, A., Migliacci, J., Karassawa Zanoni, D., Boyle, J. O., Singh, B., Wong, R. J., et al. (2017). Complications Following Transoral Robotic Surgery (TORS): A Detailed Institutional Review of Complications. *Oral Oncol.* 67, 160–166. doi:10.1016/j.oraloncology.2017.02.022

Herrero, R., Castellsagué, X., Pawlita, M., Lissowska, J., Kee, F., Balaram, P., et al. (2003). Human Papillomavirus and Oral Cancer: The International Agency for Research on Cancer Multicenter Study. *J. Natl. Cancer Inst.* 95, 1772–1783. doi:10.1093/jnci/djg107

Huang, S. H., Perez-Ordonez, B., Liu, F. F., Waldron, J., Ringash, J., Irish, J., et al. (2012). Atypical Clinical Behavior of P16-Confirmed HPV-Related Oropharyngeal Squamous Cell Carcinoma Treated with Radical

Radiotherapy. *Int. J. Radiat. Oncol. Biol. Phys.* 82, 276–283. doi:10.1016/J.IJROBP.2010.08.031

Huang, S. H., Perez-Ordonez, B., Weinreb, I., Hope, A., Massey, C., Waldron, J. N., et al. (2013). Natural Course of Distant Metastases Following Radiotherapy or Chemoradiotherapy in HPV-Related Oropharyngeal Cancer. *Oral Oncol.* 49, 79–85. Available at:https://www.sciencedirect.com/science/article/pii/S1368837512002436?via%3Dihub (Accessed September 13, 2018). doi:10.1016/j.oraloncology.2012.07.015

Huang, S. H., Xu, W., Waldron, J., Siu, L., Shen, X., Tong, L., et al. (2015). Refining American Joint Committee on Cancer/Union for International Cancer Control TNM Stage and Prognostic Groups for Human Papillomavirus-Related Oropharyngeal Carcinomas. *J. Clin. Oncol.* 33, 836–845. doi:10.1200/JCO.2014.58.6412

Hutcheson, K. A., Warneke, C. L., Yao, C. M. K. L., Zaveri, J., Elgohari, B. E., Goepfert, R., et al. (2019). Dysphagia after Primary Transoral Robotic Surgery with Neck Dissection vs Nonsurgical Therapy in Patients with Low- to Intermediate-Risk Oropharyngeal Cancer. *JAMA Otolaryngol. Head Neck Surg.* 145, 1053–1063. doi:10.1001/jamaoto.2019.2725

Kelly, J. R., Husain, Z. A., and Burtness, B. (2016). Treatment De-intensification Strategies for Head and Neck Cancer. *Eur. J. Cancer* 68, 125–133. doi:10.1016/j.ejca.2016.09.006

Kimple, R. J., Smith, M. A., Blitzer, G. C., Torres, A. D., Martin, J. A., Yang, R. Z., et al. (2013). Enhanced Radiation Sensitivity in HPV-Positive Head and Neck Cancer. *Cancer Res.* 73, 4791–4800. doi:10.1158/0008-5472.CAN-13-0587

Klein, C., Dokic, I., Mairani, A., Mein, S., Brons, S., Häring, P., et al. (2017). Overcoming Hypoxia-Induced Tumor Radioresistance in Non-small Cell Lung Cancer by Targeting DNA-dependent Protein Kinase in Combination with Carbon Ion Irradiation. *Radiat. Oncol.* 12, 208. doi:10.1186/s13014-017-0939-0

Kong, C. S., Narasimhan, B., Cao, H., Kwok, S., Erickson, J. P., Koong, A., et al. (2009). The Relationship between Human Papillomavirus Status and Other Molecular Prognostic Markers in Head and Neck Squamous Cell Carcinomas. *Int. J. Radiat. Oncol. Biol. Phys.* 74, 553–561. doi:10.1016/J.IJROBP.2009.02.015

Laban, S., Gangkofner, D. S., Holzinger, D., Schroeder, L., Eichmüller, S. B., Zörnig, I., et al. (2019). Antibody Responses to Cancer Antigens Identify Patients with a Poor Prognosis Among HPV-Positive and HPV-Negative Head and Neck Squamous Cell Carcinoma Patients. *Clin. Cancer Res.* 25, 7405–7412. doi:10.1158/1078-0432.CCR-19-1490

Langendijk, J. A., Doornaert, P., Rietveld, D. H., Verdonck-de Leeuw, I. M., Leemans, C. R., and Slotman, B. J. (2009). A Predictive Model for Swallowing Dysfunction after Curative Radiotherapy in Head and Neck Cancer. *Radiother. Oncol.* 90, 189–195. doi:10.1016/J.RADONC.2008.12.017

Lassen, P., Eriksen, J. G., Hamilton-Dutoit, S., Tramm, T., Alsner, J., and Overgaard, J. (2010). HPV-associated P16-Expression and Response to Hypoxic Modification of Radiotherapy in Head and Neck Cancer. *Radiother. Oncol.* 94, 30–35. doi:10.1016/J.RADONC.2009.10.008

Lassen, P., Overgaard, J., and Eriksen, J. G. (2013). Expression of EGFR and HPV-Associated P16 in Oropharyngeal Carcinoma: Correlation and Influence on Prognosis after Radiotherapy in the Randomized DAHANCA 5 and 7 Trials. *Radiother. Oncol.* 108, 489–494. doi:10.1016/j.radonc.2013.08.036

Lee, N., Schoder, H., Beattie, B., Lanning, R., Riaz, N., McBride, S., et al. (2016). Strategy of Using Intratreatment Hypoxia Imaging to Selectively and Safely Guide Radiation Dose De-escalation Concurrent with Chemotherapy for Locoregionally Advanced Human Papillomavirus-Related Oropharyngeal Carcinoma. *Int. J. Radiat. Oncol. Biol. Phys.* 96, 9–17. doi:10.1016/j.ijrobp.2016.04.027

Lee, N. Y., Ferris, R. L., Psyrri, A., Haddad, R. I., Tahara, M., Bourhis, J., et al. (2021). Avelumab Plus Standard-Of-Care Chemoradiotherapy versus Chemoradiotherapy Alone in Patients with Locally Advanced Squamous Cell Carcinoma of the Head and Neck: a Randomised, Double-Blind, Placebo-Controlled, Multicentre, Phase 3 Trial. *Lancet Oncol.* 22, 450–462. doi:10.1016/S1470-2045(20)30737-3

Levendag, P. C., Teguh, D. N., Voet, P., van der Est, H., Noever, I., de Kruijf, W. J., et al. (2007). Dysphagia Disorders in Patients with Cancer of the Oropharynx Are Significantly Affected by the Radiation Therapy Dose to the superior and Middle Constrictor Muscle: A Dose-Effect Relationship. *Radiother. Oncol.* 85, 64–73. doi:10.1016/j.radonc.2007.07.009

Lewis, J. S., Beadle, B., Bishop, J. A., Chernock, R. D., Colasacco, C., Lacchetti, C., et al. (2018). Human Papillomavirus Testing in Head and Neck Carcinomas: Guideline from the College of American Pathologists. *Arch. Pathol. Lab. Med.* 142, 559–597. doi:10.5858/arpa.2017-0286-CP

Lydiatt, W., O'Sullivan, B., and Patel, S. (2018). Major Changes in Head and Neck Staging for 2018. *Am. Soc. Clin. Oncol. Educ. Book.* 38, 505–514. doi:10.1200/EDBK_199697

Ma, D. J., Price, K. A., Moore, E. J., Patel, S. H., Hinni, M. L., Garcia, J. J., et al. (2019). Phase II Evaluation of Aggressive Dose De-escalation for Adjuvant Chemoradiotherapy in Human Papillomavirus-Associated Oropharynx Squamous Cell Carcinoma. *J. Clin. Oncol.* 37, 1909–1918. doi:10.1200/JCO.19.00463

Machtay, M., Moughan, J., Trotti, A., Garden, A. S., Weber, R. S., Cooper, J. S., et al. (2008). Factors Associated with Severe Late Toxicity after Concurrent Chemoradiation for Locally Advanced Head and Neck Cancer: an RTOG Analysis. *J. Clin. Oncol.* 26, 3582–3589. doi:10.1200/JCO.2007.14.8841

Marur, S., Li, S., Cmelak, A. J., Gillison, M. L., Zhao, W. J., Ferris, R. L., et al. (2017). E1308: Phase II Trial of Induction Chemotherapy Followed by Reduced-Dose Radiation and Weekly Cetuximab in Patients with HPV-Associated Resectable Squamous Cell Carcinoma of the Oropharynx- ECOG-ACRIN Cancer Research Group. *J. Clin. Oncol.* 35, 490–497. doi:10.1200/JCO.2016.68.3300

Masterson, L., Moualed, D., Liu, Z. W., Howard, J. E., Dwivedi, R. C., Tysome, J. R., et al. (2014). De-escalation Treatment Protocols for Human Papillomavirus-Associated Oropharyngeal Squamous Cell Carcinoma: a Systematic Review and Meta-Analysis of Current Clinical Trials. *Eur. J. Cancer* 50, 2636–2648. doi:10.1016/j.ejca.2014.07.001

Mehanna, H., Beech, T., Nicholson, T., El-Hariry, I., McConkey, C., Paleri, V., et al. (2013). Prevalence of Human Papillomavirus in Oropharyngeal and Nonoropharyngeal Head and Neck Cancer-Ssystematic Review and Meta-Analysis of Trends by Time and Region. *Head Neck* 35, 747–755. doi:10.1002/hed.22015

Mehanna, H., Robinson, M., Hartley, A., Kong, A., Foran, B., Fulton-Lieuw, T., et al. (2019). Radiotherapy Plus Cisplatin or Cetuximab in Low-Risk Human Papillomavirus-Positive Oropharyngeal Cancer (De-ESCALaTE HPV): an Open-Label Randomised Controlled Phase 3 Trial. *Lancet* 393, 51–60. doi:10.1016/S0140-6736(18)32752-1

Mirghani, H., and Blanchard, P. (2018). Treatment De-escalation for HPV-Driven Oropharyngeal Cancer: Where Do We Stand. *Clin. Transl. Radiat. Oncol.* 8, 4–11. doi:10.1016/j.ctro.2017.10.005

Mirghani, H., Amen, F., Blanchard, P., Moreau, F., Guigay, J., Hartl, D. M., et al. (2015a). Treatment De-escalation in HPV-Positive Oropharyngeal Carcinoma: Ongoing Trials, Critical Issues and Perspectives. *Int. J. Cancer* 136, 1494–1503. doi:10.1002/ijc.28847

Mirghani, H., Casiraghi, O., Amen, F., He, M., Ma, X. J., Saulnier, P., et al. (2015b). Diagnosis of HPV-Driven Head and Neck Cancer with a Single Test in Routine Clinical Practice. *Mod. Pathol.* 28, 1518–1527. doi:10.1038/modpathol.2015.113

Misiukiewicz, K., Gupta, V., Miles, B. A., Bakst, R., Genden, E., Selkridge, I., et al. (2019). Standard of Care vs Reduced-Dose Chemoradiation after Induction Chemotherapy in HPV+ Oropharyngeal Carcinoma Patients: The Quarterback Trial. *Oral Oncol.* 95, 170–177. doi:10.1016/J.ORALONCOLOGY.2019.06.021

Mortensen, L. S., Johansen, J., Kallehauge, J., Primdahl, H., Busk, M., Lassen, P., et al. (2012). FAZA PET/CT Hypoxia Imaging in Patients with Squamous Cell Carcinoma of the Head and Neck Treated with Radiotherapy: Results from the DAHANCA 24 Trial. *Radiother. Oncol.* 105, 14–20. doi:10.1016/J.RADONC.2012.09.015

Münger, K., Baldwin, A., Edwards, K. M., Hayakawa, H., Nguyen, C. L., Owens, M., et al. (2004). Mechanisms of Human Papillomavirus-Induced Oncogenesis. *J. Virol.* 78, 11451–11460. doi:10.1128/JVI.78.21.11451-11460.2004

NCT01687413 (2012). Post Operative Adjuvant Therapy De-intensification Trial for Human Papillomavirus-Related, P16 + Oropharynx Cancer—ClinicalTrials.Gov. Available at: https://clinicaltrials.gov/ct2/show/NCT01687413 (Accessed December 26, 2019)

NCT01898494 (2013). Transoral Surgery Followed by Low-Dose or Standard-Dose Radiation Therapy with or without Chemotherapy in Treating Patients with HPV Positive Stage III-IVA Oropharyngeal Cancer. Available at: https://clinicaltrials.gov/ct2/show/NCT01898494 (Accessed December 26, 2019).

NCT02764593 (2016). Safety Testing of Adding Nivolumab to Chemotherapy in Patients with Intermediate and High-Risk Local-Regionally Advanced Head and Neck Cancer - Full Text View - ClinicalTrials.Gov. Available at: https://clinicaltrials.gov/ct2/show/NCT02764593 (Accessed December 21, 2019).

NCT02908477 (2016). Evaluation of De-escalated Adjuvant Radiation Therapy for Human Papillomavirus (HPV)-Associated Oropharynx Cancer - Full Text View - ClinicalTrials.Gov. Available at: https://clinicaltrials.gov/ct2/show/NCT02908477 (Accessed December 26, 2019).

NCT03396718 (2018). De-escalation of Adjuvant Radio (Chemo) Therapy for HPV-Positive Head-Neck Squamous Cell Carcinomas. Available at: https://clinicaltrials.gov/ct2/show/NCT03396718 (Accessed July 26, 2021).

NCT03715946 (2018). Adjuvant De-escalated Radiation + Adjuvant Nivolumab for Intermediate-High Risk P16+ Oropharynx Cancer - ClinicalTrials.Gov. Available at: https://clinicaltrials.gov/ct2/show/NCT03715946 (Accessed December 21, 2019).

NCT03799445 (2019). Ipilimumab, Nivolumab, and Radiation Therapy in Treating Patients with HPV Positive Advanced Oropharyngeal Squamous Cell Carcinoma - ClinicalTrials.Gov. Available at: https://clinicaltrials.gov/ct2/show/NCT03799445 (Accessed December 21, 2019).

NCT03952585 (2019). De-intensified Radiation Therapy with Chemotherapy (Cisplatin) or Immunotherapy (Nivolumab) in Treating Patients with Early-Stage, HPV-Positive, Non-smoking Associated Oropharyngeal Cancer - ClinicalTrials.Gov. Available at: https://clinicaltrials.gov/ct2/show/NCT03952585 (Accessed December 21, 2019).

Nelson, H. H., Pawlita, M., Michaud, D. S., McClean, M., Langevin, S. M., Eliot, M. N., et al. (2017). Immune Response to HPV16 E6 and E7 Proteins and Patient Outcomes in Head and Neck Cancer. *JAMA Oncol.* 3, 178–185. doi:10.1001/jamaoncol.2016.4500

Nguyen, N. P., Moltz, C. C., Frank, C., Vos, P., Smith, H. J., Karlsson, U., et al. (2006). Evolution of Chronic Dysphagia Following Treatment for Head and Neck Cancer. *Oral Oncol.* 42, 374–380. doi:10.1016/J.ORALONCOLOGY.2005.09.003

Nguyen, N. P., Sallah, S., Karlsson, U., and Antoine, J. E. (2002). Combined Chemotherapy and Radiation Therapy for Head and Neck Malignancies: Quality of Life Issues. *Cancer* 94, 1131–1141. doi:10.1002/cncr.10257

Nichols, A. C., Lang, P., Prisman, E., Berthelet, E., Tran, E., Hamilton, S., et al. (2020). Treatment De-escalation for HPV-Associated Oropharyngeal Squamous Cell Carcinoma with Radiotherapy vs. Trans-oral Surgery (ORATOR2): Study Protocol for a Randomized Phase II Trial. *BMC Cancer* 20, 125. doi:10.1186/s12885-020-6607-z

Nichols, A. C., Theurer, J., Prisman, E., Read, N., Berthelet, E., Tran, E., et al. (2019). Radiotherapy versus Transoral Robotic Surgery and Neck Dissection for Oropharyngeal Squamous Cell Carcinoma (ORATOR): an Open-Label, Phase 2, Randomised Trial. *Lancet Oncol.* 20, 1349–1359. doi:10.1016/S1470-2045(19)30410-3

O'Sullivan, B., Huang, S. H., Su, J., Garden, A. S., Sturgis, E. M., Dahlstrom, K., et al. (2016). Development and Validation of a Staging System for HPV-Related Oropharyngeal Cancer by the International Collaboration on Oropharyngeal Cancer Network for Staging (ICON-S): a Multicentre Cohort Study. *Lancet Oncol.* 17, 440–451. doi:10.1016/S1470-2045(15)00560-4

Owadally, W., Hurt, C., Timmins, H., Parsons, E., Townsend, S., Patterson, J., et al. (2015). PATHOS: a Phase II/III Trial of Risk-Stratified, Reduced Intensity Adjuvant Treatment in Patients Undergoing Transoral Surgery for Human Papillomavirus (HPV) Positive Oropharyngeal Cancer. *BMC Cancer* 15, 602. doi:10.1186/s12885-015-1598-x

Palma, D. A., Prisman, E., Berthelet, E., Tran, E., Hamilton, S. N., Wu, J., et al. (2021). A Randomized Trial of Radiotherapy vs. Trans-oral Surgery for Treatment De-escalation in HPV-Associated Oropharyngeal Squamous Cell Carcinoma (ORATOR2). *Int. J. Radiat. Oncology*Biology*Physics* 111, 1324–1325. doi:10.1016/J.IJROBP.2021.09.013

Parsons, J. T., Mendenhall, W. M., Stringer, S. P., Amdur, R. J., Hinerman, R. W., Villaret, D. B., et al. (2002). Squamous Cell Carcinoma of the Oropharynx: Surgery, Radiation Therapy, or Both. *Cancer* 94, 2967–2980. doi:10.1002/cncr.10567

Patel, M. A., Blackford, A. L., Rettig, E. M., Richmon, J. D., Eisele, D. W., and Fakhry, C. (2016). Rising Population of Survivors of Oral Squamous Cell Cancer in the United States. *Cancer* 122, 1380–1387. doi:10.1002/cncr.29921

Pignon, J. P., le Maître, A., Maillard, E., Bourhis, J., and Mach-Nc Collaborative Group, M.-N. C. (2009). Meta-analysis of Chemotherapy in Head and Neck Cancer (MACH-NC): An Update on 93 Randomised Trials and 17,346 Patients. *Radiother. Oncol.* 92, 4–14. doi:10.1016/j.radonc.2009.04.014

Prigge, E. S., Arbyn, M., von Knebel Doeberitz, M., and Reuschenbach, M. (2017). Diagnostic Accuracy of p16INK4a Immunohistochemistry in Oropharyngeal Squamous Cell Carcinomas: A Systematic Review and Meta-Analysis. *Int. J. Cancer* 140, 1186–1198. doi:10.1002/ijc.30516

Psyrri, A., Rampias, T., and Vermorken, J. B. (2014). The Current and Future Impact of Human Papillomavirus on Treatment of Squamous Cell Carcinoma of the Head and Neck. *Ann. Oncol.* 25, 2101–2115. doi:10.1093/annonc/mdu265

Ragin, C. C., Modugno, F., and Gollin, S. M. (2007). The Epidemiology and Risk Factors of Head and Neck Cancer: a Focus on Human Papillomavirus. *J. Dent. Res.* 86, 104–114. doi:10.1177/154405910708600202

Ragin, C. C., and Taioli, E. (2007). Survival of Squamous Cell Carcinoma of the Head and Neck in Relation to Human Papillomavirus Infection: Review and Meta-Analysis. *Int. J. Cancer* 121, 1813–1820. doi:10.1002/ijc.22851

Ramaekers, B. L., Joore, M. A., Grutters, J. P., van den Ende, P., Jong, Jd., Houben, R., et al. (2011). The Impact of Late Treatment-Toxicity on Generic Health-Related Quality of Life in Head and Neck Cancer Patients after Radiotherapy. *Oral Oncol.* 47, 768–774. doi:10.1016/J.ORALONCOLOGY.2011.05.012

Rayess, H., Wang, M. B., and Srivatsan, E. S. (2012). Cellular Senescence and Tumor Suppressor Gene P16. *Int. J. Cancer* 130, 1715–1725. doi:10.1002/ijc.27316

Rieckmann, T., Tribius, S., Grob, T. J., Meyer, F., Busch, C. J., Petersen, C., et al. (2013). HNSCC Cell Lines Positive for HPV and P16 Possess Higher Cellular Radiosensitivity Due to an Impaired DSB Repair Capacity. *Radiother. Oncol.* 107, 242–246. doi:10.1016/J.RADONC.2013.03.013

Rietbergen, M. M., Brakenhoff, R. H., Bloemena, E., Witte, B. I., Snijders, P. J., Heideman, D. A., et al. (2013). Human Papillomavirus Detection and Comorbidity: Critical Issues in Selection of Patients with Oropharyngeal Cancer for Treatment De-escalation Trials. *Ann. Oncol.* 24, 2740–2745. doi:10.1093/annonc/mdt319

Rietbergen, M. M., Snijders, P. J., Beekzada, D., Braakhuis, B. J., Brink, A., Heideman, D. A., et al. (2014). Molecular Characterization of P16-Immunopositive but HPV DNA-Negative Oropharyngeal Carcinomas. *Int. J. Cancer* 134, 2366–2372. doi:10.1002/ijc.28580

Rischin, D., King, M., Kenny, L., Porceddu, S., Wratten, C., Macann, A., et al. (2021). Randomized Trial of Radiation Therapy with Weekly Cisplatin or Cetuximab in Low-Risk HPV-Associated Oropharyngeal Cancer (TROG 12.01) - A Trans-tasman Radiation Oncology Group Study. *Int. J. Radiat. Oncol. Biol. Phys.* 111, 876–886. doi:10.1016/J.IJROBP.2021.04.015

Rischin, D., Young, R. J., Fisher, R., Fox, S. B., Le, Q. T., Peters, L. J., et al. (2010). Prognostic Significance of p16INK4A and Human Papillomavirus in Patients with Oropharyngeal Cancer Treated on TROG 02.02 Phase III Trial. *J. Clin. Oncol.* 28, 4142–4148. doi:10.1200/JCO.2010.29.2904

Rosenthal, D. I., Harari, P. M., Giralt, J., Bell, D., Raben, D., Liu, J., et al. (2016). Association of Human Papillomavirus and P16 Status with Outcomes in the IMCL-9815 Phase III Registration Trial for Patients with Locoregionally Advanced Oropharyngeal Squamous Cell Carcinoma of the Head and Neck Treated with Radiotherapy with or without Cetuximab. *J. Clin. Oncol.* 34, 1300–1308. doi:10.1200/JCO.2015.62.5970

Rosenthal, D. I., Mendoza, T. R., Fuller, C. D., Hutcheson, K. A., Wang, X. S., Hanna, E. Y., et al. (2014). Patterns of Symptom burden during Radiotherapy or Concurrent Chemoradiotherapy for Head and Neck Cancer: A Prospective Analysis Using the University of Texas MD Anderson Cancer Center Symptom Inventory-Head and Neck Module. *Cancer* 120, 1975–1984. doi:10.1002/cncr.28672

Sadeghi, N., Khalife, S., Mascarella, M. A., Ramanakumar, A. V., Richardson, K., Joshi, A. S., et al. (2019). Pathologic Response to Neoadjuvant Chemotherapy in HPV-associated Oropharynx Cancer. *Head Neck* 42, 417–425. doi:10.1002/hed.26022

Schache, A. G., Liloglou, T., Risk, J. M., Filia, A., Jones, T. M., Sheard, J., et al. (2011). Evaluation of Human Papilloma Virus Diagnostic Testing in Oropharyngeal Squamous Cell Carcinoma: Sensitivity, Specificity, and Prognostic Discrimination. *Clin. Cancer Res.* 17, 6262–6271. doi:10.1158/1078-0432.CCR-11-0388

Seiwert, T. Y., Foster, C. C., Blair, E. A., Karrison, T. G., Agrawal, N., Melotek, J. M., et al. (2019). OPTIMA: a Phase II Dose and Volume De-escalation Trial for Human Papillomavirus-Positive Oropharyngeal Cancer. *Ann. Oncol.* 30, 297–302. doi:10.1093/annonc/mdy522

Senkomago, V., Henley, S. J., Thomas, C. C., Mix, J. M., Markowitz, L. E., and Saraiya, M. (2019). Human Papillomavirus-Attributable Cancers - United States, 2012-2016. *MMWR Morb Mortal Wkly Rep.* 68, 724–728. doi:10.15585/MMWR.MM6833A3

Sethia, R., Yumusakhuylu, A. C., Ozbay, I., Diavolitsis, V., Brown, N. V., Zhao, S., et al. (2018). Quality of Life Outcomes of Transoral Robotic Surgery with or without Adjuvant Therapy for Oropharyngeal Cancer. *Laryngoscope* 128, 403–411. doi:10.1002/lary.26796

Shi, W., Kato, H., Perez-Ordonez, B., Pintilie, M., Huang, S., Hui, A., et al. (2009). Comparative Prognostic Value of HPV16 E6 mRNA Compared with *In Situ* Hybridization for Human Oropharyngeal Squamous Carcinoma. *J. Clin. Oncol.* 27, 6213–6221. doi:10.1200/JCO.2009.23.1670

Shinn, J. R., Davis, S. J., Lang-Kuhs, K. A., Rohde, S., Wang, X., Liu, P., et al. (2021). Oropharyngeal Squamous Cell Carcinoma with Discordant P16 and HPV mRNA Results: Incidence and Characterization in a Large, Contemporary United States Cohort. *Am. J. Surg. Pathol.* 45, 951–961. doi:10.1097/PAS.0000000000001685

Singhi, A. D., and Westra, W. H. (2010). Comparison of Human Papillomavirus *In Situ* Hybridization and P16 Immunohistochemistry in the Detection of Human Papillomavirus-Associated Head and Neck Cancer Based on a Prospective Clinical Experience. *Cancer* 116, 2166–2173. doi:10.1002/cncr.25033

Spreafico, A., Sultanem, K., Chen, B., Bratman, S. V., Ringash, J., Louie, A. V., et al. (2018). A Randomized Phase II Study of Cisplatin Plus Radiotherapy versus Durvalumab Plus Radiotherapy Followed by Adjuvant Durvalumab versus Durvalumab Plus Radiotherapy Followed by Adjuvant Tremelimumab and Durvalumab in Intermediate Risk, HPV-Positive, Locoregionally Advanced Oropharyngeal Squamous Cell Cancer (LA-OSCC) (Canadian Cancer Trials Group HN.9). *Ann. Oncol.* 29, viii399. doi:10.1093/annonc/mdy287.080

Stokes, W., Ramadan, J., Lawson, G., Ferris, F. R. L., Holsinger, F. C., and Turner, M. T. (2021). Bleeding Complications after Transoral Robotic Surgery: A Meta-Analysis and Systematic Review. *Laryngoscope* 131, 95–105. doi:10.1002/lary.28580

Tanaka, H., Suzuki, M., Takemoto, N., Fukusumi, T., Eguchi, H., Takai, E., et al. (2022). Performance of Oral HPV DNA, Oral HPV mRNA and Circulating Tumor HPV DNA in the Detection of HPV-Related Oropharyngeal Cancer and Cancer of Unknown Primary. *Int. J. Cancer* 150, 174–186. doi:10.1002/IJC.33798

Toustrup, K., Sørensen, B. S., Lassen, P., Wiuf, C., Alsner, J., and Overgaard, J. (2012). Gene Expression Classifier Predicts for Hypoxic Modification of Radiotherapy with Nimorazole in Squamous Cell Carcinomas of the Head and Neck. *Radiother. Oncol.* 102, 122–129. doi:10.1016/J.RADONC.2011.09.010

Trotti, A. (2000). Toxicity in Head and Neck Cancer: a Review of Trends and Issues. *Int. J. Radiat. Oncol. Biol. Phys.* 47, 1–12. doi:10.1016/s0360-3016(99)00558-1

Venuti, A., and Paolini, F. (2012). HPV Detection Methods in Head and Neck Cancer. *Head Neck Pathol.* 6 Suppl. 1, S63–S74. doi:10.1007/s12105-012-0372-5

Wirth, L. J., Burtness, B., Nathan, C. O., Grégoire, V., and Richmon, J. (2019). Point/Counterpoint: Do We De-escalate Treatment of HPV-Associated Oropharynx Cancer Now? and How. *Am. Soc. Clin. Oncol. Educ. Book* 39, 364–372. doi:10.1200/EDBK_238315

Yom, S. S., Torres-Saavedra, P., Caudell, J. J., Waldron, J. N., Gillison, M. L., Xia, P., et al. (2021). Reduced-Dose Radiation Therapy for HPV-Associated Oropharyngeal Carcinoma (NRG Oncology HN002). *J. Clin. Oncol.* 39, 956–965. doi:10.1200/JCO.20.03128

Zhan, K. Y., Eskander, A., Kang, S. Y., Old, M. O., Ozer, E., Agrawal, A. A., et al. (2017). Appraisal of the AJCC 8th Edition Pathologic Staging Modifications for HPV-Positive Oropharyngeal Cancer, a Study of the National Cancer Data Base. *Oral Oncol.* 73, 152–159. doi:10.1016/J.ORALONCOLOGY.2017.08.020

Conflict of Interest: BT: None to report. JD: Research Grant; Siemens Health Care GmbH, Solution Akademia Gmbh, Viewray Inc., CRI The Clinical Research Institute GmbH, Accuray International Sari, RaySearch Laboratories AB, Vision RT Limited, Merck Serono GmbH, Astellas Pharma GmbH, Astra Zeneca GmbH, Egomed PLC Surrey Research Park, Quintiles GmbH, Pharmaceutical Research Associates Gm. AA: Research Grant; Merck KGaA, FibroGen, Bayer. Consulting or Advisory Role; Roche, Merck KGaA, Merck Serono, FibroGen, BMS Brazil, Bayer Health.

Publisher's Note: All claims expressed in this article are solely those of the authors and do not necessarily represent those of their affiliated organizations, or those of the publisher, the editors, and the reviewers. Any product that may be evaluated in this article, or claim that may be made by its manufacturer, is not guaranteed or endorsed by the publisher.

Copyright © 2022 Tawk, Debus and Abdollahi. This is an open-access article distributed under the terms of the Creative Commons Attribution License (CC BY). The use, distribution or reproduction in other forums is permitted, provided the original author(s) and the copyright owner(s) are credited and that the original publication in this journal is cited, in accordance with accepted academic practice. No use, distribution or reproduction is permitted which does not comply with these terms.

frontiers in Pharmacology

REVIEW
published: 20 January 2022
doi: 10.3389/fphar.2021.747895

Molecular Targets for Novel Therapeutics in Pediatric Fusion-Positive Non-CNS Solid Tumors

Wen-I Chang[1,2,3]*, *Claire Lin*[1], *Nicholas Liguori*[1], *Joshua N. Honeyman*[1,3,4], *Bradley DeNardo*[2,3] and *Wafik El-Deiry*[1,3,5,6,7]*

[1]Laboratory of Translational Oncology and Experimental Cancer Therapeutics, The Warren Alpert Medical School, Brown University, Providence, RI, United States, [2]Pediatric Hematology/Oncology, The Warren Alpert Medical School, Brown University, Providence, RI, United States, [3]The Joint Program in Cancer Biology, Brown University and Lifespan Health System, Providence, RI, United States, [4]Pediatric Surgery, The Warren Alpert Medical School, Brown University, Providence, RI, United States, [5]Department of Pathology and Laboratory Medicine, The Warren Alpert Medical School, Brown University, Providence, RI, United States, [6]Cancer Center at Brown University, The Warren Alpert Medical School, Brown University, Providence, RI, United States, [7]Hematology/Oncology Division, Department of Medicine, Lifespan Health System and Brown University, Providence, RI, United States

OPEN ACCESS

Edited by:
Anne Lorant, Laboratoire de Biologie Moléculaire et Cellulaire du Cancer (LBMCC), Luxembourg

Reviewed by:
Lawrence Panasci, Segal Cancer Centre, Canada
Pankaj Pathak, National Institutes of Health (NIH), United States

***Correspondence:**
Wen-I Chang
wen-i_chang@brown.edu
Wafik El-Deiry
wafik@brown.edu

Specialty section:
This article was submitted to Pharmacology of Anti-Cancer Drugs, a section of the journal Frontiers in Pharmacology

Received: *27 July 2021*
Accepted: *03 December 2021*
Published: *20 January 2022*

Citation:
Chang W-I, Lin C, Liguori N, Honeyman JN, DeNardo B and El-Deiry W (2022) Molecular Targets for Novel Therapeutics in Pediatric Fusion-Positive Non-CNS Solid Tumors. Front. Pharmacol. 12:747895. doi: 10.3389/fphar.2021.747895

Chromosomal fusions encoding novel molecular drivers have been identified in several solid tumors, and in recent years the identification of such pathogenetic events in tumor specimens has become clinically actionable. Pediatric sarcomas and other rare tumors that occur in children as well as adults are a group of heterogeneous tumors often with driver gene fusions for which some therapeutics have already been developed and approved, and others where there is opportunity for progress and innovation to impact on patient outcomes. We review the chromosomal rearrangements that represent oncogenic events in pediatric solid tumors outside of the central nervous system (CNS), such as Ewing Sarcoma, Rhabdomyosarcoma, Fibrolamellar Hepatocellular Carcinoma, and Renal Cell Carcinoma, among others. Various therapeutics such as CDK4/6, FGFR, ALK, VEGF, EGFR, PDGFR, NTRK, PARP, mTOR, BRAF, IGF1R, HDAC inhibitors are being explored among other novel therapeutic strategies such as ONC201/TIC10.

Keywords: sarcoma, pediatric, fusion-positive, molecular targets, solid tumors

INTRODUCTION

Pediatric cancer rates have been rising the past few decades, and approximately 400,000 new cases are diagnosed globally each year (Ward et al., 2019a). While the overall 5-year survival rate for pediatric oncology patients in the United States is 84%, outcomes are generally worse in pediatric solid tumors outside of the central nervous system (CNS), especially in cases of up-front metastases, recurrence, or progressive disease (Siegel et al., 2020). Pediatric sarcomas account for approximately 10% of all childhood tumors, and include both soft tissue and bone-related tumors. Pediatric carcinomas, including liver tumors such as fibrolamellar hepatocellular carcinoma, are less common. Of all pediatric sarcoma patients, recurrence occurs in 30–40% of cases, with patients facing poor event-free survival odds after relapse (Stahl et al., 2011; Duchman et al., 2015; Smeland et al., 2019). Similarly, pediatric carcinoma patients who present

with up-front metastasis can have an overall survival rate of less than 20% (Schmid and von Schweinitz, 2017).

A subset of extra-cranial pediatric solid tumors are fusion-positive tumors, which are characterized by abnormal chromosomal rearrangements (e.g., translocations, insertions, inversions, and deletions) that result in the fusion of two disparate genes. Fusion genes can lead to constitutively activated oncogenes when a proto-oncogene is upregulated by the promoter and activator sequences of the partner gene in the fusion (Dupain et al., 2017). Additionally, the encoded chimeric oncoprotein can act as an aberrant transcription factor, driving downstream activation of pathways involved in tumorigenesis. Gene fusions may also result in deletion of tumor-suppressor genes, allowing for cancer cell transformation (Dupain et al., 2017).

In the past few decades, detection of these fusions has been of great interest in both basic cancer research and in the clinical setting, as fusions can be used as diagnostic markers, prognostic indicators, and therapeutic targets in the treatment of disease (**Table 1**). Clinical utility with screening fusion panels in pediatric solid tumors and hematological malignancies has been previously demonstrated, highlighting the need for targeted therapies in fusion-positive pediatric cancers (Chang et al., 2019).

Current therapeutic strategies focus on decreasing long-term treatment toxicity while maintaining excellent outcomes for low-risk patients, while improving outcomes for high-risk patients, often through treatment intensification. In pediatric solid tumors, the combination of cytotoxic chemotherapy, radiation, and surgery has been the standard in pediatric patients for over 2 decades. With the advent of precision medicine, and subsequent increasing understanding of molecular drivers of disease, such as fusion oncogenes, emphasis is currently placed on investigating targeted treatment options.

EWING SARCOMA

Ewing Sarcoma (ES) is the second most common pediatric bone cancer. ES tumors are thought to arise from mesenchymal progenitor cells in bones and soft tissues in both children and adolescents. ES is most frequently driven by the fusion of a FET/TET family of RNA-binding proteins and an ETS family of transcription factors, with approximately 85–90% of ES cases harboring a common *EWSR1-FLI1* fusion (Brohl et al., 2014). These tumors have relatively quiet genome with a low mutational burden, as most of the tumors only have fusion gene rearrangements identified. *STAG2* loss is identified in 15% of ES (Brohl et al., 2014). There is inconsistent information about whether mutations in *STAG2*, *CDKN2A* and *TP53* lead to less favorable prognoses (Honoki et al., 2007; Brohl et al., 2014; Lerman et al., 2015; Brohl et al., 2017).

ES disease progression can be further monitored using a liquid biopsy technique (Hayashi et al., 2016). Liquid biopsies detect circulating tumor DNA (ctDNA) in the peripheral blood. There are promising initial results using capture based next generation sequencing or digital droplet PCR to function as a disease monitoring tool. Circulating tumor DNA has been shown to be effective at detecting disease. One study of ctDNA in the blood found detectable levels in 53% patients tested (Shulman et al., 2018). Detectable ctDNA is associated with inferior outcomes in these patients and can inform how to proceed with management of the disease (Shulman et al., 2018).

Treatment of ES is *via* a three-pronged approach. Surgery, radiation, and chemotherapy are the mainstays of up-front therapy in ES. Surgery to remove the tumor requires a wide resection (Adzhubei et al., 2010). ES has also expressed sensitivity to radiation therapies in attempts to treat and manage the disease (Ewing, 19211972). It is possible to use radiation therapies as definitive local control for inoperable tumors and radiation may also be used pre- or post-operatively to combat tumor progression or in the setting of marginal or intralesional resection (Zöllner et al., 2021). The optimal utilization of radiation therapy is unclear prior to surgery, but the benefit can be significant (Zöllner et al., 2021). This multimodal treatment strategy of combining cytotoxic chemotherapy with radiation and/or surgery has resulted in a 5-year survival rate of 65–75% in patients with localized disease. In addition, patients with metastatic disease suffer from a survival rate of less than 30% with no appreciable improvements over the past 30 years (Gaspar et al., 2015).

The EWSR1-FLI1 oncoprotein acts as an aberrant transcription factor that binds to the canonical ETS binding site and GGAA microsatellite sequences, thereby deregulating cell cycle genes involved in checkpoint control. Genes regulating cell function, cell migration, signal transduction, and chromatin structure are also affected, leading to malignant transformation.

Several studies have shown the oncogenic effect of the *EWSR1-FLI1* fusion, as inhibition of ES cell growth occurs when the EWSR1-FLI1 fusion protein is depleted (Herrero-Martín et al., 2009). This makes for a valuable target for therapies aimed at treating this disease. Despite being recognized as a valuable therapeutic target over 25 years ago, there have been relatively few steps towards inhibiting its tumorigenic characteristics.

Lysine-specific histone demethylase 1 (LSD1) is a part of the nucleosome remodeling and deacetylase (NuRD) co-repressor complex. It is recruited by *EWSR1-FLI1* to regulate transcription. *In vitro* and *in vivo* experiments with LSD1 inhibition have resulted in reversal of the EWSR1-FLI1 oncogenic activity (Sankar et al., 2013; Sankar et al., 2014). Several of the LSD1 inhibitors have begun to enter clinical trials.

The insulin-like growth factor 1 receptor (IGF-1R) pathway is deregulated by the *EWSR1-FLI1* translocation and is an exciting potential target for targeted therapies. There are currently trials ongoing that display at least a partial response in 11.7% of participants, when the IGF-1R inhibitor is administered alone or in combination (van Maldegem et al., 2016). However, a phase II trial combining an IGF-1R inhibitor with an mTOR inhibitor did not show any benefit (Malempati et al., 2012).

The poly (ADP-ribose) polymerase (PARP) pathway is essential for detection of DNA repair and detection of DNA stand breakage in tumor cells. A phase II trial examined 12 patients with ES who were administered 400 mg of oral olaparib, a PARP inhibitor, twice, daily (Choy et al., 2014). While there were no significant toxicities to report, tumor response was not seen in any of the 12 patients, although four of the 12 patients reported stable disease with a

TABLE 1 | Different gene fusions and their corresponding tumor and current significance(s).

Gene fusion	Tumor	Significance
EWS-FLI1	Ewing sarcoma	Prognostic de Alava et al. (2000) Direct therapeutic target García-Domínguez et al. (2018), Spriano et al. (2019)
PAX-FOXO1	Alveolar rhabdomyosarcoma	Diagnostic Wexler and Ladanyi (2010) Prognostic Arnold and Barr (2017)
ETV6-NRTK3	Infantile fibrosarcoma	Diagnostic Bourgeois et al. (2000) Direct therapeutic target Dunn (2020)
TFE3-ASPSCR1	Alveolar soft part sarcoma	Diagnostic Aulmann et al. (2007)
Fusion partner-*ALK*	Inflammatory myofibroblastic tumor	Diagnostic Cook et al. (2001) Direct therapeutic target Trahair et al. (2019), Fordham et al. (2020)
DNAJB1-PRKACA	Fibrolamellar hepatocellular carcinoma	Diagnostic Honeyman et al. (2014)
Fusion partner-*TFE3*	Renal cell carcinoma	Diagnostic Akgul et al. (2021)
SS18-SSX	Synovial sarcoma	Diagnostic Clark et al. (1994), Shipley et al. (1994)
EWS-WT1	Desmoplastic small round cell tumors (DSRCT)	Diagnostic Ladanyi and Gerald (1994)
EWS-ATF1	Clear cell sarcoma	Diagnostic Antonescu et al. (2002)

median time for progression-free survival (PFS) of 5.7 weeks (Choy et al., 2014). Additionally, there is an open clinical study ongoing testing the PARP inhibitor niraparib to refine dosing and determine dose-limiting toxicities. Similarly, this trial also evaluates escalating doses of temozolomide and/or irinotecan in patients who have recurrent or progressive Ewing Sarcoma that has failed previous treatment (clinicaltrials.gov, NCT 02044120).

There is optimism in a novel ES treatment that focuses on the combination of epigenetic drugs vorinostat and HCI-2509 to inhibit EWSR1-FLI1 and suppress tumor growth. This study analyzed proliferation and cell viability in ES cell lines, showing a synergistic combination of the two epigenetic drugs. These drugs also increased the amount of apoptosis induced in these tumor cells (García-Domínguez et al., 2018). The mechanistic interaction between these epigenetic therapies and EWSR1-FLI1 is not currently well known. However, many of the tumor cells analyzed were stuck in their G1 phase, and apoptosis was induced (García-Domínguez et al., 2018). Treatment with these agents, individually or in combination, resulted in a significant decrease in levels of *EWSR1-FLI1* mRNA and protein (García-Domínguez et al., 2018). This result was also confirmed in patient-derived xenograft mice.

Additionally, preclinical work examining the effect of small molecule inhibitors on ETS-transcription factors is ongoing. The molecule YK-4-279 is a small molecule inhibitor that binds to EWSR1-FLI1 and blocks its interaction with RNA helicase A (RHA) (Spriano et al., 2019). RHA is required for efficient EWSR1-FLI1 activity. When the RHA- EWSR1-FLI1 interaction is blocked, ES cellular growth is inhibited, and tumor proliferation is halted. This interaction results in cell cycle inhibition and promotion of apoptosis, resulting in reduced growth in tumor cells (Erkizan et al., 2009). RHA-EWSR1-FLI1 interactions serve as a unique point of optimism in development of ES targeted therapies. The clinical derivative of YK-4-279, known as TK-216, is currently in Phase I clinical trials for patients with refractory or relapsed ES (clinicaltrials.gov, NCT02657005).

Further investigation into the efficacy of targeted therapies and their impact on ES outcomes is needed. There are currently numerous clinical trials underway that are focusing on molecular targets to effectively treat ES and result in better outcomes. Unlike kinase fusions, the *EWSR1-FLI1* translocation has yet to be successfully targeted with novel therapies. This represents an area of research that needs further investigation and analysis of *in vivo* and *in vitro* studies, as well as clinical trial protocols. Perhaps most intriguing are studies involving small molecule-based therapies. These trials are summarized in **Table 2** and are a point of optimism in advancing ES treatment options.

Abemaciclib is a small molecule inhibitor of CDK4 and CDK6, and it is currently FDA approved for HR+/HER2− advanced breast cancer (Dowless et al., 2018). Additionally, it is available in lung cancer and other solid tumors. In the laboratory, abemaciclib showed tumor suppression in ES cell lines by blocking the G1 phase of the cell cycle (Dowless et al., 2018). Additionally, when cytokine secretion, antigen presentation, and interferon pathway upregulation were measured, abemaciclib was shown to have anti-inflammatory effects (Dowless et al., 2018).

This small molecule is currently being evaluated in two phase I clinical trials in pediatric solid tumors, including ES, either as monotherapy, or in combination with temozolomide and irinotecan, or with temozolomide alone.

Another therapy, recently approved by the FDA in 2020, is lurbinectedin. Lurbinectedin is an inhibitor of RNA polymerase II and induces DNA breaks in cells that result in apoptosis (Markham, 2020). This small molecule therapy covalently binds to guanine, located centrally in the minor groove of DNA, forming adducts capable of inducing DNA double-strand breaks (Markham, 2020). Lurbinectedin is also being investigated as to whether it may induce immunogenic cell death and increase anti-tumor immunity. This is potentially due to the fact that lurbinectedin has been associated with a reduction in tumor associated macrophages and monocytes in pre-clinical *in vitro* and *in vivo* models (Markham, 2020). Lurbinectedin has been shown to be an effective anti-tumor treatment in solid tumors, and it is well tolerated by patients. Currently there is one current trial testing lurbinectedin in combination with irinotecan against solid tumors in adults but not in the pediatric population (clinicaltrials.gov, NCT02611024). The trial is based on 2016 laboratory studies where lurbinectedin was shown to cause nuclear redistribution of the *EWSR1-FLI1*

TABLE 2 | Small Molecule Clinical Trials that are Recruiting or Active for Adolescent or Pediatric Ewing Sarcoma Patients (All Data from ClinicalTrials.gov).

Name of study	Phase	Target	Small molecule treatment	Identifier
9-ING-41 with Chemotherapy in Sarcoma	II	GSK-3β	9-ING-41	NCT05116800
Cabozantinib-S-Malate in treating younger patients with recurrent, refractory, or Newly diagnosed Sarcomas, Wilms Tumor, or Other Rare Tumors	II	AXL, MET, RET, VEGFR2	Cabozantinib-s-malate	NCT02867592
Ensartinib in treating patients with relapsed or Refractory advanced solid Tumors, Non-Hodgkin Lymphoma, or Histiocytic disorders with ALK or ROS1 genomic alterations (A Pediatric MATCH Treatment Trial)	II	ALK	Ensartinib	NCT03213652
Targeted therapy directed by Genetic testing in treating pediatric patients with relapsed or Refractory advanced solid Tumors, Non-Hodgkin Lymphomas, or Histiocytic disorders (The Pediatric MATCH Screening Trial)	II	FGFR, ALK, IDH1, NTRK, PARP, CDK4/6, PI3K/mTOR, RET, MEK, EZH2, HRAS, MAPK, BRAF	Ensartinib, erdafitinib, ivosidenib, larotrectinib, olaparib, palbociclib, samotolisib, selpercatinib, selumetinib, tazemetostat, tipifarnib, ulixertinib, vemurafenib	NCT03155620
Erdafitinib in treating patients with relapsed or Refractory advanced solid Tumors, Non-Hodgkin Lymphoma, or Histiocytic Disorders with FGFR Mutations (A Pediatric MATCH Treatment Trial)	II	FGFR	Erdafitinib	NCT03210714
Ivosidenib in Treating Patients with Advanced Solid Tumors, Lymphoma, or Histiocytic Disorders with IDH1 Mutations (A Pediatric MATCH Treatment Trial)	II	IDH1	Ivosidenib	NCT04195555
Larotrectinib in Treating Patients with Relapsed or Refractory Advanced Solid Tumors, Non-Hodgkin Lymphoma, or Histiocytic disorders with NTRK Fusions (A Pediatric MATCH Treatment Trial)	II	NTRK	Larotrectinib	NCT03213704
Olaparib in treating patients with relapsed or Refractory advanced solid Tumors, Non-Hodgkin Lymphoma, or Histiocytic disorders with defects in DNA damage repair genes (A Pediatric MATCH Treatment Trial)	II	PARP	Olaparib	NCT03233204
Palbociclib in treating patients with relapsed or Refractory Rb positive advanced solid Tumors, Non-Hodgkin Lymphoma, or Histiocytic disorders with activating alterations in cell cycle genes (A Pediatric MATCH Treatment Trial)	II	CDK4/6	Palbociclib	NCT03526250
Palbociclib + Ganitumab in Ewing Sarcoma	II	CDK4/6, IGF1R	Palbociclib, Ganitumab	NCT04129151
SARC024: A Blanket Protocol to study oral Regorafenib in patients with selected sarcoma subtypes	II	VEGFR, PDGFR-β, FGFR, KIT, RET, RAF	Regorafenib	NCT02048371
A Phase II study evaluating efficacy and safety of Regorafenib in patients with Metastatic Bone Sarcomas (REGOBONE)	II	VEGFR, PDGFR-β, FGFR, KIT, RET, RAF	Regorafenib	NCT02389244
Samotolisib in treating patients with Relapsed or Refractory Advanced Solid Tumors, Non-Hodgkin Lymphoma, or Histiocytic disorders with TSC or PI3K/MTOR mutations (A Pediatric MATCH Treatment Trial)	II	PI3K, mTOR	Samotolisib	NCT03213678
Selpercatinib for the treatment of Advanced Solid Tumors, Lymphomas, or Histiocytic disorders with activating RET gene alterations, a Pediatric MATCH Treatment Trial	II	RET	Selpercatinib	NCT04320888
Sirolimus in combination with Metronomic Chemotherapy in children with recurrent and/or refractory solid and CNS Tumors (AflacST1502)	II	mTOR	Sirolimus	NCT02574728
Tazemetostat in treating patients with Relapsed or Refractory Advanced Solid Tumors, Non-Hodgkin Lymphoma, or Histiocytic disorders with EZH2, SMARCB1, or SMARCA4 Gene Mutations (A Pediatric MATCH Treatment Trial)	II	EZH2, SMARCB1, SMARCA4	Tazemetostat	NCT03213665
Tipifarnib for the Treatment of Advanced Solid Tumors, Lymphoma, or Histiocytic Disorders with HRAS Gene Alterations, a Pediatric MATCH Treatment Trial	II	HRAS	Tipifarnib	NCT04284774

(Continued on following page)

TABLE 2 | (*Continued*) Small Molecule Clinical Trials that are Recruiting or Active for Adolescent or Pediatric Ewing Sarcoma Patients (All Data from ClinicalTrials.gov).

Name of study	Phase	Target	Small molecule treatment	Identifier
Vemurafenib in treating patients with Relapsed or Refractory Advanced Solid Tumors, Non-Hodgkin Lymphoma, or Histiocytic disorders with BRAF V600 Mutations (A Pediatric MATCH Treatment Trial)	II	BRAF	Vemurafenib	NCT03220035
Dasatinib, Ifosfamide, Carboplatin, and Etoposide in treating young patients with Metastatic or Recurrent Malignant Solid Tumors	I/II	BCR/ABL, Src Family Tyrosine kinase (SFK)	Dasatinib	NCT00788125
Study of entrectinib (Rxdx-101) in children and Adolescents with locally Advanced or Metastatic Solid or Primary CNS Tumors and/or Who have no satisfactory treatment options (STARTRK-NG)	I/II	NTRK, ROS1, ALK	Entrectinib	NCT02650401
Study of lenvatinib in combination with Everolimus in recurrent and refractory pediatric solid tumors, including central nervous system tumors	I/II	VEGFR, mTOR	Lenvatinib, everolimus	NCT03245151
Pharmacokinetic Study of PM01183 in Combination with Irinotecan in Patients with Selected Solid Tumors	I/II	DNA minor groove	Lurbinectedin	NCT02611024 (not pediatric)
Study of Onivyde with Talazoparib or Temozolomide in children with Recurrent Solid Tumors and Ewing Sarcoma	I/II	PARP	Talazoparib, Onivyde (irinotecan liposomal)	NCT04901702
Abemaciclib in children with DIPG or Recurrent/ Refractory Solid Tumors (AflacST1501)	I	CDK4/6	Abemaciclib	NCT02644460
A study of Abemaciclib in combination with Temozolomide and Irinotecan and Abemaciclib in combination with Temozolomide in children and young adult participants with Solid Tumors	I	CDK4/6	Abemaciclib	NCT04238819
Cabozantinib with Topotecan-Cyclophosphamide	I	AXL, MET, RET, VEGFR2	Cabozantinib	NCT04661852
Dose Escalation study of CLR 131 in children, Adolescents, and young adults with Relapsed or Refractory Malignant Tumors including but not limited to Neuroblastoma, Rhabdomyosarcoma, Ewing Sarcoma, and Osteosarcoma (CLOVER-2)	I	Lipid rafts	CLR 131 (phospholipid drug conjugate)	NCT03478462
Phase I study of Olaparib and Temozolomide for Ewing Sarcoma or Rhabdomyosarcoma	I	PARP	Olaparib	NCT01858168
Study of Palbociclib combined with Chemotherapy in Pediatric patients with Recurrent/Refractory Solid Tumors	I	CDK4/6	Palbociclib	NCT03709680
Pbi-shRNA™ EWS/FLI1 Type 1 LPX in subjects with advanced Ewing's Sarcoma	I	Type 1 junction EWS-FLI1 translocation	pbi-shRNA™ EWS/FLI1 Type 1 LPX	NCT02736565
A Phase I dose finding study in children with Solid Tumors Recurrent or Refractory to standard therapy	I	VEGFR, PDGFR-β, FGFR, KIT, RET, RAF	Regorafenib	NCT02085148
Clinical Trial of SP-2577 (Seclidemstat) in patients with Relapsed or Refractory Ewing or Ewing-related Sarcomas	I	LSD1	Seclidemstat	NCT03600649
TK216 in patients with Relapsed or Refractory Ewing Sarcoma	I	EWS-FLI1	TK216	NCT02657005
Vorinostat in combination with Chemotherapy in Relapsed/Refractory Solid Tumors and CNS Malignancies (NYMC195)	I	HDAC	Vorinostat	NCT04308330

translocation, resulting in less activity at the promoter and lower levels of mRNA and protein (Harlow et al., 2016). This effect was confirmed in xenograft studies, and when lurbinectedin was combined with irinotecan, there was a complete reversal of EWSR1-FLI1 tumorigenic activity, as ES cells were replaced with benign fat cells. The elimination of tumors in 30–70% of mice in only 11 days from the inception of treatment was observed (Harlow et al., 2016). The targeted therapies discussed above for ES are summarized in **Figure 1**.

Rhabdomyosarcoma

Rhabdomyosarcoma (RMS), derived from primitive mesenchymal cells in the striated skeletal muscle lineage and myogenic progenitors, is the most common soft tissue sarcoma in children.

For localized RMS cases, gross surgical resection of the primary tumor plus radiation therapy and chemotherapy is considered standard-of-care, although long-term toxicities from RT is a concern in younger patients. Over 90% of low-

risk localized RMS patients have relapse-free survival with cytotoxic multi-agent chemotherapy. Most recently vinorelbine and low-dose cyclophosphamide maintenance therapy was trialed in high-risk localized RMS patients and demonstrated improvement in overall survival (Chen et al., 2019). However, overall survival for metastatic and recurrent RMS remains low at 21 and 30%, respectively, indicating the need for novel targeted therapies to improve survival outcomes (Chen et al., 2019).

Alveolar RMS (ARMS), harboring an oncofusion, is the most aggressive subtype due to its high metastasis and recurrence rates (van Erp et al., 2018). ARMS tumors are characterized by the presence of a chromosomal translocation, either the *PAX3-FOXO1* fusion gene or the *PAX7-FOXO1* fusion gene. The *PAX3-FOXO1* rearrangement fuses the DNA-binding domain of paired box gene 3 (*PAX3*) on chromosome 2 to the transactivation domain of forkhead box protein O1 (*FOXO1*) on chromosome 13 (van Erp et al., 2018). The PAX-FOXO1 fusion protein is an aberrant oncogenic transcription factor, resulting in downstream transcription and translation of proteins involved in oncogenic transformation (Chen et al., 2019).

The PAX-FOXO1 transcription factor, which is both upstream to many of the signal cascades that promote RMS tumorigenesis, is a direct and promising target, although inhibitors that bind to PAX-FOXO1 with good specificity and affinity have yet to be designed. Another way to suppress PAX-FOXO1 transcription factor activity is through epigenetic targets, with therapy aimed at inhibiting the co-regulators and chromatin-remodeling complexes involved in transcription. Small molecule inhibitors such as JQ1 that target the BET bromodomain-containing protein (BRD4), an epigenetic reader that mediates transcription, can disrupt BRD4 and PAX3-FOXO1 interaction, leading to degradation of PAX3-FOXO1 and reduced transcription of the oncogenic fusion protein (Gryder et al., 2017). Histone deacetylase (HDAC) inhibitors such as entinostat, panobinostat, and vorinostat have also been shown to delay tumor growth in xenograft RMS models (Hedrick et al., 2015).

Receptor tyrosine kinases (RTKs), such as IGFR1, VEGFR, EGFR, FGFR4, and PDGFRα become constitutively activated and cause downstream tumorigenic effects in the presence of PAX-FOXO1 gene fusions and have also been identified as potential targets in RMS. Recently completed and currently ongoing clinical trials that target these RTKS are summarized in **Table 3**.

A phase II clinical trial compared the IGF-1R inhibitor cixutumumab to conventional multi-agent chemotherapy in pediatric and adult patients with metastatic alveolar and embryonal RMS. Event-free survival (EFS) at 18 months was initially higher in patients receiving cixutumumab treatment (68%) compared to combinational chemotherapy (39%), but at 3-year follow-up, cixutumumab therapy had an event-free survival rate of 16% (Malempati et al., 2015; van Erp et al., 2018; Malempati et al., 2019). A phase II trial of the IGF-1R inhibitor ganitumab in combination with the Src Family Kinase (SFK) inhibitor dasatinib is ongoing in patients with relapsed or refractory RMS (clinicaltrials.gov, NCT03041701).

In a phase II clinical trial comparing conventional chemotherapy against an experimental arm adding the VEGFR inhibitor bevacizumab to cytotoxic chemotherapy in pediatric and adolescent patients with metastatic RMS and soft-tissue sarcomas, median EFS was higher in patients treated with bevacizumab (20.6 months, compared to 14.9 months for chemotherapy only). Higher objective response with bevacizumab was also observed at 54%, compared to 36% in the chemotherapy cohort, but findings were not statistically significant (Chisholm et al., 2017). In another phase I clinical trial evaluating the efficacy of bevacizumab with sorafenib and low-dose cyclophosphamide, 1 of 2 patients with refractory/recurrent RMS experienced a partial response (Navid et al., 2013).

EGFR is over-expressed in about 15–20% of ARMS tumors. Although no *in vivo* experiments targeting EGFR have been conducted yet, *in vitro* experiments in ARMS cell lines found that combination therapy of the anti-EGFR antibody cetuximab and the standard chemotherapy dactinomycin had synergistic effects in inhibiting cell growth and inducing apoptosis, with greater anticancer toxicity than dactinomycin alone (Yamamoto et al., 2013).

PAX3-FOXO1 also amplifies *FGFR4* expression in ARMS, and *FGFR4* has been implicated in resistance to apoptosis in tumors treated with therapeutics targeting the IGF1R-PI3K-mTOR pathway. However, the FGFR4 inhibitor BGJ398 showed synergy with IGF-1R inhibitor AEW54 in an ARMS cell line, suggesting that FGFR4 may be a promising target in treatment resistance prevention (Wachtel et al., 2014). Relapsed ARMS has also been shown to be responsive to pazopanib, a multi-kinase inhibitor currently in use for soft tissue sarcomas (Heske and Mascarenhas, 2021).

In the Children's Oncology Group phase II clinical trial ARST0921, treatment of first-relapse RMS patients with a vinorelbine and cyclophosphamide chemotherapy backbone in combination with either the mTOR inhibitor temsirolimus or the VEGFR inhibitor bevacizumab resulted in 6-month event-free survival rates of 69 and 55%, respectively, with a greater proportion of partial responses in patients treated with temsirolimus (Heske and Mascarenhas, 2021). This data was promising enough to lead to further investigation of temsirolimus in the upfront setting for patients with newly diagnosed intermediate-risk RMS. This randomized phase III trial compares conventional cytotoxic chemotherapy with VAC/VI (alternating vincristine, dactinomycin, cyclophosphamide, and vincristine, irinotecan), with the addition of temsirolimus to the conventional VAC/VI chemotherapy backbone (Heske and Mascarenhas, 2021).

Developmental pathways may also provide therapeutic targets in RMS. GLI transcription factor activation through the constitutively active Hedgehog signaling pathway in RMS is involved in tumorigenesis. ERMS and ARMS xenograft models treated with GLI1/2 inhibitor GANT-61 combined with either temsirolimus or vincristine showed inhibition of proliferation via cell cycle arrest at the G0/G1 phase and significant reductions in tumor growth (Srivastava et al., 2014). Further research is needed to establish the potential of GLI inhibitors in RMS treatment.

TABLE 3 | Small Molecule Clinical Trials that are Recruiting or Active for Pediatric and Adolescent Rhabdomyosarcoma Patients (All Data from ClinicalTrials.gov).

Name of study	Phase	Target(s)	Small molecule treatment	Identifier
9-ING-41 with Chemotherapy in Sarcoma	II	GSK-3β	9-ING-41	NCT05116800
Ensartinib in treating patients with Relapsed or Refractory Advanced Solid Tumors, Non-Hodgkin Lymphoma, or Histiocytic disorders with ALK or ROS1 Genomic alterations (A Pediatric MATCH Treatment Trial)	II	ALK	Ensartinib	NCT03213652
Targeted Therapy Directed by Genetic testing in Treating Pediatric patients with Relapsed or Refractory Advanced Solid Tumors, Non-Hodgkin Lymphomas, or Histiocytic disorders (The Pediatric MATCH Screening Trial)	II	FGFR, ALK, IDH1, NTRK, PARP, CDK4/6, PI3K/mTOR, RET, MEK, EZH2, HRAS, MAPK, BRAF	Ensartinib, erdafitinib, ivosidenib, larotrectinib, olaparib, palbociclib, samotolisib, selpercatinib, selumetinib, tazemetostat, tipifarnib, ulixertinib, vemurafenib	NCT03155620
Erdafitinib in Treating Patients with Relapsed or Refractory Advanced Solid Tumors, Non-Hodgkin Lymphoma, or Histiocytic Disorders with FGFR Mutations (A pediatric MATCH Treatment Trial)	II	FGFR	Erdafitinib	NCT03210714
Ivosidenib in treating patients with Advanced Solid Tumors, Lymphoma, or Histiocytic Disorders with IDH1 Mutations (A Pediatric MATCH Treatment Trial)	II	IDH1	Ivosidenib	NCT04195555
Larotrectinib in treating patients with Relapsed or Refractory Advanced Solid Tumors, Non-Hodgkin Lymphoma, or Histiocytic disorders with NTRK Fusions (A Pediatric MATCH Treatment Trial)	II	NTRK	Larotrectinib	NCT03213704
Olaparib in Treating Patients with Relapsed or Refractory Advanced Solid Tumors, Non-Hodgkin Lymphoma, or Histiocytic Disorders with Defects in DNA Damage Repair Genes (A Pediatric MATCH Treatment Trial)	II	PARP	Olaparib	NCT03233204
Palbociclib in Treating Patients with Relapsed or Refractory Rb Positive Advanced Solid Tumors, Non-Hodgkin Lymphoma, or Histiocytic Disorders with Activating Alterations in Cell Cycle Genes (A Pediatric MATCH Treatment Trial)	II	CDK4/6	Palbociclib	NCT03526250
SARC024: A Blanket Protocol to study oral Regorafenib in patients with selected Sarcoma subtypes	II	VEGFR, PDGFR-β, FGFR, KIT, RET, RAF	Regorafenib	NCT02048371
Samotolisib in treating patients with Relapsed or Refractory Advanced Solid Tumors, Non-Hodgkin Lymphoma, or Histiocytic disorders with TSC or PI3K/MTOR Mutations (A Pediatric MATCH Treatment Trial)	II	PI3K, mTOR	Samotolisib	NCT03213678
Selpercatinib for the Treatment of Advanced Solid Tumors, Lymphomas, or Histiocytic disorders with activating RET Gene alterations, a Pediatric MATCH Treatment Trial	II	RET	Selpercatinib	NCT04320888
Sirolimus in combination with Metronomic Chemotherapy in children with recurrent and/or refractory Solid and CNS Tumors (AflacST1502)	II	mTOR	Sirolimus	NCT02574728
Tipifarnib for the Treatment of Advanced Solid Tumors, Lymphoma, or Histiocytic Disorders with HRAS Gene alterations, a Pediatric MATCH Treatment Trial	II	HRAS	Tipifarnib	NCT04284774
Vemurafenib in treating patients with Relapsed or Refractory Advanced Solid Tumors, Non-Hodgkin Lymphoma, or Histiocytic disorders with BRAF V600 Mutations (A Pediatric MATCH Treatment Trial)	II	BRAF	Vemurafenib	NCT03220035
Insulin-like Growth Factor 1 Receptor (IGF-1R) Antibody AMG479 (Ganitumab) in combination with the Src family kinase (SFK) inhibitor dasatinib in people with Embryonal and Alveolar Rhabdomyosarcoma	I/II	IGF1R, SFK	Ganitumab, dasatinib	NCT03041701
Vincristine and Temozolomide in combination with PEN-866 for Adolescents and young adults with Relapsed or Refractory Solid Tumors	I/II	HSP90	PEN-866	NCT04890093
	I/II	CHK1, CHK2	Prexasertib	NCT04095221

(Continued on following page)

TABLE 3 | (*Continued*) Small Molecule Clinical Trials that are Recruiting or Active for Pediatric and Adolescent Rhabdomyosarcoma Patients (All Data from ClinicalTrials.gov).

Name of study	Phase	Target(s)	Small molecule treatment	Identifier
Prexasertib, Irinotecan, and Temozolomide in people with Desmoplastic small round cell Tumor and Rhabdomyosarcoma				
Onivyde with Talazoparib or Temozolomide in children with recurrent Solid Tumors and Ewing Sarcoma	I/II	PARP	Talazoparib	NCT04901702
A study of Abemaciclib in combination with Temozolomide and Irinotecan and Abemaciclib in combination with Temozolomide in children and young adult participants with Solid Tumors	I	CDK4/6	Abemaciclib	NCT04238819
Dose Escalation Study of CLR 131 in children, Adolescents, and young adults with Relapsed or Refractory Malignant Tumors Including but not limited to Neuroblastoma, Rhabdomyosarcoma, Ewing Sarcoma, and Osteosarcoma (CLOVER-2)	I	Lipid rafts	CLR 131 (phospholipid drug conjugate)	NCT03478462
Mocetinostat with Vinorelbine in Children, Adolescents and young adults with Refractory and/or Recurrent Rhabdomyosarcoma	I	HDAC	Mocetinostat	NCT04299113
Phase I study of Olaparib and Temozolomide for Ewing Sarcoma or Rhabdomyosarcoma	I	PARP	Olaparib	NCT01858168
Study of Palbociclib Combined with Chemotherapy in Pediatric Patients with Recurrent/Refractory Solid Tumors	I	CDK4/6	Palbociclib	NCT03709680
Vorinostat in combination with Chemotherapy in Relapsed/Refractory Solid Tumors and CNS Malignancies (NYMC195)	I	HDAC	Vorinostat	NCT04308330

Therapeutic targets may also lie in the apoptosis pathway. The Bcl-2 family of apoptotic proteins is involved in cancer cell survival and proliferation, and combination of Bcl-2 inhibitor ABT-737 and mTOR inhibitor AZD8055 was highly synergistic in inducing caspase-dependent apoptosis in ARMS and ERMS cells (Preuss et al., 2013).

Numerous targets for RMS are being investigated, yet there are currently no clinically impactful novel agents for the treatment of RMS. Inhibitors of the PAX-FOXO1 fusion protein have yet to be developed as well, despite the discovery of this oncogenic driver since 1993 (Galili et al., 1993). As prognosis for recurrent and metastatic RMS remains poor, this is an area of research that greatly needs further investigation and analysis of both *in vivo* and *in vitro* studies and clinical trials. The targeted therapies discussed above for RMS are summarized in **Figure 2**.

NTRK-Fused Infantile Fibrosarcoma

Infantile fibrosarcoma (IFS) is a soft tissue sarcoma that presents as a localized, but large and rapidly growing tumor in the neonatal setting. IFS accounts for 24.5% of all soft tissue sarcomas found in children under the age of one. IFS has a very good overall prognosis, with studies demonstrating a 5-year survival rate of approximately 90%.

The optimal form of treatment for IFS is surgical resection, but wide local excision often results in mutilating surgery. In particular cases, neoadjuvant chemotherapy may be used to improve the probability of achieving a complete surgical resection; radiotherapy is used when surgical resection is deemed impossible (Parida et al., 2013). Thus there is a need for novel therapies in those IFS patients with extensive or unresectable disease, as well as those with metastatic IFS.

Nearly all IFS tumors harbor a neurotrophic tyrosine receptor kinase (*NTRK*) fusion, with 70% of IFS cases containing the ETS Variant Transcription Factor 6 (*ETV6*)-*NTRK3* gene rearrangement (Knezevich et al., 1998). In *NTRK* rearrangements, the 5' fusion partner induces ligand-independent constitutive activation of the tropomyosin receptor kinase (TRK). This leads to uninterrupted downstream signaling of the RAS/RAF/MEK/ERK and PI3K/AKT pathways, which promote cancer cell survival, invasion, and proliferation (Amatu et al., 2019).

Larotrectinib is a TRKA, TRKB, and TRKC inhibitor that prevents neurotrophin-TRK interaction and activation, inducing apoptosis and inhibition of tumor growth. Larotrectinib has been approved by the FDA for use in children and adults with *NTRK*-fusion-positive tumors that are metastatic and/or will result in severe morbidity upon surgical removal and do not have any resistance mutations (Dunn, 2020).

Various clinical trials have shown efficacy of larotrectinib against *ETV6-NTRK3* fusion-positive IFS with negligible toxicity. In a phase I clinical trial, a 16-month-old female patient with refractory IFS was treated with larotrectinib. One month later, MRI scans revealed a reduction in tumor size by over 90%, and continued clinical response was also observed in later cycles of therapy (Nagasubramanian et al., 2016). Multiple phase 1 studies and case reports show reduction in tumor size, facilitating complete surgical resection, and remarkable reduction in size in other cases without surgical intervention (Caldwell et al., 2020).

Larotrectinib can also be used as a pre-surgical therapy to reduce tumor size, preventing radical and disfiguring surgeries.

Larotrectinib treatment resulted in rapid and durable tumor regression and allowed for limb-sparing surgeries in patients who otherwise would have undergone amputations, confirming larotrectinib as a promising therapy for *ETV6-NTRK3* fusion-positive IFS (DuBois et al., 2018). In a multi-center, phase I clinical study enrolling eight NTRK-fusion-positive IFS patients between 1 month and 21 years of age, larotrectinib was well-tolerated and demonstrated antitumor activity in all eight patients. Four patients avoided disfiguring surgery and instead underwent R0 (negative resection margins with no tumor at marked resection region) and R1 (microscopic residual tumor at resection margin) surgical resection following larotrectinib treatment, indicating that larotrectinib may represent a new standard of care in controlling disease without morbid surgery (Laetsch et al., 2018).

Another gene fusion identified in IFS is the non-classical *LMNA-NTRK1* fusion. Crizotinib, an ALK inhibitor, has been shown to be effective in treating these tumors. Case reports show patients with refractory and metastatic IFS on crizotinib therapy had responses ranging from stable disease to complete and durable responses (Wong et al., 2016; Bender et al., 2019). The targeted therapies discussed above for IFS are summarized in **Figure 3**.

Alveolar Soft Part Sarcoma

Alveolar soft part sarcoma (ASPS) is a rare, slow-growing but highly-angiogenic soft tissue sarcoma that often remains undetected until metastasis. ASPS is characterized by the *TFE3-ASPSCR1* fusion gene, which induces overexpression of the MET receptor tyrosine kinase. This leads to downstream activation of MEK1/2 and AKT, which promote tumor cell proliferation and angiogenesis (Mitton and Federman, 2012).

The 5-year survival rates of localized and metastasized ASPS are 80% and 10–40%, respectively. The main form of treatment for ASPS is surgical removal; radiation therapy may also be used to prevent regrowth following surgery. For unresectable tumors, however, ASPS is resistant to conventional chemotherapies, indicating the need for novel therapeutic targets such as receptor tyrosine kinase inhibitors and other anti-angiogenic agents in the treatment of ASPS (Mitton and Federman, 2012).

Tivantinib (ARQ 197), a selective inhibitor of MET receptor tyrosine kinase, has been investigated in a Phase II clinical trial involving 27 patients ≥13 years with metastatic and/or surgically unresectable ASPS. After 10 cycles of tivantinib, 78% of ASPS patients had stable disease for at least 4 months, and median PFS was 6 months (Wagner et al., 2012).

Sunitinib, a PDGFR and VEGFR tyrosine kinase inhibitor that reduces tumor angiogenesis and triggers cancer cell apoptosis, has demonstrated efficacy in controlling progressive metastatic ASPS in adults. In a case series of 10 adult patients, with a median age of 24, treated with daily sunitinib, treatment was well-tolerated and induced long-lasting responses. Partial response and stable disease were confirmed in 9 cases after 6 months, and median PFS was 17 months (Stacchiotti et al., 2011). A further case study reporting a patient with refractory metastatic ASPS treated with sunitinib described complete primary tumor regression and stabilization of the metastases (Ghose et al., 2012). These anecdotal reports of sunitinib efficacy in adult ASPS tumors suggest a potential therapeutic role of sunitinib in pediatric ASPS patients as well.

Cediranib, a potent inhibitor of VEGFR tyrosine kinase, has also been evaluated in treating adult ASPS. In a phase II clinical trial involving 46 patients, with a median age of 27, with unresectable and metastatic ASPS, 35% had partial response and 60% had stable disease after 24 weeks of daily cediranib treatment (Kummar et al., 2013).

Inflammatory Myofibroblastic Tumor

Inflammatory myofibroblastic tumors (IMT) are rare soft tissue neoplasms made up of myofibroblastic spindle cells, typically characterized by benign local recurrence and rare metastasis. The standard treatment for IMT is complete surgical resection, which has favorable prognosis with most patients surviving past 10 years after complete tumor removal. However, therapy remains lacking for malignant unresectable IMT, especially since chemotherapy and radiation are not particularly effective (Maruyama et al., 2017).

About half of all IMTs are anaplastic lymphoma kinase (ALK) fusion-positive, consisting of cells that express an *ALK* gene rearranged with over 30 different identified 5' fusion partners (Coffin et al., 2001). Rearrangement of *ALK* over-activates ALK receptor tyrosine kinase, which leads to downstream activation of the PI3K/AKT, JAK/STAT, and Ras/ERK pathways, increasing cancer cell proliferation and survival.

Crizotinib, a receptor tyrosine kinase inhibitor, inhibits ALK phosphorylation and its downstream signaling pathways, leading to G1/S cell cycle arrest and apoptosis. Crizotinib is currently used to treat *ALK*-rearranged cancers, such as anaplastic large-cell lymphoma (ALCL) and non-small cell lung cancer (NSCLC), and crizotinib has demonstrated efficacy in treating ALK-positive IMT as well.

In a 2017 study involving 14 unresectable, ALK-positive IMT pediatric patients who were given two doses of oral crizotinib daily, complete and partial responses were observed in five and seven patients, respectively (Mossé et al., 2017). In a cohort of eight ALK-positive IMT patients diagnosed with IMT between 2009-2016 and treated with crizotinib, four achieved a complete response, 3 a partial response, and one patient had stable disease. When preoperative crizotinib was used to decrease tumor size prior to surgical resection, 2 of the 3 partial responses achieved complete response. Furthermore, seven of eight patients were still alive at long-term follow-up, with no evidence of disease in six patients. Crizotinib was also found to be well-tolerated. As such, crizotinib combined with surgical resection appears to be effective in long-term disease control of ALK-positive IMT (Trahair et al., 2019).

For patients with *RANBP2-ALK* fusion positive epithelioid inflammatory myofibroblastic sarcoma (eIMS), a malignant variant of *ALK*-fusion-positive IMT, CD30 and ALK combination therapy may have high therapeutic potency. *RANBP2-ALK* eIMS xenografts treated with brentuximab-vedotin, targeting $CD30^{+}$ tumor cells, and crizotinib resulted in tumor shrinkage and prolonged disease-free survival. In the diagnosis eIMS model, the majority of mice were confirmed as tumor-free 180 days past the study end date. However, disease

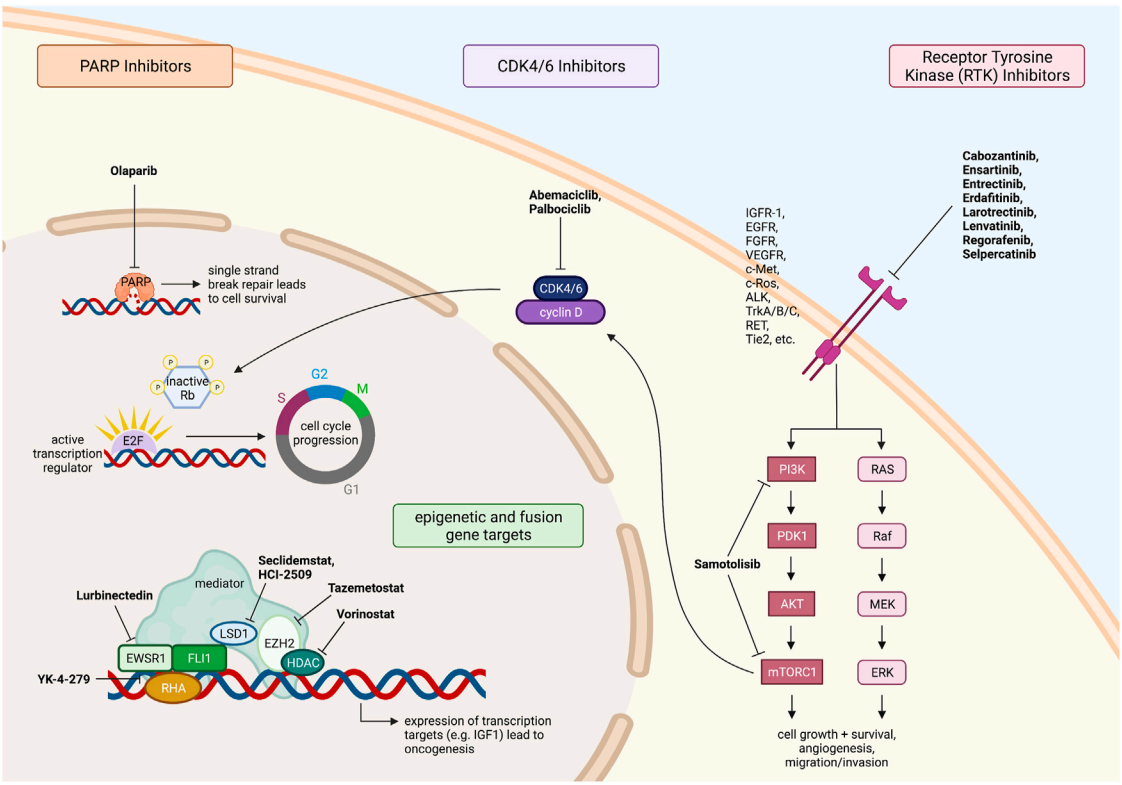

FIGURE 1 | Fusion driven pediatric solid tumors with clinically actionable targets. Ewing sarcoma therapeutic targets and drugs under investigation. All figures were created with BioRender.com.

recurrence was observed in all mice in the relapsed eIMS model, indicating that CD30 and ALK combination therapy may be most effective as early treatment for eIMS (Fordham et al., 2020).

Ceritinib, another ALK receptor tyrosine kinase inhibitor, has demonstrated efficacy against crizotinib-resistant tumors, with stronger potency in both crizotinib-naïve and crizotinib-refractory patients. Ceritinib is currently approved for use in ALK-positive NSCLC, but it has also shown excellent disease control in various ALK-positive IMT case studies (Santarpia et al., 2017). Recent case reports also show response in stage IV IMT or unresectable IMTs with ceritinib therapy and tumor response, allowing for surgical resection or complete response with ceritinib therapy alone (Mittal et al., 2021).

Alectinib is another ALK-inhibitor that has demonstrated efficacy against ALK-fusion-positive IMT. A case study in which a 26-year-old male with hyper-progressive ALK-fusion-positive IMT experienced a significant and durable response to treatment with alectinib was reported in 2017 (Saiki et al., 2017).

Entrectinib is an inhibitor of TRK, ROS1, and ALK, and has been shown to induce rapid and durable anti-cancer responses in NTRK, ROS1, and ALK-fusion tumors. A 16-year-old female patient with unresectable DCTN1-ALK-fusion-positive IMT had a complete response to entrectinib therapy, which controlled disease with low toxicity (Ambati et al., 2018).

Other gene translocations observed in IMT include proto-oncogene tyrosine-protein kinase (*ROS1*) fusions, which lead to tumorigenesis in mechanisms similar to ALK fusions. In a case study reported in 2021, the ALK- and ROS1-inhibitor lorlatinib was reported successful in treating a patient with refractory *TFG-ROS1* fusion-positive IMT (Carcamo et al., 2021).

Fibrolamellar Hepatocellular Carcinoma

Fibrolamellar hepatocellular carcinoma (FL-HCC) is a rare form of hepatocellular carcinoma (HCC), affecting adolescents and young adults with no prior history of liver disease or risk factors for live cancer. In FL-HCC, a ~400 kilobase deletion on chromosome 19 gives rise to the DnaJ Heat Shock Protein Family (HSP40) Member B1 (DNAJB1)-Protein Kinase CAMP-Activated Catalytic Subunit Alpha (PRKACA) fusion gene, and the corresponding *DNAJB1-PRKACA*-fusion protein has upregulated protein kinase activity to promote tumorigenesis (Honeyman et al., 2014).

Current treatments for FL-HCC remain in development. Chemotherapy for unresectable hepatocellular carcinoma (HCC) is a combination of atezolizumab and bevacizumab, but this therapy showed no clinical benefits in case studies in

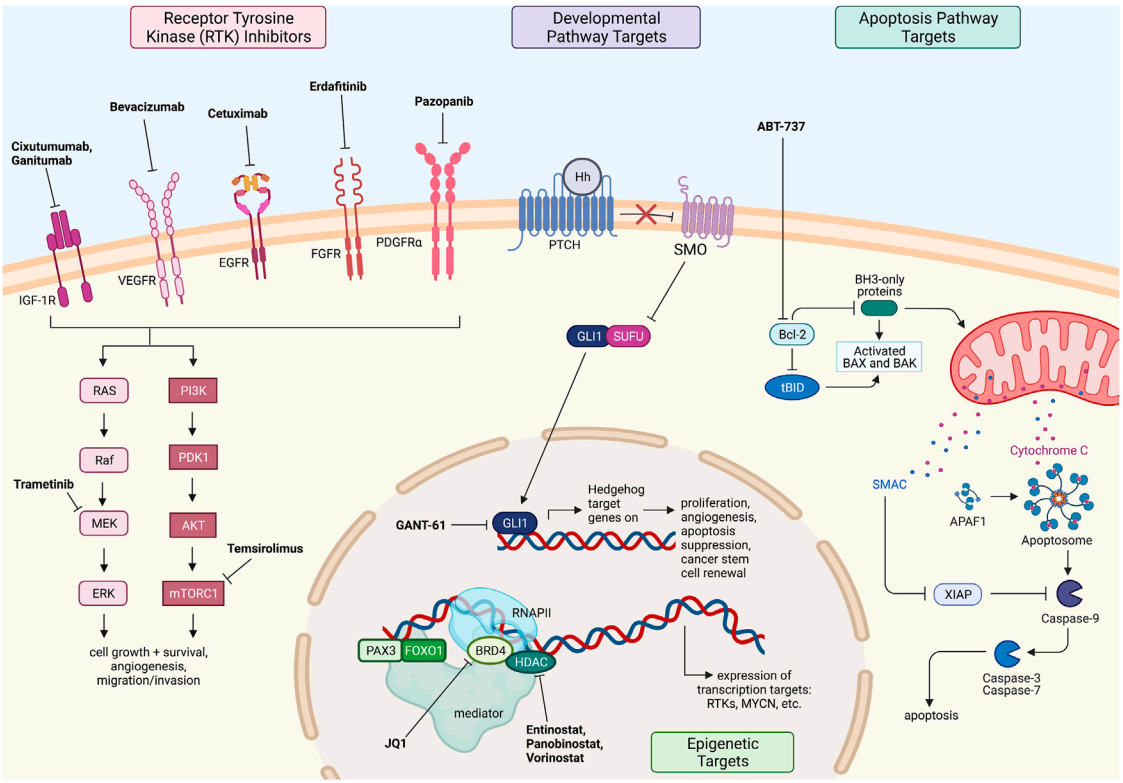

FIGURE 2 | Fusion driven pediatric solid tumors with clinically actionable targets. Rhabdomyosarcoma therapeutic targets and drugs under investigation. All figures were created with BioRender.com.

two patients with advanced FL-HCC (Al Zahrani and Alfakeeh, 2021). Sorafenib is another multi-tyrosine kinase inhibitor in use against advanced HCC; however, sorafenib has limited efficacy against FL-HCC, with only delayed progression of disease as the best response (Ang et al., 2013).

The only potentially curative treatment for FL-HCC is liver resection or liver transplantation; if the tumor is not completely removed, likelihood of recurrence is high. For patients with metastatic and/or unresectable disease, there are no effective treatments available and FL-HCC is progressive and fatal; median survival time is less than 12 months (Kassahun, 2016).

However, novel combination and targeted therapies are being investigated in the treatment of FL-HCC. In a phase II trial of continuous IV fluorouracil and thrice weekly recombinant interferon alfa-2b administered to eight FL-HCC patients, one patient had complete response while four had partial responses, and overall median survival was 23.1 months (Patt et al., 2003). In a case study involving a 27-year-old woman with FL-HCC, 10 cycles of gemcitabine and oxaliplatin were administered, and 5 years after the regimen had been completed, the woman remained in complete remission (Gras et al., 2012).

The PRKACA kinase domain was also found to play an essential role in FL-HCC tumor formation, suggesting the potential for small molecule PRKACA-inhibitors as a therapy for FL-HCC (Kastenhuber et al., 2017). However, further research is needed to investigate the efficacy and viability of PRKACA inhibitors against FL-HCC.

Renal Cell Carcinoma

Pediatric translocation renal cell carcinoma (tRCC) is a rare kidney cancer found in children, accounting for 2–5% of all childhood renal neoplasms. Less-advanced tRCC tumors can be treated via surgical resection, whereas more-advanced tRCC is treated with targeted therapies.

The most common mutation associated with RCC is the *TFE3*-fusion gene, where the *TFE3* gene on chromosome Xp11.12 is rearranged with a fusion partner (i.e., PRCC, ASPSCR1, NONO, CLTC, SFPQ, etc.) from a different chromosome. The *TFE3*-fusion gene is a constitutively active promoter, causing dysregulated transcriptional TFE3 activity that leads to tumorigenesis through downstream upregulation of the PI3K/AKT/mTOR signaling pathway (Damayanti et al., 2018).

Cabozantinib is a small-molecule VEGFR2 and MET tyrosine kinase inhibitor that has already been approved for use in medullary thyroid cancer and renal cell carcinoma. For tRCC tumors that express MET, cabozantinib has been shown to regress disease with tolerable toxicity. In a 16-year-old female patient presenting with refractory, locally recurrent *TFE3*-fusion-positive tRCC with lung metastases, treatment with cabozantinib led to prompt and durable

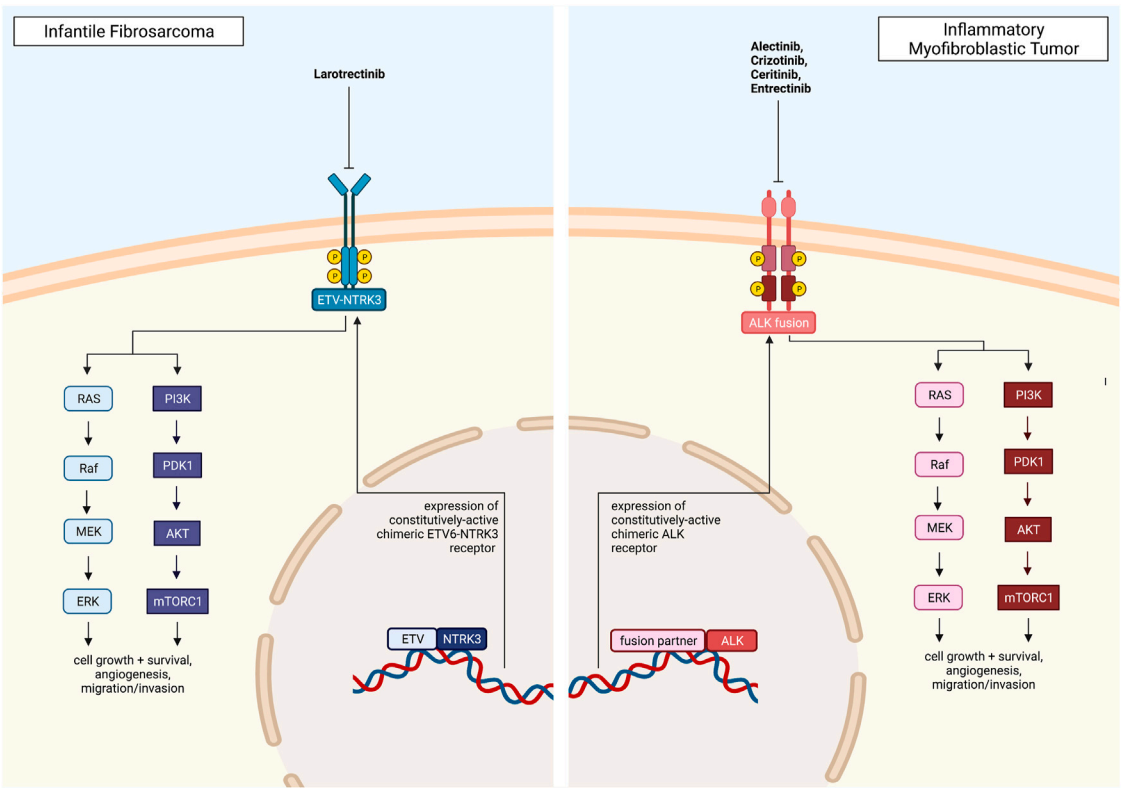

FIGURE 3 | Pediatric solid tumors with a direct, targetable fusion kinase, including Infantile Fibrosarcoma and Inflammatory Myofibroblastic Tumor, and clinically approved drugs. All figures were created with BioRender.com.

disease control. The patient was also noted to have reduction in pain, weight gain of 90% of weight previously lost on chemotherapy, and improved quality of life. In a 12-year-old male patient with stage IV *TFE3*-fusion-positive tRCC, treatment with cabozantinib demonstrated excellent disease control, including reduced pain just after 3 months and halted disease progression even 18 months later (Wedekind et al., 2017).

VEGFR tyrosine kinase and mTOR inhibitors, which are used in metastatic RCC therapies, have also demonstrated efficacy in disease control of tRCC. In a case study of 53 patients with tRCC, 21 patients who were *TFE3*-fusion-positive received targeted therapy. Fourteen patients treated with sunitinib had a median PFS of 8.2 months, with seven patients achieving either a partial or complete response. Eight patients treated with sorafenib had a median PFS of more than 6 months. Two pediatric patients had partial responses with single agent therapy of either sunitinib or sorafenib, and both patients continued with stable disease after 29 months. For patients that experienced disease progression while being treated with VEGFR inhibitors, switching to mTOR inhibitors temsirolimus and everolimus resulted in stable disease (Malouf et al., 2010).

Synovial Sarcoma

Synovial sarcoma (SS) is a rare soft tissue sarcoma that occurs in adolescents and young adults, with a pathognomonic t (X; 18) (p11.2; q11.2) chromosomal translocation, fusing the *SS18* (formerly known as *SYT*) gene with the *SSX1*, *SSX2*, or *SSX4* gene (Clark et al., 1994; Shipley et al., 1994). Therapeutic approaches involve systemic chemotherapy with doxorubicin and ifosfamide combined with radiation therapy and/or surgery for local control.

The SS18-SSX fusion protein acts as an epigenetic modifier, driving tumorigenesis in SS cells (Kadoch and Crabtree, 2013). SWItch Sucrose Non-Fermentable (SWI/SNF) chromatin remodeling complexes, containing the BAF (BRG1 or BRM associated factors) complex, are disrupted in SS cells when the SS18-SSX fusion protein competitively replaces the wild-type SS18 in the BAF complex (Kadoch and Crabtree, 2013). The fusion SS18-SSX protein is found to co-localize with Polycomb Repressive Complexes 1 and 2 (PRC1, PRC2) (Soulez et al., 1999; Lubieniecka et al., 2008). PRC2 silences chromatin with its catalytic subunit, the histone methyltransferase Enhancer of Zeste 2 (EZH2) (Wilson et al., 2010). The relocalization of oncogenic BAF complexes to PRC repressed domains, recruitment of RNA Polymerase II, and initiation of transcription leads to epigenetic reprogramming and drives tumorigenesis (McBride et al., 2018).

Preclinical studies using EZH2 inhibitors in SS cell lines were promising, showing a decrease in cellular proliferation and migration *in vitro*, and with decreased tumor burden in xenograft models (Kawano et al., 2016; Shen et al., 2016). However, in a phase II clinical trial in adult patients with synovial sarcoma, the selective EZH2 inhibitor tazemetostat

exhibited less promising preliminary results. Tazemetostat was well tolerated by patients with few adverse events, but the best response observed was stable disease, which occurred in 33% of patients (Schoffski P et al., 2017).

Other Novel Approaches Such as Immunotherapy and ONC201/TIC10

Various strategies have been employed to promote the immune response against pediatric solid tumors. These include oncolytic virus-based therapy, antibody-dependent cellular cytotoxicity (ADCC), bispecific antibodies, immune checkpoint inhibitors, tumor microenvironment targeted therapies (cancer-associated fibroblasts, macrophages), cytokines, growth factors and CAR-T cells (Marayati et al., 2019).

TRAIL-Inducing Compound #10 (TIC10)/ONC201 is a novel agent that activates a potent innate immune pro-apoptotic anti-cancer response through the integrated stress response (Allen et al., 2013; Kline et al., 2016; Wagner et al., 2018; Prabhu et al., 2020). ONC201 has potential for further development in pediatric solid tumors including in combination with epigenetic modulators (Chang et al., 2020; Chang et al., 2021; Honeyman et al., 2021; Zhang et al., 2021).

CONCLUSION

Pediatric non-CNS solid tumors are a diverse group of tumors that are best managed with a multi-disciplinary approach. Combinations of chemotherapy, surgery and radiation have improved patient outcomes (Ward et al., 2019b), but these approaches have changed little in the previous 2 decades. In addition, patients with unresectable, metastatic, and recurrent disease typically face dismal outcomes with current multimodal therapy. With the ability to analyze the genomes of individual patients and identify molecular drivers specific to an individual cancer, opportunities for clinical trials, such as the Pediatric MATCH trial run by the Children's Oncology group, are now available. Currently, there exists promising novel therapies in preclinical investigation as well as ongoing clinical trials. Investigation continues in these targeted therapies, their toxicities, and administration in the pediatric population. Novel therapies, including small molecule agents, targeted therapies, and other precision medicine-based treatments, can offer an opportunity to examine unique mechanisms in treating pediatric sarcomas and other solid tumors.

Preclinical strategies to target gene fusions include both the utilization of existing inhibitors as well as the development of novel drugs through rational design approaches. The development of novel therapies requires a significant development time and multidisciplinary effort that includes expertise in genomics, molecular biology, pharmacology, clinical trials, and clinical oncology. Using these resources more effectively will not only help drive the development of novel therapies, but also better inform individual patient treatment decisions. As our understanding of the molecular drivers of pediatric fusion-positive cancers increases, so do our abilities to tailor therapies toward better outcomes for this patient population.

DATA AVAILABILITY STATEMENT

The original contributions presented in the study are included in the article/Supplementary Material, further inquiries can be directed to the corresponding authors.

AUTHOR CONTRIBUTIONS

All authors listed have made a substantial, direct, and intellectual contribution to the work and approved it for publication.

FUNDING

This work was supported by a grant from the Rhode Island Foundation (W-IC) and an NIH grant (CA173453) to WE-D. WE-D is an American Cancer Society Research Professor and is supported by the Mencoff Family University Professorship at Brown University.

ACKNOWLEDGMENTS

All figures were created with BioRender.com.

REFERENCES

Adzhubei, I. A., Schmidt, S., Peshkin, L., Ramensky, V. E., Gerasimova, A., Bork, P., et al. (2010). A Method and Server for Predicting Damaging Missense Mutations. *Nat. Methods* 7 (4), 248–249. doi:10.1038/nmeth0410-248

Akgul, M., Williamson, S. R., Ertoy, D., Argani, P., Gupta, S., Caliò, A., et al. (2021). Diagnostic Approach in TFE3-Rearranged Renal Cell Carcinoma: a Multi-Institutional International Survey. *J. Clin. Pathol.* 74 (5), 291–299. doi:10.1136/jclinpath-2020-207372

Al Zahrani, A., and Alfakeeh, A. (2021). Fibrolamellar Hepatocellular Carcinoma Treated with Atezolizumab and Bevacizumab: Two Case Reports. *J. Med. Case Rep.* 15 (1), 132. doi:10.1186/s13256-021-02695-8

Allen, J. E., Krigsfeld, G., Mayes, P. A., Patel, L., Dicker, D. T., Patel, A. S., et al. (2013). Dual Inactivation of Akt and ERK by TIC10 Signals Foxo3a Nuclear Translocation, TRAIL Gene Induction, and Potent Antitumor Effects. *Sci. Transl Med.* 5 (171), 171ra17. doi:10.1126/scitranslmed.3004828

Amatu, A., Sartore-Bianchi, A., Bencardino, K., Pizzutilo, E. G., Tosi, F., and Siena, S. (2019). Tropomyosin Receptor Kinase (TRK) Biology and the Role of NTRK Gene Fusions in Cancer. *Ann. Oncol.* 30 (Suppl. l_8), viii5–viii15. doi:10.1093/annonc/mdz383

Ambati, S. R., Slotkin, E. K., Chow-Maneval, E., and Basu, E. M. (2018). Entrectinib in Two Pediatric Patients with Inflammatory Myofibroblastic Tumors Harboring ROS1 or ALK Gene Fusions. *JCO Precis Oncol.* 2018, 1–6. doi:10.1200/PO.18.00095

Ang, C. S., Kelley, R. K., Choti, M. A., Cosgrove, D. P., Chou, J. F., Klimstra, D., et al. (2013). Clinicopathologic Characteristics and Survival Outcomes of Patients with Fibrolamellar Carcinoma: Data from the Fibrolamellar Carcinoma Consortium. *Gastrointest. Cancer Res.* 6 (1), 3–9.

Antonescu, C. R., Tschernyavsky, S. J., Woodruff, J. M., Jungbluth, A. A., Brennan, M. F., and Ladanyi, M. (2002). Molecular Diagnosis of clear Cell Sarcoma: Detection of EWS-ATF1 and MITF-M Transcripts and Histopathological and Ultrastructural Analysis of 12 Cases. *J. Mol. Diagn.* 4 (1), 44–52. doi:10.1016/S1525-1578(10)60679-4

Arnold, M. A., and Barr, F. G. (2017). Molecular Diagnostics in the Management of Rhabdomyosarcoma. *Expert Rev. Mol. Diagn.* 17 (2), 189–194. doi:10.1080/14737159.2017.1275965

Aulmann, S., Longerich, T., Schirmacher, P., Mechtersheimer, G., and Penzel, R. (2007). Detection of the ASPSCR1-TFE3 Gene Fusion in Paraffin-Embedded Alveolar Soft Part Sarcomas. *Histopathology* 50 (7), 881–886. doi:10.1111/j.1365-2559.2007.02693.x

Bender, J., Anderson, B., Bloom, D. A., Rabah, R., McDougall, R., Vats, P., et al. (2019). Refractory and Metastatic Infantile Fibrosarcoma Harboring LMNA-NTRK1 Fusion Shows Complete and Durable Response to Crizotinib. *Cold Spring Harb Mol. Case Stud.* 5 (1). doi:10.1101/mcs.a003376

Bourgeois, J. M., Knezevich, S. R., Mathers, J. A., and Sorensen, P. H. (2000). Molecular Detection of the ETV6-NTRK3 Gene Fusion Differentiates Congenital Fibrosarcoma from Other Childhood Spindle Cell Tumors. *Am. J. Surg. Pathol.* 24 (7), 937–946. doi:10.1097/00000478-200007000-00005

Brohl, A. S., Patidar, R., Turner, C. E., Wen, X., Song, Y. K., Wei, J. S., et al. (2017). Frequent Inactivating Germline Mutations in DNA Repair Genes in Patients with Ewing Sarcoma. *Genet. Med.* 19 (8), 955–958. doi:10.1038/gim.2016.206

Brohl, A. S., Solomon, D. A., Chang, W., Wang, J., Song, Y., Sindiri, S., et al. (2014). The Genomic Landscape of the Ewing Sarcoma Family of Tumors Reveals Recurrent STAG2 Mutation. *Plos Genet.* 10 (7), e1004475. doi:10.1371/journal.pgen.1004475

Caldwell, K. J., De La Cuesta, E., Morin, C., Pappo, A., and Helmig, S. (2020). A Newborn with a Large NTRK Fusion Positive Infantile Fibrosarcoma Successfully Treated with Larotrectinib. *Pediatr. Blood Cancer* 67 (9), e28330. doi:10.1002/pbc.28330

Carcamo, B., Bista, R., Wilson, H., Reddy, P., and Pacheco, J. (2021). Rapid Response to Lorlatinib in a Patient with TFG-ROS1 Fusion Positive Inflammatory Myofibroblastic Tumor of the Chest Wall Metastatic to the Brain and Refractory to First and Second Generation ROS1 Inhibitors. *J. Pediatr. Hematol. Oncol.* 43 (5), e718–e722. doi:10.1097/MPH.0000000000002185

Chang, F., Lin, F., Cao, K., Surrey, L. F., Aplenc, R., Bagatell, R., et al. (2019). Development and Clinical Validation of a Large Fusion Gene Panel for Pediatric Cancers. *J. Mol. Diagn.* 21 (5), 873–883. doi:10.1016/j.jmoldx.2019.05.006

Chang, W.-i., Zhou, L., Seyhan, A. A., Prabhu, V. V., and El-Deiry, W. S. (2021). Abstract 1060: Combinatorial Therapy of Imipridones and Histone Deacetylase Inhibitors in Ewing Sarcoma Cell Lines Demonstrates Synergistic Cell Death. *Cancer Res.* 81 (13 Suppl. ment), 1060. doi:10.1158/1538-7445.am2021-1060

Chang, W.-I., Zhou, L., Seyhan, A. A., Zhang, Y., and El-Deiry, W. S. (2020). Abstract 3902: Novel Therapeutic Targeting of Epigenetic Aberrations in Pediatric Sarcomas through Combination of ONC201 and HDAC Inhibitors. *Cancer Res.* 80 (16 Suppl. ment), 3902. doi:10.1158/1538-7445.am2020-3902

Chen, C., Dorado Garcia, H., Scheer, M., and Henssen, A. G. (2019). Current and Future Treatment Strategies for Rhabdomyosarcoma. *Front. Oncol.* 9, 1458. doi:10.3389/fonc.2019.01458

Chisholm, J. C., Merks, J. H. M., Casanova, M., Bisogno, G., Orbach, D., Gentet, J. C., et al. (2017). Open-label, Multicentre, Randomised, Phase II Study of the EpSSG and the ITCC Evaluating the Addition of Bevacizumab to Chemotherapy in Childhood and Adolescent Patients with Metastatic Soft Tissue Sarcoma (The BERNIE Study). *Eur. J. Cancer* 83, 177–184. doi:10.1016/j.ejca.2017.06.015

Choy, E., Butrynski, J. E., Harmon, D. C., Morgan, J. A., George, S., Wagner, A. J., et al. (2014). Phase II Study of Olaparib in Patients with Refractory Ewing Sarcoma Following Failure of Standard Chemotherapy. *BMC Cancer* 14, 813. doi:10.1186/1471-2407-14-813

Clark, J., Rocques, P. J., Crew, A. J., Gill, S., Shipley, J., Chan, A. M., et al. (1994). Identification of Novel Genes, SYT and SSX, Involved in the t(X;18)(p11.2;q11.2) Translocation Found in Human Synovial Sarcoma. *Nat. Genet.* 7 (4), 502–508. doi:10.1038/ng0894-502

Coffin, C. M., Patel, A., Perkins, S., Elenitoba-Johnson, K. S., Perlman, E., and Griffin, C. A. (2001). ALK1 and P80 Expression and Chromosomal Rearrangements Involving 2p23 in Inflammatory Myofibroblastic Tumor. *Mod. Pathol.* 14 (6), 569–576. doi:10.1038/modpathol.3880352

Cook, J. R., Dehner, L. P., Collins, M. H., Ma, Z., Morris, S. W., Coffin, C. M., et al. (2001). Anaplastic Lymphoma Kinase (ALK) Expression in the Inflammatory Myofibroblastic Tumor: a Comparative Immunohistochemical Study. *Am. J. Surg. Pathol.* 25 (11), 1364–1371. doi:10.1097/00000478-200111000-00003

Damayanti, N. P., Budka, J. A., Khella, H. W. Z., Ferris, M. W., Ku, S. Y., Kauffman, E., et al. (2018). Therapeutic Targeting of TFE3/IRS-1/PI3K/mTOR Axis in Translocation Renal Cell Carcinoma. *Clin. Cancer Res.* 24 (23), 5977–5989. doi:10.1158/1078-0432.CCR-18-0269

de Alava, E., Panizo, A., Antonescu, C. R., Huvos, A. G., Pardo-Mindán, F. J., Barr, F. G., et al. (2000). Association of EWS-FLI1 Type 1 Fusion with Lower Proliferative Rate in Ewing's Sarcoma. *Am. J. Pathol.* 156 (3), 849–855. doi:10.1016/S0002-9440(10)64953-X

Dowless, M., Lowery, C. D., Shackleford, T., Renschler, M., Stephens, J., Flack, R., et al. (2018). Abemaciclib Is Active in Preclinical Models of Ewing Sarcoma via Multipronged Regulation of Cell Cycle, DNA Methylation, and Interferon Pathway Signaling. *Clin. Cancer Res.* 24 (23), 6028–6039. doi:10.1158/1078-0432.CCR-18-1256

DuBois, S. G., Laetsch, T. W., Federman, N., Turpin, B. K., Albert, C. M., Nagasubramanian, R., et al. (2018). The Use of Neoadjuvant Larotrectinib in the Management of Children with Locally Advanced TRK Fusion Sarcomas. *Cancer* 124 (21), 4241–4247. doi:10.1002/cncr.31701

Duchman, K. R., Gao, Y., and Miller, B. J. (2015). Prognostic Factors for Survival in Patients with Ewing's Sarcoma Using the Surveillance, Epidemiology, and End Results (SEER) Program Database. *Cancer Epidemiol.* 39 (2), 189–195. doi:10.1016/j.canep.2014.12.012

Dunn, D. B. (2020). Larotrectinib and Entrectinib: TRK Inhibitors for the Treatment of Pediatric and Adult Patients with NTRK Gene Fusion. *J. Adv. Pract. Oncol.* 11 (4), 418–423. doi:10.6004/jadpro.2020.11.4.9

Dupain, C., Harttrampf, A. C., Urbinati, G., Geoerger, B., and Massaad-Massade, L. (2017). Relevance of Fusion Genes in Pediatric Cancers: Toward Precision Medicine. *Mol. Ther. Nucleic Acids* 6, 315–326. doi:10.1016/j.omtn.2017.01.005

Erkizan, H. V., Kong, Y., Merchant, M., Schlottmann, S., Barber-Rotenberg, J. S., Yuan, L., et al. (2009). A Small Molecule Blocking Oncogenic Protein EWS-FLI1 Interaction with RNA Helicase A Inhibits Growth of Ewing's Sarcoma. *Nat. Med.* 15 (7), 750–756. doi:10.1038/nm.1983

Ewing, J. (19211972). Classics in Oncology. Diffuse Endothelioma of Bone. James Ewing. Proceedings of the New York Pathological Society, 1921. *CA Cancer J. Clin.* 22 (2), 95–98. doi:10.3322/canjclin.22.2.95

Fordham, A. M., Xie, J., Gifford, A. J., Wadham, C., Morgan, L. T., Mould, E. V. A., et al. (2020). CD30 and ALK Combination Therapy Has High Therapeutic Potency in RANBP2-ALK-Rearranged Epithelioid Inflammatory Myofibroblastic Sarcoma. *Br. J. Cancer* 123 (7), 1101–1113. doi:10.1038/s41416-020-0996-2

Galili, N., Davis, R. J., Fredericks, W. J., Mukhopadhyay, S., Rauscher, F. J., Emanuel, B. S., et al. (1993). Fusion of a fork Head Domain Gene to PAX3 in the Solid Tumour Alveolar Rhabdomyosarcoma. *Nat. Genet.* 5 (3), 230–235. doi:10.1038/ng1193-230

García-Domínguez, D. J., Hontecillas-Prieto, L., Rodríguez-Núñez, P., Pascual-Pasto, G., Vila-Ubach, M., García-Mejías, R., et al. (2018). The Combination of Epigenetic Drugs SAHA and HCI-2509 Synergistically Inhibits EWS-FLI1 and Tumor Growth in Ewing Sarcoma. *Oncotarget* 9 (59), 31397–31410. doi:10.18632/oncotarget.25829

Gaspar, N., Hawkins, D. S., Dirksen, U., Lewis, I. J., Ferrari, S., Le Deley, M. C., et al. (2015). Ewing Sarcoma: Current Management and Future Approaches through Collaboration. *J. Clin. Oncol.* 33 (27), 3036–3046. doi:10.1200/JCO.2014.59.5256

Ghose, A., Tariq, Z., and Veltri, S. (2012). Treatment of Multidrug Resistant Advanced Alveolar Soft Part Sarcoma with Sunitinib. *Am. J. Ther.* 19 (1), e56–8. doi:10.1097/MJT.0b013e3181e70d20

Gras, P., Truant, S., Boige, V., Ladrat, L., Rougier, P., Pruvot, F. R., et al. (2012). Prolonged Complete Response after GEMOX Chemotherapy in a Patient with Advanced Fibrolamellar Hepatocellular Carcinoma. *Case Rep. Oncol.* 5 (1), 169–172. doi:10.1159/000338242

Gryder, B. E., Yohe, M. E., Chou, H. C., Zhang, X., Marques, J., Wachtel, M., et al. (2017). PAX3-FOXO1 Establishes Myogenic Super Enhancers and Confers BET Bromodomain Vulnerability. *Cancer Discov.* 7 (8), 884–899. doi:10.1158/2159-8290.CD-16-1297

Harlow, M. L., Maloney, N., Roland, J., Guillen Navarro, M. J., Easton, M. K., Kitchen-Goosen, S. M., et al. (2016). Lurbinectedin Inactivates the Ewing Sarcoma Oncoprotein EWS-FLI1 by Redistributing it within the Nucleus. *Cancer Res.* 76 (22), 6657–6668. doi:10.1158/0008-5472.CAN-16-0568

Hayashi, M., Chu, D., Meyer, C. F., Llosa, N. J., McCarty, G., Morris, C. D., et al. (2016). Highly Personalized Detection of Minimal Ewing Sarcoma Disease

burden from Plasma Tumor DNA. *Cancer* 122 (19), 3015–3023. doi:10.1002/cncr.30144

Hedrick, E., Crose, L., Linardic, C. M., and Safe, S. (2015). Histone Deacetylase Inhibitors Inhibit Rhabdomyosarcoma by Reactive Oxygen Species-dependent Targeting of Specificity Protein Transcription Factors. *Mol. Cancer Ther.* 14 (9), 2143–2153. doi:10.1158/1535-7163.MCT-15-0148

Herrero-Martín, D., Osuna, D., Ordóñez, J. L., Sevillano, V., Martins, A. S., Mackintosh, C., et al. (2009). Stable Interference of EWS-FLI1 in an Ewing Sarcoma Cell Line Impairs IGF-1/IGF-1R Signalling and Reveals TOPK as a New Target. *Br. J Cancer* 101 (1), 80–90. doi:10.1038/sj.bjc.6605104

Heske, C. M., and Mascarenhas, L. (2021). Relapsed Rhabdomyosarcoma. *J. Clin. Med.* 10, 804. doi:10.3390/jcm10040804

Honeyman, J. N., Simon, E. P., Robine, N., Chiaroni-Clarke, R., Darcy, D. G., Lim, I. I., et al. (2014). Detection of a Recurrent DNAJB1-PRKACA Chimeric Transcript in Fibrolamellar Hepatocellular Carcinoma. *Science* 343 (6174), 1010–1014. doi:10.1126/science.1249484

Honeyman, J. N., Chang, W-I., Prabhu, V. V., Allen, J. E., Zhou, L., and El-Deiry, W. S. (2021). Abstract 1040: Imipridones Exhibit Synergy with Sorafenib, HDAC Inhibition, PARP Inhibition, and Proteasome Inhibition in Liver Cancer Cell Lines. *Cancer Res.* 81 (13 Suppl. ment), 1040. doi:10.1158/1538-7445.am2021-1040

Honoki, K., Stojanovski, E., McEvoy, M., Fujii, H., Tsujiuchi, T., Kido, A., et al. (2007). Prognostic Significance of P16 INK4a Alteration for Ewing Sarcoma: a Meta-Analysis. *Cancer* 110 (6), 1351–1360. doi:10.1002/cncr.22908

Kadoch, C., and Crabtree, G. R. (2013). Reversible Disruption of mSWI/SNF (BAF) Complexes by the SS18-SSX Oncogenic Fusion in Synovial Sarcoma. *Cell* 153 (1), 71–85. doi:10.1016/j.cell.2013.02.036

Kassahun, W. T. (2016). Contemporary Management of Fibrolamellar Hepatocellular Carcinoma: Diagnosis, Treatment, Outcome, Prognostic Factors, and Recent Developments. *World J. Surg. Oncol.* 14 (1), 151. doi:10.1186/s12957-016-0903-8

Kastenhuber, E. R., Lalazar, G., Houlihan, S. L., Tschaharganeh, D. F., Baslan, T., Chen, C. C., et al. (2017). DNAJB1-PRKACA Fusion Kinase Interacts with β-catenin and the Liver Regenerative Response to Drive Fibrolamellar Hepatocellular Carcinoma. *Proc. Natl. Acad. Sci. U S A.* 114 (50), 13076–13084. doi:10.1073/pnas.1716483114

Kawano, S., Grassian, A. R., Tsuda, M., Knutson, S. K., Warholic, N. M., Kuznetsov, G., et al. (2016). Preclinical Evidence of Anti-tumor Activity Induced by EZH2 Inhibition in Human Models of Synovial Sarcoma. *PLoS One* 11 (7), e0158888. doi:10.1371/journal.pone.0158888

Kline, C. L., Van den Heuvel, A. P., Allen, J. E., Prabhu, V. V., Dicker, D. T., and El-Deiry, W. S. (2016). ONC201 Kills Solid Tumor Cells by Triggering an Integrated Stress Response Dependent on ATF4 Activation by Specific eIF2α Kinases. *Sci. Signal.* 9 (415), ra18. doi:10.1126/scisignal.aac4374

Knezevich, S. R., McFadden, D. E., Tao, W., Lim, J. F., and Sorensen, P. H. (1998). A Novel ETV6-NTRK3 Gene Fusion in Congenital Fibrosarcoma. *Nat. Genet.* 18 (2), 184–187. doi:10.1038/ng0298-184

Kummar, S., Allen, D., Monks, A., Polley, E. C., Hose, C. D., Ivy, S. P., et al. (2013). Cediranib for Metastatic Alveolar Soft Part Sarcoma. *J. Clin. Oncol.* 31 (18), 2296–2302. doi:10.1200/JCO.2012.47.4288

Ladanyi, M., and Gerald, W. (1994). Fusion of the EWS and WT1 Genes in the Desmoplastic Small Round Cell Tumor. *Cancer Res.* 54 (11), 2837–2840.

Laetsch, T. W., DuBois, S. G., Mascarenhas, L., Turpin, B., Federman, N., Albert, C. M., et al. (2018). Larotrectinib for Paediatric Solid Tumours Harbouring NTRK Gene Fusions: Phase 1 Results from a Multicentre, Open-Label, Phase 1/2 Study. *Lancet Oncol.* 19 (5), 705–714. doi:10.1016/S1470-2045(18)30119-0

Lerman, D. M., Monument, M. J., McIlvaine, E., Liu, X. Q., Huang, D., Monovich, L., et al. (2015). Tumoral TP53 And/or CDKN2A Alterations Are Not Reliable Prognostic Biomarkers in Patients with Localized Ewing Sarcoma: a Report from the Children's Oncology Group. *Pediatr. Blood Cancer* 62 (5), 759–765. doi:10.1002/pbc.25340

Lubieniecka, J. M., de Bruijn, D. R., Su, L., van Dijk, A. H., Subramanian, S., van de Rijn, M., et al. (2008). Histone Deacetylase Inhibitors Reverse SS18-SSX-Mediated Polycomb Silencing of the Tumor Suppressor Early Growth Response 1 in Synovial Sarcoma. *Cancer Res.* 68 (11), 4303–4310. doi:10.1158/0008-5472.CAN-08-0092

Malempati, S., Weigel, B., Ingle, A. M., Ahern, C. H., Carroll, J. M., Roberts, C. T., et al. (2012). Phase I/II Trial and Pharmacokinetic Study of Cixutumumab in Pediatric Patients with Refractory Solid Tumors and Ewing Sarcoma: a Report from the Children's Oncology Group. *J. Clin. Oncol.* 30 (3), 256–262. doi:10.1200/JCO.2011.37.4355

Malempati, S., Weigel, B. J., Chi, Y. Y., Tian, J., Anderson, J. R., Parham, D. M., et al. (2019). The Addition of Cixutumumab or Temozolomide to Intensive Multiagent Chemotherapy Is Feasible but Does Not Improve Outcome for Patients with Metastatic Rhabdomyosarcoma: A Report from the Children's Oncology Group. *Cancer* 125 (2), 290–297. doi:10.1002/cncr.31770

Malempati, S. W., Anderson, J., Parham, D., Teot, L. A., Rodeberg, D. A., Yock, T. I., et al. (2015). Early Results from Children's Oncology Group (COG) ARST08P1: Pilot Studies of Cixutumumab or Temozolomide with Intensive Multiagent Chemotherapy for Patients with Metastatic Rhabdomyosarcoma (RMS). *J. Clin. Oncol.* 33 (15), 10015. doi:10.1200/jco.2015.33.15_suppl.10015

Malouf, G. G., Camparo, P., Oudard, S., Schleiermacher, G., Theodore, C., Rustine, A., et al. (2010). Targeted Agents in Metastatic Xp11 translocation/TFE3 Gene Fusion Renal Cell Carcinoma (RCC): a Report from the Juvenile RCC Network. *Ann. Oncol.* 21 (9), 1834–1838. doi:10.1093/annonc/mdq029

Marayati, R., Quinn, C. H., and Beierle, E. A. (2019). Immunotherapy in Pediatric Solid Tumors-A Systematic Review. *Cancers (Basel)* 11 (12), 2022. doi:10.3390/cancers11122022

Markham, A. (2020). Lurbinectedin: First Approval. *Drugs* 80 (13), 1345–1353. doi:10.1007/s40265-020-01374-0

Maruyama, Y., Fukushima, T., Gomi, D., Kobayashi, T., Sekiguchi, N., Sakamoto, A., et al. (2017). Relapsed and Unresectable Inflammatory Myofibroblastic Tumor Responded to Chemotherapy: A Case Report and Review of the Literature. *Mol. Clin. Oncol.* 7 (4), 521–524. doi:10.3892/mco.2017.1383

McBride, M. J., Pulice, J. L., Beird, H. C., Ingram, D. R., D'Avino, A. R., Shern, J. F., et al. (2018). The SS18-SSX Fusion Oncoprotein Hijacks BAF Complex Targeting and Function to Drive Synovial Sarcoma. *Cancer Cell* 33 (6), 1128–e7. doi:10.1016/j.ccell.2018.05.002

Mittal, A., Gupta, A., Rastogi, S., Barwad, A., and Sharma, S. (2021). Near-complete Response to Low-Dose Ceritinib in Recurrent Infantile Inflammatory Myofibroblastic Tumour. *Ecancermedicalscience* 15, 1215. doi:10.3332/ecancer.2021.1215

Mitton, B., and Federman, N. (2012). Alveolar Soft Part Sarcomas: Molecular Pathogenesis and Implications for Novel Targeted Therapies. *Sarcoma* 2012, 428789. doi:10.1155/2012/428789

Mossé, Y. P., Voss, S. D., Lim, M. S., Rolland, D., Minard, C. G., Fox, E., et al. (2017). Targeting ALK with Crizotinib in Pediatric Anaplastic Large Cell Lymphoma and Inflammatory Myofibroblastic Tumor: A Children's Oncology Group Study. *J. Clin. Oncol.* 35 (28), 3215–3221. doi:10.1200/JCO.2017.73.4830

Nagasubramanian, R., Wei, J., Gordon, P., Rastatter, J. C., Cox, M. C., and Pappo, A. (2016). Infantile Fibrosarcoma with NTRK3-ETV6 Fusion Successfully Treated with the Tropomyosin-Related Kinase Inhibitor LOXO-101. *Pediatr. Blood Cancer* 63 (8), 1468–1470. doi:10.1002/pbc.26026

Navid, F., Baker, S. D., McCarville, M. B., Stewart, C. F., Billups, C. A., Wu, J., et al. (2013). Phase I and Clinical Pharmacology Study of Bevacizumab, Sorafenib, and Low-Dose Cyclophosphamide in Children and Young Adults with Refractory/recurrent Solid Tumors. *Clin. Cancer Res.* 19 (1), 236–246. doi:10.1158/1078-0432.CCR-12-1897

Parida, L., Fernandez-Pineda, I., Uffman, J. K., Davidoff, A. M., Krasin, M. J., Pappo, A., et al. (2013). Clinical Management of Infantile Fibrosarcoma: a Retrospective Single-Institution Review. *Pediatr. Surg. Int.* 29 (7), 703–708. doi:10.1007/s00383-013-3326-4

Patt, Y. Z., Hassan, M. M., Lozano, R. D., Brown, T. D., Vauthey, J. N., Curley, S. A., et al. (2003). Phase II Trial of Systemic Continuous Fluorouracil and Subcutaneous Recombinant Interferon Alfa-2b for Treatment of Hepatocellular Carcinoma. *J. Clin. Oncol.* 21 (3), 421–427. doi:10.1200/JCO.2003.10.103

Prabhu, V. V., Morrow, S., Rahman Kawakibi, A., Zhou, L., Ralff, M., Ray, J., et al. (2020). ONC201 and Imipridones: Anti-cancer Compounds with Clinical Efficacy. *Neoplasia* 22 (12), 725–744. doi:10.1016/j.neo.2020.09.005

Preuss, E., Hugle, M., Reimann, R., Schlecht, M., and Fulda, S. (2013). Pan-mammalian Target of Rapamycin (mTOR) Inhibitor AZD8055 Primes Rhabdomyosarcoma Cells for ABT-737-Induced Apoptosis by Down-Regulating Mcl-1 Protein. *J. Biol. Chem.* 288 (49), 35287–35296. doi:10.1074/jbc.M113.495986

Saiki, M., Ohyanagi, F., Ariyasu, R., Koyama, J., Sonoda, T., Nishikawa, S., et al. (2017). Dramatic Response to Alectinib in Inflammatory Myofibroblastic

Tumor with Anaplastic Lymphoma Kinase Fusion Gene. *Jpn. J. Clin. Oncol.* 47 (12), 1189–1192. doi:10.1093/jjco/hyx133

Sankar, S., Bell, R., Stephens, B., Zhuo, R., Sharma, S., Bearss, D. J., et al. (2013). Mechanism and Relevance of EWS/FLI-mediated Transcriptional Repression in Ewing Sarcoma. *Oncogene* 32 (42), 5089–5100. doi:10.1038/onc.2012.525

Sankar, S., Theisen, E. R., Bearss, J., Mulvihill, T., Hoffman, L. M., Sorna, V., et al. (2014). Reversible LSD1 Inhibition Interferes with Global EWS/ETS Transcriptional Activity and Impedes Ewing Sarcoma Tumor Growth. *Clin. Cancer Res.* 20 (17), 4584–4597. doi:10.1158/1078-0432.CCR-14-0072

Santarpia, M., Daffinà, M. G., D'Aveni, A., Marabello, G., Liguori, A., Giovannetti, E., et al. (2017). Spotlight on Ceritinib in the Treatment of ALK+ NSCLC: Design, Development and Place in Therapy. *Drug Des. Devel Ther.* 11, 2047–2063. doi:10.2147/DDDT.S113500

Schmid, I., and von Schweinitz, D. (2017). Pediatric Hepatocellular Carcinoma: Challenges and Solutions. *J. Hepatocell Carcinoma* 4, 15–21. doi:10.2147/JHC.S94008

Schoffski P, A. M., Stacchiotti, S., Davis, L. E., Villalobos, V. M., Italiano, A., George, S., et al. (2017). Phase 2 Multicenter Study of the EZH2 Inhibitor Tazemetostat in Adults with Synovial Sarcoma (NCT02601950). *J. Clin. Oncol.* 35 (15), 11057. doi:10.1200/jco.2017.35.15_suppl.11057

Shen, J. K., Cote, G. M., Gao, Y., Choy, E., Mankin, H. J., Hornicek, F. J., et al. (2016). Targeting EZH2-Mediated Methylation of H3K27 Inhibits Proliferation and Migration of Synovial Sarcoma *In Vitro*. *Sci. Rep.* 6, 25239. doi:10.1038/srep25239

Shipley, J. M., Clark, J., Crew, A. J., Birdsall, S., Rocques, P. J., Gill, S., et al. (1994). The t(X;18)(p11.2;q11.2) Translocation Found in Human Synovial Sarcomas Involves Two Distinct Loci on the X Chromosome. *Oncogene* 9 (5), 1447–1453.

Shulman, D. S., Klega, K., Imamovic-Tuco, A., Clapp, A., Nag, A., Thorner, A. R., et al. (2018). Detection of Circulating Tumour DNA Is Associated with Inferior Outcomes in Ewing Sarcoma and Osteosarcoma: a Report from the Children's Oncology Group. *Br. J Cancer* 119 (5), 615–621. doi:10.1038/s41416-018-0212-9

Siegel, D. A., Richardson, L. C., Henley, S. J., Wilson, R. J., Dowling, N. F., Weir, H. K., et al. (2020). Pediatric Cancer Mortality and Survival in the United States, 2001-2016. *Cancer* 126 (19), 4379–4389. doi:10.1002/cncr.33080

Smeland, S., Bielack, S. S., Whelan, J., Bernstein, M., Hogendoorn, P., Krailo, M. D., et al. (2019). Survival and Prognosis with Osteosarcoma: Outcomes in More Than 2000 Patients in the EURAMOS-1 (European and American Osteosarcoma Study) Cohort. *Eur. J. Cancer* 109, 36–50. doi:10.1016/j.ejca.2018.11.027

Soulez, M., Saurin, A. J., Freemont, P. S., and Knight, J. C. (1999). SSX and the Synovial-sarcoma-specific Chimaeric Protein SYT-SSX Co-localize with the Human Polycomb Group Complex. *Oncogene* 18 (17), 2739–2746. doi:10.1038/sj.onc.1202613

Spriano, F., Chung, E. Y. L., Gaudio, E., Tarantelli, C., Cascione, L., Napoli, S., et al. (2019). The ETS Inhibitors YK-4-279 and TK-216 Are Novel Antilymphoma Agents. *Clin. Cancer Res.* 25 (16), 5167–5176. doi:10.1158/1078-0432.CCR-18-2718

Srivastava, R. K., Kaylani, S. Z., Edrees, N., Li, C., Talwelkar, S. S., Xu, J., et al. (2014). GLI Inhibitor GANT-61 Diminishes Embryonal and Alveolar Rhabdomyosarcoma Growth by Inhibiting Shh/AKT-mTOR axis. *Oncotarget* 5 (23), 12151–12165. doi:10.18632/oncotarget.2569

Stacchiotti, S., Negri, T., Zaffaroni, N., Palassini, E., Morosi, C., Brich, S., et al. (2011). Sunitinib in Advanced Alveolar Soft Part Sarcoma: Evidence of a Direct Antitumor Effect. *Ann. Oncol.* 22 (7), 1682–1690. doi:10.1093/annonc/mdq644

Stahl, M., Ranft, A., Paulussen, M., Bölling, T., Vieth, V., Bielack, S., et al. (2011). Risk of Recurrence and Survival after Relapse in Patients with Ewing Sarcoma. *Pediatr. Blood Cancer* 57 (4), 549–553. doi:10.1002/pbc.23040

Trahair, T., Gifford, A. J., Fordham, A., Mayoh, C., Fadia, M., Lukeis, R., et al. (2019). Crizotinib and Surgery for Long-Term Disease Control in Children and Adolescents with ALK-Positive Inflammatory Myofibroblastic Tumors. *JCO Precis Oncol.* 3 (3), 1–11. doi:10.1200/PO.18.00297

van Erp, A. E. M., Versleijen-Jonkers, Y. M. H., van der Graaf, W. T. A., and Fleuren, E. D. G. (2018). Targeted Therapy-Based Combination Treatment in Rhabdomyosarcoma. *Mol. Cancer Ther.* 17 (7), 1365–1380. doi:10.1158/1535-7163.MCT-17-1131

van Maldegem, A. M., Bovée, J. V., Peterse, E. F., Hogendoorn, P. C., and Gelderblom, H. (2016). Ewing Sarcoma: The Clinical Relevance of the Insulin-like Growth Factor 1 and the Poly-ADP-Ribose-Polymerase Pathway. *Eur. J. Cancer* 53, 171–180. doi:10.1016/j.ejca.2015.09.009

Wachtel, M., Rakic, J., Okoniewski, M., Bode, P., Niggli, F., and Schäfer, B. W. (2014). FGFR4 Signaling Couples to Bim and Not Bmf to Discriminate Subsets of Alveolar Rhabdomyosarcoma Cells. *Int. J. Cancer* 135 (7), 1543–1552. doi:10.1002/ijc.28800

Wagner, A. J., Goldberg, J. M., Dubois, S. G., Choy, E., Rosen, L., Pappo, A., et al. (2012). Tivantinib (ARQ 197), a Selective Inhibitor of MET, in Patients with Microphthalmia Transcription Factor-Associated Tumors: Results of a Multicenter Phase 2 Trial. *Cancer* 118 (23), 5894–5902. doi:10.1002/cncr.27582

Wagner, J., Kline, C. L., Zhou, L., Campbell, K. S., MacFarlane, A. W., Olszanski, A. J., et al. (2018). Dose Intensification of TRAIL-Inducing ONC201 Inhibits Metastasis and Promotes Intratumoral NK Cell Recruitment. *J. Clin. Invest.* 128 (6), 2325–2338. doi:10.1172/JCI96711

Ward, Z. J., Yeh, J. M., Bhakta, N., Frazier, A. L., and Atun, R. (2019). Estimating the Total Incidence of Global Childhood Cancer: a Simulation-Based Analysis. *Lancet Oncol.* 20 (4), 483–493. doi:10.1016/S1470-2045(18)30909-4

Ward, Z. J., Yeh, J. M., Bhakta, N., Frazier, A. L., and Atun, R. (2019). Estimating the Total Incidence of Global Childhood Cancer: a Simulation-Based Analysis. *Lancet Oncol.* 20 (4), 483–493. doi:10.1016/S1470-2045(18)30909-4

Wedekind, M. F., Ranalli, M., and Shah, N. (2017). Clinical Efficacy of Cabozantinib in Two Pediatric Patients with Recurrent Renal Cell Carcinoma. *Pediatr. Blood Cancer* 64 (11). doi:10.1002/pbc.26586

Wexler, L. H., and Ladanyi, M. (2010). Diagnosing Alveolar Rhabdomyosarcoma: Morphology Must Be Coupled with Fusion Confirmation. *J. Clin. Oncol.* 28 (13), 2126–2128. doi:10.1200/JCO.2009.27.5339

Wilson, B. G., Wang, X., Shen, X., McKenna, E. S., Lemieux, M. E., Cho, Y. J., et al. (2010). Epigenetic Antagonism between Polycomb and SWI/SNF Complexes during Oncogenic Transformation. *Cancer Cell* 18 (4), 316–328. doi:10.1016/j.ccr.2010.09.006

Wong, V., Pavlick, D., Brennan, T., Yelensky, R., Crawford, J., Ross, J. S., et al. (2016). Evaluation of a Congenital Infantile Fibrosarcoma by Comprehensive Genomic Profiling Reveals an LMNA-NTRK1 Gene Fusion Responsive to Crizotinib. *J. Natl. Cancer Inst.* 108 (1). doi:10.1093/jnci/djv307

Yamamoto, Y., Fukuda, K., Fuchimoto, Y., Matsuzaki, Y., Saikawa, Y., Kitagawa, Y., et al. (2013). Cetuximab Promotes Anticancer Drug Toxicity in Rhabdomyosarcomas with EGFR Amplification *In Vitro*. *Oncol. Rep.* 30 (3), 1081–1086. doi:10.3892/or.2013.2588

Zhang, Y., Zhou, L., Safran, H., Borsuk, R., Lulla, R., Tapinos, N., et al. (2021). EZH2i EPZ-6438 and HDACi Vorinostat Synergize with ONC201/TIC10 to Activate Integrated Stress Response, DR5, Reduce H3K27 Methylation, ClpX and Promote Apoptosis of Multiple Tumor Types Including DIPG. *Neoplasia* 23 (8), 792–810. doi:10.1016/j.neo.2021.06.007

Zöllner, S. K., Amatruda, J. F., Bauer, S., Collaud, S., de Álava, E., DuBois, S. G., et al. (2021). Ewing Sarcoma-Diagnosis, Treatment, Clinical Challenges and Future Perspectives. *J. Clin. Med.* 10 (8), 1685. doi:10.3390/jcm10081685

Conflict of Interest: WE-D is a co-founder of Oncoceutics, Inc., a subsidiary of Chimerix. WE-D has disclosed his relationship with Oncoceutics and potential conflict of interest to his academic institution/employer and is fully compliant with NIH and institutional policy that is managing this potential conflict of interest.

The remaining authors declare that the research was conducted in the absence of any commercial or financial relationships that could be construed as a potential conflict of interest

Publisher's Note: All claims expressed in this article are solely those of the authors and do not necessarily represent those of their affiliated organizations, or those of the publisher, the editors and the reviewers. Any product that may be evaluated in this article, or claim that may be made by its manufacturer, is not guaranteed or endorsed by the publisher.

Copyright © 2022 Chang, Lin, Liguori, Honeyman, DeNardo and El-Deiry. This is an open-access article distributed under the terms of the Creative Commons Attribution License (CC BY). The use, distribution or reproduction in other forums is permitted, provided the original author(s) and the copyright owner(s) are credited and that the original publication in this journal is cited, in accordance with accepted academic practice. No use, distribution or reproduction is permitted which does not comply with these terms.

Advantages of publishing in Frontiers

OPEN ACCESS
Articles are free to read for greatest visibility and readership

FAST PUBLICATION
Around 90 days from submission to decision

HIGH QUALITY PEER-REVIEW
Rigorous, collaborative, and constructive peer-review

TRANSPARENT PEER-REVIEW
Editors and reviewers acknowledged by name on published articles

Frontiers
Avenue du Tribunal-Fédéral 34
1005 Lausanne | Switzerland

Visit us: www.frontiersin.org
Contact us: frontiersin.org/about/contact

REPRODUCIBILITY OF RESEARCH
Support open data and methods to enhance research reproducibility

DIGITAL PUBLISHING
Articles designed for optimal readership across devices

FOLLOW US
@frontiersin

IMPACT METRICS
Advanced article metrics track visibility across digital media

EXTENSIVE PROMOTION
Marketing and promotion of impactful research

LOOP RESEARCH NETWORK
Our network increases your article's readership